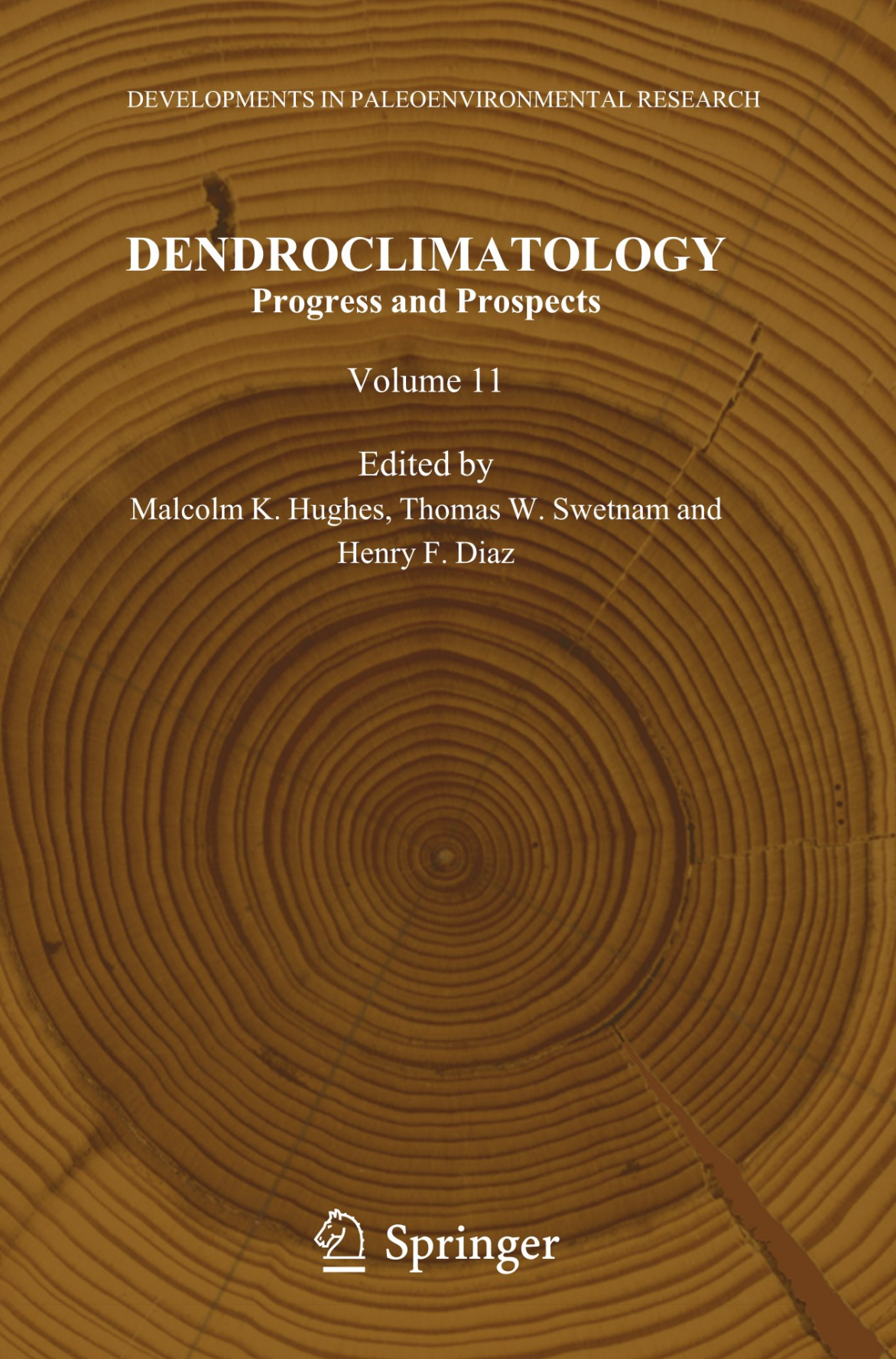
DEVELOPMENTS IN PALEOENVIRONMENTAL RESEARCH
DENDROCLIMATOLOGY
Progress and Prospects
Volume 11
Edited by
Malcolm K. Hughes, Thomas W. Swetnam and
Henry F. Diaz
Springer

Dendroclimatology

Developments in Paleoenvironmental Research

VOLUME 11

Aims and Scope:
Paleoenvironmental research continues to enjoy tremendous interest and progress in the scientific community. The overall aims and scope of the *Developments in Paleoenvironmental Research* book series is to capture this excitement and document these developments. Volumes related to any aspect of paleoenvironmental research, encompassing any time period, are within the scope of the series. For example, relevant topics include studies focused on terrestrial, peatland, lacustrine, riverine, estuarine, and marine systems, ice cores, cave deposits, palynology, isotopes, geochemistry, sedimentology, paleontology, etc. Methodological and taxonomic volumes relevant to paleoenvironmental research are also encouraged. The series will include edited volumes on a particular subject, geographic region, or time period, conference and workshop proceedings, as well as monographs. Prospective authors and/or editors should consult the series editor for more details. The series editor also welcomes any comments or suggestions for future volumes.

For further volumes:
http://www.springer.com/series/5869

Dendroclimatology

Progress and Prospects

Edited by

Malcolm K. Hughes

University of Arizona, Tucson, AZ, USA

Thomas W. Swetnam

University of Arizona, Tucson, AZ, USA

Henry F. Diaz

University of Colorado, Boulder, CO, USA

Springer

Editors
Prof. Malcolm K. Hughes
University of Arizona
Laboratory of Tree-Ring Research
85721 Tucson Arizona
USA
mhughes@ltrr.arizona.edu

Prof. Thomas W. Swetnam
University of Arizona
Laboratory of Tree-Ring Research
85721 Tucson Arizona
USA
tswetnam@ltrr.arizona.edu

Prof. Henry F. Diaz
University Colorado
CIRES
Broadway 325
80305-3328 Boulder Colorado
USA
Henry.F.Diaz@noaa.gov

ISSN 1571-5299
ISBN 978-1-4020-4010-8 e-ISBN 978-1-4020-5725-0
DOI 10.1007/978-1-4020-5725-0
Springer Dordrecht Heidelberg London New York

Library of Congress Control Number: 2010936678

Cover illustration: Inner rings (first ring AD 521) of a Douglas-fir beam from Broken Flute Cave, Arizona. Photo by Thomas W. Swetnam, copyright Laboratory of Tree-Ring Research, The University of Arizona.

Printed on acid-free paper

Springer is part of Springer Science+Business Media (www.springer.com)

Preface

This collection is the latest of a series of efforts to evaluate the contributions of dendroclimatology, the study of past climate using tree rings, to climatology and to other fields and activities. The origins of dendroclimatology as a collaborative international field may be traced to two meetings held at the Laboratory of Tree-Ring Research (LTRR), University of Arizona, in April 1974 and June 1977. The First International Workshop on Dendroclimatology (April 1974), inspired and organized by Harold C. Fritts, set the scene for a scientific venture of remarkable ambition—the development of networks of fully dated, adequately replicated, and documented tree-ring chronologies throughout the temperate and subarctic regions of both the Northern and Southern Hemispheres. It was at this meeting, attended by scientists from ten countries, that the International Tree-Ring Data Bank (ITRDB) was established, with an interim committee chaired by Fritts and including Bernd Becker (Germany), Zdzisaw Bednarz (Poland), Jon Pilcher (UK), and Charles Stockton (USA). The foundation of the ITRDB (now part of the World Data Center for Paleoclimatology, operated by the US National Oceanic and Atmospheric Administration, NOAA), signaled the acceptance by most of the active practitioners around the world of a shared minimum set of criteria for the development and recording of dendroclimatic data. This in turn made it possible to conceive of many individual efforts, leading to the establishment of internally consistent networks at national, continental, and eventually, global scales.

The June 1977 meeting, organized with the support of the National Science Foundation (NSF), had the goal of reviewing Harold Fritts's pioneering dendroclimatic reconstruction projects. Most of the participants at the meeting were climatologists interested in a topic that had received very little attention up to that time—high-resolution paleoclimatology. Those present included Roger Barry, Ray Bradley, Henry Diaz, Mick Kelly, John Kutzbach, Murray Mitchell, Jr., and Harry van Loon. The meeting led to several productive long-term scientific collaborations, which in turn led to, among other things, the creation of baseline comprehensive instrumental climate databases for studying climatic variations over the past century and a half. From today's viewpoint, it is difficult to imagine how little was known about interannual- to century-scale variability in the climate system at that time, with published sketches of the spectrum of climatic variability exhibiting little or no power between bidecadal and millennial frequencies. Recall, the El Niño/Southern

Oscillation (ENSO) phenomenon was not as well understood then as it is now, and the view of longer fluctuations had changed little since the early twentieth-century work of Sir Gilbert Walker. The last 35 years have seen an extraordinary growth of interest in the very topics of climatology and broader environmental science to which tree-ring studies can contribute most—variability on interannual to century timescales. The tree-ring record has become more and more important to the understanding of the climate system as we learn about things like decadal and longer patterns, and it is central to the issue of whether current climate changes are extraordinary, and if so, on what scale.

This volume arose from a workshop titled, 'Tree Rings and Climate: Sharpening the Focus,' held in Tucson, Arizona, April 6–9, 2004, although it contains much material developed since the workshop. There were forty oral presentations and twenty-two poster presentations at the workshop, with participants coming from many countries, and including 'users' of dendroclimatic information, such as climatologists, as well as 'producers.' The primary aim of the meeting was to review what has been learned, by using tree rings, about natural climate variability and its environmental and social impacts. This was done by reviewing and synthesizing the results of the last 35 years, and identifying the strengths and weaknesses of dendroclimatology and the needs for and the opportunities for future work. Thanks are due to the following bodies for financial and other support for the meeting, and hence for making this volume possible: the Paleoclimatology Program in the Division of Atmospheric Sciences at the US National Science Foundation; the Climate Change Data and Detection Program, US National Oceanic and Atmospheric Administration; the Past Global Changes (PAGES) project of the International Geosphere-Biosphere Program; the Institute for the Study of Planet Earth, University of Arizona; the Office of the Vice President for Research, University of Arizona; and the Laboratory of Tree-Ring Research, University of Arizona.

We are also particularly grateful to the colleagues who kindly undertook the task of providing peer reviews for the chapters in this collection, and to the authors for their good grace in awaiting its publication. Diana Miller has done us all a great favor by her meticulous and constructive copyediting of the manuscripts.

Finally, thanks are due to those who set this ball rolling: Andrew Douglass in the early twentieth century, Edward Schulman and Bruno Huber in the mid-twentieth century, and, notably, Harold C. Fritts, who made the global venture possible, and to whom this volume is dedicated.

Tucson, Arizona — Malcolm K. Hughes
Tucson, Arizona — Thomas W. Swetnam
Boulder, Colorado — Henry F. Diaz

Contents

Contributors

Kevin J. Anchukaitis Laboratory of Tree-Ring Research, The University of Arizona, Tucson, AZ, USA; Lamont-Doherty Earth Observatory, Columbia University, Palisades, NY 10964, USA, kja@ldeo.columbia.edu

Juan Carlos Aravena Centro de Estudios Cuaternarios (CEQUA), Universidad de Magallanes, Casilla 113-D, Punta Arenas, Chile, juan.aravena@cequa.cl

Jaime Argollo Laboratorio de Dendrocronología e Historia Ambiental, Facultad de Ciencias Geológicas, Universidad Mayor de San Andrés, Calle 27, Cota Cota, La Paz, Bolivia, jargollo@ceibo.entelnet.bo

Franco Biondi Department of Geography, University of Nevada, Reno MS 156, Reno, NV 89557, USA, fbiondi@unr.edu

Jose Boninsegna Departamento de Dendrocronología e Historia Ambiental, Instituto Argentino de Nivología, Glaciología y Ciencias Ambientales (IANIGLA), CONICET, CC 330, 5500, Mendoza, Argentina, pbonin@lab.cricyt.edu.ar

Raymond S. Bradley Department of Geosciences, Climate System Research Center, University of Massachusetts, Amherst, MA 01003-9297, USA, rbradley@geo.umass.edu

Keith R. Briffa Climatic Research Unit, University of East Anglia, Norwich, NR4 7TJ, UK, k.briffa@uea.ac.uk

Peter M. Brown Rocky Mountain Tree-Ring Research, 2901 Moore Lane, Fort Collins, CO 80526, USA, pmb@rtrr.org

Julian Cerano-Paredes Instituto Nacional de Investigaciones Forestales y Agropecuarias, INIFAP CENID-RASPA, Km 6.5 Margen Derecha del Canal Sacramento, Gómez Palacio, Durango, 35140, México, cerano.julian@inifap.gob.mx

Malcolm Cleaveland Tree-Ring Laboratory, Department of Geosciences, University of Arkansas, Ozark Hall 113, Fayetteville, AR 72701, USA, mcleavel@uark.edu

Edward R. Cook Tree-Ring Laboratory, Lamont-Doherty Earth Observatory, 61 Route 9W, Palisades, NY 10964, USA, drdendro@ldeo.columbia.edu

Rosanne D. D'Arrigo Tree-Ring Laboratory, Lamont-Doherty Earth Observatory, Columbia University, Palisades, NY 10964, USA, rdd@ldgo.columbia.edu

Jeffrey S. Dean Laboratory of Tree-Ring Research, University of Arizona, Tucson, AZ 85721, USA, jdean@ltrr.arizona.edu

Henry F. Diaz Laboratory of Tree-Ring Research, University of Arizona, Tucson, AZ 85721, USA; NOAA Cooperative Institute for Research in Environmental Sciences, Earth System Research Laboratory, University of Calorado, 325 Broadway, Boulder, CO 80309, USA, Henry.F.Diaz@noaa.gov

Michael N. Evans Laboratory of Tree-Ring Research, The University of Arizona, Tucson, AZ, USA; Department of Geology and Earth System Science Interdisciplinary Center, The University of Maryland, College Park, MD 20742, USA, mevans@geol.umd.edu

Mary Gagen Department of Geography, School of the Environment and Society, Swansea University, Singleton Park, Swansea, SA2 8PP, UK, m.h.gagen@swansea.ac.uk

Nicholas E. Graham Hydrologic Research Center, 12780 High Bluff Drive, 250 La Jolla, CA 92130-3017, USA, ngraham@hrc-lab.org

Peter Hartsough Department of Land, Air and Water Resources, University of California, Davis, CA 95618, USA, phartsough@ucdavis.edu

Malcolm K. Hughes Laboratory of Tree-Ring Research, University of Arizona, Tucson, AZ 85721, USA, mhughes@ltrr.arizona.edu

Gordon Jacoby Tree-Ring Laboratory, Lamont-Doherty Earth Observatory, Columbia University, Palisades, NY 10964, USA, druid@ldeo.columbia.edu

Antonio Lara Laboratorio de Dendrocronología, Instituto de Silvicultura, Universidad Austral de Chile, Casilla 567, Valdivia, Chile, antoniolara@uach.cl

Carlos LeQuesne Laboratorio de Dendrocronología, Instituto de Silvicultura, Universidad Austral de Chile, Casilla 567, Valdivia, Chile, clequesn@uach.cl

Neil J. Loader Department of Geography, School of the Environment and Society, Swansea University, Singleton Park, Swansea SA2 8PP, UK, N.J.Loader@swansea.ac.uk

Brian H. Luckman Department of Geography, University of Western Ontario, London, ON N6A 5C2, Canada, luckman@uwo.ca

Guillermo Martinez Pastur Centro Austral de Investigaciones Científicas (CADIC), CONICET, Tierra del Fuego, Argentina, cadicforesta1@cadic.gov.ar

Mariano Masiokas Departamento de Dendrocronología e Historia Ambiental, Instituto Argentino de Nivología, Glaciología y Ciencias Ambientales (IANIGLA), CONICET, CC 330, 5500 Mendoza, Argentina, mmasiokas@mendoza-conicet.gov.ar

Guillermina Massacchesi Parque Nacional Tierra del Fuego, Administración de Parques Nacionales, San Martín N° 1395 – Ushuaia – Tierra del Fuego, Argentina, gmassaccesi@apn.gov.ar

Danny McCarroll Department of Geography, School of the Environment and Society, Swansea University, Singleton Park, Swansea, SA2 8PP, UK, D.McCarroll@swansea.ac.uk

David M. Meko Laboratory of Tree-Ring Research, University of Arizona, Tucson, AZ 85721, USA, dmeko@LTRR.arizona.edu

Thomas M. Melvin Climatic Research Unit, University of East Anglia, Norwich, NR4 7TJ, UK, t.m.melvin@uea.ac.uk

Mariano S. Morales Departamento de Dendrocronología e Historia Ambiental, Instituto Argentino de Nivología, Glaciología y Ciencias Ambientales (IANIGLA), CONICET, CC 330, 5500 Mendoza, Argentina, mmorales@mendoza-conicet.gov.ar

Jorge Moya Laboratorio de Dendrocronología, Instituto de Silvicultura, Universidad Austral de Chile, Casilla 567, Valdivia, Chile, jorgemoya@uach.cl

Jeanette Pacajes Laboratorio de Dendrocronología e Historia Ambiental, Facultad de Ciencias Geológicas, Universidad Mayor de San Andrés, Calle 27, Cota Cota, La Paz, Bolivia, jane_pacajes@yahoo.com

Neil Pederson Department of Biological Sciences, Eastern Kentucky University, 521 Lancaster Avenue, Richmond, KY 40475, USA, neil.pederson@eku.edu

Iain Robertson Department of Geography, School of the Environment and Society, Swansea University, Singleton Park, Swansea SA2 8PP, UK, i.robertson@swansea.ac.uk

Fidel Roig Departamento de Dendrocronología e Historia Ambiental, Instituto Argentino de Nivología, Glaciología y Ciencias Ambientales (IANIGLA), CONICET, CC 330, 5500 Mendoza, Argentina, froig@lab.cricyt.edu.ar

Claudia Soliz Laboratorio de Dendrocronología e Historia Ambiental, Facultad de Ciencias Geológicas, Universidad Mayor de San Andrés, Calle 27, Cota Cota, La Paz, Bolivia, SolizGamboa@uu.nl

David W. Stahle Department of Geosciences, University of Arkansas, Fayetteville, AR 72701, USA, dstahle@uark.edu

Thomas W. Swetnam Laboratory of Tree-Ring Research, The University of Arizona, Tucson, AZ 85721, USA, tswetnam@ltrr.arizona.edu

Matthew Therrell Geography & Environmental Resources, Faner Hall-Mail Code 4514, Southern Illinois University, Carbondale, IL 62901, USA, therrell@siu.edu

Rocio Urrutia Laboratorio de Dendrocronología, Instituto de Silvicultura, Universidad Austral de Chile, Casilla 567, Valdivia, Chile, rociourrutia@uach.cl

Eugene A. Vaganov Rectorate, Siberian Federal University, Krasnoyarsk, Russia, rectorat@sfu-kras.ru

Ricardo Villalba Departamento de Dendrocronología e Historia Ambiental, Instituto Argentino de Nivología, Glaciología y Ciencias Ambientales (IANIGLA), CONICET, CC 330, 5500 Mendoza, Argentina, ricardo@mendoza-conicet.gob.ar

Jose Villanueva-Diaz Instituto Nacional de Investigaciones Forestales y Agropecuarias, INIFAP CENID-RASPA, Km 6.5 Margen Derecha del Canal Sacramento, Gómez Palacio, Durango, 35140, México, villanueva.jose@inifap.gob.mx

Emma Watson 17 Dawson Crescent, Aurora, Ontario, L4G4T6, Canada, emma.watson@rogers.com

Gregory Wiles The College of Wooster, Wooster, OH 44691, USA, gwiles@wooster.edu

Robert J.S. Wilson Department of Geography, University of Saint Andrews, St Andrews, Scotland, UK, rjsw@st-andrews.ac.uk

Connie A. Woodhouse Laboratory of Tree-Ring Research, The University of Arizona, Tucson, AZ, 85721, USA; Department of Geography and Regional Development, University of Arizona, Tucson, AZ 85721, USA, Conniew1@arizona.edu

Part I
Introductory Section

Chapter 1
High-Resolution Paleoclimatology

Raymond S. Bradley

Abstract High resolution paleoclimatology involves studies of natural archives as proxies for past climate variations at a temporal scale that is comparable to that of instrumental data. In practice, this generally means annually resolved records, from tree rings, ice cores, banded corals, laminated speleothems and varved sediments. New analytical techniques offer many unexplored avenues of research in high resolution paleoclimatology. However, critical issues involving accuracy of the chronology, reproducibility of the record, frequency response to forcing and other factors, and calibration of the proxies remain. Studies of proxies at high resolution provide opportunities to examine the frequency and magnitude of extreme events over time, and their relationships to forcing, and such studies may be of particular relevance to societal concerns.

Keywords Climate dynamics · Natural archives · Paleoclimate · Proxies

1.1 Introduction

Paleoclimatology uses natural archives to reconstruct climate in the pre-instrumental period. The longest instrumental records are from Western Europe, and a few of these extend back into the early eighteenth (or even late seventeenth) century. However, for most regions, continuous instrumental measurements rarely extend beyond the early nineteenth century, with some remote (desert or polar) regions having barely 50 years of observations (Fig. 1.1). Consequently, our instrumental perspective on climate variability is extremely limited. In particular, it is unlikely

R.S. Bradley (✉)
Department of Geosciences, Climate System Research Center, University of Massachusetts, Amherst, MA 01003-9297, USA
e-mail: rbradley@geo.umass.edu

M.K. Hughes et al. (eds.), *Dendroclimatology*, Developments in Paleoenvironmental Research 11, DOI 10.1007/978-1-4020-5725-0_1,

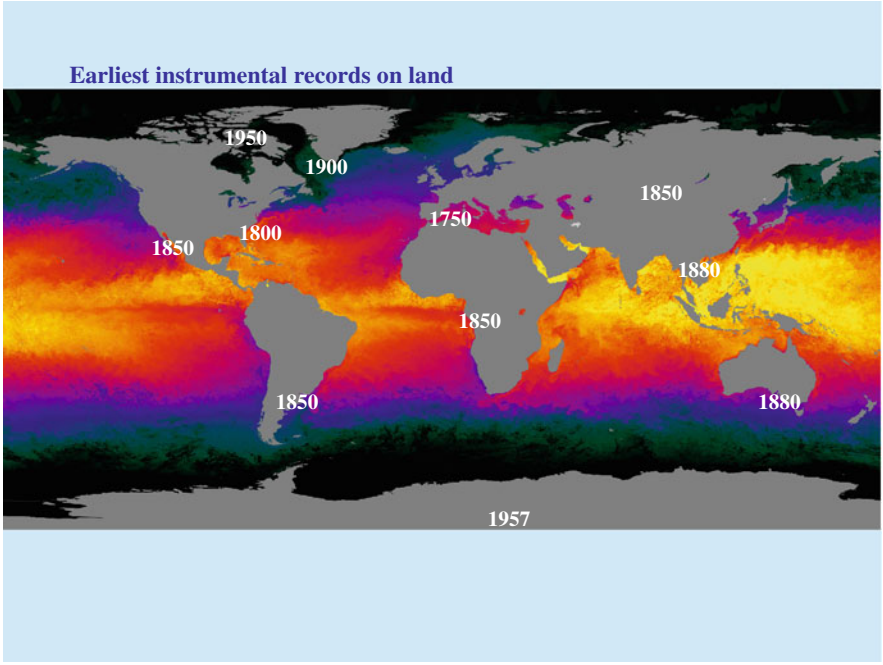

Fig. 1.1 Approximate earliest date of continuous instrumental records, which defines the need for high-resolution proxy-based data prior to these dates

that we understand the full spectrum of variability of the most important climate modes (such as the El Niño/Southern Oscillation [ENSO], Pacific Decadal Oscillation [PDO], North Atlantic Oscillation [NAO]. etc). High-resolution paleoclimatology addresses this issue by focusing on climate proxies that can be resolved at seasonal to annual resolutions. These proxy records may extend back continuously from the present, or provide discrete windows into the past, to shed light on modes of variability in earlier times. By providing data at a resolution comparable to that of the instrumental record, high-resolution paleoclimatology plays an important role in resolving anthropogenic effects on climate. Specifically, it helps to place contemporary climate variability in a long-term perspective (*detection*, in the parlance of the Intergovernmental Panel on Climate Change [IPCC]), and it enables climatic changes to be examined in terms of forcing mechanisms (*attribution*). High-resolution paleoclimatology also provides targets (either time series or maps of past climatic conditions) with which models (general circulation models [GCMs] or energy balance models [EBMs]) can be tested and validated, and it offers the opportunity to explore climate dynamics (modes of variability, abrupt climate changes, climate system feedbacks) over long periods of time. Thus, high-resolution paleoclimatology naturally interfaces with, and complements, the research priorities of the climate dynamics community.

1.2 Data Sources for High-Resolution Paleoclimatology

The critical requirements for high-resolution paleoclimatology are that:

- An accurate chronology can be established; this generally requires replication of the archive being sampled.
- The archive can be sampled in detail, ideally at seasonal to annual resolutions, but at least at the resolution of a few years.
- The parameter being measured is reasonably well understood in terms of its relationship to climate (i.e., its mechanistic and seasonal response) so that it can be calibrated in terms of climate, by using the instrumental record as a yardstick for interpreting the paleorecord.
- The relationship between the proxy and climate observed today has been similar in the past (the principle of uniformitarianism).
- The record captures variance of climate over a wide range of frequencies, or at least the window of variance that the proxy does capture is known.

In the next section, these issues are examined with reference to the main archives that are available for high-resolution paleoclimatology: tree rings, corals, speleothems, ice cores, and varved sediments. This examination is followed by a discussion of the opportunities and challenges in high-resolution paleoclimatology, with particular reference to dendroclimatology.

1.3 Chronology and Replication

An accurate timescale is essential in high-resolution paleoclimatology. A chronology is commonly obtained by counting annual increments, by using variations in some parameter to mark the passage of time. This might be the cyclical ^{18}O maximum in a coral record, registering the sea surface temperature (SST) minimum over each annual cycle; or the presence of a 'clay cap' in varved lacustrine sediments, marking each winter's sediment layer; or the width of a tree ring between the large, open-walled spring cells that form each year. However, simply counting these recurrent features in a sample (even if they are counted several times by different analysts) does not guarantee an accurate chronology. The best procedure is to replicate the record by using more than one sample (core), to eliminate potential uncertainties due to 'missing' layers and to avoid misinterpretation of dubious sections. On this matter, dendroclimatic studies have a clear and unambiguous advantage over most other paleoclimate proxies. Duplicate cores are easily recovered, and crossdating using one or more samples is routinely done. Tree-ring chronologies are thus as good as a natural chronometer can be, at least for those regions where there is an annual cycle of temperature or rainfall and trees are selected to record such changes in their growth. However, for those vast areas of equatorial and tropical forests, where trees are not under climatic stress and so do not produce annual rings,

establishing a chronology has been far more challenging. Recent analytical improvements using continuous flow isotope mass spectrometry have made feasible the almost continuous sampling of wood, so that annual changes in isotopic properties can be identified, even in wood that appears to be undifferentiated in its growth structure (Evans and Schrag 2004; Poussart et al. 2004). This technique opens up the possibility of using trees for paleoclimatic reconstruction in regions that were hitherto unavailable. However, replication of samples from nearby trees is still necessary to reduce chronological uncertainties in these newer records.

In the case of most other high-resolution proxies, replication is rarely carried out. This is generally related to the cost of sample recovery (in terms of logistics or time) or because of the analytical expense of duplicating measurements. Most coral records, for example, are based on single transects through one core, though the veracity of the chronology may be reinforced through the measurement of multiple parameters, each of which helps confirm the identification of annual layering in the coral. Similarly, in ice cores, multiparameter glaciochemical analyses can be especially useful in determining a secure chronology (McConnell et al. 2002a; Souney et al. 2002). In addition, in some locations more than one core may be recovered to provide additional ice for analysis and to help resolve uncertainties in chronology (Thompson 1993). It may also be possible to identify sulfate peaks in the ice, related to explosive volcanic eruptions of known age. Such chronostratigraphic horizons can be very helpful in confirming an annually counted chronology (Stenni et al. 2002). Varved sediments are sometimes analyzed in multiple cores, but sample preparation (such as impregnation of the sediments with epoxy, thin section preparation, etc.) is expensive and very time-consuming, so duplication is not commonly done. Where radioactive isotopes from atmospheric nuclear tests conducted in the late 1950s and 1960s can be identified in sediments (and in ice cores), such horizons can be useful time markers. Tephra layers (even finely dispersed cryptotephra) can be useful in confirming a sedimentary chronology if the tephras can be geochemically fingerprinted to a volcanic eruption of known age (e.g., Pilcher et al. 2005). Finally, where annual layer counting is not feasible—as in many speleothems—radioactive isotopes (^{210}Pb, ^{14}C, and uranium-series) can be used to obtain mean deposition/accumulation rates, though there may have been variations in those rates between dated levels.

1.4 High-Resolution Sampling

Advances in analytical techniques have now made sub-annual sampling and measurements fairly routine in most high-resolution proxies. Whereas tree rings were generally measured in terms of total annual increments, densitometry now enables measurements of wood density and incremental growth in early and latewood sections of each annual ring. Image analysis provides further options in terms of analyzing cell growth parameters (Panyushkina et al. 2003). Isotopic dendroclimatic studies require subannual sampling resolution to determine growth increments. In corals, such detailed sampling is now routine; often 10 or more samples will be

obtained per annual increment (e.g., Mitsuguchi et al. 1996; Quinn and Sampson 2002). Stalagmite research has rarely achieved such detail, with sampling intervals (in most studies) of a few years at best. However, some studies have established chronologies by counting annual layers on polished sections under a microscope, and new analytical approaches (using an electron microprobe, secondary ionization mass spectrometry [SIMS], or excimer laser ablation–inductively coupled plasma–mass spectrometry [ELA-ICP-MS]) have made it feasible to identify annual layers through seasonal changes in trace elements (such as Mg, Ca, Sr, Ba, and U), along multiple transects of a sample (e.g., Fairchild et al. 2001; Desmarchelier et al. 2006). Image analysis of varved sediments (via impregnated thin sections examined under a petrographic or scanning electron microscope) can reveal intra-annual sediment variations that may be associated with seasonal diatom blooms or rainfall events (Dean et al. 1999). In ice cores, it is now possible to make continuous multiparameter measurements, providing extremely detailed time series (McConnell et al. 2002a, b). Thus, in most natural archives available for high-resolution paleoclimatology, detailed measurements can be made both to define annual layers or growth increments and to characterize changes therein. However, it is not necessarily the case that an annual layer fully represents conditions over the course of a year. Much of the sediment in a varve, for example, may result from brief periods of runoff. Similarly, annual layers in an ice core represent only those days when snowfall occurred. Indeed, they may not even do that, if snow was subsequently lost through sublimation or wind scour. Coral growth increments may result from more continuous growth, and trees may also grow more continuously, at least during the growing season. Speleothems accumulate from water that has percolated through the overlying regolith, and so short-term variations related to individual rainfall episodes are likely to be 'smoothed out.' Nevertheless, there is some evidence that extreme rainfall episodes can be detected in the carbon isotopes of speleothems in areas where the throughflow of water is rapid (Frappier et al. 2007).

1.5 Relationships Between Natural Archives and Climate

Extracting a climatic signal from individual archives requires an understanding of the climatic controls on them. Analysis of the temporal relationships between variables may provide a statistical basis for calibration, but a theoretical basis for such a relationship is also required, to direct some light into the statistical black box. This may require in situ process-based studies to understand the factors controlling the proxy signal. Even if such studies are short-term, they can provide valuable insights into how climate influences the system being studied, and hence improve our understanding of the paleoclimatic record. For example, studies of meteorological conditions at the ice-coring site on Sajama, Bolivia, demonstrated strong seasonality in snow accumulation, with much of the snowfall that accumulated late in the accumulation season being subsequently lost through sublimation (Hardy et al. 2003). Consequently, the ice core record is made up of sections of snow that accumulated for (at most) a few months each year, demonstrating that division of

such records into 12 monthly increments is not appropriate (cf. Thompson et al. 2000a). Similarly, hydrological studies in the Arctic have shown that in some lakes, much of the runoff and associated sediment may be transferred into the lake over the course of only a few weeks. For example, measurements at Sophia Lake (Cornwallis Island, Nunavut, Canada) showed that 80% of the runoff and 88% of the annual sediment flux occurred in the first 33 days of the 1994 melt season (Braun et al. 2000). This sediment was subsequently distributed across the lake floor, forming an annual increment (varve), but the climatic conditions that mobilized the sediment were brief and perhaps unrepresentative of the summer season (and the year as a whole). Other studies of arctic lakes indicate that watersheds containing glaciers provide more continuous runoff and associated sediment flux throughout each summer, and thus provide a better proxy for summer climatic conditions (e.g., Hardy et al. 1996). Thus, understanding the environment from which the proxy archive is extracted is critically important for proper interpretation of the paleoclimate record. Process-based studies (often derided as simply 'monitoring') have also provided insights into climatic controls on corals, showing strong nonlinearities at high water temperatures (Lough 2004). In situ measurements within caves, aimed at gaining a better understanding of paleoclimate records, are now also being carried out (e.g., McDonald et al. 2004; Cruz et al. 2005). By comparison, dendroclimatology is far advanced because ecophysiological studies of tree growth have a long history. Consequently, factors influencing tree growth increments are well understood (Fritts 1996; Schweingruber 1996; Vaganov et al. 2006), providing a very strong foundation for paleoclimatic studies using tree rings.

1.6 Uniformitarianism

Perhaps because of the rapidity of recent climate change, many archives are no longer responding to climate in a manner that typifies much of the past. This phenomenon was first noted by Briffa et al. (1998), who showed that some trees that were formerly strongly influenced by temperature were no longer so influenced, or at least not to the same extent. Figure 1.2 shows the geographical distribution of this effect. Briffa et al. (2004) speculated that this response might be related to recent increases in ultraviolet radiation resulting from the loss of ozone at high elevations. Others have argued it might reflect the fact that trees in some areas have reached a threshold, perhaps now being affected more by drought stress than was formerly the case. Whatever the reason, it raises the question of whether such conditions might have occurred in the past, and if so, whether it would be possible to recognize such a 'decoupling' of the proxy archive from the ('normal') climate driver. Paleoclimate reconstruction is built on the principle of uniformitarianism, in which the present is assumed to provide a key to the past. If modern conditions (during the calibration period) are not typical of the long term, this assumption will be invalid. It is thus important to resolve the reasons for such changes and determine if additional parameters (such as cell growth features) might provide clues about when such stresses may have overwhelmed the typical climate response.

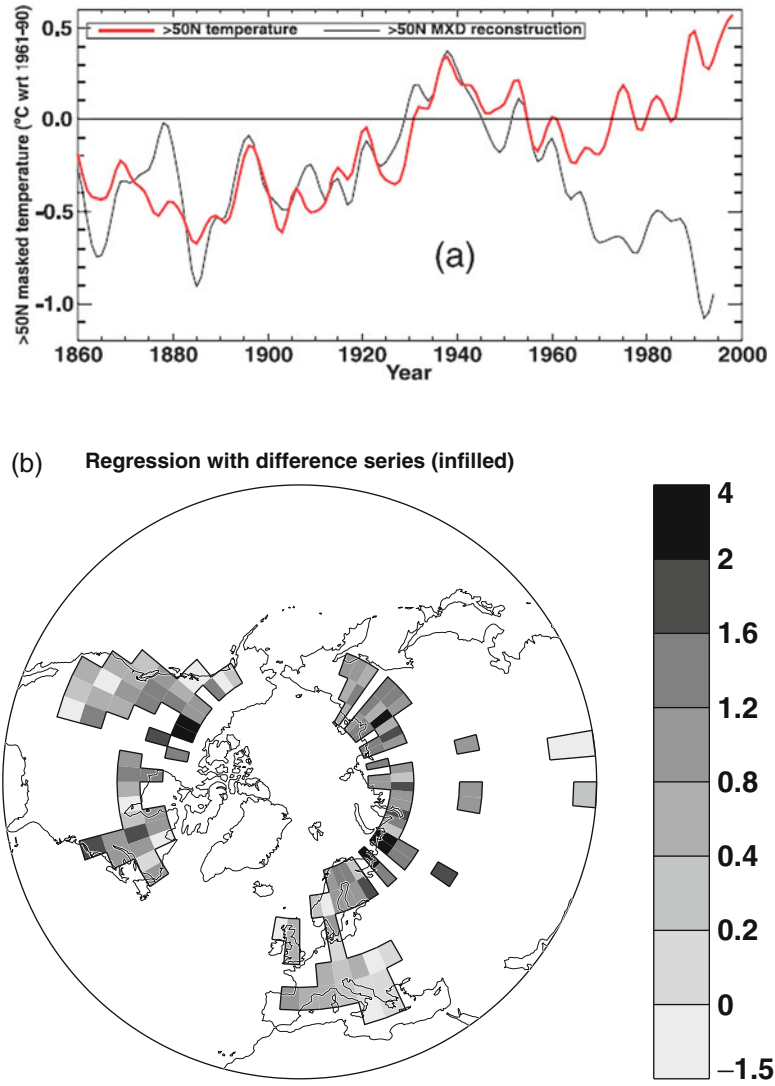

Fig. 1.2 (**a**) Instrumental temperatures (*heavier line; red in on-line version*) and tree-ring density reconstructions of temperature (*thinner line; black in on-line version*) averaged over all land grid boxes north of 50°N, smoothed with a 5-year low-pass filter. (**b**) Map showing where the average temporal pattern of divergence between tree-ring density chronologies and mean warm season temperatures is most apparent. The smoothed difference between the thin line (*black in on-line version*) and the thicker line (*red*) in (**a**) were regressed against the local difference curves produced from the averages of data in each grid box. Where the regression slope coefficients are progressively >1.0 (the increasingly darker boxes, generally the most northerly locations), the greater is the local difference between density and temperature. In the areas shown as lighter colored boxes (generally areas further south), the difference is apparent, but of lower magnitude. The areas shown in the lightest color (basically the most southern regions) do not show the divergence (redrawn from Briffa et al. 2004)

On a related point, it is clear that many natural archives are being detrimentally affected by recent changes in climate. Thus, many high-elevation ice caps in the tropics have been affected by surface melting and strong sublimation, so that the recent isotopic record has been degraded or even lost entirely (Thompson et al. 2000b). Similarly, corals in many areas were greatly affected by exceptionally high sea surface temperatures associated with the 1997–1998 El Niño (Wilkinson et al. 1999). Many century-old *Porites* colonies in the Great Barrier Reef were killed at this time.

1.7 Frequency Response

High-resolution records may have certain low-frequency characteristics that differ from the spectrum of the climatic environment in which they are situated. Such effects may be due to long-term biological growth (in the case of trees, and perhaps corals), compaction (ice, sediments), non-climatic changes in depositional environments (lake sediments, speleothems), and other proxy records. This issue is especially important as efforts are made to extend paleoclimatic reconstructions further back in time, to reveal changes in climate over thousands of years. Sediments are certainly affected by compaction, but this effect can be relatively easily corrected for by examining changes in density. This is also true in ice cores. Diffusion of isotopes within firn leads to a reduction in the amplitude of isotopic values that must also be considered. Deposition rates in speleothems are determined by radiocarbon or uranium series dates, and such analysis is generally sufficient to determine if deposition has been continuous over time. Certainly, there are no compression issues to be concerned with here, so in that sense speleothems do offer a very good option for identifying low-frequency changes in climate. This is illustrated well in the Dongge Cave record of Wang et al. (2005) (Fig. 1.3). The record shows an underlying low-frequency decline in monsoon precipitation, related to orbital forcing, on which decadal- to centennial-scale variations are superimposed, which appear to be (at least in part) related to variations in solar irradiance.

The issue of determining low-frequency changes in climate has been most problematical in dendroclimatology. The biological growth function of trees must first be removed before climatic information can be extracted. When this procedure is done, some low-frequency information may be lost. Furthermore, since most tree-ring series are short, assembling a composite long time series from many short records makes it even more problematical to obtain low-frequency information over timescales longer than the typical segment length (Cook et al. 1995). New approaches to standardization of tree-ring series have been developed, and these help to preserve more low-frequency information than do more traditional methods. However, such approaches require very large datasets and so cannot be applied in all cases. Another approach involves combining different proxies, some that may contain more low-frequency information with others that capture well higher-frequency information, so that together they cover the full spectrum of climate variability

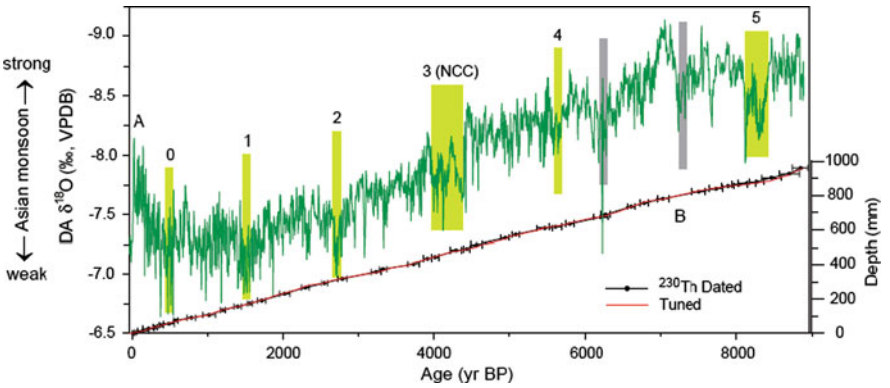

Fig. 1.3 (**a**) $\delta^{18}O$ time series of a Dongge Cave (China) stalagmite (*thin line*). Six vertical shaded bars denote the timing of Bond events 0–5 in the North Atlantic. Two *vertical gray bars* (without numbers) indicate two other notable weak Asian monsoon periods that can be correlated to ice-rafted debris events. Higher frequency variability appears to be related to solar (irradiance) forcing. NCC is the Neolithic Culture of China, which collapsed at the time indicated. (**b**) Age-depth relationship. *Black error bars* show ^{230}Th dates with 2σ errors. Two different age-depth curves are shown, one employing linear interpolation between dated depths and the second slightly modified by tuning to INTCAL98 within the ^{230}Th dating error (from Wang et al. 2005). On-line version shows this figure in color

(Moberg et al. 2005). This approach has much promise, and further fine-tuning will likely lead to a better understanding of large-scale climate variability over recent millennia.

1.8 High-Resolution Proxies: Challenges and Opportunities

High-resolution paleoclimatic records provide unique opportunities to better understand the climate system because they extend the limited sampling interval that is available from short instrumental records. This longer perspective is especially important for studies of rare events, such as explosive volcanic eruptions or the occurrence of extreme climatic conditions such as droughts or floods. Ice cores reveal (through sulfate and electrical conductivity measurements) that there have been much larger explosive volcanic eruptions in the past than during the period of instrumental records (Zielinski et al. 1994; Castellano et al. 2005); by identifying these events, it is then possible to explore the relationship between eruption size and location and the subsequent climatic effects (e.g., D'Arrigo and Jacoby 1999). Many dendroclimatic studies have recognized the connection between explosive eruptions and cold growing season conditions, which sometimes have led to frost damage in trees (e.g., LaMarche and Hirschboeck 1984; Baillie and Munro 1988; Briffa et al. 1990; D'Arrigo et al. 2001). Proxy records of volcanic forcing also provide a much larger database of eruption events than is available for the instrumental

period; compositing climatic conditions following such events increases the signal-to-noise ratio, giving a clearer view of the climate system response to such events. Thus Fischer et al. (2007) were able to show that summer conditions in Europe have tended to be both cold and dry after major tropical volcanic eruptions; but in winter, a positive NAO circulation has generally been established, resulting in mild, wet conditions in northern Europe and well below average precipitation in the Alps and Mediterranean region.

Dendroclimatic research has been especially important in documenting the frequency, geographical extent, and severity of past drought episodes, as well as periods of unusually high rainfall amounts; such studies have been especially extensive in the United States (e.g., Stahle and Cleaveland 1992; Hughes and Funkhouser 1998; Cook et al. 2004). These studies have shown that there has often been a strong connection between severe droughts in the southwestern United States and the occurrence of La Niña episodes, although the precise geographical pattern of each drought has varied over time (Stahle et al. 2000; Cole et al. 2002). Tree-ring research has also been applied to reconstructing modes of circulation in the past, such as the North Atlantic Oscillation (Cook et al. 1998; Cullen et al. 2001), Pacific Decadal Oscillation (Gedalof and Smith 2001), and Atlantic Multidecadal Oscillation (AMO) (Gray et al. 2004). In all of these cases, the paleoclimatic reconstructions have expanded our understanding of the spectrum of variability of these modes of circulation and provided insight into how large-scale teleconnections (and interactions between Atlantic- and Pacific-based circulation regimes) may lead to persistent, large-amplitude anomalies over North America and other regions.

Great strides have been made in constructing hemispheric- and global-scale patterns of past climate variability by combining many different types of high-resolution paleoclimatic records, using a variety of statistical methods (Mann et al. 1998, 1999, 2005; Moberg et al. 2005; Rutherford et al. 2005). These studies have demonstrated the importance of volcanic and solar forcing, and of the increasingly dominant effects of anthropogenic forcing over the last 150 years. Nevertheless, such studies rely largely on the most extensive database of paleoclimatic reconstructions that is currently available—that provided by dendroclimatology. On the one hand, this is good because the physiological basis for how trees respond to climate is well understood, thanks to decades of careful studies, and tree rings provide the most accurate chronologies available. However, the use of tree rings in long-term paleoclimate reconstructions is dogged by questions of uniformitarianism (a question not unique to dendroclimatology, of course), but more significantly by the difficulty of resolving the full spectrum of climate variability from overlapping, relatively short, tree-ring series. This matter can be resolved by obtaining longer records where possible, expanding the tree-ring database to improve data density back in time, and developing new statistical approaches; all these methods are necessary to ensure that long-term paleoclimatic reconstructions are as reliable as possible. New isotopic and image analysis techniques applied to tree growth may add further information about past climate variations in regions that were formerly off-limits to dendroclimatologists, thereby extending the geographical domain for large-scale climate reconstruction. New proxies, especially from lake sediments and speleothems,

will likely further supplement this expansion of high-resolution records, providing records with more robust low-frequency characteristics that can be combined with proxies that are exceptionally good at capturing high-frequency climate variability (e.g., Moberg et al. 2005). In this way, the next decade of high-resolution paleoclimatology will likely see paleoclimatic reconstructions with far less uncertainty, covering more geographical regions, and providing meaningful estimates of climate sensitivity before the 'Anthropocene'.

Acknowledgements I gratefully acknowledge the support of my research by the National Oceanic and Atmospheric Administration (NOAA, NA050AR4311106), the National Science Foundation (NSF, ATM-0402421), and the U.S. Department of Energy (DOE, DE-FG02-98ER62604).

References

Baillie MGL, Munro MAR (1988) Irish tree-rings, Santorini and volcanic dust veils. Nature 332:344–346

Braun C, Hardy DR, Bradley RS, Retelle M (2000) Streamflow and suspended sediment transport into Lake Sophia, Cornwallis Island, Nunavut, Canada. Arctic Antarctic Alpine Res 32: 456–465

Briffa KR, Bartholin TS, Eckstein D, Jones PD, Karlen W, Schweingruber FH, Zetterberg P (1990) A 1400 year tree-ring record of summer temperatures in Fennoscandia. Nature 346:434–439

Briffa KR, Osborn TJ, Schweingruber FH (2004) Large-scale temperature inferences from tree rings: a review. Global Planet Change 40:11–26

Briffa KR, Schweingruber FH, Jones PD, Osborn TJ, Shiyatov SG, Vaganov EA (1998) Reduced sensitivity of recent tree-growth to temperatures at high northern latitudes. Nature 391:678–682

Castellano E, Becagli S, Hansson M, Hutterli M, Petit JR, Rampino MR, Severi M, Steffensen JP, Traversi R, Udisti R (2005) Holocene volcanic history as recorded in the sulfate stratigraphy of the European Project for Ice Coring in Antarctica Dome C (EDC96) ice core. J Geophys Res 110:D06114. doi:10.1029/2004JD005259

Cole JE, Overpeck JT, Cook ER (2002) Multiyear La Niña events and persistent drought in the contiguous United States. Geophys Res Lett 29:1647. doi:10.1029/2001GL013561

Cook ER, Briffa KR, Meko DM, Graybill DS, Funkhouser G (1995) The 'segment length curse' in long tree-ring chronology development for paleoclimatic studies. Holocene 5:229–237

Cook ER, D'Arrigo RD, Briffa KR (1998) The North Atlantic Oscillation and its expression in circum-Atlantic tree ring chronologies from North America and Europe. Holocene 8:9–17

Cook ER, Meko DM, Stahle, DW, Cleaveland MK (1999) Drought reconstructions for the continental United States. J Climate 12:1145–1162

Cook ER, Woodhouse CA, Eakin CM, Meko DM, Stahle DW (2004) Long-term aridity changes in the western United States. Science 306:1015–1018

Cruz FW Jr, Karmann I, Viana O Jr, Burns SJ, Ferrari JA, Vuille M, Moreira MZ, Sai NF (2005) Stable isotope study of cave percolation waters in subtropical Brazil: implications for paleoclimate inferences from speleothems. Chem Geol 220:245–262

Cullen HM, D'Arrigo RD, Cook ER, Mann ME (2001) Multiproxy reconstructions of the North Atlantic Oscillation. Paleoceanography 16:27–39

D'Arrigo RG, Jacoby JC (1999) Northern North American tree-ring evidence for regional temperature changes after major volcanic events. Climatic Change 41:1–15

D'Arrigo R, Frank D, Jacoby G, Pederson N (2001) Spatial response to major volcanic events in or about A.D. 536, 934 and 1258: frost rings and other dendrochronological evidence from Mongolia and northern Siberia. Climatic Change 49:239–246

Dean JM, Kemp AES, Bull D, Pike J, Patterson G, Zolitschka B (1999) Taking varves to bits: scanning electron microscopy in the study of laminated sediments and varves. J Paleolimnology 22:121–136

Desmarchelier J, Hellstrom JM, McCulloch MT (2006) Rapid trace element analysis of speleothems by ELA-ICP-MS. Chem Geol 231:102–117

Evans MN, Schrag DP (2004) A stable isotope-based approach to tropical dendroclimatology. Geochim Cosmochim Acta 68:3295–3305

Fairchild IJ, Baker A, Borsato A, Frisia S, Hinton RW, McDermott F, Tooth AF (2001) Annual to sub-annual resolution of multiple trace-element trends in speleothems. J Geol Soc London 158:831–841

Fischer, EM, Luterbacher J, Zorita E, Tett SFB, Casty C, Wanner H (2007) European climate response to tropical volcanic eruptions over the last half millennium. Geophys Res Lett 34, doi:10.1029/2006GL/027992

Frappier A, Sahagian D, Carpenter SJ, Gonzáles LA, Frappier BR (2007) Stalagmite stable isotope record of recent tropical cyclone events. Geology 35:111–114

Fritts HC (1996) Tree rings and climate. Academic Press, San Diego

Gedalof Z, Smith D (2001) Inter-decadal climate variability and regime-scale shifts in Pacific North America. Geophys Res Lett 28:1515–1518

Gray ST, Graumlich LJ, Betancourt JL, Pederson GT (2004) A tree ring-based reconstruction of the Atlantic Multidecadal Oscillation since A.D. 1567. Geophys Res Lett 31, doi:10.1029/2004GL019932

Hardy DR, Bradley RS, Zolitschka B (1996) The climatic signal in varved sediments from Lake C-2, northern Ellesmere Island, Canada. J Paleolimnology 16:227–238

Hardy DR, Vuille M, Bradley RS (2003) Variability of snow accumulation and isotopic composition on Nevado Sajama, Bolivia. J Geophys Res-Atmospheres 108: D22, 4693. doi:10.1029/2003JD003623

Hughes MK, Funkhouser G (1998) Extremes of moisture availability reconstructed from tree rings for recent millennia in the Great Basin of western North America. In: Innes M, Beniston JL (eds) The impacts of climate variability on forests. Springer, Berlin, Heidelberg, New York, pp 99–107

LaMarche VC, Hirschboeck K (1984) Frost rings in trees as records of major volcanic eruptions. Nature 307:121–126

Lough JM (2004) A strategy to improve the contribution of coral data to high-resolution paleoclimatology. Palaeogeog Palaeoclimatol Palaeoecol 204:115–143

Mann ME, Bradley RS, Hughes MK (1998) Global-scale temperature patterns and climate forcing over the past six centuries. Nature 378:266–270

Mann ME, Bradley RS, Hughes MK (1999) Northern Hemisphere temperatures during the past millennium: inferences, uncertainties, and limitations. Geophys Res Lett 26:759–762

Mann ME, Rutherford S, Wahl E, Ammann C (2005) Testing the fidelity of methods used in proxy-based reconstructions of past climate. J Climate 18:4097–4107

McConnell JR, Lamorey GW, Hutterli MA (2002a) A 250-year high-resolution record of Pb flux and crustal enrichment in central Greenland. Geophys Res Lett 29:2130–2133

McConnell JR, Lamorey GW, Lambert SW, Taylor KC (2002b) Continuous ice-core chemical analyses using inductively coupled plasma mass spectrometry. Environ Sci Technol 36:7–11

McDonald J, Drysdale R, Hill D (2004) The 2002–2003 El Niño recorded in Australian cave drip waters: implications for reconstructing rainfall histories using stalagmites. Geophys Res Lett 31: L22202. doi:10.1029/2004GL020859

Mitsuguchi T, Matsumoto E, Abe O, Uchida T, Isdale PJ (1996) Mg/Ca thermometry in coral skeletons. Science 274:961–963

Moberg A, Sonechkin DM, Holmgren K, Datsenko NM, Karlén W (2005) Highly variable Northern Hemisphere temperatures reconstructed from low- and high-resolution proxy data. Nature 433:613–617

Panyushkina IP, Hughes MK, Vaganov EA, Munro MAR (2003) Summer temperature in northeastern Siberia since 1642 reconstructed from tracheids dimensions and cell numbers of *Larix cajanderi*. Can J Forest Res 33:1–10

Pilcher J, Bradley RS, Francus P, Anderson L (2005) A Holocene tephra record from the Lofoten Islands, Arctic Norway. Boreas 34:136–156

Poussart PF, Evans MN, Schrag DP (2004) Resolving seasonality in tropical trees: multi-decade high-resolution oxygen and carbon isotope records from Indonesia and Thailand. Earth Planet Sci Lett 218:301–316

Quinn TE, Sampson D (2002) A multi-proxy approach to reconstructing sea surface conditions using coral skeleton geochemistry. Paleooceanography 17:1062. doi:10.1029/2000PA000528

Rutherford S, Mann ME, Osborn TJ, Bradley RS, Briffa KR, Hughes MK, Jones PD (2005) Proxy-based Northern Hemisphere surface temperature reconstructions: sensitivity to methodology, predictor network, target season, and target domain. J Climate 18:2308–2329

Schweingruber FH (1996) Tree rings and environment. Dendroecology. Haupt, Berne

Souney JM, Mayewski PA, Goodwin ID, Meeker LD, Morgan V, Curran MAJ, van Ommen TD, Palmer AS (2002) A 700-year record of atmospheric circulation developed from the Law Dome, East Antarctica. J Geophys Res 107: D22, 4608. doi:10.1029/2002JD002104

Stahle DW, Cleaveland MK (1992) Reconstruction and analysis of spring rainfall over the southeastern U.S. for the past 1000 years. Bull Am Meteorol Soc 73:1947–1961

Stahle DW, Cook ER, Cleaveland MK, Therrell MD, Meko DM, Grissino-Mayer HD, Watson E, Luckman BH (2000) Tree-ring data document 16th century megadrought over North America. Eos 81(12):121,125

Stenni B, Proposito M, Gragnani R, Flora O, Jouzel J, Faourd S, Frezzotti M (2002) Eight centuries of volcanic signal and climate change at Talos Dome (East Antarctica). J Geophys Res 107:D9. doi:10.1029/2000JD000317

Thompson LG (1993) Ice core evidence from Peru and China. In: Bradley RS, Jones PD (eds) Climate since AD 1500. Routledge, London, pp 517–548

Thompson LG, Henderson KA, Mosley-Thompson E, Lin P-N (2000a) The tropical ice core record of ENSO. In: Diaz HF, Markgraf V (eds) El Niño and the Southern Oscillation: multiscale variability and global and regional impacts. Cambridge University Press, Cambridge, pp 325–356

Thompson LG, Mosley-Thompson E, Henderson K (2000b) Ice core paleoclimate records in South America since the Last Glacial Maximum. J Quat Sci 15:377–394

Vaganov SG, Hughes MK, Shaskin AV (2006) Growth dynamics of conifer tree rings. Springer, Berlin, Heidelberg, New York

Wang Y, Cheng H, Edwards LR, He Y, Kong X, An Z, Wu J, Kelly MJ, Dykoski CA, Li X (2005) The Holocene Asian monsoon: links to solar changes and North Atlantic climate. Science 308:854–857

Wilkinson C, Linden O, Cesar H, Hodgson G, Rubens J, Strong AE (1999) Ecological and socioeconomic impacts of 1998 coral mortality in the Indian Ocean: An ENSO impact and a warning of future change? Ambio 28(2):188–196

Zielinski GA, Mayewski PA, Meeker LD, Whitlow SI, Twickler SM, Morrison M, Meese DA, Gow AJ, Alley RB (1994) Record of volcanism since 7000 BC from the GISP2 Greenland ice core and implications for the volcano-climate system. Science 264:948–952

Chapter 2
Dendroclimatology in High-Resolution Paleoclimatology

Malcolm K. Hughes

Abstract The characteristics of tree rings as natural archives of past climate are discussed. Special consideration is given to key issues affecting their robustness and reliability as sources of information on past climate. These issues include: the effects of sample design and in particular the importance of using networks of tree-ring records from many locations whenever possible; potentially complementary approaches to the identification of climate signal in tree rings, namely empirical-statistical and process-modeling approaches; statistical and mechanistic stability over time of the climate signal in tree rings; and the ongoing effort to isolate climate signal from noise, without introducing biases, in tree-ring based proxy records of climate.

Keywords Tree rings · Dendrochronology · Dendroclimatology · Climatology · Reconstructions

2.1 Introduction

Bradley (Chapter 1, this volume) has placed tree rings firmly in the context of high-resolution paleoclimatology, along with other natural archives such as coral growth bands, laminated and high-accumulation freshwater and marine sediments, speleothems, and annual bands in polar and high-elevation ice caps. He further identified a number of critical issues that must be faced in using properties of such natural archives as proxy records of climate variables. These were the precision and accuracy of the chronology applied to each record; the effective temporal resolution of each archive; the degree to which the processes producing each archive are understood and may be compared with observed climate; the consistency or inconsistency of response to climate throughout the period of interest; and the extent to which each

M.K. Hughes (✉)
Laboratory of Tree-Ring Research, University of Arizona, Tucson, AZ 85721, USA
e-mail: mhughes@ltrr.arizona.edu

M.K. Hughes et al. (eds.), *Dendroclimatology*, Developments in Paleoenvironmental Research 11, DOI 10.1007/978-1-4020-5725-0_2,

type of record can capture climate variability over a wide range of timescales, from interannual to millennial. In this chapter, these critical issues will be examined, with specific reference to tree rings as natural archives of past climate.

Tree rings are uniquely widespread relative to all comparable natural archives of climate. Woody plants with reliably annual rings are formed wherever the local climate imposes a single dormant season and a single growth season each and every year. Such conditions are widespread in the boreal, temperate, and subtemperate regions, and in some parts of the tropics. At middle and high latitudes or elevations, this pattern of one dormant and one growth season per year in the formation of wood is imposed by annual day length and temperature cycles. In some tropical locations, it may be imposed by the existence of a single dry season-induced dormant period each year, as in teak through much of its range in south Asia.

The abundance of potentially useful tree-ring records and the relative ease with which they may be collected has resulted in unique approaches to their use as natural archives of past climate. In this chapter some of these specific approaches, which lead to characteristic features of tree-ring records of past climate, will be described, so as to help the reader place the chapters that follow in a wider context. Specifically, consideration will be given to four key issues:

(1) sample design in dendroclimatology and the importance of networks
(2) identifying climate signal in tree rings by empirical-statistical and process-modeling approaches
(3) stability of the climate signal
(4) the quest for unbiased chronologies

2.2 Sample Design in Dendroclimatology

2.2.1 Natural Archives and Proxy Climate Records

The layer of new xylem or wood laid down each year under the bark of a tree (the annual ring) is a natural archive of growth that year. The environmental conditions influencing that growth may leave an imprint on the properties of the ring. Thus the size, structure, and composition of the ring may contain information on those conditions; for example, climate. Estimates of those properties in turn may be used as proxy climate records.

In the case of tree rings, the most commonly used properties are structural; namely, the total ring width (TRW) and maximum latewood density (MXD). There are other structural properties of tree rings that can contain climate information; for example, earlywood and latewood width measured separately, or tracheid (conifer wood cell) dimensions. Their use will likely increase as a result of technical advances in measurement (see Vaganov et al. 2006, Chapter 2, for a basic account of these structural properties and their measurement).

Many measurements of the composition of wood in annual rings could contain climate information. In recent years considerable progress has been made in using

ratios of stable isotopes, primarily of carbon and oxygen, in tree rings as proxy climate records (Gagen et al. Chapter 6, this volume). The issues of sample design, replication, removal of non-climatic variability, identification of climate signals, and the properties of networks of isotope chronologies are all being explored, and appropriate methods are emerging.

In this chapter the discussion of the four key issues mentioned in the previous section will focus on TRW and MXD because they are the subjects of most of the existing literature.

2.2.2 Single Site Chronologies

The criteria used to identify sites, species, and trees to be sampled in establishing a local reference for dating annual rings correspond to those used to capture a clear and strong climate signal. There is considerable variability in ring growth within and between trees, and so multiple samples are taken so as to 'distill' the common, presumably climatic, signal, and to 'dilute' the likely more individual non-climatic variability or noise (Fig. 2.1 shows raw data from a site where high correlations between sample series suggest a strong common climate signal). The common signal, usually expressed as some form of the mean of the individual samples' modified

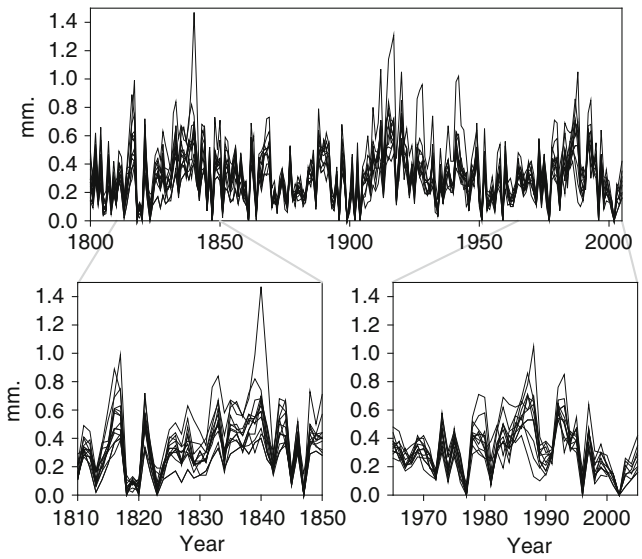

Fig. 2.1 Common pattern of variability shared by trees at one location. Raw, unmodified ring widths (millimeters) of 18 samples from Douglas-fir in Navajo Canyon, Colorado, each shown by a single fine line. Note that although absolute growth rates differ, the relative patterns of variability are similar. The *lower* panels show two 41-year periods with the horizontal scale expanded. Data provided by David M. Meko

ring series, or 'chronology,' is equally essential as a standard for dating local wood of unknown dates and as an estimate of ring growth as influenced by climate. In both cases, sites, species, and trees are sought in which the ratio of the climate (common) signal to non-climatic (primarily individual) noise is as great as possible.

It would make little sense to drill an ice core in a situation where stratigraphy is likely to be distorted—or even inverted—to sample lake sediments in locations where the record is prone to earthquake-induced slumps or extensive bioturbation, or indeed to use meteorological station data without the application of appropriate quality control standards and procedures for homogenization. In the same spirit, strategies have been developed for selecting the sites, species, variables, and individual trees most likely to show strong, consistent ring variability common to all trees, and hence a clear climate signal in their rings, and for rejecting those where there are a priori reasons to expect strong non-climatic influences that cannot be disentangled. The aim in this case is not to take a representative sample of the trees of the forest, but rather to maximize climate signal and minimize non-climatic noise.

A quite different sampling protocol would be used if the aim were to take a representative sample of the forest. An optimal record of summer temperature is likely to come from regions with cool, moist summers where drought influence on wood growth is minimal. Within such regions, sites at upper elevations close to the upper or poleward tree limit are likely to reflect regional temperatures, rather than the peculiar regime of a particular valley. In cases where the uppermost or highest-latitude trees have a stunted or dwarf growth form, they would not be sampled, as their wood anatomy is strongly influenced by mechanical rather than climatic forces. Individual trees with a lean, lightning damage, or other abnormal morphology would also be avoided. A site from which a chronology is to be developed should be as uniform as possible with respect to the small-scale conditions affecting tree growth, such as aspect, slope, and substrate. Tree species produce ring series with characteristic properties, and this too would be taken into account in designing a sampling program.

Differing properties of tree rings reflect different climate signals, according to the growth situation. Maximum latewood density of conifer tree rings in regions with cool, moist summers is usually a better proxy for summer temperature than is ring width from the same trees, for example. In regions of Mediterranean climate, ring width may be the best available proxy for growing season soil moisture, or for winter half-year precipitation, which is possibly the main determinant of early summer growth. These considerations concerning the location and design of tree-ring sampling are analogous to those that apply in choosing the best place to drill a lake or a glacier.

This approach to sample design is almost universally applied 'a priori' to the sampling of tree rings. Once the samples and data exist, the strength of the common signal within the tree-ring dataset from an individual site is analyzed by using information on the number of samples and the correlations between them (within the tree-ring data, not with a climate variable), and a decision is made whether or not to use the existing data for dendroclimatology, to reject it on the basis of a weak common signal, or to seek more samples to strengthen the signal (Wigley et al. 1984).

2.2.3 Networks and the Relationship Between Crossdating and the Emergence of Climate Signal from Networks of Tree-Ring Data

Whenever possible, chronologies are built for multiple sites in a region, forming a network of chronologies, each containing records from multiple trees. This process provides protection against undue site-specific influences, and increases the chances of capturing regional-scale climate signals, just as would be the case with meteorological station data. Chronologies for ecologically comparable sites within a region typically share many features (Fig. 2.2). Continental- and hemispheric-scale

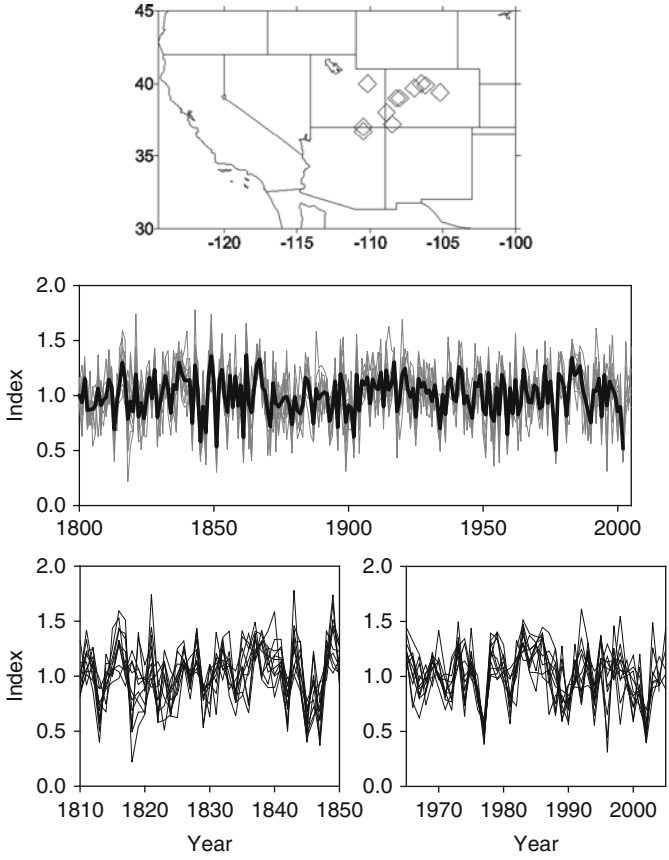

Fig. 2.2 Common pattern of variability shared by site chronologies over a distance of several hundred kilometers. Ring-width-based chronologies from 11 locations in the upper basin of the Colorado River, United States, including that based on the samples from Navajo Canyon shown in Fig. 2.1. Each chronology is the mean of multiple detrended ring-width series. (*Top*) Locations of the chronologies. (*Middle*) The 11 site chronologies for the period AD 1800–2005 shown in gray, with their mean as the thicker, black line. (*Bottom*) The 11 site chronologies for the periods AD 1810–1850 and 1965–2005. Data provided by David M. Meko; details of chronologies in Meko et al. (2007)

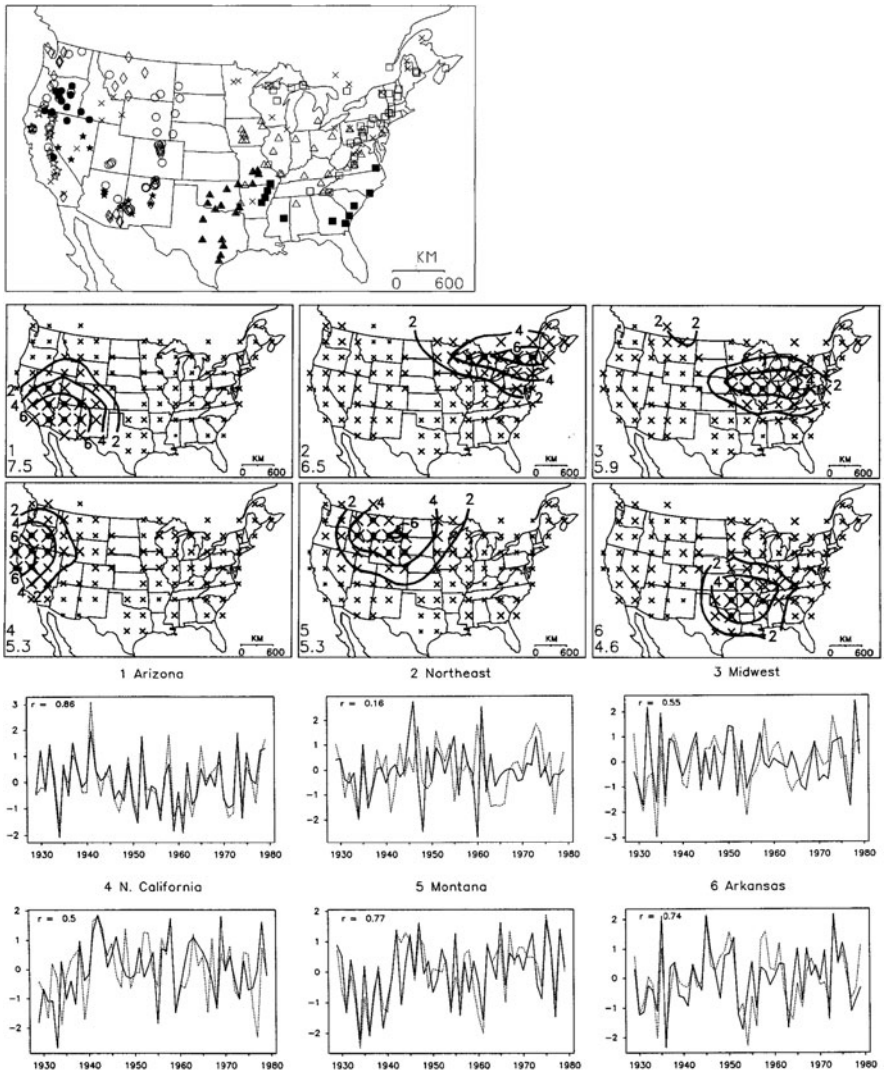

Fig. 2.3 Synoptic-scale patterns of tree-ring growth and their link to climate. Meko et al. (1993) analyzed a network of 248 drought-sensitive tree-ring chronologies using rotated principal component analysis (RPCA) 'to delineate "regions" of common tree growth variation in the period 1705–1979.' *Upper panel*: Locations of the chronologies—symbols indicate tree species. *Middle* two rows of panels: Maps of primary pattern coefficients for six of the nine obliquely rotated PCs of gridded tree-ring indices calculated by Meko et al. Principal component number and sum of squares of coefficients are shown at the lower left in each panel. In each case, the contoured area with the larger symbols indicates the region most influencing that PC. *Lower* two rows of panels: Time series of scores of the six rotated PCs (*solid*) compared with July Palmer Drought Severity Index (PDSI) (*dashed*) for from 2 to 7 grid points with highest pattern correlation with PC. Both variables were standardized to zero mean and unit standard deviation. This shows a strong relationship between large-scale patterns of tree-ring growth and growing season moisture availability in all regions except the most mesic, the Northeast. Reproduced with permission from Meko et al. (1993, © Copyright American Meteorological Society. Reprinted with permission)

networks contain robust synoptic-scale patterns (Fig. 2.3 upper and middle), which may often be interpreted in terms of climatic conditions (Fig. 2.3 lower). It is the existence of such emergent patterns that permits crossdating of tree rings, not only between trees derived from the same site but also over distances of hundreds of kilometers (Hughes and Brown 1992; Hughes et al. 2001; Kelly et al. 1989, 2002). Clearly, these tree-ring networks provide a very different kind of proxy record from that extracted from a single ice core or sediment core—they are massively replicated, precisely and accurately dated to the calendar year throughout, and eminently suitable for testing against instrumental climate data.

2.3 Climate Signal in Tree-Ring Properties

2.3.1 Identifying Signal—An Empirical-Statistical Approach

The primary methods of identifying a potential climate signal in tree-ring records have been inference based on external knowledge of the conditions controlling the formation of the rings—for example, LaMarche (1974) or Esper et al. (2002b)—and statistical exploration of the relationships of the tree-ring data with candidate climate factors.

Fritts et al. (1971) developed a general scheme in which regression models were used to relate climate variables and tree-ring series. In the first instance, models using climate variables as predictors and tree-ring records as predictands were used to identify the aspects of climate most likely to be controlling tree-ring formation. Such models were termed 'response functions.' The response functions, considered in the light of available ecological and physiological knowledge, were then used in the design of another kind of regression model known as a 'transfer function.' In this case, tree-ring records were used as candidate predictors for target climate predictands. The approach was designed to be applied on a broad spatial scale, using the climate-relevant data covering the longest possible period and most broadly available at that time. These were monthly mean temperatures and total precipitation from meteorological stations.

This approach was considered appropriate, even though Fritts was well aware of the influence of local site and ecological conditions (see Fritts 1974), because the target was the reconstruction of subcontinental-scale spatiotemporal patterns in climate, and because he was also aware of the existence of emergent patterns of tree-ring growth on scales similar to synoptic patterns in climate data (LaMarche and Fritts 1971). Moreover, more directly ecologically relevant climate data covering a sufficiently long period were extremely rare. The need to use monthly data from meteorological stations was further supported because the length of records was extremely important. Vaganov et al. (2006, p 191) point out that 'for any derived statistical model to be valid, it must have the largest possible ratio between the number of cases (years) and the number of variables (months or seasons per year

per climate parameter). A substantial literature exists in which the strengths and weaknesses of this empirical-statistical approach are investigated, and many of the most important issues are further explored by Cook and Pederson (Chapter 4, this volume). They particularly emphasize the necessity for testing the stability of any such statistical models, whether they are being used as response functions to estimate tree-ring variables or as transfer functions to estimate past climate from tree rings.

2.3.2 Identifying Climate Signal—Process-Modeling Approaches

From the inception of dendroclimatology, care has been taken to evaluate the ecological reasonableness of the statistical models used to extract climate signals from tree-ring data (Fritts 1976). The mechanistic bases for this evaluation are now summarized in simulation models; for example, those focusing on the activity of the tissue that forms wood, the vascular cambium, as discussed by Vaganov et al. (Chapter 3, this volume). Evans et al. (2006) have shown that a relatively simple process-based model (the Vaganov-Shashkin, or VS model) achieved skill comparable to that of regression models fitted to each of almost 200 chronologies from a wide range of conditions in the United States and Russia, even though the simulation model used a single set of parameters for all of these, and was not tuned chronology by chronology, unlike the statistical model. Anchukaitis et al. (2006) demonstrated that varying only a single model parameter produced a similarly impressive performance of the VS model for a combination of species and region for which it performed poorly in the Evans et al. (2006) work, underlining the generality of its applicability. This result indicates that there is a mechanistic basis for the use of tree-ring variables as proxy climate records, based primarily on the environmental control of the activity of the vascular cambium. As Vaganov et al. (2006; Chapter 3, this volume) indicate, there is a growing understanding of the ecophysiological, developmental, and even molecular mechanisms of the climatic control of tree-ring formation.

Recent progress in the observation of the timing of events in the vascular cambium of conifers in alpine and subarctic conifers has revealed a number of remarkably consistent common features of the environmental control of xylogenesis, the process of wood formation, in cool-region conifers. These features include the existence of threshold temperatures for the onset of xylogenesis (Rossi et al. 2008), which are most consistent when measurements are made at the stem, rather than in the air or soil (Rossi et al. 2007), and tend to be the same regardless of location and species. They also show a tendency for the maximum rate of cell production and xylem growth to occur close to the summer solstice, not necessarily at the warmest time of year (Rossi et al. 2006). In fact, cell division in the cambium stopped in July or August, when temperatures were still high (Rossi et al. 2008). Process modeling of the climate control of tree-ring growth can only benefit from the continuation of this kind of work and the incorporation of its results into existing and new models.

2.4 Stability of the Climate Signal

2.4.1 Temporal Stability

The existing climate reconstructions made using tree rings are based on statistically derived transfer functions using (largely) twentieth-century instrumental data for calibration and validation. Two questions arise, although the difference between them is not always recognized. First, it is necessary to test whether the transfer function is statistically stable. Second, there is a need to know if the fundamental relationship between climate and tree-ring formation is likely to have varied over the period to be reconstructed. A particularly advantageous situation arises when local climate data cover a sufficiently long period to allow for the development of statistically stable transfer functions that cover non-overlapping periods. Hughes et al. (1984) were able to perform a rigorous test of the stability of the tree-ring/temperature relationship back to the early nineteenth century, and less rigorously into part of the eighteenth century, by using two of the longest continuous instrumental records in the world—the Edinburgh, Scotland, meteorological record, and Manley's central England monthly temperature series. These were compared with tree-ring data from the Scottish Highlands. The tree-ring/temperature relationship was stable over at least 160 years, and probably over 250 years, as compared with the central England temperature record. Not only are the reconstructions derived from the separate 80-year calibrations almost identical, but the structures of the statistical models for each are similar (Hughes et al. 1984, p 341). It would, of course, be of great interest to see if this relationship stayed stable since 1970.

Conkey (1986) similarly checked her ring-width and density-based reconstructions of New England summer temperatures, calibrated and validated against twentieth-century temperature records by comparison with late eighteenth- through early nineteenth-century temperature data derived from early measurements and diaries, and found them to have been stable over the two-century period. Whereas Hughes et al. (1984) examined their seasonal transfer functions for stability, Carrer and Urbinati (2006) tested the stability of monthly correlations and response functions in larch in northern Italy against long climate data extending back to the beginning of the nineteenth century. They found tree-ring growth to be consistently most sensitive to June temperatures, but the strength of this relationship varied rather strongly. From the point of view of reconstructing past temperatures by using their tree-ring data, it would be interesting to know if this variation in sensitivity would be enhanced, unaffected, or damped when it is examined in a seasonal transfer function mode, rather than in the monthly response function mode they investigated.

2.4.2 Recent Reports of Divergence Between Temperature and Tree-Ring Density and Width

It is against this background that the results of Briffa et al. (1998) emerged. Working with hundreds of ring-width and maximum latewood density chronologies from

alpine and subarctic locations, they concluded that 'during the second half of the twentieth century, the decadal-scale trends in wood density and summer temperatures have increasingly diverged as wood density has progressively fallen.' These results apply to their network of sites chosen to be optimal for using wood density as a proxy of summer temperature. Further, the 'divergence' they report is in the decadal, not the interannual, component of the response, and this divergence has the opposite sign in parts of the middle latitudes and in the western regions of North America and of Europe (their Fig. 2.1). Bearing this in mind, Briffa and his colleagues, working with this dataset, have chosen to end their calibration period in 1960, so that the divergence could not affect their reconstructions.

Subsequently, several authors have sought to identify the cause or causes of this divergence (for example, D'Arrigo et al. 2008b; Vaganov et al. 1999). Proposed causes fall into three general classes—the emergence of new combinations of climate conditions in the late twentieth century, the intervention of non-climatic factors, such as changing atmospheric or soil composition or changed UV radiation, and previously undetected artifacts in the tree-ring chronologies introduced by the methods used to remove non-climatic variations ('standardization'), along with associated biases related to the calibration and verification periods used. This possibility of artifacts introduced by standardization methods is raised by Melvin and Briffa (2008) and is discussed by Briffa and Melvin (Chapter 5, this volume). Grudd (2008) found that increasing the number of relatively young modern trees in a multimillennial density chronology from northern Sweden caused a previously present late-twentieth-century divergence to disappear, lending support to the suggestion that at least some of the instances of divergence are artifacts of some combination of sample structure and standardization treatment.

Setting this last possibility aside for the moment, we see that the question arises, might such a divergence have occurred in earlier times, and, if so, how would we know? The Hughes et al. (1984) and Conkey (1986) studies cast light on the last 200–300 years, and in neither case is there any evidence of such instability over that time before about 1970. Büntgen et al. (2008) examined a large network of chronologies from across the European Alps, all carefully prepared to preserve low-frequency variability, in the context of climate data covering the late nineteenth and twentieth centuries. They found no evidence for any unusual late-twentieth-century divergence problem, and indeed concluded that the warmth of the late twentieth/early twenty-first century was unique in the last millennium. Esper et al. (2009) reported similar findings for a network of ring-width and density chronologies across northern Siberia, concluding that there is no divergence there between tree-ring data and temperature when appropriate methods of standardization and calibration are used.

In fact, tree-ring-network-based reconstructions of temperature over the past several centuries are remarkably consistent with those derived from independent records such as historical sources (Luterbacher et al. 2004) and the gross dynamics of large numbers of mountain glaciers (Oerlemans 2005). These results suggest that, in the context of the last several centuries, apparent divergences that survive analyses such as that reported by Esper et al. (2009) are unique to the late twentieth century

in the regions to which these studies apply. Even so, it is important to develop strategies for detecting whether such divergences have occurred in the past. This could best be done by examining whether completely independent types of natural archive yield proxy records that continue to be mechanistically and climatically consistent with one another for the periods of interest, as in the comparison of tree-ring-derived reconstructions with the work of Luterbacher et al. (2004) and Oerlemans (2005), as was mentioned above. Although the issue of unstable signal, and divergence, has mainly been discussed in the context of tree rings as archives of past temperature, this concern must apply equally to moisture-related records.

2.5 The Quest for Unbiased Chronologies

2.5.1 The Problem

Annual rings formed early in the life of a tree tend to be wider than those formed later. The main cause of this is the tree's mode of growth. Each year's new annual ring (which consists of xylem) is laid down outside the previous years'. Thus, if approximately the same volume of wood is laid down each year, and if the proportionality between radial and height growth does not change radically, the newer rings must, in general, be thinner than the older rings. As a result, there is usually an 'age-size-related trend' in ring width. In many cases, rings get larger in the first few decades of the tree's life, presumably as the tree's canopy is built and as it emerges from the shade of its neighbors. For other reasons that are likely related more to the mechanical function of wood, there is usually also a downward trend in maximum latewood density with increasing distance from the pith. These age-size-related trends can contaminate any record of climate variability to be found in the annual rings, and so must be discounted in some way.

There are several other non-climatic sources of variability in tree-ring width and maximum latewood density. The overwhelming majority of dendroclimatic reconstructions published to date have been based on measurements of TRW or MXD. In the case of trees growing close enough to influence one another's growth, and in dense enough stands for fire and other disturbances to affect growth, 'disturbance pulses' leave strong imprints on the course of growth, modifying or even completely obscuring the general age-size-related trend. In the early years of the development of dendroclimatology, primarily in the semiarid American Southwest, the trees sampled most commonly fit the description of 'open-grown'—that is, because trees were far apart there was minimal interaction between them, and disturbance pulses played only a small role. Thus, the preparation of tree-ring chronologies for use as climate records consisted mainly of detrending each sample with a simple deterministic model, such as a linear trend model or a modified negative exponential curve (Fritts 1963), and then averaging the detrended series from many trees (usually with two series per tree) to produce a mean chronology. The intention was that averaging many replicate samples from each site should result in a relative strengthening of

the common climatic signal, and a dilution of the individual effects of competition and disturbances on the resulting mean chronology, as was discussed above.

As networks were built in more mesic regions characterized by denser forests and much greater influences of competition and disturbances—in Western Europe and eastern North America, for example—it became clear that additional approaches were needed. In order to fit and hence remove growth surges or suppressions unique to single trees, more 'flexible' curves were used in detrending; for example, polynomials (Fritts 1976), flexible cubic smoothing splines (Cook and Peters 1981), and digital filters (Briffa 1984). An accessible and thorough account of these developments is given by Cook (1990) and Cook et al. (1990). It was acknowledged at an early stage that this approach could well result in the loss of climatic information on the same and longer timescales as those of the age-size-related trend (LaMarche 1974, pp 1045–1046; Fritts 1976, p 264), or on even shorter timescales when the more 'flexible' approaches were applied. Cook et al. (1995) also noted that, in building a millennia-long chronology from overlapping short segments, 'the maximum length of recoverable climate information is ordinarily related to the lengths of the individual tree-ring series used to reconstruct the millennia-long chronology.' They named this problem the 'segment length curse.' In some cases this problem was avoided by performing no detrending, specifically where there was reason to believe an age-size trend was largely absent (see, for example, LaMarche 1974). Of course, there was a concomitant need to exclude samples showing evidence of a sudden surge or suppression from inclusion prior to pretreatment, and in the example mentioned, the rapid growth of the early centuries of the tree's life was discarded.

This option is not available when individual segments are only a few centuries long, as a large fraction of each series will likely be in the fast-growing early part of the age-size curve. In such situations, those seeking to reconstruct lower-frequency climate fluctuations—for example, on multidecadal to multicentennial timescales—have long chosen to use 'stiff' detrending curves such as straight lines, the modified negative exponential, the Hugershoff curve, and very stiff splines, in detrending the original tree-ring measurement series, so as to conserve these slower variations to as great an extent as possible. Where individual segments are exceptionally long (many centuries), it has been possible to capture multicentennial features by using such techniques (for example, Hughes and Funkhouser 1998). More commonly, chronologies with segment lengths of 300 or 400 years cannot be expected to capture variability on timescales much greater than multidecadal, no matter how long the chronology.

It was in response to this problem that the approach known as regional curve standardization (RCS) was developed, or at least modified for use in dendroclimatology, initially by Briffa et al. (1992). An empirically defined age/ring-width or age/maximum latewood density curve is developed and used in place of, for example, the modified negative exponential curve to detrend each measurement series. Unlike the fitted curves, whether deterministic (e.g., negative exponential, polynomial) or stochastic (e.g., digital filters or splines), the empirical age/growth curve is positioned relative to the cambial age, not the calendar date, of each ring in the sample series being treated.

As Cook et al. (1995) state, 'The premise behind RCS is that there is a single, common age and size-related biological growth curve for a given species and site that can be applied to all series regardless of when the trees were growing.' This technique has been used for the reconstruction of summer temperatures at high-latitude or high-elevation sites or regions by using conifer ring widths (TRW) or densities (MXD) (for example, Briffa et al. 1992, 1995, 1996; Naurzbaev and Vaganov 2000; Luckman and Wilson 2005), and on much broader spatial scales (Esper et al. 2002a). It characteristically results in both more marked century-scale fluctuations and weaker correlations between individual samples after treatment, leading to greater statistical uncertainty than with 'traditional' methods (Briffa et al. 1992), unless far more samples are included. If the assumptions listed by Cook et al. (1995) are not met, the use of RCS-based chronologies in climate reconstructions will result in time-dependent biases. Briffa and Melvin (Chapter 5, this volume) examine these and other biases that can be associated with the use of RCS and related methods, and they provide suggestions for improvement of the techniques for removing non-climatic information from tree-ring series. Other recent work has dealt with suggested techniques related to RCS (Briffa et al. 2001; Esper et al. 2009), while efforts are also under way to derive methods from theoretical consideration of basal area increment (Biondi and Qeadan 2008). Perhaps the most interesting possibility is the development of a process-based standardization method based on the mechanical strength of trees (Melvin 2004).

It should be emphasized that the problem all this work is designed to solve concerns very slow climatic changes, on timescales of centuries—changes that are likely to be small in comparison to interannual and interdecadal variability (Hughes and Diaz 1994, p 120). As many available tree-ring chronologies have mean segment lengths of two, three, or four centuries, the segment length curse has little relevance to the capture of climate signal by tree rings on timescales from interannual to multiple decades, or even a single century.

2.6 Final Thoughts

One of the most spectacular achievements in dendroclimatology has been its application to the detection of modes of climate variability affecting the Americas in both the Northern and Southern Hemispheres, and hence casting light on interannual to multidecadal variability in the Pacific basin. This endeavor, to which tree rings are indispensable, is described by Villalba et al. (Chapter 7, this volume), and provides the reader with a view of the unique contributions of dendroclimatology to climatology. Considerable progress has also been made in Europe and in the boreal zone (for example, Briffa et al. 2004, 2008; Büntgen et al. 2006), Asia (for example, D'Arrigo et al. 2001; Yin et al. 2008), Australasia (for example, Cook et al. 2006), northern Africa (Esper et al. 2007; Touchan et al. 2008), and the Near East (Touchan et al. 2005), and impressive advances are being made in the tropics (for example, Buckley et al. 2007; D'Arrigo et al. 2008a).

The major contributions that dendroclimatology has made, and continues to make, to the reconstruction of global and hemispheric temperatures during recent centuries and millennia depend on the same approaches and have been covered elsewhere (e.g., Mann et al. 2008). In a review of high-resolution paleoclimatology of the last millennium, Jones et al. (2009, p 4) wrote,

> While the visibility of large-scale (average and spatially detailed) reconstructions stems from their ability to contextualize 'unprecedented' climate change in the twentieth century against a multicentury backdrop, such multiproxy reconstructions are critical to a variety of climate science studies. They provide a large-scale context with which to compare regional climate variability as reconstructed by single proxy records, which may ultimately help resolve the large-scale mechanisms of past low-frequency climate change. They also provide much-needed tests of the response of large-scale climate to a variety of climate forcings which occurred during the last millennium (most notably solar and volcanic forcing).

Its capacity to identify patterns of climate variability on various spatial scales permits the application of dendroclimatology to a remarkable range of fields of direct relevance to human concerns, in addition to their relevance to the pressing questions of current and impending climate change. As is described in this book, these include but are not limited to hydrology and the management of water resources (Meko and Woodhouse, Chapter 8, this volume), interactions of climate and ecological systems (Swetnam and Brown, Chapter 9, this volume), and the study of the relationships between climate extremes and social disasters (Stahle and Dean, Chapter 10, this volume).

In each case, the usefulness of dendroclimatology rests on:

- appropriate sample design
- precise and accurate annual chronology
- removal of non-climatic variability
- distillation of a common climate signal by sample replication and combination into site chronologies
- understanding of the mechanisms producing the tree-ring record, especially the role of climate
- the demonstration of climatically credible spatiotemporal behavior in geographic networks of site chronologies

This cascade of requirements flows directly from the peculiar nature of the potential proxy records of past climate embedded in tree rings, whether structural (for example, total ring width and maximum latewood density) or compositional (for example, stable isotopic ratios in cellulose) (see Gagen et al. Chapter 6, this volume). In spite of the presence of multiple confounding influences on all of these proxy records, the presence of common patterns of variation repeatedly emerges when the above requirements are met. This trend is seen in the time series from tens or more of trees sampled at one location, and across regions represented by tens or even hundreds of site chronologies, each 'distilled' from each location's set of multiple individual samples. Thus, although climate signals in tree rings are emergent from a complex and varying set of influences (Cook and Pederson, Chapter 4,

this volume), they are eminently susceptible to mechanistic understanding (Vaganov et al. Chapter 3, this volume).

There is a certain irony in the use of tree rings as records of past climate, with all its complexities and subtleties, in that it rests on a very simple observation for which only an increment corer, sandpaper, and a low-power dissecting microscope are needed. It is possible to date tree rings when common year-to-year patterns of ring variation can be seen (quite literally) to be shared by many trees of a species at one place, and between trees in similar places within a region. So far as a cause for these common patterns is concerned, the prime suspect is climate variability. So, in turn, where tree-ring samples 'cross-date' (share massively replicated patterns of variability), a prima facie case for their containing a climate signal has been made.

References

Anchukaitis KJ, Evans MN, Kaplan A, Vaganov EA, Hughes MK, Grissino-Mayer HD, Cane MA (2006) Forward modeling of regional scale tree-ring patterns in the southeastern United States and the recent influence of summer drought. Geophys Res Lett 33: L04705. doi:10.1029/2005GL025050

Biondi F, Qeadan F (2008) A theory-driven approach to tree-ring standardization: defining the biological trend from expected basal area increment. Tree-Ring Res 64: 81–96

Briffa KR (1984) Tree-climate relationships and dendroclimatological reconstruction in the British Isles. Dissertation, University of East Anglia, Norwich

Briffa KR, Jones PD, Bartholin TS, Eckstein D, Schweingruber FH, Karlen W, Zetterberg P, Eronen M (1992) Fennoscandian summers from AD 500: temperature changes on short and long timescales. Clim Dynam 7:111–119

Briffa KR, Jones PD, Schweingruber FH, Shiyatov SG, Cook ER (1995) Unusual twentieth century summer warmth in a 1000 year temperature record from Siberia. Nature 376:156–159

Briffa, KR, Jones PD, Schweingruber FH, Karlén W, Shiyatov SG (1996) Tree-ring variables as proxy-climate indicators: problems with low-frequency signals. In: Bradley RS, Jones PD, Jouzel J (eds) Climatic variations and forcing mechanisms of the last 2000 years. Springer, Berlin, pp 9–41

Briffa KR, Schweingruber FH, Jones PD, Osborn TJ, Shiyatov SG, Vaganov EA (1998) Reduced sensitivity of recent tree-growth to temperature at high northern latitudes. Nature 392:678–682

Briffa KR, Osborn TJ, Schweingruber FH, Harris IC, Jones PD, Shiyatov SG, Vaganov EA (2001) Low-frequency temperature variations from a northern tree ring density network. J Geophys Res 106:2929–2941

Briffa KR, Osborn TJ, Schweingruber FH (2004) Large-scale temperature inferences from tree rings: review. Global Planet Change 40:11–26

Briffa KR, Shishov VV, Melvin TM, Vaganov EA, Grudd H, Hantemirov RM, Eronen M, Naurzbaev MM (2008) Trends in recent temperature and radial tree growth spanning 2000 years across northwest Eurasia. Philos Trans R Soc Lond B Biol Sci 363:2271–2284

Buckley BM, Palakit K, Duangsathaporn K, Sanguantham P, Prasomsin P (2007) Decadal scale droughts over northwestern Thailand over the past 448 years: links to the tropical Pacific and Indian Ocean sectors. Clim Dynam 29:63–71

Büntgen U, Frank DC, Nievergelt D, Esper J (2006) Summer temperature variations in the European Alps, AD 755–2004. J Climate 19:5606–5623

Büntgen U, Frank D, Wilson R, Carrer M, Urbinati C (2008) Testing for tree-ring divergence in the European Alps. Glob Change Biol 14:2443–2453

Carrer M, Urbinati C (2006) Long-term change in the sensitivity of tree-ring growth to climate forcing in *Larix decidua*. New Phytol 170:861–872

Conkey LE (1986) Red spruce tree-ring widths and densities in eastern North America as indicators of past climate. Quaternary Res 26:232–243

Cook ER (1990) A conceptual linear aggregate model for tree rings. In: Cook ER, Kairiukstis L (eds) Methods of dendrochronology: applications in the environmental sciences. Kluwer, Dordrecht, pp 98–104

Cook ER, Peters K (1981) The smoothing spline: a new approach to standardizing forest interior tree-ring width series for dendroclimatic studies. Tree-Ring Bull 41:45–53

Cook E, Briffa K, Shiyatov S, Mazepa V (1990) Tree-ring standardization and growth-trend estimation. In: Cook ER, Kairiukstis L (eds) Methods of dendrochronology: applications in the environmental sciences. Kluwer, Dordrecht, pp 104–123

Cook ER, Briffa KR, Meko DM, Graybill DA, Funkhouser G (1995) The segment length curse in long tree-ring chronology development for palaeoclimatic studies. Holocene 5:229–235

Cook ER, Buckley BM, Palmer JG, Fenwick P, Peterson MJ, Boswijk G, Fowler A (2006) Millennia-long tree-ring records from Tasmania and New Zealand: a basis for modelling climate variability and forcing, past, present and future. J Quaternary Sci 21:689–699

D'Arrigo R, Jacoby G, Frank D, Pederson N, Cook E, Buckley B, Nachin B, Mijiddorj R, Dugarjav C (2001) 1738 years of Mongolian temperature variability inferred from a tree-ring width chronology of Siberian pine. Geophy Res Lett 28:543–546

D'Arrigo R, Allan R, Wilson R, Palmer J, Sakulich J, Smerdon JE, Bijaksana S, Ngkoimani LO (2008a) Pacific and Indian Ocean climate signals in a tree-ring record of Java monsoon drought. Int J Climatol 28:1889–1901

D'Arrigo R, Wilson R, Liepert B, Cherubini P (2008b) On the 'divergence problem' in northern forests: a review of the tree-ring evidence and possible causes. Global Planet Change 60: 289–305

Esper J, Cook ER, Schweingruber FH (2002a) Low-frequency signals in long tree-ring chronologies for reconstructing past temperature variability. Science 295:2250–2253

Esper J, Schweingruber FH, Winiger M (2002b) 1300 years of climatic history for western central Asia inferred from tree-rings. Holocene 12:267–277

Esper J, Frank D, Büntgen U, Verstege A, Luterbacher J (2007) Long-term drought severity variations in Morocco. Geophys Res Lett 34:L17702. doi:10.1029/2007GL030844

Esper J, Frank D, Buntgen U, Verstege A, Hantemirov R, Kirdyanov AV (2009) Trends and uncertainties in Siberian indicators of twentieth century warming. Glob Change Biol: 1–14. doi:10.1111/j.1365–2486.2009.01913.x

Evans MN, Reichert BK, Kaplan A, Vaganov EA, Hughes MK, Cane MA (2006) A forward modeling approach to paleoclimatic interpretation of tree-ring data. J Geophys Res 111. doi:10.1029/2006JG000166

Fritts HC (1963) Computer programs for tree-ring research. Tree-Ring B 25:2–6

Fritts HC (1974) Relationships of ring widths in arid-site conifers to variations in monthly temperature and precipitation. Ecol Monogr 44:411–440

Fritts HC (1976) Tree rings and climate. Academic Press, London

Fritts HC, Blasing TJ, Hayden BP, Kutzbach JE (1971) Multivariate techniques for specifying tree-growth and climate relationships and for reconstructing anomalies in paleoclimate. J Appl Meteorol 10:845–864

Grudd H (2008) Tornetrask tree-ring width and density AD 500–2004: a test of climatic sensitivity and a new 1500-year reconstruction of north Fennoscandian summers. Clim Dynam 31: 843–857

Hughes MK, Brown PM (1992) Drought frequency in central California since 101 BC recorded in giant sequoia tree rings. Climate Dynam 6:161–167

Hughes MK, Diaz HF (1994) Was there a Medieval Warm Period, and if so, where and when? Climatic Change 26:109–142

Hughes MK, Funkhouser G (1998) Extremes of moisture availability reconstructed from tree rings for recent millennia in the Great Basin of western North America. In: Beniston M, Innes JL (eds) The impacts of climate variability on forests. Springer, Berlin, pp 99–107

Hughes MK, Schweingruber FH, Cartwright D, Kelly PM (1984) July–August temperature at Edinburgh between 1721 and 1975 from tree-ring density and width data. Nature 308: 341–344

Hughes MK, Kuniholm PI, Eischeid, JK, Garfin G, Griggs CB, Latini C (2001) Aegean tree-ring signature years explained. Tree-Ring Res 57:67–73

Jones PD, Briffa KR, Osborn TJ, Lough JM, Van Ommen TD, Vinther BM, Lutherbacher J, Wahl ER, Zwiers FW, Mann ME, Schmidt GA, Ammann CM, Buckley BM, Cobb KM, Esper J, Goosse H, Graham N, Jansen E, Kiefer T, Kull C, Kuttel M, Mosley-Thompson E, Overpeck JT, Riedwyl N, Schulz M, Tudhope AW, Villalba R, Wanner H, Wolff E, Xoplaki E (2009) High-resolution palaeoclimatology of the last millennium: a review of current status and future prospects. Holocene 19:3–49

Kelly PM, Munro MAR, Hughes MK, Goodess CM (1989) Climate and signature years in west European oaks. Nature 340:57–60

Kelly PM, Leuschner HH, Briffa KR, Harris IC (2002) The climatic interpretation of Pan-European signature years in oak ring-width series. Holocene 12:689–694

LaMarche VC (1974) Paleoclimatic inferences from long tree-ring records. Science 183: 1043–1088

LaMarche VC, Fritts HC (1971) Anomaly patterns of climate over the western United States, 1700–1930, derived from principle component analysis of tree-ring data. Mon Weather Rev 99:138–142

Luckman BH, Wilson RJS (2005) Summer temperatures in the Canadian Rockies during the last millennium: a revised record. Clim Dynam 24:131–144

Luterbacher J, Dietrich D, Xoplaki E, Grosjean M, Wanner H (2004) European seasonal and annual temperature variability, trends, and extremes since 1500. Science 303:1499–1503

Mann ME, Zhang, Z, Hughes MK, Bradley RS, Miller SK, Rutherford S, Ni Fenbiao (2008) Proxy-based reconstructions of hemispheric and global surface temperature variations over the past two millennia. Proc Natl Acad Sci USA 105(36):13252–13257

Meko DM, Cook ER, Stahle DW, Stockton CW, Hughes MK (1993) Spatial patterns of tree-growth anomalies in the United States and southeastern Canada. J Clim 6:1773–1786

Meko DM, Woodhouse CA, Baisan CA, Knight R, Lukas JL, Hughes MK, Salzer MW (2007) Medieval drought in the upper Colorado River Basin. Geophysical Research Letters 34:L10705. doi:10.1029/2007GL029988

Melvin T (2004) Historical growth rates and changing climatic sensitivity of boreal conifers. Dissertation, University of East Anglia, Norwich

Melvin TM, Briffa KR (2008) A 'signal-free' approach to dendroclimatic standardisation. Dendrochronologia 26:71–86

Naurzbaev MM, Vaganov EA (2000) Variation of early summer and annual temperature in East Taymir and Putoran (Siberia) over the last two millennia inferred from tree rings. J Geophys Res-Atm 105:7317–7326

Oerlemans J (2005) Extracting a climate signal from 169 glacier records. Science 308:675–677

Rossi S, Deslauriers A, Anfodillo T, Morin H, Saracino A, Motta R, Borghetti M (2006) Conifers in cold environments synchronize maximum growth rate of tree-ring formation with day length. New Phytol 170:301–310

Rossi S, Deslauriers A, Anfodillo T, Carraro V (2007) Evidence of threshold temperatures for xylogenesis in conifers at high altitudes. Oecologia 152:1–12

Rossi S, Deslauriers A, Gricar J, Seo JW, Rathgeber CBK, Anfodillo T, Morin H, Levanic T, Oven P, Jalkanen R (2008) Critical temperatures for xylogenesis in conifers of cold climates. Global Ecol Biogeogr 17:696–707

Touchan R, Xoplaki E, Funkhouser G, Luterbacher J, Hughes MK, Erkan N, Akkemik U, Stephan J (2005) Reconstructions of spring/summer precipitation for the eastern Mediterranean from tree-ring widths and its connection to large-scale atmospheric circulation. Clim Dynam 25:75–98

Touchan R, Anchukaitis KJ, Meko DM, Attalah S, Baisan C, Aloui A (2008) Long term context for recent drought in northwestern Africa. Geophys Res Lett 35:L13705. doi:10.1029/2008GL034264

Vaganov EA, Hughes MK, Kirdyanov AV, Schweingruber FH, Silkin PP (1999) Influence of snowfall and melt timing on tree growth in subarctic Eurasia. Nature 400:149–151

Vaganov EA, Hughes MK, Shashkin AV (2006) Growth dynamics of conifer tree rings: images of past and future environments. Springer, Berlin, Heidelberg, New York

Wigley TML, Briffa KR, Jones PD (1984) On the average value of correlated time series, with applications in dendroclimatology and hydrometeorology. J Clim Appl Meteorol 23:201–213

Yin ZY, Shao XM, Qin NS, Liang E (2008) Reconstruction of a 1436-year soil moisture and vegetation water use history based on tree-ring widths from Qilian junipers in northeastern Qaidam Basin, northwestern China. Int J Climatol 28:37–53

Part II
Scientific Bases of Dendroclimatology

Chapter 3
How Well Understood Are the Processes that Create Dendroclimatic Records? A Mechanistic Model of the Climatic Control on Conifer Tree-Ring Growth Dynamics

Eugene A. Vaganov, Kevin J. Anchukaitis, and Michael N. Evans

Abstract We develop an observational and conceptual basis for modeling conifer cambial processes as a direct but nonlinear and multivariate response to external environmental conditions. The model, here termed Vaganov–Shashkin (VS), reproduces the critical features linking climate variability to tree-ring proxy formation. We discuss recent test simulations of tree-ring width data from a variety of sites and spatiotemporal scales. Our experiments demonstrate that the model skillfully reproduces observed patterns of tree-ring growth across a range of environments, species, and scales. Model performance is found to be robust to parameter estimation. We discuss present and future applications of the VS model, including exploration of the biological basis of emergent phenomena and prediction of the influence of climate change on conifer tree growth dynamics.

Keywords Tree growth · Biological basis · Cambium · Simulation · Process model

3.1 Introduction

Climatic variation is a major factor affecting tree-ring growth and wood formation. Accordingly, a significant amount of dendroclimatology research has been focused on the extraction and validation of climatic variability from tree-ring data series (Fritts 1966; Cook and Jacoby 1977; Fritts et al. 1979; Hughes et al. 1984; more recently, see, for example, Stahle and Cleaveland 1992; Grissino-Mayer 1996; Villalba et al. 1998; Briffa et al. 2001; Cook et al. 2002; Hughes 2002; Briffa et al. 2004; Pederson et al. 2004; Watson and Luckman 2004; Salzer and Kipfmueller 2005). The main morphological and anatomical characteristics of tree rings bearing the climatic signal have been described: tree-ring width, density profile, cell diameter, and cell wall thickness (Vaganov 1996a). Although stable isotope methods and

E.A. Vaganov (✉)
Rectorate, Siberian Federal University, Krasnoyarsk, Russia
e-mail: rectorat@sfu-kras.ru

M.K. Hughes et al. (eds.), *Dendroclimatology*, Developments in Paleoenvironmental Research 11, DOI 10.1007/978-1-4020-5725-0_3,

models are increasingly valuable (McCarroll and Loader 2004), the most widely used tree-ring characteristics for climate reconstructions have been tree-ring width and maximum latewood density. Such reconstructions have relied almost entirely on statistical covariation of the proxy observations and climate data during the modern period.

But Harold C. Fritts saw the vital importance of concurrent research into the anatomical pattern of tree-ring formation in response to changing environment. He was one of the first to make a careful study of tree-ring formation in ponderosa pine on the anatomical level, showing how the current and previous weather conditions affect the seasonal growth and cell dimensions of tree rings (Fritts 1966, 1976). Studies like this have provided broad knowledge about which processes in the growing tree control cell production and which determine the characteristics of those cells which are produced. Briefly, tree-ring formation occurs in the active vegetation season, and the processes involved in tree-ring formation integrate the prior and current seasonal conditions. Growth starts with cambial zone activation (activation of the fast divisions of cells). Newly produced cells progress to enlargement, and finally to cell wall thickening. At this stage the cell loses the protoplast and transforms to the 'dead' element of the water conductive system of the tree.

The focus of much anatomical research since Fritts' early work has been on cambial activity (the workings of the 'cambial machine'). Detailed observations and analyses of basic processes of wood formation allowed Wilson and Howard (1968), Howard and Wilson (1972), and Wilson (1973) to offer a 'mimic' model for the quantitative description of tree-ring formation. While this model reproduced the structures formed in the tree stem during the growing season, it required an enormous number of variables and seasonal observational data that had to be specifically defined for any particular tree ring. Furthermore, the model did not include external environmental parameters. Despite the lack of explicit modeling of the external environmental influence on the processes of tree-ring growth, or perhaps because of it, the nature of the environmental control of wood formation has often simply been assumed. The implicit hypothesis has been that environmental factors influence tree-ring formation indirectly, through hormone and substrate balance produced by the apical meristems of shoots, and probably roots (Larson 1964; Denne and Dodd 1981).

3.1.1 The Substrate Source-Sink Hypothesis

In his pioneering work on the biological basis for dendroclimatology, Fritts (1976) included extensive descriptions of the role of both metabolic and cambial processes as mediators of the environmental control on annual tree growth and ring formation. Metabolic approaches often rely on a source-sink understanding of the influence of climate on tree-ring width, which assumes that the environment indirectly determines annual xylem increment as a function of the amount of carbon available for secondary growth. Because secondary basal growth is interpreted to be a low priority for the apportionment of the available whole plant resources (Savidge 2000a), wider

rings would arise as a result of optimal climatic conditions for photosynthesis, while a narrow ring would signal a deficit of carbohydrates and environmental conditions that restrict photosynthetic capacity. Clearly, given that a large quantity of complex carbohydrates, in the form of cellulose, lignin, and hemicelluloses and other polysaccharides, form the bulk of tree biomass, the availability of a source of carbon is an obvious prerequisite for secondary growth. Consistent with a carbon source–limited understanding of secondary growth, it has been observed that plant resources allocated to reproduction can result in a reduction of overall basal growth (Wheelwright and Logan 2004). Defoliation can also induce basal growth suppression and narrow tree rings (Speer et al. 2001), presumably through limitations on available carbohydrates (Ericsson et al. 1980).

Ecophysiological modeling of the environmental controls on the annual incremental basal growth has generally made use of this carbon-balance, source-sink approach (Bassow et al. 1990; Makela 1990). In essence, this type of model focuses on how the external environment controls carbon fixation and the production of other metabolites by trees in the canopy (buds and leaves) and how these are then allocated to various plant parts. Carbon-balance models may include calculations of photosynthesis as a function of tree age, foliage and crown composition, height, and root mass (Bassow et al. 1990). Assimilated carbon is then partitioned into branch, bole, root, and crown growth, as well as to respiration. Explicit models linking environmental conditions to resultant tree-ring characteristics have been developed.

Perhaps the most complete of these models (albeit still considered overly simplistic by Fritts), incorporating processes linking environmental conditions to tree-ring characteristics via photosynthesis, respiration, carbon storage, and cambial processes, is TREERING2000 (Fritts et al. 1999). This model was developed and refined exhaustively using, in part, tree-ring data and meteorological observations from the Santa Catalina Mountains in southern Arizona. Such models provide explicit tests of our understanding of the processes governing tree-ring formation and variation, and have been a critical component of the science of dendrochronology. It is important to note that TREERING2000, is not purely ecophysiological. It uses photosynthesis and assimilation to modify the rates of cellular processes in the cambium (see next section), and is therefore a hybrid carbon-balance and cellular process model (Fritts et al. 1999). The MAIDEN model (Misson 2004) uses a stand-level ecophysiological approach, which simulates the environmental control on photosynthesis and respiration, using both climate and allometric data to determine carbon fixation and mean bole increment diameter, which can be interpreted as analogous to tree-ring width for comparison with dendroecological data.

A drawback to this approach is that modeling the partitioning of carbon within a tree depends strongly on parameters that are not completely understood or described (see LeRoux et al. 2001 for a review and critique). Further, there is evidence of age-related trends in partitioning coefficients (Makela 1990). Many allocation processes will scale with tree height, a non-climatic, age-dependent metric that is itself at least partially a function of stand-level competition for nutrients, sunlight, and water.

A further challenge to modeling the environmental control on tree growth is that our understanding of the nature of the relationship between the concentration of carbohydrates in the developing xylem and the eventual ring width as mediated by the external environment (climate, photoperiod, exogenous ecological factors) remains incomplete (Savidge 2000a, b). Earlier research found the amount of carbohydrates in the cambium was positively correlated with the period of greatest tracheid production (Parkerson and Whitmore 1972). However, Sundberg et al. (1993) revealed that the relative concentration of sucrose could not explain ring width differences between two populations of *Pinus sylvestris*. Similarly, a study of the effect of pruning *Eucalyptus grandis* trees revealed that the loss of stems and foliage does not reduce tree diameter (Thomas et al. 2006). Even extreme insect defoliation has been observed to not result in reduced-diameter growth or tree-ring width (Jones et al. 2004), even in one case despite a 50% reduction in the number of leaves, presumably because stored starches can compensate to some degree for the immediate loss of photosynthetic capacity (Hoogesteger and Karlsson 1992). Dickson et al. (2000) have hypothesized that the export of photosynthate could be generally sink limited as opposed to excess source mediated; that is, environmental constraints may reduce developing tissues' demand for metabolic products prior to the point in time at which photosynthesis or total carbohydrate availability becomes truly limiting. Körner (1998) examined potential environmental controls on alpine tree-line position and found that trees in these environments were not limited by carbon availability and photosynthetic rate, but rather apparently directly by temperature. In a recent paper, Körner (2003) is even more direct:

> It is concluded that, irrespective of the reason for its periodic cessation, growth does not seem to be limited by carbon supply. Instead, in all the cases examined, sink activity and its direct control by the environment or developmental constraints restricts biomass production of trees under current ambient CO_2 concentrations.

3.1.2 The Cambial Control Hypothesis

A different understanding of the environmental control on the characteristics of annual tree rings is that cellular processes in the cambium are directly influenced by environmental conditions. It is recognized that these cellular processes of growth, division, differentiation, maturation, and death, which do ultimately give rise to the structure and size of the annual tree ring, are controlled by gene expression and hormonal stimulus, and that they can respond to both external (environmental) and internal (developmental) influences (Savidge 2000a; Plomion et al. 2001; Schrader et al. 2003). Rossi et al. (2007) concluded that the minimum threshold temperature for growth they observed in tree-line larch, pine, and spruce was directly limiting secondary growth at the cellular level, and that below this temperature the sink for nonstructural carbohydrates in the secondary xylem was reduced. Numerous experiments have shown that direct heating of stems can initiate cambial activity after the onset of winter dormancy (Gričar et al. 2006). Abe et al. (2003) found that cell expansion rate in the cambium decreases as a direct consequence

of water deficit, which results in an overall decrease in cell production as cambial activity subsequently declines. Cellular processes in the cambium can therefore be directly inhibited by climate, through temperature or pressure (via water potential) influences on the cell cycle. The impetus to avoid cavitation and cell embolism in vascular tissues would not require mediation through carbohydrate availability and could act as a developmental determinant on the cambium itself.

Hormones and other substrates clearly play an important role in cellular growth and differentation in the cambium, although the exact mechanisms through which they influence these processes continue to be investigated (Savidge 1983, 1996, 2000a; Dengler 2001). Recent research on the genetic controls on xylem differentiation by Schrader et al. (2003) has shown that hormone gradients across the cambial zone are associated with differential gene expression and the specific stage of cellular development. Because of this, cambial processes and development of new xylem cells are inherently related to their position in the cellular file. Schrader et al. (2003) also concluded that the hormonal gradients across the cambium could change rapidly, potentially in response to external environmental influences. Similarly, Uggla et al. (2001) found concentration gradients of sucrose and indole-3-acetic acid (IAA) across developing vascular plant tissue that corresponded to different stages of cellular development, and moreover that the onset of latewood formation did not correspond to any seasonal change in overall carbohydrate availability. The importance of positional information and the rate of cellular processes, particularly division, in the developing xylem will be discussed below in the context of the physiological and observational basis for our model. Certainly, xylogenesis cannot occur without the provisioning of sucrose and hormones from the canopy, which in turn depends on access to water and nutrients provided by the roots. However, cellular processes in the meristem and developing xylem directly regulate cambial activity, and secondary xylem development involves spatiotemporal gradients of cellular growth and regulation, which can reflect the direct influence of climate on these processes and patterns.

For dendroclimatology, it would be desirable to create a tractable forward model that mechanistically includes only the critical processes that are minimally necessary to link climate variables to tree-ring formation, but whose application worldwide is not sensitive to the choice of a limited set of tunable parameters. Such a class of models can be used to validate statistically based reconstructions of local climate variations, the assumptions behind which may not always be valid (Cook and Pederson, Chapter 4, this volume). For example, such models could predict a change in the dominant environmental influence on tree-ring width variations, which can be compared against actual observations. Such phenomena can only be diagnosed from ad hoc statistical analyses, and Cook and Pederson (Chapter 4, this volume) caution against a priori interpretation of tree-ring data when statistical uncertainty and emergent behavior cannot be distinguished from one another.

Here, we introduce and briefly detail the processes that control ring development in the context of the seasonal kinetics of cambial activity. We discuss the mechanisms and controls on the production, expansion, and maturation of xylem cells, and show how these may be externally influenced by climate. A mechanistic tree-ring

model that integrates the primary environmental controls on conifer cambial activity is described, and we provide examples of its application in dendroclimatology. A version of this model, here referred to as Vaganov–Shashkin (VS), also forms the core of the cambial simulation portion of the more complete TREERING2000 model of conifer tree growth (Fritts et al. 1999). We review recent applications of the VS model to the interpretation of tree-ring observations in a number of regions, environments, and climate change scenarios. Implicit in this review is the assumption that the VS model includes the most important processes required to successfully simulate observed characteristics of tree rings, if it can be shown that the simulations are consistent with observations. Finally, we discuss the role of forward models in the development, calibration, and interpretation of tree-ring-based estimates of climate variability and change.

3.2 Cambial Activity

The formation of mature xylem cells is usually considered as a process that occurs in three stages: the division of cells, the growth of cells by radial expansion, and the maturation of tracheids, when cell walls thicken and the protoplast is autolysed. All stages are divided in space and in time, although they may overlap partially (Gamaley 1972). In the majority of plants, xylem is a complex tissue consisting of differentiated cells of more than one type, generated by a secondary meristem, the cambium. Plant meristems and cambium in particular, by virtue of their accessibility, became a subject of research with the appearance of the first microscope. The history of cambium research is well described; for example, in Larson's book (1994). However, until now our knowledge of the factors initiating and regulating the origin of tissue from meristems and the physiology of meristem has been rather fragmentary. This has led to the absence of a uniform nomenclature (Wilson 1966; Schmid 1976; Catesson 1984; Larson 1994).

Cambium has common features intrinsic to all meristematic tissues and has, as a highly specialized secondary meristem, specific features:

1. It is a self-sustaining cell-like system; that is, it retains its various functions for extended periods of time, frequently throughout the life of the plant, which may last centuries or millennia.
2. In woody plants the cambium grows at the expense of the growth of the tree. An increase in the number of cambial cells happens at the expense of the division and differentiation of those cells and of the primary (apical) meristem.
3. Cambial derivatives can be differentiated into various types of xylem and phloem cells.
4. Cambium has a strictly ordered spatial organization.

The cambial cells form a continuous layer, covering the trunk, branches, and roots. Therefore, the cambium, on the one hand, is distributed in space, and, on the other hand, it is a linked system, where the adjacent cells are in direct contact. The

spatial organization of the cambial zone is important from the point of view of regulation of its activity, as it imposes a number of specific requirements on regulation and control. Another, but not less significant, aspect of the spatial organization of the cambium is that it is the basis of the spatial cell-like organization of xylem and phloem. For example, it orders the radial tracheid files, the formation of the vessel system, and so on.

The growth of a tree ring is the result of periclinal divisions of cells in the cambial zone and of their differentiation. The growth rate depends on the number of cells in the cambial zone and their rate of division. In coniferous species, the growth of a tree ring during a season is always accompanied by a change in the number of cambial cells, which has characteristic dynamics that are general for all species (Wilson 1966; Gregory 1971; Skene 1972; Kutscha et al. 1975; Vaganov et al. 1985). In dormancy, the size of the cambial zone reaches a minimum and usually includes 4–5 cells but can reach up to 10 (Larson 1994). The radial diameter of cells in the cambial zone is equal to 5–6 μm in average but does not exceed 10 μm (Bannan 1955; Alfieri and Evert 1968; Vaganov et al. 1985). Activation of the cambial zone starts with a swelling of cells, and then the first divisions appear. After activation the size of the cambial zone is increased, and the number of cells in it increases and reaches maximum values up to 20 (15–16 on average for different species) (Larson 1994). There is evidence for a relationship between the number of cells in the cambial zone during the dormant period (and at the starting date) and the total annual production of xylem. So, Gregory (1971) found that this relationship for Alaskan white spruce is described as $N_{\text{camb}} = 3.82 + 0.05 \times N (R^2 = 0.75; n = 37; p < 0.001)$. Sviderskaya (1999) obtained similar results from seasonal observations of tree-ring formation in Scots pine (*Pinus sylvestris*) and Siberian fir (*Abies sibirica*) in the Siberian taiga (Fig. 3.1).

All the available data on the duration of the cell cycle, as well as of separate phases of it, show significant variability between samples taken in different parts of a tree during a growing season, especially for the size of the cambial zone. This essential variability is determined by the weather conditions of the season and other factors. Thus it is clear that the length of the cell cycle in the cambial zone changes during the growth season. Combining this statement with the observed curvilinear relationship between the number of cells in the cambial zone and annual xylem increment, we are led to the following conclusion: the regulation of cell production by the cambial zone can be achieved by increasing the number of cells in the cambial zone as well as by increasing the rate of cell division in the cambial zone.

We can summarize the results concerning the kinetics parameters of cambial activity in xylem cell production observed in different conifer species:

1. The number of cambial cells in dormant cambium and active cambium is rather different. There is a significant relationship between the number of dormant cells in the cambial zone and subsequent annual xylem increment (Skene 1972; Sviderskaya 1999).
2. The number of cells in the cambial zone varies during a season due to internal and external factors (Fig. 3.1). The average duration of the cell cycle in the cambial

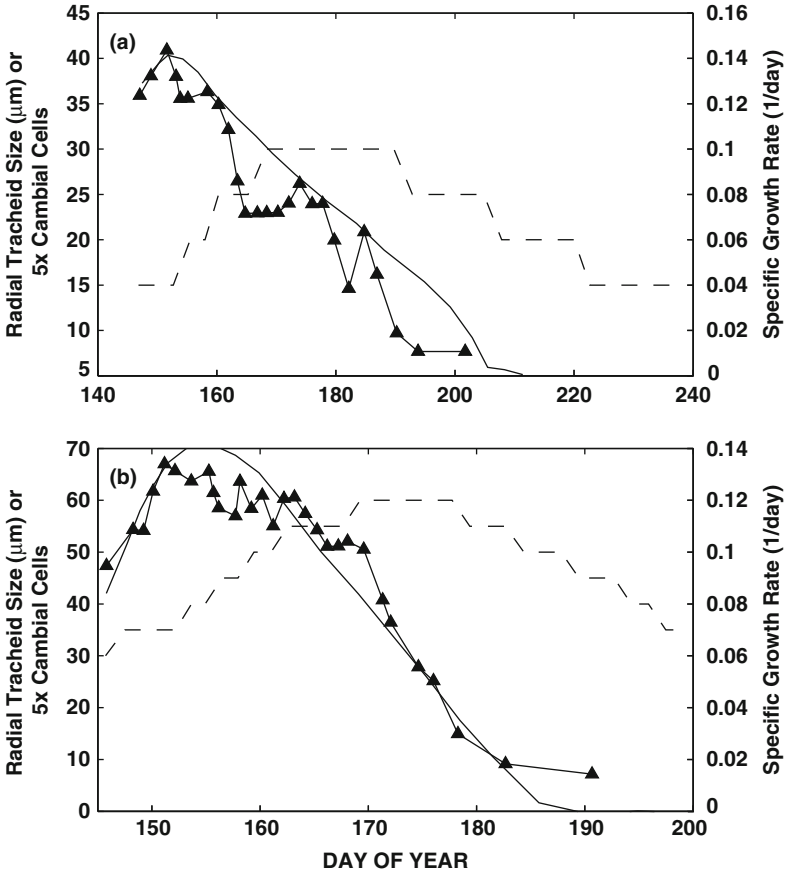

Fig. 3.1 Seasonal dynamics of radial tracheid size (*filled triangles*), cell number in cambial zone (*dashed line*, divide by 5), and specific growth rate (*solid line*) in (**a**) *Abies sibirica* and (**b**) *Pinus sylvestris* (from Sviderskaya 1999). A good relationship is seen between the intraseasonal changes in the specific growth rate and changes in the size of tracheids leaving the cambium at that time. The radial tracheid dimension is primarily determined by the average radial growth rate in the cambial zone or by the average rate of cell division within the cambial zone, and therefore also corresponds quite well to the magnitude of cell production

zone varies during a season. Usually the cycle is shorter when earlywood cells form and longer during formation of latewood cells, especially at the end of the growing season.

3. The total annual xylem cell production is closely related to the number of cells in the cambial zone. There is, however, a curvilinear relationship between the cell number of annual xylem increment and the average cambial cell number (Skene 1972) or the maximum cell number in the cambial zone (Vaganov et al. 1985; Sviderskaya 1999). This relationship indicates that a low rate of cell production during a season is supported mainly by an increase of the cambial zone (more

xylem mother cells), but a higher rate of cell production during a season must also be associated with an increase in the rate of cell division or faster cycling of xylem mother cells.

4. There is a typical distribution of measured mitotic index along the cambial zone: moving inward from the last phloem cells produced, the mitotic index increases to a maximum approximately one-third the distance across the cambial zone and then decreases, either slowly or rapidly depending on whether the cambial zone is wide or narrow (that is, depending on the number of cells in the cambial zone) (Bannan 1957; Wilson 1964).
5. There are differences in the rates of cell production even if the relationship between the number of cells produced during a season and the number of cells in the cambial zone is the same (Gregory and Wilson 1968). These differences are associated with higher or lower mitotic index.
6. In conifers, the first cell divisions (in the growing season) are evident in cambial cells near to or often adjoining the last differentiated tracheids of the previous year's growth ring (Bannan 1955; Grillos and Smith 1959; Bannan 1962; Zimmermann and Brown 1971; Savidge 1993).

What can we say about the possible control of each characteristic? One possibility is that the specific growth rate distribution within the cambial zone depends on tree species as well as the geographical zone of growth (regional climate). There is some evidence for this from observations (Gregory and Wilson 1968; Sviderskaya 1999). From the dendrochronological point of view, these characteristics are more or less stable through a long period of growth and do not affect interannual variations of cell production. The dormant and especially the starting size of the cambial zone may be closely related to the previous growth and tree vigor (Dodd and Fox 1990; Sviderskaya 1999). Dendroclimatic analysis based on 'cell chronologies' of larch and spruce near the northern timberline shows the significant effect of starting conditions (temperature and soil melting) on production of cells and tree-ring width (Hughes et al. 1999; Vaganov et al. 1999). These characteristics affect the interannual variability in tree-ring width and cell production. However, the starting number of cells in the cambial zone may also be affected by growth conditions in the previous year and, so, might be responsible for autocorrelation in tree-ring series that appear, at first sight, to have no climate cause (Fritts 1976). The main possible environmental control is related to intraseasonal variations of size of the cambial zone and the specific growth rate of xylem mother cells. This thesis is supported by practically all experimental data, which show close correlation between average and maximal size of the cambial zone and annual xylem increment (see Wilson 1964; Gregory 1971; Skene 1972; Vaganov et al. 1985). In combination with cell cycle distribution across the cambial zone, these seasonal variations may explain much of the interannual deviation in total cell production and tree-ring width.

Analysis of the data shows that there are two determinants of variability in the sizes of the cambial zone: one that is more or less constant over many years, determined by the condition of the tree as a whole (growth class, vigor, energy of growth, age, position in stand, etc.); and a second, an intraseasonal component, which is

determined by change of the specific growth rate of xylem mother cells and on which their number also simultaneously depends (Vaganov 1996b). The first determinant can be considered as a constant on the long-term scale of the life span of a tree (some years, some decades); the second depends on current environments (climatic conditions within a season).

The assumption that the cell cycle is equal along the cambial zone throughout the season leads to the following conclusion: in order to control division it is necessary to control the size (or width) of the cambial zone (the number of dividing cells) and their specific growth rate. This means that two mechanisms are involved in control. One is clearly positional, and the other may have dependence on concentration or have some other nature. Formally, the unequal (and, in the case of the hypothesis presented here, increased) cell growth rate across the cambial zone needs only one control—positional, which is easily described in mathematical terms and the corresponding equations. Of course, nature does not always conform to the simplicity of its mathematical description.

3.3 Cell Expansion

Expansion of the radial size of cells after they leave the cambial zone is the next main stage of the cytodifferentiation of xylem (Gamaley 1972; Roberts 1976). Roberts (1976) noted that at this stage, 'the cells exhibit high variability in the extent and regulation of expansion. The deposition of primary wall material during expansion requires the synthesis of primary wall monomers. Protein synthesis occurs. DNA replication involving endoreplication and gene amplification may occur' (Roberts 1976, pp 36–37). The visible result of the enlargement is greatly increased radial cell size. In earlywood the radial dimension of tracheids reaches 50–60 μm; in latewood it is about 15–25 μm. So, during the formation of earlywood the radial size of tracheids increases up to 7–8 times, in latewood, up to 2–3 times in comparison with the starting size of a cell in a cambial zone, which is about 7–8 μm on the average.

Most experimental results indicate that final tracheid size is not determined by the rate of radial expansion (Wodzicki 1971; Skene 1972; Vaganov et al. 1985; Dodd and Fox 1990; Sviderskaya 1999; but see Antonova et al. 1995), thus we must look elsewhere. It is obvious, however, that such a search must focus on the period prior to radial cell expansion; namely, on cell production. Sviderskaya (1999) estimated the specific growth rate of cells within the cambial zone using cell production data and the size of the cambial zone over the course of the growing season (Fig. 3.1). A good relationship was found between the intraseasonal changes in the specific growth rate and changes in the size of tracheids leaving the cambium with a given growth rate. This means that the radial tracheid dimension is primarily determined by the average radial growth rate in the cambial zone or by the average rate of cell division within the cambial zone. In other words, radial tracheid dimension corresponds to the magnitude of cell production in the cambial zone.

Summarizing published data on the variability of radial tracheid dimension within conifer tree rings, we can say (Vaganov 1996a):

1. Radial tracheid dimension shows a clear seasonal trend (from earlywood to latewood) except in some subtropical and tropical trees (Vaganov et al. 1985).
2. Radial tracheid dimension shows variability due to climatic factors operating within a growing season that combine with the seasonal trend (a typical example of this is the formation of 'false' rings caused by intraseasonal drought) (Fritts 1976; Schweingruber 1988, 1996).
3. The average radial tracheid dimension is more or less constant over a long period of tree growth. This constancy results in the close linear relationship between tree-ring width and the number of cells produced annually (Gregory 1971; Vaganov et al. 1985, 1992).
4. The range of variation in radial tracheid dimension in tree rings of different conifer species is usually limited—from 8 to 70 μm (Vaganov et al. 1985).

What indirect data confirm the suggestion that the final radial tracheid dimension cannot be effectively controlled by external influences during enlargement? They come mainly from measurements of tracheidograms (Vaganov et al. 1985, 1992). Narrow layers including only two to three tracheids with small radial dimension and thin cell walls can often be observed in wide tree rings from dry conditions (Fritts 1976; Shashkin and Vaganov 1993). The appearance of those cells in the earlywood zone may, in most cases, be the result of periods of moisture deficit lasting only from several days to a very few weeks. Obviously, the existence of such a layer of small, thin-walled cells cannot be due to the effect of water stress on cells that were enlarging at that time. On the other hand, if water stress affects the cells that have only just started to enlarge, then why are the other cells in the enlargement zone not affected?

There are several lines of evidence that apparently conflict with the idea that the environmental control of the final radial dimension achieved by a tracheid acts on the enlargement stage. It is, however, possible to explain this evidence if this control acts on cell production; that is, it is effective in the cambial zone, not in the enlargement zone. The evidence for the relationship between the growth rate of cambial cells and the final radial dimension of the tracheids they produce is obtained by means of a kinetic approach. It needs to be tested by other direct and indirect sets of data, because not all the questions that arise have been answered. Most questions come from the enormous volume of research on hormonal control of wood formation (see Zimmermann 1964; Barnett 1981; Creber and Chaloner 1984; Savidge 1996; Kozlowski and Pallardy 1997). There are many examples of specific and nonspecific effects of hormones and other plant growth regulators (auxin, IAA, gibberellin, ethylene, and others) on the production rate of tracheids as well as on their size. Some of this work is based on saplings, and may be of limited applicability to mature trees in natural stands. Furthermore, we do not believe these data are necessarily contradictory to the statements made above.

We do not know the precise mechanism by which the kinetics of cell production and growth in the cambial zone determine the ultimate radial dimension of a

tracheid. Recent work on root development may, however, indicate the kinds of mechanisms that may be involved. Baluska et al. (1994, 1996, 2001) hypothesized and substantiated the existence in growing roots of a so-called 'transition zone' between the root meristem and the elongation zone. The main significance of this 'transition zone' is as a sensory zone of the root that monitors diverse environmental parameters and effects appropriate responses (Baluska et al. 1996, 2001). For example, gravistimulation significantly changes the distribution of the relative elemental growth rate pattern along the growing root (Mullen et al. 1998). The real mechanisms are still unclear. Perhaps they operate through interactions of the gene expression responsible for the control of coordinated growth processes with hormones and growth regulators (Savidge 2000a; Baluska et al. 2001). For our purposes the definition of such a special zone is very likely. This is because the results we have presented here lead us to expect the existence of some specific mechanisms of external control of cell production and enlargement at the edge of the cambial zone. We can only hypothesize that such mechanisms are related to growth rate and 'movement' of cells through the cell cycle, especially through the G_1-phase. These mechanisms would provide the link between growth rate near the edge of the cambial zone and further radial enlargement. Using a simplified scheme (i.e., that the division rate at the edge of the cambial zone controls the ultimate radial diameter of the tracheid) clarifies the positional control of cell growth within the cambial and enlargement zones. Both zones (dividing cells and enlargement) are characterized by a high rate of primary wall expansion (elongation), although the second stage has a higher rate of linear growth.

The importance of auxin in this process is clear (Rayle and Cleland 1992; Casgrove 1993; Brett and Waldron 1996). Precise determinations of gradients of IAA distribution within growing xylem and phloem show that IAA can be the hormonal signal for positional control of cell growth (Uggla et al. 1996, 1998, 2001). The results clearly indicate that IAA concentration is higher within the cambial zone with dividing cells and decreases to zero at the end of the zone of enlargement (Uggla et al. 1996, 1998, 2001). We have not here entered the discussion of the origin and maintenance of a constant level or the total value of IAA (is its control external, from the shoot—or internal, from the cambial zone itself?). Such a picture of the distribution of one of the main hormones that is closely related to cell wall growth and cell growth regulation supports some of the assumptions we have made in a way we cannot get from direct evidence. Uggla et al. (2001) describe graphically the generalized distribution pattern of IAA, carbohydrates, and sucrose-metabolizing enzyme activities across the cambial zone, zones of enlargement and maturation. If we compare the measured concentration of IAA from experiments by Uggla et al. (1996, 1998, 2001) and specific growth rate from our evaluations, we see that the maximal linear extension growth rate of cells in the enlargement zone coincides with decreasing IAA concentration (Uggla et al. 2001, Fig. 1). The sucrose concentration decreases in the same direction, and SuSy (sucrose synthase, an enzyme) activity increases in the enlargement zone and falls during cell wall thickening.

All the main processes involved in the radial growth of developing tracheids, as well as in the formation of the secondary wall, are coordinated by the position of the

cell in the file. The simplest explanation for the IAA pattern is that the expanding cells that have left the cambial zone use up the amount of IAA produced within the cambial zone by the dividing cells. This implies that IAA mediates the positioning signal from the cambial zone to the enlargement zone. IAA is also under the higher-level control of the shoot (and root) meristems, and so it can be the mediator of the external control of cell growth within the cambial and enlargement zones. The main differences between earlywood and latewood formation are related to seasonal changes in illumination, temperature, and water supply, so changes in hormone gradients between the early and later parts of the growing season indirectly show the results of environmental control of wood formation, although the main patterns remain largely similar through the season (Uggla et al. 2001, Fig. 5). Quantitative variations are primarily related to the width of the cambial zone and the position of cells. This relationship indirectly supports the hypothesis defining xylem formation as a partially independent system after the external signal from higher levels of regulation has been accepted.

3.4 Cell Wall Thickening

The last stage of differentiation of the xylem elements that form the water-lifting system of the plant is characterized by completion of a rigid secondary wall with the consequent autolysis of the protoplasm. The secondary wall contains cellulose microfibrils, xylan, protein, and lignin. They provide a strictly ordered structure on the exterior of the cell membrane. The three main layers in the secondary wall are distinguished by the orientation of cellulose microfibrils (Preston 1974). First there is S1, then a main, much thicker layer, S2, in which cellulose microfibrils are oriented along the axis of the cell and will frequently display spiral structures. Then comes S3, a layer that is absent in compression wood. The completion of the secondary wall involves a complex of intracellular processes and systems: the endomembrane system for transport, specialization of certain areas of the cytoplasmic diaphragm and elements of the cytoskeleton, expression of new genes, activation of numerous enzymes, biophysical processes connected to between-cell gradients, and properties of membranes and organization of the cell wall (Catesson 1994; Demura and Fukuda 1994; Fukuda 1994; Savidge 1996).

The completion of the secondary wall with its consequent lignification can be considered as the final stage in the biogenesis of the cell wall, which happens continuously during the closing stage of tracheid differentiation. Actually, the tangential and radial walls of cambial cells represent two levels of the process of maturation of primary cell walls (Catesson 1990, 1994). Tangential walls have a more rigid polysaccharide matrix in comparison with radial walls, the chemical composition and ultrastructure of which arise from the mechanical properties radial walls need for subsequent radial growth (Roland 1978; Catesson and Roland 1981). The initial heterogeneity of cambial cell walls disappears during the first stage of tracheid maturation, when the radial growth of cells is completed. It is supposed that the ratio of synthetic rates of different types of polysaccharide and their selective inclusion in radial and tangential walls predetermines the fate of the cells (Catesson

1990, 1994). For example, the earlier beginning and fast rate of xylan synthesis, mainly included in radial walls, can increase radial growth and result in formation of large tracheids or vessels. On the contrary, the synthesis of cellulose reduces an initial nonuniformity of the wall and so hinders radial growth (Catesson 1990, 1994).

All mature xylem elements (except parenchyma cells) have a thick secondary cell wall. However, thickness can noticeably differ in tracheids formed at different times in the growth season. In earlywood tracheids, the cell wall is noticeably thinner (1.5–3.0 μm). In latewood tracheids, cell wall thickness can reach 7–8 μm. As well as tracheid sizes, the thickness of a cell wall can vary greatly, especially in latewood cells in various tree rings, and also in various parts of the tree (Zahner 1968; Larson 1969; Creber and Chaloner 1984; Vaganov et al. 1985). The greater cell wall thickness compared with tracheids differentiated at the beginning of the growing season is one of the main criteria of definition of latewood. As of now the issue has not been solved as to how the transition from formation of earlywood to formation of latewood is regulated. In any case such a transition is connected with the control of synthesis of the secondary wall. External and internal factors can influence formation of the secondary wall. Experimental research shows that seasonal change of external factors, such as light exposure, photoperiod, water deficit, nutrients, or temperature influence both the quantity of latewood cells and the thickness of their cell walls (see Brown and Sax 1962; Wilson 1964; Zahner 1968; Larson 1969; Denne and Dodd 1981; Creber and Chaloner 1984; Vaganov et al. 1985; Carlquist 1988a, b; Downes and Turvey 1990; Antonova and Stasova 1993; Lev-Yadun and Aloni 1995; Savidge 1996).

In early works conducted by Wodzicki (1971), Skene (1972), and Denne (1971) it was pointed out that the rate of cell wall deposition varied relatively little within a growing season. For example, in spite of differences in the growth rates of individual trees (different tree vigor), the actual rate of deposition of cell wall material was about 0.1–0.2 μm^2 per day and seemed to show little change during the course of the season in *Tsuga canadensis* (Skene 1972). The time period required for lysis of the cytoplasm was about 4 days, with no evidence of any changes with tree vigor (Skene 1972). For tree rings of Douglas-fir (*Pseudotsuga menziesii*) it was 4–5 μm^2/day, and in trees with a well-developed crown at the beginning of a season, 6–7 μm^2/day (Dodd and Fox 1990). These authors have compared rates of radial growth and formation of the cell wall in young trees distinguished by development of the crown, and for different heights in the stem. The differences are not marked, except in the case of the growth rate in the second half of a season in trees with a well-developed crown. The experimental data of Wodzicki (1971) have shown that the rate of maturation has no clear influence on the radial size and thickness of the cell wall, and the main role is played by the duration of these stages of differentiation. The average value of the rate of cell wall deposition in *Pinus sylvestris* was a little more than in *Tsuga* and *Pseudotsuga,* reaching 5–10 μm^2/day. Similarly, Sviderskaya (1999) obtained a rate of cell wall deposition of 5–7 μm^2/day in observations of seasonal tree-ring formation in three coniferous species (*Pinus sylvestris, Picea obovata, Abies sibirica*). So, as in the case of the

radial cell dimension of the tracheid, the experimental data on the kinetics of cell wall deposition indicate that the average rate of deposition of cell wall does not differ much during the growing season and supports the statement that the leading role in determining final cell wall thickness is played by the duration of this process and by the radial size of the tracheid in which the cell wall was deposited. Mechanisms for the control of tracheid radial expansion through the predetermination of final tracheid radial dimension and cell wall thickness may be mediated through control of the rates of synthesis of different components of the tangential and radial walls.

The process of tracheid differentiation is, as a matter of fact, a process of implementation of the genetic program of differentiation, starting at the level of cambial cells and finishing with secondary cell wall formation (Fukuda 1996; Graham 1996; Hertzberg et al. 2001; Chaffey et al. 2002; Ito and Fukuda 2002; Goujon et al. 2003; Kirst et al. 2003; Nieminen et al. 2004). Schrader et al. (2003), for example, showed that the expression of specific members of the auxin transport genes are associated with different stages of vascular cambium development and demonstrated that trees have developed mechanisms to modulate auxin transport in meristem in response to developmental and environmental cues. A variety of anatomical parameters of tracheids among trees and years indicate that the eventual result is not absolutely determined, and that it depends on the local conditions where the differentiation occurs. The process of differentiation can be presented as a series of events, in which the duration and intensity of each stage depend on the previous one. Then, in changed conditions, if two events are carried on further in space and in time, their deterministic relationship may change. If we identify processes most sensitive to the influence of external factors, we see that the external signal should be most clearly perceived by the cambial zone. These external effects will leave their mark on further processes of differentiation and, ultimately, the anatomical characteristics of tracheids. As a result, the direct influence of environmental conditions on the process of tracheid enlargement, as recorded in their final anatomical characteristics, will be significantly smaller. There are a number of indirect data that indicate that the events occurring during cell division in the cambial zone can have a strong influence on the ultimate sizes of tracheids. Already, at this early stage of differentiation, biochemical changes of the primary cell wall are necessary for radial growth of cells and determination of its rate (Taiz 1984; Catesson 1990, 1994; Pritchard 1994).

In a recent review, Somerville et al. (2004) stated that progress integrating biophysical, developmental, and genetic information into useful models of plant cell wall will require a system-based approach. They presented a cyclical diagram which emphasizes that the expansion of the cell wall and integration of a new cell plate during cytokinesis are components of the cell cycle. ‘Thus, we infer that many of the genes involved in primary cell wall synthesis and modification will be found to be controlled by factors that control other aspects of the cell cycle’ (Somerville et al. 2004, p 2210). This process determines the bridge between the first and last stages of tracheid differentiation through the activity of genes involved in the cell cycle and cell wall thickening.

3.5 Effect of Climatic Factors on Tree-Ring Structure (Light, Temperature, and Water)

3.5.1 Temperature

Dendrochronologists have made many investigations of the effect of temperature on radial tree growth and wood density (Fritts 1976; Hughes et al. 1982; Schweingruber 1996). Significantly less data are available for the temperature effect on the anatomical features of tree rings. Much of the relevant research was conducted on trees growing at high latitudes where temperature is presumably a leading limiting factor. Some research concerning anatomical structure was made on seedlings in controlled conditions. There are some common findings:

1. Temperature is the most important factor for growth initiation in boreal and temperate climates (Creber and Chaloner 1984; Iqbal 1990). At high latitudes, growth (new cell production) ceases in about the middle of August and the duration of the season of wood production is mainly determined by the starting date of cambial activity (Mikola 1962). Leikola (1969) showed that a 0.5°C deviation in the mean April–May temperature caused significant shifts in the starting date of cambial activity. For the Siberian subarctic, we found early summer (mid-June to mid-July) temperature and snowmelt timing to be very important for the variation in radial growth of larch trees (Hughes et al. 1999; Vaganov et al. 1999; Kirdyanov et al. 2003). Wood production ceases at a much higher temperature than is necessary for its initiation (Denne 1971).

   One of the best examples of environmentally controlled tracheid production and differentiating were given in a recent study of Deslauriers et al. (2003). Analyzing the kinetics of cells in each phase of tree-ring formation (division, expansion, wall thickening) during seasonal growth and development in *Abies balsamea* L. growing in boreal forest, they demonstrated a high degreee of variation in the timing of the beginning of the growing season (about one month), the earlywood-latewood transition (around half of a month), and the end of the growing season (about one month). This result is in a good agreement with other high-latitude observations and simulations (Vaganov et al. 1999; Kirdyanov et al. 2003). On the other hand, Deslauriers et al. (2003) estimated a duration of cell expansion in the stage of cell enlargement that gave significantly shorter times (less than one week for earlywood and 5–10 days for latewood) than those recorded in lower latitudes (Wodzicki 1971; Skene 1972; Antonova et al. 1995; Vaganov et al. 2006). These differences could be genetically determined because of the short season for tree-ring growth and maturation of the tracheids. Deslauriers and Morin (2005) found that cell production in the cambium was correlated with the temperature during the same period. Artificially lagging the daily temperature data even by a single day decreased the correlation with cell production substantially, indicating that the cambium reacted quickly to external environmental variability.

2. At high latitudes, tree-ring width variations correlate well with average summer (June–August) temperature, but maximum density shows a significant correlation with temperature for a larger part of the growing season—for example, May–September (Briffa et al. 1990, 1992, D'Arrigo et al. 1992). A longer growing season due to high temperatures will definitely increase the percentage of latewood in tree rings (Larson 1964).
3. Denne (1971), in experiments with Scots pine (*Pinus sylvestris*) seedlings, showed that a temperature increase from 17.5 to 27.5°C produced only a 10% increase in tracheid diameter. Contrary to this, we found a significant increase of tracheid diameter in the earlywood of larch tree rings near the northern timberline associated with a long-term summer temperature increase (Vaganov 1996c). Note that these effects of early summer temperature on earlywood tracheid diameter occur in the temperature range 5–14°C. In more southerly sites where the early summer temperatures were higher (between 12 and 19°C), the effect of temperature on tracheid diameter was diminished because the temperature was no longer in the range where it was clearly limiting (Vaganov 1996c). Under conditions close to optimal temperature (as in Denne's experiments), the limiting effect of temperature on tracheid diameter is probably small.
4. Temperature and tracheid wall thickness were inversely correlated in several conifer species (Wodzicki 1971). Similar data were obtained by Antonova and Stasova (1993, 1997). This result contradicts results from maximum latewood density, which is mainly determined by cell wall thickness. At the upper elevations or northern timberlines, rings with thin-walled cells in the latewood (so-called 'light rings'), are produced by a cold autumn or sharp cooling at the end of summer (Filion et al. 1986; Schweingruber 1993).

Many of the contradictions in publications on the effect of temperature on tracheid dimensions (diameter, wall thickness) are caused by other uncontrolled but important external factors, such as water supply or light intensity, and by uncertainties in the ranges of strong limitation of one factor and alteration of the limit by another factor. For example, Denne (1971) chose a temperature range that is close to optimal for growth. Thus there is no pronounced effect of temperature on anatomical structure. In the case of Antonova and Stasova (1993, 1997), there was no control of the soil water content during the production and formation of latewood tracheids. Hence the apparent negative effect of temperature could come from its indirect effect on water loss from soil due to increased evapotranspiration.

3.5.2 Water

The availability of soil water may affect the growth rate and formation of wood, both at long timescales and within a season (Zahner and Oliver 1962; Kozlowski 1968; Zahner 1968; Creber and Chaloner 1984; Bräuning 1999). For example, pine in marshy conditions forms not only narrower tree rings, but rings with smaller absolute size and proportion of latewood. In periods of suppressed growth, a tree

ring may have only one or two cells of earlywood and one small-sized, thin-walled latewood cell in each file. Considerable variability of cell size and cell wall thickness may occur within wide tree rings grown in favorable conditions. 'False' rings may be produced when small, thick-walled cells are seen at the beginning of the latewood zone and are followed by larger, thin-walled cells. The formation of 'false' rings is a common phenomenon when intraseasonal droughts occur in a precisely designated rainy season, as seen, for example, in the mountains of the American Southwest. The layer of larger cells is produced in response to the arrival of the rains at the northern fringes of the Mexican monsoon in early July. However, during certain years, the trees can completely stop growth in the 'pre-summer' drought period; and in such a case a 'false' ring identified on anatomical features does not differ from the annual ring.

3.5.3 Light

Even if we may reasonably assume that temperature and water availability have direct effects on cambial activity, in the case of light the effect is undoubtedly indirect, being mediated through the photosynthetic tissues. The control of growth by light intensity and photoperiod (day length) has been examined in several monographs and textbooks (Alexeev 1975; Howe et al. 1995; Kozlowski and Pallardy 1997). It is not possible here to review much of the work in which the effect of light on the height or diameter growth (and tree-ring width) of trees was studied. We will briefly consider some results concerning the influence of light intensity and photoperiod on the anatomy of conifer tree rings.

Richardson (1964) showed a clear positive effect of light intensity and day length on tracheid cell wall thickness and mean lumen diameter in xylem formed in stems of Sitka spruce (*Picea sitchensis*) seedlings. Larson (1962, 1964) showed an obvious effect of photoperiod on anatomical characteristics of tracheids in xylem formed in *Pinus resinosa* seedlings. He found that, on a long day, the formation of larger tracheids was associated with greater needle length. He showed that this effect was clearly photoperiodic rather than simply photosynthetic. Day length influences wood density by controlling the formation of earlywood and latewood cell types through the types of cambial derivatives, rather than the width of the xylem increment (Waisel and Fahn 1956). The growth and formation of earlywood was resumed if the trees were returned to the long day-length condition (Wareing and Roberts 1956).

3.6 Toward a Quantitative Description of Cambial Activity and Xylem Differentiation Under Environmental Control

Thus, to correctly describe the transformation of climatic signal to tree-ring growth and wood structure, it is necessary (according to the hormonal theory) to describe the mechanism of substrate and hormonal regulation of cambial growth and

differentiation. This hypothesis of 'independent' external control of wood formation offered by Larson (1964) is, however, a barrier to the creation of process-based models for dendroclimatology.

The hypothesis of 'independent control' can be illustrated by the following. In a period of active wood formation, cells are in all three main stages (but at different locations within the forming tree ring); i.e., the external signal may affect cells in all stages at the same time. According to this we may write that

$$\begin{aligned} \frac{d\mathrm{N}}{d\mathrm{t}} &= f_1\{\mathrm{x_i(t_j)}\} \\ \frac{d\mathrm{D}}{d\mathrm{t}} &= f_2\{\mathrm{x_i(t_j)}\} \\ \frac{d\mathrm{CWT}}{d\mathrm{t}} &= f_3\{\mathrm{x_i(t_j)}\} \end{aligned} \tag{3.1}$$

Where i indicates the factors or processes affected, and all three functions are assumed to be different and have a different time dependence. Then in the final tree ring, each of its subdivisions (portions) will contain the climatic signal, integrated in time, accumulated in cell number (N), cell dimension (D), and cell wall thickness (CWT).

$$\mathrm{TR_{portion}} = f\{f_1[x_i(t_j),\ f_2[x_i(t_{j+k})],\ f_3[x_i(t_{j+m})]\} \tag{3.2}$$

Here, j, k, and m are the time intervals between the processes of production, cell enlargement, and wall thickening. The values of j, k, and m vary significantly during a season, and show a significant relation with the total number of cells in the cambial zone and total production (tree-ring width). Taking into account that the process of enlargement of a single cell can continue up to 3 weeks, and that wall thickening takes 2–3 weeks, leads to the conclusion that each portion of a tree ring integrates the growth conditions over about 1.5 months (without any delays in passing the hormonal signal from apical meristem to cambium). The most complex aspect of this analysis is the necessity of defining each function in the equations (3.1), which are assumed to be different.

According to this statement, the maximum density of the last forming portion of a tree ring must be determined only by the climatic conditions at the end of the growing season because all processes involved occur at this particular time. This means that even in strong temperature-limited conditions, the maximum density must be related strongly to August–September temperatures, when the last forming tracheids enlarge and thicken. But almost all results in dendroclimatic interpretation of maximum density show that maximum density is better than even the tree-ring width as an indicator of the whole summer temperature because of significant correlation with the early season as well as with late season temperatures (commonly with April–September temperature) (Briffa et al. 2001, 2004).

An alternative hypothesis is that the main target of environmental control in tree-ring seasonal formation is the cambial zone, and then this signal is transformed into further processes of cell differentiation (enlargement and cell wall thickening). This hypothesis suggests that the main target of environmental control is the first process;

i.e., the cambial zone plays the main role as the target of environmental influence and then transforms this influence to the next stages of cell differentiation (Vaganov et al. 1985; Vaganov 1996a). Reflecting this, equation (3.1) can be rewritten:

$$\begin{aligned} \frac{dN}{dt} &= f_1\{x_i(t_j)\} \\ \frac{dD}{dt} &= f_2\{f_1\} \\ \frac{dCWT}{dt} &= f_3\{f_1, f_3\} \end{aligned} \tag{3.3}$$

From this, several theoretical and experimental considerations follow:

1. The hierarchy of control simplifies the common mechanism of environmental control.
2. There is much evidence of a close relationship between the rate of cell production and the anatomical characteristics of the cells produced; i.e., the relationship between two consecutive stages of cell differentiation.
3. The cell dimensions (radial diameter and cell wall thickness) are mainly determined by the duration of these processes rather than their speed.
4. There is evidence of a nonrandom relationship between the radial dimension and cell wall thickness (i.e., a relationship between the second and third main processes of cell differentiation).
5. From measurements of interannual variability of tree-ring characteristics, there is a decrease in variability from a maximum for tree-ring index (width), to a minimum for radial cell dimension (diameter, cell wall thickness, maximum density). This result suggests a decreasing influence of climatic variations if one considers the within-ring components, in contrast to interannual rings with variability.

In the case of hierarchy control, the quantitative description becomes simpler because only one function must be defined in relation to environmental variables, and to do this we have enough experimental data from biophysical and physiological research of tree growth. This background allows us to create a simple version of the process-based model of tree-ring formation under changing climatic conditions (weather conditions), and to test this model by simulation of climatically induced variations of tree-ring width and cell dimension in different climates (from northern timberline to semiarid regions) (Vaganov et al. 1990; Fritts et al. 1991; Shashkin and Vaganov 1993; Evans et al. 2006; Vaganov et al. 2006). The basic premise of the model is the principle of a limiting factor, well known in the physiology of plant growth. The model is restricted by application only to the quantitative description of climatically induced growth variations, which means that we do not use this approach for other factors controlling tree growth, like fertilization (either carbon dioxide or nitrogen), within-stand competition, growth release after forestry management, etc.

A significant property of this model is its use of available, commonly measured meteorological characteristics available from any meteorological station. The model, therefore, consolidates and compresses our recent knowledge concerning the

climatic influence on tree growth, and on the other hand, improves our understanding of the tree growth–climate relationship. There are several examples and issues that illustrate the advance in tree growth–climate relationships resulting from the use of the model as a research tool.

3.7 Process Model Description

The Vaganov–Shashkin model makes use of a limited number of equations relating daily temperature, precipitation, and sunlight to the kinetics of secondary xylem development (Vaganov et al. 2006) in order to model tree-ring growth and the internal characteristics (density, cell sizes) of annual rings. The model consists of two primary modules, or blocks. The Growth (or Environmental) Block calculates a daily external growth rate based on climatic variability, including temperature, soil moisture balance, and solar irradiance. The Cambial Block uses this external growth rate to simulate the rate and timing of growth and division of cells in the cambium following the hierarchical model described above. In this way, the kinetics of xylem formation are explicitly modeled as a function of climate variability modified by parameterized environmental and cambial processes.

3.7.1 Growth (Environmental) Block

Relative growth rate calculations made by the model are used to determine the rate of the growth and division of cells during xylogenesis, as well as the timing of the transition between stages. Daily growth rates themselves are determined by comparing daily temperature and soil moisture (calculated from precipitation, transpiration, and soil drainage) to piecewise linear approximations of parabolic growth functions (Fig. 3.2, inset). Four parameters define the shape of the trapezoidal growth functions—a minimum ($g(t) = 0$), lower and upper optimal bounds ($g(t) = 1$), and a maximum ($g(t) = 0$). Between the minimum (or maximum) and the lower (or upper) bounds of the optimal values for the climate parameter (temperature, sunlight, or soil moisture), growth rates will be between 0 and 1. Relative growth rates are calculated for precipitation ($g_W(t)$), temperature ($g_T(t)$), and sunlight ($g_E(t)$). The determination of the overall growth rate $G(t)$ for any given day t is calculated as

$$G(t) = g_E(t) \cdot \min[g_T(t), g_W(t)] \tag{3.4}$$

Water balance is computed daily by the model as a function of precipitation (as well as snowmelt), evaporation (which is a function of temperature), and runoff (Thornthwaite and Mather 1955). Solar irradiance is determined by the model from the latitude of the meteorological station from which the input data are taken. Because of the minimization term in the calculation of the growth rate, and the

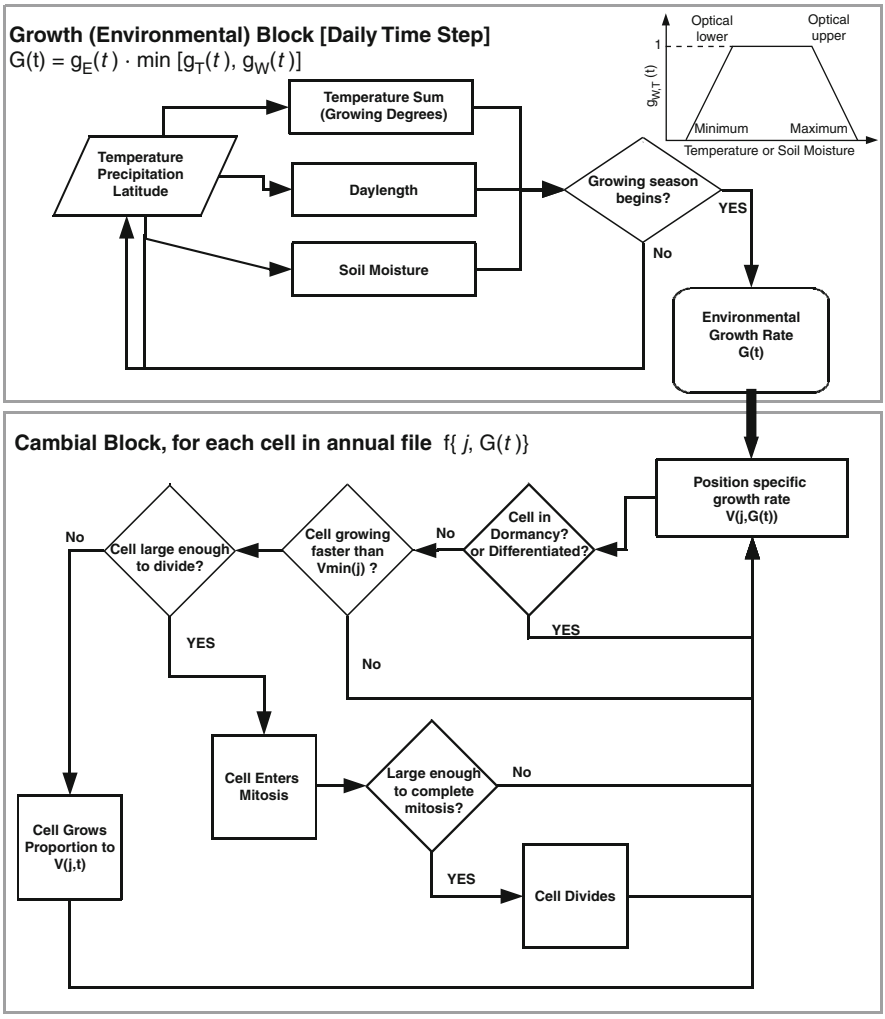

Fig. 3.2 Vaganov–Shashkin growth and cambial model block processes. Daily external (environmental) growth rates are determined by comparing daily temperature and soil moisture (calculated from precipitation, transpiration, and soil drainage) to piecewise linear approximations of parabolic growth functions (see *inset*) in the Growth (Environmental) Block. This growth rate is used in the Cambial Block to calculate the cellular growth rate $V(j, G(t))$,which is a function of the environmental growth rate and the position of the cell in the radial file. Each cell is permitted to be dormant, differentiate, grow, or divide on an intraday time interval. When a nondifferentiated cell reaches a critical size, it enters and completes the mitotic cycle, continuing its subsequent growth at a constant, environmentally independent growth rate until division occurs, resulting in two cells, each half the size of the original mother cell. Once differentiated, cells can no longer divide and go on to complete the subsequent stages of expansion and cell wall thickening

piecewise approximation of the nonlinear growth function, the model behaves stoichiometrically—that is, it is controlled by the most limiting factor (e.g., Fritts 1976)—at a daily resolution.

A recent study of intra-annual radial growth rates in trees of different species located in different sites and environmental conditions reveals that maximum growth rate of weekly cell production and variations in stem circumference at high-latitude sites occurred around the time of maximum day length (Rossi et al. 2006). These data were obtained by smoothing seasonal growth curves by using the Gompertz equation and transferring the cumulative curves into differential rates of cell division, expansion, and maturation. These data in general are in good agreement with what we assume in equation (3.4), although equation (3.4) has more flexibility because of the combination of day length and temperature for determining the maximum growth rate. Observations at high latitudes indicate that the maximum growth rate, as well as the beginning of the growing season, may vary greatly, even as late as the summer solstice (Deslauriers et al. 2003; Vaganov et al. 2006). Use of the Gompertz equation for quantitative description of tree-ring growth is ultimately a statistical tool and not a biological model, but it is potentially useful for combining subannual observations of cambial dynamics and diameter growth with mechanistic modeling at daily to weekly resolutions.

3.7.2 Cambial Block

The Cambial Block uses the output from the Growth Block to determine the rate at which cambial cells grow and divide (Figs. 3.2 and 3.3). Each cell in the Cambial Block is characterized by two variables at each daily step—its position (j) in the cellular file and its diameter. The growth rate $G(t)$ calculated in the prior block is used to derive a specific growth rate, $V(j,t)$, for each cell based on its position (Fig. 3.2). For cambial cells, diameter increases in the G_1 phase until a maximum size when division occurs, or until the cell loses the ability to divide as its growth rate falls below a minimum threshold $V_{\min}(j)$ for the cell's position in the radial file. Cells that lose the ability to divide pass out of the cambium, and complete the cell cycle, including elongation and cell wall thickening. Daily cellular growth rates below a critical minimum threshold (V_{cr}) send the cambium into dormancy. The cells in the cambium at the end of one simulated growing season will therefore be those which first grow and divide in the subsequent year, and therefore influence the cambial dynamics and tree-ring structure of the following year. Activity in the cambium is initiated each year when the sum of temperatures above a certain threshold over a specified period of time (i.e., growing degree days) reaches a critical threshold.

The Vaganov–Shashkin model explicitly integrates the essential features of cambial dynamics as previously described. Annual xylem cell production is related to the number of cells in the cambial zone, the size of which varies over the course of the year in response to environmental variability. Specific cellular growth rates are positional and depend on the distance of the simulated cell from the cambial initial,

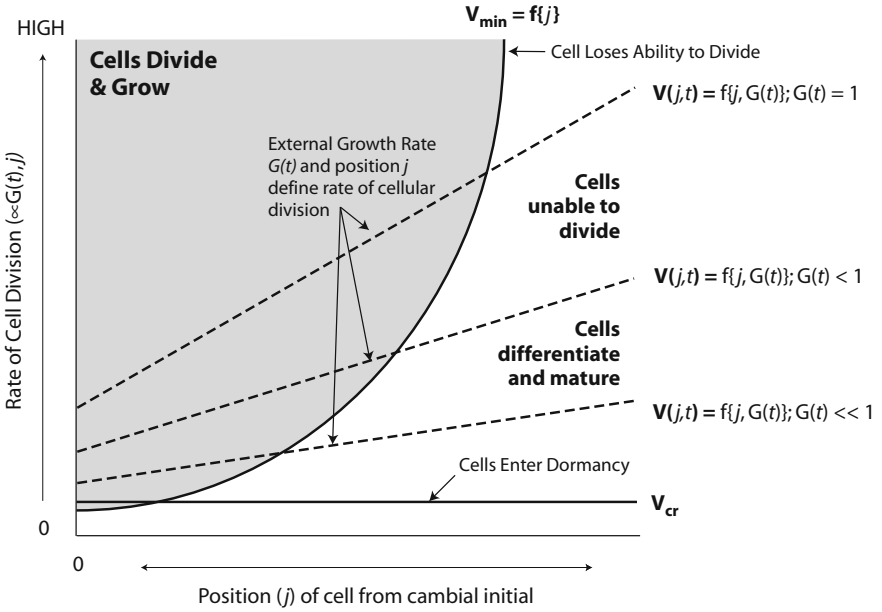

Fig. 3.3 Schematic diagram showing the functions that control cell division and transitions in the Vaganov–Shashkin model. The rate of cambial cell division (which is proportional to the cellular growth rate $V(j,t)$) is a linear function of the position (j) of the cell in the cellular file and the daily external environmental growth rate $G(t)$. The division rate increases with distance from the cambial initial. The exponential function $V_{\min}(j)$ defines the threshold rate of division, below which cells lose the ability to divide and mature to xylem cells. The size of the actively dividing cambial zone is therefore a nonlinear function of the rate of cellular division. The third function, V_{cr}, defines the division rate at which cells still in the cambium enter dormancy

with maximum rates of cell division observed tangential to the zone of radial expansion (the 'cambial edge'). Radial tracheid dimension is mainly determined during cell production and at the beginning of expansion.

The model uses daily precipitation and temperature from meteorological stations as its required input data. The 28 primary model parameters are based on empirical and experimental data, whose selection is discussed in detail by Vaganov et al. (2006). The output, consisting of standardized synthetic tree-ring width chronologies, simulated growth rates, and number of cambial cells, are solely a function of those environmental and biological activities modeled in the Growth and Cambial Blocks. Hence, simulations do not reflect direct growth influences due to increasing atmospheric CO_2 concentration over the past 150 years. Nor are additional biological or ecological influences on patterns of tree-ring formation modeled, including those caused by tree age or geometry, interseasonal carbon storage, canopy and root activity, or stand-level competition and disturbance. In a sense the simulations can be considered 'idealized' mean site tree-ring chronologies with respect to the modeled processes.

3.8 Model Applications

Temporal variability in the relationship between climate and tree-ring-derived proxies has been identified in a range of species and locations (Briffa et al. 1998a, b; Biondi 2000; Jacoby et al. 2000; Aykroyd et al. 2001; Wilmking et al. 2004, 2005). Such instability might be particularly important in environments where both temperature and precipitation can be important controls on tree growth (Anchukaitis et al. 2006), where the timing of the onset of growth or the length of the growing season strongly influences tree-ring proxies (Vaganov et al. 1999; Aykroyd et al. 2001; Vaganov et al. 2006; Evans et al. 2006), and for high-latitude or high-elevation temperature-sensitive trees under anthropogenic climate forcing (Jacoby et al. 2000; Wilmking et al. 2004, 2005). The Vaganov–Shashkin model produces synthetic chronologies that would be expected if climate, mediated by cambial processes, were the only external control on tree growth. This characteristic potentially allows dendroecologists to evaluate the importance of hypothesized ecological factors that might be responsible for differences observed between actual tree-ring chronologies and simulations. For instance, it can also be used to develop null hypotheses against which to test theories about the influences of insects, disease, CO_2 enrichment, carbon storage, pollution, and disturbance on tree growth. Furthermore, because the Vaganov–Shashkin model has the ability to simulate nonlinear relationships between tree-ring formation and the environment, it can be used to determine whether observed variability in climate–tree growth relationships arise as a function of climate itself, as a stochastic feature without a determinant cause, or through possibly unobserved influences by biological or ecological changes not related to climate.

The Vaganov–Shashkin model has recently been applied to simulate tree-ring proxies across a range of environments for a variety of species and using several complementary approaches. The particular methodology for developing and analyzing synthetic chronologies depends in part on the research questions posed and the availability of meteorological and tree-ring data with which to drive and evaluate the model. The simplest approach to modeling tree-ring chronologies is to use single meteorological stations close to the actual tree-ring chronology site. Several studies have demonstrated that using appropriately chosen local meteorological stations can produce simulations that skillfully reproduce actual tree-ring width patterns (Vaganov et al. 1999; Evans et al. 2006; Vaganov et al. 2006). These studies target cases in which direct model-data intercomparisons are easily made, but do not assess the extent to which model skill is general across environments and species. An intermediate approach exploits spatiotemporal techniques like principal components analysis (PCA), which decompose a large set of time series into a few low-order empirical functions that contain the primary modes of robust common variance in networks of observed and simulated tree-ring data networks (Anchukaitis et al. 2006). A third approach is to compare tree-ring datasets to meteorological datasets on a large scale for assessing model robustness and the general suitability of the tree-ring dataset for climate monitoring (Evans et al. 2006). These nonlocal approaches permit assessment of the suitability of the proxy data

network for the reconstruction of large-scale features of paleoclimatic fields, but the comparison suffers from differences in the meteorological and dendrochronological observing networks (Anchukaitis et al. 2006; Evans et al. 2006), which make direct comparisons impossible. We stress that implicit in our interpretation of the model results presented here is the following assumption: If we can establish that the simulations are consistent with the corresponding observed chronologies, the VS model includes the most critical processes linking climate to annual tree-ring formation.

3.8.1 Local Simulations

Evans et al.(2006) reported tree-ring width simulations performed for eight high-latitude Russian sites (Vaganov et al. 2006) spanning 60 degrees of latitude (Fig. 3.4), and using the same set of fixed parameters and closely collocated meteorological station data. Despite neglecting adjustment of model parameters to fit local site characteristics, seven of eight simulations are significantly correlated with actual chronologies at or above the 95% confidence level. Four of eight correlations between 5-year means of the simulations and actual chronologies were significant at or above the 90% confidence level. Cook and Pederson (Chapter 4, this volume) discuss the problem of emergent phenomena in dendrochronology and the resulting uncertainties in statistically modeling tree-ring data, using as a case study tree-ring chronologies of a number of species and locations from near the Mohonk Lake, New York, meteorological station. Their work raises the question: How do we separate empirically demonstrated emergence, pervasive in the biological sciences, from incomplete understanding of the system at hand? In an effort to address this question, we simulated the NY004r.crn Mohonk Lake tree-ring width residual chronology (http://www.ncdc.noaa.gov/paleo/) using the Vaganov–Shashkin model and Mohonk Lake station daily meteorological data (NCDC Cooperative Station 305426).

We found that with only an increase in the soil moisture drainage rate (all other model parameters at default 'Russian' settings; Anchukaitis et al. 2006; Vaganov et al. 2006), the simulation was sufficient to explain the gross features of this data series (annual r up to 0.57 ($p < 0.05$); Fig. 3.5c). The significance of r was not highly sensitive to the exact value of the soil moisture drainage parameter we chose. Correlation functions for simulated and actual chronologies are similar (Fig. 3.5a,b). The most important of these are (1) positive correlation with current-year May–July precipitation, (2) negative correlation with current-year May temperature; (3) positive correlation with current-year March–April temperature; (4) positive correlation with prior-year September–October precipitation. Lower-frequency model skill may be a consequence of the influence of the size of initial cambial cells from the prior growing season on the ring width of the following year (results not shown).

Although Cook and Pederson (Chapter 4, this volume) pointed to observation (3) above as an example of an emergent phenomenon, it is predicted with the VS model simulation. Examination of the growth-limiting functions G_T, G_E, G_W, and the integrated growth function G broadly confirm these results for an average year

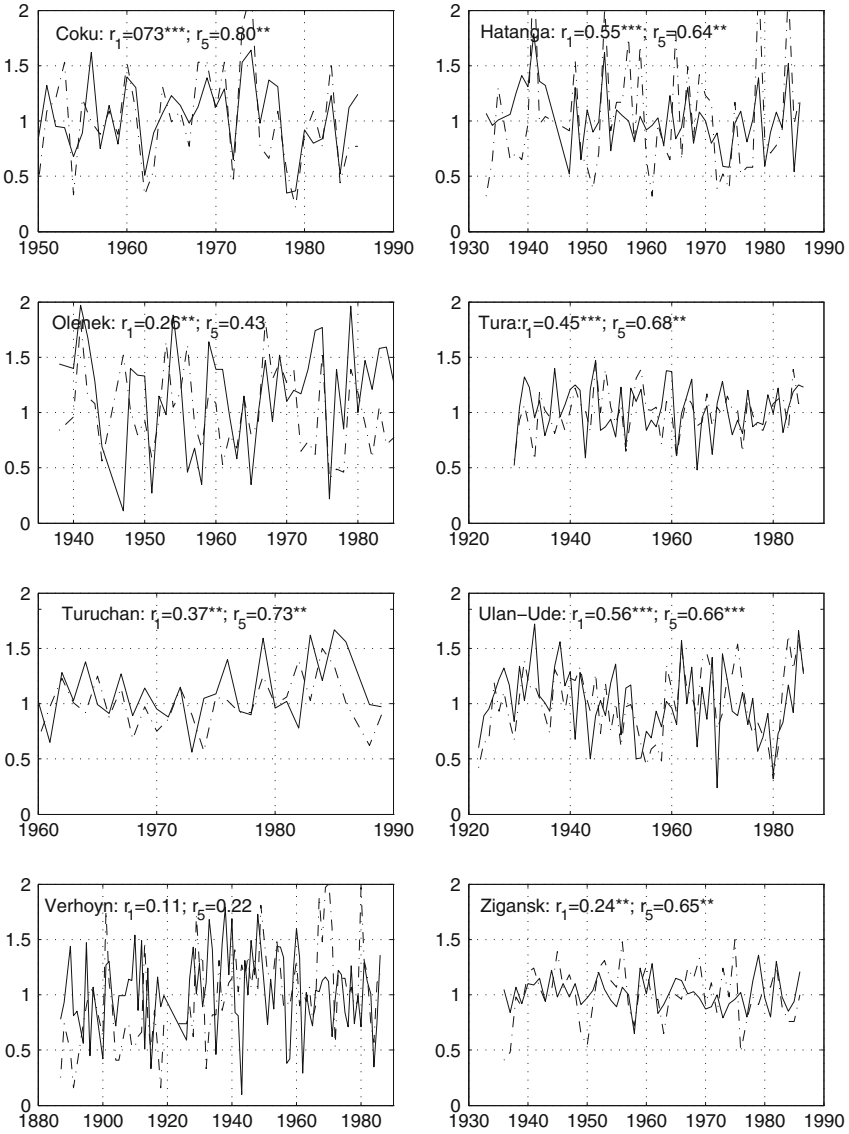

Fig. 3.4 Time series of Vaganov–Shashkin model simulations (*dashed lines*) compared with actual ring width chronologies (*solid lines*) from high-latitude sites across Russia. Correlations are for annual and five year averages. *, **, *** indicate one-tailed significance at $p < 0.1, 0.05, 0.01$ levels, respectively, considering effective degrees of freedom given series lag-1 autocorrelations. Chokurdakh (Coku) (147.9°E, 70.6°N). Hatanga (102.5°E, 72°N). Olenek (112.4°E, 68.5°N). Tura (100.0°E, 64.2°N). Turuchan (88.0°E, 65.8°N). Ulan-Ude (107.4°E, 51.8°N). Verhoyn (133.4°E, 67.6°N). Zigansk (123.4°E, 66.8°N). Results from Evans et al. (2006)

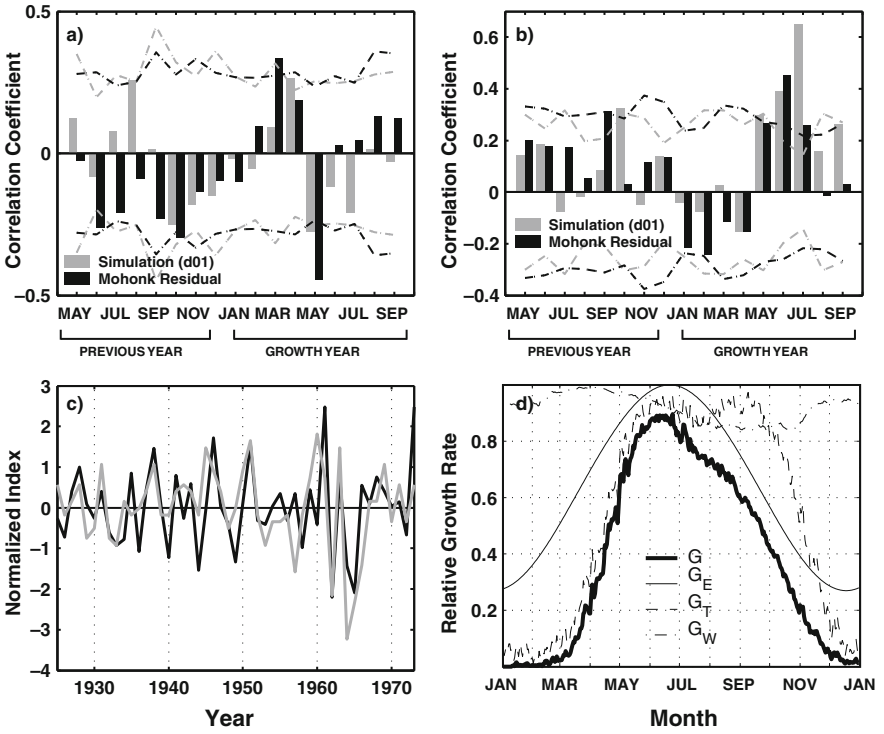

Fig. 3.5 Simulation of Mohonk Lake tree-ring width chronology. Correlation of previous and current year tree-ring widths with (**a**) temperature and (**b**) precipitation show similar patterns for both simulated and actual chronologies. *Dashed lines* of the same color show the 95% two-tailed confidence intervals from bootstrapping (1,000 draws with replacement; Biondi and Waikul [2004]). Values above these lines can be considered statistically significant, accounting for the number of independent predictors (**c**) The simulation (*black line*) is correlated with the actual chronology (*gray line*) at $r = 0.57 (p < 0.05)$. (**d**) Growth functions G_T, G_W, G_E, and overall growth function G from daily simulation output averaged for 1925–1973. See text, Section 3.8.1, for discussion

based on 1925–1973 simulations (Fig. 3.5d). The modeling results suggest that early season growth is strongly tied to the timing of early spring (March) warming, unless such warming is strong enough by early summer (May), in which case warm conditions lead to growth limitation by moisture stress. The way in which the VS model simulates such a phenomenon is described in Evans et al. (2006). Given these results, maybe in this specific case it's not emergence after all. Our tentative conclusion is that current-generation multivariate linear regression models may be unable to completely describe the environmental controls on tree-ring variations because of intraseasonal-interannual changes in the limiting factors controlling tree growth (see also the example from Anchukaitis et al. [2006], described below). Forward modeling exercises like this can complement statistical model verification procedures, assess the influence of such effects in linear paleoclimate inversions, increase confidence in our interpretation of the data ('What do we expect to see?'),

and help further distinguish emergence (the complex and potentially unexpected interaction of biotic and abiotic elements) from statistics (uncertainty arising from random noise).

3.8.2 Mesoscale Network Simulations

Anchukaitis et al. (2006) used the modified parameter described for the Mohonk simulations above to simulate tree-ring widths across the southeastern United States. They demonstrated that the leading principal component time series of simulated and real conifer chronologies is well correlated and that both reflect the regional importance of spring rainfall for interannual variability in tree-ring widths (Fig. 3.6). Anchukaitis et al. (2006) further apply the model to detecting and attributing changes in climate/tree-ring growth relationships related to climate. Using the eight simulations from the southeastern United States validated against the leading temporal pattern of variability in actual tree-ring chronologies, they hypothesize that tree-ring growth should become increasingly limited by summer precipitation. Model findings are verified by using a new tree-ring chronology, excluded from

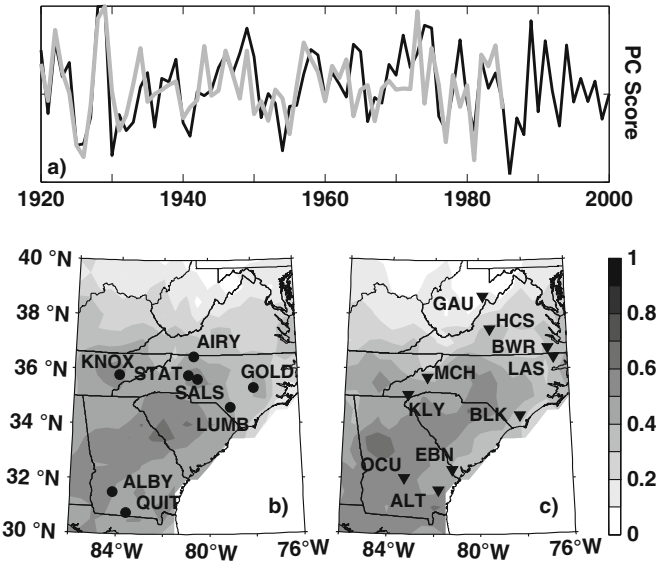

Fig. 3.6 Intercomparison of synthetic and actual tree-ring width chronologies from the southeast United States. (**a**) Leading time series expansions from PCA on simulated and actual regional ring width data (*black* and *gray lines*, respectively). Correlation fields between the spring (March–April–May, MAM) precipitation and the first principal component for the (**b**) simulated and (**c**) real tree-ring width chronologies for the full period of overlap (1920–1985). Four-letter identifiers mark eight meteorological stations in (**b**); three-letter identifiers denote 10 ring width chronology sites in (**c**). Reprinted with permission from Anchukaitis et al. (2006)

the original dataset, which shows a similar pattern of increased growth sensitivity to summer precipitation, and is consistent with analysis of trends in regional climate and broad-scale forcing (Anchukaitis et al. 2006). Additional tree-ring data, updated through the most recent quarter century, should show the same behavior, if the model-based hypothesis is correct. The results point to larger-scale predictive studies using the VS model driven by general circulation model (GCM) output.

3.8.3 Large Network Intercomparisons

Evans et al. (2006) used a continental-scale set of meteorological stations and tree-ring chronologies to assess the skill of the Vaganov–Shashkin model across a broad range of species and environments. They utilized a 500 km search radius around each of 190 tree-ring chronologies to evaluate simulated chronologies derived from the Global Historical Climatology Network (Peterson and Vose 1997) within that area. This approach allowed the model to choose the station within the given search radius which resulted in the best simulation, and presumably best reflecting climate conditions at the actual tree-ring chronology site. This approach assumes that a single station exists within the search radius that best approximates the mean conditions over a given region. A similar search radius approach has been successfully used in point-to-point regression-based reconstructions of the Palmer Drought Severity Index (PDSI) using tree rings (Cook et al. 1999, 2004). Evans et al. (2006) found that the model-simulated chronologies were correlated at the 95% significance level with actual tree-ring chronologies in 176 out of 190 cases (Fig. 3.7). The results were not dependent on the size of the search radius, with similar findings for a 200 km search area (Evans et al. 2006, results not shown). Process model skill was about the same as that achieved for verification-period statistical modeling of the same chronologies using robust linear multiple regression methods common in dendroclimatology. Skillful decadal simulations were only made in a minority of simulations either by statistical modeling or process modeling approaches, suggesting that paleoclimatic interpretations of decadal climate variability from tree-ring width data should be made with caution. Additional studies designed to identify and remove such non-climatic biases from candidate proxy dendroclimatic datasets are under way.

3.8.4 Uncertainties and Caveats

There are several important caveats that should accompany the interpretation of existing simulation experiments as well as the future applications of the VS model to new research questions in dendroclimatology. One of the strengths of the model is that it operates on a daily timescale, and is therefore capable of accurately simulating the response of trees to rapidly changing seasonal climate conditions (e.g. Deslauriers and Morin 2005). The daily data requirements of the model, however, restrict both its temporal and spatial application, due the limited length and

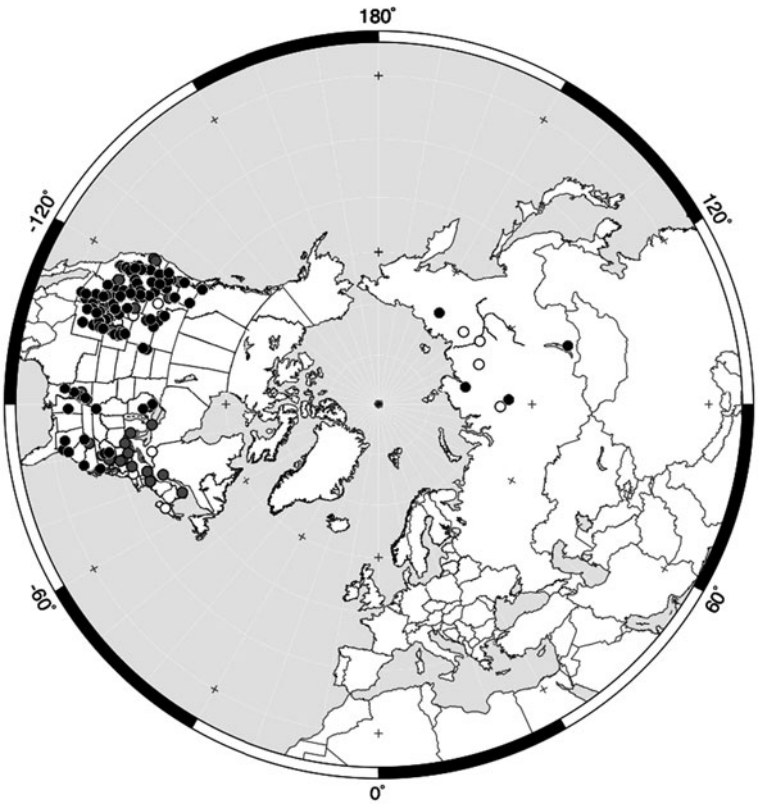

Fig. 3.7 Significance of annual correlations of simulated and actual tree-ring width data for eight sites across Russia (Fig. 3.4) and 190 sites in North America from the Mann et al. (1998) dataset. *Black* and *gray circles* show correlations with significances at or above the 99 and 95% levels, respectively; white circles show significances below the 90% level. Reprinted with permission from Evans et al. (2006)

general unavailability of meteorological observations of the appropriate timescale, particularly from the remote alpine or tree line regions of particular interest to dendroclimatologists. Even where daily meteorological data can be found, stations may be located at considerable distance from the tree-ring chronology site, almost always at a lower elevation, and often with different exposure and topography. While differences in temperature between site and station can usually be evaluated and reasonably corrected, it is quite difficult to do so for precipitation. The length of the daily meteorological records also limits the period over which model skill can be evaluated against the available tree-ring chronologies. At the same time, many tree-ring chronologies in many parts of the world were originally collected in the 1970s and 1980s and have not yet been updated, further limiting the overlap between simulated and actual tree-ring data.

Additional uncertainties derive from model parameter specification. The model has 31 adjustable parameters (Vaganov et al. 2006), many of which were originally developed from empirical research on cold (Siberia) or dry (Arizona) environments, but which are potentially poorly constrained in other regions. With our collaborators, we are currently developing and testing two complementary approaches to evaluating and reducing uncertainties associated with parameter choices. Ongoing studies in Siberia are focused on improving the empirical basis for model parameterization across a range of environments and site conditions. Another approach is to use Monte Carlo bootstrapping techniques to develop probabilistic estimates of the sensitivity of simulation results to parameter choices, and to identify those that are most important. An additional complication is the potential for species-specific parameters. Although we have successfully applied the model with the default ('Siberian') parameters to a range of species (Evans et al. 2006), there are indications that the model performs better for some species than for others. We are currently investigating the extent to which this differential skill is a consequence of site environment or species characteristics.

As was discussed in the previous section, our specific research questions as well as data requirements have led us to use a variety of approaches in simulating tree-ring width chronologies. Evaluations of the model skill as compared with observations have therefore employed a range of statistical techniques, including correlation, principal components (Anchukaitis et al. 2006), and spatiotemporal analysis of large overlapping networks (Evans et al. 2006). Each of these approaches necessarily has its own underlying assumptions and potential biases, which must be kept in mind in testing the model against existing tree-ring data.

3.9 Conclusion

The biological, chemical, and physical processes that link the external environment to the characteristics of annual growth rings in trees form the necessary basis for dendroclimatological research. Although ultimately the incremental basal diameter growth of trees cannot proceed without biochemical pathways, structures, and substrates associated with both the crown and the roots, the fundamental processes that give rise to basal growth and the characteristics and anatomical features of the annual ring are those associated with cellular growth and division in the cambium. Here, we have demonstrated that understanding and modeling the environmental controls on tree-ring formation as arising in part from direct climatic influences on the dynamic cambium allow us to reproduce the observed phenomenonology of intra-annual patterns of tree growth as well as the annual and interannual patterns of ring width variability as observed in a variety of species and sites, and across different spatial scales. However, much future work is necessary at the intersection of dendrochronology, tree physiology, and biochemistry in order to better describe and understand the relationships between photosynthesis, carbon assimilation and storage, and tree-ring width, as well as the cellular processes or structures that might

account for and permit the direct environmental influences on dividing and growing cells in the cambium.

By linking the external environmental controls on the formation of tree-ring proxies to processes that primarily influence the cambial zone, the VS model allows us to produce synthetic tree-ring series that can be compared directly to actual tree-ring-based proxy observation of climate variability. In cases where robust coherence between model results and actual data is found, we can use the model to mechanistically interpret the basis of variations in the actual tree-ring data. Local, regional, and synoptic-scale intercomparisons of model results and data suggest the VS model explains gross features of interannual tree-ring width variability that are relatively insensitive to parameter estimation. These results can be used to better understand the processes underlying behavior of the actual data. In the case studies discussed here, for instance, the apparent emergence of behavior such as the dependence of eastern hemlock ring width variations on spring temperatures, and the increasing dependence of ring width variations in the southeastern United States on summertime soil moisture can be explained in terms of intra-annual to multidecadal changes in environmental conditions, as mediated by cambial processes. Future applications of the model may include further exploration of the biological basis of emergent phenomena, study of the nature of decadal-scale variability in tree-ring data, prediction of the influence of future climate change on conifer forest growth, objective process-based removal of potential non-climatic biases in tree-ring data prior to paleoclimatic inversions, and the allowance for varying climate–tree growth relationships as a constraint in paleoclimatic modeling and reconstruction activities using tree-ring data as input.

Acknowledgements KJA was supported by a graduate training fellowship from the NSF IGERT Program (DGE-0221594) and a Graduate Research Environmental Fellowship (to KJA) from the US Department of Energy.

References

Abe H, Nakai T, Utsumi Y, Kagawa A (2003) Temporal water deficit and wood formation in Cryptomeria japonica. Tree Physiol 23(12):859–863

Alexeev VA (1975) The light regime in forests (in Russian). Nauka, Leningrad, 227 pp

Alfieri FJ, Evert RF (1968) Seasonal development of the secondary phloem in Pinus. Am J Bot 55:518–528

Anchukaitis KJ, Evans MN, Kaplan A, Vaganov EA, Hughes MK, Grissino-Mayer HD, Cane MA (2006) Forward modeling of regional scale tree-ring patterns in the southeastern United States and the recent influence of summer drought. Geophys Res Lett 33:L04705. doi:10.1029/2005GL025050

Antonova GF, Stasova VV (1993) Effects of environmental factors on wood formation in Scots pine stems. Trees 7:214–219

Antonova GF, Stasova VV (1997) Effects of environmental factors on wood formation in larch (Larix sibirica Ldb.) stems. Trees 11:462–468

Antonova GF, Cherkashin VP, Stasova VV, Varaksina TN (1995) Daily dynamics in xylem cell radial growth of Scots pine (*Pinus sylvestris*). Trees 10:24–30

Aykroyd RG, Lucy D, Pollard AM, Carter AHC, Robertson I (2001) Temporal variability in the strength of proxy-climate correlations. Geophys Res Lett 28:1559–1562

Baluska F, Barlow PW, Kubica S (1994) Importance of the post-mitotic growth (PIG) region for growth and development of roots. Plant Soil 167:31–42
Baluska F, Volkmann D, Barlow PW (1996) Specialized zones of development in roots: view from the cellular level. Plant Physiol 112:3–4
Baluska F, Volkmann D, Barlow PW (2001) A polarity crossroad in the transition growth zone of maize root apices: cytoskeletal and developmental implications. Plant Growth Regul 20:170–181
Bannan MW (1955) The vascular cambium and radial growth in Thuja occidentalis L. Can J Bot 33(2):113–138
Bannan MW (1957) The relative frequency of the different types of anticlinal divisions. Can J Bot 35:875–884
Bannan MW (1962) The vascular cambium and tree-ring development. In: Kozlovski TT (ed) Tree growth. Ronald Press, New York, pp 3–21
Barnett JR (ed) (1981) Xylem cell development. Castle House Publications, Tunbridge Wells, Kent, 307 pp
Bassow S, Ford E, Kiester AR (1990) A critique of carbon-based tree growth models. In: Dixon R, Meldahl R, Ruark G, Warren W (eds) Process-modeling of forest growth responses to environmental stress. Timber Press, Portland, Oregon, pp 50–57
Biondi F (2000) Are climate-tree growth relationships changing in North-Central Idaho, USA? Arctic Alpine Res 32:111–116
Biondi F, Waikul K (2004) DENDROCLIM2002: a C++ program for statistical calibration of climate signals in tree-ring chronologies. Comput Geosci 30(3):303–311
Bräuning A (1999) Dendroclimatological potential of drought-sensitive tree stands in southern Tibet for the reconstruction of monsoon activity. IAWA J 20:325–338
Brett C, Waldron K (1996) Physiology and biochemistry of plant cell wall, 2nd edn. Chapman and Hall, London, 255 pp
Briffa KR, Bartholin TS, Eckstein D, Jones PD, Karlen W, Schweingruber FH, Zetterberg PA (1990) A 1,400-year tree ring record of summer temperatures in Fennoscandia. Nature 346:434–439
Briffa KR, Jones PD, Schweingruber FH (1992) Tree-ring density reconstructions of summer temperature patterns across western North America since 1600. J Climate 5:735–754
Briffa KR, Schweingruber FH, Jones PD (1998a) Trees tell of past climates: but are they speaking less clearly today? Phil Trans R Soc 352: 65–73
Briffa KR, Schweingruber FH, Jones PD, Osborn TJ, Shiyatov SG, Vaganov EA (1998b) Reduced sensitivity of recent tree-growth to temperature at high northern latitudes. Nature 391:678–682
Briffa KR, Osborn TJ, Schweingruber FH, Harris IC, Jones PD, Shiyatov SG, Vaganov EA (2001) Low-frequency temperature variations from a northern tree ring density network. J Geophys Res 106:2929–2941
Briffa KR, Osborn TJ, Schweingruber FH (2004) Large-scale temperature inferred from tree rings: a review. Global Planet Change 40:11–26
Brown CL, Sax K (1962) The influence of pressure on the differentiation of secondary tissues. Am J Bot 49:693
Carlquist S (1988a) Comparative wood anatomy: systematic, ecological and evolutionary aspects of dicotyledon wood. Springer-Verlag, Berlin, Heidelberg, New York, 460 pp
Carlquist S (1988b) Near-vesselessness in Ephedra and its significance. Am J Bot 75:598–601
Casgrove DJ (1993) How do plant cell walls extend? Plant Physiol 102:1–6
Catesson AM (1984) La dynamique cambial. Ann Sci Nat Bot 13(6):23–43
Catesson AM (1990) Cambial cytology and biochemistry. In: Iqbal M (ed) The vascular cambium. Research Studies Press, Taunton, England, pp 63–112
Catesson AM (1994) Cambial ultrastructure and biochemistry: changes in relation to vascular tissue differentiation and the seasonal cycle. Int J Plant Sci 155(3):251–261
Catesson AM, Roland JC (1981) Sequential changes associated with cell wall formation and fusion in the vascular cambium. IAWA Bull 2:151–162

Chaffey N, Cholewa E, Regan S, Sundberg B (2002) Secondary xylem development in Arabidopsis: a model for wood formation. Physiol Plantarum 114:594–600
Cook ER, Jacoby GC (1977) Tree-ring-drought relationships in the Hudson Valley, NY. Science 198:399–401
Cook ER, Meko DM, Stahle DW, Cleaveland MK (1999) Drought reconstructions for the continental United States. J Climate 12:1145–1162
Cook ER, Palmer JG, D'Arrigo, RD (2002) Evidence for a 'Medieval Warm Period' in a 1,100 year tree-ring reconstruction of past austral summer temperatures in New Zealand. Geophys Res Lett 29(14). doi:10.1029/2001GL014580
Cook ER, Woodhouse CA, Eakin CM, Meko DM, Stahle DW (2004) Long-term aridity changes in the western United States. Science 306(5698):1015–1018
Creber GT, Chaloner WG (1984) Influence of environmental factors on the wood structure of living and fossil trees. Bot Rev 50:357–448
D'Arrigo RD, Jacoby GC, Free RM (1992) Tree-ring width and maximum latewood density at the North American tree line: parameters of climatic change. Can J Forest Res 22:1290–1296
Demura T, Fukuda H (1994) Novel vascular cell-specific genes whose expression is regulated temporally and spatially during vascular system development. Plant Cell 6:967–981
Dengler N (2001) Regulation of vascular development. Plant Growth Regul 20(1):1–13
Denne MP (1971) Temperature and tracheid development in *Pinus sylvestris* seedlings. J Exp Bot 22:362–370
Denne MP, Dodd RS (1981) The environmental control of xylem differentiation. In: Barnett JR (ed) Xylem cell development. Castle House Publishing, Tunbridge Wells, Kent, pp 237–255
Deslauriers A, Morin H (2005) Intra-annual tracheid production in balsam fir stems and the effect of meteorological variables. Trees-Struct Funct 19(4):402–408
Deslauriers A, Morin H, BéginY (2003) Cellular phenology of annual ring formation of Abies balsamea in the Québec boreal forest (Canada). Can J Forest Res 33:190–200
Dickson RE, Tomlinson PT, Isebrands JG (2000) Partitioning of current photosynthate to different chemical fractions in leaves, stems, and roots of northern red oak seedlings during episodic growth. Can J Forest Res 30:1308–1317
Dodd RS, Fox P (1990) Kinetics of tracheid differentiation in Douglas-fir. Ann Bot 65:649–657
Downes GM, Turvey ND (1990) The effect of nitrogen and copper on the characteristics of woody tissue in seedling of Pinus radiata. Can J Forest Res 20: 369–377
Ericsson A, Larsson S, Tenow O (1980) Effects of early and late season defoliation on growth and carbohydrate dynamics in Scots pine. J Appl Ecol 17(3):747–769
Evans MN, Reichert BK, Kaplan A, Anchukaitis KJ, Vaganov EA, Hughes MK, Cane MA (2006) A forward modeling approach to paleoclimatic interpretation of tree-ring data. Geophys Res 111:G03008. doi:10.1029/2006JG000166
Filion L, Payette S, Gauthier L, Boutin Y (1986) Light rings in subarctic conifers as a dendrochronological tool. Quaternary Res (NY) 26:272–279
Fritts HC (1966) Growth rings of trees: their correlation with climate. Science 154:973–979
Fritts HC (1976) Tree rings and climate. Academic, New York, 567 pp
Fritts HC, Lofgren GR, Gordon GA (1979) Variations in climate since 1602 as reconstructed from tree rings. Quaternary Res 12(1):18–46
Fritts HC, Vaganov EA, Sviderskaya IV, Shashkin AV (1991) Climatic variation and tree-ring structure in conifers: a statistical simulative model of tree-ring width, number of cells, cell wall-thickness and wood density. Climate Res 1(6):37–54
Fritts HC, Shashkin AV, Downes GM (1999) A simulation model of conifer ring growth and cell structure. In: Wimmer R, Vetter RE (eds) Tree-ring analysis. Cambridge University Press, Cambridge, UK, pp 3–32
Fukuda H (1994) Redifferentiation of single mesophyll cells into tracheary elements. Int J Plant Sci 155(3):262–271
Fukuda H (1996) Xylogenesis: initiation, progression, and cell death. Ann Rev Plant Physiol and Plant Mol Biol 47:299–325

Gamaley YuV (1972) Cytological basics of xylem differentiation. Nauka, Leningrad, 208 pp (in Russian)
Goujon T, Minic Z, Amrani AE, Lerouxel O, Aletti E, Lapierre C, Joseleau J-P, Jouanin L (2003) AtBXL1, a novel higher plant (*Arabidopsis thaliana*) putative beta-xylosidase gene, is involved in secondary cell wall metabolism and plant development. Plant J 33(4):677–690
Graham IA (1996) Carbohydrate control of gene expression in higher plants. Res Microbiol 147:572–580
Gregory RA (1971) Cambial activity in Alaskan white spruce. Am J Bot 58(2):160–171
Gregory RA, Wilson BF (1968) A comparison of cambial activity of white spruce in Alaska and New England. Can J Bot 46:733–734
Gričar J, Zupančič M, Čufar K, Koch G, Schmitt U, Oven P (2006) Effect of local heating and controlling on cambial activity and cell differentiation in the stem of Norway spruce (*Picea abies*). Ann Bot 97:943–951
Grillos SJ, Smith FH (1959) The secondary phloem of Douglas-fir. Forest Sci 5:377–388
Grissino-Mayer HD (1996) A 2129-year reconstruction of precipitation for northwestern New Mexico, USA. In: Dean JS, Meko DM, Swetnam TW (eds) Tree-rings, environment and humanity. Radiocarbon. University of Arizona Press, Tucson, Arizona, pp 191–204
Hertzberg M, Aspeborg H, Schrader J, Andersson A, Erlandsson R, Blomqvist K, Bhalerao R, Uhlen M, Teeri TT, Lundberg J, Sundberg B, Nilsson P, Sandberg G (2001) A transcriptional roadmap to wood formation. Proc Natl Acad Sci USA 98:14732–14737
Hoogesteger J, Karlsson PS (1992) Effects of defoliation on radial stem growth and photosynthesis in the mountain birch (*Betula pubescens* ssp. tortuosa). Funct Ecol 6(3):317–323
Howard RA, Wilson BF (1972) A stochastic model for cambial activity. Bot Gaz 133:410–414
Howe GT, Hackett WP, Furnier GR, Klevorn RE (1995) Photoperiodic responses of a northern and southern ecotype of black cottonwood. Physiol Plantarum 93:695–708
Hughes MK (2002) Dendrochronology in climatology—the state of the art. Dendrochronologia 20:95–116
Hughes MK, Kelly PM, Pilcher JR, La Marche VC (eds) (1982) Climate from tree rings. Cambridge University Press, Cambridge, 223 pp
Hughes MK, Schweingruber FH, Cartwright D, Kelly PM (1984) July–August temperature at Edinburgh between 1721 and 1975 from tree-ring density and width data. Nature 308(5957):341–344
Hughes MK, Vaganov EA, Shiyatov S, Touchan R, Funkhouser G (1999) Twentieth-century summer warmth in northern Yakutia in a 600-year context. Holocene 9(5):603–608
Iqbal M (ed) (1990) The vascular cambium. Wiley, New York, 246 pp
Ito J, Fukuda H (2002) ZEN1 is a key enzyme in the degradation of nuclear DNA during programmed cell death of tracheary elements. Plant Cell 14:3201–3211
Jacoby GC, Lovelius NV, Shumilov OI, Raspopov OM, Karbainov JM, Frank DC (2000) Long-term temperature trends and tree growth in the Taymir region of northern Siberia. Quaternary Res 53:312–318
Jones B, Tardif J, Westwood R (2004) Weekly xylem production in trembling aspen (*Populus tremuloides*) in response to artificial defoliation. Can J Bot 82(5):590–597
Kirdyanov A, Hughes MK, Vaganov E, Schweingruber F, Silkin P (2003) The importance of early summer temperatures and date of snow melt for tree growth in Siberian subarctic. Trees 17: 61–69
Kirst M, Johnson AF, Bancom C, Ulrich E, Hubbard K, Straggs R, Paule C, Retzel E, Whetten R, Sederoff R (2003) Apparent homology of expressed genes from wood forming tissues of loblolly pine (*Pinus taeda* L.) with *Arabidopsis thaliana*. Proc Natl Acad Sci USA 100:7383–7388
Körner C (1998) A re-assessment of high elevation treeline positions and their explanation. Oecologia 115(4):445–459
Körner C (2003) Carbon limitation in trees. J Ecol 91(1):4–17
Kozlowski TT (ed) (1968) Water deficits and plant growth, vol 1. Academic, New York, 398 pp

Kozlowski TT, Pallardy SG (1997) Growth control in woody plants. Academic, San Diego, 641 pp
Kutscha NP, Hyland F, Schwarzmann JM (1975) Certain seasonal changes in balsam fir cambium and its derivatives. Wood Sci Technol 9:175–188
Larson PR (1962) The indirect effect of photoperiod on tracheid diameter in *Pinus resinosa*. Am J Bot 49:132–137
Larson PR (1964) Some indirect effects of environment on wood formation. In: Zimmermann M (ed) The formation of wood in forest trees. Academic, New York, pp 345–366
Larson PR (1969) Wood formation and the concept of wood quality. School of Forestry and Environmental Studies, Bull No 74. Yale University, New Haven, Connecticut, USA, pp 3–17
Larson PR (1994) The vascular cambium: development and structure. Springer-Verlag, New York, Berlin, Doldrecht, 725 pp
Leikola M (1969) The influence of environmental factors on the diameter growth of young trees. Acta For Fenn 92:1–44
LeRoux X, Laconinte A, Escobar-Guitierrez A, LeDizès S (2001) Carbon-based models of individual tree-growth: a critical appraisal. Ann For Sci 58:469–506
Lev-Yadun S, Aloni R (1995) Differentiation of the ray system in woody plants. Bot Rev 61:45–84
Makela A (1990) Modeling structural-functional relationships in whole-tree growth: resource allocation. In: Dixon R, Meldahl R, Ruark G, Warren W (eds) Process-modeling of forest growth responses to environmental stress. Timber Press, Portland, Oregon, pp 81–95
Mann ME, Bradley RS, Hughes MK (1998) Global-scale temperature patterns and climate forcing over the past six centuries. Nature 392:779–787
McCarroll D, Loader NJ (2004) Stable isotopes in tree rings. Quaternary Sci Rev 23:771–801
Mikola P (1962) Temperature and tree growth near the northern timberline. In: Kozlowski TT (ed) Tree growth. Ronald, New York, pp 265–287
Misson L (2004) Maiden: a model for analyzing ecosystem processes in dendroecology. Can J Forest Res 34:874–887
Mullen JL, Ishikawa H, Evans ML (1998) Analysis of changes in relative elemental growth rate patterns in the elongation zone of Arabidopsis roots upon gravistimulation. Planta 206:598–603
Nieminen KM, Kauppinen L, Helariutta Y (2004) A weed for wood? Arabidopsis as a genetic model for xylem development. Plant Physiol 135:653–659
Parkerson RH, Whitmore F (1972) A correlation of stem sugars, starch, and lipid with wood formation in eastern white pine. Forest Sci 18:178–183
Pederson N, Cook ER, Jacoby GC, Peteet DM, Griffin KL (2004) The influence of winter temperatures on the annual radial growth of six northern-range-margin tree species. Dendrochronologia 22:7–29
Peterson TC, Vose RS (1997) An overview of the global historical climatology network temperature database. B Am Meteorol Soc 78:2837–2849
Plomion C, Leprovost G, Stokes A (2001) Wood formation in trees. Plant Physiol 127:1513–1523
Preston RD (1974) The physical biology of plant cell walls. Chapman and Hall, London, 250 pp
Pritchard J (1994) The control of cell expansion in roots. New Phytol 127:3–26
Rayle DL, Cleland RE (1992) The acid growth theory of auxin-induced cell elongation is alive and well. Plant Physiol 99:1271–1274
Richardson DD (1964) The external environment and tracheid size in conifers. In: Zimmermann M (ed) The formation of wood in forest trees. Academic, New York, pp 367–388
Roberts LW (1976) Cytodifferentiation in plants: xylogenesis as a model system. Cambridge University Press, Cambridge, 160 pp
Roland JC (1978) Early differences between radial walls and tangential walls of actively growing cambial zone. IAWA Bull 1:7–10
Rossi S, Deslauriers A, Anfodillo T, Morin H, Saracino A, Motta R, Borghetti R (2006) Conifers in cold environments synchronize maximum growth rate of tree-ring formation with day length. New Phytol 170:301–310
Rossi S, Deslauriers A, Anfodillo T, Carraro V (2007) Evidence of threshold temperatures for xylogenesis in conifers at high altitudes. Oecologia152:1–12

Salzer M, Kipfmueller KF (2005) Reconstructed temperature and precipitation on a millennial timescale from tree-rings in the southern Colorado Plateau, USA. Climatic Change 70(3):465–487

Savidge RA (1983) The role of plant hormones in higher plant cellular differentiation. II. Experiments with the vascular cambium, and sclereid and tracheid differentiation in the pine, *Pinus contorta*. Histochem J 15(5):447–466

Savidge RA (1993) Formation of annual rings in trees. In: Rensing L (ed) Oscillations and morphogenesis. Marcel Dekker, New York, pp 343–363

Savidge RA (1996) Xylogenesis, genetic and environmental regulation. IAWA J 17(3):269–310

Savidge RA (2000a) Intrinsic regulation of cambial growth. Plant Growth Regul 20:52–77

Savidge RA (2000b) Biochemistry of seasonal cambial growth and wood formation—an overview of the challenges. In: Savidge RA, Barnett JR, Napier R (eds) Cell and molecular biology of wood formation. Bios Scientific Publishers, Oxford, pp 1–30

Schmid R (1976) The elusive cambium—another terminological contribution. IAWA Bull 4:51–59

Schrader J, Baba K, May ST, Palmek K, Bennett M, Bhalerao RP, Sandberg G (2003) Polar auxin transport in the wood forming tissues of hybrid aspen is under simultaneous control of developmental and environmental signals. Proc Natl Acad Sci USA 100(17):10096–10101

Schweingruber FH (1988) Tree ring: basics and applications of dendrochronology. Reidel, Dordrecht, 276 pp

Schweingruber FH (1993) Trees and wood in dendrochronology. Springer, Berlin, Heidelberg, New York, 386 pp

Schweingruber FH (1996) Tree rings and environment. Dendroecology. Paul Haupt, Berne, Stuttgart, Vienna, 609 pp

Shashkin AV, Vaganov EA (1993) Simulation model of climatically determined variability of conifers annual increment (on the example of Scots pine in the steppe zone). Russ J Ecol 24(5):275–280

Skene DS (1972) The kinetics of tracheid development in Tsuga canadensis Carr and its relation to tree vigour. Ann Bot 36:179–187

Somerville C, Bauer S, Brininstool G, Facette M, Hamann T, Milne J, Osborne E, Paredez A, Persson S, Raab T, Vorwerk S, Youngs H (2004) Towards a systems approach to understanding plant cell wall. Science 306:2206–2211

Speer J, Swetnam T, Wickman B, Youngblood A (2001) Changes in Pandora moth outbreak dynamics during the past 622 years. Ecology 82(3):679–697

Stahle DW, Cleaveland MK (1992) Reconstruction and analysis of spring rainfall over the southeastern US for the past 1000 years. B Am Meteorol Soc 73:1947–1961

Sundberg B, Ericsson A, Little C, Nasholm T, Gref R (1993) The relationship between crown size and ring width in *Pinus sylvestris* L. stems: dependence on indole-3-acetic acid, carbohydrates and nitrogen in the cambial region. Tree Physiol 12(4):347–62

Sviderskaya IV (1999) Histometric analysis of patterns of seasonal formation of conifer wood. PhD Dissertation, IF SB RAS, Krasnoyarsk, 167 pp (in Russian)

Taiz L (1984) Plant cell expansion: regulation of cell wall mechanical properties. Annu Rev Plant Phys 35:583–657

Thomas D, Montagu K, Conroy J (2006) Effects of leaf and branch removal on carbon assimilation and stem wood density of Eucalyptus grandis seedlings. Trees-Struct Funct 20(6):725–733

Thornthwaite CW, Mather JR (1955) The water balance. Publ Climatol 8, 104 pp

Uggla C, Moritz T, Sandberg G, Sundberg B (1996) Auxin as a positional signal in pattern formation in plants. Proc Natl Acad Sci USA 93:9282–9286

Uggla C, Mellerowicz EJ, Sundberg B (1998) Indole-3-acetic acid controls cambial growth in Scots pine by positional signaling. Plant Physiol 117:113–121

Uggla C, Magel E, Moritz T, Sundberg B (2001) Function and dynamics of auxin and carbohydrates during earlywood/latewood transition in Scots pine. Plant Physiol 125:2029–2039

Vaganov EA (1996a) Mechanisms and simulation of tree ring formation in conifer wood. Lesovedenie (Russ J For Sci) 1:3–15 (in Russian)

Vaganov EA (1996b) Analysis of a seasonal growth patterns of trees and modelling in dendrochronology. In: Dean J, Swetnam T, Meko D (eds) Tree-rings, climate and humanity. Radiocarbon 1996:73–87
Vaganov EA (1996c) Recording of warming in current century by tracheids of the annual tree rings. Dokl Biol Sci 351:281–283
Vaganov EA, Shashkin AV, Sviderskaya IV, Vysotskaya LG (1985) Histometric analysis of woody plant growth. Nauka, Novosibirsk, 102 pp (in Russian)
Vaganov EA, Sviderskaya IV, Kondrateva EN (1990) The weather conditions and tree ring structure: the simulation model of tracheidogram. Lesovedenie (Russ J For Sci) 2: 37–45 (in Russian)
Vaganov EA, Shashkin AV, Sviderskaya IV (1992) Seasonal growth and formation of tree rings: the kinetics approach and simulation modeling. In: Giterson II (ed) Biophysics of cell populations and organisms' systems. Nauka, Novosibirsk, pp 140–150 (in Russian)
Vaganov EA, Hughes MK, Kirdyanov AV, Schweingruber FH, Silkin PP (1999) Influence of snowfall and melt timing on tree growth in subarctic Eurasia. Nature 400:149–151
Vaganov EA, Hughes MK, Shashkin AV (2006) Growth dynamics of tree rings: an image of past and future environments. Springer-Verlag, Berlin, 368 pp
Villalba R, Grau HR, Boninsegna J, Jacoby G, Ripalta A (1998) Tree-ring evidence for long-term precipitation changes in subtropical South America. Int J Climatol 18:1463–1478
Waisel Y, Fahn A (1956) The effect of environment on wood formation and cambial activity in *Robinia pseudoacacia* L. New Phytol 64:436–442
Wareing PF, Roberts DL (1956) Photoperiodic control of cambial activity in Robinia pseudoacacia L. New Phytol 55:356–366
Watson E, Luckman B (2004) Tree-ring based reconstructions of precipitation for the southern Canadian Cordillera. Climatic Change 65(1–2):209–241
Wheelwright N, Logan B (2004) Previous-year reproduction reduces photosynthetic capacity and slows lifetime growth in females of a neotropical tree. Proc Natl Acad Sci USA 101(21):8051–8055
Wilmking M, Juday GP, Barber VA, Zald HSJ (2004) Recent climate warming forces contrasting growth responses of white spruce at treeline in Alaska through temperature thresholds. Global Change Biol 10:1724–1736
Wilmking M, D'Arrigo R, Jacoby GC, Juday G (2005) Increased temperature sensitivity and divergent growth trends in circumpolar boreal forests. Geophys Res Lett 32(L15):715. doi:10.1029/2005GL023331
Wilson BF (1964) A model for cell production by the cambium of conifers. In: Zimmermann MH (ed) The formation of wood in forest trees. Academic, New York, pp 19–34
Wilson BF (1966) Mitotic activity in the cambial zone of *Pinus strobus*. Am J Bot 53:364–372
Wilson BF (1973) A diffusion model for tracheid production and enlargement in conifers. Bot Gaz 134:189–196
Wilson BF, Howard RA (1968) A computer model for cambial activity. Forest Sci 14:77–90
Wodzicki TJ (1971) Mechanism of xylem differentiation in *Pinus sylvestris* L. Exp Bot 22:670–687
Zahner R (1968) Water deficits and growth of trees. In: Kozlowski TT (ed) Water deficits and plant growth, II. Academic, New York London, pp 191–254
Zahner R, Oliver WW (1962) The influence of thinning and pruning on the date of summerwood initiation in red and jack pines. Forest Sci 8:51–63
Zimmermann MH (1964) The formation of wood in forest trees. Academic, New York, 562 pp
Zimmermann MH, Brown CL (1971) Trees: structure and function. Springer-Verlag, Berlin, 336 pp

Chapter 4
Uncertainty, Emergence, and Statistics in Dendrochronology

Edward R. Cook and Neil Pederson

Abstract Some fundamental concepts of dendrochronological analysis are reviewed in the context of statistically modeling the climatically related environmental signals in cross-dated tree-ring series. Significant uncertainty exists due to our incomplete mechanistic understanding of radial growth of most tree species in the natural world, one where environmental effects are unobserved, uncontrolled, and steadily changing over time. This biological uncertainty cascades into the realm of statistical uncertainty in ways that are difficult to quantify even though the latter may be well constrained by theory. Therefore, great care must be taken to apply the many well-developed and tested statistical methods of dendrochronology in ways that reduce the probability of making false inferences. This is especially true in the case of biological emergence. This is a special case of uncertainty that arises from the way in which trees as complex organisms can have properties expressed in their ring widths that are impossible to predict from a basic understanding of lower-level physiological processes. Statistical modeling must be conducted in ways that allow for the discovery of such phenomena and, at the same time, protect from the incorrect acceptance of spurious emergent properties. To reduce the probability of the latter, we argue that model verification be an important part of any dendrochronological inquiry based on statistics. Correlation and response function analysis is used to illustrate some of the concepts discussed here. The value of empirical signal strength statistics as predictors of climatic signal strength in tree rings is also investigated.

Keywords Dendrochronology · Uncertainty · Emergence · Statistics · Response functions · Verification

E.R. Cook (✉)
Tree-Ring Laboratory, Lamont-Doherty Earth Observatory, 61 Route 9W, Palisades, NY 10964, USA
e-mail: drdendro@ldeo.columbia.edu

M.K. Hughes et al. (eds.), *Dendroclimatology*, Developments in Paleoenvironmental Research 11, DOI 10.1007/978-1-4020-5725-0_4,

4.1 Introduction

The science of dendrochronology resides in a physical and biological world dominated by *uncertainty* and *emergence*. The relative importance of each will vary considerably from study to study, but neither uncertainty nor emergence can be assumed to be absent from most, if not all, tree-ring studies, especially those that seek to identify and extract environmental signals from tree rings. The closest thing we have to absolute certainty in dendrochronology is the assignment of calendar year dates to annual tree rings by an experienced tree-ring scientist using some accepted method of crossdating (e.g., Huber 1943; Douglass 1946; Ghent 1952; Stokes and Smiley 1968; Baillie and Pilcher 1973; Heikkenen 1984; Wigley et al. 1987; Schweingruber et al. 1990; Yamaguchi 1991; Yamaguchi and Allen 1992; Fowler 1998). Without this foundation, dendrochronology ceases to exist as a legitimate science.

Yet even here, dendrochronologists have not been immune from accusations of less dating certainty than is claimed (i.e., *zero* dating uncertainty), hence the importance of the paper by LaMarche and Harlan (1973) that documented the accuracy of the tree-ring dating of semiarid site bristlecone pine in California for calibration of the radiocarbon (^{14}C) timescale. A similar study by Pilcher et al. (1984) further illustrated the power of crossdating for absolute dating of tree rings in their documentation of the dating accuracy of the long European oak tree-ring chronology. In turn, high-precision ^{14}C measurements of independently crossdated bristlecone pine and European oak wood over the same time period have yielded very similar long-term ^{14}C variations (Linick et al. 1985). This and the confirmation of the radiocarbon Suess (1965) 'wiggles' in dendrochronologically dated wood (de Jong et al. 1979) have independently validated the robustness of crossdating as a geochronological dating tool. These studies have collectively established crossdating as the most precise and accurate dating method in geochronology.

Since that time, quality control programs like COFECHA (Holmes 1983) have become indispensable tools for objectively testing the quality of crossdating and the correct assignment of calendar year dates to tree rings. These computer-assisted tools have convinced all but the most intransigent critics of dendrochronology that crossdating works as claimed when it is applied by properly trained individuals. This being the case, it is useful to briefly define and discuss now both uncertainty and emergence in generic terms before proceeding to the heart of this chapter. Simply put, *uncertainty* means that we do not know as much as we would like about the information contained in the tree rings we are studying, and *emergence* means that those same tree rings are likely to contain totally unexpected and inherently unpredictable information about environmental effects on tree growth. The effects of these principles on dendrochronological research will be examined in the context of statistically identifying and extracting climatic signals from tree rings, but they truly span the entire science of dendrochronology and its myriad applications.

4.2 Uncertainty

Uncertainty arises from the fact that tree-ring analysis is usually applied as a retrospective study of radial tree growth formed in an unobserved, uncontrolled, and steadily changing environment over some years in the past. Consequently, we rarely know with much certainty the kinds and details of the environmental signals contained in tree rings prior to analysis. And even after our best analyses, we can only make our best 'guess' of what those signals are. This acknowledgment of uncertainty ought not be viewed negatively, because this is the way science works. The great Nobel Prize-winning physicist Richard Feynman viewed it as a necessary part of science: 'Nothing is certain or proved beyond all doubt. And as you develop more information in the sciences, it is not that you are finding out the truth, but that you are finding out that this or that is more or less likely.' (Feynman 1999, p. 248). So, here we have a clear statement that scientific 'truth' is really probabilistic and, thus, always associated with some degree of uncertainty, which in Feynman's view should be embraced as central to scientific inquiry.

This fact does not mean that dendrochronologists cannot make useful a priori inferences about the likely environmental signals in tree-ring series. Thus, we might be able to accurately infer the most likely dominant signal(s) expressed in the growth variations of an annual ring width series based on the tree species being studied (e.g., Douglas-fir [*Pseudotsuga menziesii*] or white spruce [*Picea glauca*]), the growth metric being studied (e.g., ring width or maximum latewood density), and the growth environment in which it is growing (e.g., lower or upper forest border limits). For example, ring widths of semiarid site conifers growing at a lower forest border limit site are likely to reflect variations in available soil moisture supply and evapotranspiration demand (Fritts 1971), and maximum latewood densities of high-elevation conifers are likely to reflect variations in growing season temperatures (Schweingruber et al. 1987). However, we must be honest in saying that such inferences are nothing more than educated guesses that must be modeled and verified (Fritts 1976; Snee 1977) in some justifiable way, with the understanding that we could still be wrong. In addition, we should always be ready for surprises; i.e., unexpected discoveries that may point the way to rich new research opportunities.

Thus far, this discussion has dealt essentially with biological uncertainty because we are dealing with the problem of identifying environmental signals in a biological time series, again with an emphasis here on climatic influences on tree growth. However, a completely different form of uncertainty also exists in tree-ring data that is associated with the development of annual tree-ring chronologies most frequently used for further study. This uncertainty is statistical rather than biological, although some of the statistical uncertainty in a chronology may be generated by the tree growth properties of a particular tree species (e.g., variable ring boundaries and poor circuit uniformity). Typically, such chronologies are mean-value functions of crossdated tree-ring series from many individual trees on a site. Given that the tree-ring data used in the mean-value function all crossdate to an acceptable degree,

perhaps as determined by COFECHA (Holmes 1983), this is an explicit indication that some perhaps very complicated common environmental signal exists in those tree rings. In turn, we can expect the averaging process to concentrate the common signal in the mean-value function by averaging out the noise. The act of averaging is a powerful way of getting rid of unwanted noise in tree rings, but it is never perfect; i.e., the noise is never completely eliminated. Therefore, some measure of empirical signal strength is useful because it tells us how well we have estimated the underlying common signal and eliminated the unwanted noise.

The pioneering dendroclimatologist Edmund Schulman was aware of signal strength issues and suggested that the ratio of the mean sensitivity of the average chronology (MSc) to the average mean sensitivity of the individual series (MSs) in the chronology be used as a signal strength diagnostic (Schulman 1956, pp. 20–24). This ratio he defined as coefficient R. With no noise present in the series, MSc = MSs, so $R = 1.0$. With any noise present between series, MSc < MSs because the averaging process reduces variance, so $R < 1.0$. Thus, the lower the average chronology mean sensitivity is relative to the average of the individual series, the lower the empirical signal strength. In Schulman's examples for semi-arid site conifers, $R > 0.80$ was common. Schulman even described how to use R for evaluating the signal strength in subsets of tree-ring series from a site to assess the long-term stability of the chronology signal. This idea presaged the subsample signal strength (SSS) statistic derived by Wigley et al. (1984).

Mean sensitivity has continued to be used as a diagnostic signal strength statistic, along with tree-ring chronology standard deviation and first-order autocorrelation (e.g., Fritts and Shatz 1975; DeWitt and Ames 1978). These statistics do not provide explicit estimates of statistical uncertainty in the chronology mean-value function, however. So, with the growing power and availability of computers in the 1960s, Harold C. Fritts introduced the use of analysis of variance (ANOVA) to quantitatively describe the sources of tree-ring chronology uncertainty (Fritts 1963), and through his %Y term, its relative signal strength. An excellent example of the interpretive use of ANOVA in tree-ring research can be found in Fritts (1969). Later, the average correlation between series (RBAR) was shown to be effectively equivalent to %Y as a measure of percent variance in common between series (Fritts 1976, p. 294). These results were in turn extended to include explicit estimates of signal-to-noise ratio in tree-ring chronologies (Cropper 1982a). Shortly thereafter, Wigley et al. (1984) explicitly derived the theory underlying the use of RBAR as an estimate of percent common variance between series, demonstrated its mathematical equivalence to %Y, and extended those results to the derivation of the expressed population signal (EPS), which provides an estimate of how closely a mean chronology based on a finite number of trees expresses its hypothetically perfect chronology based on an infinite number of trees. In addition, Wigley et al. (1984) derived the subsample signal strength statistic, which quantifies the changing uncertainty in a tree-ring chronology due to changing sample size. For more details and additional extensions of these extremely valuable and widely used measures of empirical signal strength, see Briffa and Jones (1990). A complementary method of expressing tree-ring chronology uncertainty is the development of annual confidence intervals

for tree-ring chronologies. This is easily done by using parametric methods or the data-adaptive bootstrap (Cook 1990).

Quantifying generic statistical uncertainty in annual tree-ring chronologies is standard practice now in dendrochronology, principally through the use of the RBAR, EPS, and SSS statistics. The methods for doing so are theoretically sound and well tested, but unfortunately they still tell us exactly nothing about the true strength of the environmental signal(s) in any given tree-ring chronology. It is up to the dendrochronologist to determine what those signals are, but considerable biological uncertainty still exists in knowing what they truly are and how they are expressed in the ring widths. Process-based forward models of cambial growth based on first principles of tree physiology have successfully modeled the effects of climate on radial growth of certain tree species (e.g., Fritts et al. 1991; Fritts and Shashkin 1995; Fritts et al. 1999; Shashkin and Vaganov 1993; Anchukaitis et al. 2006; Evans et al. 2006; Vaganov et al. 2006). The results to date are very promising, but the challenge remains to make these models more adaptable to the likely presence of biological uncertainty and emergence in many tree-ring studies.

4.3 Emergence

Emergence is the greatest source of biological uncertainty in dendrochronology because it represents a property or signal in a tree-ring series that cannot be predicted, even in principle, from our best understanding of the fundamental physiological and environmental processes that control radial growth in trees. Emergent properties arise in tree rings as a function of the inherent complexity of trees as living things and the ways in which they interact with and are constrained by their operational environment (Fritts 1976, pp. 48–50).

Examples of emergence in the fields of dendroclimatology and dendroecology are the almost universal positive correlation of March temperatures with subsequent radial growth of eastern hemlock (*Tsuga canadensis*), which appears to be independent of site characteristics and location within that species' range (Cook and Cole 1991), the almost universal positive correlation between December–January temperatures and subsequent radial growth of high-elevation red spruce (*Picea rubens*) in the northern Appalachian Mountains (Cook and Johnson 1989), the importance of winter temperatures on annual radial growth of six northern range margin tree species (Pederson et al. 2004), and the phylogenetic separation of *Quercus* species by subgenus (Erthrobalanus vs. Leucobalanus) in the West Gulf Coast forests of Texas and Louisiana, even when these oak subgenera grow together on the same site (Cook et al. 2001). None of these well-replicated statistical properties would have been predicted based on previous studies, and it is unlikely that they would ever be deduced from our best understanding of the underlying physiological processes that directly result in annual ring formation. The interactions between tree genetics and the tree's operational environment render such emergent properties inherently difficult, if not impossible, to predict. It also does not matter that some of these emergent climate signals, like the March temperature response in eastern hemlock, are of no

immediate interest for climate reconstruction. The presence of such signals is telling us something much more fundamental about how a given tree species has adapted to its climatic environment over time. That in itself is worth knowing.

Other forms of emergence in dendrochronology are arguably the effectively linear association commonly found between tree rings and local climate and the existence of crossdating itself. It is well known that the physiological processes and rates of reactions that lead to ring formation are often strongly nonlinear. A classic example is the nonlinear relationship between net photosynthesis and daily temperature (Fig. 4.1), which is caused by the differential effects of increasing temperature on rates of primary photosynthesis and dark respiration (Kozlowski et al. 1991, p. 189). The former becomes more quickly limited by increasing temperature than the latter, which results in the roughly quadratic form of the net photosynthesis curves as a function of temperature. A similar nonlinear relationship is found between net photosynthesis and leaf water potential (Kozlowski et al. 1991, p. 39). Remarkably, the aggregate expression of the many interacting nonlinear, rate-limited processes within a tree is often an effectively linear response to local climate (e.g., precipitation and temperature) in its ring widths.

This being said, certain kinds of nonlinearity may be found in tree-ring/climate relationships when a particular growth-limiting factor such as available soil moisture becomes saturated and tree growth is no longer responsive to it. Consequently, nonlinear artificial neural networks (ANNs; Guiot et al. 1995) may perform better than linear models in modeling and reconstructing precipitation and drought signals in tree-ring chronologies (e.g., D'Odorico et al. 2000; Ni et al. 2002, although there apparently can be a problem of overfitting using ANNs in relatively low signal-to-noise cases (e.g., Woodhouse 1999). The fact that the linear models developed in these examples still produced acceptable precipitation reconstructions suggests that the overall nonlinearity of tree-ring/climate relationships is not large. Vaganov et al. (1999) and Anchukaitis et al. (2006) also demonstrated how a mechanistic nonlinear model can in certain cases outperform best-fit linear statistical models when a change in local climate alters the way in which the trees respond. Such changes in climate response can also be modeled by using dynamic linear regression modeling

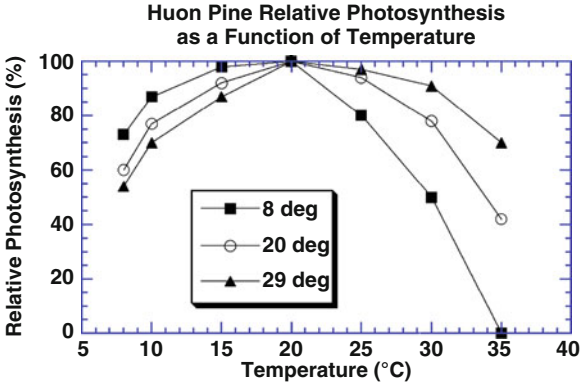

Fig. 4.1 Relative photosynthesis as a function of temperature for Huon pine in Tasmania. Three curves are based on different initial temperature acclimatizations. Adapted from Read and Busby (1990)

based on the Kalman filter (Visser and Molenaar 1988; Cook and Johnson 1989). Thus, one does not necessarily have to abandon the linear model to demonstrate a change in the way that trees respond to climate. However, the clear strength of the process-based model is that it provides insights into why the change occurred. The Kalman filter cannot do this in any obvious way.

The existence of crossdating between trees is likewise remarkable when it is viewed from microenvironmental and tree physiological perspectives. A schematic from Harold C. Fritts' seminal book *Tree Rings and Climate* (Fritts 1976) nicely illustrates the complex ways that high temperature and low precipitation affect physiological processes within the tree to produce a narrow annual ring (Fig. 4.2). This schematic applies to a tree of a given species within a stand, but the individuals of the same species within the stand undoubtedly experience different levels of environmental forcing on growth. Each tree, situated on a variable landscape, will experience different levels of available soil moisture; different levels of insolation and evapotranspiration demand; different levels of soil nutrient status; and in closed-canopy forests, different levels of competition with neighboring trees for available resources for growth. These varying external growth-limiting factors result in variable absolute growth rates between trees in any given year. Yet, the resulting secondary growth on the bole of each tree produces a common pattern of annual ring width over time; i.e., the trees crossdate, and this crossdating among the same and closely related tree species can extend over remarkably large regions (Fritts 1965; Cropper and Fritts 1982). Admittedly, crossdating is not universal among all tree

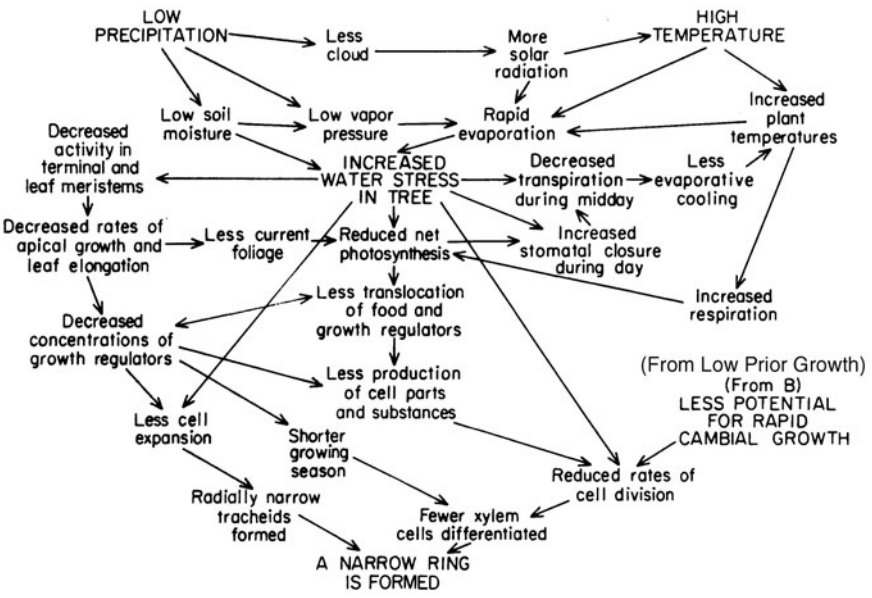

Fig. 4.2 A schematic showing how low precipitation and high temperature jointly contribute to the formation of a narrow annual ring in trees. Reproduced from Fritts (1976) with kind permission

species. However, its occurrence over a broad range of taxa growing in extremely diverse habitats worldwide indicates that crossdating is a property of tree growth that frequently *emerges* from the radial growth increments of trees being subjected to a highly variable set of microenvironmental conditions that contain within it a secondary set of common external growth-limiting factors.

The principle of emergence in biological systems might be regarded as a fundamental flaw in the current state of biological theory, one that could be eliminated if biologists knew how to develop exquisite mathematical models with high predictive skill, like those produced by physicists using classical reductionist methods to explain much of the physical world. However, the physical world is also filled with emergent properties that can never be predicted from underlying theory, even in principle. This fact was pointed out by the great evolutionary biologist Ernst Mayr, in a May 1997 interview published in the magazine *Natural History* (Angier 1997):

> It's now so clear that every time you have a more complex system, new qualities appear that you could not have predicted from the components. That's the principle of emergence. I once gave a lecture in Copenhagen, and I said something I now realize to be wrong. I said emergence is characteristic only of biology. That was in 1953, when emergence was very suspect, nobody believed it. The famous physicist Niels Bohr got up to object, and I thought he'd say emergence was metaphysical and supernatural and all sorts of things. Instead he said, 'We have emergence all over the inanimate world,' and he gave the famous example of water. If you know all the characteristics of hydrogen and all the characteristics of oxygen, you still couldn't predict that the product would be liquid.

Mayr went on to say, 'So that's the end of reductionism' (Angier 1997), a highly provocative statement that is admittedly not readily accepted by many physicists and biologists who are still committed to reductionism in science.

Among others, Hatcher and Tofts (2004) have countered Ernst Mayr's provocative statement in their recent paper *Reductionism Isn't Functional*. In it, the authors propose a solution to the emergence-versus-reductionism problem based on a mathematical theorem in concurrency theory, a branch of theoretical computer science. This theorem 'proves that all possible systems can be reasoned about in terms of their subcomponents' based on methods of process algebra. Doing the modeling this way replaces underlying functions with objects, 'i.e., every object in the system is represented by an object in the model' (Hatcher and Tofts 2004). This approach accepts the validity of constitutive reductionism in biology, which states that 'systems are composed of systems or entities at a lower level and conform to the laws governing the latter' (Hatcher and Tofts 2004). If this statement is true, then object-based methods of process algebra naturally lead to the conclusion that 'all systems can be explained in terms of the sum (composition) of their parts' (Hatcher and Tofts 2004). This conclusion thus formally rejects the fundamental premise of emergence, i.e., the whole is greater than the sum of its parts, which allows for completely unexpected properties to emerge from the collective. Because constitutive reductionism is based on 'objects' and not 'functions,' it differs from classical explanatory reductionism used in theoretical physics to deduce higher-order properties from more fundamental processes. In this sense, constitutive reductionism is a weaker form of reductionism, with little or no implied deductive ability.

For object-based models to work in the way described by Hatcher and Tofts (2004), 'every object in the system' must be known. This we maintain is the fundamental flaw of constitutive reductionism if one were to apply it to tree-ring research. We do not have a complete understanding of the evolution of a given tree species that has resulted in its genotypic definition as a species, its phenotypic expression as an organism, and its expressible range of phylogenetic responses to its operational environment. Consequently, many properties of tree-ring series can only be discovered by experiment. So in our view, the proposed method of Hatcher and Tofts (2004) does not solve the emergence-versus-reductionism problem in tree-ring analysis in favor of constitutive reductionism, because there will never be enough known 'objects in the system' to model tree growth at the genus and species levels needed for dendrochronology. Nor is it likely that their approach will even work in the physical world, where theory has historically been based on mathematically rigorous forms of explanatory reductionism.

Nobel Prize-winning physicist Robert Laughlin and coauthor David Pines (Laughlin and Pines 2000) argue convincingly in their paper *The Theory of Everything* that reductionist methods 'have succeeded in reducing all of ordinary physical behavior to a simple, correct Theory of Everything only to discover that it has revealed *exactly nothing* about many things of great importance' (emphasis added), and they give several examples in physics where this is undoubtedly the case. Laughlin and Pines (2000) go on to state that 'emergent physical phenomena regulated by higher organizing principles have a property, namely their *insensitivity to microscopics*, that is directly relevant to the broad question of what is knowable in the deepest sense of the term' (emphasis added). This means that even if we know the exact laws of physics at microscopic scales, we cannot use them to deduce the macroscopic properties of something as common as a crystalline solid, because the macroscopic world is 'regulated by higher organizing principles' that are distinct from those at the microscopic level. This harkens back to Ernst Mayr's earlier reference to Neils Bohr's comment about water. Consequently, 'living with emergence means, among other things, *focusing on what experiment tells us* about candidate scenarios for the way a given system might behave before attempting to explore the consequences of any specific model' (Laughlin and Pines 2000; emphasis added). Even earlier, Nobel Prize-winning physicist Philip Anderson (1972) made similar arguments in his paper *More is Different*, which stimulated much of the thinking that went into the paper by Laughlin and Pines (2000). Those interested in this very important topic are strongly encouraged to read the papers by Anderson (1972), Laughlin and Pines (2000), and the recently published book *A Different Universe: Remaking Physics from the Bottom Down* (Laughlin 2005).

Emergence is an inherent macroscopic property of complex systems in both the physical and biological worlds that cannot be ignored or rejected by reductionist arguments. Its presence in dendrochronological studies should therefore be expected and, indeed, welcomed because it means that we can expect surprises in our tree-ring studies that make the science of dendrochronology fun and thought provoking. Thus, we should approach our analyses with a good deal of exploration in mind and follow statistician John Tukey's exhortation that we be *data detectives* (Tukey 1977).

4.4 Statistics

Our rather lengthy, somewhat philosophical, discussions of uncertainty and emergence have set the stage now for our discussion of statistical analysis in dendrochronology. Dendrochronology is predominantly an empirical science that is deeply rooted in statistical modeling and its attendant probabilistic nature. Therefore, biological uncertainty and emergence are generally still expressed through statistical descriptions of the data. This approach places an added burden on the results and interpretations of dendrochronological analyses because, as we all know, statistical analysis can lead to the incorrect acceptance of apparently strong, yet utterly false, statistical associations. Hence the famous quote from Mark Twain's autobiography (Twain 1924, p. 246): 'There are three kinds of lies: lies, damned lies, and statistics.' Clearly, Mark Twain did not have much trust in statistics!

In statistical jargon, the generic way in which we test empirical associations is through *hypothesis testing*. We start out by assuming that no experimental treatment effect or association exists between the statistical samples or variables being compared. This is our *null hypothesis*. The *alternate hypothesis* is simply the converse of the null hypothesis; i.e., that the experimental treatment effect or association is detectable with some level of confidence. In standard statistical notation, the null and alternate hypotheses are expressed as H_0: $\rho = 0$ and H_a: $\rho \neq 0$, respectively, where ρ is the statistic being tested, such as the Pearson correlation coefficient r. We then test the statistical significance of the treatment effect or association via an appropriate statistical test. When the null hypothesis is falsely rejected, this is known as a Type-1 error in statistics. In other words, we have concluded that the tested effect or association is true, when in fact it is not true. This is a serious mistake that can lead us down the wrong scientific path. To counterbalance Type-1 error, there is Type-2 error, which is the false rejection of the alternate hypothesis when it is true. This mistake is also serious, but in a different way, because now we may have missed an important scientific discovery.

The balancing act between Type-1 and Type-2 errors is generally based on the chosen α-level probability used for rejecting the null hypothesis. Commonly, $\alpha = 0.05$ is selected (a 1-in-20 chance of being wrong), which is equivalent to the 95% significance level ($1 - \alpha$), but there is no theoretical reason for picking any particular α-level. It all depends on how willing the analyst being wrong is in not accepting the null hypothesis as true. The '1-in-20 chance of being wrong' example also illustrates the way in which statistical hypothesis testing is generally weighted towards accepting the null hypothesis. What also matters is the choice of a one-tailed or two-tailed hypothesis test. If the sign of the outcome has no a priori expectation (e.g., the correlation r may be either positive or negative to be statistically significant), a two-tailed hypothesis test is used. Conversely, if the sign of the outcome can only be positive or negative to be meaningfully significant, a one-tailed hypothesis test is used. In this case, the alternate hypothesis notation changes from H_a: $\rho \neq 0$ to either H_a: $\rho < 0$ or H_a: $\rho > 0$ to account for the sign of the outcome being important. In our later examples of modeling the climate signals in tree rings, we do not assume that we know the signs of the statistical associations a priori and, thus, we

will use a two-tailed hypothesis test. For examples of using a one-tailed hypothesis test in modeling the effects of temperature on tree growth in dendrochronology, see Pederson et al. (2004).

The interpretation of any given α-level probability is complicated by the fact that we often mine tree-ring data for statistically significant associations with climate through multiple tests of the same statistic. This is because we do not know what to expect more often than we would like. For example, if we wish to calculate the monthly correlations between tree rings and climate over, say, a 16-month dendroclimatic year (Fritts 1976; Blasing et al. 1984) beginning in the May of the previous year and ending in August of the current year of growth, and we do this for both temperature and precipitation, we are making 32 tests simultaneously and then looking for any statistically significant correlations to tell us how to interpret the tree-ring series as a function of climate. Unfortunately, this *multiplicity* of tests weakens the a priori α-level probability for any given correlation out of the 32 candidates based on a standard *t*-test for *r*, and one can therefore no longer legitimately claim that any given correlation is truly significant at the a priori 1 – α level. Most reported associations between tree rings and climate in the literature ignore this multiplicity problem in describing statistically significant months in climate correlation functions.

A simple correction for the effects of multiplicity on significance levels can be made as $P = 1 - (1 - p)^m$, where p is the a priori probability (same as our α-level described above), m is the number of tests being made, and P is the resulting a posteriori probability (Mitchell et al. 1966; Yamaguchi 1994). In our hypothetical correlation function example, if $p = 0.05$ and $m = 32$, then $P = 0.806$, which does not instill much confidence in our statistical interpretations if the correlations barely exceed the a priori 95% significance level to begin with. To achieve an a posteriori probability $P = 0.05$ requires an approximate a priori probability p ~0.001 in our hypothetical case. This is equivalent to an a priori 95% significance level for r of ~0.25 and an a posteriori 95% significance level of ~0.46 for all 32 correlations considered jointly. This correction for multiplicity would render many correlations between tree rings and climate reported in the literature (including ours!) not statistically significant. As will be shown by example below, we should not err on the side of excessive statistical rigor at this stage, because those same climate correlations may yet have significant dendroclimatic meaning even if most of them do not exceed the a priori 95% significance level, let alone the stringent correction for multiplicity. So what do we mean here? An example of correlation and response function analysis applied to an annual tree-ring chronology will serve as an illustration.

4.5 Correlation and Response Function Analysis

Consider the case where few, if any, simple correlations are statistically significant ($p < 0.05$) after correction for multiplicity. Figure 4.3 shows such an example for an eastern hemlock (*Tsuga canadensis*) tree-ring chronology from a xeric, quartzite conglomerate, talus slope site located near Mohonk Lake, Ulster County, New York (41.76°N, 74.15°W; elev. 379 m). Correlation and response functions (Fritts 1976;

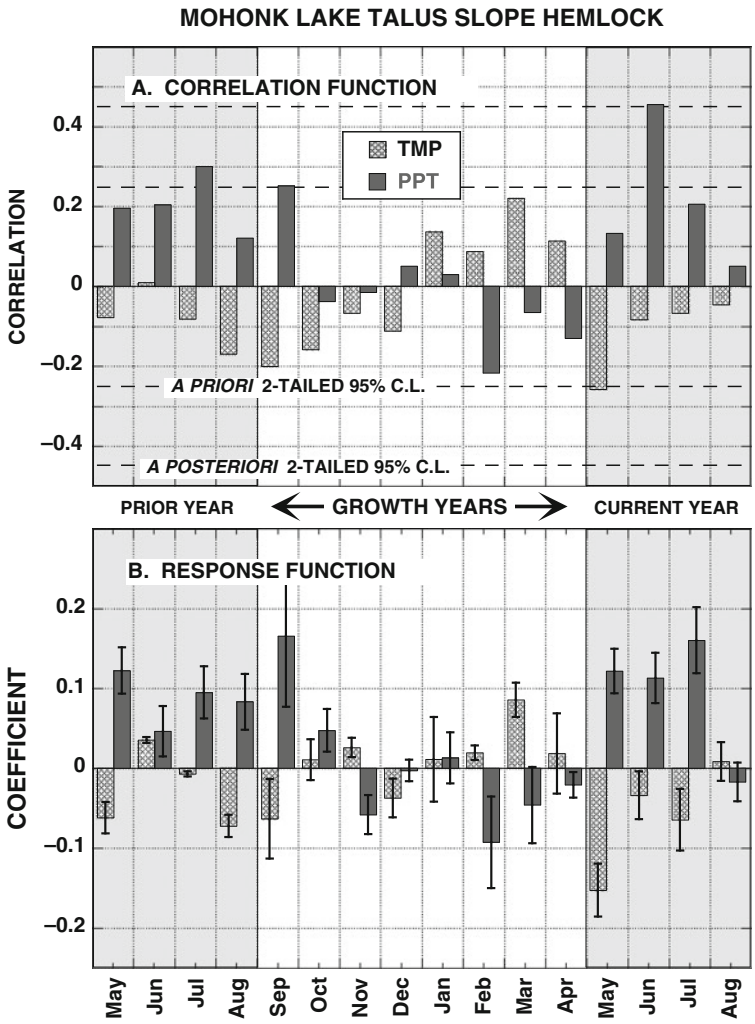

Fig. 4.3 Correlation function (*top panel*) and response function (*bottom panel*) analyses of an eastern hemlock tree-ring chronology located near Mohonk Lake, New York

Blasing et al. 1984) have been computed for this hemlock chronology by using monthly climate data from the Mohonk Lake cooperative weather station located about one kilometer from the tree-ring site at nearly the same elevation. The tree-ring and climate records cover the periods 1850–1996 and 1896–2004, respectively. So the joint period covered by the two datasets is 1896–1996. The correlation and response functions shown here were calculated and tested as follows:

1. The correlation and response functions span a 'dendroclimatic year' (Fritts 1976) that begins in May of the previous growing season and ends in August of the current growing season. This 16-month year is arranged to include two complete

radial growth seasons (roughly May–August) and the intervening 'dormant' season. As a consequence, the first year of climate data was used in creating the prior year portion of the 1897 dendroclimatic year, which resulted in the first analysis year being 1897.

2. The tree-ring data used were first prewhitened with a best-fit first-order autoregressive (AR) model (Box and Jenkins 1976) to remove the effect of persistence on degrees of freedom and the determination of statistical significance. The monthly climate data had very little, if any, persistence in the monthly variables. Consequently, the climate data were not prewhitened and the first analysis year remained 1897.
3. The correlation and response functions were computed by using data only over the 1931–1996 interval. This 66-year interval provides 64 degrees of freedom for the simple correlations, which yields a two-tailed a priori 95% confidence limit of ±0.25 and an a posteriori 95% confidence limit of ±0.45 (each shown as dashed lines in Fig. 4.3a).
4. The response function was based on retaining as candidate predictors the eigenvectors of climate with eigenvalues >1.0 (the EV1 rule; Guttman 1954; Kaiser 1960) and the best-fit regression model was determined by using the minimum Akaike information criterion (AIC; Akaike 1974; Hurvich and Tsay 1989). The actual goodness-of-fit is expressed in terms of the classical coefficient of multiple determination or R^2 statistic used in regression analysis as a measure of explained variance.
5. The pre-1931 data were reserved for statistical validation tests of the response function estimates. The validation tests used were the square of the Pearson correlation coefficient (RSQ), the reduction of error (RE), and coefficient of efficiency (CE) (Cook et al. 1999).

The correlation function (Fig. 4.3a) reveals that only 4 out of the 32 monthly correlations have exceeded the two-tailed a priori 95% confidence limits (prior-July, prior-September, and current June precipitation, and current May temperature), while only one month (current June precipitation) exceeds the a posteriori limit. Does this result mean that only current June precipitation truly matters to these trees? Based on the most rigorous statistical considerations described above, the answer would appear to be 'Yes.' However, there may be much more physiological meaning in the structure of the correlation function than purely statistical considerations would suggest, because the response function (Fig. 4.3b), which was explicitly estimated from the matrix of these monthly correlations, has many more 'significant' coefficients, 24 to be exact. This result in itself is tricky to interpret because of the way the response function and its confidence limits are calculated as a regression-weighted, linear combination of fitted climate eigenvectors (Fritts 1976; Guiot et al. 1982; Fekedulegn et al. 2002). Indeed, even the estimation of the response function confidence limits has been somewhat controversial. There is good reason to believe that the original method of Fritts (1976) produced confidence limits that were a bit too narrow. This problem has been rectified in two different ways: (1) by using bootstrap resampling to generate empirical confidence intervals (Guiot

1991; Biondi and Waikul 2004) and (2) by using a *t*-test derived from principal components regression theory (Fekedulegn et al. 2002). We use the *t*-test described by Fekedulegn et al. (2002) here.

The number of climate eigenvectors included in the response function (four in our example) also affects the number of resulting 'significant' variables. This effect is illustrated in the four steps used in calculating the final response function. The Step-1 response function (Fig. 4.4a) is based on only one eigenvector that explains 19.5% of the variance. Yet, all 32 monthly variables are 'significant' based on the calculated 95% confidence limits. Step-2 cumulatively explains 25% of the variance, but now has only 26 'significant' variables. Step-3 cumulatively explains 30.3% of the variance and has 27 'significant' variables. Final Step-4 cumulatively explains 34.2% of the variance and now has only 24 significant variables. So, from Step-1 to Step-4, the explained variance increases by 75%, but the number of significant variables decreases by 25%. A similar result can be found in Fritts (1976, Fig. 7.13, p. 367). This tendency for an inverse dependence between the number of eigenvectors in a response function model and the resulting number of 'significant' monthly variables means that one must be careful about interpreting response functions based on few climate eigenvectors because the number of 'significant' months may be inflated; this will be especially the case when only one climate eigenvector is used.

Using simulation methods, Cropper (1982b) illustrated how the number of 'significant' months can be inflated in response functions. This inflation occurs in part because the monthly patterns of the climate eigenvectors are determined by the intercorrelations between the monthly variables themselves. Some of these climate intercorrelations will be based on true physical associations (e.g., temperature may be inversely correlated with precipitation for a given month or season). However, some of the intercorrelations will also be unique to the analysis period or occur by chance alone, and thus have little or no true physical meaning. Yet, they will show up in the monthly patterns of the climate eigenvectors and may be carried into the response function when they are part of the climate eigenvectors that best explain tree growth. We must always keep in mind that the climate eigenvectors are mathematically defined orthogonal modes that are not constrained to have any physical meaning whatsoever (although they will often have some in practice) and certainly do not have *any* inherent biological meaning. So the number of statistically significant months in a response function is not a good diagnostic for determining the successful application of the method. Response function monthly confidence intervals also do not take into account the multiplicity problem described earlier. Gray et al. (1981) tackled this problem by using the binomial distribution to determine the minimum number of significant ($p < 0.05$) months needed for a response function to have overall significance ($P < 0.05$). For response functions based on 32 monthly coefficients (Fig. 4.3b), one needs a minimum of four to five significant coefficients ($p < 0.05$) to claim that the response function is significant (overall response function $P < 0.05$), which in our example is the case. Our correlation function would barely pass this test, however.

This finding brings up another issue that can greatly affect the estimation of response functions. Fekedulegn et al. (2002) note that response function analysis

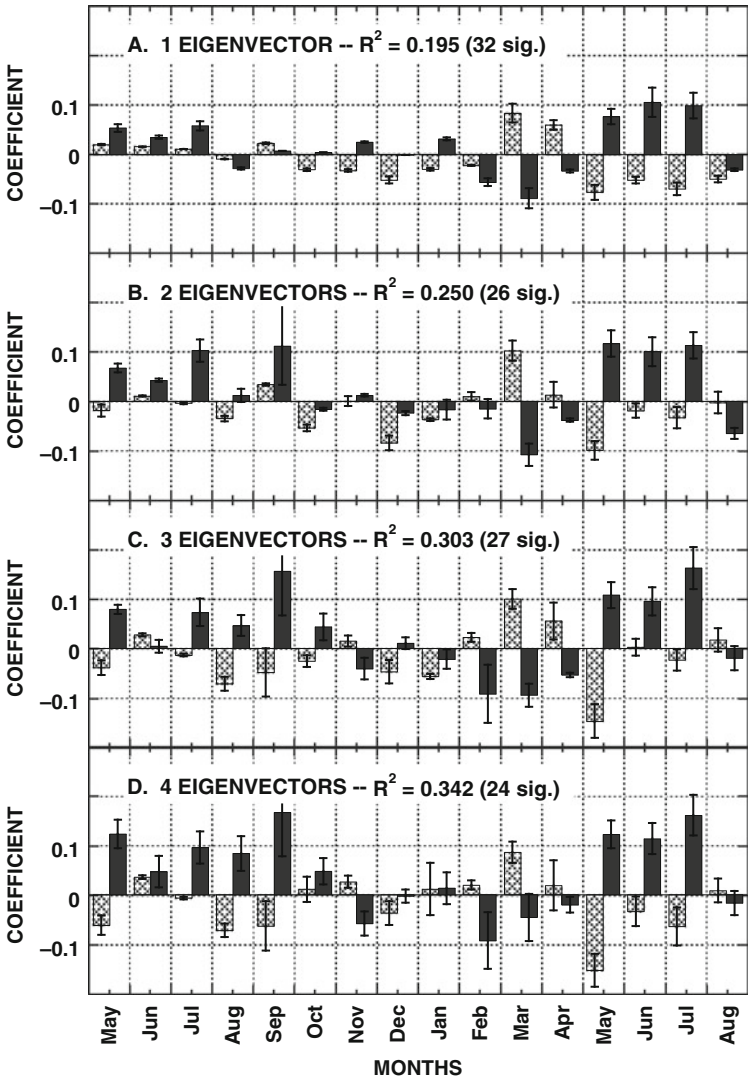

Fig. 4.4 The stepwise development of the hemlock response function shown in Fig. 4.3b. The progressive changes in fractional variance explained (R^2) and the number of significant coefficients are indicated

is highly sensitive to (1) the number of eigenvectors retained as candidate predictors in regression analysis and (2) the criterion for entering eigenvectors into the regression model. Fritts (1976), Guiot et al. (1982), and Fekedulegn et al. (2002) argue for retaining a large number of candidate eigenvectors, ones that may explain up to 90–95% of the total variance in the climate data correlation matrix. An objective

way for doing so is to use the cumulative eigenvalues product (PVP in French) criterion (Guiot et al. 1982), which is based on the cumulative product of the eigenvalues, one way of calculating the determinant of a matrix. The actual cutoff occurs where PVP drops below 1.0, the value of the determinant of a random correlation matrix of equal rank. In contrast, the EV1 cutoff occurs at the point where the remaining eigenvectors cannot explain as much variance as those extracted from an equal-rank random correlation matrix. Both PVP and EV1 are based on appealing asymptotic arguments that relate to expected values of random correlation matrices. Yet, they yield quite different results in practice.

In our example, the EV1 cutoff retained 13 of 32 eigenvectors as candidate predictors, which cumulatively explained 73.4% of the total climate variance. If the PVP cutoff had been used, it would have retained 25 of the 32 eigenvectors (equal to 96.5% of the total variance) as candidate predictors. So, is one cutoff better than the other? Support for EV1 comes from the fact that Monte Carlo estimates of eigenvalue confidence limits based on 'Rule N' (Preisendorfer et al. 1981; Preisendorfer 1988) always select a cutoff that is consistent with the asymptotic argument underlying EV1. On the other hand, there may be some useful climate information in the deleted eigenvectors below the EV1 cutoff, which is the principal argument for using PVP (or some other criterion) to retain more candidate eigenvectors (cf. Jolliffe 1973). This argument is appealing because the total information in the original climate correlation matrix is contained in the complete set of eigenvectors. See Fritts (1976, p. 357) for this mathematical equivalence. However, the increasing orthogonality constraints imposed on the higher-order eigenvectors are likely to distort the climatic meaning of those modes increasingly away from physical reality, which may make them more sensitive to chance correlations within the original intercorrelation matrix of climate variables. This and our 'Rule N' argument above are the reasons why we prefer the EV1 cutoff.

The choice of EV1 or PVP can also be argued in terms of Type-1 and Type-2 errors. Choosing EV1 is a more conservative choice because it reduces the number of candidate predictors and the likely inflation of R^2 (Rencher and Pun 1980). However, the premium paid for protecting against inflated R^2 using EV1 is the possible loss of additional useful climate information in the higher-order climate eigenvectors that PVP would retain. Thus, EV1 reduces the chance of Type-1 error and increases the chance of a Type-2 error in response functions by eliminating more eigenvectors from the candidate predictor pool. In contrast, PVP increases the chance of Type-1 error and decreases the chance of Type-2 error by allowing more potentially spurious candidate eigenvectors to be included in the response function.

Given the selected cutoff used to retain candidate eigenvectors, the criterion for entering the eigenvectors into the regression-based response function model ultimately determines the final form of the response function. Fritts (1976), Guiot et al. (1982), and Fekedulegn et al. (2002) argue for somewhat lenient entry criteria. Fritts (1976) used an F-level = 1.0 cutoff for entering eigenvectors, which in our example has a probability $p = 0.30$. Guiot et al. (1982) suggested $p = 0.50$ for relatively short datasets ($n = 30$ years) when the number of variables is comparable to the number of observations and 0.10–0.20 for longer datasets like that used here ($n =$

66). Fekedulegn et al. (2002) suggested using $p = 0.15$ for entering eigenvectors. Here, we argue for the use of the minimum Akaike information criterion (Akaike 1974), with a correction for small sample bias (Hurvich and Tsay 1989). This is a totally objective way of determining the order of the model, one that is based on sound and well-tested information theoretic principles. For this reason, we prefer the minimum AIC cutoff. Interestingly, the original uncorrected AIC (Akaike 1974) also allows variables to enter into a model if $p < 0.15$ (Jones 1985), the same as the variable entry criterion of Fekedulegn et al. (2002). So the use of the AIC should not change the response function results nearly as much as the chosen eigenvector cutoff.

Table 4.1 provides more detail on the four steps used in calculating our hemlock response function. Eigenvectors #3, #9, #10, and #6 were added to the model in that order, with a cumulative explained variance of 34.2% and a minimum AIC of −16.63. Perhaps the most interesting result here is what is not included in the model; i.e., climate eigenvectors #1 and #2, which together explain 19.2% of the total variance in the correlation matrix of temperature and precipitation at Mohonk Lake. Even though those eigenvectors are the two most important modes of covariance among the monthly temperature and precipitation variables, they correlate extremely poorly with hemlock growth ($r = -0.01$ and 0.06, respectively). This result illustrates another aspect of response function analysis. The most important modes of monthly climate variability defined by the eigenvectors need not relate to the needs of tree growth. Thus, it is always dangerous to impose a priori expectations on how trees respond to climate. We should allow the climate response of a tree-ring series to objectively *emerge* from our analysis.

The bottom two rows of Table 4.1 provide additional steps in the response function model that would have occurred if the PVP criterion were used as the cutoff for candidate eigenvectors instead of EV1. As was mentioned earlier, PVP retains 25 of the 32 eigenvectors (96.5% of the total variance) as candidate predictors. In this case, eigenvectors #15 and #18 would have also been added to the model, with a minimum AIC now at −19.37. This result suggests that PVP is better than EV1 because the final model with six eigenvectors has a smaller AIC. Is this true? In this

Table 4.1 The four regression steps used in calculating the hemlock response function

STEP	EIG	CORR	T-STAT	PROB	PART R^2	R^2	AIC
1	3 (7.2)	0.441	3.931	0.0003	0.195	0.195	−10.09
2	9 (4.6)	0.235	1.932	0.0549	0.055	0.250	−12.57
3	10 (4.1)	−0.232	−1.907	0.0580	0.054	0.303	−15.20
4	6 (5.2)	0.197	1.605	0.1093	0.039	0.342	−16.63
5	15 (2.8)	0.197	1.605	0.1094	0.039	0.381	−18.21
6	18 (2.1)	0.183	1.490	0.1371	0.034	0.413	−19.37

STEP = response function step; EIG = the eigenvector number entered and its (percent variance); CORR = simple correlation of the eigenvector with tree rings; T-STAT = Student's t statistic for Corr; PROB = Probability of t-stat; PART R^2 = partial R^2 or fractional variance contributed by each step; R^2 = cumulative fractional variance of the model; AIC = Akaike information criterion.

case at least, the answer appears to be 'No,' but how do we know? Recall that we withheld the 1897–1930 data from response function estimation for model validation purposes. We can use these data now to objectively test each response function model for skill prior to the 1931–1996 calibration period. For comparison, we have also done this using only the significant climate months in the correlation function as predictors: the single month that exceeds the a posteriori 95% significance level (current June precipitation) and the four months that exceed the a priori 95% significance level (prior-July, prior-September, and current June precipitation, and current May temperature). The results of these runs are shown in Table 4.2.

Note that the calibration period R^2 increases as the number of predictors in the model increases. This is expected even by chance alone (Morrison 1976). In particular, there is a big jump in R^2 from one predictor (current June precipitation) to four predictors (prior-July, prior-September, and current June precipitation, and current May temperature) and a corresponding substantial reduction in the AIC. This jump in R^2 is also strongly maintained in the form of increased skill in the verification period of the four-predictor model; i.e., the RSQ, RE, and CE statistics are all substantially higher for the four-predictor model compared to that based on only one predictor. So the four monthly variables selected by a priori testing of the monthly correlations are collectively more important to eastern hemlock growth than the one variable selected by the stringent a posteriori test. In this case anyway, the multiplicity problem discussed earlier is not a problem at all!

The results of the full response function tests based on using all 32 monthly climate variables in the eigenanalysis, and using either the EV1 or PVP cutoffs for retaining candidate eigenvectors, are even more interesting. As we saw previously, the response function based on the candidate predictor pool selected by PVP resulted in a higher R^2 and smaller AIC than those selected by EV1. Yet, the verification statistics are somewhat better for the full response function based on the EV1 pool (especially for RE and CE). This result illustrates that while the AIC is useful for

Table 4.2 Comparisons of climate models used to estimate the Mohonk Lake hemlock chronology

	Calibration period statistics			Verification period statistics		
# PREDICTORS	NEIG	R^2	AIC	RSQ	RE	CE
1	1/1	0.209	−11.27	0.094	0.039	0.039
4	2/2	0.343	−21.34	0.226	0.173	0.173
32	EV1 13/4	0.342	−16.63	0.269	0.251	0.251
32	PVP 25/6	0.413	−19.37	0.248	0.111	0.110

The calibration period is 1931–1996 and the verification period is 1897–1930.
PREDICTORS = number of monthly climate variables used in each principal components regression model; NEIG = the number of candidate climate eigenvectors/the number of climate eigenvectors entered into the model; R^2 = cumulative fractional variance of the model; AIC = Akaike information criterion; RSQ = square Pearson correlation; RE = verification reduction of error; CE = verification coefficient of efficiency. Higher RSQ, RE, and CE mean better verification of the fitted model.

selecting the best subset model within a given pool of candidate predictors, it does not mean that the minimum AIC model among all competing models from differing candidate predictor pools will also select the model that verifies best. How one chooses the candidate predictor pool for response functions matters, as Fekedulegn et al. (2002) point out. This example also supports our contention that higher-order eigenvectors may be less reliable predictors of tree growth because of increasing orthogonality constraints on those extracted modes. But we have also found that response functions of other tree species sampled near Mohonk Lake sometimes verified better using PVP (see below), so our case for using EV1 is certainly not closed. More provocatively, the overall monthly *structure* (i.e., month-to-month evolution) of the correlation function appears to be physiologically meaningful to these trees, even when only 4 out of 32 variables pass the a priori 95% significance level. How might this be?

We argue that the answer lies in the difference between how the monthly correlations are treated statistically here versus how monthly climate actually affects tree growth. The monthly correlations are tested in the correlation function as if adjacent months of climate are completely independent of each other. Yet, the positive and negative correlations between tree rings and precipitation/temperature during the prior and current growing season months (Fig. 4.3a) almost certainly reflect the sensitivity of our eastern hemlock chronology to overall changes in growing season moisture supply and evapotranspiration demand that may span adjacent months. Response functions attempt to address this possible interaction between months both within and between climate variables by exploiting the eigenstructure of the climate correlation matrix, apparently with some success here. This effect is best revealed by comparing the current growing season May–June–July correlations in Fig. 4.3a with the coefficients of the response function for the same months based on the single most important climate eigenvector in Fig. 4.4a. The response function coefficients are more uniformly positive for precipitation and negative for temperature over those growing season months. This result implies that the simple correlations are not measuring the strength of the tree growth response to climate as fully as the response function. The significant verification statistics of the final response function model support this conclusion (Table 4.2; EV1 results). Thus, the appearance of more statistically significant response function coefficients during the growing season months (Fig. 4.3b) does not appear to be a statistical artifact of the method in this example.

4.6 Response Functions and Empirical Signal Strength

As was noted earlier, our successful demonstration of the EV1 cutoff does not necessarily mean that it will always perform better than the PVP cutoff. To demonstrate this, we have calculated response functions for a total of seven tree species, all located near Mohonk Lake and its cooperative weather station. The tree species are eastern hemlock (*Tsuga canadensis*; TSCA), pitch pine (*Pinus rigida*; PIRI), chestnut oak (*Quercus prinus*; QUPR), black oak (*Quercus velutina*; QUVE), pignut

hickory (*Carya glabra*; CAGL), tulip poplar (*Liriodendron tulipifera*; LITU), and black birch (*Betula lenta*; BELE). This selection covers a diverse range of conifer and deciduous hardwood tree genera and subgenera. The tree-ring chronologies are based on crossdated ring width series from 6 to 14 trees/12–20 cores per species (Table 4.3). In addition, 6–10 paired cores per tree were included to allow for the calculation of within-tree correlations. The total sample size per chronology is admittedly somewhat modest (especially for PIRI), but the selected samples allowed for a consistent assessment of chronology signal strength over the same 1931–1996 period used for climate calibration. This enabled us to directly compare the empirical signal strength statistics with the response function results. For comparative purposes, all ring width series were also standardized with fixed 50-year smoothing splines (Cook and Peters 1981). In addition, the response functions and signal strength statistics were calculated from the tree-ring chronologies after removal of autocorrelation based on best-fit, low-order autoregressive models (the residual chronology from program ARSTAN; Cook 1985). Doing so eliminated different levels of autocorrelation in the original chronologies that might obscure the interspecies comparisons presented here.

Table 4.3 provides a suite of 10 descriptive statistics for each tree-ring chronology. MS is mean sensitivity; SD is standard deviation; R1 is first-order autocorrelation; ESR is Edmund Schulman's *R*; RTOT is the average correlation between all series, including within-tree replicate cores; RWT is the average correlation of the within-tree replicate cores; RBT is the average correlation of only the between-tree cores; REFF is a weighted average correlation based on RWT and RBT; EPS is the expressed population signal; and SNR is the signal-to-noise ratio. Refer to our earlier discussion of these statistics and also Briffa and Jones (1990). Explicit mathematical definitions of these statistics are also included in an Appendix of this chapter for those who are unfamiliar with them.

MS, SD, R1, and the correlation-based signal strength statistics for our tree species all fall in the typical range occupied by tree-ring data from eastern North America (ENA) (cf. Fritts and Shatz 1975; DeWitt and Ames 1978). For example, our average MS is 0.166, which compares well with 0.175 for ENA tree-ring chronologies in DeWitt and Ames (1978, their Table II, p. 10). In contrast, average MS for western North America chronologies is 0.365 in DeWitt and Ames (1978) and 0.390 in Fritts and Shatz (1975). Estimates of common signal strength for ENA chronologies (mean %Y = 0.289) in DeWitt and Ames (1978) are much lower than those presented here (mean RBT = 0.460 and REFF = 0.527), but this is an unfair comparison. Both %Y and the RBAR-based signal strength statistics (RBT, RWT, REFF) are highly sensitive to how the tree-ring data have been processed. Estimating signal strength from prewhitened tree-ring data, as was done here, will in general increase those statistics. The method of detrending will also have an effect. In contrast, MS is relatively insensitive to how the tree-ring data are processed; e.g., MS of standardized (detrended) tree-ring indices is the same as that of the original ring width measurements. The MS statistics in Table 4.3 also show the danger in using this statistic as a direct measure of climate sensitivity. All of our tree species have been subjected to the same macroclimatic effects and most are

Table 4.3 Chronology descriptive statistics and measures of empirical signal strength

SPECIES	T/C/P	MS	SD	R1	ESR	RTOT	RWT	RBT	REFF	EPS	SNR
TSCA	10/16/6	0.161	0.165	0.334	0.671	0.439	0.623	0.429	0.484	0.926	12.509
PIRI	6/12/6	0.245	0.248	0.316	0.605	0.522	0.718	0.502	0.569	0.923	12.016
QUPR	9/18/9	0.107	0.152	0.520	0.633	0.544	0.687	0.535	0.634	0.955	21.441
QUVE	14/20/6	0.106	0.131	0.511	0.716	0.439	0.723	0.429	0.456	0.940	15.626
CAGL	11/20/9	0.152	0.156	0.275	0.664	0.433	0.727	0.418	0.470	0.938	15.250
LITU	10/20/10	0.176	0.223	0.569	0.759	0.503	0.695	0.492	0.581	0.953	20.248
BELE	11/20/9	0.214	0.252	0.603	0.606	0.422	0.589	0.414	0.497	0.936	14.613

See the text and the Appendix in the chapter for details.
Column headings: SPECIES = tree species used: eastern hemlock (TSCA), pitch pine (PIRI), chestnut oak (QUPR), black oak (QUVE), pignut hickory (CAGL), tulip poplar (LITU), black birch (BELE); T/C/P = number of trees/number of cores/number of trees with paired cores; MS = mean sensitivity; SD = standard deviation; R1 = first-order autocorrelation; ESR = Edmund Schulman's *R*; RTOT = average correlation between all series including within-tree replicate cores; RWT = average correlation of the within-tree replicate cores; RBT = average correlation of only the between-tree cores; REFF = weighted average correlation based on RWT and RBT; EPS = expressed population signal; SNR = signal-to-noise ratio.

growing on well-drained to xeric sites. The greatest exception is the tulip poplar site growing along a stream bottom. Yet, the range of MS is quite large, with PIRI and BELE having more than twice the MS of QUPR and QUVE. This result suggests that the expressible range of MS in trees growing in a common macroclimatic environment can be highly species dependent, which complicates the use of MS as a general measure of climate sensitivity.

Some signal strength statistics have been used in the past as qualitative predictors of climate sensitivity of tree-ring chronologies (e.g., MS and RBT). Since they are based on the same prewhitened tree-ring data as the response functions, the signal strength statistics can be tested as predictors of the response function modeling results (cf. Cropper 1982a). This was done for response functions based on the EV1 and PVP eigenvector cutoffs, with model selection determined by the minimum AIC. Those results are provided in Table 4.4. With respect to calibration R^2, all of the response functions calibrated a significant amount of tree-ring variance, with PVP always outperforming EV1 because the former resulted in the entry of more model predictors. This difference ranges from one to five additional predictors and 0.037 to 0.164 in additional fractional variance explained. The verification statistics (RSQ, RE, CE) tell a more mixed story. As before, the hemlock (TSCA) response function verifies strongly for all three statistics, with EV1 verifying somewhat better than PVP. The next best result is for chestnut oak (QUPR), which has a statistically significant verification RSQ ($p < 0.01$) for the PVP model. Tulip poplar (LITU) and black birch (BELE) also have verification RSQs that are weakly significant ($p < 0.10$), again for the PVP model, and pignut hickory (CAGL) performs slightly better with EV1. None of the other species/models verify in any useful way for either EV1 or PVP, although the RE and CE tend to be less negative for the EV1 models. Taken together, these results marginally support PVP over EV1 as an eigenvector cutoff criterion, but the difference is not large.

Given the way that certain tree-ring statistics have often been used as predictors of climate sensitivity (e.g., MS; Fritts and Shatz 1975), we have tested that capacity using the EV1 and PVP response function modeling results. The statistics used as predictors of response function R^2 are MS, REFF, SNR, and ESR in Table 4.3. The other signal strength statistics are either biased by the high within-tree core correlations (RTOT) or are absorbed in the estimate of REFF (RWT, RBT). EPS also includes REFF in its estimate and asymptotes quickly towards 1.0, making it not very sensitive for our tests. These comparisons assume that there are no 'species effects' in our results; i.e., the joint distributions of our predictors of climate sensitivity with the response function results are independent of the species being tested. This is unlikely to be the case here because of our diverse taxa, but without within-species replication we have no way of directly testing for 'species effects.' Also, we have only seven cases to test (5 degrees of freedom), so no claims of statistical significance will be made. However, the results are interesting enough to warrant additional study using many more within- and between-species tests.

Figure 4.5 shows the four x-y scatterplots with fitted bivariate regression curves and simple correlations. REFF correlates with R^2 (Fig. 4.5a) at levels that suggest a predictive relationship between them: r equals 0.644 for EV1 and 0.548 for PVP.

Table 4.4 Response function modeling statistics for seven tree species growing near Mohonk Lake

SPECIES	CUTOFF	NEIG	EIGENVECTORS	R^2	AIC	RSQ	RE	CE
TSCA	EV1	4	**3**,9,**10**,**6**	0.342	−16.63	0.269	0.251	0.251
	PVP	6	**3**,9,**10**,**6**,15,18	0.413	−19.37	0.248	0.111	0.110
PIRI	EV1	4	**3**,11,8,**10**	0.350	−17.44	0.001	−0.349	−0.349
	PVP	5	**3**,11,19,8,**10**	0.389	−19.05	0.002	−0,403	−0.403
QUPR	EV1	8	**6**,**3**,**10**,11,13,9,7,8	0.527	−28.16	0.062	−0.152	−0.154
	PVP	11	**6**,**3**,**10**,11,13,9,15,7,8,20,19	0.610	−32.22	0.159	−0.079	−0.081
QUVE	EV1	3	**3**,**6**,**10**	0.184	−4.75	0.003	−0.114	−0.114
	PVP	4	**3**,**6**,**10**,14	0.221	−5.51	0.008	−0.114	−0.114
CAGL	EV1	2	**3**,**6**	0.200	−8.36	0.040	−0.042	−0.043
	PVP	5	**3**,**6**,21,14,25	0.323	−12.35	0.020	−0.345	−0.356
LITU	EV1	3	**3**,**6**,**10**	0.250	−10.37	0.038	−0.073	−0.082
	PVP	5	**3**,25,15,**6**,**10**	0.360	−16.06	0.064	−0.355	−0.367
BELE	EV1	4	**3**,**6**,9,**10**	0.420	−24.93	0.005	−0.249	−0.262
	PVP	9	**3**,**6**,21,9,**10**,17,22,5,13	0.584	−33.95	0.051	−0.493	−0.508

The tree species are eastern hemlock (*Tsuga canadensis*; TSCA), pitch pine (*Pinus rigida*; PIRI), chestnut oak (*Quercus prinus*; QUPR), black oak (*Quercus velutina*; QUVE), pignut hickory (*Carya glabra*; CAGL), tulip poplar (*Liriodendron tulipifera*; LITU), and black birch (*Betula lenta*; BELE). The three most important eigenvectors—#3, #6, and #10—are highlighted as bold numbers.

SPECIES = tree species abbreviations; CUTOFF = eigenvalue cutoff used to retain candidate eigenvectors; NEIG = number of eigenvectors entered into each response function model. EIGENVECTORS = list of entered eigenvectors in their order of entry; R^2 = cumulative fractional variance of the model; AIC = Akaike information criterion; RSQ = square Pearson correlation; RE = verification reduction of error; CE = verification coefficient of efficiency. Higher RSQ, RE, and CE mean better verification of the fitted model.

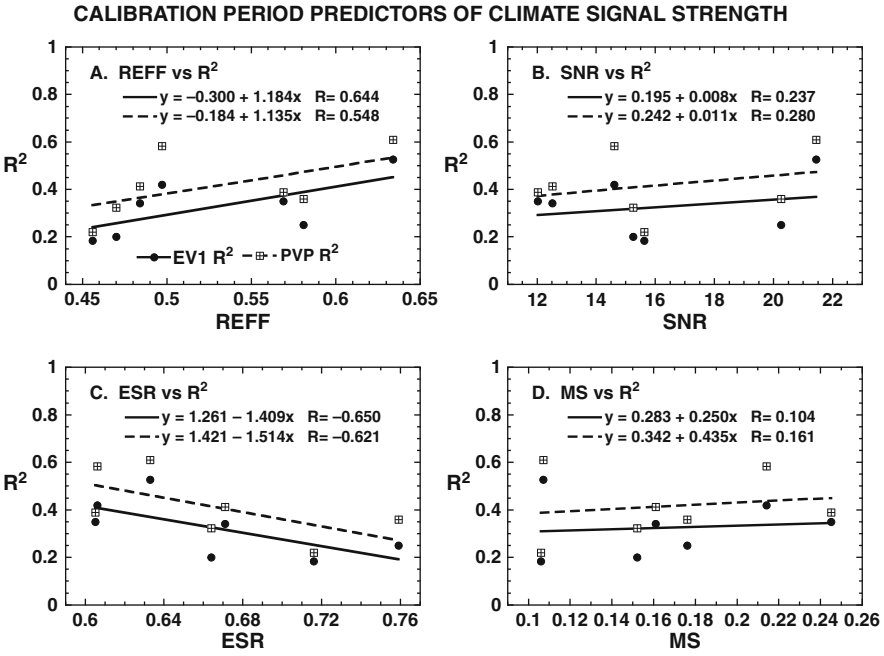

Fig. 4.5 Relationships between four empirical measures of signal strength (REFF, SNR, ESR, MS) and explained variance (R^2) by response functions based on the EV1 and PVP eigenvector cutoff criteria. The signal strength and R^2 statistics are described in the text and their values come from Tables 4.3 and 4.4

That relationship weakens considerably when SNR is used to predict R^2 (Fig. 4.5b), probably because of the strongly nonlinear behavior of SNR. Interestingly, ESR also correlates highly with R^2 (Fig. 4.5c), but in an inverse sense: r equals −0.650 for EV1 and −0.621 for PVP. As far as we know, ESR has never been used before as a diagnostic of chronology signal strength since Schulman (1956) first described it, but intuitively we would have expected positive correlations like those between REFF and R^2. If this inverse relationship between ESR and R^2 were to hold up, it would suggest that loss of MS in the mean-value function is good. This is counterintuitive if we accept the premise that high common MS among trees in the chronology is a true measure of signal strength. Thus, the ESR result could be reflecting a 'species effect' here, because MS varies considerably between the tree species used: 0.106–0.245 (Table 4.3). Interestingly, the weakest relationship of all is between chronology MS and R^2 (Fig. 4.5d): r equals 0.104 for EV1 and 0.161 for PVP. Again, we could have a 'species effect' here that weakens this relationship because of differences in how conifers and hardwoods produce secondary growth in the form of annual tree rings. In any case, the results presented here provide limited support for REFF as a predictor of climate sensitivity. This result supports the findings of Cropper (1982a), but many more test cases must be studied to determine just how useful it really is for that purpose.

4.7 Additional Response Function Interpretations

Table 4.4 lists the actual eigenvectors used in each response function in order of entry into the models. Given the disappointing verification results, these tree species have still clearly 'voted' for the most important cross-taxa climate eigenvectors. For six of the seven species, eigenvector #3 enters first; for the remaining species it enters second (refer to Table 4.4). The second most important is climate eigenvector #6, which enters either first or second in five of seven species models, all deciduous hardwoods (refer to Table 4.4). The third most important is climate eigenvector #10, which often enters third or fourth into the models (refer to Table 4.4). After that, the selected eigenvectors vary much more between species and models.

We stated earlier that the more important climate eigenvectors probably have some physical meaning due to the intercorrelations between monthly temperature and precipitation, but they are not constrained to have any biological meaning at all. While this is true, the results of our response function analyses also indicate that eigenvectors #3, #6, and #10, at least, are likely to have significant biological meaning to the trees, given their associations with ring width. For this reason, we will examine these climate eigenvectors for some biological meaning.

Climate eigenvector #3 (Fig. 4.6a) reveals an oppositional pattern between monthly temperature and precipitation that is strongest during the May–July current growing season months. This pattern is probably physically based in the sense that higher rainfall in the warm-season months should result in lower temperatures due to increased cloudiness and vice versa. It also makes biological sense as a predictor of tree growth, because our trees are growing on well-drained sites where they should have a natural sensitivity to moisture supply and evapotranspiration demand during the growing season. Thus, above-average precipitation and below-average temperature should jointly contribute to above-average radial growth, and this model applies more or less equally well to all seven tree species. Interestingly, there is a reversal in the precipitation/temperature association during the preceding March–April months that presages the start of the radial growth season. This observation indicates that warm/dry spring conditions tend to precede cool/wet late-spring/summer conditions at Mohonk Lake and vice versa. The physical meaning of this spring-summer pattern is unclear and its biological significance is even less certain. The March–April pattern could be totally unrelated to actual tree growth and simply carried into the response function because of its association with the more biologically meaningful May–July pattern in eigenvector #3. Conversely, warm/dry March–April conditions could also help in initiating early physiological activity in the trees prior to the radial growth season; i.e., it may have some phenological significance. The fact that the March–April pattern greatly diminishes in the final hemlock response function (cf. Fig. 4.4a,d) supports the former argument, but the highly significant positive March temperature response is still probably real for this species (Cook and Cole 1991). In contrast, the May–July pattern remains largely intact through all four steps of the response function calculation. Prior to March, the eigenvector loadings are uniformly lower, which means that they are more likely to be there by chance alone.

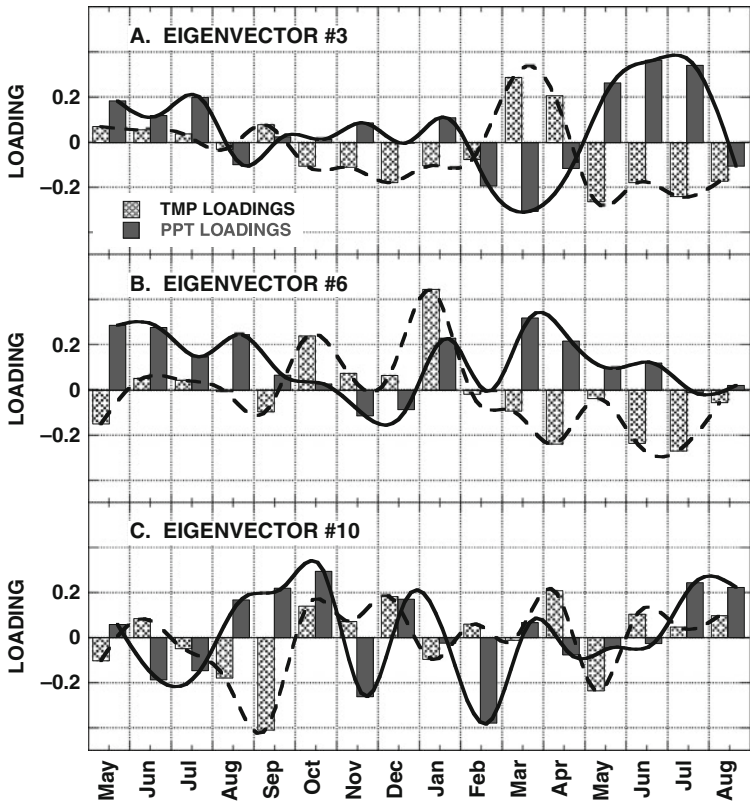

Fig. 4.6 Climate eigenvectors Nos. 3, 6, and 10. These are shown to describe the modes of climate that are most important in estimating the response functions of the seven tree species from near Mohonk Lake. A cubic spline has been applied to each eigenvector, separately for the precipitation (*solid bars*) and temperature (*hatched bars*) loadings, in order to highlight the more general structure of each eigenvector. On-line version shows this figure in color

Climate eigenvector #6 (Fig. 4.6b) is most strongly associated with the radial growth of the deciduous hardwoods. It has a significantly different pattern of monthly climate loadings that emphasizes a tendency for both prior summer and current spring precipitation to be jointly above or below average. It is unclear how much of this structure is due to orthogonality constraints alone, but it appears to be biologically meaningful nonetheless to the tree species being tested here. The added importance of prior growing season rainfall to radial growth the following year occurs even when autoregressive persistence has been removed from the tree-ring chronologies (see Fig. 4.3b for hemlock). Thus, this carryover effect of climate on ring width, from one year to the next, is not related to autocorrelation per se. Rather, it appears to be related to a discrete physiological event in a given year, like foliar budset, whose effect on radial growth can be delayed one or more years. Nonstructural carbon, which is an important component of bud construction and early leaf development, may also play a role here, as it has a residence time up to

3–5 years in oaks (Trumbore et al. 2002). The relative importance of this climate eigenvector in the response functions may also reflect some phylogenetic differences in the climate response of hardwoods and conifers. For example, the implied greater dependence on above-average precipitation during the March–April months may be related to critical early springwood vessel enlargement, particularly in the *Quercus* species. The other interesting feature of eigenvector #6 is the prominent positive loading in January. This phenomenon may be associated with the winter temperature sensitivity of certain tree species described by Pederson et al. (2004).

Climate eigenvector #10 (Fig. 4.6c) is more complicated (perhaps due to orthogonality constraints) and, therefore, more difficult to interpret from a tree physiological perspective. However, its presence in most of the response functions indicates that it does have some true biological meaning. It mainly emphasizes monthly climate variability during the late prior growing season, mainly during the prior August–October months. As a predictor of tree growth, it also appears to be more important for the hardwoods.

This evaluation of the three most important climate eigenvectors has revealed a well-understood dependence between tree growth and moisture supply/evapotranspiration demand during the current growing season of trees growing on well-drained sites, especially eigenvector #3. This common signal among all seven tree species is why they all crossdate significantly; from COFECHA (Holmes 1983), the mean correlation between all series is 0.55 (range: 0.30–0.69). Therefore, a forward model of cambial growth parameterized to model this basic water relations' effect on tree growth should produce useful first-order estimates of these tree-ring series (see Vaganov et al. Chapter 3, this volume). Details at the genus and species level might be missed by the forward model, however, unless additional climate response information suggested by eigenvector #6 (and perhaps eigenvector #10) is part of the model. Interestingly, the most poorly correlated series among the seven is pitch pine (PIRI), whose response function does not include eigenvector #6. The lack of this signal, common to all other species, may help explain why this pitch pine chronology crossdates relatively weakly with the others ($r = 0.30$).

4.8 Some Implications for Climate Reconstruction

The response function model results indicate that the seven tree species tested have statistically significant climate information in them, but with varying degrees of strength and fidelity. Based on the examinations of the most important climate eigenvectors entered into the response function models, it appears that the dominant common signal among all species is a May–July growing season response to above-average precipitation and below-average temperature. Climate eigenvectors #3 and #6 also indicate that this response occurs in both the current and prior growing seasons. Consequently, it should be possible to exploit both years of climate information in the tree rings for reconstructing past growing season climate. We have investigated this potential by reconstructing May–July total precipitation at Mohonk Lake using the mutual climate information in all seven tree-ring series. We

also did this for each species separately to see how much might be gained by using a multi-species assemblage.

Using the same principal components regression program that calculated the response functions, we reversed the order of dependence and used the seven tree-ring chronologies as predictors of May–July total precipitation. The tree-ring chronologies were lagged on themselves by one year (t and t+1 for each series) to allow for the carryover of the climate signal from one year to the next, thus creating a matrix of 14 candidate predictors. Lagging the tree-ring data resulted in the loss of one year for calibration (now 1931–1995), and the use of the now unlagged climate data resulted in a gain of one year for verification (now 1896–1930). The 14 candidate predictors were next screened for simple correlation with May–July precipitation over the calibration period. Those that did not correlate significantly ($p < 0.05$; one-tailed test) were removed from this candidate predictor pool. Of the 14 t, t+1 candidates, only 3 were rejected: PIRI t+1, QUPR t+1, and QUVE t+1. Those that passed the screening had correlations with May–July precipitation ranging from 0.272 to 0.468. The retained 11 candidate predictors were subjected to principal components analysis and the EV1 cutoff was used to retain the candidate eigenvectors. The EV1 cutoff retained 3 of 11 eigenvectors, which accounted for 65.5% of the total variance. These were used as candidate predictors in regression analysis using the minimum AIC for selecting the best-fit model. See Table 4.5 for details. The result was the entry of the first two tree-ring eigenvectors, which is consistent with what we found earlier in our evaluation of the most important climate eigenvectors associated with tree growth. The reconstruction model

Table 4.5 Comparisons of May–July total precipitation reconstructions at Mohonk Lake

	Calibration period statistics			Verification period statistics		
PREDICTORS	NEIG	R^2	AIC	RSQ	RE	CE
ALL (11)	3/2	0.436	−30.83	0.126*	−0.047	−0.112
TSCA (2, t, t+1)	2/1	0.266	−15.91	0.098*	0.040*	0.020*
PIRI (1, t)	1/1	0.213	−11.36	0.072*	−0.033	−0.097
QUPR (1, t)	1/1	0.195	−9.88	0.257*	0.256*	0.244*
QUVE (1, t)	1/1	0.128	−4.72	0.051	0.014*	−0.002
CAGL (2, t, t+1)	2/1	0.284	−17.48	0.019	−0.137	−0.155
LITU (2, t, t+1)	2/1	0.237	−13.42	0.069*	0.008*	−0.008
BELE (2, t, t+1)	2/1	0.286	−17.69	0.011	−0.262	−0.282

The calibration period is 1931–1995 and the verification period is 1896–1930.
PREDICTORS = the tree-ring variables used in each principal components regression model that passed the correlation screening with climate (all but the first row are single-species predictors); NEIG = the number of candidate tree-ring eigenvectors/the number of tree-ring eigenvectors entered into the model; R^2 = cumulative fractional variance of the model; AIC = Akaike information criterion; RSQ = square Pearson correlation; RE = verification reduction of error; CE = verification coefficient of efficiency. Higher RSQ, RE, and CE mean better verification of the fitted model.
*Means significant $p < 0.05$, RE > 0, or CE > 0.

produced a highly significant calibration R^2 of 0.436 and significant ($p < 0.05$) verification RSQ, but the RE and CE were weakly negative.

The individual species results are an interesting contrast to the joint reconstruction model (Table 4.5). None of the single-species models calibrated as much variance as the joint model. Single-species R^2 ranged from 0.128 for QUVE to 0.286 for BELE. Thus, a significant amount of additional calibrated variance has been captured by using the mutual climate information contained in the seven tree species chronologies. In terms of verification RSQ, the joint model outperforms all single-species models except that for QUPR. The RE and CE statistics show more variability between the models, but most are ± 0.05, a range that is indeterminate with respect to assessing differences in the significance of the models (Gordon and LeDuc 1981). The QUPR model is the most anomalous single-species model. It has substantially higher verification statistics even though its calibration R^2 is the second lowest one. Since the 1950s, the forests around Mohonk Lake have been subjected to episodic gypsy moth (*Lymantria dispar*) infestations that have resulted in the occasional defoliation of certain tree species, and chestnut oak is among the most favored host species. Years of notable gypsy moth population buildup and defoliation in the vicinity of Mohonk Lake were 1957, 1965–1966, 1971, 1981, and 1987–1988 (Smiley and Huth 1982; Huth 2005). So it is possible that the weak QUPR calibration is due to gypsy moth defoliation effects on the radial growth of chestnut oak.

Overall, the results presented in Table 4.5 support the use of multiple trees species for reconstructing past climate. This finding is not terribly surprising, because, as we have seen from our response function modeling results (Table 4.4) and the results from other studies (e.g., Graumlich 1993; Cook et al. 2001), tree species at the genus and subgenus levels can have different phylogenetic responses in their ring widths to nearly the same macroclimatic influences on growth. These statistically expressed differences in response to a common climate forcing are likely to enter into any climate reconstruction if it is based on only one tree species. The introduction of certain non-climatic biases into such reconstructions is therefore likely. This ought to be avoided whenever practical through the use of multiple tree species in climate reconstructions.

4.9 Concluding Remarks

Tree-ring analysis is one of the most powerful tools available for the study of environmental change and the identification of fundamental relationships between tree growth and climate. At every stage of analysis there is both statistical and biological uncertainty. In statistical analysis, we wish to reduce the uncertainty of our inferences as best as our data and analysis methods can reasonably allow, always taking into account the fact that we could be horribly wrong. To reduce the chances of making false statistical inferences, some form of model validation should therefore be conducted whenever possible (Snee 1977). Validation based on the analysis of withheld data as described here and on new tree-ring data from the same or

phylogenetically related species (e.g., Cook and Cole 1991; Graumlich 1993; Cook et al. 2001) are two recommended approaches.

Biological uncertainty is a more difficult problem to deal with because it can be due to emergent properties of tree growth that are essentially unpredictable from lower-level processes. For this reason, process-based mechanistic models may never be sufficiently complete to model the finer details of tree radial growth due to climate over a broad range of tree species and environmental conditions. Even so, simplified mechanistic models can work quite well in modeling the essentials of ring width variation due to climate for a variety of tree species (Anchukaitis et al. 2006; Evans et al. 2006; Vaganov et al. Chapter 3, this volume). Therefore, to deal with the possibility of emergent properties of tree growth that might be missed by a process-based model, we suggest that mechanistic and statistical models be used jointly to model the response of trees to climate and to test each other, because neither approach is likely to provide all the answers.

Finally, tree-ring analysis should also always contain a significant amount of data exploration, because the inherent biological uncertainty of tree growth in uncontrolled natural environments will never be eliminated. This, in our opinion, is good because it means that there will be a lot of interesting discoveries to make in the future! In turn, the results of exploratory data analysis can—and should—lead to numerous confirmatory tests of newly revealed associations that would have been otherwise missed if only a previously planned analysis were conducted. This does not eliminate the need or desire for a good a priori experimental design. Rather, it expands the scope of statistical analyses to allow for the unforeseen. As the father of exploratory data analysis, John Tukey, put it, 'restricting one's self to the planned analysis—failing to accompany it with exploration—loses sight of the most interesting results too frequently to be comfortable' (Tukey 1977, p. 3).

Acknowledgements This chapter is a contribution to the meeting 'Tree Rings and Climate: Sharpening the Focus,' held at the University of Arizona, Tucson, on April 6–9, 2004. We thank the organizing committee members (Malcolm Hughes, Henry Diaz, and Tom Swetnam) for their kind support and encouragement. This chapter is based the generous long-term support of the Lamont-Doherty Tree-Ring Laboratory (TRL)by the National Science Foundation and the National Oceanic and Atmospheric Administration Office of Global Programs. The U.S. Department of Energy Global Change Education Program also supported N. Pederson in his PhD dissertation research at the Lamont TRL that contributed to this chapter. We also thank the Mohonk Preserve (Paul Huth and John Thompson) for permission to sample trees used in this study and for access to the Mohonk Lake meteorological data, and to the remarkable naturalist Daniel Smiley of Mohonk who made all of this possible. Lamont-Doherty Earth Observatory Contribution No. 7205.

Appendix

Basic chronology statistics for tree-ring series of length n:

Arithmetic Mean:

$$\bar{x} = \frac{1}{n}\sum_{i=1}^{n} x_i$$

Standard Deviation:

$$s = \sqrt{\frac{\sum_{i=1}^{n} (x_i - \bar{x})^2}{n-1}}$$

Lag-1 Autocorrelation:

$$r_1 = \frac{\sum_{i=2}^{n} (x_i - \bar{x})(x_{i-1} - \bar{x})}{(n-1)s_x^2}$$

Mean Sensitivity:

$$\text{ms} = \frac{1}{n-1} \sum_{i=2}^{n} \left| \frac{2(x_i - x_{i-1})}{(x_i + x_{i-1})} \right|$$

Empirical signal strength statistics for m tree-ring series from t trees of length n:

Mean chronology:

$$\overline{X} = \frac{1}{m} \sum_{j=1}^{m} x_{i,j}$$

for each year, $i = 1, n$

Chronology MS:

$$\text{MS}_c = \frac{1}{n-1} \sum_{i=2}^{n} \left| \frac{2(\overline{X}_i - \overline{X}_{i-1})}{(\overline{X}_i + \overline{X}_{i-1})} \right|$$

Average *ms* of the m series:

$$\overline{\text{MS}_s} = \frac{1}{m} \sum_{j=1}^{m} \text{ms}_j$$

Edmund Schulman's R:

$$\text{ESR} = \frac{\overline{\text{MS}_s}}{\text{MS}_c}$$

For t trees and m total cores, calculate all possible between-series Pearson cross-correlations as

Pearson correlation:

$$r_{xy} = \frac{\sum_{i=1}^{n}(x_i - \bar{x})(y_i - \bar{y})}{(n-1)\, s_x\, s_y}$$

where r_{xy} is the correlation between cores x and y.

From Briffa and Jones (1990), let c_i equal the number of within-tree cores for a given tree and let RBAR be a given average correlation statistic. Then,

RBAR for all series:

$$\mathrm{RTOT} = \frac{1}{\mathrm{NTOT}} \sum_{i=1}^{t} \sum_{\substack{l=1 \\ i \neq 1}}^{t} \sum_{j=1}^{c_i} r_{ilj}$$

where

$$\mathrm{NTOT} = \frac{1}{2}\left[\sum_{i=1}^{t} c_i\right]\left\{\left[\sum_{i=1}^{t} c_i\right] - 1\right\}$$

RBAR within trees:

$$\mathrm{RWT} = \frac{1}{\mathrm{NWT}} \sum_{i=1}^{t} \left[\sum_{j=2}^{c_i} r_{ij}\right]$$

where

$$\mathrm{NWT} = \sum_{i=1}^{t} \frac{1}{2} c_i (c_i - 1)$$

RBAR between trees:

$$\mathrm{RBT} = \frac{1}{\mathrm{NBT}}(\mathrm{RTOT} \cdot \mathrm{NTOT}) - \mathrm{RWT} \cdot \mathrm{NWT})$$

where NBT = NTOT − NWT

The effective RBAR (REFF) is a weighted average of RBT and RWT that includes the added signal strength due to the within-tree correlations.

RBAR effective:

$$\mathrm{REFF} = \frac{\mathrm{RBT}}{\mathrm{RWT} + \frac{1-\mathrm{RWT}}{\mathrm{CEFF}}}$$

where

$$\frac{1}{\text{CEFF}} = \frac{1}{t}\sum_{i=1}^{t}\frac{1}{c_i}$$

The signal-to-noise ratio and expressed population signal are estimated from REFF now as

Signal-to-noise ratio:

$$\text{SNR} = \frac{t \cdot \text{REFF}}{1 - \text{REFF}}$$

Expressed population signal:

$$\text{EPS} = \frac{t \cdot \text{REFF}}{t \cdot \text{REFF} + (1 - \text{REFF})}$$

References

Akaike H (1974) A new look at the statistical model identification. IEEE Trans Automat Contr AC-19(6):716–723

Anchukaitis KJ, Evans MN, Kaplan A, Vaganov EA, Hughes MK, Grissino-Mayer HD, Cane MA (2006) Forward modeling of regional-scale tree-ring patterns in the southeastern United States and the recent emergence of summer drought stress. Geophys Res Lett 33(4):L04705. doi:10.1029/2005GL025050

Anderson PW (1972) More is different. Science 177:393–396

Angier N (1997) Ernst Mayr at 93. Nat Hist 106(4):8–11

Baillie MGL, Pilcher JR (1973) A simple cross-dating program for tree-ring research. Tree-Ring Bull 33:7–14

Biondi F, Waikul K (2004) DENDROCLIM2002: a C++ program for statistical calibration of climate signals in tree-ring chronologies. Comput Geosci 30:303–311

Blasing TJ, Solomon AM, Duvick DN (1984) Response functions revisited. Tree-Ring Bull 44: 1–15

Box GEP, Jenkins GM (1976) Time series analysis: forecasting and control. Holden Day, San Francisco, 553 pp

Briffa KR, Jones PD (1990) Basic chronology statistics and assessment. In: Cook ER, Kairiukstis LA (eds) Methods of dendrochronology: applications in the environmental sciences. International Institute for Applied Systems Analysis, Kluwer Academic Publishers, Boston, pp. 137–152

Cook ER (1985) A time series analysis approach to tree ring standardization. PhD Dissertation, University of Arizona, Tucson, 185 pp

Cook ER (1990) Bootstrap confidence intervals for red spruce ring-width chronologies and an assessment of age-related bias in recent growth trends. Can J Forest Res 20: 326–1331

Cook ER, Cole J (1991) Predicting the response of forests in eastern North America to future climatic change. Climatic Change 19:271–282

Cook ER, Johnson AH (1989) Climate change and forest decline: a review of the red spruce case. Water Air Soil Poll 48:127–140

Cook, ER, Peters K (1981) The smoothing spline: a new approach to standardizing forest interior tree-ring width series for dendroclimatic studies. Tree-Ring Bull 41: 43–53

Cook ER, Meko DM, Stahle DW, Cleaveland MK (1999) Drought reconstructions for the continental United States. J Climate 12:1145–1162
Cook ER, Glitzenstein JS, Krusic PJ, Harcombe PA (2001) Identifying functional groups of trees in west Gulf Coast forests (USA): a tree-ring approach. Ecol Appl 11(3): 883–903
Cropper JP (1982a) Comment on climate reconstructions from tree rings. In: Hughes MK, Kelly PM, Pilcher JR, LaMarche VC Jr (eds) Climate from tree rings. Cambridge University Press, Cambridge, pp 65–67
Cropper JP (1982b) Comment on response functions. In: Hughes MK, Kelly PM, Pilcher JR, LaMarche VC Jr (eds) Climate from tree rings. Cambridge University Press, Cambridge, pp 47–50
Cropper JP, Fritts HC (1982) Density of tree-ring grids in western North America. Tree-Ring Bull 42:3–10
de Jong AFM, Mook WG, Becker B (1979) Confirmation of the Suess wiggles 3200–3800 BC. Nature 280:48–49
DeWitt E, Ames M (1978) Tree-ring chronologies of eastern North America. Chronology series IV, vol 1. Laboratory of Tree-Ring Research, University of Arizona, Tucson, Arizona, 42 pp + tables
D'Odorico P, Revelli R, Ridolfi L (2000) On the use of neural networks for dendroclimatic reconstructions. Geophys Res Lett 27(6):791–794
Douglass AE (1946) Precision of ring dating in tree-ring chronologies. In: Laboratory of Tree-Ring Research Bulletin 3. University of Arizona Bull 17(3):1–21
Evans MN, Reichert BK, Kaplan A, Anchukaitis KJ, Vaganov EA, Hughes MK, Cane MA (2006) A forward modeling approach to paleoclimatic interpretation of tree-ring data. J Geophys Res-Biogeosci 111:G03008. doi:10.1029/2006JG000166
Fekedulegn BD, Colbert JJ, Hicks RR Jr, Schuckers ME (2002) Coping with multicollinearity: an example on application of principal components regression in dendroecology. Research paper NE-721. U.S. Department of Agriculture, Forest Service, Northeastern Research Station, Newtown Square, Pennsylvania, 43 pp
Feynman RP (1999) The relation of science and religion. In: The pleasure of finding things out. Helix Books, Perseus, Cambridge, Massachusetts, pp 245–257
Fowler A (1998) XMATCH98: an interactive tree-ring crossdating program. Occasional paper 38. University of Auckland, Department of Geography, pp 1–29
Fritts HC (1963) Computer programs for tree-ring research. Tree-Ring Bull 25(3–4):2–7
Fritts HC (1965) Tree-ring evidence for climatic changes in western North America. Mon Weather Rev 93(7):421–443
Fritts HC (1969) Bristlecone pine in the White Mountains of California. Growth and ring-width characteristics. Papers of the Laboratory of Tree-Ring Research 4. University of Arizona Press, Tucson, Arizona, pp 1–44
Fritts HC (1971) Dendroclimatology and dendroecology. Quaternary Res 1(4):419–449
Fritts HC (1976) Tree rings and climate. Academic, London, 567 pp
Fritts HC, Shashkin AV (1995) Modeling tree-ring structure as related to temperature, precipitation, and day length. In: Lewis TE (ed) Tree rings as indicators of ecosystem health. CRC, Boca Raton, pp 17–57
Fritts HC, Shatz DJ (1975) Selecting and characterizing tree-ring chronologies for dendroclimatic analysis. Tree-Ring Bull 35:31–40
Fritts HC, Vaganov EA, Sviderskaya IV, Shashkin AV (1991) Climatic variation and tree-ring structure in conifers: empirical and mechanistic models of tree-ring width, number of cells, cell size, cell-wall thickness and wood density. Climate Res 1(2):97–116
Fritts HC, Shashkin A, Downes GM (1999) A simulation model of conifer ring growth and cell structure. In: Wimmer R, Vetter RE (eds) Tree-ring analysis: biological, methodological, and environmental aspects. CABI, Oxon, UK, pp 3–32
Ghent AW (1952) A technique for determining the year of the outside ring of dead trees. Forest Chron 28(4):85–93

Gordon GA, LeDuc SK (1981) Verification statistics for regression models. Seventh conference on probability and statistics in atmospheric sciences, Monterey, California, USA
Gray BM, Wigley TML, Pilcher JR (1981) Statistical significance and reproducibility of tree-ring response functions. Tree-Ring Bull 41:21–35
Graumlich LJ (1993) Response of tree growth to climatic variation in the mixed conifer and deciduous forests of the upper Great Lakes region. Can J Forest Res 23:133–143
Guiot J (1991) The bootstrapped response function. Tree-Ring Bull 51:39–41
Guiot J, Berger AL, Munaut AV (1982) Response functions. In: Hughes MK, Kelly PM, Pilcher JR, LaMarche VC (eds) Climate from tree rings. Cambridge University Press, Cambridge, UK, pp 38–45
Guiot J, Keller T, Tessier L (1995) Relational databases in dendroclimatology and new non-linear methods to analyse the tree response to climate and pollution. In: Ohta S, Fujii T, Okada N, Hughes MK, Eckstein D (eds) Tree rings: from the past to the future. Proceedings of the international workshop on Asian and Pacific dendrochronology. Forestry and Forest Products Research Institute Scientific Meeting Report, vol 1, pp 17–23
Guttman L (1954) Some necessary conditions for common-factor analysis. Psychometrika 19: 149–161
Hatcher MJ, Tofts C (2004) Reductionism isn't functional. Unpublished paper. Trusted Systems Laboratory, HP Laboratories, Bristol. www.hpl.hp.com/techreports/2004/HPL-2004-222.pdf
Heikkenen HJ (1984) Tree-ring patterns: a key-year technique for cross-dating. J Forest 82: 302–305
Holmes RL (1983) Computer-assisted quality control in tree-ring dating and measurement. Tree-Ring Bull 43:69–78
Huber B (1943) Über die Sicherheit jahrringchronologische Datierung (On the accuracy of dendrochronological dating). Holz als Roh und Werkstoff, 6(10/12):263–268
Hurvich CM, Tsay CL (1989) Regression and time series modeling in small samples. Biometrika 76:297–307
Huth P (2005) Personal communication on an updated history of gypsy moth defoliation in Ulster County, New York. Daniel Smiley Research Center, Mohonk Preserve, Mohonk Lake, New Paltz, New York
Jolliffe IT (1973) Discarding variables in a principal component analysis II: real data. Appl Stat 22:21–31
Jones RH (1985) Time series analysis—time domain. In: Murphy AH, Katz RW (eds) Probability, statistics and decision making in the atmospheric sciences. Westview, Boulder, Colorado, pp 223–259
Kaiser HF (1960) The application of electronic computers to factor analysis. Educ Psychol Meas 20:141–151
Kozlowski TT, Kramer PJ, Pallardy SG (1991) The physiological ecology of woody plants. Academic, London, 657 pp
LaMarche VC Jr, Harlan TP (1973) Accuracy of tree-ring dating of bristlecone pine for calibration of the radiocarbon time scale. J Geophys Res 78(36):8849–8858
Laughlin RB (2005) A different universe: remaking physics from the bottom down. Basic Books, New York
Laughlin RB, Pines D (2000) The theory of everything. Proc Natl Acad Sci USA 97:28–31
Linick TW, Suess HE, Becker B (1985) La Jolla measurements of radiocarbon on south German oak tree ring chronologies. Radiocarbon 27(1):20–30
Mitchell JM Jr, Dzerdzeevskii B, Flohn H, Hofmeyr WL, Lamb HH, Rao KN, Walléen CC (1966) Climatic change. WMO technical note no 79
Morrison DF (1976) Multivariate statistical methods, 2nd edn. McGraw-Hill, New York
Ni F, Cavazos T, Hughes MK, Comrie AC, Funkhouser G (2002) Cool-season precipitation in the southwestern USA since AD 1000: comparison of linear and nonlinear techniques for reconstruction. Int J Climatol 22:1645–1662

Pederson N, Cook ER, Jacoby GC, Peteet DM, Griffin KL (2004) The influence of winter temperatures on the annual radial growth of six northern range margin tree species. Dendrochronologia 22:7–29

Pilcher JR, Baillie MGL, Schmidt B, Becker B (1984) A 7272-year tree-ring chronology for western Europe. Nature 312(5990):150–152

Preisendorfer RW (1988) Principal component analysis in meteorology and oceanography. Elsevier Science, Amsterdam, 426 pp

Preisendorfer RW, Zwiers FW, Barnett TP (1981) Foundations of principal components selection rules. SIO reference series 81-4, Scripps Institution of Oceanography, La Jolla, California, USA, 192 pp

Read J, Busby JR (1990) Comparative responses to temperature of the major canopy species of Tasmanian cool temperate rainforest and their ecological significance. II. Net photosynthesis and climate analysis. Aust J Bot 38:185–205

Rencher AC, Pun FC (1980) Inflation of R^2 in best subset regression. Technometrics 22:49–53

Schulman E (1956) Dendroclimatic changes in semiarid America. University of Arizona Press, Tucson, 142 pp

Schweingruber FH, Bräker OU, Schär E (1987) Temperature information from a European dendroclimatological sampling network. Dendrochronologia 5:9–33

Schweingruber FH, Eckstein D, Serre-Bachet F, Bräker OU (1990) Identification, presentation and interpretation of event years and pointer years in dendrochronology. Dendrochronologia 8:9–38

Shashkin AV, Vaganov EA (1993) Simulation model of climatically determined variability of conifers' annual increment (on the example of common pine in the steppe zone). Russ J Ecol 24:275–280

Smiley D, Huth P (1982) Gypsy moth defoliation in vicinity of Mohonk Lake 1956–1981. Unpublished research report. Mohonk Preserve, Inc

Snee RD (1977) Validation of regression models: methods and examples. Technometrics 19: 415–428

Stokes MA, Smiley TL (1968) An introduction to tree-ring dating. University of Chicago Press, Chicago, Illinois, 73 pp

Suess HE (1965) Secular variations of the cosmic-ray-produced carbon-14 in the atmosphere and their interpretation. J Geophys Res 70:5937–5952

Trumbore S, Gaudinski JB, Hanson PJ, Southon JR (2002) Quantifying ecosystem-atmosphere carbon exchange with a 14C label. Eos 83:265, 267–268

Tukey JW (1977) Exploratory data analysis. Addison-Wesley, London, 688 pp

Twain M (1924) Mark Twain's autobiography, vol 1. Harper & Brothers, New York, 368 pp

Vaganov EA, Hughes MK, Kirdyanov AV, Schweingruber FH, Silkin PP (1999) Influence of snowfall and melt timing on tree growth in subarctic Eurasia. Nature 400:149–151

Vaganov EA, Hughes MK, Shashkin AV (2006) Growth dynamics of tree rings: images of past and future environments. Springer-Verlag, Berlin, Heidelberg, New York

Visser H, Molenaar J (1988) Kalman filter analysis in dendroclimatology. Biometrics 44(4): 929–940

Wigley TML, Briffa KR, Jones PD (1984) On the average value of correlated time series, with applications in dendroclimatology and hydrometeorology. J Clim Appl Meteorol 23:201–213

Wigley TML, Jones PD, Briffa KR (1987) Cross-dating methods in dendrochronology. J Archaeol Sci 14:51–64

Woodhouse CA (1999) Artificial neural networks and dendroclimatic reconstructions: an example from the Front Range, Colorado, USA. Holocene 9(5):521–529

Yamaguchi DK (1991) A simple method for cross-dating increment cores from living trees. Can J Forest Res 21:414–416

Yamaguchi DK (1994) More on estimating the statistical significance of cross-dating positions for 'floating' tree-ring series. Can J Forest Res 24(2):427–429

Yamaguchi DK, Allen GA (1992) A new computer program for estimating the statistical significance of cross-dating positions for 'floating' tree-ring series. Can J Forest Res 22(9):1215–1221

Chapter 5
A Closer Look at Regional Curve Standardization of Tree-Ring Records: Justification of the Need, a Warning of Some Pitfalls, and Suggested Improvements in Its Application

Keith R. Briffa and Thomas M. Melvin

Abstract Some background describing the rationale and early development of regional curve standardization (RCS) is provided. It is shown how, in the application of RCS, low-frequency variance is preserved in the mean values of individual series of tree indices, while medium-frequency variance is also preserved in the slopes. Various problems in the use of the RCS approach are highlighted. The first problem arises because RCS detrending removes the average slope (derived from the data for all trees) from each individual tree measurement series. This operation results in a pervasive 'trend-in-signal' bias, which occurs when the underlying growth-forcing signal has variance on timescales that approach or exceed the length of the chronology. Even in a long chronology (i.e., including subfossil data), this effect will bias the start and end of the RCS chronology. Two particular problems associated with the use of RCS on contemporaneously growing trees, which might represent a typical (i.e., modern) sample, are also discussed. The first is the biasing of the RCS curve by the residual climate signal in age-aligned samples and the undesirable subsequent removal of this signal variance in RCS application. The second is the 'differing-contemporaneous-growth-rate' bias that effectively imparts a spurious trend over the span of a modern chronology. The first of these two can be mitigated by the application of 'signal-free' RCS. The second problem is more insidious and can only be overcome by the use of multiple sub-RCS curves, with a concomitant potential loss of some longer-timescale climate variance. Examples of potential biasing problems in the application of RCS are illustrated by reference to several published studies.

K.R. Briffa (✉)
Climatic Research Unit, University of East Anglia, Norwich, NR4 7TJ, UK
e-mail: k.briffa@uea.ac.uk

M.K. Hughes et al. (eds.), *Dendroclimatology*, Developments in Paleoenvironmental Research 11, DOI 10.1007/978-1-4020-5725-0_5,

Further implications and suggested directions for necessary further development of the RCS concept are discussed.

Keywords Dendrochronology · Regional curve standardization · Low-frequency variance · Chronology bias · Signal-free regional curve standardization

5.1 Introduction

Among those high-resolution environmental proxies that have the potential to express aspects of climate variability with perfect dating fidelity, at annual resolution, tree-ring records remain unique in the way in which they provide information continuously spanning centuries to millennia over vast swathes of the world's extra-tropical land areas. In general, this information is most accurate in its representation of short-timescale variability; i.e., relative changes from year to year and decade to decade. It is in this high-frequency part of the variance spectrum that chronology confidence can be quantified most easily, and the empirical calibration of tree-ring chronologies, routinely achieved by regression against observed climate variability, can be more accurately facilitated and subjected to rigorous verification through comparison with independent data (Fritts 1976, Section 5.4; Fritts and Guiot 1990; Briffa 1999).

Tree-ring data series, extracted from radial tree-growth measurements, may contain information about external growth influences on multidecadal, centennial, and even longer timescales. The expression of this information in individual series of measurements is, however, obscured by trends associated with changing tree geometry over time. In localized site chronologies and in large regional average chronologies, the expression and reliability of long-timescale variance is affected by the techniques used to 'standardize' the measurements to mitigate non-climate effects and by the manner in which the resulting standardized indices are incorporated within the final chronology. In this discussion, for convenience, we define medium-frequency variability as that representing timescales of decades up to the age of a tree. We define low-frequency variability as that manifested at timescales beyond the age of a tree.

We begin this review by citing a simple example that demonstrates why, where the intention is to recover evidence of long-timescale climate variability in chronologies, it is inappropriate to use common 'data-adaptive' standardization techniques (Cook et al. 1995). We also show how the presence of medium-frequency common tree-growth influences can create distortion in the recovered climate signal, particularly at the ends of chronologies standardized by using flexible curve-fitting techniques.

We provide some background to the history and simple application of what is known today as regional curve standardization (RCS), a standardization approach that has the potential to preserve the evidence of long-timescale forcing of tree growth. We discuss a number of potential biases that arise in the simple application

of RCS. We provide some illustrative examples of potential bias issues that have arisen in selected applications of RCS in previous published work. Finally, we suggest some ways in which the potential problems we have highlighted might be addressed in future work.

5.2 Frequency Limitation in Curve-Fitting Standardization

We now know that some types of tree-ring standardization are not ideal where there is a specific requirement to compare the growth rates of trees over long periods of time. The fitting of linear or curvilinear functions, or even more flexible forms of low-pass filtering, to series of individual growth measurements and the subsequent removal of variance associated with these trends, results in the inevitable loss of longer-timescale information, even in relatively long measurement series; i.e., the so-called segment length curse (Briffa et al. 1992; Cook et al. 1995).

As an illustration of the loss of low-frequency variance incurred by fitting functions through measured growth parameter series, we show Fig. 5.1, based on Fig. 1 in Cook et al. (1995). This figure shows the 'standardization' of a pseudo-climate signal comprising the arithmetic sum of three sine waves (with periods of 250, 500, and 1000 years, each with an amplitude of two units, plotted with their phases synchronized so the curves coincide every 500 years), achieved, in the original work,

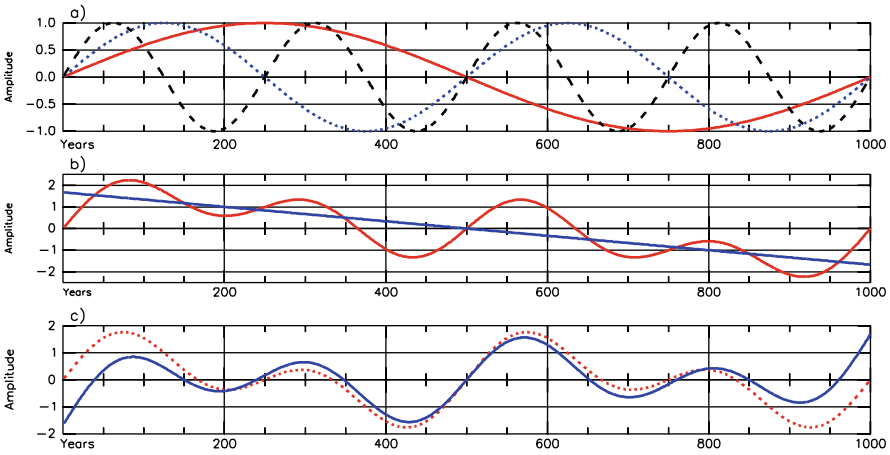

Fig. 5.1 An example of the loss of long-timescale variance resulting from simple data-adaptive standardization (in this case, linear detrending), based on the example of Fig. 1 in Cook et al. (1995): (**a**) three sine waves with periods of 1000, 500, and 250 years; (**b**) the ideal 'signal' series made as a composite of the three sine waves. A linear trend line is shown fitted through these data; (**c**) indices generated by division of the signal series values by those of the trend line (*solid line*) and a composite of the original 500- and 250-year sine waves (*dashed line*), showing the distortion apparent near the ends of the 'chronology'

by subtraction of the values of a straight line fitted through the single composite series. The loss of the original 1000-year trend in the resulting index series is plain. However, what is also clear is that the higher-frequency variance represented by the sum of the two shorter-period sine waves (dotted line in Fig. 5.1c) has been severely distorted at both ends of the chronology (compare the dotted and solid lines in Fig. 5.1c). This distortion comes about because of the localized influence of the medium-frequency signal variance at the beginning and end of the composite series on the overall fit of the standardizing line. Here the first and last values of the signal are both zero, while the first and last values of the indices are at their minimum and maximum, respectively. Had this example extended over another 500 years (i.e., 1500 years), the aggregate signal series would have had zero slope overall. Standardizing with a straight line fitted through the data would not produce any distortion of medium-frequency signal in the index series. This potential end-effect phenomenon, or 'trend distortion,' encountered in data-adaptive approaches to curve fitting in tree-ring standardization is discussed in more detail in Melvin and Briffa (2008). We return to this issue in the context of RCS later.

5.3 Background and Description of Regional Curve Standardization

The limitations in preserving evidence of long-timescale climate change in chronologies, led to the reintroduction of what is now generally known as regional curve standardization. This approach scales ring measurements by comparison against an expectation of growth for the appropriate age of ring for that type of tree in that region (Briffa et al. 1992). The tree-ring measurements acquired from multiple trees in one area are aligned by ring age (years from pith), and the arithmetic means of ring width for each ring age are calculated. The curve created from the mean of ring width for each ring age is smoothed by using a suitable mathematical smoothing function (Briffa et al. 1992; Esper et al. 2003; Melvin et al. 2007) to create smoothly varying RCS curve values for each ring age. In a simple application of RCS, each ring measurement is divided by the RCS curve value for the appropriate ring age to create a tree index (note in all cases subsequently discussed here, indices are created by division of the expected into measured values). Chronology indices are created as the arithmetic mean of tree indices for each calendar year. The value of the expected growth curve is, therefore, empirically derived as the average value, for that tree-growth parameter for the specific age of ring, based on the available sample of trees from that site or region. The reordering of the data, from calendar to relative life span age, is intended to remove the effect of climate variability on expected ring growth. In the reordered alignment of the data, this climate-related variance is assumed to be distributed randomly and expected to cancel out when the age-aligned data are averaged to form the RCS curve.

In standardization applications where the means of index series are constrained to be equal (e.g., approximately 1.0), a chronology formed by averaging these data is not capable of representing variance on timescales longer than the lengths of constituent series. The means of series of tree indices are not constrained in RCS,

and it is because the means of index series from different trees can vary through time, that the chronology constructed from them can exhibit long-timescale variance at periods up to the length of the chronology or beyond (Briffa et al. 1992; Cook et al. 1995; Briffa et al. 1996).

The use of the curve formed by calculating mean ring width of radial measurements ordered by cambial age has a long history in forestry and dendroclimatic studies, and an earlier awareness of some of the problems associated with it can be recognized. In seeking to study past climate changes in California, Huntington (1914) used a curve of growth rate plotted against ring age, which included a correction for longevity because he recognized that older trees tended to grow more slowly, even when young, compared to others. In a study of the relationship between tree growth and climate in Sweden, Erlandsson (1936) calculated growth rate curves for specific age classes of trees at various locations and applied a correction factor to enable comparison of different age classes. Mitchell (1967) showed that the shape of the mean curve by ring age varied between species and for the same species in different geographical locations. Becker (1989) used trees from generally even-aged, living stands but selected a large number of stands with as wide a range of stand ages as possible in order to eliminate the effect of 'trends according to calendar years.' Dupouey et al. (1992) developed a mean growth by age curve to model and remove the age trend while retaining long-timescale variance. Briffa et al. (1992, 1996) introduced the term 'regional curve standardization' to describe the method in the specific context of attempting to recover long-timescale climate trends but used large numbers of subfossil trees, hoping to eliminate the problem of modern climate biasing the parameters of the RCS curve.

Nicolussi et al. (1995) examined how tree-growth rates change when they are quantified for a specific ring age class through time and discussed problems associated with the interpretation of these changes. Badeau et al. (1996) examined potential sources of bias in the use of regionally based age curves. Esper et al. (2002) used two different RCS curves to standardize tree measurements from a wide range of sites being analyzed together, and Esper et al. (2003) also examined other aspects of RCS implementation. Helama et al. (2005a) examined the effect of forest density on the shape of the RCS curve.

Since its recent reintroduction for dendroclimatic studies, there has been a resurgence in the application of RCS, and it has been adopted and sometimes adapted in dendroclimatic studies intended to capture long-timescale climate variance (e.g., Rathgeber et al. 1999a; Cook et al. 2000; Grudd et al. 2002; Helama et al. 2002; Melvin 2004; Naurzbaev et al. 2004; Büntgen et al. 2005; D'Arrigo et al. 2005; Linderholm and Gunnarson 2005; Luckman and Wilson 2005; Wilson et al. 2005)

5.4 Potential Biases in RCS

Previous discussions of the recent application of RCS make it clear that the advantage offered by this approach, in terms of its potential to represent long-timescale variability in chronologies, must be weighed against the likelihood of large uncertainty associated with this information. Fritts (1976, p. 280) pointed out

problems with the use of RCS when he stated, '. . . all individuals of a species rarely attain optimum growth at the same age, and individual trees differ in their growth rates because of differences in soil factors, competition, microclimate, and other factors governing the productivity of a site.'

In practice, the simple application of RCS as described above makes sweeping assumptions about the validity of using a single, empirically derived curve to represent 'expected' radial tree growth as a function of tree age under constant climate conditions, and that this simple curve is an appropriate benchmark for scaling measured ring widths throughout the entire time span of a chronology. It is assumed that the mean of tree-growth deviations from this expectation, as observed in multiple tree samples at any one time, represents the net tree-growth response to variations in climate forcing alone. It is assumed that the form of the RCS curve is unbiased by the presence of residual climate variability in the stacked average of cambial-age-aligned samples, and that through time the growth of sample trees is not biased by some factors other than climate that would lead to a misinterpretation of the RCS chronology variability. In practice, these assumptions are unlikely to be entirely valid. The purpose of this review is to draw attention to several examples of how different potential sources of bias can affect RCS chronologies.

5.4.1 'Trend-in-Signal' Bias

The first distortion of underlying common forcing signal occurs in RCS when that signal has variance on timescales that approach or are longer than the length of the chronology. As a hypothetical example, let us say that the climate affecting tree growth has a trend over 600 years (Fig. 5.2a; actually, this series represents a negative trend with added white noise smoothed with a 10-year spline to represent short-timescale climate forcing superimposed on the long-term forcing trend). This signal series can be subdivided into five 200-year-long series, each overlapping by 100 years, to represent a set of pseudo-tree-ring measurement series (Fig. 5.2b). Aligning these series by ring age (Fig. 5.2c), averaging and smoothing, produces the RCS curve (shown in Fig. 5.2d). This RCS curve displays the mean slope of all sample series. As they all contain the underlying long-term forcing signal, the RCS curve must do likewise. Each sample measurement series is then indexed by dividing by the appropriate age value of the RCS curve. Each of the resulting standardized series (Fig. 5.2e) has no substantial overall trend (i.e., the mean series of the age-aligned index series has zero trend).

When the index series are realigned by calendar year, each series systematically underestimates the magnitude of the ideal forcing in its early section and overestimates the signal later, a potential medium-frequency bias. In the average chronology (Fig. 5.2f), the original overall signal trend is captured by the differences in the means of the index series. In our simplified example, the bias in the trends of individual index series cancel to some extent by virtue of the compensating biases in overlaps between early sections of some index series and late sections of others. In

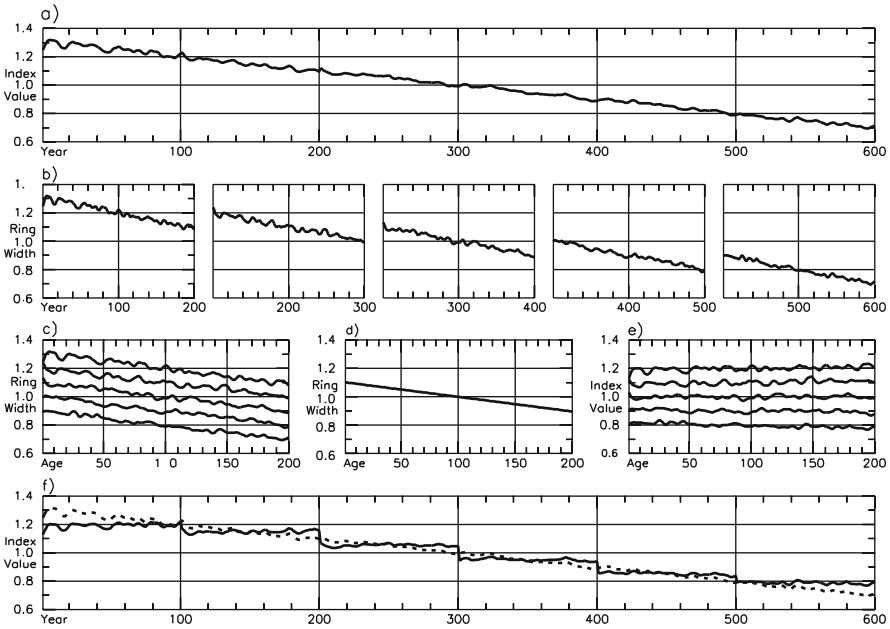

Fig. 5.2 A schematic representation of how the simple regional curve standardization (RCS) recovers long-timescale trend from the mean values of index series but with potential distortions within, and particularly at the ends, of the chronology: (**a**) an idealized chronology signal composed of an overall negative slope with superimposed medium-frequency variance; (**b**) five overlapping 200-year-long series representing simulated measurements; (**c**) the five series aligned by ring age; (**d**) the smoothed RCS curve generated by averaging these series; (**e**) the series of indices generated through division by the RCS curve; (**f**) the averages of these indices that make up the resultant chronology (*solid line*), which is shown superimposed on the ideal chronology (*dashed line*)

situations where there is a good overlap in many series, this potential bias could be averaged out. However, this cannot happen at the start and end of the chronology. In the case of a long-term declining signal, the chronology will, respectively, under- and overestimate the ideal chronology at the beginning and end. With a long-term positive forcing trend, the signs of the biases will be reversed.

Figure 5.3 illustrates a somewhat more realistic example of this problem than that shown in Fig. 5.2. The underlying forcing signal that is used here is similar to that used in Fig. 5.1, but rescaled to resemble ring measurements (white noise with mean of 1.0 and range ±5% was smoothed with a 10-year low-pass filter added to the three sine waves, each of which has an amplitude of 0.34). This aggregated sine wave signal series was sub-sampled to produce forty-one 334-year pseudo-measurement series. Their start dates are evenly distributed between year 1 and year 668, providing the potential for a 1002-year chronology with a maximum replication of 20 series (see shaded area in Fig. 5.3d). Figure 5.3a shows five of the sample series. Figure 5.3b shows the average of age-aligned measurements of all

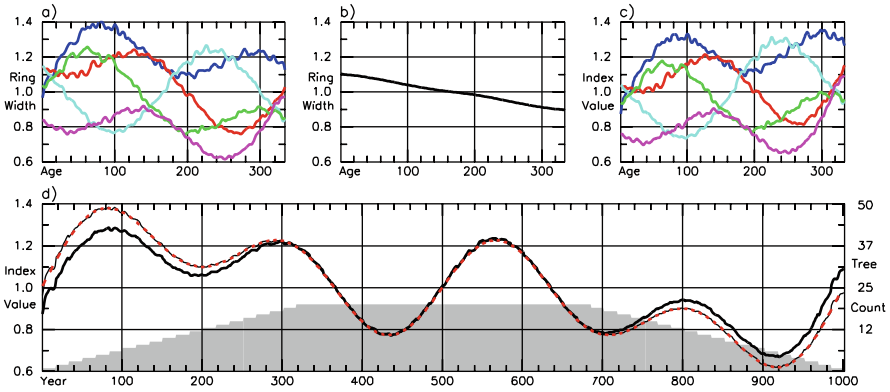

Fig. 5.3 An example of the use of regional curve standardization (RCS) where the 'signal' is the same composite of the three sine waves shown in Fig. 5.1a: (**a**) five sample series; (**b**) smoothed, mean RCS curve of all 41 series; (**c**) indices of the five example series created by division with the RCS curve; (**d**) the ideal chronology (*dashed line*; as in Fig. 5.1b), the RCS chronology (*thick line*) with 'trend-in-signal' bias apparent at the start and end of the chronology. Sample counts are shown by *grey shading*. A substantially undistorted recovery of the 1000-year trend (*thin line*), and the variance associated with the shorter-period sine waves is achieved in using the 'signal-free' approach discussed in the Appendix

41 series, and Fig. 5.3c shows the same five example series from Fig. 5.3a, after standardization with the average RCS curve. Figure 5.3d shows how the medium- and long-term trends in the underlying forcing are relatively well represented in the RCS chronology. The loss of long-timescale signal apparent in Fig. 5.1c does not occur in Fig. 5.3d. However, the systematic under- and overrepresentation of the aggregate signal (in years 1 to 300 and 700 to 1002, respectively) results from the trend-in-signal bias, similar to the biased representation of the medium-frequency signal shown in Fig. 5.1c. The trend-in-signal bias is generally manifested as an end-effect problem in both RCS and curve-fitting standardization. However (because trend distortion is the result of slope removal), while in the latter case the entire slope of an individual-tree measurement series is removed, in the case of RCS, only the mean slope over the whole length of the chronology is removed (i.e., implying a much smaller-scale problem of overall trend distortion in RCS).

Note that by applying the recently advocated 'signal-free' method of standardization (see Appendix), this problem may largely be mitigated in the RCS. For example, when applied to the data in Fig. 5.3, this approach is able to capture all of the long-timescale variance and it does so without producing this end-effect bias. For these equal-length, artificial series, the 'ideal' chronology signal is recovered without distortion as shown by the blue curve of Fig. 5.3c. However, it is important to stress that in this highly artificial example, all of the index series have the correct means and amplitude of variance, perfectly matching the hypothesized signal. In a 'real-world' situation, random variation in growth rates of trees would prevent such a perfect result.

5.4.2 'Differing-Contemporaneous-Growth-Rate' Bias

The second potential end-effect bias arises because, even within one region, there is often a variation in the growth rates of contemporaneously growing trees. The problem that a single RCS curve may not be relevant for trees with widely varying growth rates has been widely recognized (e.g., Erlandsson 1936; Nicolussi et al. 1995; Briffa et al. 1996; Rathgeber et al. 1999a; Esper et al. 2002). In a restricted geographical range where trees might be expected to experience the same regional climate, localized elevation or aspect differences can lead to variations in the climates of specific tree locations. Even where trees do experience the same common history of climate forcing during their lifetime, invariably, some trees will exhibit greater or less radial growth than others because they are influenced by non-climatic factors such as differences in soil quality or competition for light or other resources. A simple RCS approach uses a single (average) model of expected tree growth (e.g., radial ring increment or maximum latewood density) as a function of tree age, applied to all trees in one region. If trees are drawn from a wide region or one with diverse ecological conditions, differences in growth rate in contemporaneously growing trees is virtually inevitable. Within such a sample, the slope of a single average RCS curve will be systematically too shallow for relatively fast-growing trees and too steep for relatively slow-growing trees (Fig. 5.4).

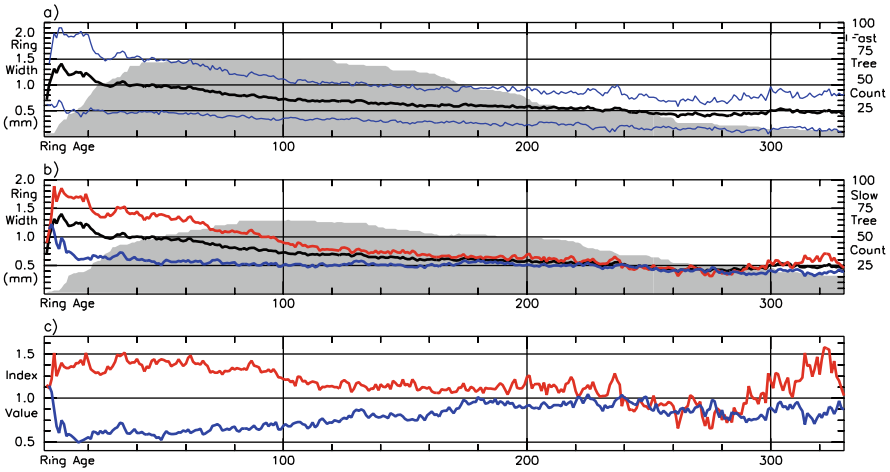

Fig. 5.4 Based on 207 measurement series, for which pith-offset estimates are available (Kershaw 2007), from the AD portion of the Swedish Torneträsk chronology (Grudd et al. 2002): (**a**) curve of mean ring width by ring age, bracketed by thin lines showing the plus and minus one standard deviation limits of the mean values; (**b**) separate curves of mean ring width by ring age for all trees (*middle line*—as in **a**), the fastest-growing third of trees (*upper line*), and the slowest-growing third of trees (*lower line*); (**c**) mean ring width indices (produced by dividing the measurements by the appropriate age values on the overall-mean regional curve standardization curve), plotted by ring age for the fastest-growing third of trees (*upper line*) and the slowest-growing third of trees (*lower line*). The *gray shading* in (**a**) and (**b**) shows sample replication for the fastest- and slowest-growing trees, respectively, where rate of growth is based on time to reach 20 cm diameter

This mismatch is most apparent for the indices that are produced from earlier years of the tree lifetime, as the sub-RCS curves for fast- and slow-grown trees (Fig. 5.4b) often tend to a common value in old age and the corresponding index series, produced as quotients from the overall mean RCS curve, display a negative trend for the early years of a fast-grown tree and a positive trend in the early years of a relatively slow-grown tree (Fig. 5.4c). In an RCS chronology, if in one period fast-grown trees outnumber slow-growing trees (or vice versa), artificial medium-frequency trends (i.e., of non-climate origin) might result. It is at the recent end of a chronology that the influence of downsloping indices, derived from fast-growing trees, may not, in general, be balanced by the upsloping index series from slower-growing trees. The result, even under constant climate conditions, is an overall negative bias, seen in the final century or most recent decades of the chronology.

5.4.3 'Modern-Sample' Bias

The next bias we discuss has been referred to by Melvin (2004, Section 5.4) as 'modern-sample bias.' We consider this of sufficient importance to identify it as a specific potential bias in its own right, but it arises as a consequence of the previously discussed bias (i.e., because of different growth rates in contemporaneous trees) and because of variations in the longevity of trees, allied to common tree sampling practice.

A naturally grown, uneven-aged forest (even if growing in an unchanging climate) will contain trees of differing ages that have roughly the same diameter. The widths of rings of a specific age from trees of the same diameter must be smaller for the older trees than for the younger trees. A plot of mean ring width for a specific ring age plotted by calendar year for a specific sampling diameter range (i.e., only for trees of a similar diameter when cored) will display a steady increase over time, independent of any common climate signal. If samples are taken only from trees alive on the sampling date, then the mean growth rate by year (as the average of each diameter class for any specific age range, which all slope upwards) must also slope upwards.

5.4.3.1 Relationship Between Growth Rate and Longevity

This bias arises if there is a relationship between average tree growth rate and tree longevity and generally applies only to trees with full circumferential growth. If we assume that the probability of tree mortality is related to tree size—i.e., large trees have a high risk of mortality—then as trees approach the largest size for a given site, they are much more likely to be killed, perhaps because of some extreme climate event. Hence, the likelihood that some random extreme event will kill a tree is higher while it is in the 'near maximum' size category. Rapidly growing trees are more likely to approach or reach the maximum size than are slower growing trees because the former need only spend a shorter time in the 'high-risk' (i.e., approaching large)

size category (Melvin 2004, Section 5.4). To grow old, a tree must grow slowly and so remain for some considerable time, safely below the maximum size by some margin.

This, of course, is a great simplification of likely tree mortality influences. It takes no account of the competition dynamics of trees growing within forest stands; i.e., self-thinning processes (Dewar 1993). Nevertheless, there is some observational evidence, particularly when competition pressures are not strong, that to become old a tree might grow slowly (Huntington 1913). Figure 5.5 is an attempt to demonstrate this concept using subfossil pine ring width data from northern Fennoscandia (Eronen et al. 2002; Grudd et al. 2002). These wood samples provide data that span the last 7500 years, but here we have excluded any data from trees that were alive after 1724. This choice precludes any human sampling influence on the life span of trees. The retained data were used to produce a single RCS curve. The measurement data for each tree sample were then summed to provide an estimated diameter, and this diameter was compared to the mean regional diameter calculated from the appropriate age point of the RCS curve to give a relative growth rate (i.e., the ratio of tree diameter at its final year to the RCS curve diameter at that year). In this way, all the individual tree measurement series were grouped into eight relative growth classes and a sub-RCS curve was constructed for each relative class. The mean growth rate (millimeters per year) by age for these eight RCS curves is shown in Fig. 5.5a, and the decay in mean growth rate is due to the reduction of ring width with age. A tendency for higher growth-rate classes to have shorter life spans can

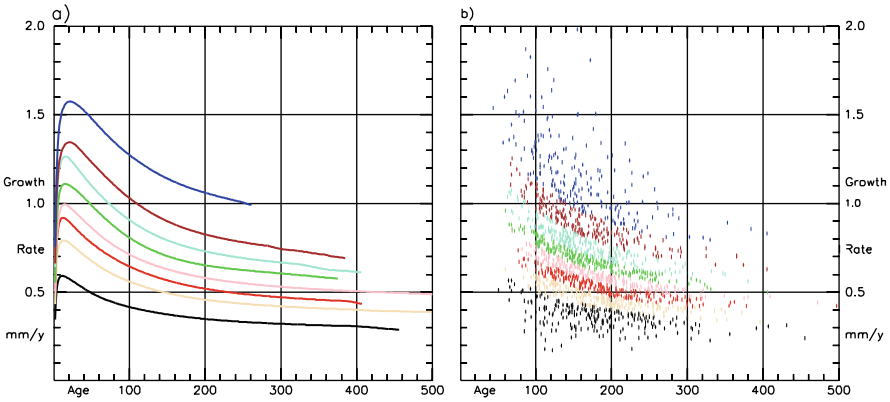

Fig. 5.5 Based on 1724 subfossil trees from Torneträsk (Grudd et al. 2002) and Finnish Lapland (Eronen et al. 2002) from the period circa 5400 BC to AD 1724; i.e., excluding trees that were alive after 1724 to avoid any anthropogenic factors and sampling bias: (**a**) all trees sorted by growth rate relative to a single regional curve standardization (RCS) curve, into eight separate RCS curves; (**b**) a scatter plot of mean growth rate for each tree plotted against final tree age. Scatter plot points are *shaded* to match their growth rate curve of (**a**). This figure illustrates the tendency for longevity to be inversely proportional to tree vigor

be discerned. Plotting the mean growth rates of individual samples by sample age (i.e., final tree diameter divided by final age) again reveals a tendency for slowly growing trees to live longer (Fig. 5.5b). The oldest trees have mean growth rates far lower than the reduction explained by the expected decrease of ring width with age shown in the curves of Fig. 5.5a. This occurs despite the fact that many subfossil tree samples lose outer rings because of erosion or degradation of the relatively soft sapwood.

5.4.3.2 Growth Rate/Longevity Association Distorts RCS Curves

Figure 5.6 illustrates a very simplified example of one distortion that occurs where a sample of even-sized (radius 26.4 cm) trees of varying age might be cored (Fig. 5.6a). Here there is an assumed constant climate forcing (horizontal dashed line of Fig. 5.6b) and the younger trees have progressively larger growth rates. The mean RCS curve is horizontal up until 240 years (the age of the youngest tree) but gets progressively lower as the lower growth rates of the older trees dominate. Thus this is a distortion of the RCS curve caused by older trees having lower growth rates. Hence individual index series aligned by calendar age then exhibit positive trends after 240 years (Fig. 5.6c), and the calendar-aligned averaged values (Fig. 5.6d) display an initial (stepped) increasing trend for the first 160 years of the mean chronology due to the oldest trees having slower growth rates, and a late increasing trend after 240 years because of distortion of the RCS curve, despite the fact that the

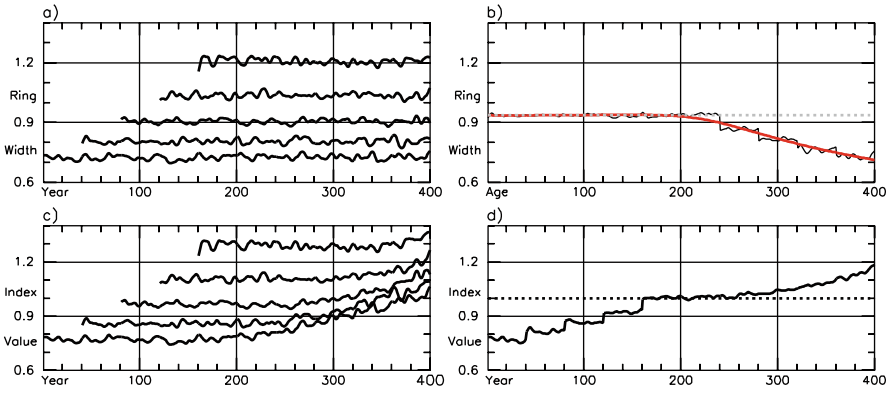

Fig. 5.6 A simple hypothetical example of the distortions to a common underlying forcing signal when a chronology is constructed by using regional curve standardization (RCS) applied to an uneven-aged group of similar-sized trees. (**a**) The measurements (mm.) from five trees of unequal length and of the same final diameter (26.4 cm), each containing the same trend in growth superimposed on the differing overall average growth. When aligned by ring age, the average RCS curve (**b**), instead of displaying the expected linear growth trend (*dotted line*) is distorted, showing narrower expected ring width for older trees. (**c**) Series of indices created through division of the simulated measurements by the RCS curve values, where all but the shortest series are distorted. (**d**) The chronology created by averaging the index series and the desired low-frequency signal (*dotted line*)

underlying forcing signal is constant. The constant mean growth rate is not realistic, but the bias shown will apply similarly to curvilinear declining ring series.

In order to demonstrate modern-sample bias, it is necessary to use series of tree indices that have no common climate signal and no common age-related growth trend. Here, 1724 trees from both Torneträsk (Grudd et al. 2002) and Finnish Lapland (Eronen et al. 2002) from the several-millennia period 5400 BCE to AD 1724 are used. Trees that were alive after 1724 are not included so as to avoid any anthropogenic factors or sample bias arising from the coring of living trees. The measurement data are all realigned so that their final growth years correspond (i.e., they are 'end-aligned' and the end year is nominally set to zero). The mean ring width of the subset of all 40- to 60-year-old rings from trees with a final radius between 12 and 14 cm (ring counts shown as gray shading) are plotted by nominal year for Fig. 5.7a. In order to reach the 12–14 cm final diameter class, the 40- to 60-year-old rings must be larger for the younger trees than in the older trees and this curve of mean ring width takes on a positive slope. Provided that there is some maximum size limit to tree growth, the sum of data for any, and hence all, size classes will also produce an upwardly sloping common signal. This bias occurs in the absence of any common climate signal, and is a result of random distribution of tree growth rates and the fact that sampling takes place at a specific point in time.

Figure 5.7b shows the yearly means of all RCS indices (based on a single RCS curve) after alignment by their final growth year (year zero). Even though these trees grew at various times over a 7000-year period, and should not, therefore, contain any common external growth-forcing signal when in this alignment, there is still evidence of a residual bias, represented by a general positive slope as tree counts increase followed by a slight decline in the final period, when tree counts remain constant. This decline is likely the result of indices of 'fast-growing' trees, with their typical negative slope (cf. Fig. 5.4), dominating over the weaker positive trend from 'slow-growing' trees.

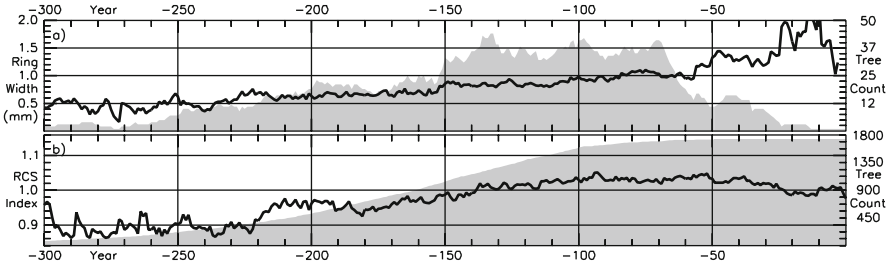

Fig. 5.7 Based on the same subfossil tree-ring dataset used in Fig. 5.5, but here with all individual series aligned on the final ring of each series (year zero): (**a**) the mean ring width of the subset of all 40- to 60-year-old rings from trees with a final radius between 12 and 14 cm; (**b**) indices, created using regional curve standardization (RCS), aligned according to their final year of growth (year zero) and averaged to form an 'end-aligned' chronology. Ring counts for each year are shown by the *gray shading*

This result demonstrates the strong likelihood of sampling bias implicit in analyses of ring width, density, or basal area increments, where the data are stratified within discrete age classes (e.g., Briffa et al. 1992; Nicolussi et al. 1995). Age band decomposition (ABD) as proposed by Briffa et al. (2001), although originally envisaged as a means of circumventing the need to define a statistical model of expected growth as a function of tree age, is in effect similar to applying RCS. This conclusion follows because the mean value for each age band, when plotted as a function of ring age, will form a stepped version of the RCS curve. In ABD, the mean value of the time series for each age band is subtracted from each average yearly value for that band, and these differences are divided by the standard deviation of the band time series to transform the data into normalized series. These series are then summed across all (or selected) age bands to form an ABD chronology. When this method is applied in this way to the data for a single species and location (e.g., see Briffa et al. 2001), it is similar to applying the RCS at a site level to a set of living-tree core samples. The results may, therefore, be affected by a modern-sample bias, bearing in mind the common practice of sampling dominant or codominant trees (Schweingruber and Briffa 1996).

Where this sampling bias exists, it is difficult to gauge the extent to which it amplifies or obscures the accompanying influence of climate variability. Note that in Fig. 5.7b, the range of the bias is only 0.14 units, likely considerably less than the range for typical chronology variances, for example, as is shown in Fig. 3 of Becker (1989) or in Fig. S4b of Esper et al. (2007), where chronologies display similar shapes (in their time variance) to that of the bias in Fig. 5.7b.

Figure 5.8 is a dramatic example of how the selection of samples, based on a minimum size criterion, can lead to a large potential bias at the ends of, even long subfossil, chronologies. Again we use measurement data provided by the ADVANCE-10 K project (Eronen et al. 2002; Grudd et al. 2002), this time including all subfossil (from lakes and dry land) and modern core data for the last 2000 years. These (more than 1000) sample series were combined to produce an RCS chronology (based on a single RCS curve) shown as the solid black line in Fig. 5.8a, with the temporal distribution of the sample series shown by gray shading. The data were sub-sampled to simulate eight hypothetical samplings during the last 2000 years, separated by 200-year intervals, the most recent of which was in the year 1980. Only trees that would have been alive and that had achieved a minimum diameter of 14 cm are included in each subsample. The subsamples form a large proportion (43%) of all rings. This is a realistic simulation of common dendroclimatic sampling strategies.

The temporal distribution of each ‘sampled’ group of trees is shown in Fig. 5.8b. The eight individual sub-chronologies, each produced as the average of the index series generated in the production of the overall mean RCS chronology, are shown superimposed on the RCS chronology produced from all 1024 series. The sub-chronologies generally underestimate the mean chronology in their early years (mainly composed of older and generally slower-growing trees) and overestimate the overall chronology in their later years (when the younger, more vigorous trees dominate the sample). This result demonstrates that sampling bias, when allied

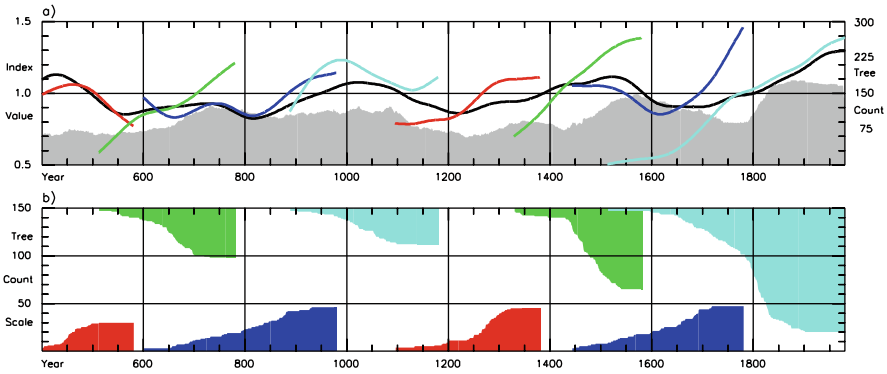

Fig. 5.8 Based on 1024 trees from AD portions of the Torneträsk and Finnish Lapland chronologies. (**a**) The simple regional curve standardization (RCS) chronology (*black line*) and associated tree counts (*gray shading*), truncated before AD 400. Simulated 'modern sample type' chronologies were created by averaging eight selected groups of tree indices (all produced by using the same single RCS curve and only where sample counts exceed 2). Each sub-chronology is made up of samples that would have been collected by using modern sampling practice with selections made on a series of specific dates (the first is AD 580 and subsequent selections are made every 200 years until 1980) and only including trees alive and with a diameter greater that 14 cm on the sampling date. (**b**) *Shaded areas* showing sample counts by year for each simulated chronology, plotted alternatively from the bottom and top of the figure for clarity. Approximately 43% of the total ring measurements are included in the 'selected' samples

with the growth rate/longevity phenomenon, imparts negative bias in the start of a chronology and positive bias in the recent period. The systematic continuous overlaps between slower- and faster-grown trees in this example compensate throughout the chronology for these biases. That is, of course, except for the early section and, most noticeably, in the most recent 100 years of the overall chronology, which appears to follow what is likely to be a biased trajectory due to an absence of small indices from young, slow-growing trees that would have gone on to become the early sections of old trees.

5.5 Particular Problems Associated with the Application of RCS to Modern (i.e., Living-Tree) Sample Data

In practice, the underlying assumption of RCS, that the averaging of measurement series aligned by ring age and subsequent smoothing of the resulting mean curve will remove all the climate-related variance, may not always be valid. This assumption cannot be true when all samples span the full length of the chronology. In such a case, the overall climate signal will be contained within the RCS curve and will be completely removed by standardization. In a modern chronology where trees are of unequal length, the average overall slope of the chronology is contained in the RCS curve and is thus removed from every tree in the final chronology. In a long

(i.e., partly subfossil) chronology, with long-timescale variation maintained in the means of each index series, this is an 'end effect.' However, where the chronology comprises one set of currently coexisting trees, as in many modern samples, the overall slope of the chronology representing the external (i.e., climate control of tree growth) will be removed. Had the chronology of Fig. 5.6 had an overall downward slope, the resultant chronology would still display an upward slope (due to modern-sample bias) because the downward slope of the chronology would be removed by RCS.

Even where an uneven-aged sample of trees covers a wide time span, a localized coincidence in the temporal spans of many samples at roughly the same stage in their life span will locally bias the RCS curve. This bias is more likely near the 'old-age' section of the RCS curve, where typical low replication of very old trees leads to greater uncertainty in the RCS curve. This bias is potentially large for modern chronologies and seriously limits the application of RCS where trees come from the same time period (Briffa et al. 1996).

In a typical 'modern' dendroclimatic sample collection, the earliest measurements will come from the oldest trees cored, which tend to be slow growing. Faster-growing trees that may have been contemporaneous with the old trees in the early years will likely not have survived long enough to be included in the modern sample. Similarly, the most recent section of the chronology produced from these sampled trees would not contain data from young, slow-growing trees because these trees would not be of sufficient diameter to be considered suitable for coring. Any relatively young trees sampled would likely have to have been vigorous and growing quickly enough to allow them to attain a reasonable size in a short time. This leads to a situation where a 'modern sample' may exclude the fastest-growing trees of the earliest period and also exclude the slowest-growing trees of the most recent period. Such a sample of uneven-aged trees will be less susceptible to trend-in-signal bias, but still prone to contemporaneous-growth-rate bias, with smaller indices at the start of the chronology and larger ones at the end, imparting a positive bias on the overall chronology slope.

Figure 5.9 illustrates the use of RCS on a 'modern' chronology and the way in which a recent (ca. 1920) increase in the radial increments can influence the shape of the RCS curve. This set of 100 measurement series (each an average of data from multiple cores) from Luosto, north Finland (Melvin 2004, Section 3.2), has a wide age range. Pith-offset estimates are available for all of these data. First, an RCS curve and corresponding chronology were produced from them (thin lines in Fig. 5.9a,b). The signal-free method (see Appendix) was used to create an unbiased (signal-free) RCS curve and corresponding chronology (thick lines in Fig. 5.9a,b). The removal of the common signal from the measurements changes the shape of the RCS curve, removing the influence of the post-1920 growth increase from recent data (see values for ages 200–240 and 340 onwards in Fig. 5.9a) and produces a relative increase in the expectation of early growth (up to age 120), and a smoother, less noisy RCS curve. The resultant chronology will still suffer from bias (see Sections 5.4.1, 5.4.2 and 5.4.3), and the overall chronology slope is to some extent 'arbitrary' as described above. However, provided there is a wide distribution of tree

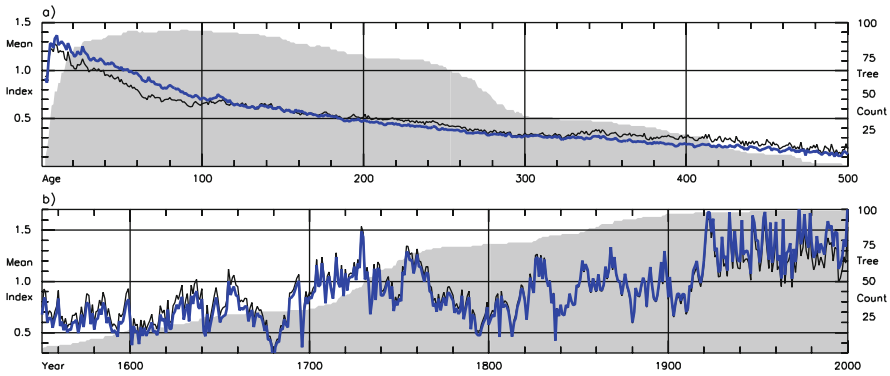

Fig. 5.9 An illustration of the use of regional curve standardization (RCS) on a 'modern' chronology and the influence on the shape of the RCS curve exerted by a recent (presumably warming related) growth rate increase. The 100 mean-tree series from Luosto, north Finland (Melvin 2004), which have a wide age range and include pith-offset estimates but, after 1920, also show a large growth increase are used here: (**a**) a simple RCS curve (*thin line*) and the 'signal-free' RCS curve (*thick line*) and (**b**) the corresponding simple RCS chronology (*thin line*) and 'signal-free' RCS chronology (*thick line*). *Gray shaded* areas show tree counts

ages, following the signal-free approach can mitigate the localized bias imparted by climate in the RCS curve without the need for large numbers of earlier subfossil tree data to 'average' away any modern climate signal.

Even the application of the signal-free technique is not able to mitigate the loss of the overall slope of the chronology, and a 'modern' chronology must therefore be considered as having a largely 'arbitrary' slope.

5.6 Examples of Issues that Arise in Various Applications of RCS

In this section, we discuss several examples of previous work, chosen here to illustrate 'potential' bias problems that are suggested by the way in which previous authors have chosen to implement, or could be interpreted as having implemented, first, simple RCS and then variations of the simple RCS. The three examples are based on work by Briffa et al. (1992), Esper et al. (2002), and Helama et al. (2005a, b).

5.6.1 Inappropriate RCS Definition

Briffa et al. (1992) constructed separate RCS curves for ring-width (TRW) and maximum-latewood-density (MXD) data aquired from temporally overlapping subfossil and living-tree pine samples from north Sweden. The chronologies spanned the 1480-year period from AD 501 to 1980. The ring-width RCS curve was built

from 425 samples, while the density data comprised measurements made on a subsample of 65 of these trees. Though both the ring-width and density chronologies spanned more than 1400 years, the greater replication of the data in the ring-width curve was considered more likely to have produced an 'unbiased' RCS curve (i.e., one that is not influenced by residual climate variance in the mean of the measurement data for any specific tree age). A curvilinear (negative exponential) curve was fitted to the ring width RCS curve, but a straight line was fitted to the density RCS curve (following Bräker 1981). The resulting ring-width and MXD RCS chronologies were found to diverge noticeably from each other after about 1800, with the density chronology exhibiting progressively lower index values. Briffa et al. (1992) 'corrected' this apparent anomaly by fitting a line through the residuals of actual minus estimated ring widths, derived from a regression using the density data over the period 501–1750 as the predictor variable, and then removing the recent apparent decline in the density chronology by adding the fitted straight line values

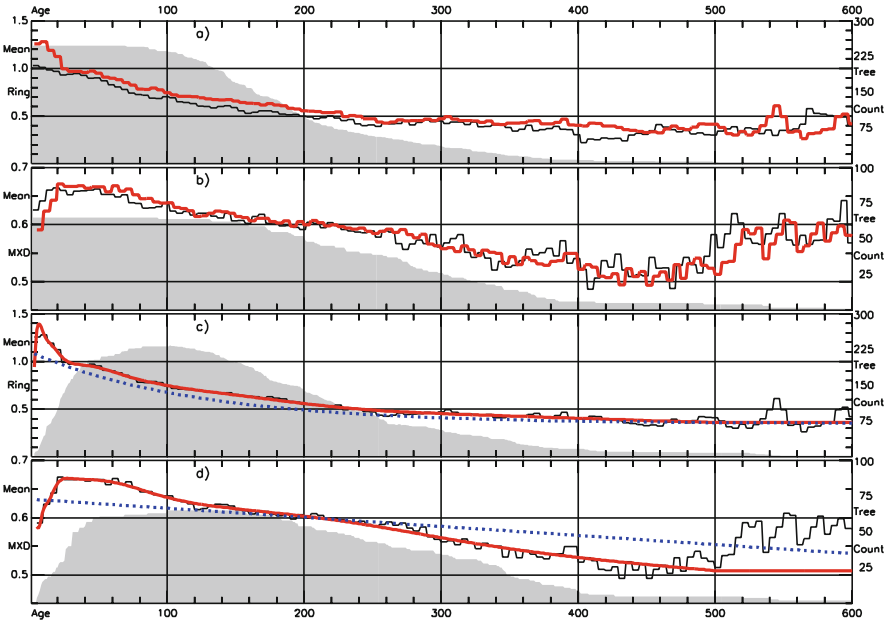

Fig. 5.10 Using the 207 ring width series (TRW) with pith-offset estimates (Kershaw 2007) from the AD portion of the Torneträsk chronology (Grudd et al. 2002) and 65 maximum latewood density series (MXD) from Torneträsk (Briffa et al. 1992): (**a**) curves of 5-year means of average TRW by ring age created without using pith-offset estimates (*thin line*) and using pith-offset estimates (*thick line*); (**b**) as (**a**) but using MXD; (**c**) 5-year means of TRW by ring age created by using pith-offset estimates (*thin line*), modified negative exponential curve fitted to the ring width means created without using pith-offset estimates (*dashed line*) and age-related spline (*thick line*), fitted to the first 500 years of ring width means and then linearly extended, created by using pith-offset estimates; (**d**) as (**c**) but using MXD. *Gray shading* shows ring counts by age without pith-offset estimates (**a** and **b**) and with pith-offset estimates (**c** and **d**)

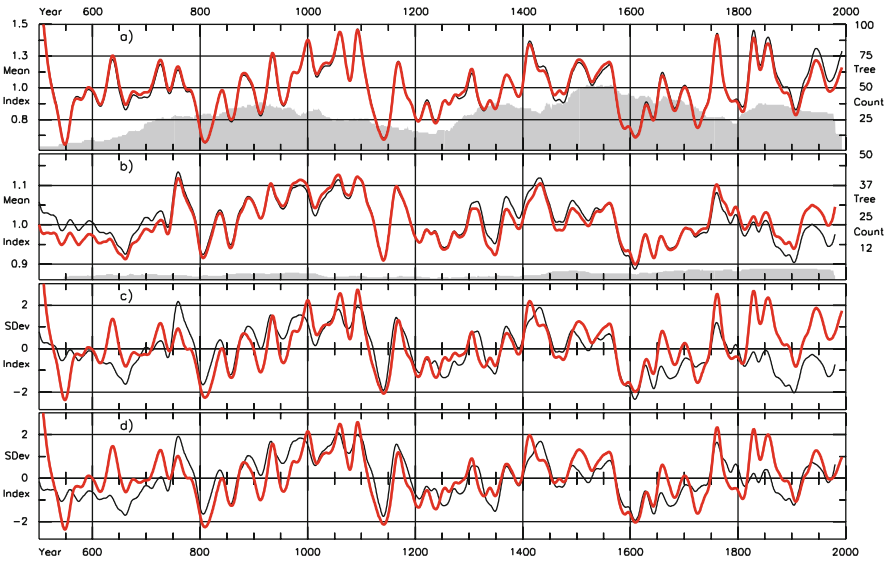

Fig. 5.11 Chronologies generated by using the measurement data and regional curve standardization (RCS) curves shown in Fig. 5.10: (**a**) ring width series (TRW) chronologies created without using pith-offset estimates and a negative-exponential RCS curve (*thin line*), and with pith-offset estimates and using age-related spline smoothed RCS curve (*thick line*); (**b**) maximum latewood density series (MXD) chronologies created without using pith-offset estimates and a linear RCS curve (*thin line*) and with pith-offset estimates and an age-related spline smoothed RCS curve (*thick line*); (**c**) chronologies created without using pith-offset estimates, and using a negative-exponential RCS curve for TRW (*thick line*) and a linear RCS curve applied to MXD (*thin line*); (**d**) chronologies created by using age-related spline smoothed RCS curves and pith-offset estimates for TRW (*thick line*) and MXD (*thin line*)

(with the sign reversed) to the chronology data for 1750–1980. This 'correction' has been termed the 'Briffa bodge' (Stahle, personal communication)! In Figs. 5.10 and 5.11, we show how this comparative anomaly in the density compared to the ring-width chronology arose, at least in part, because of an inappropriate representation of the density RCS curve. We use the same density data as used by Briffa et al. (1992) but use a subset of 207 ring-width measurement series from the original 425 series that were subsequently updated by Grudd et al. (2002). We have chosen to use this smaller set of measurement data because estimates of the pith offsets for these samples are now available (Kershaw 2007).

The new RCS curve (based on the smaller subset of measurements) for the ring-width data without pith-offset values (Fig. 5.10a) is effectively identical to that used in Briffa et al. (1992). With pith-offset values included, the RCS curve has a slightly higher juvenile growth-rate but tends to the same expected growth for old trees: the resulting RCS chronology (Fig. 5.11a) is not substantially different from that shown in Briffa et al. (1992), except that the 10-year-smoothed ring-width chronology is very slightly lower than that without pith estimates during the most recent 50 years. Figure 5.10d shows how the original linear RCS curve for the density data (dashed

line) was not a good fit to the measured data, systematically underestimating the juvenile values and overestimating the measured data for tree ages between 250 and 500. This situation arose because the linear fit was influenced by high-density values measured in relatively old-age trees, many of which experienced the relative warmth of the twentieth century in parallel in their later years. In other words, the climate signal (as represented in the final years of the chronology) was not averaged out in the later (oldest) section of the RCS curve. A more appropriate, unbiased RCS curve is derived (the thick line of Fig. 5.10d) by using a 'signal-free' approach where the chronology variance (i.e., the best estimate of the growth-forcing signal) is iteratively removed from the measurement series so that the resulting age-aligned averaged measurements contain substantially little or no variance associated with the common forcing (see Appendix, and Melvin and Briffa 2008).

The density chronology produced by using the new 'unbiased' RCS curve displays potentially higher values after about 1800, and much of the comparative recent decline in the density compared to ring width chronology is removed (Fig. 5.11d). The same correction could have been achieved in this case by excluding the longest-lived tree density samples or by fitting the RCS curve only on the data extracted from tree rings up to 500 years old and extrapolating the RCS curve to give RCS values for older trees. The relevant conclusion, however, is that it is important to use a nonbiased representation of the RCS curve. Where replication is low or when there are few samples representing the expected RCS values for old trees, and especially when the oldest rings are all from trees sampled in the same period (e.g., three of the four oldest trees in the Torneträsk MXD chronology were sampled in 1982), it is particularly necessary to guard against signal bias influencing the overall shape of the RCS curve.

5.6.2 Application of RCS Across Wide Species and Climate Ranges

In their study of ring-width changes viewed over a large area of the Northern Hemisphere, Esper et al. (2002) (see also Cook et al. 2004; Frank et al. 2007) took data from 14 different locations, from various tree species, and standardized them using one of two RCS curves constructed from a subdivision of all of the measurement series. One group of measurement data displayed the familiar negative exponential pattern of declining ring width with increasing age, while the other showed a 'weakly linear' declining trend. Two RCS curves were used because it was clear that linearly declining ring growth was not well suited to scaling by the curvilinear function and vice versa. However, by incorporating data from very different species and locations in each of the linear and nonlinear RCS curves, each is unavoidably associated with wide confidence intervals. The measurements for trees at a particular site location may be systematically over- or underestimated by the use of a multisite RCS curve.

This is an extreme case of the differing-contemporaneous-growth-rate bias discussed in Section 5.4.2. The expression of this bias in the Esper et al. (2002) context is illustrated in Fig. 5.12. This figure shows the local site chronologies for 5 of the 14

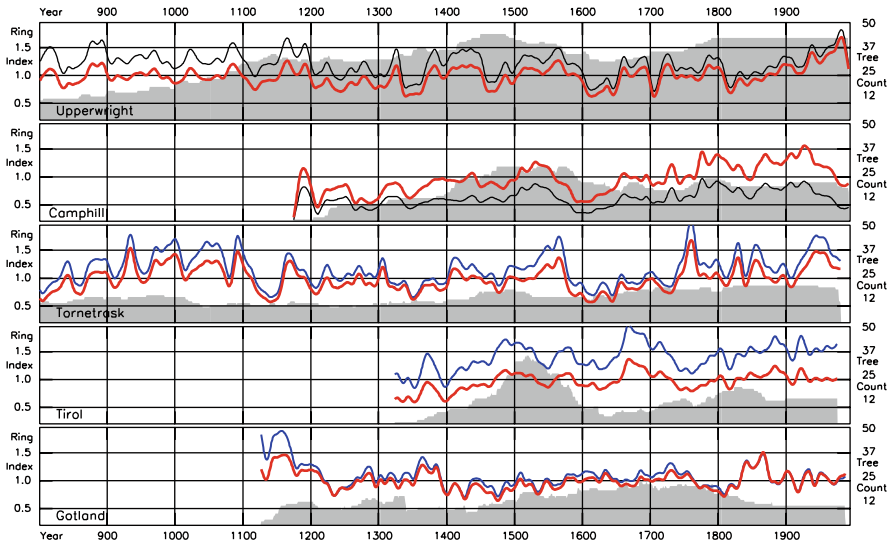

Fig. 5.12 A comparison of regional curve standardized (RCS) chronologies at various sites from among those used in Esper et al. (2002). The alternative chronologies shown for each of the selected sites illustrated here were produced using different RCS curves: either that used by Esper et al. based on multi-site data (linear model for Upperwright (*upper line*) and Camphill (*lower line*) or non-linear model for Tornetrask (*upper line*), Tirol (*upper line*) and Gotland (*upper line*)) or a single RCS curve (*thick line*) based only on the data available for that site. The difference between the two curves at each site represents a potential local bias when all chronologies are averaged to form a single 'Northern Hemisphere' series. In Esper et al. (2002) this bias was largely mitigated because each site chronology was normalized prior to averaging. For clarity all chronologies are shown as 20-year smoothed series. Sample counts are shown by *gray shading*

sites used by Esper et al. (2002), selected here to show how the use of multi-site RCS curves, whether linear or nonlinear in shape, can bias the mean of the local indices with respect to the mean indices that would have been produced by using an RCS curve derived from, and applied to, the measurement data only for the particular site. At some sites (e.g., Upperwright and Torneträsk), the bias is generally positive, while at others (e.g., Camphill) it is negative. At some sites, the mean bias is large compared to the temporal variance of the chronology (e.g., Tirol). If the regional chronologies, based on multisite-mean RCS, are simply averaged (as is implied in Esper et al. 2002), medium-frequency biases could arise in the final chronology as specific site data contained within it vary through time. In fact (though it is not apparent in Esper et al. 2002), the individual site chronologies were actually normalized prior to averaging (Ed Cook, personal communication) so that their overall means are set to a value of 1.0. This operation will mitigate much of the potential bias and effectively produce site chronologies similar to those that would be produced by using RCS applied at the site level, though medium-frequency bias will still arise where the slope of the local and multisite RCS curves differ (e.g., for Upperwright , Camphill, and Gotland; shown in Fig. 5.12).

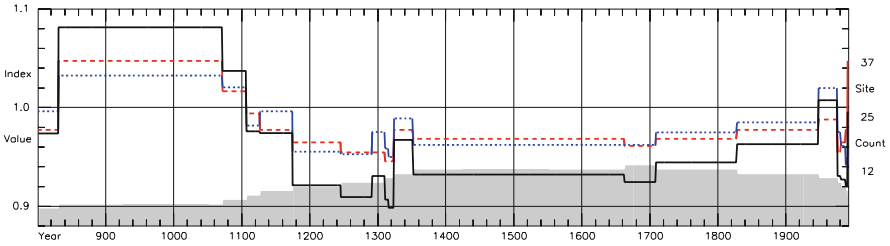

Fig. 5.13 A simplified illustration of the time dependence of separate potential biases in the grand average of all local regional curve standardized (RCS) chronologies produced in Esper et al. (2002). The dotted line represents the sum, across all sites (except Mongolia, see text) of the local difference in the means of alternative chronologies, produced either with a hemispheric-data-based RCS or a local-data-based RCS curve. The mean of all individual site chronology weightings, according to site latitude (see Esper et al. 2002), is shown as a *dashed line*. The product of these two potential biases is shown in *black*. Site counts over time are shown by *grey shading*

Figure 5.13 indicates the changing effective net bias that would be associated with the application of either the mean linear form or curvilinear RCS curves to the site measurement data had the data not been normalized prior to averaging. These biases are simply the sum over all sites of the mean differences between a chronology produced by using one of the multisite RCS curves and a chronology produced by using an RCS curve applied only at a site level. (With the exception of the Mongolia data which were not available for analysis). Normalization of the individual site series largely removes this potential bias, leaving only the time-dependent changes in average site-latitude weighting applied by Esper et al. (2002) according to the site locations (presumably following the weighting normally applied in regional averaging of gridded temperature records to take account of the change of area of grid boxes with latitude when the grid is defined according to fixed latitude and longitude spacings).

5.6.3 Adaption of RCS to Account for Non-climate Bias

In their study of northern Finnish tree growth and climate variability during more than 7000 years, Helama et al. (2005a,b) propose a modification of simple RCS, to take account of the changing density of forest cover, and hence competitional interactions among trees that they presume are sufficiently strong to alter the shape of the appropriate RCS curve through time. The progress of ring width decay for open-grown and close-packed trees will result in differences in the shape of RCS curves and could lead to bias in RCS chronologies, but can be evaluated only over a common ‘climate’ period, and it is inappropriate to disregard the background changes in the underlying climate forcing of tree growth. They first construct the basis for a conventional single RCS curve by averaging all age-aligned measurement data. To this series they fit a negative exponential with an added constant term (following Fritts et al. 1969) of the form

$$y = \mathrm{a} \times e^{-\mathrm{bx}} + \mathrm{c} \tag{5.1}$$

where the constant (a) defines the expected magnitude of the juvenile growth phase of ring growth (referred to by Helama et al. 2005a,b as the 'juvenile growth maximum'); the constant (c) defines an assumed constant growth rate of old-age trees; and constant (b) describes the rate of diminution of ring width with age (referred to by Helama et al. 2005a,b as the 'growth trend concavity').

In what they term 'environmental curve standardisation (ECS), Helama et al. (2005b) do not apply this single fitted function (5.1) to all of their measurement data. Instead, they perform time-dependent standardization by generating a series of RCS curves, each based on data from a 750-year time slice, overlapping each of its neighbors by 250 years. Each RCS curve is applied only to the data from the central 250 years of its corresponding time window. In this way, each 250-year non-overlapping period of the chronology is based on standardization with a different RCS curve. However, within each 250-year standardization application, only the RCS concavity (parameter b) is varied; the (a) and (c) parameters are maintained at the values calculated for the single, original overall period RCS curve.

They find a relationship between the number of tree samples (interpreted as spatial tree density) and the concavity (b) parameter (reported as 0.683, Helama et al. 2005b, Fig. 2d, and 0.73, Helama et al. 2005a, Fig. 5). The lack of any significant association between tree density and juvenile growth maximum (a) in these data (Helama et al. 2005b, Fig. 2c) presumably led them to conclude that concavity was independent of average tree growth rate.

In Table 5.1, we demonstrate that this conclusion is erroneous by using a subset of Finnish Lapland tree-ring measurements (Eronen et al. 2002; Helama et al. 2002) that form a major part (1087 trees) of the Helama et al. (2005b) dataset (1205 trees). Figure 5.14 shows these measurement data sorted, by relative growth rate,

Table 5.1 Parameters from modified negative exponential curves fitted to RCS curves[a]

	a	b	c	at	Bt	ct	rwr
Slowest	0.48	0.020	0.26	0.48	0.022	0.24	0.40
2nd	0.68	0.015	0.23	0.69	0.022	0.30	0.54
3rd	0.83	0.024	0.37	0.84	0.021	0.34	0.63
4th	0.95	0.014	0.29	0.95	0.019	0.37	0.75
5th	1.14	0.011	0.34	1.13	0.016	0.39	0.90
Fastest	1.41	0.011	0.36	1.36	0.013	0.47	1.18
Mean	0.92	0.016	0.31	0.91	0.019	0.35	
Mean difference				0.01	0.004	0.06	

[a]First a, b, and c are fitted to the full period of the regional curve standardization (RCS) curves, and second, at, bt, and ct are fitted to the truncated period of the RCS curves; i.e., the period with four or more series. 'rwr' is ring width reduction in the first 50 years of the truncated RCS curves. Values are shown for six growth rate classes, slowest to fastest. The means are shown and for the columns and also the mean differences between the full and truncated RCS curve parameters are shown. Growth rate is assessed as the ratio of the diameter growth of each tree to the diameter growth of the single RCS curve over the life of that tree.

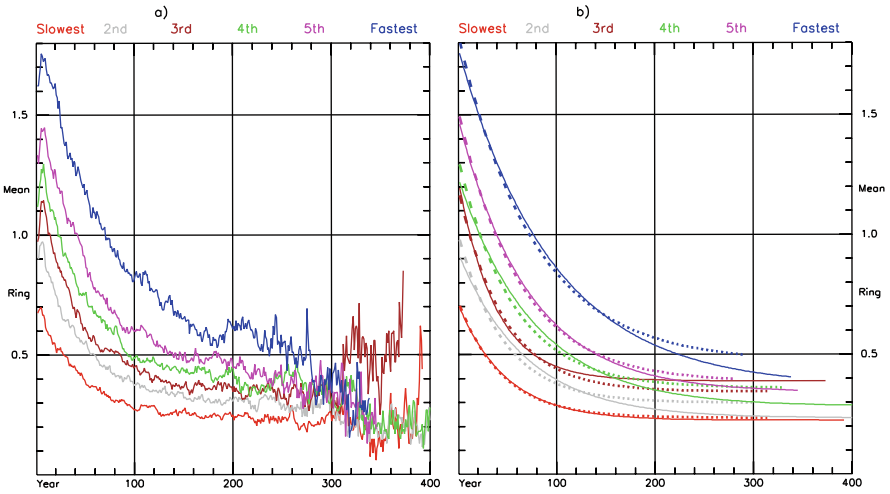

Fig. 5.14 The 1087 ring width measurement series of the Finnish Lapland chronology (Eronen et al. 2002), without pith-offset estimates, sorted into six growth rate classes (≈180 trees in each) on the basis of the ratio of final tree radius to the radius of the single regional curve standardization (RCS) curve (at that age) created from all trees Smoothing was achieved by fitting a modified negative exponential curve to the mean series. (**a**) The mean ring width by age for the six growth rate classes, slowest to fastest (*shaded*). (**b**) Smoothed RCS curves for each of the six growth rate classes when fitted first to the full mean ring width by age series (*continuous lines*) and second when fitted to the portion of these series with sample counts of four or more trees (*dotted lines*)

into six separate classes, each containing 180 or 181 trees. Growth rate was assessed according to the ratio of the radius of each tree divided by the radius of the single, overall-sample RCS curve at the point corresponding to the final age of that tree. In this way, the measurement series for all trees were divided into six groups ranging from fastest to slowest growth. For each group, a curve of mean ring width by age was produced and a modified negative exponential curve (5.1) was fitted to each (Fig. 5.14b). The coefficients are shown in Table 5.1 (the (a), (b), and (c) columns).

The low numbers of older samples generally produce large inter-tree variance in these curves. With few trees (i.e., for tree ages above about 250 years) the measurement averages are erratic, so we have also calculated the curve fits only for sections of data representing the average of at least four trees. These alternative (truncated data) curve fits and their associated coefficients are also shown in Fig. 5.14b and Table 5.1 (the [at], [bt], and [ct] columns)

These results show that there is potentially large uncertainty in estimating the (b) coefficient where the RCS curve is fitted over sections of poorly replicated data. In our truncated group fits, removal of only 0.5% of the ring measurements on average alters the (b) parameter fits by up to 20% over the six groups. Helama et al. (2005b) calculated estimates of concavity for 28 time periods, but based on fewer trees than in this sample, and there is likely to be considerable uncertainty associated with them.

Table 5.1 also shows that there is a relationship between the juvenile growth maximum (a) and concavity (b) ($r = -0.66,\ n = 6$). This relationship is very clear in the truncated group data fits between (at) and (bt) ($r = -0.96,\ n = 6$). Similarly, the diminution in ring width over the first 50 years (Table 5.1, column [rwr]) is strongly correlated with both (a) and (b). Hence, regardless of the reason, fast-growing trees will display greater reduction of ring width. Helama et al. (2005b), by varying (b) through time (where [a] and [c] are fixed) are standardizing the slower-growing trees with the 'higher growth rate' RCS curves and the faster-growing trees with 'lower growth rate' RCS curves (the curve with [a] and [c] held constant will have a higher rate of radial increase if [b] is small rather than large). The resulting mean values of the indices will be correspondingly greater for fast-growing trees and lower for slow-growing trees, in comparison to the means of indices generated by using a single fixed parameter RCS curve. The low-frequency variance in chronologies is imparted by changes in the means of index series.

Leaving aside the issue of whether a count of a relatively small number of tree samples through time is likely to be a realistic representation of between-tree competition when the sample area is very large and varies in its northern boundary by up to 80 km over past millennia, Helama et al. (2005b) are, in effect, amplifying the medium- to low-frequency variance in their ECS chronology by an amount that is directly proportional to the relative growth rate of the trees, regardless of whether there is any change in their direct competition status. This can be seen in the inverse pattern of variability through time of their concavity values, on the one hand, and in the difference in the ECS and RCS chronologies on the other (compare Fig. 4a, b in Helama et al. 2005b).

A positive association between changing concavity and tree-sample number during the last 7000 years (see Fig. 4 in Helama et al. 2005a) may reflect a common response in both variables to changing temperature forcing; i.e., warmer periods resulting in faster tree growth (and greater decay rate of ring width) and increased germination and survival of pine trees. Were this to be true, even to some extent, the deliberate biasing of the RCS curve implicit in the ECS approach could be questionable. However, even in subfossil chronologies a period with poor overlap between two groups of contemporaneous trees can result in a period affected by this 'modern' sample bias. The most recent section of a long subfossil chronology is invariably made up of a 'modern sample' from living trees, and the recent end of almost all such chronologies will suffer from modern-sample bias to some extent.

5.7 Discussion and Suggested Directions for RCS Development

It is the unavoidable loss of medium- and low-frequency variance, implicit in curve-fitting methods, which leads to the necessity of using RCS and the consequent requirement to recognize and overcome a number of problems associated with its specific implementation. Had the five sample series in Fig. 5.2b been standardized by using curve-fitting methods, the means of each series would each be set to 1.0 and

the slopes of each series would be virtually zero. All low-frequency variance would have been removed from the resulting chronology (see also Fig. 1, Briffa et al. 1996; Fig. 3, D'Arrigo et al. 2005). With curve-fitting standardization, our ability to compare the magnitude of tree growth in one decade with that in another, when they are separated by more than half the length of the constituent sample series, is potentially compromised. Hence, curve-fitting methods of tree-ring standardization are not well suited for exploring the long-term context of recent tree growth changes in response to factors such as recent temperature rises, increasing atmospheric CO_2, or other hypothesized anthropogenic influences on terrestrial ecosystems. This is the fundamental rationale for further exploring the potential, limitations, and possible improvements of RCS. A number of problems have been raised in this review, and in this final discussion we summarize several of them and point in the direction of possible solutions.

Establishing the form of the RCS curve and applying it to produce a chronology are both subject to potential biases. Bias in the form of the RCS curve arises when it erroneously tracks medium-frequency variance representing common climate signal; where the fit of expected RCS curve to the underlying age-aligned data is poor; and possibly when no allowance is made for pith offsets when aligning the underlying measurements (e.g., see Fig. 5.10d). The use of 'signal-free' methods of standardization addresses the first of these potential problems and can improve the accuracy of the RCS curve and reduce chronology error levels. These errors are generally small for long (multimillennial) chronologies but can be large for shorter chronologies. Routine implementation of signal-free methods, therefore, forms a useful extension to RCS, particularly with regard to its application in processing 'modern' chronologies. To address the second problem and to prevent loss of medium-frequency climate variance, smoothing of the RCS curve must not be too flexible, especially where sample counts are low. However, the RCS curve must be sufficiently flexible to follow the pattern of expected growth plotted against tree age accurately (Melvin et al. 2007).

The use of pith-offset estimates in generating and applying RCS curves will produce more accurate RCS curves. This increased accuracy arises because a lack of pith offsets introduces systematic bias in RCS curves, reducing the expected ring width maximum in early years of tree growth and consequently lowering the expected trend of declining growth with increasing age. Though RCS chronologies produced with and without pith offsets may be highly correlated (Esper et al. 2003; Luckman and Wilson 2005), using pith offsets may still occasionally produce more accurate chronologies (Naurzbaev et al. 2002; Melvin 2004; Büntgen et al. 2005; Esper et al. 2007), as is shown by lower chronology standard errors and a reduced frequency of local chronology bias associated with temporal concentrations of young (or old) tree samples in a chronology. The routine estimation and use of pith-offset information is, therefore, recommended.

However, other potential bias problems remain in RCS application. Any climate signal that affects the average of age-aligned sample series, e.g., the climate trend over the length of the chronology, is unavoidably removed from each series within the chronology. This trend-in-signal bias is minor for a long chronology and

is manifest only at the ends, but it can be a substantial bias affecting the whole length of a short, modern chronology. Differences in the growth rates of contemporaneously growing trees, and the inadvertent acquisition of data from younger trees that are more vigorous rather than slower-growing trees in recent times, both lead to the possibility of chronologies in which more recent chronology trends may not accurately represent the influence of climate variability. This contemporaneous-growth-rate bias will cancel in all but the ends of long chronologies, but may be a serious end-effect problem manifest equally in long subfossil and modern chronologies.

Having discussed the various sources of potential bias, we now turn to the question as to relative magnitudes. No generalizations can be made, because the specific characteristics of sample data and underlying climate signal will vary in different situations. However, in an attempt to provide some illustrative indication, we offer Table 5.2. This table lists the sources and possible relative magnitudes of different biases, and makes a guess at the overall bias for a hypothetical, but not untypical, example chronology (the detailed makeup of which is described in the caption to Table 5.2) that was assumed to have been subject to a notable increase in tree growth forcing about 50–60 years ago. All the biases are manifest at the recent end and tend to reduce the expression of the expected recent growth increase over the last century of the chronology. The net biases act to produce a spurious positive trend 400−200 years from the end of the chronology, but the relatively large negative bias, mostly associated with non-random sampling practices, is likely to dominate in the most recent centuries.

Table 5.2 Relative sizes of individual and net bias effects[a]

Type of RCS bias	Effective duration (years)	General slope of bias	Approximate magnitude
Absence of pith-offset estimates	200	Negative	0.1
Trend-in-signal bias			
Solely modern chronology	200	Negative	0.1
Longer subfossil chronology	200	Negative	Negligible
Contemporaneous-growth-rate bias			
Modern sample bias	400	Positive	0.2
Dominancy of fast-growth indices	100	Negative	0.2
Net effect	400−200	Positive	0.1
	100−0	Negative	0.2

[a]These effects are implicit in the application of simple regional curve standardization (RCS) for a hypothetical chronology. These figures are 'guesstimates' of the magnitude and effective duration of RCS biases discussed in this review. These figures are expressed for a hypothetical set of data from trees with the following characteristics: the longest trees are about 400 years old; the shortest trees are around 100 years old; the chronology indices have a range from 0.5 to 1.5; and the trees experienced a 40% growth increase, which occurred around the middle of the twentieth century. These biases are manifest as 'end effects' (i.e., all terminating at the end of the chronology). All biases, with the exception of trend-in-signal bias, will apply equally to modern and sub-fossil chronologies.

The technique of aligning and averaging tree index series by ring age allows the investigation of bias. Comparison of tree indices sorted according to different criteria (e.g., by contemporaneous growth rate (Fig. 5.4b), tree age, tree diameter, latitude, altitude, aspect, or packing density) will allow the identification of potential systematic biases in RCS chronologies. The technique of 'end-aligning' (Fig. 5.7), in which both the age-related trend and the climate signal are removed, is an additional method of identifying potential bias (Section 5.4.3.2). The signal-free method is also a tool that can be used to test for residual bias in chronologies; measurement series are divided by the final chronology and the residual signal will represent bias, or the limits of the standardization method (Melvin and Briffa 2008).

The count of trees needed to produce a 'robust' chronology is often gauged by using the mean interseries correlation to calculate the expressed population signal (EPS; Wigley et al. 1984; Briffa and Jones 1990). However, estimates of EPS are strongly influenced by (biased towards) the correspondence between index series on short (primarily interannual) timescales. Experiments using ring width data from Torneträsk (Grudd et al. 2002) and Finnish Lapland (Eronen et al. 2002) have evaluated the robustness of chronology confidence in RCS. This work (Melvin 2004, Section 6.3.3) explored the influence on the standard deviations of chronologies (the average standard deviation of all yearly values) produced by varying sample counts in differently filtered tree index series. The results suggest that if a replication of 10 trees is required for a 30-year high-pass-filtered chronology to exhibit a specific mean standard deviation, a 100-year high-pass-filtered chronology would require a replication of 18 samples, while an RCS chronology would need 62 constituent samples to achieve the same standard deviation. Increasing tree counts can improve chronology confidence, but will not remove systematic bias. Mitigating bias in RCS may improve confidence but will not remove the requirement for large sample replication.

The age band decomposition (ABD) method (Briffa et al. 2001) amounts to an alternative method of applying the RCS technique. If the mean value of each 'age band' is aligned by ring age, it will form a stepped version of the RCS curve. The ABD method therefore suffers from many of the problems of RCS, especially 'modern-sample bias,' and equal care must be taken in the use of this method and in the interpretation of the results.

Subfossil chronologies, like modern chronologies, are still susceptible to the contemporaneous-growth-rate bias. One possibility of mitigating this bias is to identify and remove the influence of fast- versus slow-grown trees, but only when they are identified in samples growing under the same climate conditions.

Some modifications of the application of RCS go some way towards obtaining these objectives, ranging from the alternative use of two sub-RCS curves (Esper et al. 2002) to the use of multiple RCS curves (Melvin 2004, Section 5.7). In the former, two different classes of RCS curve shape are identified from among those in the full dataset, and each is applied separately to the relevant group of sample series. This process removes substantial potential bias that would result from detrending series that exhibit linearly decreasing ring widths with age with an expectation of exponential decay and vice versa. However, this is an extreme

example of the use of RCS, because the original sample set comprises data from various species from widely separated locations, and even the use of sub-RCS curves will not account for the large site-to-site differences in growth rates. Each sub-RCS curve will be bracketed by very wide confidence limits, leaving scope for substantial bias in the production of chronologies. Melvin (2004, Section 5.7) advocates the use of multiple RCS, in effect dividing the data on the basis of relative growth rate into a number of RCS curves, each of which is then applied to its corresponding group of measurement series to produce (where the data are continuous) multiple parallel sub-RCS chronologies. If these chronologies are then averaged together, contemporaneous-growth-rate bias will be reduced. However, this process will also remove the potential to preserve some long-timescale variance that is contained in the relative differences of the sub-RCS chronology means. There is a particular requirement for a practical way to distinguish genuine long-timescale climate signals from spurious trends that may arise in RCS, solely as a result of non-climate-related differences in the growth rates of sample trees.

Basal area increment (BAI) is a more direct measure of wood production (especially in mature trees after height increase has reduced) and BAIs are used widely in forestry. A number of researchers have used BAI chronologies as an alternative to ring widths, some employing the RCS method (e.g., Hornbeck et al. 1988; Becker 1989; Briffa 1990; Biondi et al. 1994; Rathgeber et al. 1999b). The use of BAI will likely reduce some of the problems of RCS, such as the tendency for negatively sloping indices from relatively faster-grown trees in the recent ends of chronologies and positively sloping indices from slower-growing trees, but BAI data still suffer from differing-contemporaneous-growth-rate bias and modern-sample-bias. The use of signal-free methods and the diagnostic value in examining sub-RCS curves and chronologies are equally applicable to chronologies of BAI data and, of course, to other tree-growth parameters.

5.8 Conclusions

The conceptual and practical examples of the implementation of RCS presented here are intended to demonstrate how problematic the application of a simple concept can be in practice. The recognition of the presence of bias within a chronology and the routine exploration of the magnitudes of different biases in RCS can only provide a better foundation for quantifying and expressing RCS chronology uncertainty.

The net effect of potential biases in the application of the RCS method will vary according to the specific makeup of the samples in a chronology. Much of the potential bias may average out, especially when sample replication is high, but the particular problems associated with the reliability of the start and end of chronologies may affect chronology calibration and hinder the study of recent tree-growth forcing trends. Where, by coincidence, a chronology starts around 1000 years ago, similar problems may be associated with gauging the accurate level of tree growth

at that time and perhaps, the comparative magnitude of warmth in medieval as compared to modern times.

This is not to say that biases are manifest in all RCS chronologies produced up to this time. However, it is hoped that drawing specific attention to these potential problems will stimulate a more routine approach to investigating their likely extent. This should lead to a circumspect interpretation of RCS-based climate reconstruction and provide impetus for further work aimed at improving the RCS method.

Acknowledgements The authors are very grateful to Ed Cook, Connie Woodhouse, Malcolm Hughes and Samuli Helama for their thoughtful reviews and suggested modifications to the original manuscript. KRB acknowledges support from the UK Natural Environmental Research Council (NERC) (NER/T/S/2002/00440) under the Rapid Climate Change Program. TMM acknowledges current support from The Leverhulme Trust (A20060286). KRB also acknowledges travel support from the organizers of the Tucson conference.

Appendix: Signal-Free Standardization

In this review, we make several references to the 'signal-free' method in tree-ring standardization (see Sections 5.4.1, 5.5, 5.6.1, and 5.7). A more detailed discussion of the topic (in the context of 'data-adaptive' standardization involving 'curve fitting' to individual measured series) can be found in Melvin and Briffa (2008). However, for the convenience of the reader, a brief description of the rationale and application of the signal-free approach is provided here.

Background and Rationale

The signal-free concept stems from the observation that individual tree-ring measurement series represent a mixture of potential growth influences, among which are included first, that of climate variability through time and second, that of changing allocation processes and tree geometry that both affect the size of annual stem increments. Standardization has always aimed to remove or reduce the allocation bias; e.g., the signal of reducing ring width with age, so that the remaining variability in ring width indices over time provides a clearer representation of the influence of climate variability. Developing standardization curves from measurement series that contain the climate signal, where the standardization curve may track the climate signal, at least to some extent, will lead to the removal of some climate-related variance and so bias the resulting chronology. This bias is well known with respect to the removal of variance representing timescales longer than the typical life span of the sample trees (Cook et al. 1995). However, it can also arise where a common, externally forced growth signal influences the more localized fit of a standardization curve, resulting in the partial, or even complete, loss of a relatively short-term climate signal (in the case of more flexible standardization curves) and the distortion of medium-term climate trends in adjacent periods (where less flexible, but still 'fitted,' standardization functions are employed).

The rationale behind 'signal-free' standardization is that it should be possible to produce an improved (i.e., locally unbiased) chronology if the individual measurement series could be detrended without allowing the fitting of standardization curves to be affected by the presence of climatically forced variability. One suggestion for achieving this condition is to remove the common variability (chronology signal) from all measurement series to yield less-biased detrending curves.

Implementing Signal-Free Standardization

Melvin and Briffa (2008) describe one such approach, applied in the context of 'curve-fitting' standardization using options offered in the ARSTAN program (Cook 1985). They demonstrate how a combination of the 'segment length curse' and localized distortion of standardization curves can produce a biased ring-width chronology, apparent as a failure by the standardized chronology to express recent climatic trends. Details of their implementation of this signal-free approach, in the context of curve-fitting standardization, are given in Melvin and Briffa (2008).

When this approach is applied in the case of regional curve standardization (RCS), a first chronology is produced by division of the tree-ring measurements by the appropriate RCS curve values. Each original measurement value is then divided by the appropriate chronology value for that year to produce a first set of 'signal-free' measurements. The standardization is then repeated on these signal-free data, and a new chronology is produced from the new signal-free indices. The process is repeated until the point where the signal-free data make up a chronology that has virtually zero variance. In practice, the magnitude of residual bias (i.e., as represented by the variance of the signal-free chronology) after each iteration is 20% of its initial value. A zero-variance signal-free chronology is considered here to be one where all values are within the range 1.0 ± 0.002. This condition is achieved generally within four or five signal-free iterations. At this point, the final RCS curve is unaffected by any external growth-forcing signal and should, therefore, yield a less-biased chronology.

References

Badeau V, Becker M, Bert D, Dupouey J, Lebourgeois F, Picard JF (1996) Long-term growth trends of trees: ten years of dendrochronological studies in France. In: Spiecker H, Mielikainen K, Kohl M, Skovsgaard JP (eds) Growth trends in European forests. Springer, Berlin, pp 167–181

Becker M (1989) The role of climate on present and past vitality of silver fir forests in the Vosges Mountains of northeastern France. Can J Forest Res 19:1110–1117

Biondi F, Myers DE, Avery CC (1994) Geostatistically modeling stem size and increment in an old-growth forest. Can J Forest Res 24:1354–1368

Bräker OU (1981) Der Alterstrend bei Jahrringdichten und Jahrringbreiten von Nadelhölzern und sein Ausgleich. Mitteilungen der Forstlichen Bundesversuchsanstalt Wien 142:75–102

Briffa KR (1990) Increasing productivity of 'natural growth' conifers in Europe over the last century. Lundqua Rep 34:64–71, Lund University, Sweden

Briffa KR (1999) Interpreting high-resolution proxy climate data: the example of dendroclimatology. In: von Storch H (ed) Analysis of climate variability. Springer-Verlag, Heidelberg, pp 77–94

Briffa KR, Jones PD (1990) Basic chronology statistics and assessment. In: Cook ER, Kairiukstis LA (eds) Methods of dendrochronology. Kluwer Academic, Dordrecht/Boston/London, pp 137–152

Briffa KR, Jones PD, Bartholin TS, Eckstein D, Schweingruber FH, Karlén W, Zetterberg P, Eronen M (1992) Fennoscandian summers from AD 500: temperature changes on short and long timescales. Clim Dynam 7:111–119

Briffa KR, Jones PD, Schweingruber FH, Karlén W, Shiyatov SG (1996) Tree-ring variables as proxy-climate indicators: problems with low-frequency signals. In: Jones PD, Bradley RS, Jouzel J (eds) Climatic variations and forcing mechanisms of the last 2,000 years. Springer-Verlag, Berlin, pp 9–41

Briffa KR, Osborn TJ, Schweingruber FH, Harris IC, Jones PD, Shiyatov SG, Vaganov EA (2001) Low-frequency temperature variations from a northern tree-ring density network. J Geophys Res-Atmos 106:2929–2941

Büntgen U, Esper J, Frank DC, Nicolussi K, Schmidhalter M (2005) A 1,052-year tree-ring proxy for Alpine summer temperatures. Clim Dynam 25:141–153

Cook ER (1985) A time-series analysis approach to tree-ring standardization. PhD dissertation, The University of Arizona, Tucson

Cook ER, Briffa KR, Meko DM, Graybill DA, Funkhouser G (1995) The segment length curse in long tree-ring chronology development for paleoclimatic studies. Holocene 5:229–237

Cook ER, Buckley BM, D'Arrigo RD, Peterson MJ (2000) Warm-season temperatures since 1600 BC reconstructed from Tasmanian tree rings and their relationship to large-scale sea surface temperature anomalies. Clim Dyn 16:79–91

Cook ER, Esper J, D'Arrigo RD (2004) Extratropical Northern Hemisphere land temperature variability over the past 1,000 years. Quaternary Sci Rev 23:2063–2074

D'Arrigo R, Mashig E, Frank D, Wilson R, Jacoby G (2005) Temperature variability over the past millennium inferred from northwestern Alaska tree rings. Clim Dyn 24:227–236

Dewar RC (1993) A mechanistic analysis of self-thinning in terms of the carbon balance of trees. Ann Bot 71:147–159

Dupouey J, Denis J, Becker M (1992) A new method of standardization for examining long-term trends in tree-ring chronologies. Lundqua Rep 34:85–88, Lund University, Sweden

Erlandsson S (1936) Dendrochronological studies. Geochronology Institute Report 23, University of Upsala, 1–119

Eronen M, Zetterberg P, Briffa KR, Lindholm M, Merilainen J, Timonen M (2002) The supra-long Scots pine tree-ring record for Finnish Lapland: Part 1, chronology construction and initial inferences. Holocene 12:673–680

Esper J, Cook ER, Schweingruber FH (2002) Low-frequency signals in long tree-ring chronologies for reconstructing past temperature variability. Science 295:2250–2253

Esper J, Cook ER, Krusic PJ, Schweingruber FH (2003) Tests of the RCS method for preserving low-frequency variability in long tree-ring chronologies. Tree-Ring Res 59: 81–98

Esper J, Frank D, Büntgen U, Verstege A, Luterbacher J, Xoplaki, E (2007) Long-term drought severity variations in Morocco. Geophys Res Lett 34:L17702. doi:10.1029/2007GL030844

Frank D, Esper J, Cook ER (2007) Adjustment for proxy number and coherence in a large-scale temperature reconstruction. Geophys Res Lett 34:L16709. doi:10.1029/2007GL030571

Fritts HC (1976) The statistics of ring width and climatic data. Tree rings and climate. Academic, London, pp 246–311

Fritts HC, Guiot J (1990) Methods of calibration, verification, and reconstruction. In: Cook ER, Kairiukstis LA (eds) Methods of dendrochronology. Kluwer Academic, Dordrecht, pp 163–217

Fritts HC, Mosimann JE, Bottorff CP (1969) A revised computer program for standardizing tree-ring series. Tree-Ring B 29:15–20

Grudd H, Briffa KR, Karlén W, Bartholin TS, Jones PD, Kromer B (2002) A 7,400-year tree-ring chronology in northern Swedish Lapland: natural climatic variability expressed on annual to millennial timescales. Holocene 12:657–665

Helama S, Lindholm M, Timonen M, Meriläinen J, Eronen M (2002) The supra-long Scots pine tree-ring record for Finnish Lapland: Part 2, interannual to centennial variability in summer temperatures for 7,500 years. Holocene 12:681–687

Helama S, Lindholm M, Timonen M, Eronen M (2005a). Mid- and late-Holocene tree population density changes in northern Fennoscandia derived by a new method using megafossil pines and their tree-ring series. J Quaternary Sci 20:567–575

Helama S, Timonen M, Lindholm M, Merilainen J, Eronen M (2005b) Extracting long-period climate fluctuations from tree-ring chronologies over timescales of centuries to millennia. Int J Climatol 25:1767–1779

Hornbeck JW, Smith RB, Federer CA (1988) Growth trends in 10 species of trees in New England, 1950–1980. Can J Forest Res 18:1337–1340

Huntington E (1913) The secret of the big trees. Department of the Interior, Washington, DC

Huntington E (1914) The climate factor as illustrated in arid America. Pub. No. 192, Carnegie Institute, Washington, DC

Kershaw ZL (2007). The Torneträsk tree-ring chronology: exploring the potential for biased climate reconstructions in recent millennia. Unpublished BSc thesis, University of East Anglia, Norwich, UK

Linderholm HW, Gunnarson BE (2005) Summer temperature variability in central Scandinavia during the last 3,600 years. Geogr Ann A 87A:231–241

Luckman BH, Wilson RJS (2005) Summer temperatures in the Canadian Rockies during the last millennium: a revised record. Clim Dynam 24:131–144

Melvin TM (2004) Historical growth rates and changing climatic sensitivity of boreal conifers. Thesis. University of East Anglia, Norwich, UK. http://www.cru.uea.ac.uk/cru/pubs/thesis/2004-melvin/

Melvin TM, Briffa KR (2008) A "signal-free" approach to dendroclimatic standardisation. Dendrochronologia 26:71–86

Melvin TM, Briffa KR, Nicolussi K, Grabner M (2007) Time-varying-response smoothing. Dendrochronologia 25:65–69

Mitchell VL (1967) An investigation of certain aspects of tree growth rates in relation to climate in the central Canadian boreal forest. Technical report 33, University of Wisconsin, Department of Meteorology

Naurzbaev MM, Vaganov EA, Sidorova OV, Schweingruber FH (2002) Summer temperatures in eastern Taimyr inferred from a 2,427-year late-Holocene tree-ring chronology and earlier floating series. Holocene 12:727–736

Naurzbaev MM, Hughes MK, Vaganov EA (2004) Tree-ring growth curves as sources of climatic information. Quaternary Res 62:126–133

Nicolussi K, Bortenschlager S, Körner C (1995) Increase in tree-ring width in sub-Alpine Pinus cembra from the central Alps that may be CO_2 related. Trees-Struct Funct 9:181–189

Rathgeber C, Guiot J, Roche P, Tessier L (1999a) Augmentation de productivité du chêne pubescent en région méditerranéenne française. Ann For Sci 56:211–219

Rathgeber C, Guiot J, Roche P, Tessier L (1999b) Quercus humilis increase of productivity in the Mediterranean area. Ann For Sci 56:211–219

Schweingruber F, Briffa KR (1996) Tree-ring density networks for climatic reconstruction. In: Jones PD, Bradley RS (eds) NATO Series, Vol I 41, Climatic variations and forcing mechanisms. Springer-Verlag, Berlin

Wigley TML, Briffa KR, Jones PD (1984) On the average value of correlated time series with applications in dendroclimatology and hydrometeorology. J Clim Appl Meteorol 23:201–213

Wilson RJS, Luckman BH, Esper J (2005) A 500-year dendroclimatic reconstruction of spring-summer precipitation from the lower Bavarian Forest region, Germany. Int J Climatol 25: 611–630

Chapter 6
Stable Isotopes in Dendroclimatology: Moving Beyond 'Potential'

Mary Gagen, Danny McCarroll, Neil J. Loader, and Iain Robertson

Abstract When trees grow, they assimilate carbon from atmospheric carbon dioxide, and hydrogen and oxygen from soil water. The stable isotope ratios of these three elements carry signals that can be interpreted in terms of past climate because isotope ratios are climatically controlled by the tree's water and gas exchange budgets. The traditional tree-ring proxies form the most widespread and arguably the most valuable of the high-resolution climate archives. Here we asses the added contribution that can be made to dendroclimatology using stable isotope measurements. We describe what is involved in measuring tree-ring stable isotopes, provide a brief review of progress to date, and point to the ways in which stable isotope dendroclimatology can be used to provide something new. We conclude that stable isotope ratios sometimes provide stronger climate signals than the traditional proxies, which can be useful where sample replication is limited. Stable isotopes can also be used to access different climate signals in trees, providing a more synoptic view of past climate and may also have the potential to provide a greater proportion of the lower-frequency climate signal that is difficult to retain during statistical detrending of tree-ring width series. The use of stable isotopes may also pave the way to extracting climate signals from ringless tropical trees. We highlight the need for stable isotope dendroclimatology to move beyond papers that simply demonstrate 'potential' and to being to reconstruct the climate of the past. We suggest that this should be done in collaboration, not in competition, with traditional dendroclimatology.

Keywords Tree rings · Stable isotopes · Paleoclimate

M. Gagen (✉)
Department of Geography, School of the Environment and Society, Swansea University, Singleton Park, Swansea SA2 8PP, UK
e-mail: m.h.gagen@swansea.ac.uk

M.K. Hughes et al. (eds.), *Dendroclimatology*, Developments in Paleoenvironmental Research 11, DOI 10.1007/978-1-4020-5725-0_6,

6.1 Scope and Background

When trees grow, they assimilate carbon from atmospheric carbon dioxide, and hydrogen and oxygen from soil water. The stable isotope ratios of these three elements carry signals that can be interpreted in terms of past climate because isotope ratios are climatically controlled by the tree's water and gas exchange budgets. Mechanistic models are available that describe the fractionation of these isotopes (e.g., Farquhar et al. 1982; Roden et al. 2000), and these models help in interpreting the climate signal, but climate reconstruction still relies on the statistical techniques used in other branches of dendroclimatology.

The traditional tree-ring proxies form the most widespread and arguably the most valuable of the high-resolution climate archives. In his review of dendrochronology's contribution to climatology, Hughes (2002) poses the question: are stable isotopes worth the extra effort? He points to the climatological effectiveness of the traditional tree-ring proxies and suggests that to be a useful complement to them, stable isotopes would need to show coherent patterns of variability on spatial scales of hundreds to thousands of kilometers and contain different kinds of information. Hughes goes on to state that 'there is reason to believe that such a major effort may be worthwhile' and points to emerging evidence that these conditions could be met. Here we demonstrate that progress in recent years has shown that it is indeed worthwhile, and that stable isotope dendroclimatology has unique strengths, and is now making novel and specific contributions.

In this chapter we describe what is involved in measuring tree-ring stable isotopes, provide a brief review of progress to date, and attempt to answer Hughes (2002) by pointing to the ways in which stable isotope dendroclimatology can be used to provide something new. We conclude that the technique can sometimes be used to provide stronger climate signals than the traditional proxies, particularly where sample replication is limited. Stable isotopes can also be used to access different climate signals in trees, providing a more synoptic view of past climate and may also have the potential to provide a greater proportion of the lower-frequency climate signal that is difficult to retain during statistical detrending of tree-ring width series. The use of stable isotopes may also pave the way to extracting climate signals from ringless tropical trees. The time has come for isotope dendroclimatology to move beyond papers that simply demonstrate 'potential' and actually start to reconstruct the climate of the past, and this must be done in collaboration, not in competition, with traditional dendroclimatology.

6.2 Theoretical Background

There is a robust theoretical framework linking stable isotopes to climate, which is provided by models describing how carbon, oxygen, and hydrogen are fractionated by plants. These models provide the theory for expecting a climate signal from the stable isotope ratios of wood, the explanation for why the climatic signal varies from place to place, and why it is stronger in some areas than in others.

The proxy signal arises from the climatic regulation of isotopic discrimination in trees. Isotopic discrimination (also termed fractionation) is the selective separation of isotopes during natural physical, chemical, or biochemical processes, including evaporation, condensation, transpiration, and metabolism, primarily due to differences in their relative masses. Measurements are expressed as a ratio of two isotopes relative to an isotopic standard and expressed as per mille (‰) using the delta notation (δ):

$$\delta^{\text{heavy/light}} = 1000 \times \frac{[(\text{heavy/light})_{\text{sample}} - (\text{heavy/light})_{\text{standard}}]}{[(\text{heavy/light})_{\text{standard}}]} \tag{6.1}$$

where heavy/light refers to either $^{18}O/^{16}O$, $^{13}C/^{12}C$, or $^{2}H/^{1}H$ for $\delta^{18}O$, $\delta^{13}C$, and δD, respectively

6.2.1 Stable Carbon Isotope Theory

Discrimination (Δ) of carbon isotopes by trees, and other C_3 plants (Farquhar et al. 1982), is described by:

$$\Delta \approx a + (b - a)ci/ca \tag{6.2}$$

The constants represent the theoretical value assigned to the isotopic fractionation due to diffusion of CO_2 through stomata to the site of carboxylation ($a \approx 4.4\%$) and the isotopic fractionation when CO_2 is used by the photosynthetic enzyme ribulose-1,5-bisphosphate ($b \approx 27 - 28\%o$) and c_i and c_a are intercellular and ambient CO_2 concentrations. Fractionation is additive, acting on the isotopic composition of the source gas at each stage such that C_3 plants have an average $\delta^{13}C$ signature of $-25‰$. The isotopic ratio of the photosynthetic products ($\delta^{13}C_{\text{plant}}$) is given by:

$$\delta^{13}C_{\text{plant}} = \delta^{13}C_{\text{air}} - \Delta \tag{6.3}$$

Since the fractionation constants (a and b) do not vary in response to climate (except under relatively unusual conditions: McCarroll and Loader 2004) and the atmospheric concentration of carbon dioxide (c_a) is known, and has remained quite stable for most of the preindustrial Holocene, the carbon isotope measurements from tree rings are essentially a record of changes in the internal concentration of CO_2(c_i). The amount of CO_2 in leaves is regulated by two processes: stomatal conductance (g), and photosynthetic assimilation rate (A). These processes vary in response to environmental controls such as relative humidity, temperature, and soil moisture deficit such that stable carbon isotope series can capture a range of climatic variables depending upon which factors limit A and g. Stable carbon isotope measurements from tree rings are thus a proxy for the internal concentration of CO_2within the leaf

space as regulated by these two rates. Because the climatic signal is usually dominated by the response of either stomatal conductance or photosynthetic assimilation rate, the same $\delta^{13}C$ value can arise from different climatic forcings, in different locations (Saurer and Siegwolf 2007).

For example, a sunny growing season, at a cool, moist site, may force an increase in *A,* resulting in a drop in c_i and a larger proportion of ^{13}C moving through the pathway to be stored in that year's carbohydrate. In such a situation the carbon isotope signal would capture sunny summers as high $\delta^{13}C$ values. Alternatively, a particularly dry summer, at a more arid site, might force a reduction in g with the same effect on c_i and $\delta^{13}C$. In this case, high $\delta^{13}C$ values would record low relative humidity/antecedent precipitation. In both cases, owing to the close association typically observed between these meteorological variables, it is likely that $\delta^{13}C$ would also correlate with summer temperature.

6.2.2 Stable Oxygen and Hydrogen Isotope Theory

Stable oxygen and hydrogen isotope measurements from tree rings are a proxy for the isotopic composition of water taken up by the tree's roots (the source water), overprinted by evapotranspiration in the leaf; the latter signal is dominated by vapor pressure deficit (relative humidity).

Variability in source water isotopes is of climatological interest because these isotopes relate to local air mass characteristics (Darling 2004). Isotope fractionations during the hydrological cycle result in a strong association between isotopes in precipitation and mean annual surface air temperature, but as part of a complex system (Dansgaard 1964). The water isotope system in trees and the models describing them (e.g., Barbour et al. 2001) are more complicated than those for $\delta^{13}C$. Following uptake by the roots, water is transported through the xylem without fractionation until it reaches the leaves and other non-suberized tissues, where it undergoes evaporative enrichment via transpiration. Here, fractionation favors the loss of the lighter isotopes (^{16}O and ^{1}H), resulting in enrichment of the leaf waters. Evaporative enrichment in the leaf is diluted by a Péclet effect (Barbour 2007) whereby unenriched stem water diffuses into the leaf and replaces transpired water, attenuating enrichment. Photosynthetic fractionations are also mass dependent and act in addition to leaf-level enrichment (Barbour et al. 2001; Roden et al. 2000) so that the resulting photosynthate is enriched in ^{18}O and depleted in ^{2}H. Finally, a degree of enrichment is lost during synthesis of cellulose from sugar, due to re-exchange with xylem water (Sternberg et al. 1986).

Stable oxygen and hydrogen isotope measurements from tree rings thus provide a mixed signal. The oxygen and hydrogen isotopic ratios of tree-ring cellulose usually represent a source water isotopic signal modified by evaporative enrichment to a greater or lesser extent. Strong correlations between temperature and wood/cellulose water isotopes are sometimes found (e.g., Switsur et al. 1996) because temperature has a direct effect on the isotopic composition of precipitation and also an indirect effect on evaporative enrichment in the leaf (McCarroll and Loader 2004).

6.3 Sampling and Measurement

The early studies of stable isotopes in tree rings were carried out in specialist laboratories using very expensive, often custom-made equipment, and every sample involved many hours of preparation prior to analysis. However, there have been great advances in sample preparation and measurement techniques and most of the equipment required can now be purchased 'off the shelf,' putting isotope dendroclimatology within the reach of many traditional dendrochronology laboratories. Here we provide a brief description of the methods involved.

There are several steps in measuring stable isotopes from trees. Following sample selection, the desired component of the wood must be isolated. Earlywood, latewood, or whole-ring samples can be used, either in groups of years or as individual annual samples, depending upon the aims and objectives of the study. Samples are processed to a homogenous product, usually α-cellulose, sometimes resin-extracted or whole-wood (Leavitt and Danzer 1993; Loader et al. 1997; Brendel et al. 2000; Gaudinski et al. 2005; Rinne et al. 2005; Anchukaitis et al. 2008a). Homogenized samples are then pyrolyzed, and the isotopic ratios in the resulting CO (for oxygen) and H_2 (for hydrogen) are measured via isotope ratio mass spectrometry (IRMS). For carbon isotope analysis, samples are combusted to CO_2 prior to mass spectrometry.

The choice of species and sites for isotopic dendroclimatology should be guided by the aims of the study. As with the growth proxies, trees on dry sites are likely to respond most strongly to moisture supply, whereas those growing at high altitudes or latitudes, and where moisture is rarely limiting, will correlate more strongly with temperature. For the water isotopes it is necessary also to consider the depth of soil moisture being tapped, since deep-rooted trees may use precipitation that fell long before the growth season, smoothing any source water signal. This may be an advantage if the target climate variable is that controlling evaporative enrichment in the leaf rather than the source water signal. Shallow-rooted trees will be more responsive to changes in source water signal but may also be more sensitive to moisture stress.

Modern IRMS systems, with online elemental analyzers, allow the measurement of very small samples, so samples collected by using standard increment borers can now be used in stable isotope dendroclimatology. The change to online IRMS typically involves a reduction in sample size from around 5–7 mg of cellulose to 300–350 μm, for standard analysis, with a lower limit of around 25–50 μg. A standard 5 mm diameter core typically yields sufficient material for measurement of at least two isotope species at annual resolution, even when α-cellulose is used. It is possible for a trained technician to cut in excess of a hundred samples per day from a small increment core sample.

Ring cutting is most easily carried out using a scalpel under magnification, although this procedure puts a limit on the minimum ring width that can be sampled. It is possible to accurately cut rings of approximately 1 mm width. The question of whether to cut and combine single or multiple radii is a matter of objective. For paleoclimatic purposes, spatial variability around the circumference of the

tree (approximately 1–1.5‰; Leavitt and Long 1985) becomes relatively insignificant compared to between-tree variability (typically 2‰ or greater; McCarroll and Pawellek 1998), and there may be less to be gained from measuring multiple radii (McCarroll and Loader 2004). Any resulting 'spare' analytical capacity may be better used to increase replication.

Where the aim is to obtain a record at annual resolution, cores can be cut into either whole-ring or latewood increments. Investigation of the variability of isotope ratios within rings suggests that, for some conifers, the whole ring may provide the best signal (Helle and Schleser 2004). For deciduous species it may be necessary to separate the latewood, since earlywood is formed using reserves from previous years. After the rings have been cut, they can either be analyzed separately, or pooled together to reduce the cost and effort involved in chemical treatment and mass spectrometry. Where annual resolution is not required, groups of rings can be pooled together from several trees. Pooling material prior to analysis is attractive because it is much easier and cheaper, but there is a high cost in terms of the quality of the resulting data. A pooled record rapidly provides a single time series, but if tree rings are analyzed independently, then the usual array of statistical techniques can be used to test the signal strength, check that replication is adequate throughout the record, and to produce confidence limits around reconstructed climatic series. The common signal in isotope series is often much stronger than in ring widths or densities from the same trees (e.g., Robertson et al. 1997a, b; Gagen et al. 2004), so as few as four or five trees can provide a representative mean value. Given that high-frequency information is so readily available from ring width and density measurements, there is an argument for using multiple-year pooling to focus on capturing the lower-frequency signal that is so problematic to retain in traditional tree-ring proxies.

In trees that do not form annual rings, sampling multiple points through a year of growth allows identification of seasonal cycles in stable isotopes that can be used for both chronology and climatic signal. Cores, or a radial cut with a ~1 cm^2 cross section, are sampled at regular intervals (of a few tens of microns), by using a scalpel or a microtome. A sampling strategy should be designed to capture the seasonal variability needed for a chronology; 4–6 samples per annual cycle are suggested and these should be combined with radiocarbon or 'known' dates (Poussart et al. 2004). In order to detect interannual cycles in $\delta^{18}O$ in Costa Rican cloud forest species, Anchukaitis et al. (2008b) subsampled cores, combining ten 20 μm slices in each extraction, to give a sampling resolution of 200 μm, which captured the seasonal cycle. Trees that grow consistently throughout the year with relatively little sensitivity in growth rate are most useful in such studies because changes in ring width affect the capture of the annual signal if regular sampling increments are used. Thus, in opposition to the rules of traditional dendroclimatology, a constant growth rate is an advantage in tropical isotope dendroclimatology.

The wood component normally selected for isotopic analysis is α-cellulose; however, there is increasing evidence that whole wood might be used for $\delta^{13}C$ or $\delta^{18}O$ analysis (Verheyden et al. 2005; Cullen and Grierson 2006). In conifers, resins have

to be extracted first, because they are mobile between rings; the methods used to prepare laths for X-ray densitometry are adequate for this (Schweingruber et al. 1978). In the most commonly used method for extracting whole wood to α-cellulose, lignin is oxidized by the *in situ* generation of chlorine dioxide (ClO_2), by using acidified sodium chlorite in aqueous solution to yield holocellulose (Green 1963; Wilson and Grinsted 1977; Leavitt and Danzer 1993) or treated further to hydrolyze hemicelluloses by using sodium hydroxide to yield α-cellulose (Green 1963; Loader et al. 1997) . Most laboratories use a rapid 'batch processing' version (Loader et al. 1997; Rinne et al. 2005). An alternative method for cellulose preparation, proposed by Brendel et al. (2000), and subsequently modified by Gaudinski et al. (2005), which is even faster and uses relatively benign chemicals, has been used successfully in a number of studies (e.g., Poussart et al. 2004; Evans and Schrag 2004; Poussart and Schrag 2005; Anchukaitis et al. 2008a).

Whole-wood and cellulose stable carbon isotope ratios, although offset, seem to vary in parallel. Borella et al. (1999) concluded that a portion of signal is lost in whole wood, but Loader et al. (2003) found that cellulose and lignin $\delta^{13}C$, from oak, gave marginally weaker correlations with instrumental climate data than whole wood from the same trees. The use of whole wood is also supported for $\delta^{18}O$ analysis. Barbour et al. (2001) compared $\delta^{18}O$ analyses of different wood components in a global dataset of oak and pine to conclude that no climate information was lost in analyzing whole wood over α-cellulose and, depending upon local conditions, concluded that extraction of α-cellulose from wood samples might be unnecessary for isotope studies. Some caution is required in working with subfossil wood, due to the differential decay rates of lignin and cellulose (Schleser et al. 1999). For hydrogen isotope analysis, cellulose nitrate or isotopically equilibrated cellulose must be analyzed, owing to the propensity for isotopic exchange in approximately 30% of the hydrogen atoms. Equilibration replaces all of the exchangeable hydrogen atoms with hydrogen of known isotopic composition and, in nitration, the hydroxyl hydrogen is replaced by nitro groups (Ramesh et al. 1986; Filot et al. 2006).

Methodological choices for sampling and measurement should be made on the basis of the aims and objectives of the study and might usefully be viewed as a series of questions (Fig. 6.1) in order to choose the most efficient methodology for sample preparation.

6.3.1 A Note on New Measurement Techniques

Measurements of cellulose $\delta^{18}O$ are in fact an average of five oxygen molecules, all of which have different potentials for reexchange with stem water, by virtue of their position in the cellulose matrix. Therefore, certain of the oxygen molecules more reliably record the source water signal than others, which has been confirmed from experimental measurements on crop seedlings (Sternberg et al. 2006). For example, one molecule exchanges fully with source and trunk water (named as oxygen-2)

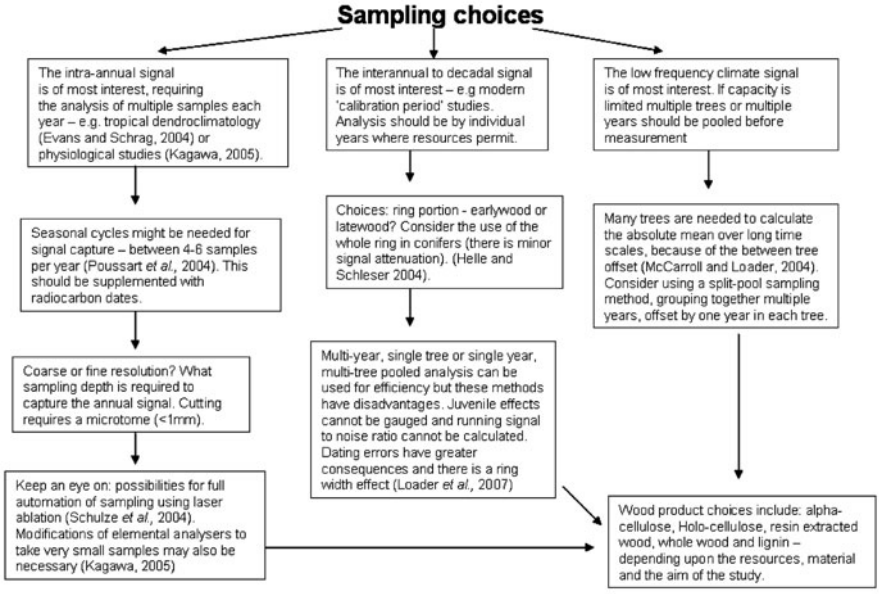

Fig. 6.1 Methodological choices in stable isotope dendroclimatology can be viewed as a flow chart of options. The aims and objectives of the study should guide: sampling resolution and pooling options, ring portion sampled (earlywood, latewood, or whole ring), and wood product choice

whilst another does not exchange with trunk water but records evaporative enrichment and the Peclét effect. The isotopic variability between these molecules is not insignificant; the fractionation of oxygen-2 differs from the average fractionation of the other molecules by 9‰ (Sternberg et al. 2006). Isolation of those oxygen molecules that hold the strongest climatic signal is known as 'position-specific analysis' and has been piloted successfully through the used of derivitized cellulose (Mullane et al. 1988; Sternberg et al. 2006). Complex synthetic organic chemistry is required to extract and separate the molecules prior to measurement. Each molecule, or group of molecules, is chemically exposed or protected in turn in order to measure its $\delta^{18}O$ value (Waterhouse, personal communication). Position-specific analysis is still in development, and it will be some time before it can be used in the measurement of long chronologies, but it is potentially an extremely powerful technique.

With evidence that whole wood, rather than cellulose, might routinely be used in stable isotope dendroclimatology, there is now scope for developing fully automated sampling systems. One of the most exciting possibilities is a coupled system using ultraviolet laser ablation. An ablating laser can be used to sample whole wood pieces, of just a few microns, from a standard core. Ablation produces an aerosol of wood particles, suspended in a helium current, which can be streamed directly into a combustion furnace and gas chromatography-IRMS (GC-IRMS) system (Schulze et al. 2004; Skomarkova et al. 2006).

6.3.2 Data Treatment of Stable Isotope Time Series

One of the great advantages of stable isotopes over the traditional growth proxies is that there appear to be no long-term age-related trends in stable isotope time series. The evidence for this conclusion is good for carbon (e.g., Gagen et al. 2007), but less certain for oxygen and hydrogen. If confirmed, this conclusion would mean that statistical detrending is not required, and the attendant problems of loss of low-frequency climate signals can be avoided. The 'segment length curse' (Cook et al. 1995), therefore, would not apply.

Stable carbon isotope series may require some treatment, to remove a 'juvenile effect' and to deal with the effect of changing atmospheric composition since industrialization.

The juvenile effect, seen as depleted but rising values for the first few decades of a tree's life (Fig. 6.2), varies with site and species, but magnitudes of ~2‰ are common over 20–40 years (e.g., Bert et al. 1997; Duquesnay et al. 1998; McCarroll and Pawellek 2001; Anderson et al. 2002; Arneth et al. 2002; Gagen et al. 2004; Raffalli-Delerce et al. 2004). In Fig. 6.2, the averaged series reveal the dramatic juvenile trend in $\delta^{13}C_{corr}$ (tree-ring $\delta^{13}C$ after atmospheric correction), which lasts for different periods of time at the two sites. After a few decades the series no longer show sharply rising $\delta^{13}C_{corr}$ values but do continue to show variability. However, crucially, there is no long-term trend pattern after the juvenile period. Over very long timescales, the presence or absence of long-term trends in $\delta^{13}C$ has not yet been assessed, but there is good evidence for the lack of age-dependent trends in the post-juvenile period.

Theories on the cause of the juvenile trend include recycling of respired CO_2, changes in hydraulic conductivity with height gain, and changes in light levels (Schleser and Jayasekera 1985; Heaton 1999; McDowell et al. 2002). The effects can simply be removed by linear detrending (e.g., Wilson and Grinsted 1977) or by using methods such as regional curve standardization (Briffa et al. 1992, 1996; Gagen et al. 2008), but the simplest solution is to remove the juvenile portion from each tree prior to analysis (e.g., Tans and Mook 1980; Arneth et al. 2002). It is advisable, at any new site, to analyze a few trees to pith, in order to correctly gauge the length of the juvenile period for a particular species and site.

Because fossil fuel–derived CO_2 is depleted in ^{13}C (Freyer and Belacy 1983), there is a nonlinear decline in the $\delta^{13}C$ of atmospheric CO_2 ($\delta^{13}C_{atm}$) since about AD 1850. Fractionation is additive (Farquhar et al. 1982), so any change in the isotopic ratio of CO_2 is incorporated into the isotopic ratio of the cellulose produced within the tree. Thus, all tree-ring $\delta^{13}C$ series, whether or not they display any trend over the industrial period, must be corrected for changes in the isotopic ratio of atmospheric CO_2. Since annual values of $\delta^{13}C_{atm}$ are available (e.g., McCarroll and Loader 2004), tree-ring $\delta^{13}C$ values can be corrected to a preindustrial (AD 1850) standard value of −6.4‰ ($\delta^{13}C_{cor}$) by using:

$$\delta^{13}C_{cor} = \delta^{13}C_{plant} - (\delta^{13}C_{atm} + 6.4) \tag{6.4}$$

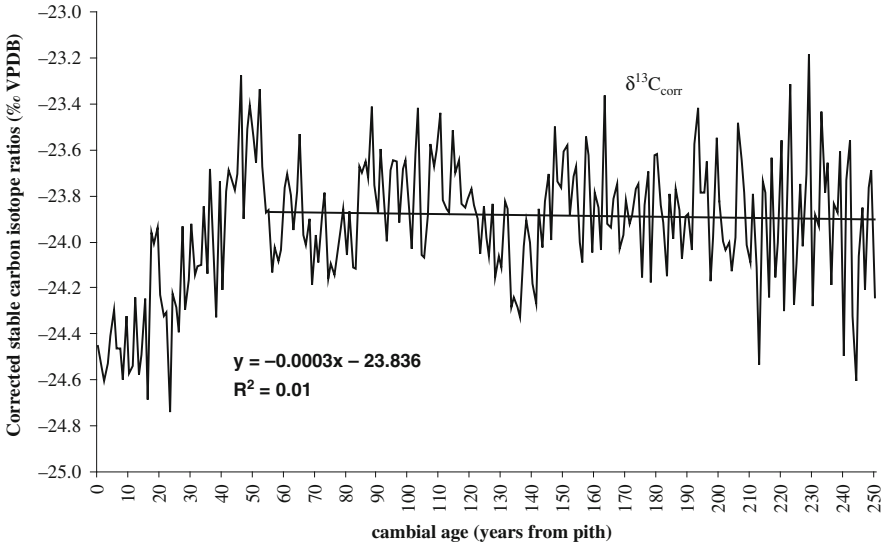

Fig. 6.2 The juvenile trend in $\delta^{13}C$ is shown when $\delta^{13}C$ ratios, corrected for changes in atmospheric CO_2 ($\delta^{13}C_{corr}$) and aligned to a common mean, are cambial age aligned. The mean of 12 *Pinus sylvestris* trees from sites at the northern tree line in Finnish Lapland is shown (the time series is from Gagen et al. 2007). A linear *trend line* indicates the lack of any long-term trend after the trees reach ~50 years in cambial age. The juvenile trend, prior to this, imparts a dramatic rise in $\delta^{13}C$

As the amount of CO_2 in the atmosphere has also increased, we might expect to see a direct response to this in trees, because it is the ratio of internal to ambient CO_2 concentrations that controls $\delta^{13}C$. If trees did not respond at all to the increase in the availability of CO_2, and the rates of stomatal conductance and assimilation remained unaffected, then $\delta^{13}C_{cor}$ values would show a marked decline since AD 1850, with an acceleration after AD 1950. However, we rarely see such a pattern in tree-ring $\delta^{13}C_{cor}$ series, suggesting that trees have actively responded to rising CO_2 by increasing their water use efficiency and keeping the ratio c_i/c_a approximately constant (Saurer et al. 1997, 2004). There is good theoretical evidence for why they might show this response (e.g., Körner 2003). The response is advantageous because it means that we do not usually need to make any correction over most of the industrial period. There is growing evidence, however, that in recent decades many trees have reached the limits of this plastic response, so that water use efficiency is no longer increasing and the $\delta^{13}C_{cor}$ values are falling rapidly (Waterhouse et al. 2004).

6.4 Progress to Date

Early studies of stable isotopes in tree rings were severely constrained by the limitations of mass spectrometry at the time and, although they made significant steps towards a mechanistic understanding of the proxy, they did not make a contribution

to climatology (Hughes 2002). Such was the time commitment involved in obtaining a few isotopic measurements, they were exclusively based upon unreplicated 'single-tree' series (e.g., Craig 1954; Farmer and Baxter 1974; Epstein and Yapp 1976; Libby et al. 1976). However, early studies provided evidence of the link between moisture stress and ^{13}C enrichment and detected a relationship between narrow rings and enrichment (Craig 1954). Craig (1954) carried out his study on *Sequoia*, from a relatively arid environment, and thus was able to identify the simple link between isotope ratios and moisture stress typically found in such an environment. Libby was perhaps a little overoptimistic in entitling her *Nature* paper 'Isotopic Tree Thermometers' (Libby et al. 1976).

Park and Epstein (1960, 1961) demonstrated that plants discriminate against the heavier carbon isotope during photosynthesis and identified the biochemical pathways where this selection occurs. Early observations also indicated that varying amounts of resins and waxes would contribute to isotopic variability in different wood components because they differ in volume (Wilson and Grinsted 1977) and are mobile between rings (Long et al. 1979) .

Epstein et al. (1977) first noted that it might be possible to transfer the work on isotope ratios in precipitation, carried out by Dansgaard (1964) and others, to look at archived oxygen and hydrogen isotope ratios in tree rings. The lack of a theoretical framework to explain stable isotope variability in plant materials meant that interpretation of these early series was often oversimplistic, with little understanding of the biological mediation of the signal (Loader et al. 2007). Thus the proxies could not be fully exploited until the development of appropriate models provided a framework for interpretation.

Leavitt and Long (1982) reviewed the current 'state of play' in stable isotope dendroclimatology and expressed concern at the apparent wide range of fractionation effects and environmental variables that could be found in measured ratios, questioning the merit of stable isotope dendroclimatology in much the same way as Hughes (2002) later did. However, publication of the 'carbon isotope model' by Farquhar et al. (1982) and a subsequent paper describing the application of the model for the interpretation of tree-ring data by Farquhar et al. (1982) effectively explained why there is natural variability between trees and why different trees can carry different climate signals. Larger sample sizes were also found to provide more coherent results (Freyer and Belacy 1983; Leavitt and Long 1984).

A mechanistic focus is also observed in the early literature on water isotopes, with measurements often carried out in conjunction with leaf water analysis using terrestrial plants (e.g., Epstein et al. 1977; Burk and Stuiver 1981) . The understanding of the relationship between $\delta^{18}O$ of cellulose and soil water was subsequently based on the idea that exchange might occur between carbohydrate and stem water, with additional fractionations during pre-cellulose remobilization (Cooper and Deniro 1989).

The need for increased replication without an increase in the cost per sample became a strong driver of multi-tree pooling methods. Many of the first stable isotope studies managed to analyze multiple trees at annual resolution, at a time when stable isotope measurement was still expensive and time consuming, by pooling

material from several trees, and this became common practice before the routine use of continuous-flow IRMS (e.g., Leavitt and Long 1984; Borella et al. 1999).

Numerous studies have attempted to express isotopic ratios as a direct linear function of temperature (i.e., as ‰ per ºC; e.g., Feng and Epstein 1995 for δD; Lipp and Trimborn 1991 for $\delta^{13}C$; Anderson et al. 1998 for $\delta^{18}O$). However, for carbon isotopes, this is an oversimplification without a firm theoretical basis (Heaton 1999). Different $\delta^{13}C$ signals are observed at different sites because of the potential for climatic control via either assimilation rate or stomatal conductance. At cool, moist, high-latitude sites, the $\delta^{13}C$ signal in tree rings tends to be dominated by those variables that are associated with controls on *A*, such as summer irradiance and temperature (McCarroll and Pawellek 2001). At dry sites the climatic signal tends to be dominated by *g*, and $\delta^{13}C$ records those variables that control soil moisture status and air humidity (Gagen et al. 2004). Site climatology and hydrology also affect the signal in δD and $\delta^{18}O$. At some sites, water isotopes in trees capture a strong source water signal and little temperature signal (e.g., Tang et al. 1999); at others, a temperature (e.g., Switsur et al. 1994) or relative humidity (e.g., Robertson et al. 2001) signal. $\delta^{18}O$ can also record precipitation effectively, via the relationship between precipitation amount and enrichment (Treydte et al. 2006).

In recent years there has been a plethora of papers that describe the relationship between tree-ring stable isotopes and climate. The vast majority of these papers are limited to trees from a single site; usually the material from several trees is pooled so that there is no estimate of signal strength, and the length of the records rarely extends beyond the period for which there are instrumental climate records (see McCarroll and Loader 2004 for a review). These papers have undoubtedly shown that stable isotope dendroclimatology has potential, but in very few cases has that potential actually been realized through climate reconstructions. There are still very few stable isotope tree-ring-based paleoclimate reconstructions that traditional dendrochronologists would recognize as well replicated, calibrated, and verified. So far, no tree-ring stable isotope data have contributed to efforts to reconstruct the climate of the last millennium over large areas.

This situation is not unexpected. Before recent advances in the rate at which tree-ring samples can be analyzed, long well-replicated chronologies were simply not feasible. However, that excuse no longer holds, and many isotope laboratories are now producing data rapidly enough to make a real contribution to climatology. In the Swansea laboratory in 1997, for example, it took approximately 144 h to extract a cellulose batch and samples were analyzed for CO_2 offline, one by one. In 2007, the value was closer to 36 h for batch cellulose extraction and IRMS autosamplers could run at the rate of about 10 min per sample, 24 h a day. The limiting step became ring cutting and the chemistry required to prepare α-cellulose, not the measurement of isotopes.

The first well-replicated stable isotope tree-ring-based paleoclimate reconstructions are now starting to appear. Treydte et al. (2006), in the most well-known recent example, reconstructed precipitation in the High Karakorum region of Pakistan from $\delta^{18}O$ cellulose derived from juniper. The reconstruction (Fig. 6.3) is based

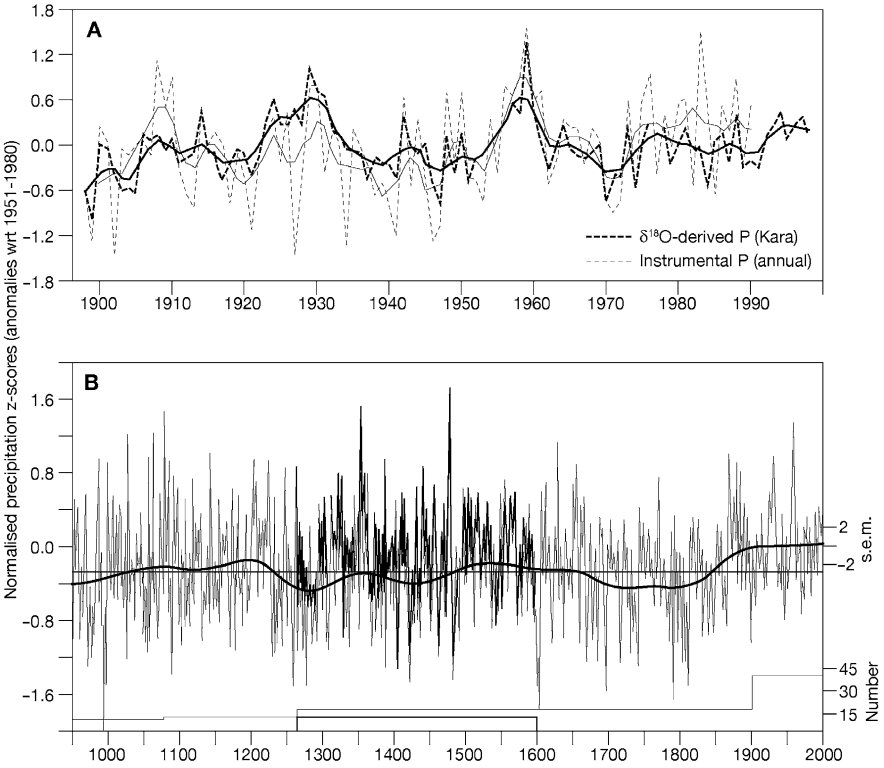

Fig. 6.3 (**a**) Annual precipitation values (AD 1898–1990) from instrumental and tree-ring δ^{18}O-derived modeled data with respect to the 1951–1980 instrumental mean. Smoothed curves (5-year Kernel filters) are shown for the δ^{18}O (*thick black*) and instrumental (*dashed gray*) series. (**b**) The δ^{18}O-based precipitation reconstruction since AD 950. Proxy data were calibrated by using a linear regression over the time period AD 1898–1990. The raw δ^{18}O series is inverted owing to the negative sign of the regression slope. The *horizontal line* is the overall mean of the reconstruction. For the period AD 1264–1599, maximum deviations are shown in *black*, when using data only from old tree rings. Replication of the reconstruction is three trees (six cores) at AD 950. Long-term variations are highlighted by using a 150-year spline (*thick black curve*). Uncertainty estimates for the low-frequency domain are indicated by two standard errors. Adapted by permission from Macmillan Publishers Ltd: Nature (Treydte et al. 2006), copyright 2006

on a correlation of $r = 0.58$ (AD 1898–1990, $P < 0.001$) with September–October instrumental precipitation values. Treydte et al. (2006) investigated the effects of developing reconstructions from different age classes of trees and found that little age-related bias was imparted into the reconstruction, though they note a slight change in the high-frequency component when only juvenile trees are used. However, the low-frequency components of the reconstruction are unaffected by tree age. The reconstruction is spatiotemporally robust, with the same signal being captured at various ecologically distinct sites, and at decadal to centennial scales. The record also shows coherence with other proxy records across the Northern

Hemisphere. This reconstruction certainly satisfies Hughes' (2002) query (and it is based on an average sample depth of 14 cores from seven trees, measured as a pooled record with a minimum *n* of 3 in its earliest portion); furthermore, it contributes significantly to climatology through evidence that changes in precipitation patterns probably exceed natural variability over the recent past (Evans 2006).

In addition to robust 'single-site' studies, 'network' stable isotope dendroclimatology projects are also providing exciting results. The European Union–funded 'ISONET' project brought together many laboratories to produce 400-year isotope chronologies from across Europe, mostly based on pooled material. Those data are being used to examine the spatial coherence of the isotope signals from tree rings (Treydte et al. 2007). Gagen et al. (2007) reconstructed the summer temperature of northern Finland back to AD 1640 based on a well-replicated $\delta^{13}C$ record, without pooling, and were able to demonstrate strong calibration and verification statistics. The EU-funded 'Millennium project' (www.millenniumproject.net) is currently building stable isotope chronologies at 12 sites across Europe, all of which will extend for at least 500 years, and most for more than 1,000 years. These isotope records will be integrated with tree-ring width, density (or blue intensity: McCarroll et al. 2002) measurements and with other proxies, including those obtained from peat mires and lake sediments, to produce multiproxy climate reconstructions.

6.5 Future Directions

Tree-ring width and density proxies have traditional geographical strongholds where it will be hard for stable isotopes to contribute more, and probably not an efficient use of resources to try. Correlations between ring width/density and climate are famously high; for example, at the northern timberline (e.g., Linderholm and Eronen 2000; Linderholm and Gunnarson 2005). Here, stable isotope records are unlikely to be able to compete as a proxy for summer temperature. Although, stable carbon isotopes do appear to display comparable results to the traditional proxies, even in the stronghold regions of the latter (Fig. 6.4), and also show equally high, sometimes higher, common signal strengths (Robertson et al. 1997a, b; McCarroll and Pawellek 1998; McCarroll et al. 2003; Gagen et al. 2004; Table 6.1). Robertson et al. (1997a, b) found that generally slightly fewer $\delta^{13}C$ series are needed than ring width series for equivalent *r* values, with high-frequency indices only. The same information is not yet known for the lower-frequency signal in stable carbon isotopes. Signal strength in $\delta^{13}C$ may well be variable both spatially and by frequency.

In the example shown in Fig. 6.4, stable carbon isotopes from latewood cellulose and maximum latewood density capture slightly different (but strongly autocorrelated) climatic variables in the southern French Alps, with density recording summer temperatures most strongly and stable isotope ratios (in a relatively dry region) responding most strongly to summer precipitation (see Gagen et al. 2004 for details). The spatial pattern of correlation with gridded climate data reveals a comparably strong climatic signal in the $\delta^{13}C$ series compared to the maximum latewood density

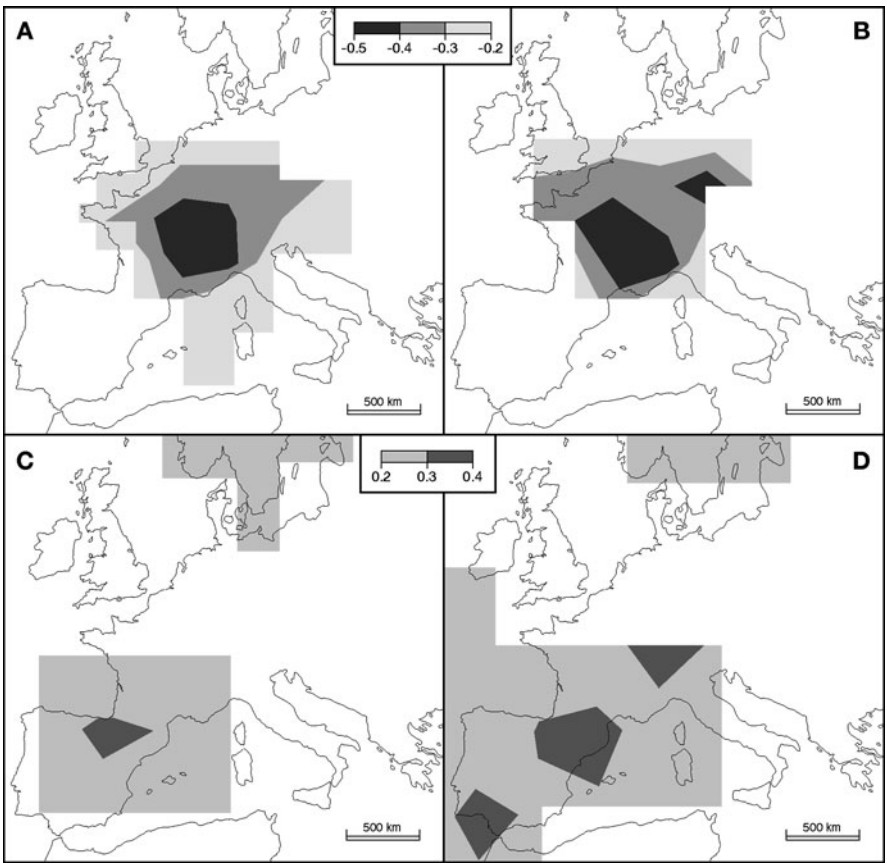

Fig. 6.4 The spatial pattern of correlation with gridded climate data revealed by maximum latewood density (MXD) ('upper site' series from Gagen et al. 2004; $n = 14$) and latewood $\delta^{13}C$ (composite upper and lower site mean series in Gagen et al. 2004; $n = 6$) from *Pinus sylvestris* and *Pinus uncinata* sampled at Montgenévre (see Gagen et al. 2004 for details). (**a**) Stable carbon isotopes and June–August precipitation (University of East Anglia, Climatic Research Unit CRU TS 2.1, 0.5° analysis, precipitation: AD 1901–1995). (**b**) Maximum latewood density and June–August precipitation (CRU TS 2.1 0.5° analysis, precipitation; AD 1901–1995). (**c**) Stable carbon isotopes and July–August temperature (AD 1901–2002; CRU TS 2.1 0.5° analysis). (**d**) MXD and July–August temperature (AD 1901–2002; CRU TS 2.1 0.5° analysis). Spatial field correlations were performed by using KNMI Climate Explorer

series, when correlated with summer precipitation; however, for summer temperatures, the signal is both stronger and more spatially homogenous with the latewood density series.

It is in situations such as this—where stable isotopes can provide a measure of a different climatic variable that might be coupled to temperature reconstructions derived from the traditional tree-ring proxies—that stable isotope dendroclimatology has much to offer.

Table 6.1 Expressed population signal (EPS) (Wigley et al. 1984) and mean *r* for a range of measured $\delta^{13}C$ series from the literature

	EPS Ring width Numbers in parentheses are *n*	EPS Maximum density Numbers in parentheses are *n*	EPS latewood $\delta^{13}C$ Numbers in parentheses are *n*
Pinus sylvestris French Alps ('upper site' in Gagen et al. 2004)	0.92 (14)	0.95 (14)	0.88 (4)
Pinus sylvestris, northern timberline, Finnish Lapland (Laanila in McCarroll et al. 2003)	0.83 (5)	0.95 (5)	0.96 (5)
Pinus sylvestris, northern timberline, Finnish Lapland (Kaamanen in McCarroll et al. 2003)	0.81 (5)	0.91 (5)	0.97 (5)
Pinus sylvestris, northern timberline, Finnish Lapland (Kevo in McCarroll et al. 2003)	0.91 (5)	0.96 (5)	0.97 (5)
	Mean inter-tree correlation coefficient (r) Ring width Numbers in parentheses indicate trees required for EPS > 0.85		Mean inter-tree correlation coefficient (r) $\delta^{13}C$ Numbers in parentheses indicate trees required for EPS > 0.85
Robertson et al. 1997b *Quercus robur,* Finland, Kasvitieteellinen Puutarha	0.57 (5)		0.79 (2)
Robertson et al. 1997b *Quercus robur,* Finland, Kansanpuisto	0.60 (4)		0.70 (3)
Robertson et al. 1997a. *Quercus robur*, England, Sandringham.	0.41 (9)		0.59 (4)

In Gagen et al.(2004) and McCarroll et al. (2003) EPS is given (*n* in parentheses). For Robertson et al. (1997a, b), mean *r* and the required number of trees for EPS ρ>0.85 are given.

There is also much to be gained from focusing stable isotope investigations on parts of the world where growth proxies do not hold a strong climate signal.

The most pressing priority for stable isotope dendroclimatology is the production of long chronologies obtained by using sampling strategies that allow the signal-to-noise ratio to be calculated and calibration and verification to be carried out using the tried and tested protocols of traditional dendroclimatology. Whilst the testing of the stable isotope proxies was, sensibly, carried out in those areas where results could be compared with existing ring width and density chronologies and using data from the last few hundred years, exploiting the proxy's specific strength now requires more imaginative study design. That is the first step in moving beyond 'potential.'

6.5.1 Climate of the Moist Midlatitudes

Most studies using tree-ring stable isotopes have concentrated on sites where growth is strongly limited by a single climate parameter—typically tree line sites for temperature and very dry sites for precipitation. However, these are precisely the types of sites where the traditional tree-ring proxies already perform very well. The strong common signal in stable isotope series means that fewer trees are required, but

where there are plenty of trees available that is no real advantage, given the extra cost and effort required for IRMS. One of the great challenges for isotope dendroclimatology is to extract climate signals from areas where traditional measurements do not perform well, such as the moist midlatitudes where, for example, climatically sensitive ring width series are often limited to high-altitude sites. Climate reconstructions from such areas are needed to redress the bias towards high latitudes in hemispheric temperature reconstructions and to test general circulation models (GCMs).

Long tree-ring chronologies already exist for many areas in the moist midlatitudes, typically constructed for dendrochronological dating, or to calibrate the radiocarbon timescale rather than for climate reconstruction (e.g., Pilcher and Baillie 1980; Suess 1980; Becker 1993; Friedrich et al. 2004). There must be some common (climatic) information in these ring width series; otherwise, they would not crossdate, but it is rarely strong enough to be useful for climate reconstruction. The common signal in isotope series is also likely to be weaker away from the ecological boundaries, and so the required replication will be greater, but preliminary results suggest that it may be possible to produce acceptable climate reconstructions based on stable isotopes (Saurer et al. 1995; Switsur et al. 1996; Loader and Switsur 1996; Robertson et al. 1997a, b; Saurer et al. 1997; Hemming et al. 1998; Loader et al. 2008). This would be a valuable contribution to climatology.

6.5.2 Different Climate Signals

The climate reconstructions that have so far been produced have not been based on mechanistic models; they have used the same statistical techniques that are used in the more traditional approaches to dendroclimatology. However, we know that this is a simplification of reality, and that none of the isotopes is really controlled by a single climate parameter in a linear fashion. Of course this is true for all proxies, and there are many factors that can influence the annual growth increment of a tree, for example. The advantage with stable isotopes, however, is that the range of parameters that can control fractionation and cellulose formation are both limited and relatively well understood.

This does not help, of course, in interpreting a single isotope series in isolation; all we can say is that there is more than one potential change in climate that could explain a rise or fall in the stable isotope values in a particular tree, in the past. However, when we combine two or more stable isotope series together, and also include the growth proxies, then we can begin to define a much smaller range of conditions under which a particular suite of proxies will covary through time.

Stable isotopes almost certainly perform best in combination with each other; there are numerous different climatic conditions that might lead to a particular $\delta^{13}C$ value, but a much smaller range of conditions will account for a specific combination of $\delta^{13}C/\delta^{18}O$ values (McCarroll and Loader 2004). The potential of this ‘multiproxy’ or ‘multiparameter’ approach to dendroclimatology looks very promising. For example, McCarroll et al. (2003) combined stable carbon isotopes

and maximum densities of pine trees in northern Finland to recognize years with very low summer rainfall, even though moisture stress did not limit the growth of the trees. Gagen et al. (2004) have shown how proxies might be expected to covary under different climate change scenarios, but so far stable isotope dendroclimatology has not been used to produce chronologies that contain any climate parameters that could not have been produced by using the traditional proxies. However, the need for reduced data treatment and statistical detrending is an attractive characteristic may provide access to a greater proportion of lower-frequency climate information and represent a unique advantage of the isotopic proxies.

6.5.3 Tropical Isotope Dendroclimatology

Traditional dendrochronology has been unable to establish itself in large parts of the tropics, and only extratropical species have contributed significantly to large-scale paleoclimate reconstructions (Mann 2002). Whilst tropical climatology may prevent the formation of an annual ring boundary, the tropics are, in fact, the only place where we potentially have a signal for the entire year, because growth does not necessarily stop. Stable isotopes are capable of capturing this signal, even where no visible ring is seen. Sites in the tropics may not exhibit the temperature seasonality needed to form rings, but in the majority of areas, there is a seasonal cycle in precipitation, arising either from wetter and dryer seasons, or from a shift in the dominant trajectory of precipitation-bearing air masses, which seems to be recorded in wood cellulose in a cyclical way. Evans and Schrag (2004) coined the term 'tropical isotope dendroclimatology' and presented empirical and theoretical evidence supporting the capture of rhythmical seasonal cycles in $\delta^{18}O$.

Seasonal cycles in precipitation isotopes may also arise from a fractionation effect in the hydrological cycle, known as the 'amount effect'—the process by which preferential rainout of the heavier water isotopes (^{18}O and ^{2}H) leaves subsequent precipitation depleted. The $\delta^{18}O$ of precipitation is negatively correlated with rainfall amount, and this effect is one of the primary features of intra-annual variability in the isotopic composition of rainfall in the tropics (Gat 1996). Layered on top of this seasonal cycle, the amount effect also captures a climate signal; the greater the amount of precipitation within a season, the more depleted the $\delta^{18}O$ signal in the wood products (Evans and Schrag 2004; Anchukaitis et al. 2008b). The amount effect can be used to explain precipitation $\delta^{18}O$ over a range of timescales such that unusually rainy years are offset as low $\delta^{18}O$ values, and unusually dry years are offset as high values (Evans and Schrag 2004). It may also be possible to use cycles in cellulose $\delta^{18}O$ derived from geographical shifts in dominant moisture source to derive climate records.

Seasonal variations in cellulose $\delta^{13}C$ also retain an annual signal. The seasonal amplitude in $\delta^{13}C$ of atmospheric CO_2 in the tropics should be between 0.4‰ and 0.6‰ (Mook et al. 1983) and a seasonal cycle in discrimination, within the tree, will layer on top of this. Poussart et al. (2004) measured interannual $\delta^{13}C$ and $\delta^{18}O$ variability in Thai *Podocarpus* species, finding greater amplitude in $\delta^{18}O$

but more strongly defined cycles in $\delta^{13}C$. Low assimilation rates at the start of the growth season (with high c_i and discrimination) give relatively depleted $\delta^{13}C$ values, as A increases, to the height of the growing season, discrimination drops and $\delta^{13}C$ rises, to a seasonal maximum. The pattern is then reversed to the end of the growing season, closing the cycle. Poussart et al. (2004) also find an association between enrichment (as a result of moisture stress) with El Niño/Southern Oscillation (ENSO) events, suggesting that chronology and signal may be derived from $\delta^{13}C$.

Whist tropical isotope dendroclimatology is still very much in development, and is only one of a range of tree-ring methods that are being used to exploit the tropical tree-ring archive (e.g., Worbes 2002; Poussart et al. 2006), in areas where the lack of a dry season prevents annual ring formation, isotope-derived hydrological proxies might be used to improve the paleoclimate picture of tropical phenomena such as ENSO (Evans and Schrag 2004). To date, replication and an indication of common signal strength has been lacking in most tropical isotope dendroclimatology studies. However, more rigorous analyses of signal strength, replication requirements, and quantitative climate calibrations are beginning to appear in the tropical isotope dendroclimatology literature (e.g., Anchukaitis et al. 2008b).

6.5.4 Long-Term Response of $\delta^{13}C$ to Rising CO_2 Concentrations

Atmospheric corrected $\delta^{13}C$ series often show a decline, particularly over recent decades, for which there is no evidence of a climatic cause (e.g., Treydte et al. 2001; Gagen et al. 2007). The decline is often site and species specific (e.g., Liu et al. 2007). The atmospheric concentration of CO_2 (c_a) is an important component of the stable carbon isotope fractionation model; $\delta^{13}C$ reflects the control of c_i relative to changes in c_a, over longer timescales. Thus, rising c_a has the potential to affect tree-ring $\delta^{13}C$, and an increasing body of evidence supports this conclusion. If the effects of changing c_a are becoming an additional source of noise in tree-ring $\delta^{13}C$, this will become a problem for proxy climate calibration.

The simplest way to correct for rising c_a is to simply add a correction factor based on average tree response. However, it is not logical to assume that all trees, at all sites, will respond in the same way to rising c_a, and there is evidence that response is highly individual (Waterhouse et al. 2004). Simply selecting different correction factors from the literature is ill-advised, as it seems to result in very different time series. Loader et al. (2007) apply correction factors from Feng and Epstein (1995), Kürschner (1996), and Treydte et al. (2001) to a $\delta^{13}C$ dataset of *Pinus sylvestris* from northern Finland and derive significantly different corrected series as a result. A reconstruction based on their different correction factors would produce either cooling or warming, depending upon which factor was selected; this is clearly a subjective and inappropriate method. It may be more appropriate to correct c_i according to how it changes through time, on a tree-by-tree basis, as c_a rises.

Whilst changes in $\delta^{13}C$ derived from shifts in c_a must be removed prior to calibration, they do reveal important information about tree response to rising CO_2 that

has relevance to the 'divergence' debate (e.g., Wilson et al. 2007). The most common tree response to rising c_a is an increase in intrinsic water use efficiency (iWUE) because, with more CO_2 available in the atmosphere, stomata are able to limit water loss without adversely affecting assimilation rate. Saurer et al. (1997) found that 125 out of 126 trees sampled for $\delta^{13}C$ across Europe showed improvements in iWUE over the recent past. As iWUE changes, it is possible that the $\delta^{13}C$-climate relationship in trees will alter, and quite possibly the relationship between tree-ring width/density and climate. As trees become less sensitive to moistures stress, they may not respond as strongly to other climatic limiting factors. The rise in c_a can be likened to moving trees from their climatically sensitive ecological limits to more mesic sites.

6.6 Is It Worth It? A Reply to Hughes (2002)

The simple answer to this question is probably 'not always.' There are many circumstances where stable isotope dendroclimatology will not really produce anything that could not be produced more cheaply and easily by using ring widths and densities. However, there are some clear strengths of the isotope approach, which could be used to good effect.

- Stable isotopes can display higher signal strengths, in comparison to equivalent ring width and density series. This does not really matter where material is abundant, but that is rarely the case in the distant past, and the early years of many reconstructions are not adequately replicated. Where isotope methods could produce strong climate signals with fewer trees, they could be used to strengthen existing long chronologies or to produce viable chronologies where material is sparse.
- It would seem that, apart from a short juvenile phase in carbon isotope series, there are no long-term age-related trends in $\delta^{13}C$, and this characteristic probably applies also to $\delta^{18}O$ and δD series. This means that the 'segment length curse' probably does not apply in extending reconstructions back in time. At present, there are too few well-replicated, long tree-ring stable isotope chronologies available to confidently comment on the low-frequency signals that they contain. We can at least say that they have the potential to retain climate information at the low frequencies that are so difficult to capture by using other approaches.
- By using more than one isotope series from the same area, and combining them with other tree-ring proxies, in a multiproxy approach to dendroclimatology, it may be possible to reconstruct a wider range of climate parameters and also to detect climatic conditions in the past that do not occur during the relatively short calibration periods for which meteorological data are available.
- Stable isotopes may provide access to climate records in tropical trees, though the very large number of samples required will necessitate a further leap in the rate at which samples can be analyzed. The most promising approach is likely to involve linking an ablating laser to an isotope ratio mass spectrometer.

In their introduction to a special issue on stable isotope dendroclimatology in *Chemical Geology*, Robertson et al. (2008) point out the contrast between the 30 isotope tree-ring papers presented at the recent Seventh International Conference on Dendrochronology (Beijing; June 11–17, 2006) compared to the two delivered at the Second International Workshop on Global Dendroclimatology in 1980. Of the 30 papers presented, however, only six were reconstruction based. There are numerous well-equipped laboratories around the world capable of rapidly producing long stable isotope-based reconstructions. As a community we need to make the correct procedural choices to enable this to happen rapidly and to ensure that the supply of appropriately robust results for climatology begins in earnest.

We believe that the analysis of stable isotopes in tree rings does indeed have something to offer to the field of climatology. However, there are also many circumstances where stable isotope dendroclimatology will produce information that can be replicated more efficiently by using ring widths or densities. If we are truly to understand past climate variability and address, as a scientific community, the challenges of future environmental change, then it is imperative that those working with stable isotopes do not do so in isolation. To do so is to risk simply replicating existing tree-ring-based paleoclimate reconstructions by using a more expensive technique. On the contrary, isotope specialists need to take their place within the broader discipline and explore the ways in which stable isotopes can add value to a field that is already providing the best high-resolution reconstructions of past climate.

Acknowledgements This work was supported by the European Union project 017008-2 GOCE (MILLENNIUM). MHG was supported by a RCUK Fellowship. NJL was supported by the NERC NE/B501504/1 and NE/C511805/1. The authors thank our colleagues at the Tree Ring Group at Swansea University and N. Jones, and A. Ratcliffe (Swansea) for their invaluable assistance.

References

Anchukaitis KJ, Evans MN, Lange T, Smith DR, Schrag DP, Leavitt SW (2008a) Consequences of a rapid cellulose extraction technique for oxygen isotope and radiocarbon analyses. Anal Chem 80:2035–2041. doi:10.1021/ac7020272

Anchukaitis KJ, Evans MN, Wheelwright NT, Schrag DP (2008b) Isotope chronology and climate signal calibration in neotropical cloud forest trees. J Geophys Res 113. doi:10.1029/2007JG000613

Anderson WT, Bernasconi SM, McKenzie JA, Saurer M (1998) Oxygen and carbon isotopic record of climatic variability in tree-ring cellulose (*Picea abies*): an example from central Switzerland (1913–1995). J Geophys Res J103(D24):31625–31636

Anderson WT, Bernasconi SM, McKenzie JA, Saurer M, Schweingruber F (2002) Model evaluation for reconstructing the oxygen isotopic composition in precipitation from tree-ring cellulose over the last century. Chem Geol 182:121–137

Arneth A, Lloyd J, Santruckova H, Bird M, Grigoryev S, Kalaschnikov YN, Gleixner G, Schulze ED (2002) Response of central Siberian Scots pine to soil water deficit and long-term trends in atmospheric CO_2 concentrations. Global Biogeochem Cy 16:1–13

Barbour MM (2007) Stable oxygen isotope composition of plant tissue: a review. Funct Plant Biol 34:83–94

Barbour MM, Andrews TJ, Farquhar GD (2001) Correlations between oxygen isotope ratios of wood constituents of Quercus and Pinus samples from around the world. Aust J Plant Physiol 28:335–348

Becker B (1993) An 11,000-year German oak and pine dendrochronology for radiocarbon calibration. Radiocarbon 35:201–213
Bert D, Leavitt SW, Dupouey J-L (1997) Variations of wood $\delta^{13}C$ and water use efficiency of Abies alba during the last century. Ecology 78:1588–1596
Borella S, Leuenberger M, Saurer M (1999) Analysis of $\delta^{18}O$ in tree rings: wood-cellulose comparison and method dependent sensitivity. J Geophys Res 104:19267–19273
Brendel O, Iannetta PPM, Stewart D (2000) A rapid and simple method to isolate pure alpha-cellulose. Phytochem Anal 11:7–10
Briffa KR, Jones PD, Bartholin TS, Eckstein D, Schweingruber FH, Karlén W, Zetterberg P, Eronen M (1992) Fennoscandian summers since AD 500: temperature changes on short and long timescales. Clim Dynam 7:111–119
Briffa KR, Jones PD, Schweingruber FH, Karlen W, Shiyatov SG (1996) Tree-ring variables as proxy-climate indicators: problems with low-frequency signals. In: Jones PD, Bradley RS, Jouzel J (eds) Climatic variations and forcing mechanisms of the last 2,000 years. Springer, Berlin, pp 9–41
Burk RL, Stuiver M (1981) Oxygen isotope ratios in trees reflect mean annual temperature and humidity. Science 211:1417–1419
Cook ER, Briffa KR, Meko DM, Graybill DA, Funkhouser G (1995) The 'segment length curse' in long tree-ring chronology development for palaeoclimatic studies. Holocene 5:229–237
Cooper LW, Deniro MJ (1989) Covariance of oxygen and hydrogen isotopic compositions in plant water: species effects. Ecology 70:1619–1628
Craig H (1954) Carbon-13 variations in Sequoia rings and the atmosphere. Science 119:141–144
Cullen LE, Grierson PF (2006) Is cellulose extraction necessary for developing stable carbon and oxygen isotopes chronologies from Callitris glaucophylla? Palaeogeogr Palaeocl 236:206–216
Dansgaard WS (1964) Stable isotopes in precipitation. Tellus B 16:436–468
Darling WG (2004) Hydrological factors in the interpretation of stable isotopic proxy data present and past: a European perspective. Quaternary Sci Rev 23:743–770
Duquesnay A, Breda N, Stievenard M, Dupouey JL (1998) Changes of tree-ring $\delta^{13}C$ and water-use efficiency of beech (*Fagus sylvatica* L.) in northeastern France during the past century. Plant Cell Environ 21:565–572
Epstein S, Yapp CJ (1976) Climatic implications of δD ratio of hydrogen in C-H groups in tree cellulose. Earth Planet Sci Lett 30:252–261
Epstein S, Thompson P, Yapp CJ (1977) Oxygen and hydrogen isotopic ratios in plant cellulose. Science 198:1209–1215
Evans MN (2006) Palaeoclimatology: the woods fill up with snow. Nature 440:1120–1121
Evans MN, Schrag DP (2004) A stable isotope-based approach to tropical dendroclimatology. Geochim Cosmochim Acta 68:3295–3305
Farmer JG, Baxter MS (1974) Atmospheric carbon-dioxide levels as indicated by the stable isotope record in wood. Nature 247:273–275
Farquhar GD, Oleary MH, Berry JA (1982) On the relationship between carbon isotope discrimination and the intercellular carbon dioxide concentration in leaves. Aust J Plant Physiol 9:121–137
Feng XH, Epstein S (1995) Climatic temperature records in δD data from tree rings. Geochim Cosmochim Acta 59:3029–3037
Filot MS, Leuenberger M, Pazdur A, Boettger T (2006) Rapid online equilibration method to determine the D/H ratios of non-exchangeable hydrogen in cellulose. Rapid Commun Mass Spectrom 20:3337–3344
Freyer HD, Belacy N (1983) $\delta^{13}C$ records in Northern Hemispheric trees during the past 500 years: anthropogenic impact and climatic super-positions. J Geophys Res 88:6844–6852
Friedrich M, Remmele S, Kromer B, Hofmann J, Spurk M, Kaiser KF, Orcel C, Küppers M (2004) The 12,460-year Hohenheim oak and pine chronology from central Europe: a unique record for radiocarbon calibration and paleoenvironment reconstructions. Radiocarbon 46(3):1111–1122
Gagen M, McCarroll D, Edouard JL (2004) Latewood width, maximum density, and stable carbon isotope ratios of pine as climate indicators in a dry subalpine environment, French Alps. Arct Antarct Alp Res 36:166–171

Gagen M, McCarroll D, Loader NJ, Robertson L, Jalkanen R, Anchukaitis KJ (2007) Exorcising the 'segment length curse': Summer temperature reconstruction since AD 1640 using non-detrended stable carbon isotope ratios from pine trees in northern Finland. Holocene 17: 435–446

Gagen M, McCarroll D, Robertson I, Loader NJ, Jalkanen R (2008) Do tree-ring $\delta^{13}C$ series from *Pinus sylvestris* in northern Fennoscandia contain long-term non-climatic trends? Chem Geol 252(1–2):42–51

Gat JR (1996) Oxygen and hydrogen isotopes in the hydrologic cycle. Annu Rev Earth Plant Sci 24:225–262

Gaudinski JB, Dawson TE, Quideau S, Schuur EAG, Roden JS, Trumbore SE, Sandquist DR, Oh S-W, Wasylishen RE (2005) Comparative analysis of cellulose preparation techniques for use with ^{13}C, ^{14}C, and ^{18}O isotopic measurements. Anal Chem 77(22):7212–7224

Green JW (1963) Wood cellulose. In: Whistler RL (ed) Methods in carbohydrate chemistry III. Academic Press, New York

Heaton THE (1999) Spatial, species, and temporal variations in the $^{13}C/^{12}C$ ratios of C3 plants: implications for palaeodiet studies. J Archaeol Sci 26:637–649

Helle G, Schleser GH (2004) Beyond CO_2-fixation by Rubisco: an interpretation of C-13/C-12 variations in tree rings from novel intra-seasonal studies on broadleaf trees. Plant Cell Environ 27:367–380

Hemming DL, Switsur VR, Waterhouse JS, Heaton THE, Carter AHC (1998) Climate and the stable carbon isotope composition of tree ring cellulose: an intercomparison of three tree species. Tellus 50B, 25–32

Hughes MK (2002) Dendrochronology in climatology: the state of the art. Dendrochronologia 20:95–116

Körner C (2003) Carbon limitation in trees. J Ecol 91:4–17

Kürschner WM (1996) Leaf stomata as biosensors of palaeoatmospheric CO_2 levels. LPP Contrib Ser 5:152

Leavitt SW, Danzer SR (1993) Method for batch processing small wood samples to holocellulose for stable-carbon isotope analysis. Anal Chem 65:87–89

Leavitt SW, Long A (1982) Stable carbon isotopes as a potential supplemental tool in dendroclimatology. Tree-Ring Bull 42:49–55

Leavitt SW, Long A (1984) Sampling strategy for stable carbon isotope analysis of tree rings in pine. Nature 311:145–147

Leavitt SW, Long A (1985) An atmospheric $\delta^{13}C$ reconstruction generated through removal of climate effects from tree-ring $\delta^{13}C$ measurements. Tellus 35B:92–102

Libby LM, Pandolfi LJ, Payton PH, Marshall J, Becker B, Giertzsienbenlist V (1976) Isotopic tree thermometers. Nature 261:284–288

Linderholm HW, Gunnarson BE (2005) Summer temperature variability in central Scandinavia during the last 3,600 years. Geogr Ann 87A:231–241

Linderholm M, Eronen M (2000) A reconstruction of mid-summer temperatures from ring-widths of Scots pine since AD 50 in northern Fennoscandia. Geogr Ann 82A:527–535

Lipp J, Trimborn P (1991) Long-term records and basic principles of tree-ring isotope data with emphasis on local environmental conditions. Paleaoklimaforschung 6:105–117

Liu XH, Shao XM, Liang EY, Zhao LJ, Chen T, Qin D, Ren JW (2007) Species-dependent responses of juniper and spruce to increasing CO_2 concentration and to climate in semiarid and arid areas of northwestern China. Plant Ecol 193:195–209

Loader NJ, Switsur VR (1996) Reconstructing past environmental change using stable isotopes in tree-rings. Bot J Scotland 48:65–78

Loader NJ, Robertson I, Barker AC, Switsur VR, Waterhouse JS (1997) An improved technique for the batch processing of small wholewood samples to alpha-cellulose. Chem Geol 136: 313–317

Loader NJ, Robertson I, McCarroll D (2003) Comparison of stable carbon isotope ratios in the whole wood, cellulose and lignin of oak tree rings. Palaeogeogr Palaeocl 196:395–407

Loader NJ, McCarroll D, Gagen M, Robertson I, Jalkanen R (2007) Extracting climatic information from stable isotopes in tree rings. In: Dawson TE, Siegwolf RTW (eds) Stable isotopes as indicators of ecological change. Elsevier, New York, pp 27–48

Loader NJ, Santillo PM, Woodman-Ralph JP, Rolfe JE, Hall MA, Gagen M, Robertson I, Wilson R, Froyd CA, McCarroll D (2008) Multiple stable isotopes from oak trees in southwestern Scotland and the potential for stable isotope dendroclimatology in maritime climatic regions. Chem Geol (in press, online proof doi:10.1016/j.chemgeo.2008.01.006)

Long A, Arnold LD, Larry D, Damon PE, Lerman JC, Wilson AT (1979) Radial translocation of carbon in bristlecone pine. In: Berger R, Suess HE (eds) Radiocarbon dating, Proceedings of the ninth international conference on radiocarbon dating, Los Angeles and La Jolla, 1976. University of California Press, Berkeley, pp 532–537

Mann ME (2002) The value of multiple proxies. Science 297:1481–1482

McCarroll D, Loader NJ (2004) Stable isotopes in tree rings. Quaternary Sci Rev 23:771–801

McCarroll D, Pawellek F (1998) Stable carbon isotope ratios of latewood cellulose in *Pinus sylvestris* from northern Finland: variability and signal strength. Holocene 8:675–684

McCarroll D, Pawellek F (2001) Stable carbon isotope ratios of *Pinus sylvestris* from northern Finland and the potential for extracting a climate signal from long Fennoscandian chronologies. Holocene 11:517–526

McCarroll D, Pettigrew E, Luckman A, Guibal F, Edouard JL (2002) Blue reflectance provides a surrogate for latewood density of high-latitude pine tree rings. Arct Antarct Alp Res 34: 450–453

McCarroll D, Jalkanen R, Hicks S, Tuovinen M, Gagen M, Pawellek F, Eckstein D, Schmitt U, Autio J, Heikkinen O (2003) Multiproxy dendroclimatology: a pilot study in northern Finland. Holocene 13:829–838

McDowell NG, Phillips N, Lunch C, Bond BJ, Ryan MG (2002) An investigation of hydraulic limitation and compensation in large, old Douglas-fir trees. Tree Physiol 22:763–774

Mook WG, Koopmans M, Carter AF, Keeling CD (1983) Seasonal, latitudinal, and secular variations in the abundance and isotopic-ratios of atmospheric carbon dioxide. 1. Results from land stations. J Geophys Res-Oc Atm 88:915–933

Mullane MV, Waterhouse JS, Switsur VR (1988) On the development of a novel technique for the determination of stable oxygen isotope ratios in cellulose. Appl Radiat Isotopes 10:1029–1035

Park R, Epstein S (1960) Carbon isotope fractionation during photosynthesis. Geochim Cosmochim Acta 21:110–126

Park R, Epstein S (1961) Metabolic fractionation of $\delta^{13}C$ in plants. Plant Physiol 36:133–138

Pilcher JR, Baillie MGL (1980) Eight modern oak chronologies from England and Scotland. Tree-Ring Bull 40:45–58

Poussart PM, Schrag DP (2005) Seasonally resolved stable isotope chronologies from northern Thailand deciduous trees. Earth Planet Sci Lett 235:752–765

Poussart PM, Evans MN, Schrag DP (2004) Resolving seasonality in tropical trees: multidecade, high-resolution oxygen and carbon isotope records from Indonesia and Thailand. Earth Planet Sci Lett 218:301–316

Poussart PM, Myneni SCB, Lanzirotti A (2006) Tropical dendrochemistry: a novel approach to estimate age and growth from ringless trees. Geophys Res Lett 33:L17711

Raffalli-Delerce G, Masson-Delmotte V, Dupouey JL, Stievenard M, Breda N, Moisselin JM (2004) Reconstruction of summer droughts using tree-ring cellulose isotopes: a calibration study with living oaks from Brittany (western France). Tellus B 56:160–174

Ramesh R, Bhattacharya SK, Gopalan K (1986) Stable isotope systematics in tree cellulose as palaeoenvironmental indicators: a review. J Geol Soc India 27:154–167

Rinne KT, Boettger T, Loader NJ, Robertson I, Switsur VR, Waterhouse JS (2005) On the purification of α-cellulose from resinous wood for stable isotope (H, C, and O) analysis. Chem Geol 222:75–82

Robertson I, Switsur VR, Carter AHC, Barker AC, Waterhouse JS, Briffa KR, Jones PD (1997a) Signal strength and climate relationships in $\delta^{13}C$ ratios of tree-ring cellulose from oak in east England. J Geophys Res 102:19507–19519

Robertson I, Rolfe J, Switsur VR, Carter AHC, Hall MA, Barker AC, Waterhouse JS (1997b) Signal strength and climate relationships in the $^{13}C/^{12}C$ ratios of tree-ring cellulose from oak in southwest Finland. Geophys Res Lett 24(12):1487–1490

Robertson I, Waterhouse JS, Barker AC, Carter AHC, Switsur VR (2001) Oxygen isotope ratios of oak in east England: implications for reconstructing the isotopic composition of precipitation. Earth Planet Sc Lett 191:21–31

Robertson I, Leavitt SW, Loader NJ, Buhay B (2008) Progress in isotope dendroclimatology. Chem Geol 252(1–2), 30 June 2008, Pages EX1–EX4

Roden JS, Lin GG, Ehleringer JR (2000) A mechanistic model for interpretation of hydrogen and oxygen isotope ratios in tree-ring cellulose. Geochim Cosmochim Acta 64:21–35

Saurer M, Siegwolf RTW (2007) Human impacts on tree-ring growth reconstructed from stable isotopes. In: Dawson TE, Siegwolf RTW (eds) Stable isotopes as indicators of ecological change. Elsevier, New York, pp 49–62

Saurer M, Siegenthaler U, Schweingruber F. (1995) The climate–carbon isotope relationship in tree rings and the significance of site conditions. Tellus 47B, 320–330

Saurer M, Borella S, Schweingruber F, Siegwolf R (1997) Stable carbon isotopes in tree rings of beech: climatic versus site-related influences. Trees-Struct Funct 11:291–297

Saurer M, Siegwolf RTW, Schweingruber FH (2004) Carbon isotope discrimination indicates improving water-use efficiency of trees in northern Eurasia over the last 100 years. Global Change Biol 10:2109–2120

Schleser GH, Jayasekera R (1985) $\delta^{13}C$ variations in leaves of a forest as an indication of reassimilated CO_2 from the soil. Oecologia 65:536–542

Schleser GH, Helle G, Lucke A, Vos H (1999) Isotope signals as climate proxies: the role of transfer functions in the study of terrestrial archives. Quaternary Sci Rev 18:927–943

Schulze B, Wirth C, Linke P, Brand WA, Kuhlmann I, Horna V, Schulze ED (2004) Laser ablation-combustion-GC-IRMS: a new method for online analysis of intra-annual variation of $\delta^{13}C$ in tree rings. Tree Physiol 24:1193–1201

Schweingruber FH, Fritts HC, Bräker OU, Drew LG, Schär E (1978) The X-ray technique as applied to dendroclimatology. Tree-Ring Bull 38:61–91

Skomarkova MV, Vaganov EA, Mund M, Knohl A, Linke P, Boerner A, Schulze ED (2006) Interannual and seasonal variability of radial growth, wood density, and carbon isotope ratios in tree rings of beech (*Fagus sylvatica*) growing in Germany and Italy. Trees-Struct Funct 20:571–586

Sternberg LSL, DeNiro MJ, Savidge RA (1986) Oxygen isotope exchange between metabolites and water during biochemical reactions leading to cellulose synthesis. Plant Physiol 82: 423–427

Sternberg L, Pinzon MC, Anderson WT, Jahren AH (2006) Variation in oxygen isotope fractionation during cellulose synthesis: intramolecular and biosynthetic effects. Plant Cell Environ 29:1881–1889

Suess HE (1980) The radiocarbon record in tree rings of the last 8,000 years. Radiocarbon 22: 200–209

Switsur VR, Waterhouse JS, Field EMF, Carter AHC, Hall M, Pollard M, Robertson I, Pilcher JR, Heaton THE (1994) Stable isotope studies of oak from the English Fenland and Northern Ireland. In: Funnell BM, Kay RLF (eds) Palaeoclimate of the last glacial/interglacial cycle. Natural Environment Research Council, pp 67–73. Reading, UK

Switsur VR, Waterhouse JS, Field EM, Carter AHC (1996) Climatic signals from stable isotopes in oak tree rings from East Anglia, Great Britain. In: Tree rings, environment, and humanity. Radiocarbon, pp. 637–645. Radiocarbon, Tucson, Arizona

Tang KL, Feng XH, Funkhouser G (1999) The $\delta^{13}C$ of tree rings in full-bark and strip-bark bristlecone pine trees in the White Mountains of California. Global Change Biol 5:33–40

Tans P, Mook WG (1980) Past atmospheric CO_2 levels and the $\delta^{13}C$ ratios in tree rings. Tellus 32:268–283

Treydte K, Schleser GH, Schweingruber FH, Winiger M (2001) The climatic significance of $\delta^{13}C$ in subalpine spruces (Lötschental, Swiss Alps). Tellus 53B:593–611

Treydte KS, Schleser GH, Helle G, Frank DC, Winiger M, Haug GH, Esper J (2006) The twentieth century was the wettest period in northern Pakistan over the past millennium. Nature 440: 1179–1182

Treydte K, Frank D, Esper J, Andreu L, Bednarz Z, Berninger F, Boettger T, D'Alessandro CM, Etien N, Filot M, Grabner M, Guillemin MT, Gutierrez E, Haupt M, Helle G, Hilasvuori E, Jungner H, Kalela-Brundin M, Krapiec M, Leuenberger M, Loader NJ, Masson-Delmotte V, Pazdur A, Pawelczyk S, Pierre M, Planells O, Pukiene R, Reynolds-Henne CE, Rinne KT, Saracino A, Saurer M, Sonninen E, Stievenard M, Switsur VR, Szczepanek M, Szychowska-Krapiec E, Todaro L, Waterhouse JS, Weigl M, Schleser GH (2007) Signal strength and climate calibration of a European tree-ring isotope network. Geophys Res Lett 34. doi:10.1029/2007GL031106

Verheyden A, Roggeman M, Bouillon S, Elskens M, Beeckman H, Koedam N (2005) Comparison between $\delta^{13}C$ of alpha-cellulose and bulk wood in the mangrove tree *Rhizophora mucronata*: implications for dendrochemistry. Chem Geol 219:275–282

Waterhouse JS, Switsur VR, Barker AC, Carter AHC, Hemming DL, Loader NJ, Robertson I (2004) Northern European trees show a progressively diminishing response to increasing atmospheric carbon dioxide concentrations. Quaternary Sci Rev 23:803–810

Wilson AT, Grinsted MJ (1977) $^{12}C/^{13}C$ in cellulose and lignin as palaeothermometers. Nature 265:133–135

Wilson R, D'Arrigo R, Buckley B, Büntgen U, Esper J, Frank D, Luckman B, Payette S, Vose R, Youngblut D (2007) A matter of divergence: tracking recent warming at hemispheric scales using tree-ring data. J Geophys Res 112:D17103. doi:10.1029/2006JD008318

Worbes M (2002) One hundred years of tree-ring research in the tropics: a brief history and an outlook to future challenges. Dendrochronologia 20:217–231

Part III
Reconstruction of Climate Patterns and Values Relative to Today's Climate

Chapter 7
Dendroclimatology from Regional to Continental Scales: Understanding Regional Processes to Reconstruct Large-Scale Climatic Variations Across the Western Americas

Ricardo Villalba, Brian H. Luckman, Jose Boninsegna, Rosanne D. D'Arrigo, Antonio Lara, Jose Villanueva-Diaz, Mariano Masiokas, Jaime Argollo, Claudia Soliz, Carlos LeQuesne, David W. Stahle, Fidel Roig, Juan Carlos Aravena, Malcolm K. Hughes, Gregory Wiles, Gordon Jacoby, Peter Hartsough, Robert J.S. Wilson, Emma Watson, Edward R. Cook, Julian Cerano-Paredes, Matthew Therrell, Malcolm Cleaveland, Mariano S. Morales, Nicholas E. Graham, Jorge Moya, Jeanette Pacajes, Guillermina Massacchesi, Franco Biondi, Rocio Urrutia, and Guillermo Martinez Pastur

Abstract Common patterns of climatic variability across the Western Americas are modulated by tropical and extra-tropical oscillatory modes operating at different temporal scales. Interannual climatic variations in the tropics and subtropics of the Western Americas are largely regulated by El Niño-Southern Oscillation (ENSO), whereas decadal-scale variations are induced by long-term Pacific modes of climate variability such as the Pacific Decadal Oscillation (PDO). At higher latitudes, climate variations are dominated by oscillations in the Annular Modes (the Arctic and Antarctic Oscillations) which show both interannual and longer-scale temporal oscillations. Here we use a recently-developed network of tree-ring chronologies to document past climatic variations along the length of the Western Cordilleras. The local and regional characterization of the relationships between climate and tree-growth provide the basis to compare climatic variations in temperature- and precipitation-sensitive records in the Western Americas over the past 3–4 centuries. Upper-elevation records from tree-ring sites in the Gulf of Alaska and Patagonia reveal the occurrence of concurrent decade-scale oscillations in temperature during the last 400 years modulated by PDO. The most recent fluctuation from the cold- to the warm-phase of the PDO in the mid 1970s induced marked changes in

R. Villalba (✉)
Departamento de Dendrocronología e Historia Ambiental, Instituto Argentino de Nivología, Glaciología y Ciencias Ambientales (IANIGLA), CONICET, CC 330, 5500, Mendoza, Argentina
e-mail: ricardo@mendoza-conicet.gob.ar

M.K. Hughes et al. (eds.), *Dendroclimatology*, Developments in Paleoenvironmental Research 11, DOI 10.1007/978-1-4020-5725-0_7,

tree growth in most extratropical temperature-sensitive chronologies in the Western Cordilleras of both Hemispheres. Common patterns of interannual variations in tree-ring chronologies from the relatively-dry subtropics in western North and South America are largely modulated by ENSO. We used an independent reconstruction of Niño-3 sea surface temperature (SST) to document relationships to tree growth in the southwestern US, the Bolivian Altiplano and Central Chile and also to show strong correlations between these regions. These results further document the strong influence of SSTs in the tropical Pacific as a common forcing of precipitation variations in the subtropical Western America during the past 3–4 centuries. Common patterns of interdecadal or longer-scale variability in tree-ring chronologies from the subarctic and subantarctic regions also suggest common forcings for the annular modes of high-latitude climate variability. A clear separation of the relative influence of tropical versus high-latitude modes of variability is currently difficult to establish: discriminating between tropical and extra-tropical influences on tree growth still remains elusive, particularly in subtropical and temperate regions along our transect. We still need independent reconstructions of tropical and polar modes of climate variability to gain insight into past forcing interactions and the combined effect on climates of the Western Americas. Finally, we also include a series of brief examples (as 'boxes') illustrating some of the major regional developments in dendrochronology over this global transect in the last 10 years.

Keywords Dendrochronology · Regional scale · Continental scale · Climate variations · Americas

7.1 Introduction

Instrumental records show that the climate system is characterized by low- and high-latitude patterns or modes of variability such as the El Niño/Southern Oscillation (ENSO) in the equatorial Pacific and the Arctic (AO) and Antarctic (AAO) Oscillations in the extratropics. The Pacific and high-latitude atmospheric circulation features associated with interannual to decadal variability of climate over the Americas exhibit large spatial and temporal variance that remains poorly documented. The resulting regional climate variability has enormous socioeconomic impacts, as was vividly demonstrated by the disastrous flooding in Paraguay and eastern Argentina, and the extended drought and massive wildfires in the southwestern United States and Mexico during the 1997–1998 El Niño event. At decadal scales, the prolonged shift in sea surface temperature (SST) patterns over the north and south Pacific Ocean after 1976 (Graham 1994) has resulted in ocean and atmospheric changes that have caused costly changes in commercial fish populations in the eastern north Pacific (Mantua and Hare 2002; Chavez et al. 2003; Beamish et al. 2004) and a greatly reduced carrying capacity for commercially important

Patagonian grasslands. These coherent interhemispheric changes in annual and decadal climate patterns associated with the Pacific Decadal Oscillation (PDO) appear to have been driven by fundamental changes in the hydrologic cycle of the tropical Pacific Ocean (Graham 1994; Evans et al. 2001a, b; Villalba et al. 2001).

Hemispheric-scale networks of instrumental and proxy climate data are needed to document and help understand these changes in the ocean-atmosphere system and their impact on the Americas.

Substantial recent effort has been devoted to the development of ocean-atmospheric monitoring arrays in the tropical Pacific (e.g., TOGA/TAO, TOPEX/POSEIDON; Wallace et al. 1998). The cost of these arrays has already been justified by the economic benefits provided by the long-lead climate forecasting associated with recent ENSO warm events. However, there is clear instrumental and paleoclimatic evidence that, for example, the frequency of warm and cold ENSO events has been subject to substantial changes over the past several centuries. The available instrumental meteorological records are simply too short to clearly define the important temporal and spatial modes inherent in the low-frequency dynamics of the Pacific and high-latitude major circulation systems. As these decade-scale changes in atmospheric circulation have strong impacts on regional climates and society, understanding these phenomena will improve the skill of long-range climate forecasting. There is increasing evidence (e.g., Gershunov and Barnett 1998) that they modulate the character of high-frequency ENSO teleconnections, producing more extreme and more predictable anomaly patterns when the two systems are in phase.

The Western America Cordilleras provide a contiguous latitudinal transect of mountainous terrain flanking the world's largest ocean that invites comparative studies of climate variations along the Americas. The American Cordilleras can provide high-quality proxy climate records over most of their lengths. Tree rings provide the most broadly distributed, annually resolved source of proxy climate data throughout the Cordillera and thereby supply the comprehensive baseline data necessary to evaluate natural climate variability on different temporal and spatial scales.

Progress in dendroclimatology across the Americas has been concerned with the geographical expansion of the research from the local to regional and continental scales. The work of Harold Fritts (1976, 1991) and co-workers in the 1970s represented the first attempt to reconstruct the patterns of spatial variation in temperature, precipitation, and atmospheric pressure across North America and the Pacific Ocean, based on 65 ring width chronologies from the western United States. Collaborative work between several research groups during the past 10 years (Meko et al. 1993; Cook et al. 1999, 2004) have extended this methodology by compiling 835 chronologies from Canada, the United States, and Mexico to reconstruct a gridded network of 297 summer Palmer Drought Severity Indices (PDSIs) across North America that spans the past 500–600 years (or longer) over much of the grid (Cook et al. 2004). Following these initiatives, new projects have continued to develop databases of tree-ring chronologies that cover large areas in the Western Americas (Fig. 7.1).

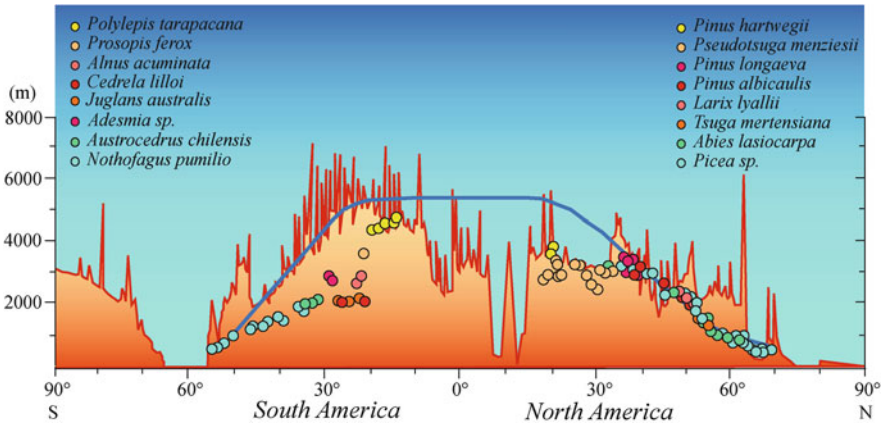

Fig. 7.1 Cross-section from the South to North Pole across the Western American Cordilleras showing changes in elevation with latitude, the approximate location of the mean annual zero degree (0°C) line, and the distribution of upper-elevation tree-ring chronologies. Major tree taxa used for developing the chronologies are also indicated

One of the Collaborative Research Networks supported by the Inter-American Institute for Global Change Research (IAI) was focused around the development of tree line chronologies from Alaska to Tierra del Fuego (Luckman and Boninsegna 2001). Using this research as a framework, we discuss in this chapter some of the most significant developments in tree-ring research across the western Americas, reviewing local- and regional-scale studies and how they contribute to our understanding of present and past variations in the circulation modes of climate variability at continental and interhemispheric scales. The Western Cordilleras of the Americas runs transverse to the generally latitudinal organization of the major climate-ocean circulation systems, and therefore past variations in the major modes of general circulation dynamics linked to El Niño/Southern Oscillation, Pacific Decadal Oscillation, the Arctic and Antarctic Oscillations can be investigated by using tree-ring records from this global-scale transect.

7.2 Oscillatory Modes of Climate Variability Across the Western Cordilleras

Instrumental records show that the climate system is characterized by low- and high-latitude patterns or modes of variability. These dominant modes of climate variability fluctuate at many different temporal scales. The best known is the El Niño-Southern Oscillation phenomenon in the tropical Pacific, which dominates global climate variations on interannual timescales, mostly ranging from 3 to 6 years (Wallace et al. 1998). On longer than interannual timescales, the dominant climate pattern in the Pacific Ocean has an ENSO-like spatial distribution of surface temperature and atmospheric circulation and has been identified as the Pacific

Decadal Oscillation in the extratropical north Pacific, the Pacific Interdecadal Mode in the whole Pacific basin, and as the Global Residual (GR) index on a global scale (Mantua et al. 1997; Garreaud and Battisti 1999; Enfield and Mestas-Nuñez 2000). Decadal variability in the climate of the Atlantic basin has also been identified (Deser and Blackmon 1993), but its interhemispheric climate effects on the Western Cordilleras are less well known.

The Arctic and Antarctic Oscillations are the dominant modes of climate variability at the highest latitudes in both hemispheres. The positive state of these annular modes is associated with intensified subtropical highs and strong polar lows, which drive a strong extratropical circulation. They also exhibit short- and long-term modes of variability.

7.2.1 El Niño/Southern Oscillation (ENSO)

Modern interannual variations in the Pacific basin and their interhemispheric effects on the Western Cordilleras have been extensively documented. The pattern of sea surface temperature associated with ENSO, measured as the SST anomalies from 6°N to 6°S, 180° to 90°W (the Cold Tongue [CT] index of Deser and Wallace 1990), are indicated by correlations mapped in Fig. 7.2. Positive correlations indicate regions where the ocean is warmer when the index is positive. As can be expected by the nature of the CT index, the strongest correlation with SST occurs in the tropical Pacific. The subtropical north and south Pacific Oceans are dominated by anomalies out of phase with the ones occurring in the tropical Pacific, forming a symmetric pattern about the equator.

The continental effects of the ENSO-related climate variations in terms of surface air temperature (SAT) and precipitation along the Western Cordilleras are remarkably symmetric about the equator (Fig. 7.3a,b). Positive temperatures in the tropical Pacific are associated with deeper than normal Aleutian lows, and the resulting steep north-south gradient in the middle latitudes brings storms and precipitation to the southwestern and southeastern parts of North America. In a rough parallel to the circulation changes in the Northern Hemisphere, the steeper gradient in pressure over the southeastern Pacific related to El Niño events, corresponds to deflections of the low-pressure systems and the associated storms towards the subtropical belt of South America, increasing precipitation in central Chile (Fig. 7.3b). Positive CT indices are associated with warmer than normal surface conditions all along the American Cordilleras (Fig. 7.3a). El Niño brings cool temperatures to the southeastern United States and to the eastern Amazon basin (Dettinger et al. 2001).

7.2.2 Pacific Interdecadal Mode

Using instrumental records, several studies have reported Pacific decadal-scale oscillatory modes (Trenberth and Hurrell 1994; Mantua et al. 1997; Zhang et al.

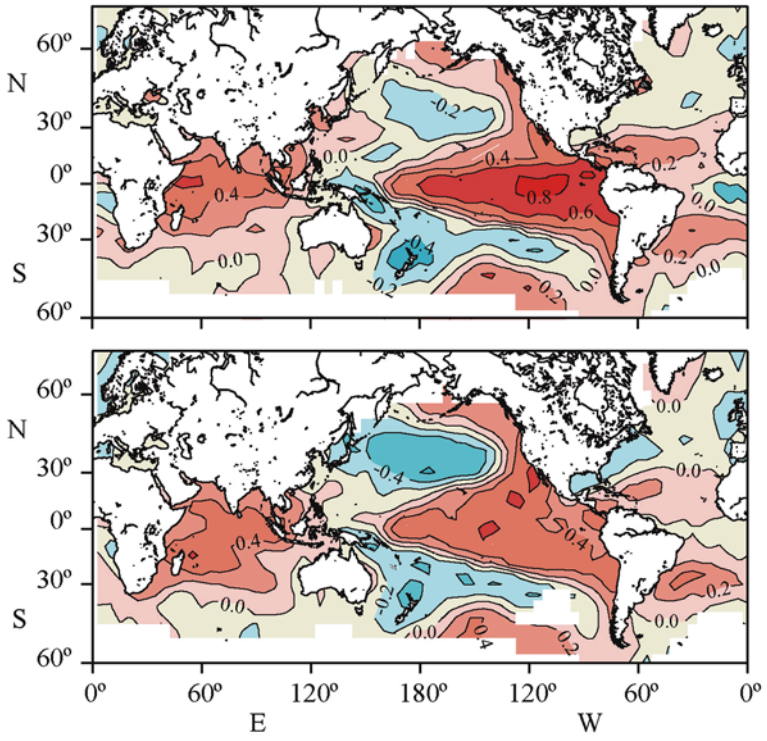

Fig. 7.2 Correlation coefficients between annual-averaged sea surface temperatures and (*upper*) Cold Tongue (CT) index (1903–1990) and (*lower*) Global Residual (GR) index (1903–1990). The contour interval is 0.2, *dashed* where negative. Correlations greater than +0.2, or less than –0.2, pass a two-tail Student's *t*-test of being different from zero at 95% significance levels (modified from Dettinger et al. 2001)

1997; Garreaud and Battisti 1999; Deser et al. 2004). The physical processes responsible for the decadal variability across the Pacific remain uncertain, but are connected to well-documented pan-Pacific changes in the atmosphere and ocean in recent decades. For example, the 1976–1977 climatic shift influenced climatic conditions all along the western Americas and is a remarkable manifestation of this Pacific decade-scale climatic variability (Ebbesmeyer et al. 1991). Sea surface temperatures along the equatorial belt and along the coast of the Americas become warmer, while further west at temperate latitudes the sea surface becomes cooler (Fig. 7.2). The array of atmospheric and oceanic changes that have been linked to these basin-wide regime shifts is collectively referred to as the Pacific Decadal Oscillation or the Pacific Interdecadal Mode (Mantua et al. 1997; Enfield and Mestas-Nuñez 2000). Warm and wet decades in the equatorial Pacific tend to be marked by extratropical circulation patterns that bring mild weather conditions to coastal Alaska and northern Patagonia. In contrast to the interannual mode of ENSO variability, the decadal mode is characterized by less pronounced anomalies in the

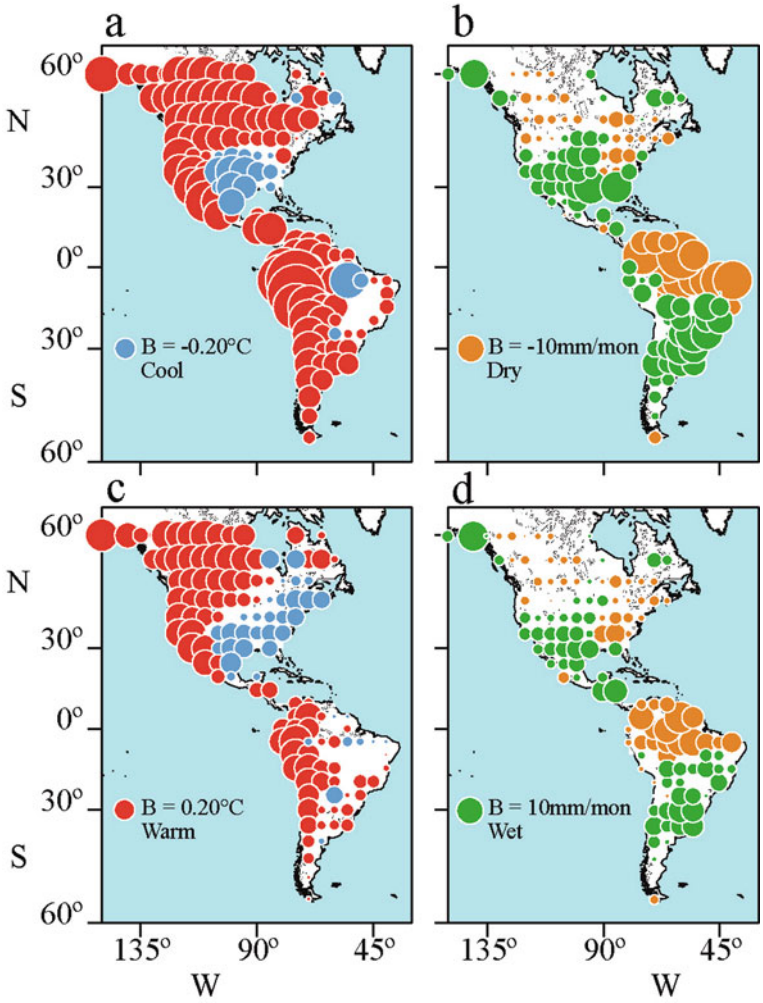

Fig. 7.3 Regression coefficients (B) estimated during the interval 1904–1990, relating Cold Tongue (CT) index to October–September (**a**) surface air temperatures, and (**b**) precipitation. Figures (**c**) and (**d**) are same as (**a**) and (**b**) but for the Global Residual (GR) index. Radii of circles are proportional to the magnitude of regression coefficients: *red* and *light blue*, respectively, for positive and negative relations with surface air temperatures; *green* and *light brown*, respectively, for positive and negative relations with precipitation. The *circles*, lower left in each diagram, indicate the scale of influences. Temperatures from an updated version of the monthly, 5° × 5°-gridded temperature anomaly set of Jones et al. (1986a, b), and land precipitation anomalies on a similar grid from Eischeid et al. (1991) were compared with CT and GR. Regression coefficients may be affected by the magnitude of the variable used in the analysis. The lack of significant regression coefficients between CT and precipitation in the central Andes along the South American Pacific coastline is likely due to the reduced precipitation across this region (modified from Dettinger et al. 2001)

eastern Pacific (the classic key ENSO region) and is not narrowly confined along the equator. The documented decadal oscillatory mode of Pacific SST shows anomalies in the western Pacific that extend to the northeast and southeast into the American subtropics.

Overall, the atmospheric expressions of the ENSO-like climate variations on both interannual and decadal timescales are remarkably symmetric about the equator, especially on the Pacific coast of western Americas (Fig. 7.3c,d). Positive variations in the CT and GR are associated with equatorward diversions of the westerlies, enhancement of the low-pressure systems, and storms from the midlatitude Pacific basin toward North and South America subtropical latitudes (Dettinger et al. 2001).

7.2.3 Annular Modes

The Northern Hemisphere (NAM) and Southern Hemisphere (SAM) Annular Modes dominate extratropical climate variability throughout their respective hemispheres (Thompson and Wallace 2000). The NAM is alternatively referred to as the North Atlantic Oscillation (NAO) (Hurrell and van Loon 1997) and the Arctic Oscillation (Thompson and Wallace 2000); whereas the SAM is alternatively referred to as the High-Latitude Mode (Karoly 1990) and the Antarctic Oscillation (Gong and Wang 1999; Thompson and Wallace 2000).The structures of the Northern Hemisphere and Southern Hemisphere Annular Modes are shown to be remarkably similar, not only in the zonally averaged geopotential height and zonal wind fields, but in the mean meridional circulations as well. Both annular modes are associated with equivalent barotropic vacillations in the strength of the zonal flow between centers of action located at ~35°−40° and ~55°−60° latitude. The SAM is moderately symmetric about the pole, but due to the more complex distribution of the northern continents, the NAM is more evident over the north Atlantic and the north Pacific Oceans (Fig. 7.4).

Periods when the zonal flow along ~55°−60° latitude is anomalously westerly (the so-called high-index polarity of the annular modes) are characterized by lower than normal geopotential heights and temperatures over the polar cap, and by higher than normal geopotential heights and temperatures in the middle latitudes centered at ~45°. As atmospheric variability in the Northern Hemisphere is largest in winter, the spatial pattern of the conventional NAM mostly reflects the winter variability (Thompson and Wallace 2000). The positive polarity of the winter AO is associated with positive surface air temperature anomalies throughout the high latitudes of Eurasia and much of North America, and negative anomalies over extreme eastern Canada, North Africa, and the Middle East. This zonally asymmetric pattern of SAT anomalies is evident throughout the year except during the Northern Hemisphere summer months (Thompson and Wallace 2000). The leading mode of the Empirical Orthogonal Function (EOF) in summer months has a smaller meridional scale than the conventional NAM. Associated summertime low-level temperature anomalies show more extended warm anomalies over the midlatitudes than the winter NAM

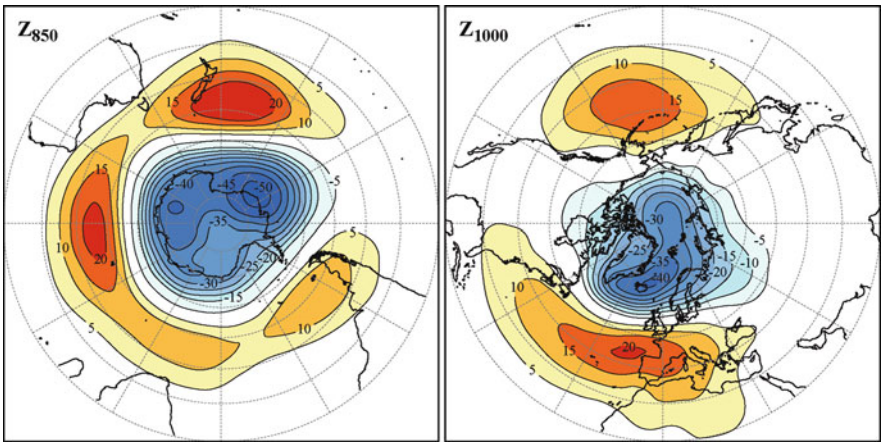

Fig. 7.4 High-latitude annular modes. The Southern Annular Mode (SAM) or Antarctic Oscillation (AAO) mode is moderately symmetric about the pole (*left*), but due to the more complex distribution of the northern continents, the Northern Annular Mode (NAM) or Arctic Oscillation (AO) is more evident over the North Atlantic and the north Pacific Oceans. Zonal-mean geopotential height fields are represented with contour intervals of 5 m (modified from Thompson and Wallace 2000)

counterpart, especially over Europe, the Sea of Okhotsk, and northern America. For example, the summer NAM pattern accounts for many of the anomalous weather features observed during the summer of 2003. Temperature anomalies over northwestern Eurasia, northeastern Siberia, and Canada during that period exceeded 3°C (Ogi et al. 2004).

The positive polarity of the Southern Hemisphere Annular Mode is associated with cold anomalies over most of Antarctica. The one notable exception is the Antarctic Peninsula and southern South America, where the enhanced westerlies related to the high SAM polarity increase the advection of relatively warm oceanic air over the lands (Thompson and Solomon 2002). The observed trend in the SAM toward stronger circumpolar flow is in the same sense as the trends that have dominated the Northern Hemisphere extratropical circulation over the past few decades. The occurrence of positive trends in both the NAM and SAM suggests that the trends reflect processes that transcend the high-latitude climate of a particular hemisphere.

7.3 Tree-Ring Records Across the Western Americas

A major result of the Collaborative Research Network has been the consolidation and expansion of tree-ring collections across the traditional research regions of North and South America, the focusing on key areas, and the start of many developments in new regions of Canada, Mexico, Peru, Bolivia, Chile, and Argentina (Boxes 7.1, 7.2, 7.3, 7.6 and 7.8). Along the western coasts of North and South

Box 7.1 Climate signals in Gulf of Alaska tree-ring records

A network of climatically sensitive tree-ring records has been compiled for the Gulf of Alaska (GOA) region, and the records have been used to develop time series of temperatures over the past one to two millennia (Box Fig. 7.1). This region is strongly sensitive to the climatic effects of the Pacific Decadal Oscillation (PDO), and the GOA chronologies show evidence for decadal-scale regime shifts, including the noteworthy 1976 transition in Pacific climate. These records have been linked to sea surface temperature (SST) variations in the Pacific and have been included in reconstructions of the PDO (e.g., D'Arrigo et al. 2001). On longer timescales, century to millennial temperature variations are evident and are linked to glacial changes in southern Alaska.

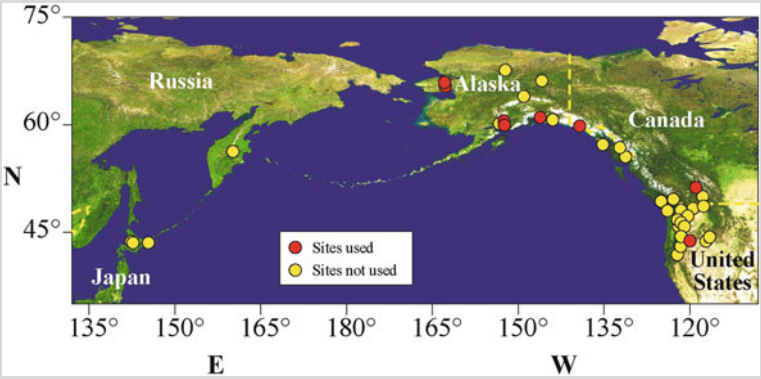

Box Fig. 7.1 Map of North Pacific region showing locations of tree-ring sites (*yellow*) used as candidate predictors of the tropical Indo-Pacific climate index (NPI). Sites in *red* are those included in the regression model used to reconstruct the NPI. Some dots represent more than one site (D'Arrigo et al. 2005)

Analyses of instrumental data demonstrate robust linkages between decadal-scale North Pacific and tropical Indo-Pacific climatic variability, yet information on the tropical–high-latitude climate connection is limited prior to the twentieth century. Gulf of Alaska and western Canadian tree-ring records were used to reconstruct the December–May North Pacific index (NPI—an index of the atmospheric circulation related to the Aleutian low-pressure cell) from 1600 to 1983 (D'Arrigo et al. 2005; Box Fig. 7.2). This NPI reconstruction shows evidence for the climatic regime shifts seen in the instrumental NPI data, and for additional events in prior centuries. It correlates significantly with both instrumental tropical climate indices and a coral-based

reconstruction of an optimal tropical Indo-Pacific climate index (OTI), supporting evidence for a tropical/North Pacific link extending as far west as the western Indian Ocean. The coral-based reconstruction (1781–1993) shows the twentieth-century regime shifts evident in the instrumental NPI and OTI, as well as previous shifts. Changes in the strength of the correlation between the NPI and OTI reconstructions over time, and the timing of regime shifts in both series prior to the twentieth century, suggest a varying tropical influence on North Pacific climate, with greater influence in the twentieth century. One likely mechanism is the low-frequency variability of the El Niño/Southern Oscillation (ENSO) and its varying impact on Indo-Pacific climate.

—R. D'Arrigo, G. Wiles, and R. Wilson

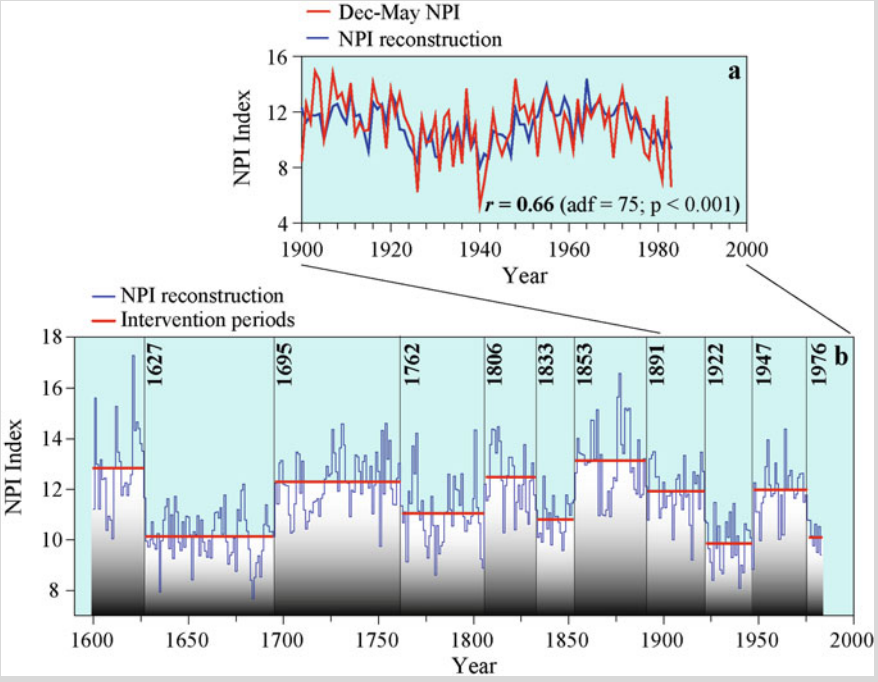

Box Fig. 7.2 Tree-ring-based reconstruction of the tropical Indo-Pacific climate index (NPI): (**a**) actual and estimated December–May NPI for the 1900–1983 calibration period, adf = adjusted degrees of freedom; (**b**) reconstruction of the December–May NPI from AD 1600 through 1983 based on North Pacific tree-ring data. The highlighted phase shifts were identified by using intervention analysis (significant at the 90% confidence level; D'Arrigo et al. 2005)

America, there is a gradual environmental gradient from the relatively dry-warm subtropics to the wet-cold high latitudes. Tree-ring records from subtropical regions, such as the southwestern United States and central Chile, are remarkably sensitive to precipitation variations (Boninsegna 1988; Cook et al. 2004; LeQuesne et al. 2006). In the transitional zones to higher latitudes, tree-ring responses to climate are largely determined by site conditions. Depending on elevation, aspect, slope, and soil characteristics, tree growth can be influenced by temperature, precipitation, or more commonly by a combination of both. In the extreme wet and cold environments at high-elevation or high-latitude upper tree lines, temperature is the major limiting factor controlling tree growth (Wiles et al. 1996; Luckman et al. 1997; Wiles et al. 1998; Aravena et al. 2002; Villalba et al. 2003; Lara et al. 2005). These changes in tree response with latitude were instrumental in setting the strategies for selecting tree-ring records sensitive to temperature and precipitation variations along the western Americas. Temperature reconstructions based on upper-elevation chronologies on mountains near the coasts around the Gulf of Alaska and northern Patagonia were selected as proxy records of temperature for North and South America, respectively. Tree-ring records from mesic to dry environments in the southern-central United States, the Bolivian Altiplano, and central Chile were used for the interhemispheric comparison of precipitation-sensitive records across the American Cordilleras (Fig. 7.1). The available data and maturity of dendroclimatological research differ considerably between regions, and therefore the kind of comparison between regional records and forcings will be different across the north-south transect.

7.3.1 Temperature-Sensitive Records

The strong cross-equatorial symmetries of SST, continental temperature, and continental precipitation patterns documented from instrumental records motivated the search in high-resolution proxy records for common spatial patterns of climate variability across the western Americas during the past centuries. Have the patterns of climate variability documented during the instrumental period been recurrent in previous centuries? Were these patterns different during the dominantly cooler conditions during the first half of the nineteenth century? Answers to these questions can provide useful information on the stationary nature of climate variations and how they could change under different global atmospheric conditions.

Box 7.2 Studies from the Canadian Cordillera

During the last 5 years, significant progress has been made in dendrochronological and dendroclimatic studies in the Canadian Cordillera (49°−65°N), building on limited earlier collections. Sampling has targeted temperature-sensitive sites at altitudinal tree line (*Picea engelmanni*, *P. glauca*, *Larix lyallii*, *Pinus albicaulis*, and *Abies lasiocarpa*) and moisture-sensitive sites at the lower forest border (*Pseudotsuga menziesii* and *Pinus ponderosa*), mainly using a network approach to isolate regional rather than local signals. Although initially focused on the southern Cordillera (ca. 125 chronologies), over 100 new sites have been sampled in the Yukon over the last 5 years. Studies at tree line in the Coast Ranges of British Columbia and Vancouver Island have developed several single- and multiple-species chronology networks (*Tsuga mertensiana*, *T. heterophylla*, and *Chamaecyparis nootkatensis*) that include sites with the potential for millennial-length reconstructions (see http://geog.uvic.ca/dept/uvtrl/uvtrl.htm). In the southern Cordillera, the network of low-elevation, moisture-sensitive sites has been used to reconstruct spatial patterns of precipitation and drought over the last three to four centuries (Watson and Luckman 2004a, 2005), and these data have been incorporated into the new gridded Palmer Drought Severity Index (PDSI) network developed by Cook et al. (2004).

New ring width and density data have been used to revise and extend a millennial-length (950–1994) summer temperature record from the Canadian Rockies (Box Fig. 7.3). Comparison with adjacent areas (e.g., Wiles et al. 2004) and global Northern Hemisphere curves suggests this is a regionally representative record. The influence of Pacific-forced decadal-scale variability in this record is more subtle, but the low-frequency signal suggests solar forcing has been an important control of summer temperature patterns in this region.

The use of multispecies networks allows the combination of temperature- and/or precipitation-sensitive chronologies to investigate climate-related phenomena that are influenced by the combined variation of temperature and precipitation. Box Figure 7.4 shows a reconstruction of glacier mass balance using independent tree-ring-derived summer and winter balances. Although winter balance (precipitation input) is strongly controlled by atmospheric circulation patterns from the Pacific, summer balance (mass loss through melt) is driven primarily by solar radiation. The major periods of positive net balance reflect a combination of higher winter inputs and cooler summers rather than summer temperatures alone. Future work can adopt similar approaches to the reconstruction of streamflow and other climate-related variables.

—B.H. Luckman, R.J.S. Wilson, and E. Watson

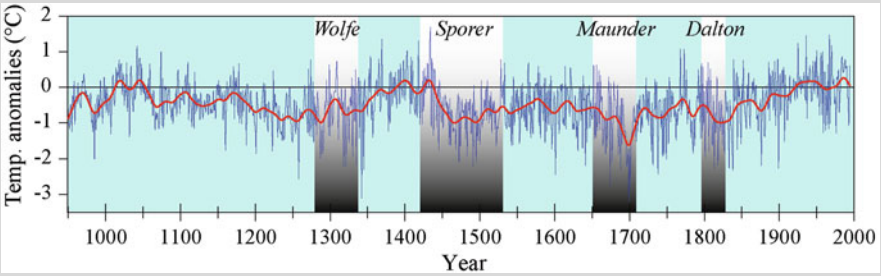

Box Fig. 7.3 Maximum May–August temperatures at the Columbia Icefield, Canadian Rockies. Temperatures are anomalies based on 1901–1980 means smoothed with a 30-year filter. Vertical bars represent significant sunspot minima (Luckman and Wilson 2005)

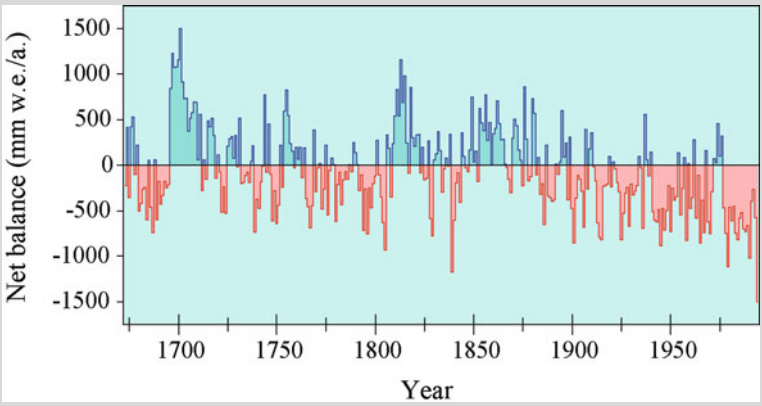

Box Fig. 7.4 Reconstructed net mass balance for Peyto Glacier, Alberta 1673–1994 (Watson and Luckman 2004b)

7.3.1.1 Extratropical Pacific Ocean

We use temperature reconstructions from coastal Gulf of Alaska and northern Patagonia to investigate past changes in the decadal oscillatory modes across the Pacific domain (Boxes 7.1 and 7.3). Wiles et al. (1998) presented a well-verified reconstruction of spring (MAM, March–May) temperature variations, based on three ring-width chronologies from coastal sites along the Gulf of Alaska, dating from 1600 to 1988. This reconstruction explains 34% of the variance in the instrumental temperature data. The decade-long variations in this reconstruction are consistent with changes in the Aleutian low-pressure system, which in turn is affected by ENSO (Dettinger et al. 2001). Spectral analysis of the temperature reconstruction shows significant peaks consistent with the ENSO-like bandwidth

(7, 8, 11, and 19 years). The reconstructed spring temperature series suggests that the recent warming exceeds temperature levels of prior centuries, extending back to AD 1600 (Wiles at al. 1998). The three coldest intervals in the spring series occurred in the seventeenth century. This cooling is consistent with the glacial record from coastal Alaska, which shows a strong advance during the late seventeenth to mid-eighteenth centuries (Wiles and Calkin 1994; Wiles 1997; Wiles et al. 2004).

A critical appraisal of surface air temperature from station records has recently been presented for southern South America (Villalba et al. 2003). Two different spatial temperature patterns were recognized in the southern Andes during the twentieth century: (1) surface cooling from 1930 to 1976 at the stations located in the northern sector of the southern Andes by the Pacific Coast (37°−42°S), and (2) a remarkable surface warming in the southern stations (south of 46°S), which intensifies at higher latitudes. Changes in the Pacific Decadal Mode around 1976 were seen in summer temperature records at most stations in the Pacific domain, starting a period with increased temperature across the southern Andes and at higher latitudes. Tree-ring records from upper tree line were used to reconstruct past temperature fluctuations for the two dominant patterns over the southern Andes. The resulting reconstructions for the northern and southern sectors of the southern Andes explain 55% and 45%, respectively, of the temperature variance over the interval 1930–1989. Cross-spectral analysis of actual and reconstructed temperatures over the common interval 1930–1989, indicates that most of the explained variance is at periods >10 years in length. Consequently, these reconstructions are especially useful for studying multidecadal temperature variations in the South American sector of the Southern Hemisphere over the past 360 years. These reconstructions show that temperatures during the twentieth century have been anomalously warm across the southern Andes. The mean annual temperatures for the northern and southern sectors during the interval 1900–1990 are 0.53°C and 0.86°C above the 1640–1899 means, respectively (Villalba et al. 2003).

Box 7.3 Climate signals in Patagonian upper-elevation tree-ring records

A great deal of progress has been made in increasing the number of upper-elevation tree-ring chronologies across the southern Andes during the past decade. This work has involved the development of more than 90 chronologies from collections of *Nothofagus pumilio*, the dominant subalpine tree in the Andes of Chile and Argentina (Villalba et al. 1997; Lara et al. 2001; Aravena et al. 2002; Villalba et al. 2003; Lara et al. 2005). These new collections have increased both the spatial coverage (ca. 35°35′ to 55°S) and the temporal span of upper-elevation records across the southern Andes (Box Fig. 7.5). The broad latitudinal distribution of *N. pumilio* across 2000 km in

a north-south direction provides the opportunity to examine the relationships between *N. pumilio* growth and climate along a temperature gradient from the subtropical central Andes to the sub-Antarctic Tierra del Fuego.

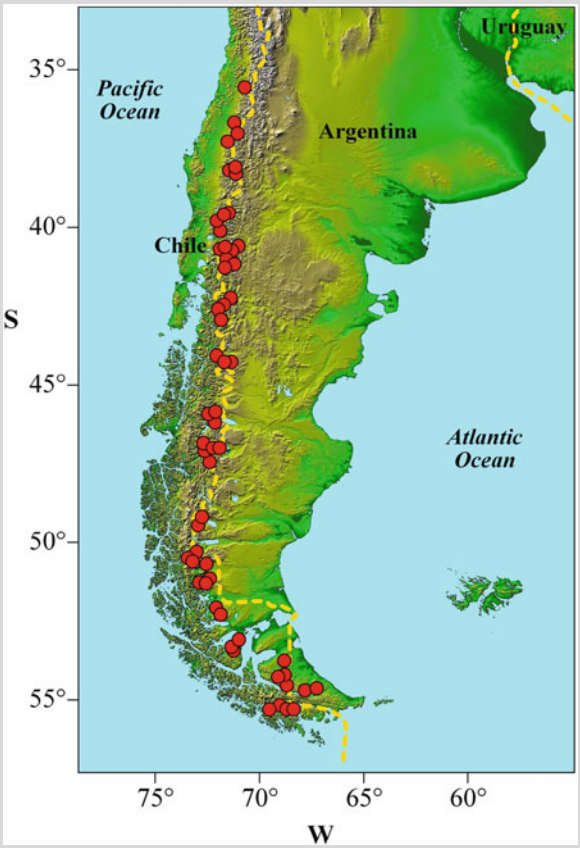

Box Fig. 7.5 *Nothofagus pumilio* chronologies in the Patagonian Andes

Nothofagus chronologies from upper tree line have been used to reconstruct past temperature fluctuations for the northern and southern sectors of the southern Andes. The reconstructions describe a well-defined cold interval from ~1640 to 1850, which conforms with the consensus view of the 'Little Ice Age' (LIA), a term commonly used to describe these cold episodes on a global scale (Bradley and Jones 1992).

Relationships between temperature reconstructions in southern South America and sea surface temperatures (SSTs) in the South Pacific and South

Atlantic Oceans clearly show that the temperature reconstructions contain information about climate variability extending over much of the tropical-subtropical Pacific and over the south Atlantic to Africa. The correlation fields between the reconstructions and SST (Box Fig. 7.6) are reminiscent of some of the global modes of SST recently derived from instrumental records. The spatial amplitudes obtained by correlating the northern Patagonian reconstruction with SSTs closely resemble the Southern Hemisphere counterpart of the interdecadal mode of the Pacific SST variability identified by Garreaud and Batistti (1999) and Enfield and Mestas-Nuñez (2000). Consistent with the documented decadal oscillatory mode of Pacific SST, the spatial field of correlations is characterized by anomalies in the western Pacific that extent to the southeast into subtropical South America. The spatial pattern that results from comparing the southern Andes reconstruction and SSTs resembles the 'global warming' mode identified by Enfield and Mestas-Nuñez (2000). According to these authors, the 'global warming' mode is the ocean counterpart to the global warming seen in surface air temperatures (SATs).

—R. Villalba, A. Lara, and M. Masiokas

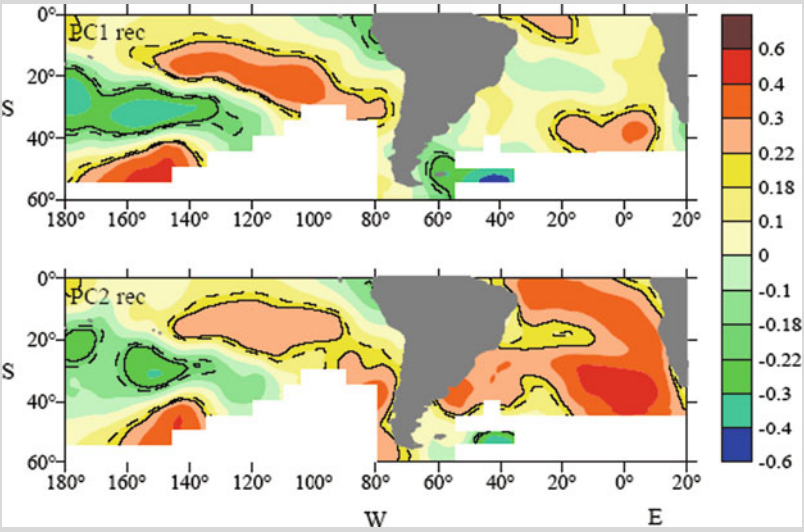

Box Fig. 7.6 Spatial correlation patterns (1857–1989) between sea surface temperature (SST) anomalies over the south Pacific and south Atlantic Oceans and the temperature reconstructions for the northern and southern sectors of the southern Patagonian Andes

The Gulf of Alaska and southern Andes reconstructions clearly show the well-documented transition from cold to warm conditions over the tropical Pacific in 1976 and are consistent with regional temperature compilations. This result reflects a comparable sensitivity of the temperature records to SST changes in the Pacific Ocean during recent decades. If decadal timescale variations in climate forced by the tropical Pacific had also affected temperature changes in the past, tree-ring-based reconstructions of temperature along the coast of North and South America should present similar oscillatory patterns. Indeed, for the common interval 1640–1989, reconstructed temperature variations from the Gulf of Alaska are significantly correlated with those of northern ($r = 0.42,\ p < 0.01$; Fig. 7.5) and southern Patagonia ($r = 0.38,\ p < 0.01$). Spatial patterns obtained by correlating the Alaska and northern Patagonia temperature reconstructions with SSTs across the Pacific and Atlantic

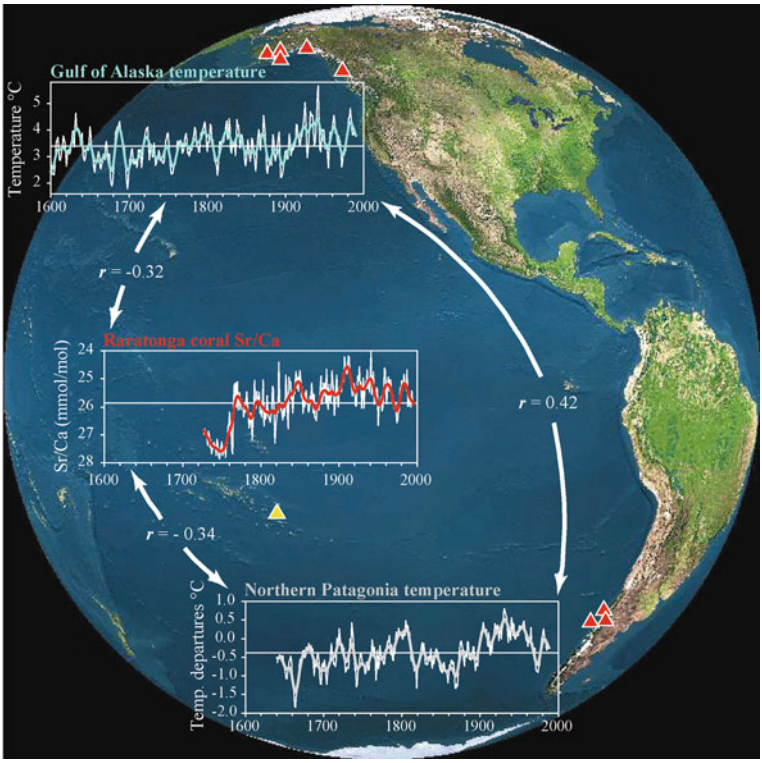

Fig. 7.5 This figure compares temperature-sensitive tree-ring records (*red triangles*) from high-latitude, western North and South America with a geochemical coral record (*yellow triangle*) from Raratonga, in the tropical South Pacific during the past three to four centuries. The series shown from top to bottom are: spring/summer Gulf of Alaska temperature reconstruction (1600–1994; Wiles et al. 1998), Sr/Ca coral record from Rarotonga (1726–1996; Linsley et al. 2004), and annual northern Patagonia temperature reconstruction (1641–1989; Villalba et al. 2003). Correlation coefficients between records are indicated. To facilitate the comparison, the Sr/Ca coral record is shown inverted

Oceans (Villalba et al. 2001) closely resemble those observed for the decadal mode of Pacific SST variability identified by Zhang et al. (1997) and Garreaud and Battisti (1999). Temperature anomalies related to ENSO-like variations are larger and more spatially consistent in northern than in southern Patagonia (Fig. 7.3c), reflecting the decrease in correlation between Alaskan and Patagonian records with increasing southern latitudes.

The Gulf of Alaska and northern Patagonia temperature reconstructions are displayed in Fig. 7.6, along with the waveforms of the two oscillatory modes that are

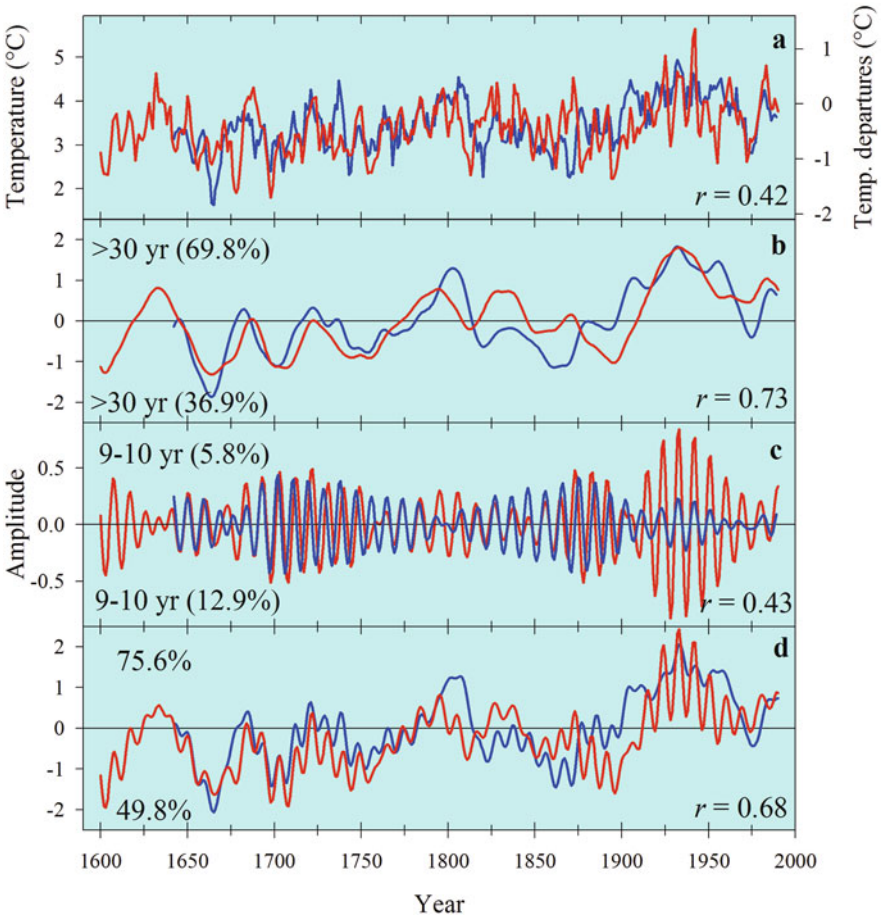

Fig. 7.6 Comparison of temperature reconstructions from northern Patagonia (*blue line*) and coastal Alaska (*red line*) and their dominant oscillations isolated by using singular spectrum analysis (SSA; panel **a**; Vautard 1995). Common oscillatory modes in both records have periods of (**b**) > 30 years, and (**c**) 9–10 years. Percentages of the original variance contributed by Patagonian and Alaskan waveforms are indicated in the upper and lower left corners, respectively. The Pearson's correlation coefficient, *r*, between the series, is shown in the lower far right. Time series included in (**d**) represent the sum of the oscillations shown in (**b**) and (**c**)

the major contributors to the common variance between these records. Waveforms were extracted from the original reconstructions by using singular spectrum analysis (SSA), basically a statistical technique related to EOF analysis, to determine oscillatory modes in the time domain (Vautard and Ghil 1989). The reconstructed waveforms, representing oscillations >30 years and approximately 10 years, reveal interesting changes in amplitude during the past 350 years. As was previously noted (Villalba et al. 2001), the temporal evolution of these components is more closely related in amplitude and intensity from 1640 to approximately 1850. After 1850, relationships between waveforms are weaker. The most remarkable feature in the long-term oscillations is the positive amplitudes during the past 100 years, reflecting the warming in the twentieth century.

7.3.1.2 Tropical Pacific Ocean

Although the temperature reconstructions from the Gulf of Alaska and northern Patagonia provide insight into the temporal evolution of the relationships between the tropical ocean and higher latitudes in the Americas, it is important to note that the variability in the records is related to tropical teleconnections along the western coasts of the Americas and not to direct forcing from the equatorial Pacific. In a first attempt to connect the extratropical tree-ring records from North and South America with climate variability in the tropical Pacific, we compared the temperature reconstructions with high-resolution coral records in the Pacific Ocean.

Long-lived corals provide continuous, high-resolution records of tropical Pacific climate that supplement the instrumental record of climate from this key region. Modern coral records from the central tropical Pacific are several centuries in length and have yielded insights into the recent history of tropical Pacific climate variability on a variety of timescales. The $\delta^{18}O$ and Sr/Ca time series from corals in the subtropical Pacific at Rarotonga (21°14′S and 159°49′W), have recently been compared with indices of climate variability in the north Pacific, suggesting some degree of cross-hemispheric symmetry of interdecadal oceanographic variability in the past centuries (Linsley et al. 2004). A tree-ring reconstruction of the north Pacific index, a measure of the intensity of the large-scale atmospheric circulation related to the Aleutian low-pressure cell, correlates significantly during the twentieth century with both instrumental tropical climate indices and a coral-based reconstruction of an optimal tropical index for the Indian and Pacific Oceans, supporting evidence for a tropical/north Pacific link that extends as far west as the western Indian Ocean (D'Arrigo et al. 2005).

The coral skeletal Sr/Ca at Rarotonga appears to be related to SST variability on annual through at least decadal timescales based on correlation with instrumental SST (Linsley et al. 2004). The coral record, which covers the period 1726–1997, is significantly correlated with both the Gulf of Alaska ($r = -0.32$, $p < 0.01$) and northern Patagonia ($r = -0.34$, $p < 0.01$) temperature reconstructions (Fig. 7.5). The low-pass fraction for each time series was isolated by using SSA (Vautard 1995), and all reconstructed components with mean frequencies longer than 20 years were summed. The results are shown in Fig. 7.7. The subtropical

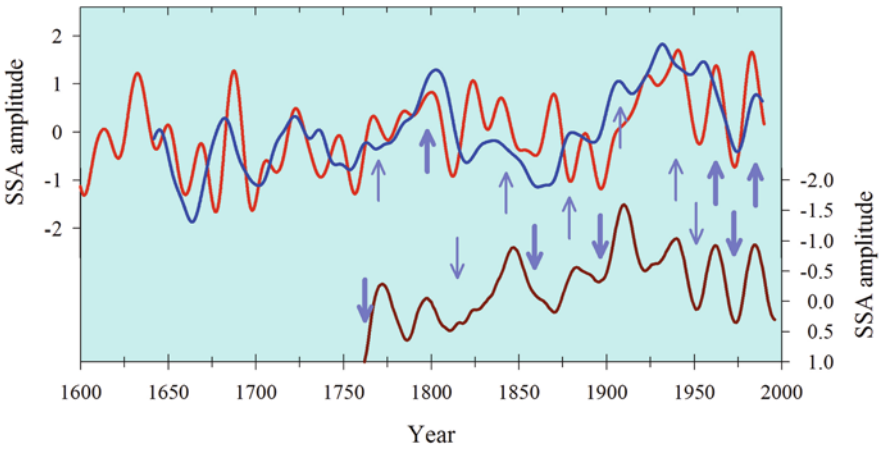

Fig. 7.7 Interdecadal to centennial variability in temperature-sensitive series from Gulf of Alaska (*red line*), northern Patagonia (*blue line*), and Raratonga (*brown line*), isolated by using singular spectrum analysis (SSA; Vautard 1995). For each record, all SSA-reconstructed components with mean frequencies longer than 20 years were summed. *Thin* and *thick arrows* indicate coincidences in oscillations between the Raratonga and one or two high-latitude records, respectively

Pacific records indicate that some of the interdecadal transitions in coral Sr/Ca temporally align with comparable transitions in the Gulf of Alaska and northern Patagonia temperature reconstructions. The remarkable shift in tropical Pacific climate during the mid-1970s is clearly captured by all three records. However, some differences are observed between interdecadal oscillations in the subtropical coral and the North and South American tree-ring records. Interdecadal temperature oscillations in northern Patagonia closely align with transitions in the Pacific coral Sr/Ca records from the 1850s to the beginning of the twentieth century, whereas the Gulf of Alaska oscillations align better with Rarotonga Sr/Ca during the second half of the twentieth century.

7.3.1.3 High-Latitude Oscillations

As was indicated in Section 7.2.3, temperature variations in high latitudes of the Northern and Southern Hemispheres are also related to changes in the NAM and SAM, respectively (Thompson and Wallace 2000; Thompson and Solomon 2002). We search for common patterns in temperature variations in the sub-Artic and sub-Antarctic regions, which in turn might provide insight on common forcings of high-latitude past climates in both hemispheres. Boreal tree-ring records from high latitudes in the Northern Hemisphere were used to provide a long-term perspective of Arctic annual temperatures (D'Arrigo and Jacoby 1993). The reconstruction was based on 12 chronologies from North America: 3 in Alaska north of 67°N, 4 in northwestern-central Canada from the Yukon to Churchill, and 5 in eastern Canada. This sub-Arctic network was complemented with five boreal

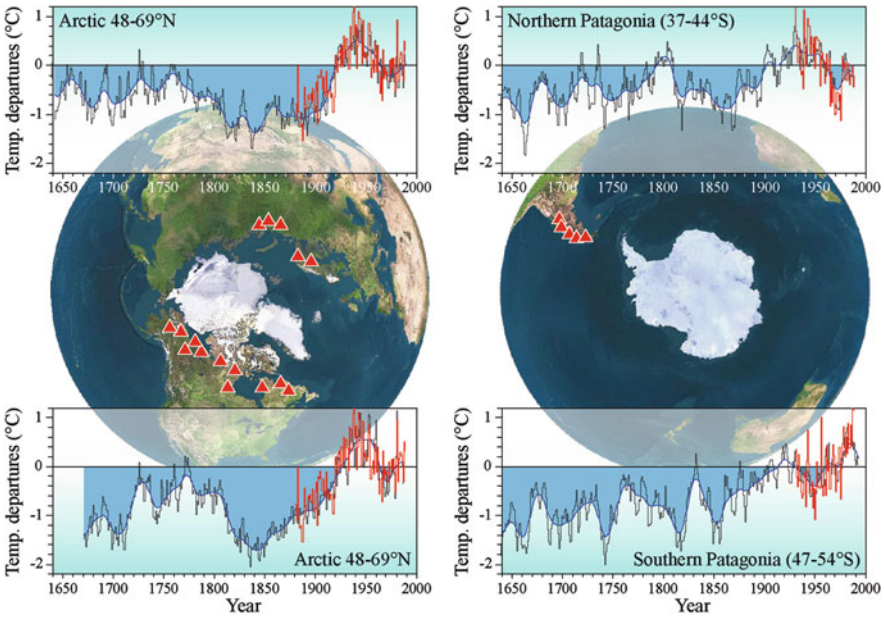

Fig. 7.8 Temperature reconstructions from Arctic and sub-Antarctic regions. The geographical locations of tree-ring chronologies (*red triangles*) used for developing the temperature reconstructions for the Arctic (*left*) and sub-Antarctic (*right*) regions are shown. See text for reconstruction details

tree-ring chronologies from Scandinavia (67°−69°N) and three from the northern Ural Mountains (Fig. 7.8). The total variance in temperature variations explained by the tree-ring chronologies during the 1880–1969 calibration period is 66%. The major low-frequency trends in the reconstructed Arctic temperatures include a cooling in the late 1600s to early 1700s, a relative warming in the 1700s, an abrupt decline in temperature in the early 1800s, a gradual warming since the middle to late 1800s, and unprecedented warming during the twentieth century. Recently, a new reconstruction of temperature variability for the Arctic has been developed with significantly improved geographical coverage and replication than previously (Gordon Jacoby, in preparation). The new temperature record reproduces most climatic events previously reconstructed, reinforcing the occurrence of major temperature changes in the sub-Arctic during the past four centuries. For comparison with the sub-Antarctic temperatures, the two reconstructions were averaged in a single Arctic temperature record.

The northern latitude record was compared with the temperature reconstructions for northern and southern Patagonia (Villalba et al. 2003, Fig. 8). For the common interval 1670–1987, the correlation coefficient between the Arctic and sub-Antarctic (average of the two southern reconstructions) is $r = 0.55$ ($p < 0.001$). For the past 400 years, striking similarities in temperature fluctuations are observed in both regions. The records exhibit their largest common variances at low frequencies

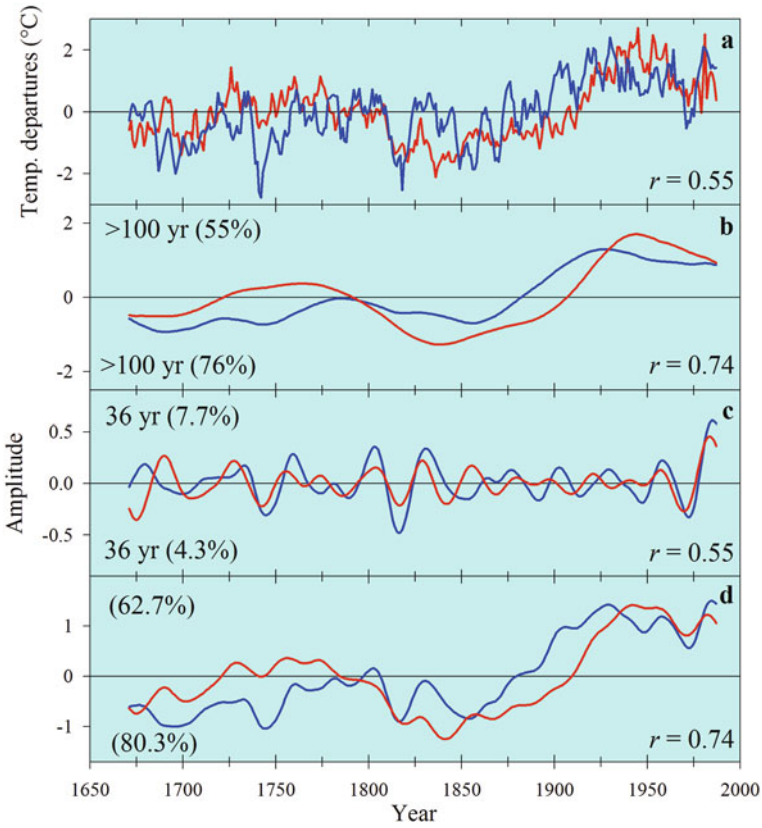

Fig. 7.9 Comparison of the amplitudes from the first principal components of the temperature reconstructions from Patagonia (*blue line*) and the Arctic (*red line*). The Patagonian and the Arctic records were obtained by averaging the temperature reconstructions shown in Fig. 7.8. Common oscillatory modes in both records have periods of (**b**) > 100 years, and (**c**) around 36 years. Time series included in (**d**) represent the sum of the oscillations shown in (**b**) and (**c**) (for explanation of the data in each panel of this figure see Fig. 7.6)

(Fig. 7.9). In both records, positive levels during twentieth-century periods exceed values back to 1670. An abrupt decrease in temperature in both regions is recorded in the 1810s, quite likely related to a series of large tropical volcanic eruptions, including an unknown source in 1809, Soufriere in 1812, and Tambora in 1815, among others (Zielinski 2000). A notable feature of temperature change revealed by the high-latitude records is the continuous transition from anomalous cold conditions in the mid-nineteenth century to anomalous warm conditions in the mid-twentieth century. In contrast, the global and hemispheric mean instrumental temperatures show almost no trend between the late 1850s and the 1910s (Jones and Moberg 2003), suggesting that high latitudes in both hemispheres share common patterns of temperature changes that are not seen at global scales.

7.3.2 Precipitation-Sensitive Records

Tree-ring chronologies from precipitation-sensitive regions across the western Americas, such as the southern United States, the Bolivian Altiplano, and central Chile, reveal common interannual to decadal-scale oscillations in precipitation variations during the past centuries (Boxes 7.4, 7.5, 7.6, 7.7 and 7.8). Spatial correlation patterns between precipitation-sensitive records and SST also show that variations in these records are strongly connected with SST anomalies in the equatorial Pacific and off the western coast of the subtropical Americas (Villalba et al. 2001).

Box 7.4 Spatial patterns of drought and wetness regimes over western North America

The network of moisture-sensitive tree-ring chronologies now available for North America has been used to reconstruct the summer (June–July–August, JJA) Palmer Drought Severity Index (PDSI) for 1200 years on 286 grid points extending from southern Mexico across the United States into southern Canada (Cook et al. 2004). These reconstructions have high temporal and spatial fidelity when compared with instrumental PDSIs on annual and decadal timescales. The average of all 286 grid points for North America indicates that the driest single year in the past 500 years occurred in 1864, and the wettest single year occurred in 1833 (Box Figs. 7.7 and 7.8). The reconstructions indicate that the twentieth century was relatively moist compared with the past 500 years, the severe Dust Bowl and 1950s droughts notwithstanding (Box Fig. 7.7).

The long-range climate influence of the El Niño/Southern Oscillation (ENSO) over western North America during the late nineteenth and twentieth centuries has been strongest in the Texas-Mexican sector of northern Mexico and the southwestern United States, with drought during La Niña events and wetness during El Niño events. The epicenter of reconstructed decadal drought was often located in the ENSO teleconnection province over the Southwest, implicating the tropical Pacific in these decadal dry regimes. The pluvials of the past 500 years were spatially heterogeneous and did not tend to recur in the ENSO teleconnection region. The notable exception was the early twentieth-century pluvial (Box Fig. 7.7), one of most extremely wet decades in 500 years, and which was concentrated in the drainage basin of the Colorado River. This period of exceptional wetness inflated expectations of surface water supplies in the Southwest, and provides a modern demonstration of the significant environmental and socioeconomic impacts associated with these decadal droughts and pluvials. The seventeenth-century Pueblo Drought lasted at least six years over the same region impacted by the twentieth-century pluvial (Box Fig. 7.7), and provides a compelling contrast to the pluvial and a strong analog for the recent multiyear drought

that has severely impacted surface water supplies in the Southwest (1999–2006). Socioeconomically, the seventeenth-century Pueblo Drought caused starvation, death, and the permanent abandonment of five Pueblo communities and other villages in New Mexico.

—D.W. Stahle and E.R. Cook

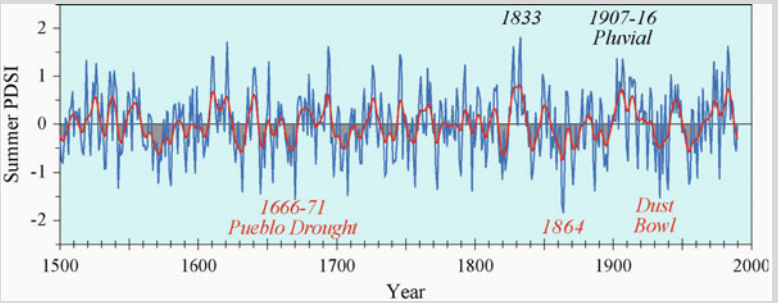

Box Fig. 7.7 North American summer Palmer Drought Severity Index (PDSI), a time series average of reconstructed PDSI from all 286 grid points over North America

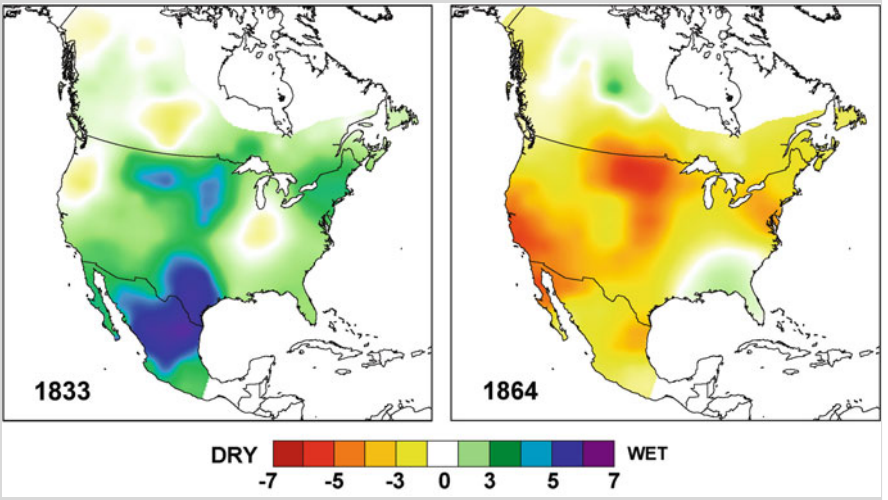

Box Fig. 7.8 Reconstructed summer Palmer Drought Severity Index (PDSI) for the wettest (1833) and driest (1864) single years in the 'North America summer PDSI' series (Box Fig. 7.7), showing the continental scale of these record moisture anomalies

Box 7.5 Western United States droughts in medieval times linked to changes over the Pacific basin

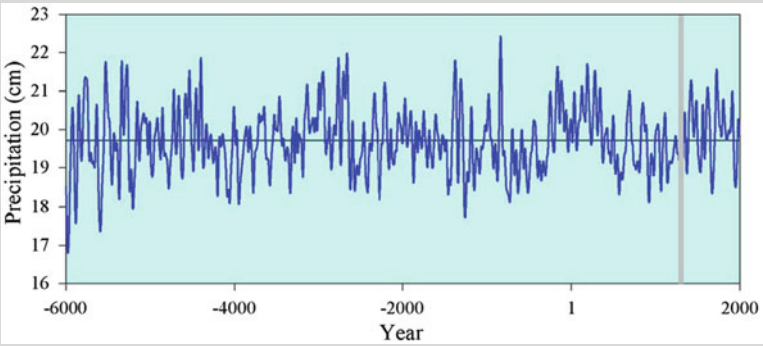

Box Fig. 7.9 Reconstructed Nevada division 3 July–June precipitation (smoothed with 50-year Gaussian filter). *Gray line* marks the transition at ~AD 1400

Several multicentury shifts in precipitation over the central Great Basin in the United States are seen in an ~8000-year reconstruction from the bristlecone pine chronology at Methuselah Walk, and in an ~1800-year reconstruction based on this and five other chronologies (Hughes and Funkhouser 1998). A remarkable, but not unique, transition from drier to wet conditions is reconstructed between the periods AD 400–1400 and AD 1400–2000 (Box Fig. 7.9). We set out to find an explanation for this transition (Graham et al. 2007). Proxy evidence from tree-ring and pollen-based reconstructions, and ocean core isotopic data suggest that the circa 1400 transition was marked by warming sea surface temperatures (SSTs) along the central California coast (Kennett and Kennett 2000; Box Fig. 7.10, plot labeled Santa Barbara Basin SST), and increasing winter precipitation with cooler summer temperatures from southern and central California into the Great Basin (Box Fig. 7.10, top plot). In today's climate, such changes are associated with El Niño episodes, suggesting the possibility that El Niño-like changes in tropical Pacific SSTs may have played a causal role in producing the mid-latitude changes suggested by the proxy records. A coral-based Niño-3.4 SST reconstruction from Palmyra Atoll in the central tropical Pacific (Box Fig. 7.10, plot 5; Cobb et al. 2003 and a foram Mg/Ca based SST reconstruction from near Mindanao in the northwest equatorial Pacific (Box Fig. 7.10, middle plot; Stott et al. 2004) support the idea of a trend towards more El Niño–like conditions at the circa 1400 transition. Analysis of the proportion of terrestrial material in a marine core taken off the coast of central Peru indicates a contemporaneous increase in river discharge associated with high-flow events (Rein et al. 2004). This

picture would be consistent with the Pacific-wide pattern proposed here. Hence, it is suggested that the proxy-inferred warming of California coastal SSTs and increasing western US precipitation around, roughly, AD 1400 resulted (at least in part) from increasing tropical Pacific SSTs and resulting changes in tropical precipitation patterns. The question now arises whether other transitions in the Nevada record (for example, around 400 BC, and in the converse direction around AD 400) have similar causes.

—Nicholas E. Graham and Malcolm K. Hughes

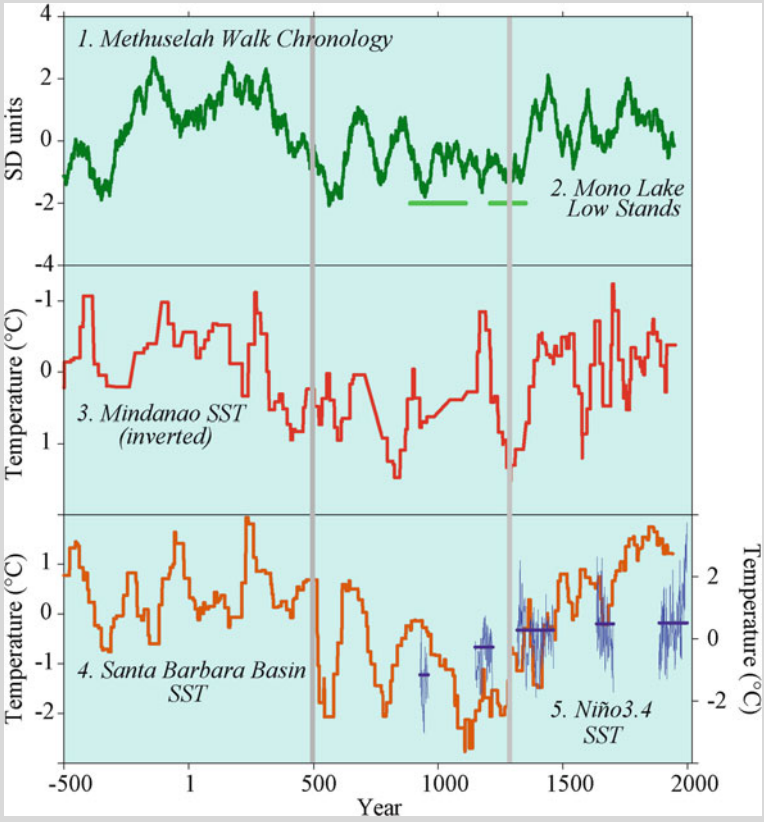

Box Fig. 7.10 Proxy records from areas in the equatorial Pacific Ocean and its eastern margin (western North America) since 500 BC. *Top Plot*: extent of Mono Lake low stands (Stine 1994) green horizontal lines, and a long tree-ring chronology from the White Mountains of California. *Middle plot*: Mg/Ca-based SST reconstruction from foraminifera near Mindanao in the northwest equatorial Pacific. Scale inverted for comparison. *Bottom Plot*: yearly values and period means (*horizontal blue lines*) of sea surface temperature (SST) (After Graham et al. 2007)

In 1999, a gridded network of 154 Palmer Drought Severity Index reconstructions for the continental United States was generated from a set of 388 tree-ring chronologies (Cook et al. 1999). More recently, the spatial and temporal coverage of the PDSI reconstructions was expanded, including 286 points in a 2.5° × 2.5° grid covering most of North America (Cook et al. 2004; Box 7.4). The new PDSI reconstructions are based on an expanded network of 835 tree-ring chronologies. The temporal coverage was also expanded to the maximum permitted by the available tree-ring data, extending back nearly 2000 years for some locations. Finally, the process of variance restoration applied to the grid point reconstructions allows for updates of those records to AD 2003 with instrumental PDSI data. In a previous work (Villalba et al. 2001), the temporal evolution of the PDSI in four cells located in the midwestern-southwestern United States were compared with precipitation-sensitive chronologies from central Chile. For the common interval 1700–1978, the correlation coefficient between the first Principal Component (PC) from the four PDSI reconstructions and tree-ring variations at El Asiento, central Chile, is $r = 0.32$ ($p < 0.001$), which was considered as an indication of common modes of variations in these series. With the increasing number of PDSI reconstructions across North America, the use of a spatial approach to study large-scale atmospheric variations connecting mid- to high-latitude precipitation changes in North and South America now appears to be feasible.

A major advance in the effort to expand the spatial coverage of tree-ring records across the Americas has been the recent development of *Polylepis tarapacana* chronologies in the Bolivian Altiplano (Argollo et al. 2004). These records, located between 17° and 20°S and above 4500 m elevation, represent the closest-to-equator tree rings in the Andes and the highest-elevation chronologies worldwide (Box 7.7). A careful examination of interannual variations in ring width and climate in the Altiplano indicate that the growth of *Polylepis* is remarkably associated with summer water balance. Most *Polylepis* records cover the past three to four centuries, but some of them extend over seven centuries. Two of the longest chronologies (Caquella and Soniquera) were merged in a single record and used for comparison with precipitation-sensitive records in other regions of the western Americas. For central Chile, a ring-width chronology from *Austrocedrus chilensis* D. Don at El Asiento (32°40′S), which represents the northernmost extent of this species in central Chile, was used for comparison with North American records (Box 7.9). Recently, the site was revisited, and series from the new cores were merged with the original data collected in 1974 by LaMarche (1975).

Box 7.6 A network of tree-ring chronologies for northern and central Mexico

The mixed conifer forests and riparian areas of northern and central Mexico contain some of the most climate-sensitive species in the North American region (Box Fig. 7.11). Douglas-fir (*Pseudotsuga menziesii*) is one of these species that has been widely recognized due to its sensitivity to climate (Fritts 1976). Douglas-fir has a native latitudinal range covering at least 38° in the Northern Hemisphere and extending well into southern Mexico at latitudes below 17°N. In Mexico, Douglas-fir occurs in scattered insolated populations of mixed conifer forests located at high elevations, thriving in cool microenvironments and scarped terrains of the Sierras Madre Occidental and Oriental (Martínez 1963). The annual ring of this species is anatomically divided into two distinct layers: the earlywood (EW) is composed of low-density, light-colored cells, whereas the latewood (LW) has smaller, darker cells with thicker walls. The development of separate EW and LW chronologies provides more information on the influence of intra-annual climate variability than using total ring width data (Cleaveland 1986; Stahle et al. 1998).

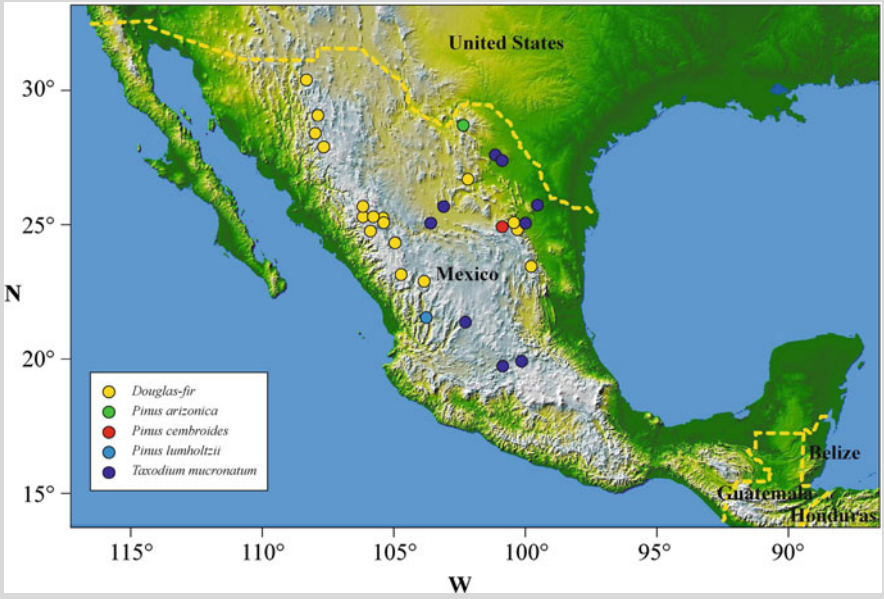

Box Fig. 7.11 Tree-ring chronologies in Mexico

Ahuehuete or Montezuma bald cypress (*Taxodium mucronatum*), a widely distributed riparian species that is considered to be the national tree of Mexico, has been used to develop the longest tree-ring chronologies in Mexico. In recent years, over 30 new tree-ring chronologies have been developed or are in process as part of the CRN03-IAI project. The Douglas-fir chronologies range between 129 and 604 years, bald cypress between 117 and 1550 years, and pinyon pine (*Pinus cembroides*) over 400 years. Some available Douglas-fir and bald cypress chronologies are being extended with the use of cross sections from subfossil wood or logged material. The EW growth of Douglas-fir trees in Mexico is influenced by dominant climatic conditions in the winter–spring period previous to growth (November to current June; Box Fig. 7.12), explaining around 70% of the variance in growth. Cool season precipitation in northern Mexico is increased by the warm phase of El Niño/Southern Oscillation (ENSO). On the other hand, the LW width is affected by the summer precipitation and the monsoon system. Annual ring width of bald cypress is influenced by the seasonal late spring to summer precipitation (June–September), explaining 52% of the variance in growth. The regions of northern and central Mexico have highly limited water resources, and paleoclimatic reconstructions are essential to understand the hydroclimatic variability that characterizes these regions. Determining past climatic variability is essential to planning proper management strategies for water use, and tree-ring studies offer the best opportunity to understand this variability over the last 1000 years.

—J. Villanueva-Diaz, J. Cerano-Paredes, D. Stahle, M. Therrell, M. Cleaveland, and B.H. Luckman

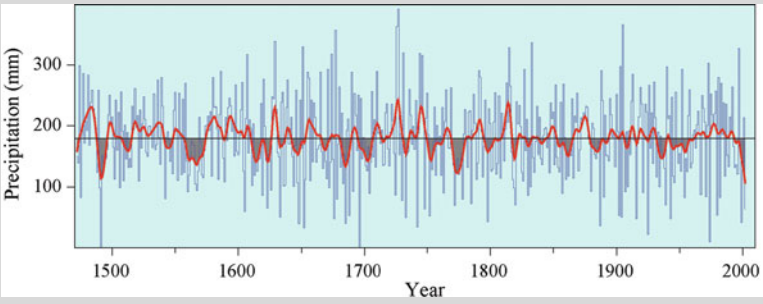

Box Fig. 7.12 The winter–spring precipitation series reconstructed from an earlywood Douglas-fir chronology in Chihuahua, Mexico. The reconstruction covers the period 1472–2002

Box 7.7 The *Polylepis tarapacana* chronologies: The highest elevation tree-ring records worldwide

Polylepis, a genus from the Rosaceae family, includes several woody species of small- to middle-sized trees that grow at very high altitudes in the tropical Andes of South America (Kessler 1995). *Polylepis tarapacana*, adapted to drier and colder conditions than other species of the same genus, reaches the highest elevation of tree growth in the world. On the slopes of the high volcanoes in Bolivia and along the Bolivian-Chilean-Argentinean border, *P. tarapacana* grows between 4100 and 5200 m elevation.

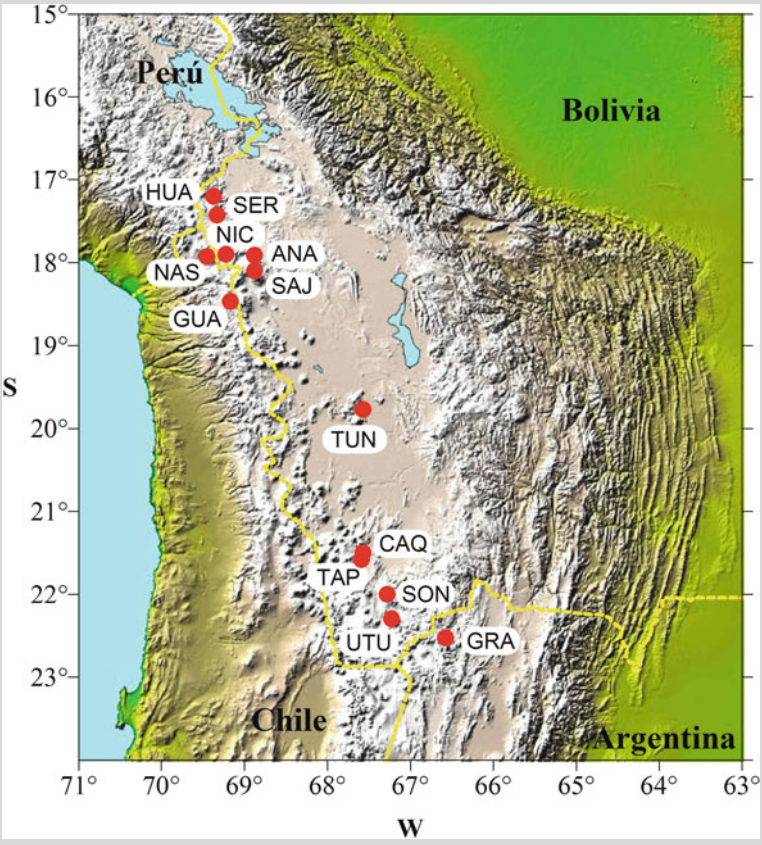

Box Fig. 7.13 *Polylepis tarapacana* chronologies in the Bolivian Altiplano and adjacent areas of Chile and Argentina. HUA: Huarinka; SER: Serke; NIC: Cerro Nicolás; ANA: Analasjchi; NAS: Nasahuento; SAJ: Sajama; GUA: Guallatire; TUN: Tunupa; CAQ: Caquella; TAP: Tapachilca; SON: Soniquera; UTU: Uturun-co; GRA: Cerro Granadas

Polylepis stands are almost exclusively restricted to volcanic slopes, with a strong preference for well-insolated north-facing slopes. Extensive collections of *P. tarapacana* were conducted in Bolivia, Chile, and Argentina (16°–22°S) as part of the IAI-CRN program to reconstruct climate variations from upper-elevation tree rings along the Americas (Box Fig. 7.13). Presently, the chronologies range between 98 and 705 years in length, and represent the highest tree-ring records worldwide (Box Fig. 7.14). In order to determine the climatic variables controlling *P. tarapacana* growth, interannual variations in tree growth were compared with regional records of precipitation and temperature. Correlation functions indicate that the radial growth of *P. tarapacana* is influenced by water balance during the summer previous to the ring formation. At the sampling sites, precipitation explains around 50% of the total variance in growth. Summer temperatures, which increase evapotranspiration and reduce soil water supply, are negatively correlated with tree growth (Argollo et al. 2004).

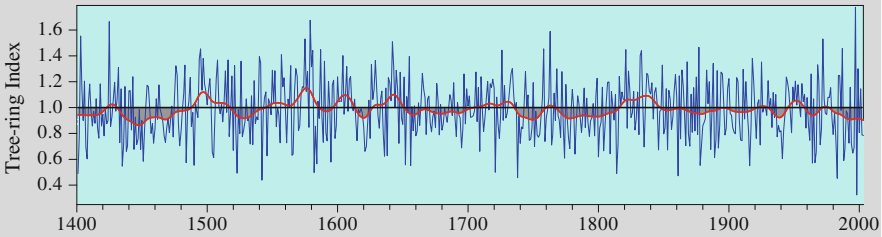

Box Fig. 7.14 Composite chronology resulting from merging the *Polylepis tarapacana* ring width series from Caquella and Soniquera in the Bolivian Altiplano

Traditionally, the wood of *Polylepis tarapacana* has been used by local populations in the Bolivian Andes for construction, particularly for house and church roofs. Wood from old buildings offers the possibility of extending the upper-elevation records of *P. tarapacana* back in time for the past millennium. These records offer the unique opportunity for reconstructing precipitation variations across the altiplano during the past five to seven centuries or more.

—Jaime Argollo, Claudia Soliz, Jorge Moya, Janette Pacajes, Mariano S. Morales, and Ricardo Villalba

7.3.2.1 Subtropical Precipitation and ENSO

Precipitation variations in the United States–Mexico, the Bolivian Altiplano, and central Chile are related to climatic changes in the tropical Pacific. It is well known that there is a strong teleconnection between SST changes in the tropical Pacific and precipitation anomalies in the southern United States and northern Mexico (Ropelewski and Halpert 1986; Kiladis and Diaz 1989; Cole and Cook 1998). Warmer SSTs in the tropical Pacific typically result in increased precipitation anomalies in this region. Spatial correlations between different indices of tropical Pacific circulation and the grid point PDSI series over the conterminous United States show that the geographic location of the highest correlation field is the southwestern United States (Cook et al. 2000), a finding that is consistent with the patterns identified by using instrumental records.

Interannual variability in precipitation over the altiplano is primarily related to changes in the mean zonal flow, reflecting changes in meridional baroclinicity between tropical and subtropical latitudes, which in turn is a response to sea surface temperature changes in the tropical Pacific (Garreaud et al. 2003). There is a general agreement that a significant fraction of interannual variability in summer precipitation is related to ENSO (e.g., Aceituno 1988; Lenters and Cook 1999; Vuille 1999; Vuille et al. 2000; Garreaud et al. 2003). All of these studies concluded that El Niño years tend to be dry, whereas La Niña years are often associated with wet conditions on the altiplano. However, dry La Niña years and wet El Niño years are not completely uncommon, which indicates that the relationship between SST anomalies in the tropical Pacific and precipitation in the central Andes is not simple (Garreaud et al. 2003). Finally, relationships between SSTs in the equatorial Pacific and precipitation anomalies in central Chile (30º−35ºS) have been reported by several authors (Quinn and Neal 1983; Aceituno 1988; Rutlland and Fuenzalida 1991; Aceituno and Montecinos 1996; Montecinos and Aceituno 2003). Positive rainfall anomalies in central Chile are associated with warmer SSTs in the tropical Pacific. Conversely, cold SSTs correspond quite closely to dry conditions in the area.

To gain insights into the long-term relationships between SST in the tropical Pacific and precipitation in the southwestern United States, the Bolivian Altiplano, and central Chile, we compared precipitation-sensitive records from these three regions with a multiproxy-based reconstruction of SST for the El Niño-3 region (Mann et al. 2000). Through exploiting the complementary information shared by a wide network of different types of proxy climate indicators, the multiproxy El Niño-3 reconstruction reduces the weaknesses in any individual type or location of indicator and makes use of the mutual strength of the diversity in the records. The reconstructed eastern equatorial Pacific Niño-3 areal-mean SST index has been previously used as a direct indication of ENSO itself for the past 400 years (Mann et al. 2000). A large proportion of the tree-ring chronologies from the southwestern United States and Mexico have been used as predictors of both the Niño-3 index and PDSI reconstructions, which make the reconstructions not statistically independent. In contrast, neither the El Asiento nor the Bolivian Altiplano chronologies have been included in the Niño-3 index reconstruction.

Box 7.8 Tree-ring chronologies from *Austrocedrus chilensis* in central Chile

Austrocedrus chilensis (D. Don, Serr et Bizz.) is the most northerly-distributed conifer species of the Andean Patagonian forests. The species occurs within a wide latitudinal range between 32º39′ and 43º40′S. The northernmost populations of the species also occupy the tree line at high elevations in the Andes of central Chile. These populations are growing on steep, rocky slopes under severe water stress in low-density, scattered stands. The trees from these marginal stands exceed 1200 years in age and exhibited typical features of long-lived species, like strip bark growth, twisted branches, and crown dieback. According to Edmund Schulman (1956), *Austrocedrus* 'was the most suitable dendrochronologic species in the southern Andes. Its ring record is as well defined as any in the drought conifers of the Rocky Mountains, and it possesses the type of cambial growth regime which leads to good crossdating quality in the ring series.'

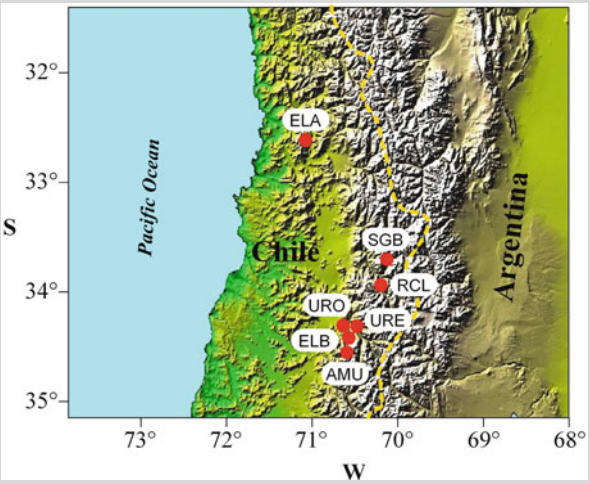

Box Fig. 7.15 *Austrocedrus chilensis* chronologies in central Chile. ELA: El Asiento; SGB: San Gabriel; RCL: Río Clarillo; URO: Urriloa Oeste; URE: Urriola Este; ELB: El Baule; AMU: Agua de la Muerte

Several tree-ring collections of *Austrocedrus chilensis* were taken in central Chile during the early years of dendrochronological studies in South America. The El Asiento site (ELA, Box Fig. 7.15) was first visited by Valmore LaMarche in 1972. After that, several collections were conducted in San Gabriel, Río Clarillo, Urriola Oeste, Urriola Este, El Baule, and Agua de

la Muerte. In recent years, new collections have been carried out in these sites to update and extend these chronologies, especially by collecting preserved relict wood (Box Fig. 7.15). Correlation function analyses show a strong climatic signal related to winter–spring precipitation during the previous and current growing seasons. A composite record consisting of El Asiento and El Baule chronologies has been used by LeQuesne et al. (2006) to develop new estimates of June–December precipitation for central Chile extending from AD 1200 to 2000 (Box Fig. 7.16).

The reconstruction suggests that the decadal variability of precipitation in central Chile was greater before the twentieth century, with more intense and prolonged dry and wet episodes. Multiyear drought episodes in the eighteenth, seventeenth, sixteenth, and fourteenth centuries exceed the estimates of decadal drought during the twentieth century. The reconstruction also indicates an increase in interannual variability after 1850. In fact, the risk of drought exceeding all thresholds increases dramatically in the reconstructed precipitation series after 1850, consistent with the drying trends indicated by selected long instrumental precipitation records.

—Carlos LeQuesne and David Stahle

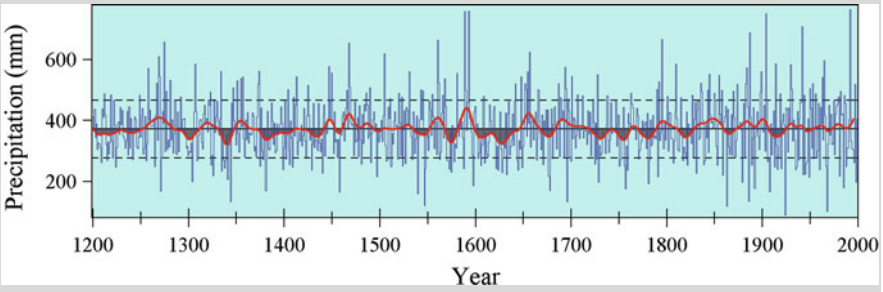

Box Fig. 7.16 Tree-ring-reconstructed precipitation for central Chile from AD 1200 to 2000. A cubic smoothing spline highlighting multidecadal variability (ca. 25 years, fit for the period 1205–1995) and the ±1.0 standard deviation thresholds are also plotted

It is important to note that based on instrumental records, the strongest teleconnections between precipitation in the southern United States–northern Mexico and SST in the tropical Pacific have been identified for the winter months (Kiladis and Diaz 1989; Stahle et al. 1998; Cleaveland et al. 2003), whereas the PSDI reconstructions are reflecting drought conditions during the summer months. On the other hand, the *Polylepis* chronologies in the Bolivian highlands and the *Austrocedrus* chronologies in central Chile are sensitive to summer and winter precipitation, respectively. Despite the limitation imposed by the differences in seasonal-window responses of trees from different regions to precipitation and the fact

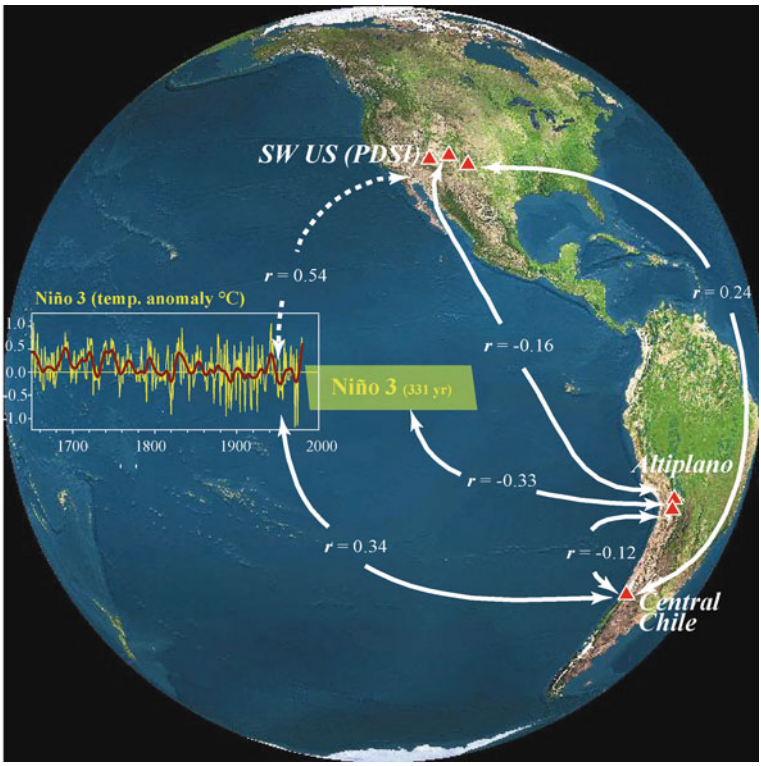

Fig. 7.10 Comparison of precipitation-sensitive tree-ring records across western America and El Niño/Southern Oscillation. The reconstruction of Niño-3 region temperature (Mann et al. 2000) was used as a proxy for tropical forcing of precipitation variations. The series used for comparison, from top to bottom, are: Tree-ring-based Palmer Drought Severity Index (PDSI) reconstructions from the southwestern United States (SW US) from Cook et al. (2004); a composite *Polylepis* record, including the Caquella and Soniquera chronologies from the Bolivian Altiplano (Argollo et al. 2004); and the El Asiento chronology in central Chile (LeQuesne et al. 2006). Correlation coefficients between records are indicated. The number of years for the comparisons is 331. The PDSI and the Niño-3 region reconstructions are not statistically independent. Some Texas-Mexican chronologies were used as predictors in both reconstructions

that we are making comparisons with an annual Niño-3 index reconstruction, the precipitation-sensitive records from the three extratropical regions in North and South America are significantly correlated with the Niño-3 index reconstruction during the 1650–1980 interval used for comparison (Fig. 7.10). The correlation coefficients between the PDSI reconstructions in the midwestern-southwestern United States and the Niño-3 index oscillate between $r = 0.20$ and $r = 0.65$. Although most correlation coefficients are remarkably high, the lack of independence between these records makes it difficult to determine the statistical significance of these relationships.

For the common interval 1650–1980, the first PC of the El Asiento chronology in year t and t+1 is significantly correlated with the Niño-3 index ($r = 0.34$, $p < 0.01$), which may be considered as a first indication of persistence in the influence of tropical SSTs on precipitation in central Chile. Long-term relationships between SST in the tropical Pacific and precipitation in the Bolivian Altiplano are also inferred from the statistically significant correlation between the two independent estimates ($r = -0.34$, $p < 0.01$).

7.3.2.2 Dominant Oscillations in Precipitation Variations

Cross-spectral analysis was used to identify coherent oscillation modes in tropical Pacific SST and precipitation variations in central Chile and the Bolivian Altiplano. Coherent oscillations between Niño-3 index and precipitation in central Chile are observed at 3.5 years, the classic El Niño frequency domain, but also at 20–28 years, an oscillation likely related to the Pacific Interdecadal Mode (Fig. 7.11). Cross-spectral analysis of the Niño-3 index and *Polylepis* records in Bolivia indicates significant coherence at 2.9, 3.2, 3.8, 8.5–10, and 19 years, a cycle also identified in the Gulf of Alaska temperature reconstructions (Fig. 7.11).

Following the previous cross-spectral analysis, we proceed to isolate the major waveforms in the precipitation-sensitive records using singular spectrum analysis (Vautard and Ghil 1989; Vautard 1995). Two dominant oscillations, representing modes of common variance at 3.6 and 28 years, were isolated from the Niño-3 and

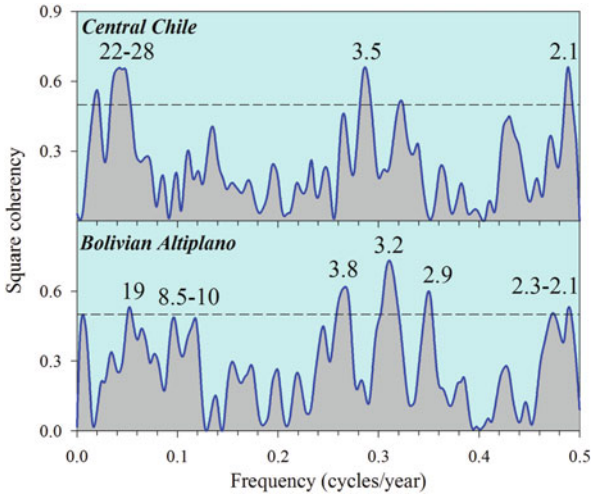

Fig. 7.11 Coherency spectra between the Niño-3 temperature reconstruction (Mann et al. 2000), and precipitation-sensitive chronologies in central Chile (*upper*) and the Bolivian Altiplano (*lower*) during the interval 1650–1981. Records are highly coherent at 3–4 years, the classic El Niño oscillations, but also at decennial-scale wavelengths longer than 10 years. *Horizontal broken lines* represent the 95% confidence level for the squared-coherency analyses. The periods are given in years for each significant coherency peak

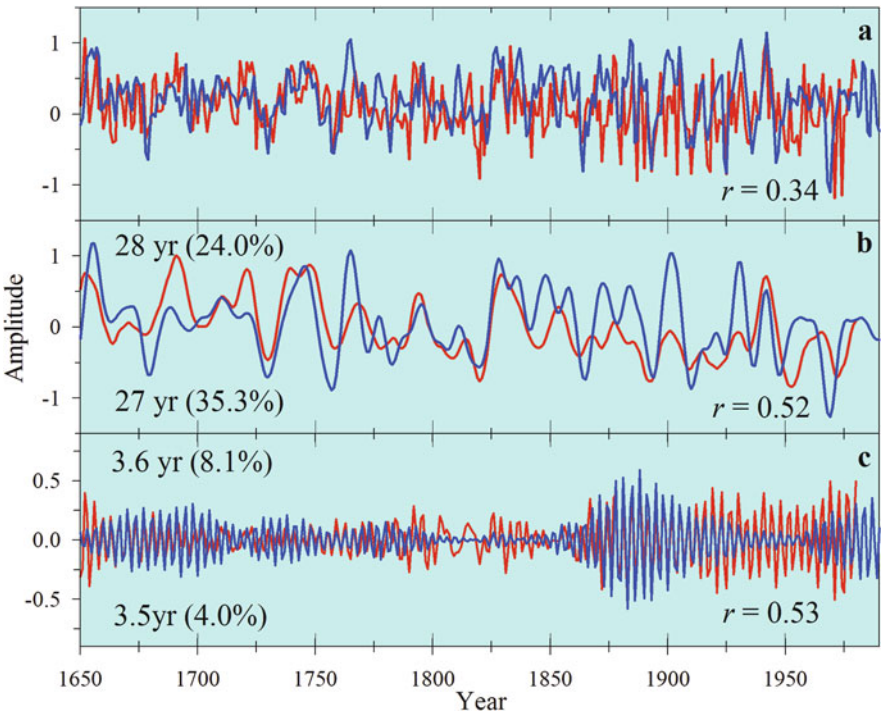

Fig. 7.12 Comparison of sea surface temperature (SST) in the tropical Pacific, represented by Niño-3 temperature reconstruction (Mann et al. 2000; *red line*), and precipitation variations in central Chile, inferred from El Asiento chronology (*blue line*), and significant correlated oscillatory modes extracted by singular spectrum analysis (SSA). Common oscillatory modes have periods of (**b**) 27–28 years, and (**c**) 3.5–3.6 years. Percentages of the original variance contributed by each of Niño-3 and El Asiento waveforms are indicated in parentheses at the upper and lower left corners of the figures, respectively. In the lower right corners, *r* is the Pearson's correlation coefficient between Niño-3 and El Asiento series. Marked increases in the interannual oscillatory modes centered at 3.6 years are observed in both series since about 1850 (**c**)

El Asiento chronology (Fig. 7.12). In general, the temporal evolution of the 28-year component shows similar fluctuations in amplitude and intensity from 1650 to 1850. After that, relationships between the 28-year waveforms are weaker. Starting around 1850, a marked increase in amplitude is observed in the 3.6-year waveforms from both the Niño-3 index and El Asiento series. Contrasting patterns in El Niño–related oscillations before and after 1850 have been noted previously by several authors (Stahle et al. 1998; Villalba et al. 2001; D'Arrigo et al. 2005).

Singular spectrum analysis of the precipitation-sensitive records from the Bolivian Altiplano also reveals common oscillatory modes with Niño-3 SST. Two major temporal patterns, centered at 3 and 4 years, are coherent with similar oscillations in tropical SSTs during the past four centuries. Similar to previous waveform comparisons, the common oscillation between the Bolivian and Niño-3 records, centered at 9.7 years, are more consistent in time and amplitude before 1850 (Fig. 7.13).

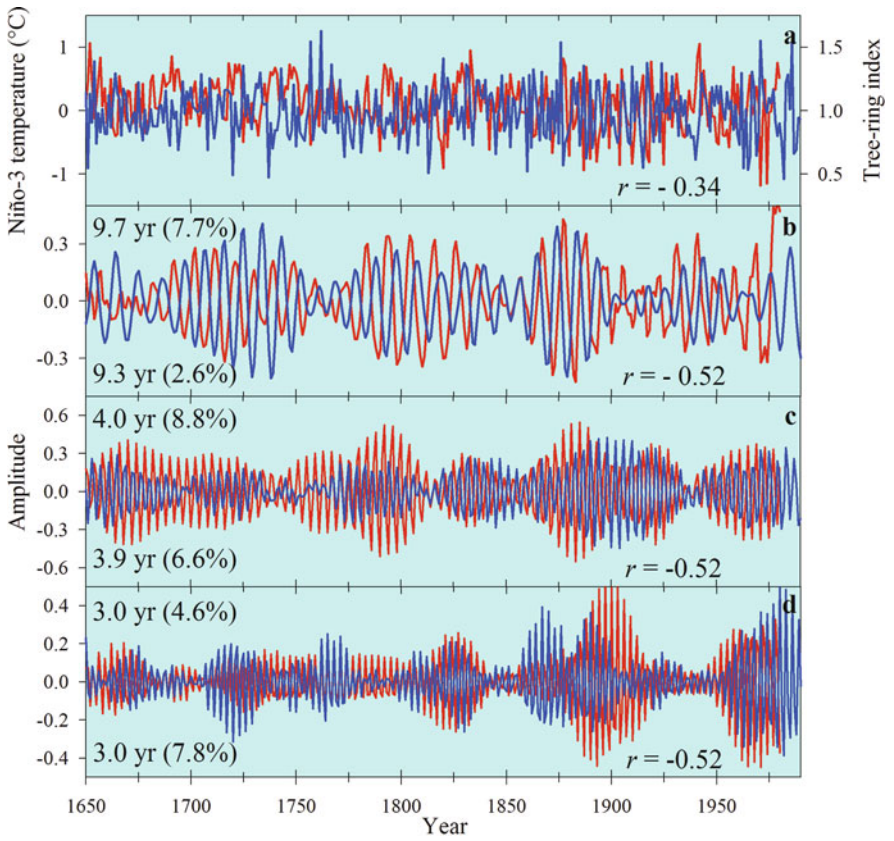

Fig. 7.13 Comparison of sea surface temperature (SST) in the tropical Pacific, represented by the Niño-3 temperature reconstruction (Mann et al. 2000; *red line*), and precipitation variations in the Bolivian Altiplano, inferred from Caquella-Soniquera composite chronology (*blue line*) lagged 1 year ($t + 1$), and significant correlated oscillatory modes extracted by singular spectrum analysis (SSA). Common oscillatory modes have periods of (**b**) 9–10 years, (**c**) 4 years, and (**d**) 3 years. Percentages of the original variance contributed by each of Niño-3 and the Bolivian waveforms are indicated in parentheses at the upper and lower left corners of the figures, respectively. In the lower right corners, r is the Pearson's correlation coefficient between Niño-3 and the Bolivian composite series

These spectral analyses basically reaffirm the existence of common oscillatory modes in tropical Pacific SST and precipitation-sensitive chronologies in subtropical North and South America, but also reveal changes in the stability of teleconnections over time. Indeed, moving correlations (using a 50-year window) between the precipitation-sensitive chronologies from South America and the El Niño-3 SST reconstruction revealed such changes in the temporal stability of the teleconnections (Fig. 7.14). Significant correlations occur for most of the sub-periods compared; however, correlation coefficients were not statistically significant during the second part of the eighteenth century between the Niño-3 SST and both the Bolivian and

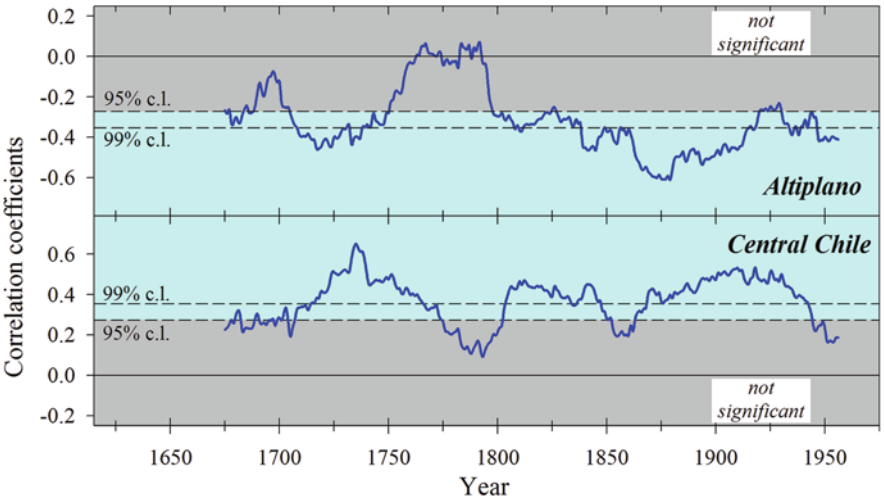

Fig. 7.14 Relationships between reconstructed Niño-3 temperature variations and interannual precipitation variability in the Bolivian Altiplano and Central Chile since 1650. Tropical influences on precipitation in both regions are evaluated by changes in the moving Pearson correlation coefficients (*blue lines*) between reconstructed Niño-3 temperatures and tree-ring width variations from *Polylepis* (*above*) and *Austrocedrus* (*below*) plotted on centroids of 50-year intervals. Lines at the 95 and 99% confidence intervals are indicated

central Chile records. This interval is characterized by low amplitudes of the interdecadal (27–28 years) oscillations in the Niño-3 and central Chile, and out-of-phase relationships in the 3- to 4-year oscillations between Niño-3 and both the central Chile and Bolivian records (Figs. 7.12 and 7.13).

The El Asiento precipitation-sensitive record from central Chile is positively correlated ($r = 0.24$ for the 350-year interval 1650–1998) with the first PC from 28 PDSI reconstructions in the midwestern-southwestern United States, the area most consistently affected by variations in tropical Pacific SST. Warm ENSO events are related to abundant precipitation in both regions. In contrast, droughts in the Bolivian Altiplano occur in years of warm ENSO events. Overall, the upper-elevation chronologies from Bolivia are consistently negatively correlated ($r = -0.16$, for the 346-year interval 1650–1998) with the first PC from 28 PDSI reconstructions from the southwestern United States and northern Mexico.

An additional indication of common ENSO influences on precipitation variations across the western Americas is provided by similarities in spatial correlation patterns between PDSI and Niño-3 index reconstructions and those resulting from the comparison between the PDSI reconstructions and precipitation-sensitive records in South America during the past 400 years. Figure 7.15 shows the teleconnection map for the Niño-3 index with reconstructed PDSI over the 1650–1980 time period common to all series. The geographical location of the highest correlation field is where one would expect based on instrumental and past proxy record analyses (Ropelewski and Halpert 1986; Kiladis and Diaz 1989; Cole and Cook 1998).

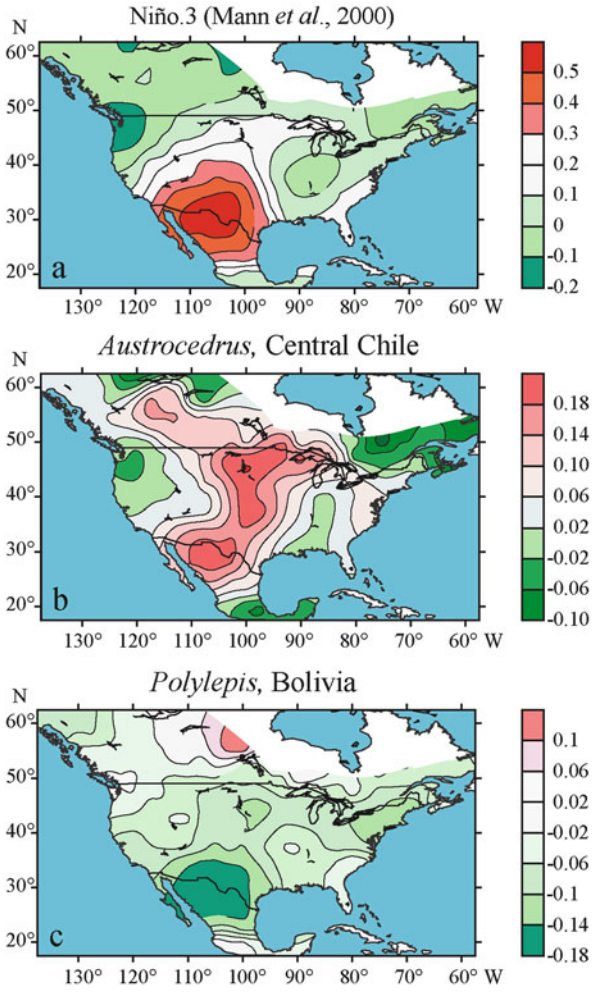

Fig. 7.15 Spatial correlation patterns between 297 Palmer Drought Severity Index (PDSI) reconstructions across North America (Cook et al. 2004) and (**a**) El Niño-3 region temperature reconstruction (Mann et al. 2000); (**b**) tree-ring variations from the precipitation-sensitive El Asiento *Austrocedrus* chronology, Central Chile; and (**c**) composite *Polylepis* chronology from Caquella and Soniquera in the Bolivian Altiplano

As was mentioned above, the tree-ring records used in the Niño-3 reconstruction are not completely independent of those used in the PDSI reconstructions, but the resulting spatial correlation pattern provides the basis for the search for commonalities with spatial patterns from comparison with the central Chile and the Bolivian Altiplano chronologies.

Figure 7.15b,c shows the spatial correlation patterns for the central Chile and altiplano chronologies with reconstructed PDSI over the 1650–1980 time period common to Niño-3 index reconstruction. Significant correlations are observed in the

southwestern United States–northern Mexico for both patterns, with the sign being positive for El Asiento and negative for the *Polylepis* records. Overall, the spatial correlation patterns produced by Niño-3 index reconstructions and the precipitation-sensitive records from South America are similar, indicating that the tree-ring estimates are capturing the interhemispheric ENSO teleconnection pattern. The significant correlations between El Asiento and PDSI are more extensive and penetrate northeastward into the central and upper Midwest of the US. This extension in the correlation pattern also has been observed by using instrumental records, particularly during the first decades of the twentieth century (Cole and Cook 1998). In contrast, the spatial pattern with the Bolivian chronologies is highly concentrated to the southwestern United States–northern Mexico region, making it remarkably similar to the pattern based on the Niño-3 index (Fig. 7.15).

7.4 Future Research

The previous results highlight the potentiality of tree rings as reliable sources of information concerning past climate variations. However, dendroclimatological studies are confronted by many challenges in the western Americas. New tree-ring chronologies in subtropical Mexico (*Pseudotsuga menziesii*, *Pinus hartwegii*, *Taxodium mucronatum*, *Pinus cembroides*, *Pinus lumholtzii*), in the high-elevation tropics of Bolivia and adjacent areas of Chile and Argentina (*Polylepis tarapacana*), and subtropical Argentina (*Prosopis ferox*) allow, for the first time, studies of annual variability in the subtropics. However, these records are still sparse and difficult to develop (Box 7.9). On the other hand, the development of climate-sensitive chronologies from the seasonally dry areas of the high- and lowland tropics remains a major task in the Americas and the world. It was only during the first years of the twenty-first century that a number of exploratory studies, mainly in coastal Peru, have established the basis for building reliable and calendar-dated chronologies from *Bursera graveolens*. The chronology, which covers the interval 1950–2002, shows an ENSO signal with an average recurrence period of about 5 years (Rodriguez et al. 2005). The search for longer records from tropical species with clear, identifiable annual rings is still a major challenge in modern dendroclimatology.

An alternative to the reliance on the presence of annual rings in tropical trees is provided by isotopic studies. An improved mechanistic understanding of controls on the oxygen isotope ratio ($\delta^{18}O$) of alpha cellulose (Roden et al. 2000) and rapid processing techniques (Brendel et al. 2000) make possible the construction of high-resolution isotope series from tropical trees that can be analyzed to provide both a chronology and paleoclimatic information, even in trees lacking annual rings (Evans and Schrag 2004). The seasonal cycle in $\delta^{18}O$ of tropical montane precipitation, primarily controlled by the difference in the amount of precipitation between wet and dry seasons, is reflected in $\delta^{18}O$ of the cellulose of trees. This seasonal rhythm can then be used for chronological control. Pilot applications of these techniques in Costa Rica, Peru, and the Amazon show annual isotope cycles as great as 4−6‰, which permit high-resolution chronological control even in the absence of annual

rings. Interannual variability up to 8‰ in $\delta^{18}O$ cellulose is associated with year-to year differences in precipitation amounts (Evans and Schrag 2004).

The seasonality in climate and tree growth is an important feature to be considered in the processes of interhemispheric comparisons. For example, ENSO matures during the boreal winter (austral summer) when the climatic anomalies set by the extratropical teleconnections are more marked. However, tree responses vary according to their location and biology, leading to wide variability between species in the total amount of the ENSO signal captured by trees during the growing season concurrent or following the event. There is a need for further investigation of the basic processes that bring about year-to-year variations in tree-ring properties, cell dimensions, wood chemistry, wood density, or ring width (Hartsough and Biondi 2003; Roig et al. 2003; see Box 7.9). Long-term monitoring that employs a combination of weather stations and dendrometers will better characterize both the climate to which the tree is responding and the season of wood formation, particularly in tropical trees. A better understanding of the relationship between tree growth and climate will facilitate the interpretation of the temporal climatic window recorded by trees, which in turn will result in better, ecophysiologically sound reconstructions of past climate variations.

Box 7.9 Monitoring of tree growth dynamics to improve dendroclimatic models

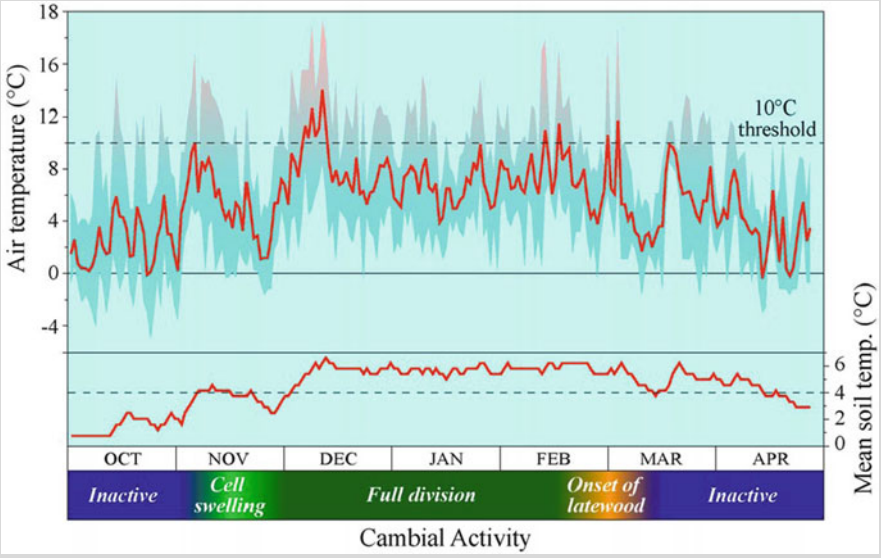

Box Fig. 7.17 Seasonal course of climate related to variations in ring morphology and leaf phenology of *Nothofagus pumilio* trees in Tierra del Fuego, as illustrated by the 2002–2003 observational period. Air temperatures are at 1.2 m above ground and soil temperatures are at 0.25 m underground (the layer with major development of the *Nothofagus* root system)

Fine-scale monitoring of tree growth dynamics is essential to improve our understanding of the climatic controls that influence both tree-ring morphology and size. Timing of the ring formation can bring clues to improve interpretation of the tree-ring growth/climate models. In recent years, we set up monitoring networks to follow tree growth and obtain in situ weather data from forest ecosystems in Argentina and Mexico. At Cerro Krund, southern Tierra del Fuego, Argentina, a network of permanent plots was established along the altitudinal gradient of *Nothofagus pumilio*, from the valley bottom to the tree line. At a given plot, the initial surge of earlywood occurs after the first formed leaves are fully expanded; later, the cambium becomes most active and then finally ceases by producing latewood cells toward the end of summer. The influence of altitude is expressed in a delay of the onset of the initial growth stages (up to 2 weeks between lower and higher plots) and in the shortening of the vegetative growth period. At lower elevations the cambium remains active for 3–4 months, compared to only 2–3 months at the tree line. Rapid changes in temperature act as the environmental catalyst to force the changes of the leaf phenological phases and the wood morphological changes through the ring. Box Figure 7.17 shows a synchrony between a sustained increase of the maximum air temperatures to values above a threshold of 10°C and the beginning of the growth phases. Toward the end of austral summer, trees slowly end their growth cycle as maximum temperatures fall below this threshold line.

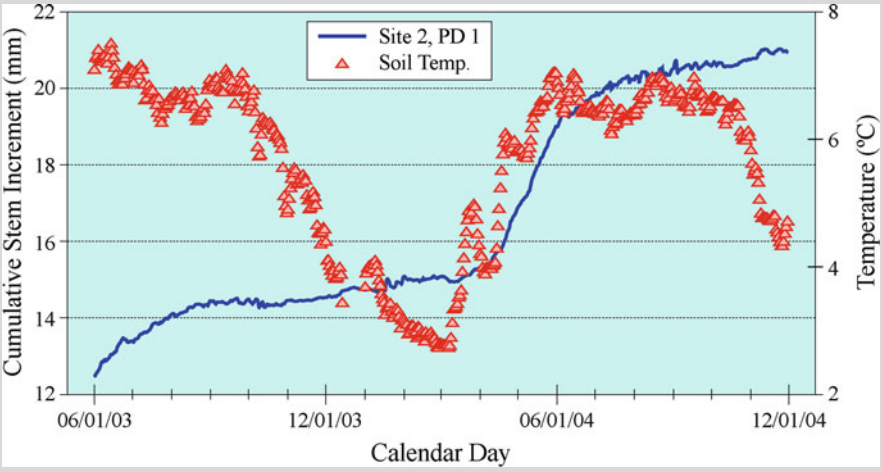

Box Fig. 7.18 Two seasons of growth are shown in the monitored *Pinus hartwegii* stand in southwestern Mexico. Onset of growth is coincident with the increase of spring temperatures above 3.6ºC. Continuation of growth is dependent on monsoon moisture

In Nevado de Colima, a 3900 m elevation site in central western México, we have been co-monitoring stem growth and weather on two plots of *Pinus hartwegii*. The monitoring network consists of a meteorological station and two sets of dendrometers installed on pure stands of *P. hartwegii* located ~100 m below tree line. This species has previously shown promise for paleoclimate analysis because of sensitivity to the North American Monsoon. Co-measuring tree growth and climate over a 3-year period has allowed a better understanding of the complex response of this species to changing environmental conditions. Box Figure 7.18 shows that the onset of spring growth is coincident with soil temperatures higher than a threshold of around 3.6ºC. Summer growth, however, is dependent on monsoon precipitation, with high correlations to precipitation and relative humidity. The pattern of growth mirrors the lull in the monsoon in late summer. We also have confirmed the cessation of growth and shutdown of cambial activity in the winter months at this high-elevation tropical site. Long-term ecological monitoring has allowed direct correlation at daily and monthly timescales between tree growth and weather. It is desirable that the monitoring previously described be continued over long time periods to better understand the radial growth behaviors.

—F. Roig, P. Hartsough, G Massacchesi, F. Biondi, and G. Martinez Pastur

In South America, the only chronologies that presently extend into the mid-Holocene are for *Fitzroya cupressoides* from southern Chile. The Volcan Apagado (41°35′S, 72°30′W) chronology is now the longest continuous chronology in the Southern Hemisphere, with a total of 5666 years (Wolodarsky-Franke et al. 2005). However, much more work is needed to develop multimillennial length chronologies encompassing most of the Holocene and employing other species in more arid regions of South America.

As in other areas of the world, it is also possible that anthropogenic activities may be subtly changing climate-growth relationships in these trees, compounding the difficulties of isolating a clear climate signal in these records. The recent high growth rates of *Nothofagus* at the upper tree line across Patagonia provide a major piece of evidence to assemble a case for anomalous regional warming in response to anthropogenic activities (Villalba et al. 2003). While this conclusion may prove to be a valid interpretation of the data, changes in the efficiency with which water is used in relation to increased atmospheric CO_2 content (fertilization), may also exert some influences on tree growth.

7.5 Discussion and Conclusions

Precisely dated, annually resolved tree-ring records from numerous sites throughout the Americas provide the basis to evaluate the changing signatures of tropical and high-latitude modes of climate variability, their time-evolving patterns, and their

interactions in the past. Based on our present knowledge of climate variations during the twentieth century, we intended this contribution to provide an interhemispheric view of interactions between large-scale modes of variability and climate along the American Cordilleras over several centuries prior to the period of instrumental observations. The striking symmetries in SSTs across the equatorial Pacific and in sea level pressure (SLP) patterns at high latitudes in both hemispheres induce similar patterns of climate variability in widely separated regions of the western Americas (Dettinger et al. 2001).

Comparisons of fire histories between the southwestern United States and northern Patagonia over the past several centuries provide additional evidence for similarities in past climate variations across the extratropical Americas (Kitzberger et al. 2001). The synchrony of fire regimes in these two distant regions has tentatively been interpreted as a response to decadal-scale changes in ENSO and PDO activities. For example, a period of decreased fire occurrence in both regions from about 1780 to 1830 was attributed to decreased amplitude and/or frequency of ENSO events.

Strong interhemispheric symmetries of ENSO and ENSO-like variations of Pacific climate on decadal timescales produce similar patterns of temperature variations in Patagonia and the Gulf of Alaska. However, the comparison of these extratropical temperature reconstructions with the Raratonga temperature-sensitive coral record from the tropical Pacific indicates that over the last 200 years, interdecadal SST variations in the Pacific alternated between times of more geographically widespread interdecadal changes—such as the shift in the mid-1970s that was recorded across the entire Pacific basin—and times of less geographically organized interdecadal changes shared by the tropics and the north or south Pacific Ocean. Our observations that interdecadal variations in SST in the tropical Pacific were more strongly connected to the north Pacific in the twentieth century than in the mid-1800s agree with previous studies by Evans et al. (2001a) and Labeyrie et al. (2003).

In addition to tropical forcings, similarities in decadal- to century-scale climate variations also result from changes in high-latitude modes of climate variability that simultaneously affect the extratropical regions of North and South America. Instrumental records show a simultaneous intensification of the AO and AAO during recent decades (Thompson and Solomon 2002).

As was shown in Section 7.3.3, the annular modes are strongly coupled with surface air temperatures over high latitudes in both hemispheres (Thompson and Wallace 2000). Sustained positive trends in both modes in recent decades may be linked to large-scale warming, particularly in Eurasia and northern Canada in the Northern Hemisphere and across Patagonia in the Southern Hemisphere (Thompson and Wallace 2000; Thompson and Solomon 2002; Ogi et al. 2004). D'Arrigo et al. (2003) presented a first reconstruction of a warm season AO temperature index during the interval 1650–1975. Values during the middle twentieth century, overlapping with the anthropogenic increase in trace gases, equal or exceed those in the prior record. Lower values are reconstructed for several colder periods, including the early nineteenth-century interval. Trends in the AO temperature index

resemble those of the tree-ring reconstructions of Arctic mean annual temperatures ($r = 0.47,\ n = 305$). According to D'Arrigo et al. (2003), the similarities between these records reflect some data overlap, but also the strong linkage between the AO and Arctic temperatures. Similarly, instrumental observations support a strong relationship between AAO and temperature in southern South America during the past 50 years, suggesting that long-term trends in temperature across Patagonia during the past centuries have also been influenced by changes in the AAO (Thompson and Solomon 2002).

As the reconstructions from high latitudes in both hemispheres indicate large similarities in temperature changes for at least the past 300 years, we could infer some common forcings of annular modes of climate variability in both hemispheres during the past centuries. Presumably, any climate change mechanism that projects onto the meridional temperature gradient between the middle and high latitudes may affect the polarity of the annular modes. Recent trends in tropical sea surface temperatures have been shown to affect the NAM (Hoerling et al. 2001), and it has been hypothesized (but not yet demonstrated) that a similar link may exist for the SAM (Hurrell and van Loon 1994).

Interactions between low- and high-latitude circulation modes are difficult to document based on the current array of climate-sensitive chronologies and forcing reconstructions. For example, interannual and decadal modes of tropical climatic variability such as ENSO and PDO strongly affect weather conditions in low latitudes of the western Americas, but their influences on the climate of the extratropics have been noted here and widely documented elsewhere. On the other hand, the annular modes have large amplitudes at extratropical latitudes, but several studies reveal that they have a substantial signature at lower latitudes as well (Thompson and Lorenz 2004).

Reflection symmetries about the equator in interdecadal ocean temperature during the past four centuries suggest that the tropical Pacific has played a pivotal role in linking westerly winds in both hemispheres through meridional teleconnections (Zhang et al. 1997; White and Cayan 1998). As has been indicated here, temperature-sensitive records from the Gulf of Alaska and northern Patagonian are coherent on long-term (>10 years) oscillatory modes, largely in response to ENSO-like decadal to interdecadal modes of variability in the Pacific Ocean. However, instrumental records show that high-latitude forcings of climate variability also affect both regions. For example, recent trends in Alaskan climate are better explained by the juxtaposition of ENSO-like and AO-related SLP variability over the north Pacific.

The 'ENSO-like' interdecadal variability, as documented in Trenberth and Hurrell (1994) and Zhang et al. (1997), has contributed to SLP declines over the north Pacific in conjunction with warming over western Canada and Alaska. Apart from that feature, SLP over the north Pacific has risen slightly during the past 30 year, consistent with the trend toward the 'high-index' state of the AO during this period. That the trend in the SAM accounts for approximately 50% of the warming over the Antarctic Peninsula and southern Patagonia attests to the importance of climate mechanisms other than ENSO over this region. In consequence, the

additive effects of low- and high-latitude forcings on climates along the American Cordilleras hamper a current estimation of past interactions between tropical and high-latitude forcings. Independent reconstructions of tropical and polar modes of variability are needed to gain insight on past forcing interactions and the combined effect on climates of the western Americas.

Teleconnections between precipitation estimates and climatic forcings evolve over time, suggesting a changing global signature of ENSO and other forcings. Our results indicate that the timing of interdecadal transitions in temperature- and precipitation-sensitive records has not always been consistent across the region. In addition, the degree of correlation between records has varied over time. Over the last 400 years, interdecadal climate variations in the Pacific alternated between times of larger amplitude and more geographically widespread interdecadal changes and times of lower amplitude and less geographically organized interdecadal changes.

Most tree-ring records suggest that the interdecadal variability in the Pacific region was particularly more organized before the mid-1800s, whereas interannual variability increased after that period. These observations point to a major reorganization of the climate modes of variability in the Pacific around 1850, the generally accepted time of the end of a particularly cool period in the 1800s, identified in some regions as the end of the Little Ice Age (LIA; Grove 1988; Bradley and Jones 1992; Luckman and Villalba 2001).

Detailed analysis of the influences of tropical and high-latitude modes of climate variability across the American Cordilleras is somewhat constrained by the current length of the proxy records. Additional insight can be gained by extending the records to cover different climatic intervals, such as the 'warmer' medieval period. Jones et al. (2001), Mann and Jones (2003), and many other authors have stressed the critical need for developing longer proxy records of both regional climate variations and hemispheric climatic forcings. Longer proxy series can be used to evaluate the long-term natural behavior of these modes of variation and their regional impacts more comprehensively. In so doing, these extended series can provide a long-term context for variability during the period of increasing trace gases, and for testing climate prediction models. Proxy climate records stand as our only means of assessing the long-term variability associated with large-scale modes of climate variability and their global influences.

Acknowledgements We gratefully acknowledge the support of the Inter-American Institute for Global Change Research through its Collaborative Research Network Program for the past 6 years. Parts of this project have also been funded by a range of national, international, and nonprofit organizations.

References

Aceituno P (1988) On the functioning of the Southern Oscillation in the South American sector. Part I: surface climate. Mon Weather Rev 116:505–524

Aceituno P, Montecinos A (1996) Assessing upper limits of seasonal predictability of rainfall in central Chile based on SST in the equatorial Pacific. Exp Long-Lead Forecast Bull 5:37–40

Aravena JC, Lara A, Wolodarsky-Franke A, Villalba R, Cuq E (2002) Tree-ring growth patterns and temperature reconstruction from *Nothofagus pumilio* (Fagaceae) forests at the upper tree line of southern Chilean Patagonia. Rev Chil Hist Nat 75:361–376

Argollo J, Soliz C, Villalba R (2004) Potencialidad dendrocronológica de *Polylepis tarapacana* en los Andes Centrales de Bolivia. Ecología en Bolivia 39:5–24

Beamish RJ, Benson AJ, Sweeting RM, Neville CM (2004) Regimes and the history of the major fisheries off Canada's west coast. Prog Oceanogr 60:355–385

Boninsegna JA (1988) Santiago de Chile winter rainfall since 1220 as being reconstructed by tree rings. Quaternary South Am Antarctic Peninsula 4:67–87

Bradley RS, Jones PD (1992) When was the 'Little Ice Age'? In: Mikami T (ed) Proceedings of the international symposium on the Little Ice Age climate. Department of Geography, Tokyo Metropolitan University, Japan, pp 1–4

Brendel O, Iannetta PPM, Stewart D (2000) A rapid and simple method to isolate pure cellulose. Phytochem Anal 11:7–10

Chavez FP, Ryan J, Llucha-Cota SE, Niquen M (2003) From anchovies to sardines and back: multidecadal change in the Pacific Ocean. Science 299:217–221

Cleaveland MK (1986) Climatic response of densitometric properties in semiarid site tree rings. Tree-Ring Bull 46:13–29

Cleaveland MK, Stahle DW, Therrell MD, Villanueva-Diaz J, Burns BT (2003) Tree-ring reconstructed winter precipitation and tropical teleconnections in Durango, Mexico. Clim Change 59:369–388

Cobb KM, Charles CD, Cheng H, Edwards RL (2003) El Niño/Southern Oscillation and tropical Pacific climate during the last millennium. Nature 424:271–276

Cole JE, Cook ER (1998) The changing relationship between ENSO variability and moisture balance in the continental United States. Geophys Res Lett 25:4529–4532

Cook ER, Meko DM, Stahle DW, Cleaveland MK (1999) Drought reconstructions for the continental United States. J Clim 12:1145–1162

Cook ER, Cole JE, D'Arrigo RD, Stahle DM, Villalba R (2000) Tree-ring records of past ENSO variability and forcing. In: Diaz HF, Markgraf V (eds) El Niño and the Southern Oscillation: multiscale variability, global and regional impacts. Cambridge University Press, Cambridge, UK, pp 297–323

Cook ER, Woodhouse CA, Eakin CM, Meko DM, Stahle DW (2004) Long term aridity changes in the western United States. Science 306:1015–1018

D'Arrigo RD, Jacoby G (1993) Secular trends in high northern latitude temperature reconstructions based on tree rings. Clim Change 25:163–177

D'Arrigo RD, Villalba R, Wiles G (2001) Tree-ring estimates of Pacific decadal climate variability. Clim Dynam 18:219–224

D'Arrigo RD, Cook ER, Mann ME, Jacoby GC (2003) Tree-ring reconstructions of temperature and sea-level pressure variability associated with the warm-season Arctic Oscillation since AD 1650. Geophys Res Lett 30(11):1549. doi:10.1029/2003GL017250

D'Arrigo R, Wilson R, Deser C, Wiles G, Cook E, Villalba R, Tudhope S, Cole J, Linsley B (2005) Tropical-north Pacific climate linkages over the past four centuries. J Clim 18:5253–5265

Deser C, Blackmon M (1993) Surface climate variations over the North Atlantic Ocean during winter: 1900–1989. J Clim 6:1743–1753

Deser C, Wallace JM (1990) Large-scale atmospheric circulation features of warm and cold episodes in the tropical Pacific. J Clim 3:1254–1281

Deser S, Phillips A, Hurrell J (2004) Pacific interdecadal climate variability: linkages between the tropics and north Pacific during boreal winter since 1900. J Clim 17:3109–3124

Dettinger MD, Battisti DS, McCabe GJ, Bitz CM, Garreaud RD (2001) Interhemispheric effects of interannual and decadal ENSO-like climate variations on the Americas. In: Markgraf V (ed) Interhemispheric climate linkages. Academic, San Diego, pp 119–140

Ebbesmeyer CC, Cayan DR, McClain DR, Nichols FH, Peterson DH, Redmond KT (1991) 1976 step in the Pacific climate: forty environmental changes between 1968–75 and 1977–84. In:

Proceedings of the seventh annual Pacific climate (PACLIM) workshop. California Department of Water Resources, pp 115–126
Eischeid JK, Diaz HF, Bradley RS, Jones JD (1991) A comprehensive precipitation data set for global land areas. DOE/ER-69017T-H1, TR051, United States Department of Energy, Carbon Dioxide Research Program, Washington, DC
Enfield DB, Mestas-Nuñez AM (2000) Global modes of ENSO and non-ENSO sea surface temperature variability and their associations with climate. In: Diaz H, Markgraf V (eds) El Niño and the Southern Oscillation: multiscale variability and global and regional impacts. Cambridge University Press, Cambridge, UK, pp 89–112
Evans MN, Schrag DP (2004) A stable isotope-based approach to tropical dendroclimatology. Geochim Cosmochim Ac 68:3295–3305
Evans MN, Cane MA, Schrag DP, Kaplan A, Linsley BK, Villalba R, Wellington GM (2001a) Support for tropically-driven Pacific decadal variability based on paleoproxy evidence. Geophys Res Lett 28:3869–3692
Evans MN, Kaplan A, Cane MA, Villalba R (2001b) Globality and optimality in climate field reconstructions from proxy data. In: Markgraf V (ed) Interhemispheric climate linkages. Academic, San Diego, pp 53–72
Fritts H (1976) Tree rings and climate. Academic, London
Fritts H (1991) Reconstructing large-scale climatic patterns from tree-ring data. University of Arizona Press, Tucson
Garreaud R, Battisti DS (1999) Interannual and interdecadal (ENSO-like) variability in the Southern Hemisphere tropospheric circulation. J Clim 12:2113–2123
Garreaud R, Vuille M, Clement A (2003) The climate of the Altiplano: observed current conditions and mechanisms of past changes. Palaeogeogr Palaeocl 194:5–22
Gershunov A, Barnett TP (1998) Interdecadal modulation of ENSO teleconnections. B Am Meteorol Soc 79:2715–2725
Gong D, Wang S (1999). Definition of Antarctic Oscillation index. Geophys Res Lett 26:459–462
Graham NE (1994) Decadal-scale climate variability in the 1970s and 1980s: observations and model results. Clim Dynam 10:135–162
Graham NE, Hughes MK, Ammann CM, Cobb KM, Hoerling MP, Xu T, Kennett DJ, Kennett JP, Rein B, Stott L, Wigand PE (2007) Tropical Pacific-mid-latitude teleconnections in Medieval times. Clim Change 83:241–285
Grove JM (1988) The Little Ice Age. Methuen, London, 498 pp
Hartsough P, Biondi F (2003) The importance of high elevation monitoring in a tropical treeline environment: a project update from southwestern Mexico. In: Fourth annual science meeting, IAI CRN03, Abstracts, p 18
Hoerling MP, Hurrell JW, Xu T (2001) Tropical origins for recent North Atlantic climate change. Science 292:90–92
Hughes MK, Funkhouser G (1998) Extremes of moisture availability reconstructed from tree rings for recent millennia in the Great Basin of western North America. In: Beniston M, Innes JL (eds) The impacts of climate variability on forests. Springer, Berlin, pp 99–107
Hurrell JW, van Loon H (1994) A modulation of the atmospheric annual cycle in the Southern Hemisphere. Tellus 46A:325–338
Hurrell JW, van Loon H (1997) Decadal variations associated with the North Atlantic Oscillation. Clim Change 36:301–326
Jones PD, Moberg A (2003) Hemispheric and large-scale surface air temperature variations: an extensive revision and update to 2001. J Clim 16:206–223
Jones PD, Raper SCB, Bradley RS, Diaz HF, Kelly PM, Wigley TML (1986a) Northern Hemisphere surface air temperature variations: 1851–1984. J Clim Appl Meteorol 25:161–179
Jones PD, Raper SCB, Wigley TML (1986b) Southern Hemisphere surface air temperature variations: 1851–1984. J Clim Appl Meteorol 25:1213–1230
Jones PD, Osborn TJ, Briffa KR (2001) The evolution of climate over the last millennium. Science 292:662–667

Karoly DJ (1990) The role of transient eddies in low-frequency zonal variations of the Southern Hemisphere circulation. Tellus 42A:41–50
Kennett DJ, Kennett JP (2000) Competitive and cooperative responses to climatic instability in coastal southern California. Am Antiquity 65(2):379–395
Kessler M (1995) The genus Polylepis (Rosaceae) in Bolivia. Candollea 50:1–172
Kiladis GN, Diaz HF (1989) Global climatic anomalies associated with extremes of the Southern Oscillation. J Clim 2:1069–1090
Kitzberger T, Swetnam TW, Veblen TT (2001) Inter-hemispheric synchrony of forest fires and the El Niño-Southern Oscillation. Global Ecol Biogeogr 10:315–326
Labeyrie L, Cole J, Alverson K, Stocker T (2003) The history of climate dynamics in the late quaternary. In: Alverson KD, Bradley RS, Pedersen TF (eds) Paleoclimate, global change and the future. IGBP Series, Springer, Berlin, pp 33–62
LaMarche VC (1975) Potential of tree rings for reconstruction of past climate variations in the Southern Hemisphere. In: Proceedings of the WMO/IAMAP symposium on long term climatic fluctuations, Norwich, England. World Meteorological Organization, WMO No. 421, Geneva, pp 21–30
Lara A, Aravena JC, Villalba R, Wolodarsky-Franke A, Luckman B, Wilson R (2001) Dendroclimatology of high-elevation *Nothofagus pumilio* forests at their northern distribution limit in the central Andes of Chile. Can J Forest Res 31:925–936
Lara A, Villalba R, Wolodarsky-Franke A, Aravena JC, Luckman BH, Cuq E (2005) Spatial and temporal variation in *Nothofagus pumilio* growth at treeline along its latitudinal range (35ºS40′ to 55ºS) in the Chilean Andes. J Biogeogr 32:879–893
Lenters JD, Cook K (1999) Summer-time precipitation variability over South America: role of the large scale circulation. Mon Weather Rev 127:409–431
LeQuesne C, Stahle DW, Cleaveland MK, Therrell MD, Aravena JC, Barichivich J (2006) Ancient ciprés tree-ring chronologies used to reconstruct central Chile precipitation variability from AD 1200–2000. J Clim 19:5731–5744
Linsley B, Wellington G, Schrag D, Ren L, Salinger M, Tudhope A (2004) Geochemical evidence from corals for changes in the amplitude and spatial pattern of South Pacific interdecadal climate variability over the last 300 years. Clim Dynam 22:1–11
Luckman BH, Boninsegna JA (2001) The assessment of present, past and future climate variability in the Americas from treeline environments. PAGES Newsletter 9:17–19
Luckman BH, Villalba R (2001) Assessing the synchroneity of glacier fluctuations in the Western Cordillera of the Americas during the last millennium. In: Markgraf V (ed) Interhemispheric climate linkages. Academic, San Diego, pp 119–140
Luckman BH, Wilson RJS (2005) Summer temperature in the Canadian Rockies during the last millennium: a revised record. Clim Dynam 24:131–144
Luckman BH, Briffa KR, Jones PD, Schweingruber FH (1997) Summer temperatures at the Columbia Icefield, Alberta, Canada, 1073–1983. Holocene 7:375–389
Mann ME, Jones PD (2003) Global surface temperatures over the past two millennia. Geophys Res Lett 30, art 1820
Mann ME, Bradley RS, Hughes MK (2000) Long-term variability in El Niño/Southern Oscillation and associated teleconnections. In: Diaz HF, Markgraf V (eds) El Niño and the Southern Oscillation: multiscale variability, global and regional impacts. Cambridge University Press, Cambridge, UK, pp 357–412
Mantua JN, Hare SR (2002) The Pacific Decadal Oscillation. J Oceanogr (Japan) 58:35–44
Mantua JN, Hare SR, Zhang Y, Wallace JM, Francis RC (1997) A Pacific interdecadal climate oscillation with impacts on salmon production. B Am Meteorol Soc 78:1069–1080
Martínez M (1963) Las pináceas mexicanas, 3rd edn. Instituto de Biología, Universidad Nacional Autónoma de México, México
Meko D, Cook ER, Stahle DW, Stockton CW, Hughes MK (1993) Spatial patterns of tree-growth anomalies in the United States and southeastern Canada. J Clim 6:1773–1786

Montecinos A, Aceituno P (2003) Seasonality of the ENSO-related rainfall variability in central Chile and associated circulation anomalies. J Clim 16:281–296

Ogi M, Yamazaki K, Tachibana Y (2004) The summertime annular mode in the Northern Hemisphere and its linkage to the winter mode. J Geophys Res 109:D20114. doi:10.1029/2004JD004514

Quinn WH, Neal VT (1983) Long-term variations in the Southern Oscillation, El Niño, and the Chilean subtropical rainfall. Fish B 81:363–374

Rein B, Lueckge A, Sirocko F (2004) A major Holocene ENSO anomaly in the medieval period. Geophys Res Lett 31, L17211. doi:10.1029/2004GL020161

Rein B, Lueckge A, Reinhardt L, Sirocko F, Wolf A, Dullo W-C (2005) El Niño variability off Peru during the last 20,000 years. Paleoceanography 20. doi:10.1029/2004PA001099

Roden JS, Lin G, Ehleringer JR (2000) A mechanistic model for interpretation of hydrogen and oxygen ratios in tree-ring cellulose. Geochim Cosmochim Ac 64:21–35

Rodriguez R, Mabres A, Luckman B, Evans M, Masiokas M, Ektvedt T (2005) 'El Niño' events recorded in dry-forest species of the lowlands of northwest Peru. Dendrochronologia 22:181–187

Roig FA, Martínez Pastur G, Massaccesi G, Pinedo L (2003) Toward an interpretation of the interactions between cambial activity, phenology and climate in *Nothofagus pumilio* forests of Tierra del Fuego, Argentina. In: Fourth annual science meeting, IAI CRN 03, Abstracts, pp 33–34

Ropelewski CF, Halpert MS (1986) North American precipitation and temperature patterns associated with El Niño/Southern Oscillation (ENSO). Mon Weather Rev 115: 1606–1626

Rutlland J, Fuenzalida H (1991) Synoptic aspects of the central Chile rainfall variability associated with the Southern Oscillation. Int J Climatol 11:63–76

Stahle DW, D'Arrigo RD, Krusic PJ, Cleaveland MK, Cook ER, Allan RJ, Cole JE, Dunbar RB, Therrell MD, Gay DA, Moore MD, Stokes MA, Burns BT, Villanueva-Diaz J, Thompson LG (1998) Experimental dendroclimatic reconstruction of the Southern Oscillation. B Am Meteorol Soc 79(10):2137–2152

Stine S (1994) Extreme and persistent drought in California and Patagonia during mediaeval time. Nature 369:546–549

Stott LD, Cannariato KG, Thunell R, Haug GH, Koutavas A, Lund S (2004) Decline of surface temperature and salinity in the western tropical Pacific Ocean in the Holocene epoch. Nature 431:56–59

Thompson DWJ, Lorenz DJ (2004) The signature of the annular modes in the tropical troposphere. J Clim 17:4330–4342

Thompson DWJ, Solomon S (2002) Interpretation of recent Southern Hemisphere climate change. Science 296:895–899

Thompson DWJ, Wallace JM (2000) Annular modes in the extratropical circulation. Part I: Month-to-month variability. J Clim 13:1000–1016

Trenberth K, Hurrell J (1994) Decadal atmospheric-ocean variations in the Pacific. Clim Dynam 9:303–19

Vautard R (1995) Patterns in time: SSA and MSSA. In: von Storch H, Navarra A (eds) Analysis of climate variability, applications of statistical techniques. Springer, Berlin, pp 259–279

Vautard R, Ghil M (1989) Singular spectrum analysis in nonlinear dynamics, with applications to paleoclimatic time series. Physica D35:395–424

Villalba R, Boninsegna JA, Veblen TT, Schmelter A, Rubulis S (1997) Recent trends in tree-ring records from high elevation sites in the Andes of northern Patagonia. Clim Change 36:425–454

Villalba R, D'Arrigo RD, Cook ER, Wiles G, Jacoby GC (2001) Decadal-scale climatic variability along the extratropical western coast of the Americas: evidences from tree-ring records. In: Markgraf V (ed) Interhemispheric climate linkages. Academic, San Diego, pp 155–172

Villalba R, Lara A, Boninsegna JA, Masiokas M, Delgado S, Aravena JC, Roig FA, Schmelter A, Wolodarsky A, Ripalta A (2003) Large-scale temperature changes across the southern Andes: twentieth-century variations in the context of the past 400 years. Clim Change 59: 177–232

Vuille M (1999) Atmospheric circulation over the Bolivian Altiplano during dry and wet periods and extreme phases of the Southern Oscillation. Int J Climatol 19:1579–1600

Vuille M, Bradley RS, Keimig F (2000) Interannual climate variability in the central Andes and its relation to tropical Pacific and Atlantic forcing. J Geophys Res 105:12447–12460

Wallace JM, Rasmusson EM, Mitchell TP, Kousky VE, Sarachik ES, von Storch H (1998). On the structure and evolution of ENSO-related climate variability in the tropical Pacific: lessons from TOGA. J Geophys Res 103:12241–14259

Watson E, Luckman BH (2004a) Tree-ring based reconstructions of precipitation for the southern Canadian Cordillera. Clim Change 65:209–241

Watson E, Luckman BH (2004b) Tree-ring estimates of mass balance at Peyto Glacier for the last three centuries. Quaternary Res 62:9–18

Watson E, Luckman BH (2005) Spatial patterns of pre-instrumental moisture variability in the southern Canadian Cordillera. J Clim 18:2847–2863

White W, Cayan DR (1998) Quasi-periodicity and global symmetries in interdecadal upper ocean temperature variability. J Geophys Res 103:21335–21354

Wiles GC (1997) North Pacific atmosphere-ocean variability over the past millennium inferred from coastal glaciers and tree rings. In: Preprint volume, Eighth symposium on global change studies. American Meteorological Society, 2–7 February 1997, Long Beach, California. pp 218–220

Wiles GC, Calkin PE (1994) Late Holocene, high-resolution glacial chronologies and climate, Kenai Mountains, Alaska. Geol Soc Am Bull 106:281–303

Wiles GC, D'Arrigo RD, Jacoby GC (1996) Temperature changes along the Gulf of Alaska and the Pacific Northwest coast modeled from coastal tree rings. Can J Forest Res 26:474–481

Wiles GC, D'Arrigo RD, Jacoby GC (1998) Gulf of Alaska atmosphere-ocean variability over recent centuries inferred from coastal tree-ring records. Clim Change 38:289–306

Wiles GC, D'Arrigo RD, Villalba R, Calkin PE, Barclay DJ (2004) Century-scale solar variability and Alaskan temperature change over the past millennium. Geophys Res Lett 31:L15203. doi:1029/2004GL020050

Wolodarsky-Franke A, Moreno P, Lara A, Pino M, Villarosa G (2005) Tree-ring, stratigraphic, and palynological evidence for volcanic and climatic controls on *Fitzroya cupressoides* forests in southern Chile, over the last 5700 years. In: Piovano EL, Leroy S (eds) Holocene environmental catastrophes in South America: from the lowlands to the Andes. Abstract volume and field guide. 11–17 Third joint meeting of the International Council for Science, Dark Nature and the International Geological Correlation Programme 490, March 2005, Miramar-Córdoba

Zhang Y, Wallace JM, Battisti DS (1997) ENSO-like interdecadal variability: 1900–93. J Clim 10:1004–1020

Zielinski GA (2000) Use of paleo-records in determining variability within the volcanism-climate systems. Quaternary Sci Rev 19:417–438

Part IV
Applications of Dendroclimatology

Chapter 8
Application of Streamflow Reconstruction to Water Resources Management

David M. Meko and Connie A. Woodhouse

Abstract Streamflow reconstruction—the statistical augmentation of streamflow time series using tree-ring data—has been increasingly applied as a planning and research tool in water resources studies over the past few decades. Streamflow reconstruction in North America has evolved from a largely qualitative science in the first half of the twentieth century into a highly quantitative science that draws heavily on probabilistic theory. The historical development of streamflow reconstruction from a western United States perspective is reviewed, with an emphasis on developments of the last 30 years. Contributions to the study of water resources are discussed. Temporal extension of gauge flow records is the central contribution of the paleo record, but the statistical summary of those records and their manner of presentation are important factors in determining the value to water resources management. Probabilistic interpretations of flow reconstructions are needed because of uncertainty stemming both from limitations of the basic data and from the reconstruction process itself. Case studies are presented for the Colorado River, at the large spatial scale, and for the water-supply region of a metropolitan area—Denver, Colorado—at the smaller scale. Interaction of the tree-ring scientists with water managers and the public is a hallmark of modern applied reconstruction studies. Aspects receiving increased attention are the extent to which seasonal flows can be resolved, and how water managers and planners concerned with future conditions can overlay impacts of expected climate change on the natural hydroclimatic variability of the past as reflected in the tree-ring record.

Keywords Dendrohydrology · Tree rings · Streamflow · Water resources · Drought

D.M. Meko (✉)
Laboratory of Tree-Ring Research, University of Arizona, Tucson, AZ 85721, USA
e-mail: dmeko@LTRR.arizona.edu

M.K. Hughes et al. (eds.), *Dendroclimatology*, Developments in Paleoenvironmental Research 11, DOI 10.1007/978-1-4020-5725-0_8,

8.1 Introduction

With the narrowing gap between water supply and demand in many of the world's river basins has come an increased interest in the susceptibility of agriculture, industry, hydropower, and municipal development to climatic fluctuations. Paleoclimatic data have played a major role in convincing hydrologists and water resources planners that the snapshot of climatic variation provided by the short instrumental record may not be sufficient to capture all modes of variability important to the planning horizon. An obvious contribution of dendroclimatology is augmentation of hydrologic records—precipitation and streamflow—on which water resources planning relies. Tree-ring data are ideally suited for this purpose. Tree growth and natural runoff respond similarly to changes in net precipitation, or the residual of precipitation and evapotranspiration. Moisture-sensitive trees are widely distributed over large portions of watersheds, especially in the temperate latitudes, and frequently are most plentiful in mountainous areas, which contribute most of the runoff in semiarid watersheds.

Dendrohydrology has been defined as 'a subfield of dendroecology which utilizes dated tree rings to study and date hydrologic phenomena, such as river flow, lake level changes, and flooding history' (Kaennel and Schweingruber 1995). Because some applications of tree rings to hydrology address ecology only peripherally, it is perhaps also reasonable to regard dendrohydrology as a subfield of dendrochronology on equal footing with dendroecology. We restrict our treatment in this chapter mainly to streamflow reconstruction, a particular subfield of dendrohydrology relevant to water resources planning on the river-basin scale. Streamflow reconstruction—the statistical augmentation of streamflow time series using tree-ring data—has had a particularly rich history of application in the semiarid western United States. In keeping with the 'sharpening the focus' theme of this book, we confine the presentation to selected aspects of streamflow reconstruction we consider novel in the time frame of the last 30 years.

It is perhaps useful at the outset to distinguish streamflow reconstruction from other types of dendroclimatic reconstruction, which are thoroughly covered in other chapters. The distinction is indeed blurred, as climatic variability is a central issue in streamflow reconstruction. Droughts are commonly the focus of streamflow reconstructions and of dendroclimatic reconstructions of precipitation, drought indices, and atmospheric circulation patterns. Streamflow reconstruction is most often concerned with hydrologic drought, as manifested by unusually low streamflow over some time interval. A hydrologic drought would be mirrored by a meteorological drought, perhaps manifested in anomalous precipitation or patterns of atmospheric circulation responsible for moisture delivery. The relative severity of a particular drought by hydrologic and meteorological measures would likely differ, however, depending on many factors, including the exact drought metrics used, the watershed initial conditions, and the spatial scale of the basin.

A streamflow reconstruction study also usually includes the tailoring of analysis to some specific interest of water users, and considerable feedback from water resources planners or the agency or entity requiring the long-term information.

In this chapter we place emphasis on the interactive aspect of streamflow reconstruction with the water user or stakeholder. The statistical methodology of reconstruction is addressed only peripherally, as that has been thoroughly reviewed by Loaiciga et al. (1993). Examples of recent modeling approaches adopted can be found in recent papers (e.g., Hidalgo et al. 2000; Gedalof et al. 2004; Woodhouse et al. 2006).

This chapter begins with a brief historical background of streamflow reconstruction, followed by a section describing contributions of streamflow reconstruction to the study of water resources. Case studies on a probabilistic approach to interpretation of reconstructions (Colorado River, western United States) and on the application of reconstructions to water resource management (Denver Water Board) are then described. We close with a discussion of current challenges to streamflow reconstruction and to the adoption of reconstructions by water managers.

8.2 Historical Background of Streamflow Reconstructions

In North America, dendrohydrological studies in the 1930s began to explore the relationships between tree growth and streamflow, and the possible uses of tree-ring records for extending gauge records (Hardman and Reil 1936; Hawley 1937; Keen 1937). Hardman and Reil's (1936) work concerning the flow of the Truckee River, California–Nevada, was the first to examine these relationships in view of possible applications to water resource management, particularly in the agricultural regions of the Truckee River basin. In the 1940s, Schulman's (1945a, b, 1947, 1951, 1956) interest in dendrohydrology led him to compare variations in ring widths and annual runoff along the Pacific coast, in the Colorado River basin, the Missouri River, and for several southern California rivers. Schulman's work in the Colorado River basin was in part driven by the need to assess the long-term reliability of power generation at Hoover Dam, and the record provided by a regional tree-ring index allowed such an assessment (Schulman 1945a; Stockton and Jacoby 1976). In work for the Denver Water Board, Potts (1962) collected and analyzed tree-ring data to examine relationships with South Platte River, Colorado, annual flow and to document recurrence of droughts. The Denver Water Board was interested in estimating future storage requirements for the City of Denver's water supply and hoped to use the record of past hydroclimatic variability from tree-ring data to support these estimates. Tree-ring-based analyses to this point consisted of comparisons of ring widths and annual runoff, quantified by using correlation coefficients, and frequently smoothed to account for persistence in annual runoff and tree growth (Stockton and Jacoby 1976 and references within).

Stockton's dendrohyrolologic work in the 1970s was the first to take advantage of a suite of new quantitative methods whose routine use was made possible by the development of high-speed computers. The methods included multivariate statistical analysis for evaluating the climatic signal in tree-ring records and for reconstructing climate (Fritts et al. 1971), and standardized protocol for field sampling and tree-ring

chronology development (Stokes and Smiley 1968; Fritts 1976). Stockton (1975) incorporated these techniques in his tree growth/runoff analysis and reconstructions for sub-basins of the Gila and Colorado Rivers, demonstrating the usefulness of dendrochronological methods for reconstructing records of past runoff in the southwestern United States. Building on this work, Stockton and Jacoby (1976) went on to develop a suite of annual runoff reconstructions for upper Colorado River gauges with new tree-ring chronology collections and improved estimates of natural flow for calibration. Stockton and Jacoby's 1976 report directly addressed the implication of the resulting reconstructions for water management in the Colorado River basin. Specifically, the report identified the early decades of the twentieth century, the portion of the gauge record upon which the 1922 Colorado River Compact was based, as the wettest period in the past 450 years. Stockton and Jacoby (1976) concluded that the apparent overallocation of water resources, based on this wet period, could soon lead to water demands that exceeded water supplies.

The work of Stockton and Jacoby (1976) clearly demonstrated the value of extended records of streamflow for water resource planning and management, particularly for evaluating twentieth-century hydrology in a long-term context. In the early 1980s, due largely to the efforts of Charles Stockton and W.R. Boggess, inroads were made on communication of the potential value of streamflow record augmentation by tree rings to river-basin management (Stockton and Boggess 1980a, 1980b, 1982). A number of studies followed, many focusing on the assessment of droughts and the potential applications to water resources management. These studies included reconstructions of streamflow for the Potomac River, Maryland (Cook and Jacoby 1983); the Occoquan River, Virginia (Phipps 1983); and the White River, Arkansas (Cleaveland and Stahle 1989; Cleaveland 2000). In the western United States, streamflow reconstructions of the Sacramento River, California, were made for the California Department of Water Resources (Earle and Fritts 1986), and reconstructions of the Salt and Verde Rivers, Arizona, were made for the US Army Corps of Engineers (Smith and Stockton 1981).

More recently, reconstructions have been generated for an array of rivers in western North America, ranging from the Canadian prairie region (Saskatchewan River; Case and MacDonald 2003) and the Pacific Northwest of the United States (Columbia River; Gedalof et al. 2004) to the northern and central Rockies (Yellowstone River in Montana, Graumlich et al. 2003; Boulder Creek in Colorado, Woodhouse 2001; Jain et al. 2002), the southwestern United States (Gila River in Arizona; Meko and Graybill 1995), and Gulf of California continental watersheds in Mexico (Brito-Castillo et al. 2003). Several efforts have recalculated upper Colorado River flows (Michaelsen et al. 1990; Hidalgo et al. 2000) using the same or similar data used by Stockton and Jacoby (1976) but different calibration approaches. Most recently, a number of Stockton and Jacoby's (1976) Colorado River basin reconstructions for gauges on the Green, Colorado, and San Juan Rivers, including Lees Ferry, have been updated by using a new set of tree-ring chronologies and a longer calibration period (Woodhouse et al. 2006).

Several studies have more specifically addressed management and decision-making issues with streamflow reconstructions. The first of these was

a multidisciplinary study of the potential impact of severe sustained drought on the Colorado River; the worst-case scenarios were framed around tree-ring estimates of annual flow at Lees Ferry (Young 1995). Partly in response to the severe 1987–1992 drought in the Sierra Nevada Mountains of California, the California Department of Water Resources commissioned an updated tree-ring study of the Sacramento River, California, with a key objective being the estimation of long-term probabilities of low flows (Meko et al. 2001; Meko 2001). The Salt River Project (SRP), the third largest public power utility in the United States, and the largest water supplier for the Phoenix Arizona region, commissioned a tree-ring study of the synchroneity of drought in two important source runoff-producing areas—the upper Colorado River basin and the Salt-Verde River basins, Arizona (Hirschboeck et al. 2005). To facilitate use of the results by the water resources professionals and public, the final report, as well as basic data, were included in a Web site using a simple 'question and answer' format (http://fp.arizona.edu/kkh/srp.htm). An ongoing project, 'Enhancing Water Supply Reliability through Improved Predictive Capacity and Response,' sponsored by the US Bureau of Reclamation, has as one of its goals the identification of strategies for incorporating tree-ring information in river-flow modeling for the lower Colorado River basin (Jacobs et al. 2005). Public outreach and communication, in the form of meetings and a quarterly newsletter, are important elements of the project. Motivated by the 2002 drought in Colorado and in response to the needs of two major Colorado Front Range water providers, Woodhouse and Lukas (2006) tailored a network of reconstructions based on gauges in the Colorado headwaters region and the South Platte basin. These reconstructions were used as input into the providers' water system models to test the ability of the system to meet demands under a broader range of hydrologic conditions than in the gauge records alone.

Although the focus of a large number of streamflow reconstructions has been on arid and semiarid regions or areas dependent on snow-fed water supplies in western North America, there have been several recent efforts in other parts of the world. These include reconstructions for Mongolia (Pederson et al. 2001), and exploratory work on the potential for hydrologic reconstructions in the Southern Hemisphere in Argentina, Chile, and New Zealand (Boninsegna 1992; Norton and Palmer 1992). Streamflow reconstruction may be especially valuable in the Middle East, where increasing population and scarce water supplies make efficient water management essential. Application in this region is feasible, as precipitation has already been successfully reconstructed in Jordan and Turkey (Touchan et al. 1999; D'Arrigo and Cullen 2001; Touchan et al. 2003).

Many other hydrologic metrics besides streamflow have been reconstructed. In western North America alone, these include changes in lake levels, flood magnitude and occurrence, and glacier mass balance. Changes in lake level have been inferred or reconstructed for several lakes, including Lake Athabasca, Crater Lake, and the Great Salt Lake (Stockton and Fritts 1973; Meko and Stockton 1988; Peterson et al. 1999; Meko 2002, 2006). Tree growth responses to floods have been found to document both the frequency and magnitude of flood events. This work was pioneered by Sigafoos (1964) along the Potomac River in the eastern United

States, and since then numerous studies have used dendrochronological techniques to record flood events in many regions, including northern California, the southwestern United States, Colorado, South Dakota, British Columbia, and Manitoba (see review in Yanosky and Jarrett 2002). Tree-ring-based mass-balance estimates have been generated for Peyto Glacier, Alberta, Canada (Watson and Luckman 2004), and tree-ring proxies for winter glacial accumulation and summer ablation at Glacier National Park have been used to assess recent glacier retreat in a 300-year context (Pederson et al. 2004).

8.3 Contributions to the Study of Water Resources

8.3.1 Extensions of Gauge Flow Records

Observed streamflow records in the western United States are seldom as long as a century, and so cannot represent multicentury fluctuations due to climate variability, should such fluctuations exist. Moreover, the gauge records in a sense are a snapshot in time of one particular part of the long-term hydroclimatic history, and the snapshot may well be unrepresentative of extreme conditions (e.g., low-flow years) that may have occurred. It should also be recognized that gauged flow records are themselves imperfect measures of the volume of water passing the stream gauge, and that the accuracy of the gauged record can change over time depending on the type of gauge installed and the location of the gauge in the stream channel (Rantz 1982).

The immediate aim of streamflow reconstruction is the temporal extension of a time series of streamflow beyond the instrumented gauge record. Specifically, reconstruction targets streamflow unaffected by works of humans, which include artificial diversions, storage, modifications of the drainage network, and other factors. Streamflow defined in this way is sometimes also called 'natural flow,' 'virgin flow,' or 'runoff' (Chow 1964). The initial requirement in a streamflow reconstruction study is a time series of natural flow for statistical calibration with tree-ring records. For basins with little impact of humans, the gauged flows may provide a suitable calibration time series. For example, gauged flows for the Salt River near Roosevelt, Arizona, were judged sufficiently free of anthropogenic effects for direct use in a reconstruction model (Smith and Stockton 1981). If human influence cannot be dismissed as negligible, a modified time series of streamflow, adjusted to natural conditions by restoring reservoir evaporation losses, artificial diversions, etc., must be used in the reconstruction. Adjusted flow series were used; for example, in reconstructions for the Colorado River at Lees Ferry, Arizona (Woodhouse et al. 2006), and the Sacramento River, California (Meko et al. 2001).

The extended streamflow series provided by tree-ring analysis have contributed in many ways to a greater appreciation of the natural variability of streamflow and the susceptibility of water resources to climatic fluctuations (Table 8.1). Direct input of time series of reconstructed flows into river management models to test robustness of the system to extreme climatic variation is one natural application. An

Table 8.1 Summary of some published streamflow reconstructions in western North America (annual, water year, or summer)

River Reference	Mean flow^{+} (m^3/s)	Reconstruction period	Hydrologic change
South Saskatchewan, Alberta, Canada Case and MacDonald (2003)*	303	1470–1992	Relatively high mean flows in twentieth century. Droughts more severe in 1840s than in twentieth century.
Columbia, Oregon Gedalof et al. (2004)	5407	1750–1987	1840s most severe low flow of the past 250 years, but 1930s nearly as extreme. Runoff affected by land-use changes in twentieth century.
Sacramento, California Earle and Fritts (1986)*	340	1560–1979	Both highest (1854–1916) and lowest (1917–1950) flow periods occurred in the past 150 years.
Sacramento, Yuba, Feather, American (sum), California Meko et al. (2001)*	746	869–1977	Lowest average (10–50 years) means near 1300. Extreme single year low flows in late 1500s.
Yellowstone, Wyoming Graumlich et al. (2003)	88	1706–1977	Relatively high mean flows in twentieth century (except 1930s). Drought of 1930s more severe than any reconstructed drought.
Colorado River, Arizona Stockton and Jacoby (1976)*	588	1520–1961	Longest period of high-flow years 1907–1930. Drought in late 1500s longer and more severe than any in twentieth century.
Colorado River, Arizona Woodhouse et al. (2006)*	588	1490–1997	Severity of recent drought (2000–2004) likely exceeded six times in past 5 centuries, and as recently as the 1850s.
South Platte, Colorado Woodhouse and Lukas (2006)*	11	1685–1987	Record low twentieth-century flows are exceeded in severity in the late 1840s. Anomalous and persistent high flows in the early twentieth century
Middle Boulder Creek, Colorado Woodhouse (2001)	1.5	1703–1987	Low flows less persistent in twentieth century than nineteenth century. Multiyear drought in 1840s more severe than any in twentieth century.

Table 8.1 (continued)

River Reference	Mean flow[+] (m^3/s)	Reconstruction period	Hydrologic change
Salt, Arizona Smith and Stockton (1981)*	25	1580–1979	Frequency of high flows relatively high in twentieth century. Most severe sustained periods of low flow before twentieth century.
Gila, Arizona Meko and Graybill (1995)	13	1663–1985	Clustering of high-flow years in early twentieth century. Drought in 1950s most severe on record.
White, Arkansas Cleaveland (2000)	842	1023–1985	Twentieth century has more extreme low-flow and a larger number of high-flow years than prior centuries, perhaps due to human activities.
Potomac, Maryland Cook and Jacoby (1983)	271	1730–1977	Severity of 1960s multiyear low-flow period has not been exceeded in 248 years. 1850–1873 longest period of below median flow.

*More than one river was reconstructed in this study, but only one reconstruction is featured in this table. [+]Mean annual observed flows, intended to show order-of-magnitude differences in basins studied; means either taken directly from the publication listed or computed from online sources (gaged or natural flow) using all available years.

early example is the routing of Stockton and Jacoby's (1976) reconstructed flows through the Colorado River simulation model (Harding et al. 1995; Tarboton 1995). The model simulates operations specific to the Colorado River, including water allocation, reservoir operations, evaporation, hydropower generation, salinity, flood control releases, and legal and institutional constraints tied to the Law of the River (Harding et al. 1995). For a worst-case scenario in that study, the reconstructed flows for the most severe multiyear drought (1579–1600) were rearranged in decreasing order (lowest-flow year last) and input into the simulation model. Results indicated that such a drought has an estimated return period of perhaps 2000–10,000 years, and would result in Lake Powell being drawn down to dead level storage.

Two recent applications of tree-ring data in river models have utilized the time persistence properties of the tree-ring data in combination with magnitudes of flow from the observed flows. Prairie (2006), citing reconstructions of Colorado River flow illustrated in Woodhouse et al. (2006), judged that the tree-ring information on the hydrologic state (wet or dry) is very reliable, but that the magnitudes of reconstructed flows are too uncertain to justify their use in water management modeling. He applied a two-stage process to come up with realistic simulations of flow that took advantage of the perceived strengths of the observed and reconstructed data. First, the reconstructed annual flows were used in a Markov chain model to generate the hydrologic state. Second, sequences of annual flows were generated by nonparametric bootstrapping of the observed flows conditioned on the hydrologic state. The simulations of annual flow were then spatially and temporally disaggregated into monthly inputs to a basin-wide decision model. He applied this method using as input the Colorado River reconstructions of flow at Lees Ferry, Arizona, from Woodhouse et al. (2006). The example effectively demonstrated how annual streamflow reconstructions can help determine risk and reliability of various components of a water resources system.

In the second application drawing on the persistence properties of tree-ring data, Shamir et al. (2007) demonstrated how tree-ring information can be incorporated into a system of hydrologic modeling modules for water-supply risk assessment in an arid region where the water supply comes primarily from relatively shallow aquifers (micro-basins) along an ephemeral stream. The method was developed for the Santa Cruz River, just north of the US-Mexico border in Arizona. The hydrologic modules included (1) stochastic generation of hourly precipitation, (2) transformation of the precipitation into daily streamflow, and (3) surface-groundwater interaction to account for alluvial groundwater recharge. Winter wetness categories (wet, medium, and dry) were used in the precipitation module. One scenario utilized a 319-year tree-ring reconstruction of winter precipitation to establish wetness categories to guide the Monte Carlo precipitation sampling and the generation of daily flows. Results of the exercise suggested the risk of low water levels in the alluvial aquifers is greater than indicated by the relatively short instrumental precipitation and streamflow record.

The more typical direct application of streamflow reconstructions has been to place statistics of the gauged flow record in a long-term context. Most papers on streamflow reconstructions include tables summarizing the most extreme conditions

in terms of single-year flows or flows averaged over several years (e.g., Cleaveland and Stahle 1989; Meko et al. 2001; Woodhouse et al. 2006). The length of selected averaging periods may include some consideration of the multiyear storage capacity of reservoirs on the river (e.g., Woodhouse et al. 2006). The mean, variance, and first-order autocorrelation of reconstructed flows generally receive much scrutiny because those statistics are widely used by hydrologists to summarize and simulate streamflow series (Salas et al. 1980). Considerable attention has therefore been given in streamflow reconstruction models to minimizing any distortion of these statistics by the biological system of tree growth and by the reconstruction modeling process.

The long-term mean annual flow is a commonly used statistic for describing the volume of water available 'on average' from a watershed. The mean is highly susceptible to sampling error, and can be severely misleading when the length of a streamflow series is short or the climatic epoch sampled by the series is especially wet or dry. Tree-ring data have, for example, consistently indicated that the long-term mean of the Colorado River at Lees Ferry, Arizona, is considerably less than suggested by the gauged flow records that start in the late nineteenth and early twentieth centuries (e.g., Stockton and Jacoby 1976; Hidalgo et al. 2000; Woodhouse et al. 2006). In applying tree-ring data to study long-term means of streamflow, it is important to recognize the limitations imposed by size-related or age-related ring width trend, which must be removed before hydrologic interpretation (Fritts 1976). Stringent quality control in the detrending of ring widths (e.g., Cook and Briffa 1990) and other tree-ring variables is required before changes in the long-term mean can be examined.

Variance, or the size of departures from the mean, is important in estimates of severity of low flows and other statistics related to water supply. Streamflow reconstructions derived by regression necessarily are compressed in variance, and so tend to underestimate the severity of dry and wet periods. Rescaling the variance such that the variances of observed and reconstructed time series are equal for the calibration period is one possible approach to circumventing the variance bias in reconstructions (e.g., Cook et al. 2004). This approach essentially treats noise (unexplained variance in regression) as signal, and so runs the risk of overemphasizing the importance of tree-ring variations unrelated to climate, but can be useful as long as it is accompanied by clear information about the reconstruction uncertainty. Noise-added reconstructions (described in a later section) are another possible approach to dealing with the unexplained variance and its effect on inferred severity of hydrologic droughts and frequency of hydrologically significant events in the reconstruction (Meko et al. 2001).

Autocorrelation is especially important in streamflow series because autocorrelation directly affects the likelihood of a negative departure following a negative departure (dry year following a dry year), and vice versa. Autocorrelation is also important to the amplitude of low-frequency fluctuations that are often of great interest in water resources planning. Comparison of autocorrelation of long-term reconstructed flows with that of the reconstructed flows for the period of the gauged record can give at least qualitative information on possible bias of the instrumental

record as a long-term estimator of autocorrelation of streamflow (Meko and Graybill 1995). In reconstruction methods, much attention has been paid to minimizing the distortion of autocorrelation in streamflow reconstructions. For example, in a reconstruction of annual flows of the Sacramento River, California, Meko et al. (2001) filtered standard tree-ring indices in a preliminary step with a first-order autoregressive model, iteratively fit such that the flow series and filtered tree-ring series had approximately the same first-order autocorrelation coefficient for their overlap period.

Another approach to dealing with autocorrelation of tree-ring data was taken by Cleaveland and Stahle (1989) in their reconstruction of the White River, Arkansas. Autoregressive (AR) modeling was applied separately to tree-ring series and flow to produce AR residual time series. The AR residual flows were then regressed on the AR residual tree-ring series, the residual flows were reconstructed, and the AR flow model was applied to reintroduce persistence into the reconstruction. A third method of dealing with autocorrelation in flow reconstruction, applied to the Gila River, Arizona, was to use residual tree-ring chronologies as predictors of flow in a distributed-lag regression model (Meko and Graybill 1995). It is important to note that streamflow reconstruction models employing residual tree-ring chronologies as predictors without lags in the model are prone to underestimation of the persistence in reconstructed flows when gauged values do contain significant persistence. This point is emphasized in a sensitivity analysis in reconstruction of the Colorado River at Lees Ferry (Woodhouse et al. 2006).

Tree-ring information on streamflow has been extended in some studies to include the complete empirical distribution function of annual flow. For example, Jain et al. (2002) identified differences in the probability density function (PDF) signatures of two prominent 31-year reconstructed low-streamflow periods for middle Boulder Creek, Colorado. One period showed a general shift of the PDF to the left, reflecting generally lower mean flows. Another period showed a focused shift toward an increase in more severe low flows, but with only slightly lower average flows than the full record. The differences were presented as an example of information that could be important to water resources system management on typical planning horizons (30–50 years).

The technique of 'runs analysis' has gained popularity in recent decades as a tool for summarizing drought properties of reconstructions of streamflow and other hydroclimatic variables. In the terminology of runs analysis, a run is a series of consecutive values below some threshold; the run length is the number of consecutive years in the run; the severity, or run sum, is the sum of departures from the threshold; and the average intensity is the quotient of the run sum and run length (Dracup et al. 1980; Salas et al. 1980). Runs analysis was first applied descriptively in dendrohydrology to summarize the co-occurrence of drought in different parts of the western United States (Meko et al. 1995). A shortcoming of the method is the somewhat artificial delimitation of the temporal extent of a drought, which can be 'ended' with a single year of normal moisture conditions. The drought tally is also sensitive to the subjective choice of a drought threshold. The theory of runs analysis has recently been extended in a tree-ring context to develop a method to place any

climatic episode in a temporal perspective (Biondi et al. 2005). In this method, a stochastic model is used to describe the joint distribution of run sum and run length (severity and duration).

Streamflow series have been observed to have long-term persistence, which increases the overall variability of the series and compounds the problem of prediction from a short record (Dunne and Leopold 1978). Long-term persistence cannot be effectively summarized by simple low-order autoregressive models, as described above, and requires different analysis approaches. The Hurst coefficient, or rescaled adjusted range, has long been used by hydrologists to describe long-term persistence (Hosking 1985). A tree-ring reconstruction of the Gila River, Arizona, was analyzed to place the Hurst coefficient of the gauged record in a long-term context (Meko and Graybill 1995). The empirical distribution of sample Hurst coefficients for 254 overlapping 70-year segments of the reconstruction indicated that the most recent 70-year segment provides a slightly biased (high) estimate of the long-term persistence of annual flow.

The continued development of networks of tree-ring chronologies over the past several decades has expanded the possibilities for studying multi-basin aspects of streamflow and runoff. In semiarid regions, such studies are especially relevant to water resources planning because of inter-basin transfers of water. The starting data for such studies might be existing streamflow reconstructions. For example, co-occurrence of drought episodes in the Sierra Nevada of California and the Rocky Mountains of Colorado was summarized in an analysis of reconstructions for the Sacramento River, California, and Blue River, Colorado (Meko and Woodhouse 2005). An evolutive cross-spectral analysis was used in that study to point out subperiods of enhanced coherence in runoff in the two regions. The extended records provided by the reconstructions strengthened the statistical evidence for a greater-than-chance joint occurrence of extreme low flows. Joint drought was also the subject of the previously mentioned study for the Salt River Project (SRP) (Hirschboeck et al. 2005). The focus in that study was the potential for drastically reduced runoff simultaneously in the upper Colorado River basin and Salt-Verde River system of Arizona. The motivation was SRP's dependence on imported Colorado River water from the Central Arizona Project (CAP) to buffer against reduced runoff on the Salt and Verde Rivers in times of drought. Results emphasized that severe drought years and clusters of drought years are strongly coherent across the two river systems, and suggest that drought-induced shortages in local Arizona water supply are unlikely to be offset by excessive runoff in the upper Colorado.

8.3.2 Probabilistic Interpretation of Streamflow Reconstructions: Example for the Colorado River

Streamflow reconstructions are statistical estimates of what the flow might have been in any given year, and the uncertainty associated with these estimates is usually displayed in the form of error bars. The user of the reconstruction can directly refer

to the error bars to judge how much importance to attach to any particular reconstructed flow, and can use the error variance of the reconstructed annual flows to derive appropriate error bars for relatively simple statistical summary statistics of annual flows, such as the *n*-year mean flow (e.g., Meko et al. 2001; Woodhouse et al. 2006).

For more complicated statistical summary statistics, mathematical derivation of the error bars may not be straightforward. An alternative approach is to dispense with interpretation of the reconstruction itself and resort to probabilistic analysis of a large number of plausible realizations of true flow derived from the annual reconstructed values and their uncertainty. Such realizations have been called 'noise-added' reconstructions (Meko et al. 2001), referring to their generation by the equation:

$$\hat{\mathbf{u}}_i = \hat{\mathbf{y}} + \mathbf{e_i} \tag{8.1}$$

where $\hat{\mathbf{y}}$ is a vector time series of reconstructed flows and $\mathbf{e}_i$ is a sample of random noise of the same length drawn from a normal distribution with appropriate variance.

A large number (e.g., 1000) of such noise-added reconstructions constitutes a plausible ensemble of 'true' flows, which can be analyzed probabilistically for streamflow statistics. Noise-added reconstructions can be used to estimate probabilities of past occurrence of any hydrologic 'event' that can be quantitatively defined. For example, in the fourth year of a drought, we might be interested in the probability that 4 consecutive low-flow years are followed by a fifth low-flow year.

The following example utilizes the updated reconstruction Lees-B of annual streamflow for the Colorado River at Lees Ferry, Arizona (Woodhouse et al. 2006), to place the recent severe 5-year drought (2000–2004) in a long-term perspective. The reconstruction was derived by multiple linear regression from a network of standard tree-ring chronologies, extends over the period 1490–1998, and is based on a 1906–1995 calibration period. The regression model explained 84% of the variance of flows for the calibration period, verified well, and had residuals that conformed reasonably well to the regression assumptions (Woodhouse et al. 2006). The Lees Ferry observed flow for the period 1906–2004 has a mean of 18,540 million cubic meters (mcm) and standard deviation of 5368.6 mcm.

Two essential steps in the analysis of the 2000–2004 drought are the definition of the 'event' and the statement of a null hypothesis:

1. Event: flow less than a specified drought threshold for at least 5 consecutive years
2. H0: at least one event occurred in the period 1490–1988

The 'event' defined for this example is the occurrence of 5 or more consecutive years of flow below a drought threshold, which is arbitrarily specified as the 0.25 quantile of observed annual flows for 1906–2004. The 0.25 quantile adopted as the drought threshold is equal to 14,365 mcm, or roughly 77% of the mean annual flow. The event is of interest because five consecutive extremely low flows indeed did occur on the Colorado River in water years 2000–2004, resulting in

steeply dropping reservoir levels and concerns among water resources professionals about the resilience of the Colorado River system to severe drought. The question rephrased in nonstatistical terms then, is how unusual was the low-flow period 2000–2004 in the context of the 509-year tree-ring record that extends over the years 1490–1998?

The severity of the recent drought is clearly evident in the time series plots of annual observed flows (Fig. 8.1, top). The period 2000–2004 is the longest run, or consecutive sequence, of years below the drought threshold. If the reconstructed flow series (Fig. 8.1, bottom) is taken at face value, it must also be concluded that the 2000–2004 drought is unprecedented in the tree-ring record, as the longest sequence of years below the threshold is 4 years. Considering the uncertainty in the tree-ring reconstruction, however, it is impossible to say categorically that there has not been another 5-year sequence of such low flows in the period 1490–1998. A more valid interpretation considers the probabilistic nature of the reconstruction. By this interpretation, the true flow in any year has some nonzero probability of being higher or lower than the reconstructed value. Depending on the reconstruction errors, which are unknown, the sequence of true flows will be somewhat different than the reconstruction itself.

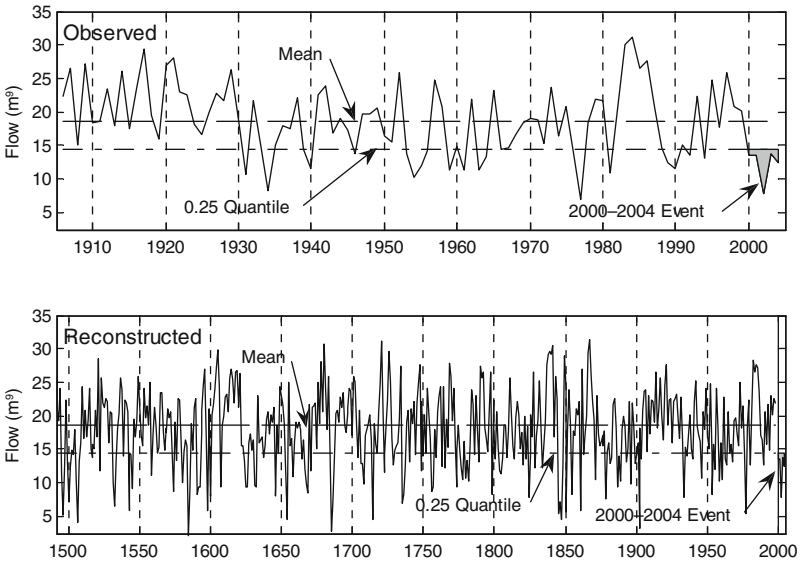

Fig. 8.1 Time series plots of observed (*top*) and reconstructed (*bottom*) annual flow of Colorado River at Lees Ferry. The mean and 0.25 quantile of the 1906–2004 observed flows are marked on both plots, along with an observed 2000–2004 'event' of 5 consecutive years below the 0.25 quantile. The maximum number of consecutive reconstructed flows below the 0.25 quantile of the observed flows is 4 years. Sources of data: observed flows are natural flow series from US Bureau of Reclamation, and reconstructed series is reconstruction Lees-B from Woodhouse et al. (2006)

To proceed with the noise-added reconstruction of Lees-B, 1000 random sequences of length 509 years were drawn from a normal distribution with mean zero and standard deviation equal to the cross-validation root-mean-square error ($RMSE_v$) of the reconstruction model. Note that in using $RMSE_v$ instead of the standard error of the estimate or the standard error of prediction to compute the error variances, we are imposing a larger error component than might be suggested by calibration statistics. The validation error is $RMSE_v = 2337.1$ mcm, or about 44% of the standard deviation of the observed flows.

The 1000 noise sequences were each added to Lees-B to get 1000 separate noise-added reconstructions of length 509 years. Each noise-added reconstruction was then checked for occurrences of 5 or more consecutive years below the drought threshold. A count of the number of noise-added reconstructions with a drought event yields an estimated probability for rejection of the null hypothesis. For example, if just one noise-added sequence out of the 1000 generated series has a drought of at least 5 consecutive years, we can conclude the there is only a 1/1000, or 0.001, probability that the tree-ring record contains at least one event. In that case we would clearly reject H0 at the 0.01 α-level.

Results revealed that 510 of the noise-added series contained at least one drought event. The empirical probability that another sequence of 5 or more consecutive years of low flow occurred before the most recent drought is therefore $p = 0.51$, indicating that the recent 5-year drought is likely not unprecedented in the long-term record. Two examples of the noise-added reconstructions are shown in Fig. 8.2. As

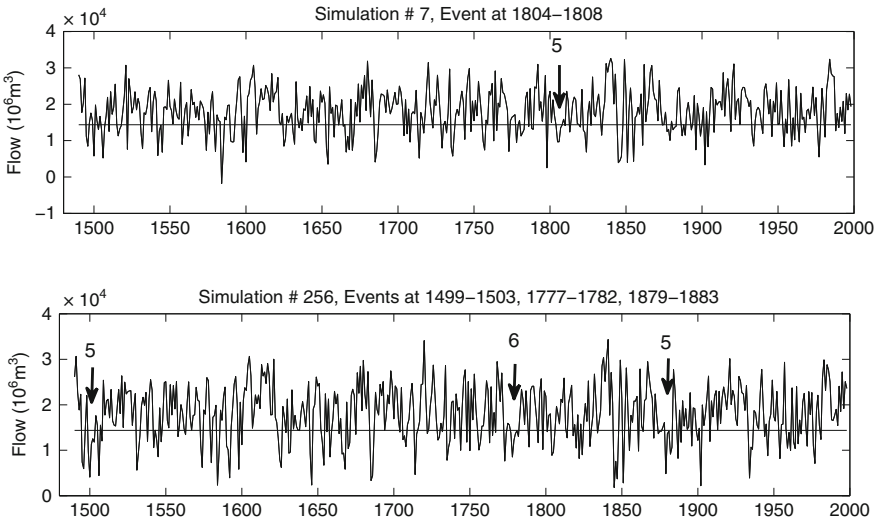

Fig. 8.2 Sample of 2 out of 1000 noise-added reconstructions illustrating occurrence of low-flow events. A low-flow event is defined as 5 or more consecutive years of flow below the 0.25 quantile drought threshold of the observed flows, 1906–2004 (*horizontal line*). The simulation at the top contains a single 5-year run below the threshold and the simulation at the bottom contains two 5-year runs and one 6-year run. A total of 510 of the 1000 simulations had such events

is indicated, some simulations may have drought events longer than 5 years, and some may have more than one event. The null hypothesis is phrased to treat all such series equally, in that each series with at least one event contributes equally to the probability. It may seem surprising that the noise-added reconstructions give such a high probability when the reconstruction itself has no events. The reason is that in years of reconstructed flow above but near the threshold, the chance is not negligible that the true flow was actually below the threshold. The noise-added series incorporate this uncertainty.

Probability estimates of hydrologic events from tree-ring reconstructions are unlikely to be used by water resources professionals without some context of comparable information from the better-understood observed flow record. The Colorado River example is extended here to illustrate how this may be done. The observed flows are limited to the period 1906–2004, but the statistics of the observed flows can be used to simulate flows as long as the tree-ring reconstruction. Differences in probabilities based on the simulated flows and the noise-added reconstruction may highlight the 'new' information provided by the tree-ring record. Conversely, similarities may attest to longer-term relevance of the short observed record.

Because the most recent years of the Colorado River observed flows have been among the lowest on record, flow statistics for designing simulation are sensitive to the truncation year for analysis. Histograms of observed flows for subperiods 1906–1999 and 1906–2004 show barely noticeable differences solely due to the low flows of the 2000–2004 drought event (Fig. 8.3). The sample mean is about 2% higher

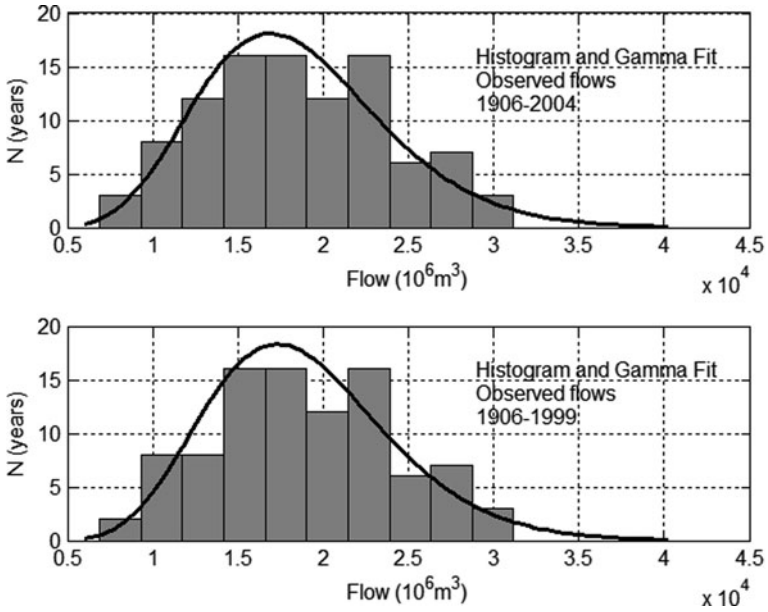

Fig. 8.3 Histograms and gamma-fit probability density functions (PDFs) of Colorado River at Lees Ferry annual flows for different analysis periods. Dropping the years of the most recent drought (2000–2004) results in a barely noticeable rightward shift in the fitted density function

for the shorter subperiod. The histograms differ only on the left side, as expected, from the addition of the 4 low-flow years to the longer sample. Probability density functions for fitted gamma distributions to the two samples look quite similar, but differences in basic statistics are large enough to be important to the simulation results, as described below.

For comparison with the probabilities from the noise-added reconstructions, the observed flows were simulated in two ways. First was bootstrapping, in which the observed flows were sampled, with replacement, to generate 1000 time series of length 509 years, corresponding to the length of the tree-ring reconstruction. Bootstrapping in this way destroys the time dependence in observations, which may indeed be important in creating persistent droughts like the 2000–2004 drought. The observed flows are significantly autocorrelated at a lag of 1 year ($r_1 = 0.28, p < 0.05,\ N = 99,$ one-tailed). The second method used for simulation was autoregressive modeling (Salas et al. 1980). A first-order, or AR(1), model was found reasonable for this modeling. The bootstrapping and AR modeling were each repeated for the two sample periods 1906–1999 and 1906–2004 to test the sensitivity of results to including the most recent drought in the sample for designing the simulation model.

The sets of 1000 simulated flow series by bootstrapping and AR modeling were analyzed for occurrence of drought events, as described previously for the noise-added reconstructions. The empirical probability of at least one event in a 509-year series is graphed in Fig. 8.4, with results from the noise-added reconstructions included for comparison. The importance of base period for the modeling of observed flows is obvious: roughly a doubling of the probability is created by choosing the base period that includes the most recent drought. The tree-ring results are most consistent with probabilities from the drier (longer) series of observed flows, and the drought probability from the tree-ring record is higher than from simulated observed flows. The results imply that the observed flow record may be slightly biased toward underestimating the probability of drought events such as occurred in 2000–2004, and that the observed record including those drought years is more representative of long-term conditions than the observed record before 2000.

8.3.3 Applications to Water Resource Management: A Case Study Using the Denver Water Board

The Denver Water Board is the oldest and largest water provider in Colorado, serving over 1 million people across the Denver metropolitan region. Denver Water holds water rights to water supplies both in the South Platte River basin, east of the Continental Divide, and in the upper Colorado River basin, west of the Divide. A complex network of diversions, tunnels, reservoirs, and treatment plants make up the Denver Water system and is used to provide water services to their customers.

One of Denver Water's key concerns with regard to water supply is whether the instrumental gauge records (for which natural flows have been estimated back to

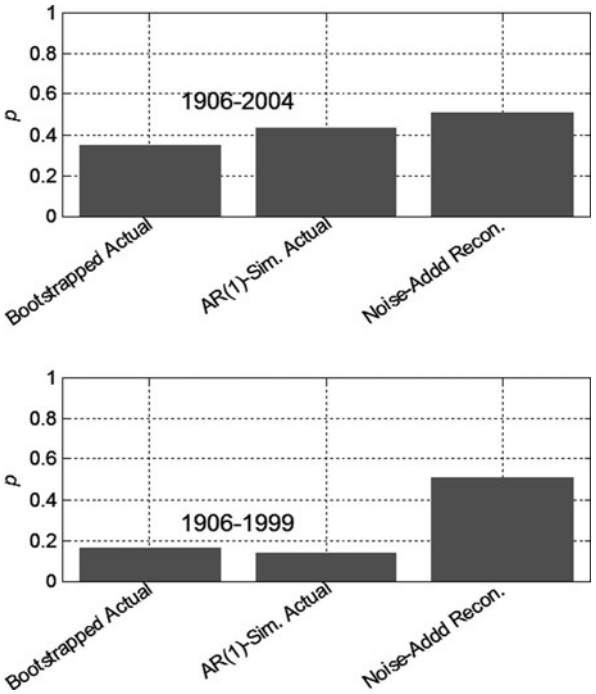

Fig. 8.4 Histograms illustrating differences in probability of drought event estimated from observed and reconstructed flows. *Y*-axis is probability (*p*) of at least one event in a 509-year period, where an event is five or more consecutive flows below the drought threshold (see text). Leftmost two bars are based on analysis of the observed flows. Rightmost bar is from noise-added reconstructions. Analysis periods for bootstrapping and autoregressive modeling of observed flows are 1906–2004 (*top*) and 1906–1999 (*bottom*)

1916) are an adequate frame of reference for future water resource planning and decision making. Denver Water planners have used the 1950s drought (1953–1956) as the 'worst-case scenario,' but the recent drought (2000–2004) called into question the appropriateness of this drought as a baseline. Are more severe droughts possible, and how would Denver Water's system perform under those conditions? Motivated by this drought, Denver Water's planning division began to consider taking another look at tree-ring-based streamflow reconstructions (after Potts' 1962 work) and their usefulness in addressing these concerns. The reconstructions would indicate if more severe droughts occurred in past centuries, and the range of their characteristics (intensity, duration, magnitude). Although the reconstructions are not used as a predictive tool, it is reasonable to assume that if extreme drought events occurred in past centuries, events of similar magnitude could occur in the future.

A meeting between a team of paleoscientists from the National Oceanic and Atmospheric Administration (NOAA) and the University of Colorado, and Denver Water planning division personnel in the summer of 2002 (the peak of the 2000–2004 drought) began a collaborative process, which evolved over the next 3 years.

In the initial meeting, paleoscientists learned of the key questions Denver Water hoped to address with tree-ring reconstructions and their concerns regarding the use of proxy streamflow data from tree rings. In turn, they endeavored to convey the science behind the reconstructions and the limitations of the proxy data. In subsequent meetings, a number of issues surfaced. These included: the availability and reliability of estimated natural flows, which would be used to calibrate models; the problem of disaggregating reconstructed annual values into the daily values needed for water system model input; and the ability of the tree-ring reconstructions to match the extreme low flows, critical for drought assessment and planning.

Some specific challenges emerged. To begin with, Denver Water wanted to know precisely how well the drought years of 2000–2002, and 2002 in particular, could be reconstructed with tree rings. The extreme low-flow year of 2002 was treated as a test case for assessing the skill of the tree-ring reconstructions. A related challenge was to evaluate the replication of other droughts in the twentieth century by the tree-ring reconstructions, and to explore techniques to better match these extremes. With regard to the uncertainty in the estimated flows, although it is known that reconstructed values more closely match the gauge values in very dry years compared to very wet years (growth is more uniformly limited in dry years; Fritts 1976), Denver Water wanted a demonstration of this in order to more closely assess the accuracy of the dry year reconstructed values. Finally, besides estimates of past water supply, Denver Water was interested in the possibility of estimating demand, using an index based on water usage, primarily in summer.

After preliminary proof-of-concept reconstructions were generated, work was begun to update western Colorado tree-ring chronologies to include the 2002 ring, and then to develop updated water year streamflow reconstructions through 2002 for Denver Water's three upper Colorado River basin gauges. Results indicated that tree growth in 2002 very well reflected 2002 low flows, and subsequent reconstructions provided estimates that closely matched the values of the 2000–2002 flows. After updating and expanding tree-ring collections for the South Platte River basin and generating streamflow reconstructions for those gauges through 2002, reconstructions resulted that were of similar high quality, especially in the replication of the 1950s and recent droughts. Along with the reconstructions, work was begun to explore approaches to refine estimates of low flow and to better describe the uncertainty related to the tree-ring-based estimates of flow. One approach was the development of an 'ensemble' reconstruction, in which reconstruction models were calibrated on numerous subsets of calibration years (Webb and Woodhouse 2003). When the ensemble members were plotted (30–40 members for the South Platte River), it was possible to see years in which all solutions converged (typically the driest years) and years in which the estimates were more variable. In several cases early in the gauge record, tree-ring estimates for a particular year all indicated dry conditions while the gauge value indicated an average or wet year. Denver Water personnel suggested errors in the estimation of the natural flows could be the cause of the mismatch in those years, something the paleoscientists had not considered. The range of scenarios presented by this ensemble approach provided a means to explore uncertainties related to statistical modeling and the

sensitivity of the reconstruction to different calibration years and the quality of gauge data.

Denver Water engineers are still in the process of incorporating these results into their water system model, a major undertaking. The general approach used is to pair pre-gauge reconstructed estimates with the closest analog year in the set of 45 years (1947–1991) with known daily hydrology for the model's 450 locations to obtain the input needed for their model. In cases where reconstructed years have no analog, values for the closest year are scaled accordingly. In this way, the extended records from the streamflow reconstructions are being incorporated into the Denver Water's water system model, ultimately allowing the system to be tested by using a longer record of hydroclimatic variability than is afforded by the gauge record. A companion reconstruction of water demand, which largely reflects maximum summer temperatures and the occurrence of rainfall events at two thresholds, was also generated, allowing a comparison of long-term records of supply and demand, and the frequency of a joint concurrence of high demand and low flow to be assessed.

8.3.4 Informing the Public

Dendrohydrologic reconstructions of streamflow have played an important role in raising awareness among water managers, policy makers, and the general public that the range of variability in gauge records is just a subset of the long-term natural variability over multiple centuries. The late 1990s through early 2000s drought in the western United States caught the attention of many, and because it was the worst drought on record in many areas (depending on variable and length of time considered), it led to questions such as, 'How often do we have a drought this severe and have there been worse droughts in the past?' The public interest level was high, especially where outdoor water use was restricted, and was further heightened by media attention to the drought. Water managers had a practical interest in getting answers to these questions, while policy makers were made acutely aware that water resource and drought planning needed to consider more than the worst drought in the twentieth century.

This situation created a rare window of opportunity for dendrohydrologists to assist in addressing these questions. It also presented an excellent opportunity to inform the general public about the usefulness of tree-ring reconstructions of hydroclimatic variability. Many groups—from the Audubon Society to the local soil conservation district to continuing education law students—were interested in hearing about droughts of the past. The challenge was to present information on the tree-ring-based reconstructions regarding the current drought and droughts of the past in a way that was readily understandable by a range of audiences. New approaches to data display and visualization were considered to improve ways to convey information about hydrological reconstructions. For example, the time series of reconstructed streamflow typically shown are not readily understood by

all audiences. Alternative ways to describe the long-term records of flow may be more meaningful. In particular, graphics that showed how often a year like 2002 or a sequence of dry years has occurred were of primary interest. Two examples of different ways to graphically depict streamflow reconstructions that have been well received by general public audiences are show in Figs. 8.5 and 8.6.

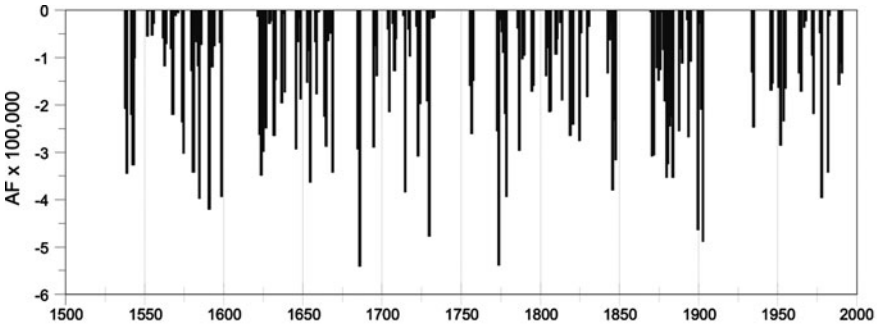

Fig. 8.5 Droughts are not evenly distributed through time. This graph shows periods of drought in the reconstructed Rio Grande River (Del Norte gauge) annual streamflow, 1536–1999. Only the years in which 2 or more consecutive years are below the mean are shown, as departures in hundred thousand acre-feet from the long-term mean

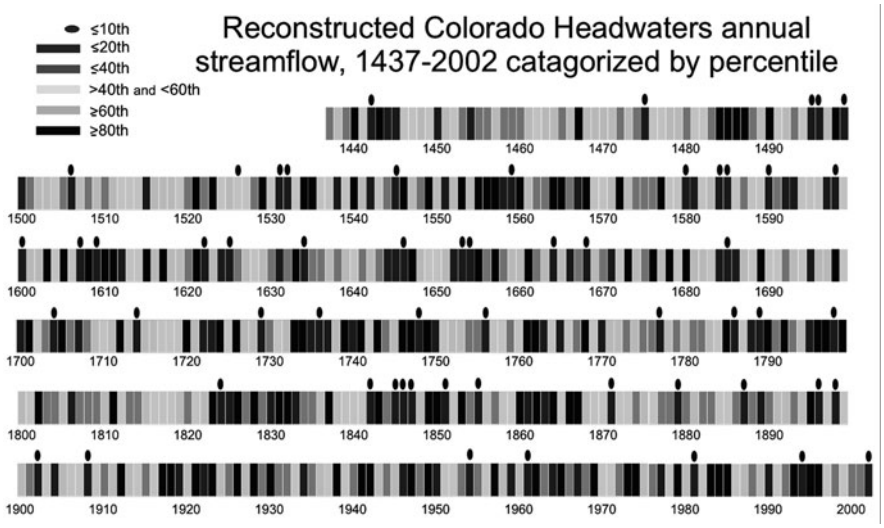

Fig. 8.6 Reconstructed Colorado headwaters streamflow (Blue, Fraser, and Williams Fork Rivers, averaged). Values are shading-coded according to percentiles of flow. The years with *dots* are the driest 10% of flows. 2002 was in this category, as were 6 years in the twentieth century. In contrast, 12 extremely dry years occurred in the nineteenth century

8.4 Challenges

8.4.1 High Flows

Attempts to reconstruct annual streamflow totals from tree-ring indices by regression methods often run up against the obstacle of heteroscedastic errors, in which the variance of the regression errors increases with the magnitude of the estimated flows (e.g., Meko and Graybill 1995; Meko et al. 2001). This is especially true the smaller the basin and the more arid the climate. To satisfy regression assumptions, one solution is log transformation of the flows before regression analysis. The reconstruction is then in log units of flow, and in such units the residuals may not be heteroscedastic. But water resources planners do not compute their water budgets in log flow units, and when reconstructions are back-transformed to original units, the heteroscedasticity returns. The problem essentially is that for basins with 'flashy' flow regimes (e.g., rapid runoff from heavy storms in arid regions), tree-ring data are unlikely to accurately distinguish magnitudes of high flows (Meko et al. 1995). The runoff events may simply occur too rapidly to leave a strong signature in soil moisture in the root zone of the trees, and in tree growth. At the same time, high flows are of great importance in water resources planning because they often contribute the pulses of runoff that refill storage reservoirs.

8.4.2 Seasonality

Cool season precipitation and snowmelt contribute proportionally more water to streamflow than warm season precipitation, especially for large watersheds. Reasons include the higher evapotranspiration losses and requirements for soil moisture recharge in the summer season, as well as the generally spotty nature of summer convective storms. Improvement of the seasonal resolution of precipitation or soil moisture signal from tree rings is therefore likely to yield more accurate streamflow reconstructions. Separate measurements of earlywood width and latewood width have proved useful in various regions for seasonal resolution of precipitation variations (e.g., Lodewick 1930; Meko and Baisan 2001; Cleaveland et al. 2003). A different issue related to seasonality concerns streamflow reconstructions in areas where the climate signal in tree growth and the main climatic contribution to annual flow do not correspond as well as they do across most of the western United States. In the Pacific Northwest, the main source of runoff is winter precipitation, while low-elevation moisture-sensitive trees are more tuned to summer precipitation (Gedalof et al. 2004). In the eastern United States, species such as bald cypress also tend to be more sensitive to summer conditions, making reconstructions of summer low flows a more appropriate hydrologic variable for reconstruction than annual flows (Cleaveland 2000).

8.4.3 Uncertainty

Uncertainty is inherent to tree-ring reconstructions of streamflow. Tree-ring data are imperfect recorders of climate, and so even a dense tree-ring network of moisture-sensitive chronologies distributed ideally over the important runoff-producing parts of a watershed will not result in an error-free reconstruction. Noise-added reconstructions, described earlier, are one possible approach to summarizing uncertainty, assuming the model is correct. The ensemble reconstructions described in the case study for Denver Water address that part of the uncertainty due to model selection given different years in the calibration set. Concisely and clearly communicating the uncertainty in reconstructions to water resources professionals is a continuing challenge to dendrohydrologists. This task is further complicated when multiple tree-ring reconstructions appear to yield widely disparate estimates for the magnitude of multiyear low-flow events and other features in the long-term record (Hidalgo et al. 2000; Woodhouse et al. 2006). Important differences in reconstructions can always be traced to differences in basic tree-ring data, hydrologic data, and modeling choices. The importance of the 'observed' flow record used for calibrating the reconstruction model is illustrated in the Colorado River reconstruction of Stockton and Jacoby (1976). These researchers reported estimated long-term mean annual flows ranging from 13.06 million acre-feet (maf) to 14.15 maf, depending on which of two existing virgin flow records were used and whether the earliest, least reliable, years of the flow record were included in the calibration. A 'best' estimate of 13.5 maf was finally adopted as a compromise based on the two versions of the reconstruction deemed most reliable. (Note: 1 maf is approximately 1.23 billion cubic meters.)

Statistical reconstruction methods, such as multiple linear regression, yield an estimate of the reconstruction uncertainty in terms of the error variance. The error variance reflects the goodness of fit of the reconstruction model, and is critical to the interpretation of the reconstructed streamflow statistics. The biases and standard errors of reconstructed streamflow drought statistics have been found to depend in degree on the goodness of fit, calibration sample length, reconstruction sample length, and autocorrelation of the reconstructed flows (Brockway and Bradley 1995). Monte Carlo studies have shown that a drought statistic derived from an observed flow record is more stable (lower standard error) than the same statistic estimated from a much longer reconstructed flow (Brockway and Bradley 1995). Reduction of the error variance of streamflow reconstructions is a major challenge in getting reconstructions to be accepted and utilized in water resources planning.

The reconstruction error variance, as useful as it is in assessing reconstruction uncertainty, summarizes only part of this uncertainty for most streamflow reconstructions. Additional uncertainty arises from the time-varying makeup of tree-ring chronologies, which can lead to reconstructed flow values based on predictors (tree-ring variables) that are essentially different from those used to calibrate the reconstruction model. An extreme example would be chronologies formed by splicing time series of indices from living trees with those of remnant wood or

archaeological samples. Methods for quality-controlling and adjusting chronologies for time-varying sample size are available (Wigley et al. 1984; Osborn et al. 1997), and should be more routinely adopted in streamflow reconstruction. Another possible strategy is to tailor reconstruction models so that the equation yielding a reconstructed flow in any given year is based on a calibration model using the identical (or similar) tree-ring cores (e.g., Meko 1997).

As tree-ring chronologies are updated and additional chronologies are developed, reconstructions for the same flow record can be expected to change: the revised flow estimates will be a different linear combination of tree-ring indices from the estimates in previous reconstructions. Illustrations of such changes for reconstructions of streamflow for the Colorado River can be found in Woodhouse et al. (2006). Moreover, choices of tree-ring processing (e.g., residual or standard indices, lags or no lags, indices or principal components) can lead to different reconstructions from the same basic tree-ring measurements. Because the 'true' model relating flow to tree-ring indices is an abstraction and is unknown, it is important that more research address the sensitivity of reconstructed streamflow features to modeling choices.

Uncertainty in the low-frequency component of streamflow variability is another aspect of streamflow reconstruction that cannot be satisfactorily addressed with calibration and validation statistics of reconstruction models. First, the flow record for the period used to calibrate and validate the model simply may not be representative of the low-frequency behavior of the long-term record. In that case, we do not know how well the tree rings might track the low-frequency flow variations, and we must assume that low-frequency features—such as broad swings above and below the mean in tree growth—reflect similar variations in flow. Second, the detrending operation in conventional standardization places a lower limit on the frequency of climatic variation resolvable with the tree-ring index. That limit depends on the length of the tree-ring series and choices of detrending curve by the researcher developing the chronology (Cook et al. 1990, 1995). Regional curve standardization (RCS), which depends on identification of a generally applicable function of expected ring width with tree age, has been applied in dendrohydrology in an attempt to circumvent the frequency-response limitation (e.g., St. George and Nielsen 2002). Unfortunately, RCS requires intensive sampling, with trees of various ages represented throughout the period of record (Briffa et al. 1996). Few river basins may afford such a luxury of moisture-sensitive trees.

Uncertainty can never be completely eliminated from streamflow reconstructions. A streamflow reconstruction relies on a statistical relationship between streamflow (observed or adjusted to natural flows) and tree-ring chronologies distributed over the basin. Increased tree-ring site coverage and improved statistical methodology may increase the strength of the relationship. Uncertainty may eventually be reduced by incorporating information from tree-ring variables other than ring width index in the reconstruction model. Variables might include wood density (e.g., Briffa et al. 1988), stable isotope ratios in tree rings (e.g., Leavitt and Wright 2002) and the anatomical features of cambial cells (e.g., Vaganov 1990; Vaganov et al. 2006). Such efforts can never arrive at a perfect reconstruction, but improvements in accuracy may enhance the usefulness of the reconstruction for water resource management.

Possible changes in basin characteristics over the period covered by the tree-ring record impose on streamflow reconstructions a layer of uncertainty not amenable to assessment with statistics on calibration accuracy or validation accuracy. Reconstruction models assume that the statistical relationships derived for the calibration period are stable over the long term, and this assumption may be violated if basin conditions have changed. For example, if the vegetative cover of the basin was drastically reduced (e.g., by fire) during some intervals, the runoff from the basin at those times would be greater than expected from a statistical model calibrated under modern conditions. On the other hand, an error of this kind may be unimportant to water managers who are interested in the possible effects of climate variability on runoff given existing vegetation coverage.

8.4.4 Communication

The extended records of hydroclimatic variability provide valuable information about the range of natural variability beyond that provided by gauge records alone. This information has important implications for water resource planning and policy making. The challenge is to move from these implications to determine the ways these data can actually be applied to water resource management. Collaborative work between water management agencies and paleoscientists, as described in the example above with Denver Water, has demonstrated the potential usefulness of these data in planning and management. In the spring of 2002, a workshop was held in Tucson, Arizona (Garrick and Jacobs 2005), that brought together paleoscientists and water management agency personnel with interests in the Colorado River basin. Group discussions during the workshop brought to the forefront some of the challenges in applying paleodata to water resource planning and management. First and foremost was the need for better communication between paleoscientists and water management personnel to improve scientists' understanding of management decision-making concerns, as well as water managers' understanding of the science behind the data. Part of that challenge is finding water managers willing to look beyond traditional management tools, and dendrohydrologists willing to think about alternative approaches to standard dendrohydrological methods. Forming successful partnerships is a time-consuming process for all parties involved. However, due to the impact of recent droughts, coupled with increased demands on water supplies and the potential for anthropogenic climate change, the water resource community has begun to recognize the value of these extended records. Our challenge is to improve communications with water management personnel so that we can find better ways to provide the data and information needed for planning and decision making.

8.4.5 Climate Change

The regional impacts of climate change on water resources are becoming evident in the declining snowpack in the mountains of the western United States, and

particularly in the Pacific Northwest (Mote et al. 2005). The decline is mostly attributed to warming winter temperatures, even with periodic and regional increases in precipitation (Mote et al. 2005). Effects of this reduction of snowpack on hydrology include earlier runoff dates and changes in the distribution of runoff over the course of the water year, with more runoff earlier in the water year (Stewart et al. 2004). These changes could result in greater losses due to evaporation and an overall reduction in water year flows, if not compensated for elsewhere in the hydrologic cycle. Future climate projections suggest large-scale warming on the order of 1−2°C across the western United States over the next half century (Barnett et al. 2004).

These trends and projections bring up the question, is the record of past hydroclimatic variability an appropriate analog to future conditions? In some respects, the climate of the future will be unlike the climate of the past; however, natural hydroclimatic variability is likely to continue, superimposed on changes in climate due to anthropogenic activities. An understanding of natural hydroclimatic variability on decadal and longer timescales can be obtained only from centuries-long reconstructed records, and is critical for understanding the large-scale, slowly varying oceanic/atmospheric drivers of climate. These large-scale controls are likely to continue to operate in the future, and a baseline knowledge of the role of oceanic/atmospheric conditions in long-term regional hydroclimatic variability is necessary to understand how the climate system operates now and how it will under warmer conditions. The challenge will be to blend the knowledge gleaned from the past with projections for climate under climate change scenarios to get a better indication of the range of hydroclimatic conditions and events to expect in the future.

8.5 Conclusion

A.E. Douglass, in the foreword to Edmund Schulman's (1945a) landmark report on tree-ring hydrology of the Colorado River basin, wrote that he believes Schulman 'offers something of novel importance and value to the hydrologists of the West,' and that the report will 'carry over to the managers of hydroelectric and reclamation projects about the world a good idea of the type of information that may be secured from properly selected and analysed [sic] trees.' Some 50 years later, we see that much has been accomplished but that the potential of tree-ring analysis in hydrology has only begun to be tapped. Early studies were most intensive in the western United States, with groundwork for quantitative streamflow reconstructions laid by H.C. Fritts and C.W. Stockton. The geographic scope has expanded with the growth of dendrochronology as a science, the development of tree-ring laboratories in various countries, and the spatial extension of tree-ring networks. The contributions of dendrohydrology continue at an accelerating pace as human demands on limited water resources increase and the need for efficient long-term planning in water

management becomes more urgent worldwide. In the western United States, severe and widespread drought conditions in recent years have only served to increase the demand for streamflow reconstructions by water management personnel who have recognized the value of the extended records.

New methods are constantly under development to better synthesize the information from streamflow reconstructions for use by water resources professionals. An overriding goal is the adoption of quantitative reconstructions in water resources planning and operations. To this end, perhaps as important as the scientific advances is a proactive approach to communication that includes much direct interaction of tree-ring researchers with water resources professionals and the public to emphasize the potential value of augmented time series of streamflow.

References

Barnett T, Malone R, Pennell W, Stammer D, Semtner B, Washington W (2004) The effects of climate change on water resources in the West: introduction and overview. Climatic Change 62:1–11

Biondi F, Kozubowski TJ, Panorska AK (2005) A new model for quantifying climate episodes. Int J Climatol 25:1253–1264

Boninsegna JA (1992) South American dendroclimatological records. In: Bradley RS, Jones PD (ed) Climate since AD 1500. Routledge, London, pp 446–462

Briffa KR, Jones PD, Schweingruber FH (1988) Summer temperature patterns over Europe: a reconstruction back to AD 1750 based on maximum latewood density indices of conifers. Quaternary Res 30:35–52

Briffa KR, Jones PD, Schweingruber FH, Karlen W, Shiyatov SG (1996) Tree-ring variables as proxy-climate indicators: problems with low-frequency signals. In: Jones PD, Bradley RS, Jouzel J (eds) Climatic variations and forcing mechanisms of the last 2,000 years, NATO ASI Series, vol 141. Springer-Verlag, Berlin, Heidelberg, pp 9–41

Brito-Castillo L, Diaz-Castro S, Salinas-Zavala CA, Douglas AV (2003) Reconstruction of long-term winter streamflow in the Gulf of California continental watershed. J Hydrol 278:39–50

Brockway CG, Bradley AA (1995) Errors in streamflow drought statistics reconstructed from tree-ring data. Water Resour Res 31(9):2279–2293

Case RA, MacDonald GM (2003) Tree-ring reconstructions of streamflow for three Canadian prairie rivers. J Am Water Resour Assoc 39(3):703–716

Chow VT (1964) Runoff. In: Chow VT (ed) Handbook of applied hydrology: a compendium of water-resources technology. McGraw-Hill, New York, pp 14.1–14.54

Cleaveland MK (2000) A 963-year reconstruction of summer (JJA) streamflow in the White River, Arkansas, USA, from tree rings. Holocene 10(1):33–41

Cleaveland MK, Stahle DW (1989) Tree-ring analysis of surplus and deficit runoff in the White River, Arkansas. Water Resour Res 25(6):1391–1401

Cleaveland MK, Stahle DW, Therrell MD, Villanueva-Diaz J, Burns BT (2003) Tree-ring reconstructed winter precipitation and tropical teleconnections in Durango, Mexico. Climatic Change 59:369–388

Cook ER, Briffa K (1990) A comparison of some tree-ring standardization methods. In: Cook ER, Kairiukstis LA (ed) Methods of dendrochronology: applications in the environmental sciences. Kluwer, London, pp 153–162

Cook ER, Jacoby GC (1983) Potomac River streamflow since 1730 as reconstructed by tree rings. J Clim Appl Meteorol 22(10):1659–1672

Cook ER, Shiyatov S, Mazepa V (1990) Estimation of the mean chronology. In Cook ER, Kairiukstis LA (ed) Methods of dendrochronology: applications in the environmental sciences. Kluwer, London, pp 123–132

Cook ER, Briffa KR, Meko DM, Graybill DA, Funkhouser G (1995) The 'segment length curse' in long tree-ring chronology development for palaeoclimatic studies. Holocene 5(2): 229–237

Cook ER, Woodhouse C, Eakin CM, Meko DM, Stahle DW (2004) Long-term aridity changes in the western United States. Science 306:1015–1018

D'Arrigo R, Cullen HM (2001) A 350-year (AD 1628–1980) reconstruction of Turkish precipitation. Dendrochronologia 19(2):169–177

Dracup J, Lee KS, Paulson EG (1980) On the definition of droughts. Water Resour Res 16(2): 297–302

Dunne T, Leopold LB (1978) Water in environmental planning. W.H. Freeman, New York, 818pp

Earle CJ, Fritts HC (1986) Reconstructed riverflow in the Sacramento River basin since 1560. Report to California Department of Water Resources, Agreement No. DWR B55398, Laboratory of Tree-Ring Research, University of Arizona, Tucson

Fritts HC (1976) Tree rings and climate. Academic, London

Fritts HC, Blasing TJ, Hayden BP, Kutzbach JE (1971) Multivariate techniques for specifying tree growth and climatic relationships and for reconstructing anomalies in paleoclimate. J Appl Meteorol 10(5):845–864

Garrick D, Jacobs K (2005) Tree-ring record informs water management decisions. Southwest climate outlook, May 2005, Climate Assessment for the Southwest (CLIMAS), University of Arizona, Tucson, pp 2–3

Gedalof Z, Peterson DL, Mantua NJ (2004) Columbia River flow and drought since 1750. J Am Water Resour Assoc 40:1579–1592

Graumlich LJ, Pisaric MFJ, Waggoner LA, Littell JS, King JC (2003) Upper Yellowstone River flow and teleconnections with Pacific basin climate variability during the past three centuries. Climatic Change 59:245–262

Harding BL, Sangoyomi TB, Payton EA (1995) Impacts of a severe sustained drought on Colorado River water resources. Water Resour Bull 316(5):815–824

Hardman G, Reil OE (1936) The relationship between tree-growth and stream runoff in the Truckee River basin, California–Nevada. Agricultural Experiment Station, Bulletin no 141, January. University of Nevada, Reno, Nevada, 38pp

Hawley FM (1937) Relationship of southern cedar growth to precipitation and runoff. Ecology 18(3):398–405

Hidalgo HG, Piechota TC, Dracup JA (2000) Alternative principal components regression procedures for dendrohydrologic reconstructions. Water Resour Res 36(11):3241–3249

Hirschboeck KK, Meko DM, Morino K, Welti J, Czyzowska E (2005) Collaboration between water managers and tree-ring researchers to evaluate long-term extreme streamflow episodes in the Salt-Verde and upper Colorado River basins. Oral presentation, Association of American Geographers annual meeting, April 5, Denver, Colorado

Hosking JRM (1985) Fractional differencing modeling in hydrology. Water Resour Bull 21(46):677–682

Jacobs K, Meko D, Nijssen B, Colby B (2005) Enhancing water supply reliability through improved predictive capacity and response. Oral presentation in session, Drought analysis, prediction, and impact mitigation, American Geophysical Union 2005 fall meeting, December 7, San Francisco

Jain S, Woodhouse CA, Hoerling MP (2002) Multidecadal streamflow regimes in the interior western United States: implications for the vulnerability of water resources. Geophys Res Lett 29:2036–2039. doi:10.1029/2001GL014278

Kaennel M, Schweingruber FH (1995) Multilingual glossary of dendrochronology. Paul Haupt, Berne

Keen FP (1937) Climate cycles in eastern Oregon as indicated by tree rings. Mon Weather Rev 98:142–153

Leavitt SW, Wright WE (2002) Spatial expression of ENSO, drought, and summer monsoon in seasonal Del^{13}C of ponderosa pine tree rings in southern Arizona and New Mexico. J Geophys Res 107(D18):1–10

Loaiciga HA, Haston L, Michaelsen J (1993) Dendrohydrology and long-term hydrologic phenomena. Rev Geophys 31:151–171

Lodewick JE (1930) Effect of certain climatic factors on the diameter growth of longleaf pine in western Florida. J Agr Res 41(5):349–363

Meko DM (1997) Dendroclimatic reconstruction with time varying subsets of tree indices. J Climate 10:687–696

Meko DM (2001) Reconstructed Sacramento River system runoff from tree rings. Report prepared for the California Department of Water Resources under agreement no. B81923-SAP # 4600000193. Tucson, Arizona. Available from: California Department of Water Resources, P.O. Box 942836, Room 1601, Sacramento, California 94236–0001

Meko DM (2002) Tree-ring study of hydrologic variability in the Peace-Athabasca Delta, Canada. Report summarizing research project contracted to University of Arizona by law firm of Lawson Lundell, 1600 Cathedral Place, 925 West Georgia St., Vancouver, British Columbia, Canada V6C3L2

Meko DM (2006) Tree-ring inferences on water-level fluctuations of Lake Athabasca. Can Water Resour J 31(4):229–248

Meko DM, Baisan CH (2001) Pilot study of latewood-width of conifers as an indicator of variability of summer rainfall in the North American Monsoon region. Int J Climatol 21:697–708

Meko DM, Graybill DA (1995) Tree-ring reconstruction of upper Gila River discharge. Water Resour Bull 31(4):605–616

Meko DM, Stockton CW (1988) Tree-ring inferences on historical changes in the level of Great Salt Lake. In: Kay PA, Diaz HF (eds) Problems and prospects for predicting Great Salt Lake level. Center for Public Affairs and Administration, University of Utah, Salt Lake City, Utah, pp 63–76

Meko DM, Woodhouse CA (2005) Tree-ring footprint of joint hydrologic drought in Sacramento and upper Colorado River basins, western USA. J Hydrol 308:196–213

Meko DM, Stockton CW, Boggess WR (1995) The tree-ring record of severe sustained drought. Water Resour Bull 31(5):789–801

Meko DM, Therrell MD, Baisan CH, Hughes MK (2001) Sacramento River flow reconstructed to AD 869 from tree rings. J Am Water Resour Assoc 37(4):1029–1040

Michaelsen J, Loaiciga HA, Haston L, Garver S (1990) Estimating drought probabilities in California using tree rings. California Department of Water Resources report B-57105, Department of Geography, University of California, Santa Barbara

Mote PW, Hamlet AF, Clark MP, Lettenmaier DP (2005) Declining mountain snowpack in western North America. Bull Am Meteorol Soc 86:39–49

Norton DA, Palmer JG (1992) Dendroclimatic evidence from Australasia. In Bradley RS, Jones PD (eds) Climate since AD 1500. Routledge, London, pp 463–482

Osborn TJ, Briffa KR, Jones PD (1997) Adjusting variance for sample-size in tree-ring chronologies and other regional mean time series. Dendrochronologia 15:89–99

Pederson N, Jacoby GC, D'Arrigo RD, Cook ER, Buckley BM (2001) Hydrometeorological reconstructions for northeastern Mongolia derived from tree rings: 1651–1995. J Climate 14:872–881

Pederson GT, Fagre DB, Gray ST, Graumlich LJ (2004) Decadal-scale climate drivers for glacial dynamics in Glacier National Park, Montana, USA. Geophys Res Lett 31(12):L12203. doi:10.1029/2004GL019770

Peterson DL, Silsbee DG, Redmond KT (1999) Detecting long-term hydrological patterns at Crater Lake, Oregon. Northwest Sci 73(2):121–130

Phipps RL (1983) Streamflow of the Occoquan River in Virginia as reconstructed from tree-ring series. Water Resour Bull 19(5):735–743

Potts HL (1962) A 600-year record of drought recurrences. First water resources engineering conference, American Society of Civil Engineers, May 16, 1962, Omaha, Nebraska

Prairie JR (2006) Stochastic nonparametric framework for basin-wide streamflow and salinity modeling: application for the Colorado River basin. PhD dissertation, University of Colorado, Department of Civil, Environmental, and Architectural Engineering, 142pp

Rantz SE (1982) Measurement and computation of streamflow: vol 1, measurement of stage and discharge. Geological Survey water-supply paper 2175. US Government Printing Office, Washington, DC

Salas JD, Delleur JW, Yevjevich VM, Lane WL (1980) Applied modeling of hydrologic time series. Water Resources Publications, Littleton, Colorado

Schulman E (1945a) Tree-ring hydrology of the Colorado River basin. University of Arizona bulletin XVI(4). University of Arizona, Tucson, 51pp

Schulman E (1945b) Runoff histories in tree rings of the Pacific Slope. Geogr Rev 35:59–73

Schulman E (1947) Tree-ring hydrology in southern California. University of Arizona bulletin XVIII(3). University of Arizona, Tucson, 36pp

Schulman E (1951) Tree-ring indices of rainfall, temperature, and river flow. In: Compendium of meteorology, American Meteorological Society, Boston, pp 1024–1029

Schulman E (1956) Dendroclimatic changes in semiarid America. University of Arizona Press, Tucson, Arizona, 142pp

Shamir E, Meko DM, Graham NE, Georgakakos KP (2007) Hydrologic model for water resources planning in the Santa Cruz River, southern Arizona. J Am Water Resour Assoc 437(5): 1155–1170

Sigafoos RS (1964) Botanical evidence of floods and flood-plain deposition. US Geological Survey professional paper 485-A. Washington, DC

Smith LP, Stockton CW (1981) Reconstructed streamflow for the Salt and Verde Rivers from tree-ring data. Water Resour Bull 17(6):939–947

St. George S, Nielsen E (2002) Hydroclimatic change in southern Manitoba since AD 1409 inferred from tree rings. Quaternary Res 58(2):103–111

Stewart IT, Cayan DR, Dettinger MD (2004) Changes in snowmelt runoff timing in western North America under a 'business as usual' climate change scenario. Climatic Change 62:217–232

Stockton CW (1975) Long-term streamflow records reconstructed from tree rings. Papers of the Laboratory of Tree-Ring Research 5. University of Arizona Press, Tucson, Arizona, 111pp

Stockton CW, Boggess WR (1980a) Tree rings: a proxy data source for hydrologic forecasting. In: North RM, Dworsky LB, Allee DJ (eds) Symposium proceedings, unified river basin management. American Water Resources Association, Minneapolis, Minnesota, pp 609–624

Stockton CW, Boggess WR (1980b) Augmentation of hydrologic records using tree rings. In: Henry WP (ed) Improved hydrologic forecasting: how and why. American Society of Civil Engineers, New York, pp 239–265

Stockton CW, Boggess WR (1982) Climatic variability and hydrologic processes: an assessment for the southwestern United States. In: Proceedings of the international symposium on hydrometeorology, American Water Resources Association, June 13–17, 1982, Denver, Colorado, pp 317–320

Stockton CW, Fritts HC (1973) Long-term reconstruction of water level changes for Lake Athabasca by analysis of tree rings. Water Resour Bull 9(5):1006–1027

Stockton CW, Jacoby GC (1976) Long-term surface-water supply and streamflow trends in the upper Colorado River basin. Lake Powell Research Project Bulletin No 18, Institute of Geophysics and Planetary Physics, University of California at Los Angeles, 70pp

Stokes MA, Smiley TL (1968) An introduction to tree-ring dating. The University of Arizona Press, Tucson

Tarboton DG (1995) Hydrologic scenarios for severe sustained drought in the southwestern United States. Water Resour Bull 31(5):803–813

Touchan R, Meko DM, Hughes MK (1999) A 396-year reconstruction of precipitation in southern Jordan. J Am Water Resour Assoc 35(1):49–59

Touchan R, Garfin GM, Meko DM, Funkhouser G, Erkan N, Hughes MK, Wallis BS (2003) Preliminary reconstructions of spring precipitation in southwestern Turkey from tree-ring width. Int J Climatol 23:157–171

Vaganov EA (1990) The tracheidogram method in tree-ring analysis and its application. In: Cook ER, Kairiukstis LA (eds) Methods of dendrochronology: applications in the environmental sciences. Kluwer, London, pp 63–76

Vaganov EA, Hughes MK, Shashkin AV (2006) Growth dynamics of conifer tree rings: images of past and future environments. Springer, New York

Watson E, Luckman BH (2004) Tree-ring-based mass-balance estimates for the past 300 years at Peyto Glacier, Alberta, Canada. Quaternary Res 62(1):9–18

Webb RS, Woodhouse CA (2003) Tree ring-derived ensembles of streamflow reconstructions for the Gunnison River basin. Eos Trans. AGU, 84(46), Fall Meet. Suppl., Abstract GC52B-04, 2003

Wigley TML, Briffa KR, Jones PD (1984) On the average value of correlated time series, with applications in dendroclimatology and hydrometeorology. J Clim Appl Meteorol 23:201–213

Woodhouse CA (2001) A tree-ring reconstruction of streamflow for the Colorado Front Range. J Am Water Resour Assoc 37(3):561–570

Woodhouse CA, Lukas JJ (2006) Multi-century tree-ring reconstructions of Colorado streamflow for water resource planning. Climatic Change 78(2–4):293–315

Woodhouse CA, Gray ST, Meko DM (2006) Updated streamflow reconstructions for the upper Colorado River basin. Water Resour Res 42:W05415. doi:10.1029/2005WR004455

Yanosky T, Jarrett RD (2002) Dendrochronologic evidence for the frequency and magnitude of paleofloods. In: House PK, Webb R, Baker VR, Levish DR (eds) Ancient floods, modern hazards: principles and applications of paleoflood hydrology, water science and application, Water Science and Application Series. American Geophysical Union, vol 5. Washington, DC, pp 77–89

Young RA (1995) Coping with a severe sustained drought on the Colorado River: introduction and overview. Water Resour Bull 316:779–788

Chapter 9
Climatic Inferences from Dendroecological Reconstructions

Thomas W. Swetnam and Peter M. Brown

Abstract Tree rings have long been employed by ecologists to study the local-scale dynamics of forest stands and woodlands, but only recently have network approaches been applied to evaluate regional and broader-scale processes. As with dendroclimatic data (e.g., ring-width and ring-density chronologies), climatic drivers become much more evident in dendroecological data aggregated at broad spatial scales (relative to local-scale data). Study of dendroecology networks has led to new insights on climatic variability and change and their impacts on ecosystems. In addition to the power of network approaches, dendroecology has advanced in recent decades because of the ready availability of, and comparison with, high quality, independent dendroclimatic reconstructions of various hydro-climatic parameters (e.g., drought indices, precipitation and temperature) and ocean-atmosphere indices (e.g., ENSO, PDO, and AMO). Dendroecological reconstructions that have been most commonly employed in climate-related analyses are disturbance histories (e.g., fire and insect outbreaks). We review examples of these applications from our studies in the Southwestern United States. We also compile and describe here, for the first time, a regional network of ponderosa pine (*Pinus ponderosa*) establishment dates from the Southwest, and we show that episodic natality patterns are probably associated with decadal wet periods. Using another example of decadal variability in forest fire histories—specifically a hiatus in fire occurrence in the circa 1780–1840 time period—we make a case that regional to continental-scale dendroecological reconstructions can provide useful insights about 'ecologically-effective climate change'. We define this type of climatic variability as the patterns of climate at interannual, decadal and centennial scales that are most distinctly reflected in synchronous ecological responses at regional and broader scales. In the context of dendroclimatology, primary values of the investigation of specific climatic patterns that elicit regional and broader ecological responses

T.W. Swetnam (✉)
Laboratory of Tree-Ring Research, The University of Arizona, Tucson, AZ 85721, USA
e-mail: tswetnam@ltrr.arizona.edu

M.K. Hughes et al. (eds.), *Dendroclimatology*, Developments in Paleoenvironmental Research 11, DOI 10.1007/978-1-4020-5725-0_9,

is that these studies provide insights about climate variability that is relevant to ecosystems, and in turn, human concerns about future climate change impacts on ecosystems.

Keywords Dendroecology · Forest fires · Insect outbreaks · Tree demography

9.1 Introduction

Dendroecology—the application of tree-ring analysis to ecological questions—is a rapidly expanding subfield of dendrochronology with increasing relevance to the study of past and present ecosystems and climatic variations. Ecologists have typically focused on short-term studies (<10 years) at fine spatial scales (<1000 m^2), but the importance of long-term and broadscale processes is increasingly appreciated (Ricklefs 1987; Levin 1992; Turner et al. 1993; Brown 1995). Many ecosystem processes, especially those affected by climate changes, manifest themselves only over longer time periods and broader spatial scales than encompassed in typical ecological studies. Understanding the dynamics of long-lived organisms and ecosystems—and the role of climate in controlling these dynamics—requires decadal to centennial and landscape- to regional-scale perspectives. Various types of tree-ring data can provide the depth of temporal and spatial information needed for multiscale, comparative analyses to fully evaluate climatic effects on ecosystems (Fritts and Swetnam 1989; Schweingruber 1996; Swetnam et al. 1999).

The most common types of dendroecological datasets with relevance to studies of climate effects are disturbance histories (e.g., chronologies of forest fires and insect outbreaks) and demographic histories of tree populations (chronologies of tree natality and/or mortality). For both of these types of datasets, there are—or there is the potential for development of—broad networks of data from multiple sites that allow for regional-scale analyses. Disturbance and demographic processes are driven by both internal system dynamics (e.g., species life histories and community dynamics, such as competition) as well as by external factors such as climate. Generally, evidence for climate effects emerges only at larger spatial and longer temporal scales because of the 'noise' introduced by local, internal ecological processes. There have been a variety of dendroecological studies that primarily focused on internal stand or community ecological dynamics (e.g., Spencer 1964; Clark et al. 1975; Lorimer 1985; Frelich and Graumlich 1994; Kneeshaw and Bergeron 1998; Morneau and Payette 2000). These studies were carried out at the stand or watershed scales and climatic analyses were not included, or they were limited because of the fine spatial scale of the datasets. In contrast, broader studies examining climate effects on ecosystem dynamics have used network-based approaches involving many sites distributed across mountain ranges or regions (i.e., 10^4 to $>10^6$ km^2; e.g., Kitzberger et al. 1997; Villalba and Veblen 1997a; Kitzberger and Veblen 1998; Swetnam and Betancourt 1998; Veblen et al. 1999, 2000; Brown and Shepperd 2001; Brown 2006; Sibold and Veblen 2006; Kitzberger et al. 2007).

Networks of well-dated disturbance and demographic chronologies can be aggregated at multiple spatial scales to enhance common patterns, just as is done in regional networks of ring-width or ring-density chronologies. Climatic influence emerges as patterns of synchrony (or asynchrony) of events, oscillations, or trends. Very broadscale synchrony (at $>10^4$ km^2 scales) is typically related to climate variability affecting the co-occurrence of ecological events in many places, because most ecological disturbances or processes are not capable of physically spreading over such large areas. For example, fires generally can not burn across the enormous desert valleys and canyons that separate forested mountain ranges in the American Southwest. Therefore, synchrony of annual fire events (or absence of fire events) among these widely dispersed mountain ranges has to be related to regional-scale, fire-inducing (or -suppressing) climatic conditions, such as regional drought (wet) events (Swetnam and Baisan 1996).

In general, synchrony of disturbance events and demographic processes at regional or broader scales can be inferred to reflect climatic influences. An apt analogy is crossdating of tree-ring measurements among trees and sites. In the case of tree-ring widths or densities, it is understood that numerous unique or local factors (e.g., soils, competition, genetics, human land uses, etc.) at the scales of trees and forest stands may affect cambial growth and thereby introduce nonsynchronous, non-climatic signals in tree-ring time series (Cook 1990). However, when sites and trees are carefully selected to maximize climatic sensitivity and ring series from many locations are combined, the existence of broadscale crossdating (i.e., synchrony) of ring patterns across regions is logically and demonstrably related—both statistically and mechanistically—to climatic variations (e.g., Fritts 1976). Likewise, disturbance and demographic events are affected by numerous local factors, but if common, synchronous patterns emerge across broadscale networks, those ecological patterns are most probably climatic in origin. Interpretations of these causal relations are most robust when coupled with mechanistic understanding of climatic/ecological processes, such as the effects of water balance on fuel productivity, fuel moisture content and fire occurrence (e.g., Swetnam and Betancourt 1998; Westerling et al. 2006).

Assembly of regional- to continental-scale networks of disturbance and tree demographic histories is just beginning (see the International Multiproxy Paleofire Database at: http://www.ncdc.noaa.gov/paleo/impd/). Analogous development of tree-ring width networks in North America and South America began in the 1950s with Edmund Schulman's work (Schulman 1956), and continued through the 1970s and 1980s with Harold Fritts' efforts (Fritts 1976, 1991). Many other dendrochronologists have assembled tree-ring data networks and contributed these to publicly accessible databases (see the International Tree-Ring Data Bank at http://www.ncdc.noaa.gov/paleo/treering.html). These datasets have now been applied in continental to global-scale dendroclimatic reconstructions (e.g., Fritts 1991; Briffa et al. 1994; Mann et al. 1998, 1999; Cook et al. 1999, 2004). In addition to providing an example for dendroecology of the power of the network approach, dendroclimatic networks provide a tremendous source of comparative data. Replicated time series of reconstructed hydroclimate variables or global

circulation indices are often used to evaluate the effects of annual to multicentennial climate variability and change on ecosystems. The easy availability of these climate reconstructions is now stimulating a surge of dendroecological research with a climatic focus.

The fact that synchronous ecological processes occur at very broad spatial scales (e.g., Hawkins and Holyoak 1998; Koenig and Knops 1998), and that this synchrony is driven in part by climatic variability (e.g., Swetnam 1993; Villalba and Veblen 1997a; Swetnam and Betancourt 1998; Brown and Wu 2005), raises important questions for both ecology and climatology:

- How can chronologies and networks of ecological patterns be used to study past climate variability and change?
- How does climate entrain ecological disturbance events and population dynamics (natality and mortality) at regional and broader scales?
- When and in what manner do climate-forced effects override internal or local factors (e.g., competition, predation, random variations) in determining the dynamics of ecosystems?
- How can we use our understanding of past climate influences on ecosystems at long-term and broad scales to predict impacts of future climate change on ecosystem structure, function, and disturbance dynamics?

In this chapter we describe several examples of ecological disturbances and population dynamics that are influenced by climatic variations. In particular, we illustrate how spatial networks are useful for evaluating climatic and ecological relationships by drawing upon our own fire history, insect outbreak, and tree population studies in the western United States. In addition to describing and discussing the ecological insights and implications of these tree-ring studies, we also focus on their relevance for climatological investigations. We compile both regional tree recruitment and fire occurrence data to highlight an unusual hiatus of forest fire occurrence in the western United States and southern South America during the early 1800s as an example of what we term here as an 'ecologically effective climate change.'

9.2 Examples of Dendroecological-Climate Reconstructions

9.2.1 Fire History and Fire Climatology

Fire history studies using crossdated fire-scarred trees are the most common type of dendroecological analysis involving assessments of climatic effects. There are numerous examples of subregional to continental (and even intercontinental) studies of fire climatology using fire-scar chronologies and various hydroclimatic reconstructions (e.g., see summaries in Veblen et al. 2003). Fire-scarred trees are a fortuitous ecological and physical phenomenon, whereby past fire events (primarily low-intensity surface fires) create very distinctive lesions within tree-ring series

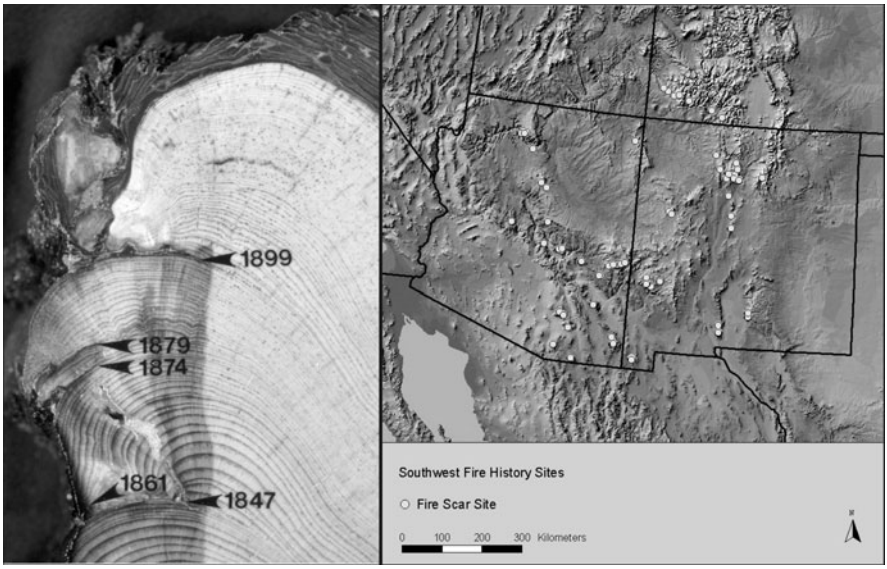

Fig. 9.1 Photograph of a cross section of a fire-scarred ponderosa pine (*left*), and map of locations of 120 fire-scar collection sites in the southwestern United States (*right*). The arrows on the cross section point to fire scars created when surface fires burned near the base of this tree. After each fire left a scar, subsequent tree rings grew over the dead tissue. The last fire scar in 1899, and subsequent century of growth with no fire scars, reflects the effects of fire suppression and the exclusion of widespread surface fires

(Fig. 9.1). The ubiquitous presence of fire-scarred trees in many forests worldwide has provided evidence to reconstruct detailed chronologies of fire history in hundreds of forest stands (e.g., Kitzberger et al. 2007). Fire history networks are now the most developed among dendroecological data networks, with more than 400 fire-scar time series included in the International Multiproxy Paleofire Database (http://www.ncdc.noaa.gov/paleo/impd/).

The power of a dendroecological network for assessing fire/climate relationships is illustrated here with an example from the southwestern United States. At present, there are a total of 120 crossdated fire-scar chronologies that have been compiled from sites in Arizona and New Mexico (Fig. 9.1). Site chronologies typically are composed of sets of 20 or more fire-scarred trees sampled in forest stands of about 10–100 hectares in size (see Swetnam and Baisan 1996, 2003, and references therein for details of site selection and other details). Compilation of fire dates recorded among multiple sites results in a regional fire chronology, which documents years when both highly synchronous fires were burning in many sites across the region as well as years when few fires occurred (Fig. 9.2).

The Southwestern regional fire chronology documents strong relationships both with hydroclimatic variables and with ocean-atmosphere indices, such as the El Niño/Southern Oscillation (ENSO; Figs. 9.3 and 9.4). Regional fire years—defined as years when fire scars were recorded on trees at more than 20 sites—mainly

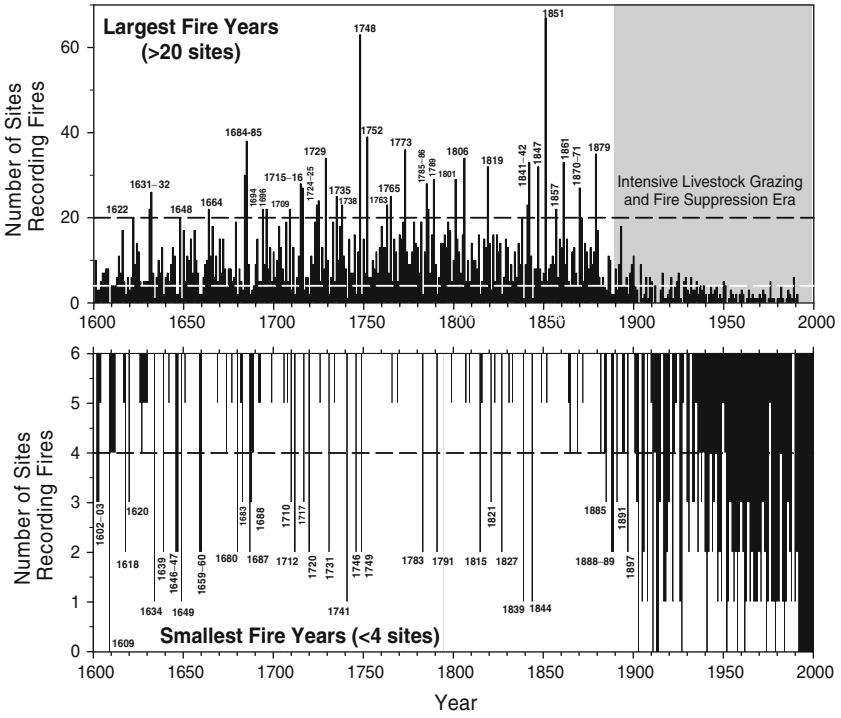

Fig. 9.2 The number of sites recording fire scars in the southwestern United States from 1600 to 2000. This chronology of regional fire occurrence is based on the 120-site network shown in Fig. 9.1. The largest regional fires are labeled in the *upper* plot, and the *dashed lines* show the threshold of >20 sites and <4 sites used to identify 'large' and 'small' regional fire years, respectively. The *lower* plot shows the smallest fire years. Note that the values in the *upper* plot are shown as *black vertical bars* on a white background, and in the *lower* plot the values are *white vertical bars* on a black background. Because these were mainly surface fires burning through grass and herbaceous fuels, the widespread introduction of livestock grazing that accompanied Euro-American settlement in the late 1800s led to the decline of fires in virtually all sites

occurred during relatively dry years of a set of gridded, independently derived reconstructions of summer Palmer Drought Severity Indices (PDSIs; Cook et al. 2004; Fig. 9.3, top panel). In contrast, years during which almost no fires were recorded around the region tended to occur during relatively wet years. Regional fire years also tended to occur during years of cool sea surface temperature (SST) conditions (low Niño-3, an index of ENSO, which are La Niña years), while all but one of the small fire years occurred during warm sea surface temperature conditions (Fig. 9.3, bottom panel; El Niño years).

These patterns are supported by superposed epoch analysis (SEAs; Fig. 9.4). Superposed epoch analysis is used to compare average annual climate anomalies for the set of regional fire years to climate for the entire period of the climate reconstructions (Swetnam 1993). Superposed epoch analysis also is used to compare climate

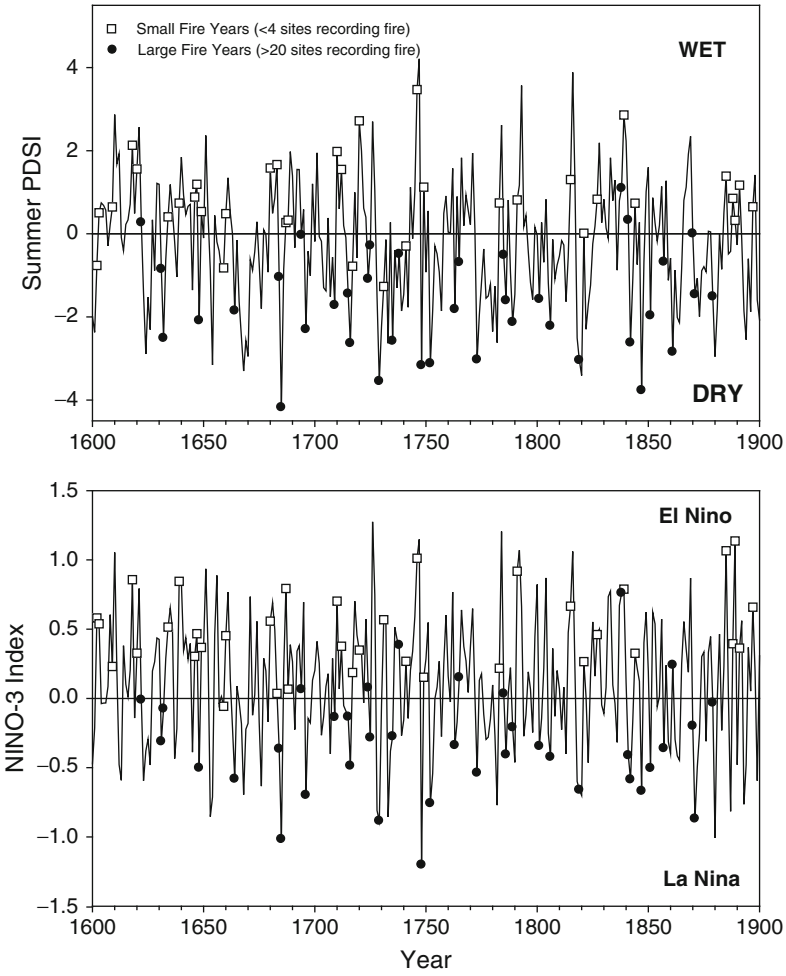

Fig. 9.3 (*Upper plot*) Tree-ring-reconstructed summer (July–August) Palmer Drought Severity Index (PDSI; *solid line*) (from Cook et al. 2004), shown with the largest and smallest regional fire years identified from the 120-site fire-scar network from the southwestern United States (*lower plot*). Tree-ring reconstructed Niño-3 index of sea surface temperatures (SSTs; Cook 2000), shown with the same set of largest and smallest regional fire years

during years prior to fire years to assess antecedent conditions that may have been important for fire occurrence. Significant climate anomalies are assessed by using bootstrapped confidence intervals based on distributions of annual climate values. Results of SEA from the Southwest regional data confirm that, on average, the larger fire years occurred during drought years and La Niña events, and that the small fire years occurred during the opposite patterns of pluvial years and El Niño events (Fig. 9.4). Interestingly, SEA also often shows that there were significant lagging relationships in climate/ecosystem dynamics, with fire years typically following

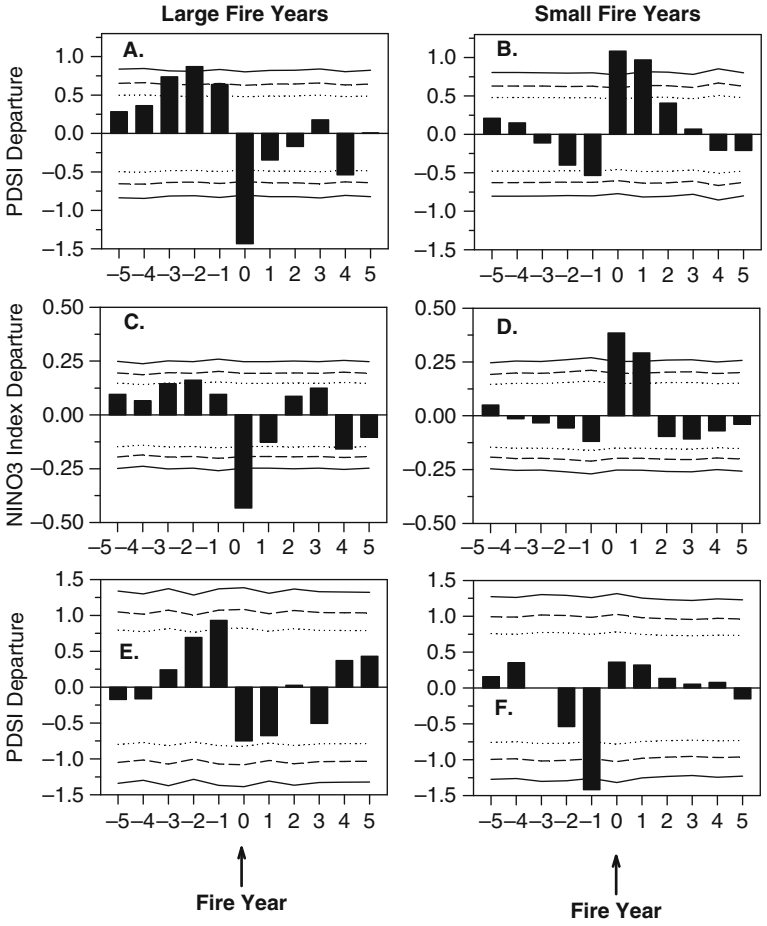

Fig. 9.4 Superposed epoch analysis (SEA) of large and small regional fire years in relation to summer Palmer Drought Severity Indices (PDSIs) in the southwestern United States and Niño-3 sea surface temperature (SST). Plots **A** and **B** show results for largest (38) and smallest (36) fire years during the period 1600–1900, using tree-ring width reconstructions of southwestern PDSI (Cook et al. 2004). Plots **C** and **D** show results from SEA using the same sets of fire years against a reconstruction of Niño-3, an index of the El Niño/Southern Oscillation (ENSO) (Cook 2000). Plots **E** and **F** show SEA results using modern PDSI based on instrumental data and the largest (19) and smallest (23) fire years from area burned records from all federal, state, and private lands in Arizona and New Mexico during the period 1905–2004. Lines in each plot represent the 0.05, 0.01, and 0.001 confidence intervals based on Monte Carlo simulations of random distributions of annual climate conditions for PDSI and Niño-3

1–3 years of wet conditions. These fires were mainly surface fires, burning in grasses and herbaceous fuels, and wet conditions would have resulted in more continuous and denser fuels that would have burned more readily and have been widespread during subsequent drought years (e.g., Brown and Wu 2005).

Overall, the Southwest climate and fire comparisons (Figs. 9.3 and 9.4) not only illustrate the close coupling between wet/dry patterns and fire in this region, but they also provide a strong confirmation of the high fidelity of these two types of dendrochronological reconstructions. The regional reconstructed climate and fire time series are based on independently collected and quite different types of tree-ring data. The climate-sensitive trees used to develop the drought and Niño-3 reconstructions generally come from dry, rocky sites where fire spread is unlikely, and ring widths are the measured variable. The fire-scar records generally come from ponderosa pine and mixed conifer forests in the same region, but typically in sites where grass and pine needle understories could carry widespread fires. Fire scars are the primary observed variable in these time series. Despite these differences, the remarkable coincidence of extreme regional dry (wet) years and high (low) fire occurrence suggests that the two kinds of network-based reconstructions are accurately identifying ecologically effective climatic conditions at annual resolutions.

9.2.2 Western Spruce Budworm Outbreaks and Climatic Entrainment

One of the most widespread forest defoliators in the western United States is the western spruce budworm (*Choristoneura occidentalis*). During its larval stage, this Lepidopteran moth is a voracious feeder on the buds and needles of true firs (*Abies* species) and Douglas-fir (*Pseudotsuga menziesii*) trees. The name 'spruce' budworm is a bit of a misnomer, because although spruce trees (*Picea* spp.) are minor hosts, the true firs and Douglas-fir typically suffer much heavier defoliation and higher mortality rates than spruces. Another closely related budworm species (*Choristoneura fumiferana*) occurs throughout eastern Canada and parts of the northeastern United States, where it is the most widespread and important defoliator of conifers. Numerous tree-ring studies have reconstructed outbreak histories of eastern and western spruce budworm (e.g., Blais 1981; Hadley and Veblen 1993; Morin et al. 1993; Swetnam and Lynch 1993; Krause 1997; Jardon 2001; Ryerson et al. 2003), making this an excellent candidate for development of regional (and perhaps continental) networks of outbreak chronologies.

The tree-ring basis for developing outbreak chronologies is the observation of very sharply reduced ring growth in the host species during the defoliation episode, which typically lasts for a decade or longer (Fig. 9.5). The methods involve multiple steps for confidently identifying reduced growth periods as outbreaks (including distinguishing the outbreak signals from potentially confounding climate effects; e.g., droughts), and compiling the observations into stand-level chronologies of outbreak events and subregional composites (see Swetnam et al. 1985; Swetnam and Lynch 1993; and Ryerson et al. 2003). Specifically, the process we have followed includes: (1) the separate development of 'host' and 'non-host' tree species ring-width chronologies from nearby sites, (2) detailed graphical and statistical comparisons of these chronologies against each other and with independent

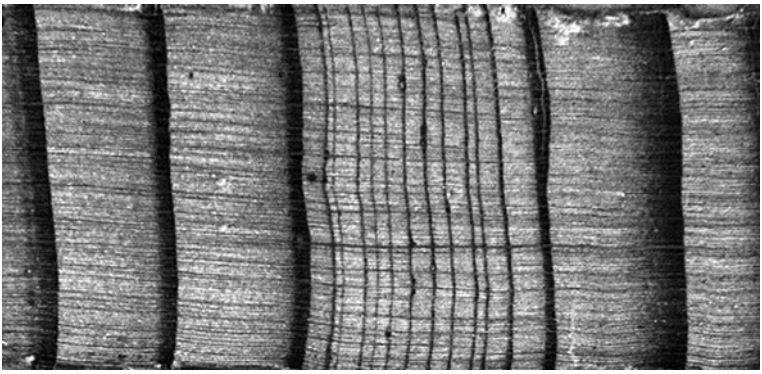

Fig. 9.5 Photograph of reduced tree-ring growth in a Douglas-fir tree due to a defoliation event by western spruce budworm. This type of rapid and sustained growth reduction over a distinct period of time, often followed by a growth surge, is characteristic of defoliation events, and generally is not typical of drought responses

instrumental climate data, (3) the use of the non-host chronologies (if comparison tests are satisfactory) to 'correct' the host chronologies (i.e., to remove most or all of the climate effects from the host chronologies), and (4) validation of the corrected chronologies with independent forest entomology records (e.g., maps and observations of defoliation and/or insect population measurements). The correction procedure involves subtraction of a variance rescaled version of the non-host chronology (index values) from the host chronology.

Resulting 'corrected' budworm-affected chronologies from individual trees or stand averages can then be combined into network composites for subregions. Our original work on this focused primarily on stand-level averages of corrected host ring-width chronologies, and the subregional composites were expressed as 'number of chronologies (stands) recording outbreaks' each year (Fig. 9.6). In subsequent work we found that an 'epidemiological approach,' focusing more on the responses of individual trees and their collective responses, rather than solely on stand averages, was more effective in revealing outbreak timing and magnitudes. Composites of these data are expressed as numbers or percentages of trees (by site or in the whole network) recording an outbreak each year (Fig. 9.6).

One of the consistent findings of our western spruce budworm studies in four subregions of the western United States is a general correspondence between budworm outbreaks and wet periods, coupled with reduced budworm outbreaks (endemic periods) during drought episodes (Fig. 9.6). In detailed analysis of precipitation and temperature variables in the southern Rocky Mountains of New Mexico, Swetnam and Lynch (1993) found that a wetter spring through early summer season (March to June) was best correlated with the regional budworm composite record. In addition to concurrence of wet periods and outbreaks, in cross-correlation and cross-spectral analyses we found that increased wet conditions usually preceded the outbreaks by several years up to a decade. These findings suggest that wet conditions predispose trees and forests to budworm outbreaks.

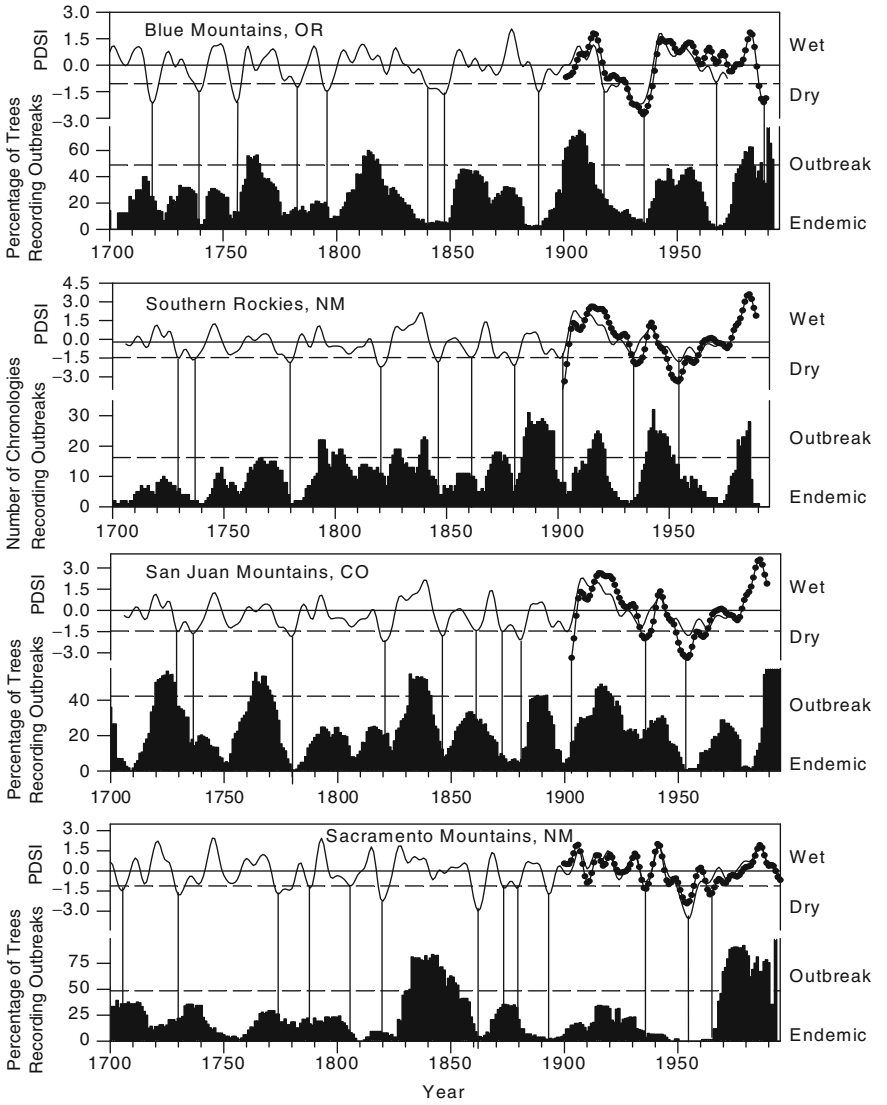

Fig. 9.6 Composite western spruce budworm histories from four subregions in the western United States, compared with smoothed (13-year symmetrical weighted low pass filter) summer (July–August) Palmer Drought Severity Index (PDSI) reconstructions from independent tree-ring width chronologies (Cook et al. 1999). The smoothed PDSI line in the upper graph is tree-ring reconstructed and the smoothed *dotted line* is based on twentieth century instrumental data. *Vertical lines* connect the PDSI and budworm axes at the minimum (1 standard deviation) years of the smoothed PDSI. The Blue Mountains, Oregon, budworm data are partly described in Swetnam et al. (1995). The other budworm datasets are described in Swetnam and Lynch (1993; southern Rockies, New Mexico); Ryerson et al. (2003; San Juan Mountains, Colorado); and Swetnam, Archambault, and Lynch (unpublished; Sacramento Mountains, New Mexico)

The subject of potential climate entrainment of insect outbreaks—and on animal population dynamics in general—has been debated in the ecological literature for decades (e.g., White 1976; Royama 1984; Martinat 1987; Mattson and Haack 1987). A variety of theories have emerged, including the famous 'Moran effect,' based on Moran's theorizing about the oscillatory behavior and regionally synchronized lynx-hare populations of Canada (Moran 1953). In the case of the western spruce budworm, it seems likely that favorable moisture conditions may act through an increase in the quantity and improvement in the quality of tree foliage, the food base for these defoliators (Swetnam and Lynch 1993). Although the exact mechanisms remain unidentified, we think the consistent, coincident patterns in the tree-ring data of wet periods/outbreaks, and droughts/endemic phases over multiple centuries and large regions are quite compelling evidence that decadal moisture variability is an important driver of budworm populations.

Notable features of forest insect outbreak reconstructions from tree rings are the remarkable cycles or quasi-cycles that are evident in these time series (e.g., see Speer et al. 2001). The famous larch budmoth (*Zeiraphera diniana*) of central Europe is the clearest example of relatively strong cyclicity in forest insect populations. These outbreaks produce a distinct tree-ring signature of defoliation events, evident as sharply reduced ring widths and densities that have allowed for reconstructions of up to 1200 years in length (Weber 1997; Esper et al. 2007). The recent work of Esper et al. (2007) demonstrates a remarkable regularity and stability of larch budmoth cycles in the European Alps over the past millennium, with an average period of 9.3 years between outbreaks. The most notable finding in this paper is that the larch budmoth reconstruction (832–2004 CE) reveals the recent period (since 1981) is the most unusual in the entire reconstruction, with an unprecedented absence of outbreaks. Esper et al. (2007) show that this period corresponds to an unprecedented increase in temperatures in this region (from an independent tree-ring reconstruction), and conclude that nutrient cycling and other ecosystem processes operating in the Alps may be undergoing a drastic alteration. Although the exact mechanisms of this change are not known, they speculate that warming winter temperatures may have led to earlier emergence of larvae from their eggs in the late winter or spring before larch tree needles have emerged, leading to starvation and failure of the larch budmoth populations to enter an outbreak phase.

Our regional time series of western spruce budworm typically show more variable oscillatory behaviors than is the case with larch budmoth, with considerable variability in the periods between budworm outbreaks. Hence, budworm population fluctuations appear not to be very strongly cyclic. Nevertheless, as much as 50% to 60% of the variance of the regional composite time series is explained by cycles of about 25–35 years (Swetnam and Lynch 1993; Ryerson et al. 2003). Considering that these data are derived from tree rings, where cycles of this strength are virtually never observed in raw ring-width series from non-host trees, this in itself is a remarkable characteristic of defoliated host trees. Moreover, in cross-correlation and cross-spectral analyses there appears to be some coherence of these moderate-strength outbreak periodicities, and much weaker but similar periodicities in climate reconstructions (Swetnam and Lynch 1993).

A notable example of the use of tree rings in evaluations of animal population dynamics and cyclic environmental variables are the studies of Sinclair et al. (1993; Sinclair and Gosline 1997) of hare populations, climate, and sunspot cycles in Canada. Unfortunately, the physical tree-ring basis of the hare population reconstructions (feeding scars on aspen stems) seems obscure and is not well illustrated or described in these papers. Some of the quantitative time series analyses are also difficult to evaluate. More research in this area, particularly with employment of more rigorous dendrochronological sampling and analysis procedures, may be fruitful in evaluating previous findings, and shedding light on the role of climate and animal population dynamics. New and powerful statistical-analytical tools that are increasingly employed by dendrochronologists and paleoclimatologists might be usefully employed in this endeavor (e.g., univariate and bivariate singular spectrum analysis (SSA), or wavelet analysis; e.g., Speer et al. 2001; Esper et al. 2007).

The periodic and aperiodic behaviors evident in tree-ring-based insect outbreak reconstructions, and their potential coherence with climate, deserve much more study. Most insect population dynamics studies have relied on much shorter observational datasets, which in some cases include only one to a few insect outbreaks (e.g., Royama 1984; Myers 1998) or population 'eruptions' (e.g., Ranta et al. 1997). Tree-ring-based insect outbreak and climate reconstructions for population dynamics research are of potentially great value because numerous population oscillations over periods of centuries can be identified at numerous locations over regions, and even continents. We think there are opportunities here for breakthroughs in our understanding of how climatic variations and oscillations act as potential synchronizing (e.g., the Moran effect) or disrupting factors in plant and animal population dynamics. Given recent enormous outbreaks of bark beetles in concert with climatic changes in North America (e.g., Logan et al. 2003; Breshears et al. 2005), and Esper et al.'s (2007) findings about changes in larch budmoth and temperature in the Alps, the importance of this topic is likely to increase in coming years.

9.2.2.1 Confounding of Dendroclimatic Signals by Insect Outbreaks

One final point regarding insect outbreaks is important in the context of this chapter and book; i.e., the potential confounding influence of insect outbreaks/defoliation on dendroclimatic interpretations from host trees. Dendroclimatologists have long been aware of this as a potential problem (e.g., Morrow and LaMarche 1978), and as a general practice they seek to avoid sampling sites and trees that have a known history of past outbreaks (Fritts 1976). A recent paper by Trotter et al. (2002) evaluated this issue in some detail in pinyon pine (*Pinus edulis*) stands near Flagstaff, Arizona, defoliated by pinyon pine needle scale (*Matsucoccus acalyptus*). They concluded that, indeed, chronic or episodic effects of this insect could alter the dendroclimatic estimates of drought if one were to use tree-ring width series from affected trees.

It is our opinion that the large majority of tree-ring width series that have been sampled and measured for dendroclimatic studies in the western United States do not have a great risk of being confounded with insect outbreak (or chronic insect feeding) signals. This is because most of the major episodic defoliators of conifers

(e.g., western spruce budworm and Douglas-fir tussock moth) generally tend to feed in stands that have relatively closed-canopy conditions, in moderate to highly mesic sites, and at mid-elevations. Stands with *Abies* as a dominant or codominant species, for example, are more vulnerable than pure Douglas-fir stands. In general, these kinds of stands are infrequently sampled for dendroclimatic purposes. The classic western United States drought-sensitive site is an open-canopy conifer stand, in a xeric site, at the lower forest border, with steep slopes and shallow soils (Schulman 1956; Fritts 1976). These are typically the least likely stands to be attacked by western spruce budworm. High-elevation, near-tree-line stands that are often sampled for temperature reconstructions also are generally not affected by budworm or other major defoliators. Although some insect defoliators and stem feeders (e.g., bark beetles) can affect large areas, to the best of our knowledge, past outbreaks have tended to occur in a relatively small proportion of the range of host species.

In addition to the reasons listed above, episodic or chronic defoliation, or past insect-induced mortality within stands is usually visually obvious on trees within the stands, or in the sampled ring-width series (e.g., Fig. 9.6; but see Ryerson et al. 2003 for a case study where outbreak signals were not often visually obvious in the 'uncorrected' ring width series). Within stands, past defoliation events are usually apparent in the presence of trees with old dead tops (spikes), and new dominant crown leaders, and many dead branches that are not simply the result of great age. Also, dead trees from past killing events may be present, and in the case of bark beetles, telltale feeding and egg-laying galleries may be visible on the stems of dead trees for many years after the event (e.g., Perkins and Swetnam 1996).

In summary, the potential confounding effects on tree-ring series of past insect attacks—and other disturbances such as fires—are an important consideration that dendroclimatologists should be more keenly aware of than they generally are. Precautions should be taken to investigate what is known from documentary sources and local experts about the potential occurrence of past outbreaks in areas to be sampled. Dendroclimatologists should have some field and laboratory training and experience in identifying signs of past outbreaks within stands and on tree-ring specimens. We encourage greater awareness of this issue by dendroclimatologists. We also recommend further study of the potential 'contamination' of dendroclimatic databases with insect and other disturbance signals. Perhaps a screening of existing dendroclimatic databases is warranted for potentially unknown insect outbreak signals that may exist in some chronologies from host species in areas with known outbreaks. However, it is our expectation that if there are any such problem chronologies, they are likely to be few.

9.2.3 Regional Tree Demography and Climate Effects

Ecologists have long recognized that time series of tree births and deaths are of fundamental value for understanding forest and woodland dynamics (Blackburn and Tueller 1970; Henry and Swan 1974; Harper 1977). Estimating the age of a tree by counting its annual rings is probably the best-known tree-ring application in history,

extending at least back to the writings of Aristotle. However, from a dendroecological perspective, the determination of tree ages is more complex than simply counting rings, and understanding forest demographic patterns requires much more than merely sampling what one suspects are the oldest trees in a forest. Because rigorous dendroecological analyses of tree demography are somewhat less well described in the literature than disturbance history methods (e.g., fire-scar and fire-history methods), we briefly describe here some key aspects of this tree-ring application in the context of studies that are relevant to climatic influences on forests and woodlands.

There are several important considerations in determining ages of individual trees and hence the age distribution of a forest stand or landscape. First, obtaining accurate dates for tree-ring sequences is of primary importance for ecological and climatic studies, since identification of synchrony of events and processes requires high temporal resolution (Baumgartner et al. 1989; Fritts and Swetnam 1989). Dendrochronological crossdating of ring sequences (Stokes and Smiley 1968; Swetnam et al. 1985) should always be used (or at least attempted) to derive absolute dates for tree-ring sequences. Even in studies where temporal precision of recruitment dates is on the order of 10–20 years, it is usually impossible to know how much error is involved in ring-counted data without first crossdating at least some of the tree-ring sequences. Crossdating is particularly critical for demographic studies in forests that have been selectively harvested (Brown and Cook 2006). Sampling of only living trees in harvested stands may give a biased perspective on the age distribution of the historical forest, as larger (and, hence, generally older) trees are often removed in selective harvest procedures.

In practice it is difficult to determine the exact germination dates of trees. This is due both to limitations in the ability to obtain ring series at the exact point of seedling germination (the 'root-shoot' boundary) and typically indistinct growth patterns in the very earliest years of seedling growth that make identification of annual ring boundaries difficult. Using the most intensive techniques and under the best circumstances, obtaining annual or nearly annual resolution tree germination dates is possible by destructively sampling and re-sectioning trees at multiple levels across the root/shoot boundary (Savage et al. 1996; League and Veblen 2006). However, most studies are limited to pith dates on ring sequences taken from some height above the original germination point; i.e., above the root-shoot boundary (e.g., Villalba and Veblen 1997b; Brown and Wu 2005; Brown 2006). These studies have generally used the terms 'tree establishment' or 'tree recruitment' to refer to the date or period when a tree became successfully rooted as a seedling, rather than the exact date of germination. Often establishment periods of 5–20 years' resolution are used to reflect the relatively low precision in estimates of tree ages.

It is also often difficult to obtain exact death dates of remnant trees. Reasons include difficulties in obtaining usable tree-ring samples from often highly decayed wood, and irregular ring characteristics near the outside, especially in very old trees that were stressed at the time of death. Death dates on remnant trees are also often difficult to determine because sapwood typically decays rapidly after tree death (especially in logs on the ground), which removes an unknown number of rings from the outside of the stem. Again, however, using the most intensive techniques

and with careful consideration of available evidence, annual or near-annual resolution of death dates can be obtained for examination of stand- to landscape-scale mortality events (e.g., Margolis et al. 2007).

Another requirement of tree demographic studies is an adequate sample size. However, no studies to our knowledge have addressed how many trees may be needed to adequately characterize population age structure in varying forests, and more work is needed in this regard. In old, uneven-aged forests, sometimes hundreds of trees must be sampled to obtain adequate characterization of age structure distributions. This requirement is mainly due to the decline in survivorship of trees as they age (often following an inverse J-shaped curve). This decline in quantity or quality of evidence with increasing time before the present is what has been referred to as the 'fading-record' problem, and it is common to paleoecological studies. The oldest trees that represent germination pulses, or 'cohorts,' in the earliest periods may not be detected unless numerous trees are sampled, but again, few studies have addressed this question in any type of systematic manner (but see Johnson et al. 1994). Furthermore, many studies have found relatively poor relationships between tree size and age. Therefore, some sort of systematic sampling procedure should be used to select trees for aging rather than merely selecting the largest trees in a stand.

Similar to tree recruitment dates, preservation of dead trees is a declining function with time before present, and obtaining estimates of past mortality events depends both on persistence of woody material and the ability to adequately sample the material to obtain death dates. Old forests usually contain complex recruitment and mortality patterns, and to temporally resolve the different pulses and hiatus periods of establishment and mortality events often requires very large sample sizes and careful sample techniques, particularly with sampling difficulties of obtaining the bark rings on dead trees.

However, despite these and other difficulties in obtaining high-resolution tree demographic data, concentrated efforts have resulted in very useful time series for evaluating population dynamics related to climatic influences. One of the most successful of these studies to date is the work of Villalba and Veblen (1997a) on *Austrocedrus chilensis* woodlands in Argentina. They demonstrated a clear set of linkages between favorable moisture conditions promoting regional tree cohort establishment, and unfavorable (drought) conditions promoting reduced tree establishment and mortality (Fig. 9.7). Another successful example is a recent study by Brown and Wu (2005) that illustrated the contingent effects of climate and fire occurrence on tree establishment in a ponderosa pine (*Pinus ponderosa)* forest in southwestern Colorado (Fig. 9.8).

Examples of regional- to landscape-scale tree natality, mortality, and climate associations found by Villalba and Veblen (1997a), Brown and Wu (2005), and Brown (2006) inspired us to undertake a 'meta-analysis' of regional tree establishment data in ponderosa pine forests from the southwestern United States. For this analysis, we compiled data from 12 studies that sampled hundreds of ponderosa pine trees distributed around the Southwest (Fig. 9.9). Some of these studies estimated stand densities (number of stems or trees per hectare) from a sampling of trees, while others reported total counts of trees establishing by date or period over

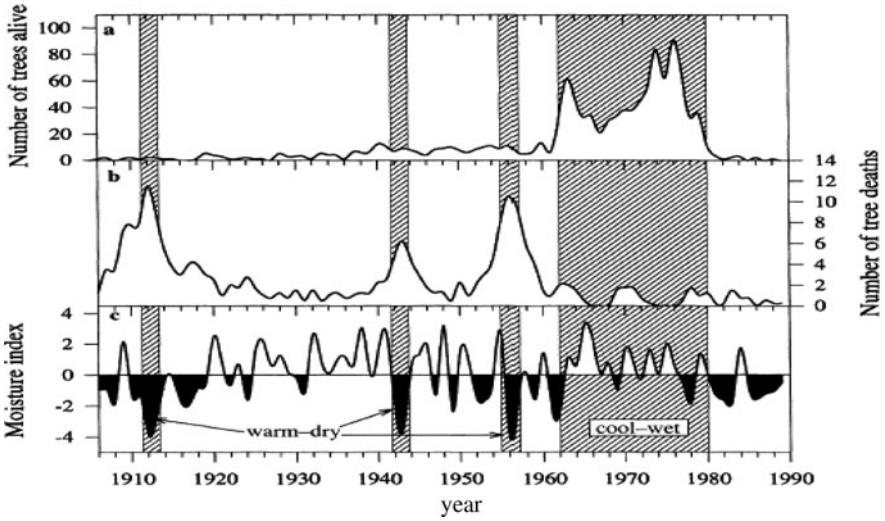

Fig. 9.7 Tree establishment and mortality dates from *Austrocedrus chilensis* woodlands in northern Argentina driven by fluctuations in effective moisture (Villalba and Veblen 1997a). (Reprinted from Villalba and Veblen, with permission from Journal of Ecology, Wiley-Blackwell)

a certain size class within fixed plots or belt transects. There were also differences in the establishment date (period) resolution in the datasets, including 5-, 10-, and 20-year periods.

Regional patterns of synchrony emerge in an overall compilation of the 12 time series in a ponderosa pine 'establishment index' (Fig. 9.10). This time series was derived from the logarithms of the time series values (tree numbers and tree densities; 1.0 was added to all values so that logarithms could be computed for years/decades with zero values) and the ratio of each log-transformed value to the mean of the entire log-transformed series. The regional time series is the average of all the establishment indices computed for each series (site). Logarithmic transformations are useful here because there is a strong tendency for recent periods (especially after 1900) to have one to several orders of magnitude more trees establishing (or surviving) than before this period. Hence, to evaluate relative patterns, the log transform and ratio index help to standardize all datasets for visual comparisons and combination in the regional index time series.

Overall, the regional composite (Fig. 9.10) shows that ponderosa pine forests are typically uneven-aged and the age structures are often dominated by episodes of tree establishment (cohorts) that alternated with multi-decade periods when relatively fewer trees established in the stands. Moreover, the composite suggests that there was substantial regional synchrony of these episodes of establishment (and lack of trees establishing), indicating the likely influence of broadscale climate forcing. In general, the largest cohorts correspond with wetter conditions, as is shown in the comparison with dendroclimatic reconstructions of drought indices (Cook et al. 2004) from the region (Fig. 9.10). In particular, the 1810s–1860s and 1890s–1930s cohorts coincide with exceptionally wet periods. Decreases in establishment

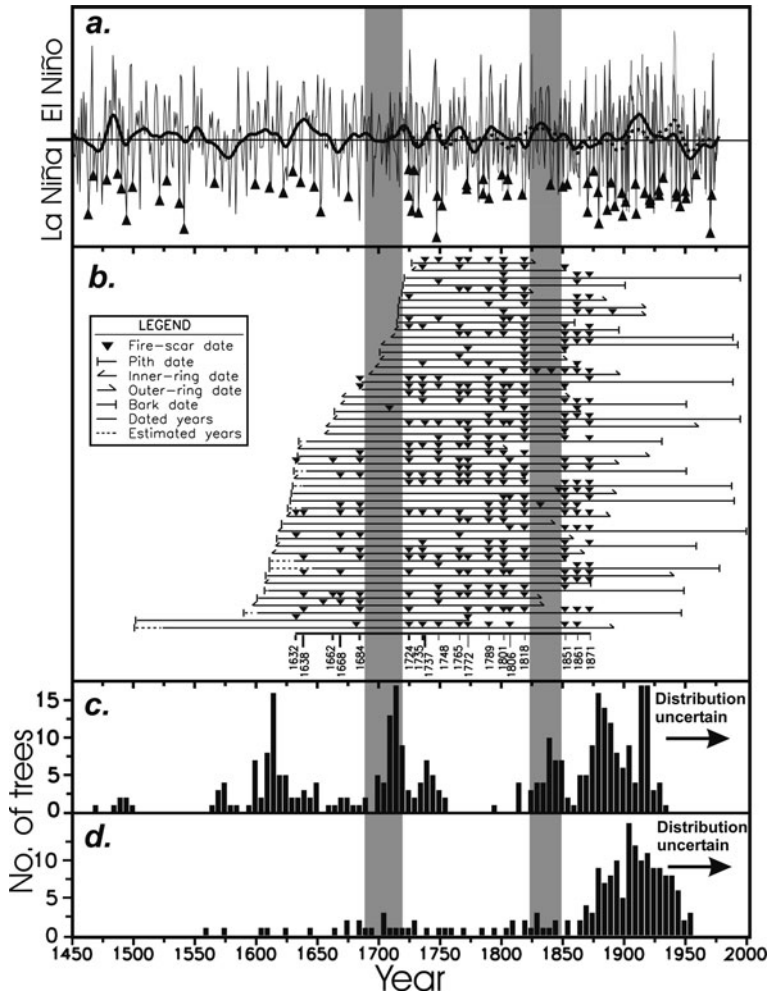

Fig. 9.8 Fire history, age structure, and climate variations in a ponderosa pine forest in southwestern Colorado, United States (Brown and Wu 2005). (**a**) ENSO time series (*thin solid line* is Niño-3 sea surface temperature (SST) index [D'Arrigo et al. 2005]; *thin dashed line* is Southern Oscillation Index [SOI, Stahle et al. 1998]). SOI is reversed to be consistent with other moisture indices. Years of significant triennial wet/dry oscillations identified by superposed epoch analyses (SEA) are shown by up *arrowheads* centered on the drought years. Biennial oscillations also were tested and found to be largely absent during the fire-quiescent periods of 1684–1724 and 1818–1851. *Thick solid* and *dashed lines* show reconstructed hydroclimate time series, smoothed with 20-year cubic splines. The *solid line* shows the annual precipitation in northeastern New Mexico (Grissino-Mayer 1996), and the *dashed line* shows the Palmer Drought Severity Index (PDSI) for the Four Corners area (Cook et al. 2004). (**b**) Fire-year chronology for Archuleta Mesa. *Horizontal lines* mark time spans of individual trees, with fire scars designated by inverted triangles. Fire years at bottom are those recorded on more than two trees. (**c**, **d**) Tree recruitment dates by 5-year periods for (**c**) ponderosa pine and (**d**) other tree species. The *shaded vertical bars* connecting graphs in (**a**)–(**d**) mark relatively quiescent ENSO variability, wet periods, reduced fire occurrence and pulses of recruitment in ponderosa pine (modified from Brown and Wu 2005, reprinted with permission of Ecology, Ecological Society of America)

1.Manitou Experimental Forest, CO, Boyden et al. 2005.

2. Turkey Springs, San Juan Mountains, CO, Romme unpublished

3. Archuleta Mesa, NM, Brown and Wu 2005.

4. Monument Canyon Research Natural Area, NM, Falk and Swetnam, unpublished.

5.Chuska Mountains, AZ, Savage 1991.

6. Powell Plateau, Grand Canyon National Park, AZ, Fule et al. 2002.

7. Walhalla Plateau, Grand Canyon National Park, AZ, Mast & Wolf 2004.

8. Gus Pearson Natural Area, AZ, Mast et al. 1999.

9. Maverick Fort Apache Reservation, AZ, Cooper 1960.

10. Malay gap, San Carlos Reservation, AZ, Cooper 1960.

11. Santa Catalina Mountains, Iniquez and Swetnam, unpublished.

12. Rhyolite Canyon, Chiricahua National Monument, AZ, Barton et al. 2001.

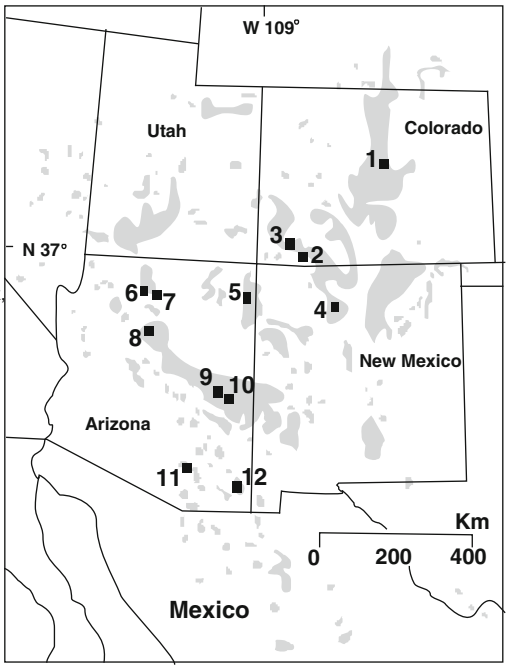

Fig. 9.9 Map of the Southwest and southern Rocky Mountains showing locations of the 12 sites where ponderosa pine age structure data have been collected and composted for analysis in this chapter. The *gray shaded* area is the approximate range of ponderosa pine in this region

of trees also appear to approximately coincide with drier periods in the 1750s–1760s, 1850s–1860s, and 1950s–1960s. Note also that a most recent cohort in the 1980s–1990s also coincides with a wet period in the Southwest that occurred from approximately 1977 to 1992 (Swetnam and Betancourt 1998), although many of the datasets used here lack counts of tree seedlings and saplings in these recent decades. Earlier wet periods (1610s–1640s and 1690s–1710s) may coincide with very slight establishment episodes, but these cohorts are not well resolved, probably because fewer trees overall are included in this earlier part of the record.

Although this is a relatively coarse-scale spatial and temporal analysis of ponderosa pine age structure patterns in the Southwest, the results (Fig. 9.10) suggest that there are several key features of local to regional recruitment dynamics that were responsive to climatic variability. It is well known that ponderosa pine produces large cone crops only erratically, and that successful germination of the seeds is enhanced by warm, wet summers (Pearson 1950; Savage et al. 1996). Successful establishment and survival of seedlings into saplings is dependent on (1) favorable moisture conditions (i.e., lack of drought), (2) the absence of surface fires for a sufficient length of time to allow the saplings to develop thicker, more heat-resistant bark (e.g., Fig 9.8), and (3) sufficient time for meristems to be elevated above grasses and

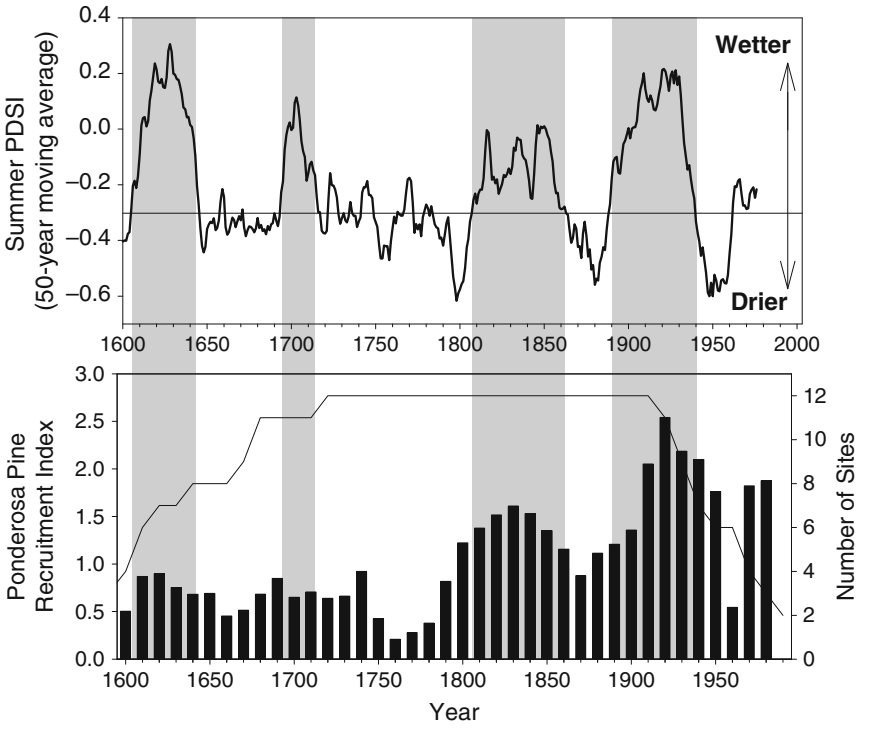

Fig. 9.10 Composite age structure data from a network of 12 ponderosa pine stands and reconstructed summer Palmer Drought Severity Index (PDSI) from corresponding grid points in the southwestern United States (Cook et al. 1999, 2004)

other surface fuels. Hence, it seems quite likely that historically, the favorable germination and establishment periods of ponderosa pine in the Southwest corresponded with wetter conditions for the reasons described above; i.e., more successful germination and survival during these periods, and relatively longer intervals between fires during these wet periods (see also Fig. 9.8). It is likely that climate affected recruitment in many of these forests both through direct effects on demographic processes (seed production, germination, and seedling growth) as well as by modifying fire frequency and timing (and perhaps other disturbances, such as insect outbreaks; e.g., Fig. 9.6). In a later section of this chapter, we will discuss timing of longer fire-free intervals, and their relationships to both climate and patterns of regional tree recruitment shown in Fig. 9.10.

As in most dendrochronological studies involving networks of chronologies, regional-scale emergent patterns of ecological synchrony may be reasonably interpreted to reflect, at least in part, the important role of climatic variability. This is not to discount the important role of local factors in causing unique disturbances or demographic peculiarities at the tree or stand level. Interactions between

disturbances and demography (e.g., fire, insect outbreaks, and tree mortality and subsequent natality) can add multiple layers of complexity and non-climatic signals in composite, ecological time series. Nevertheless, depending on the extent and degree of spatial coherence and synchrony of disturbances or demographic patterns, the relative role of climate can be assessed by the nature of the aggregated time series, and their relations to independent climate reconstructions. The moderate degree of regional synchrony in southwestern US ponderosa pine establishment over the past several centuries, and approximate correspondence with reconstructed drought indices (Fig. 9.10), suggests that climate is at least partly controlling. We recognize, however, that multiple other environment factors probably also determine the nonsynchronous variations, especially at finer spatial scales of individual stands.

9.3 The Late Eighteenth-Century, Early Nineteenth-Century Fire Gap

We close our discussion of dendroecological and climate reconstructions with a specific example of an interesting climatic episode that has been identified in multiple fire chronologies. Fire historians in North and South America have long recognized a very interesting 'gap,' or hiatus, in fire events during the period from about 1780 to 1840. The gap appears as an unusually long interval (relative to average intervals in the rest of the chronologies) between fire events. This gap is evident in many forest stands from the Southwest (e.g., Swetnam and Dieterich 1985; Fig. 9.11; see also Fig. 9.8), Baja California (Stephens et al. 2003; Fig. 9.12), and northeastern Oregon (Heyerdahl et al. 2002). The gap seems to be detectable primarily in the intermediate fire frequency fire regimes (i.e., mean fire return intervals between about 7 and 15 years). The timing and length of the gap varies somewhat from area to area, starting or ending some years earlier or later, but generally within the period from the late 1700s through the middle1800s.

Kitzberger et al. (2001) noted that a similar gap of reduced fire frequency was present during approximately the same time period (i.e., 1780s–1840s) in fire histories from *Austrocedrus chilensis* woodlands in northern Patagonia, Argentina (Fig. 9.13). Perhaps most remarkably, the regional fire-scar time series from the Southwest and Patagonia were statistically coherent (i.e., synchronous), especially in the frequency range of about 2–7 years (determined in a bivariate spectral analysis). Kitzberger et al. (2001) hypothesized that the common response of fire regimes in the Southwest and Patagonia to the El Niño/Southern Oscillation (Swetnam and Betancourt 1990; Kitzberger et al. 1997; Veblen et al. 1999, 2000; Veblen and Kitzberger 2002) was likely the reason for coherence of the two fire occurrence time series from different hemispheres. Moreover, they proposed that the hiatus during the late eighteenth and early nineteenth centuries could be due to a combination of (1) reduced amplitude and/or frequency of ENSO events (especially La Niña events) during this period (Fig. 9.14; see also Fig. 9.8), and (2) a coincidence of this period with a major global cooling phase in the early 1800s (i.e., 1810s–1820s),

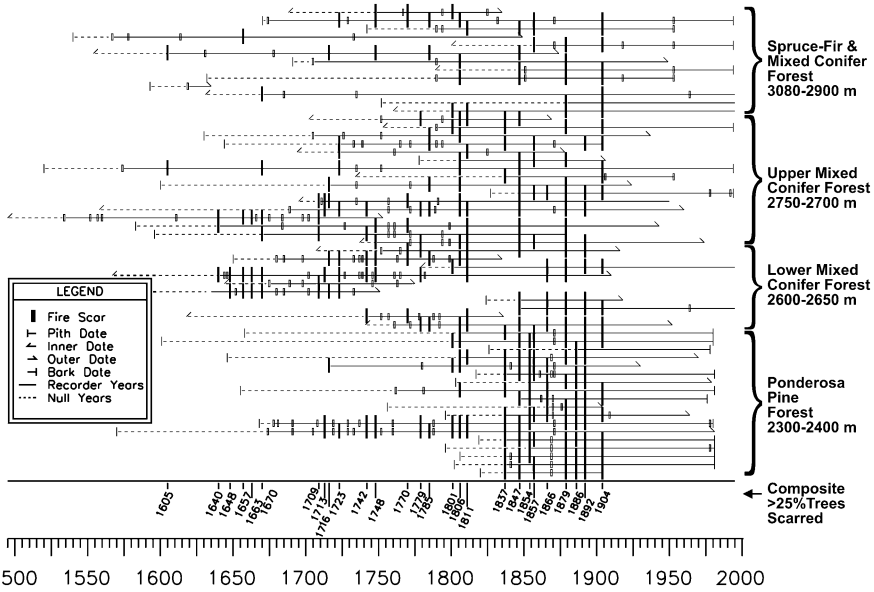

Fig. 9.11 Fire-scar chronologies from ponderosa pine and mixed-conifer forests in the Gila Wilderness, New Mexico (Swetnam and Dieterich 1985; Abolt 1997). *Horizontal lines* are tree-ring records from individual fire-scarred trees along an elevational gradient, and the *vertical tick marks* are the fire-scar dates recorded on the trees. Note the 'gap' in fire occurrence in the period 1811–1837. The lack of fire scars after 1904 was due to livestock grazing and fire exclusion by government firefighters, and is a common feature of many surface fire chronologies in the western United States

which might have been associated with volcanic eruptions, and is clearly indicated in Northern Hemisphere temperature reconstructions (e.g., Mann et al. 1998, 1999).

Additional detailed analysis of the Southwest regional fire-scar series (Fig. 9.2), and a subset of this series, offers further insight on the nature and possible causes of the gap. Swetnam and Baisan (1996) found that an index of regional fire occurrence in the Southwest based on 63 fire-scar sites was highly correlated with tree-ring-width-based Palmer Drought Severity Index reconstructions from the region during the early to mid-1700s and after the mid-1800s (Pearson's $r > 0.8$). However, this correlation declined precipitously during the late 1700s and early 1800s ($r < 0.3$) before rising again after about 1850. This finding seems to support the interpretation that interannual climate variations were reduced, perhaps associated with a quiescent ENSO, and this may have caused an uncoupling from the fire occurrence pattern in the Southwest (see also Fig. 9.8, and Brown and Wu [2005] findings of reduced 'biennial' oscillations during this period).

Other dendroecological evidence also points to possible shifts in fire regimes during the late eighteenth- and early nineteenth-century period. An analysis of a subset of fire-scar chronologies from the El Malpais area of west-central New Mexico

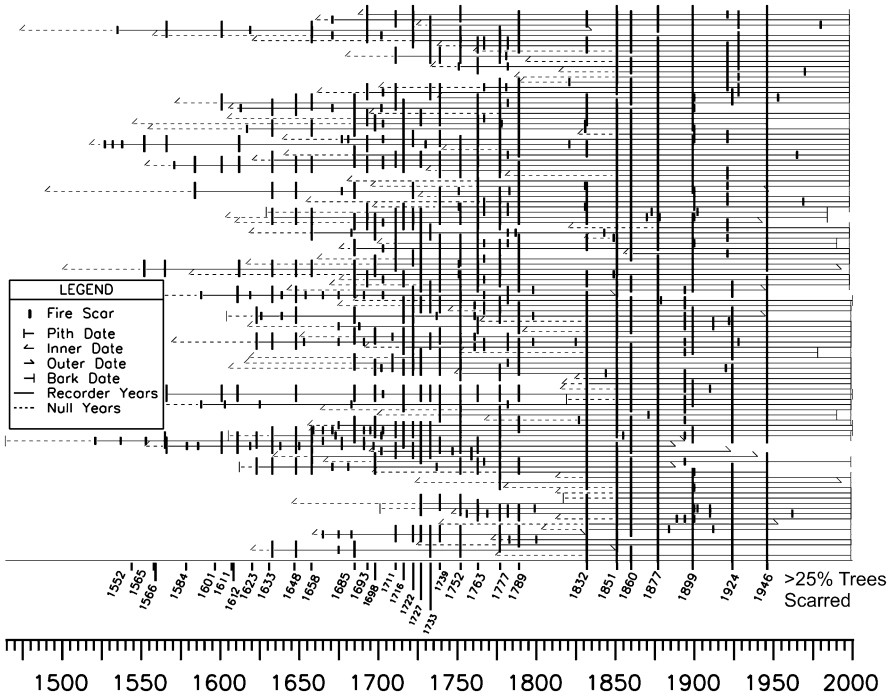

Fig. 9.12 Fire-scar chronology from Sierra San Pedro Mártir, Baja California (Stephens et al. 2003). Note the gap in fire occurrence from about 1790 to 1830. Stephens et al. suggest the gap may be related to climate, or potentially land-use history (i.e., early livestock grazing by Spanish missionaries). Note that in contrast with the Gila Wilderness chronologies (Fig. 9.11), fires generally continue to burn in this area during the twentieth century, probably indicating that livestock grazing and/or fire suppression were minimal in this area of northern Mexico until after about 1950 (modified from Fig. 1 in Stephens et al. [2003], reprinted with permission from Canadian Journal of Forest Research, NRC Research Press)

indicated that the seasonal timing of fires also shifted during the late eighteenth century (Grissino-Mayer and Swetnam 2000). This analysis of the distribution of fire-scar seasonality found that late season scars were more prevalent in the period before the late 1700s than after. In this remote and rugged area (with impassable lava flows in places), human-set fires were unlikely. It is probable that climate shifts were responsible for a change in seasonal timing of fires. Grissino-Mayer and Swetnam (2000) hypothesized that the arid fore-summer/monsoon pattern may have strengthened after the late 1700s, resulting in more fires during the early to middle growing season (i.e., the arid fore-summer, May and June), but fewer fires during and after the late summer monsoon (July to August). Prior to this time, a weaker monsoon may have persisted for some decades (early to mid-1700s), allowing more fires to occur later in the growing season (i.e., July to August).

Other synoptic climate patterns also may have played a role in the fire gap. In recent multivariate and contingency analyses of 238 fire-scar chronologies from

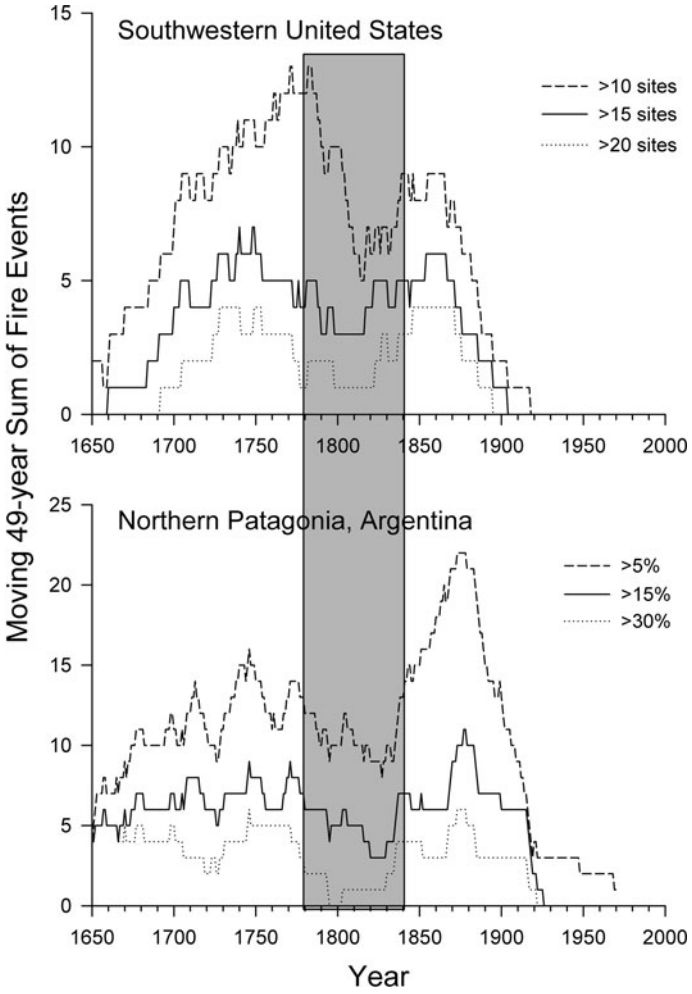

Fig. 9.13 Fire frequency changes in Patagonia, Argentina, and the southwestern United States. Both regional composites from fire-scar networks show reduced fire frequency during the 1780s–1840s period (*vertical shaded bar*) (Kitzberger et al. 2001). The *dashed* and *solid lines* show 'moving' fire frequencies, computed as the sum of fire events that were synchronously recorded by the indicated numbers or percentage of sites within the networks during 49-year windows, plotted on the central (25th) year of the window (reprinted from *Global Ecology and Biogeography*, permission granted from Wiley-Blackwell)

across western North America, extending from southern British Columbia to northern Mexico, Kitzberger et al. (2007) showed that the most coherent regional signal in the fire-scar dataset was well correlated with ENSO (Pearson $r = -0.47$, $p < 0.001$, between the first principal component of the 238 series and the D'Arrigo et al. [2005] reconstruction of the Niño-3 sea surface temperature index). An independent

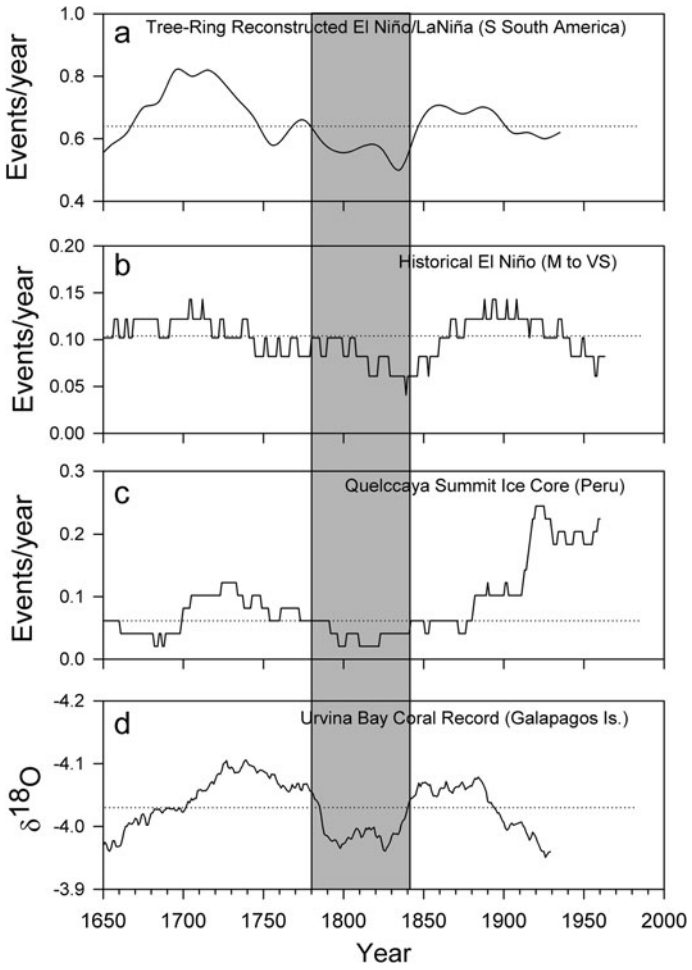

Fig. 9.14 Multiple reconstructions of the El Niño/Southern Oscillation (ENSO) show a reduced occurrence or amplitude during the 1780s–1840s period (*vertical shaded bar*) (Kitzberger et al. 2001). (**a**) La Niña and El Niño events reconstructed from tree-ring chronologies in Patagonia and central Chile (Villalba 1994). (**b**) Recurrence of moderate to very strong El Niño events reconstructed from archival documents (Quinn and Neal 1992). (**c**) El Niño recurrence based on years when $d^{18}O$ was > –16‰ (i.e., warm events) in the Quelccaya summit ice core record (Michaelsen and Thompson 1992). Plots are mean number of events per year based on moving 49-year sums of all indices. (**d**) Record of ENSO-related central Pacific upwelling based on $d^{18}O$ (‰) coral from Urvina Bay, Galapagos Islands (Dunbar et al. 1994; 49-year running mean). In all cases the horizontal dotted line represents long-term mean values (reprinted from *Global Ecology and Biogeography*, permission granted from Wiley-Blackwell)

tree-ring reconstruction of the Pacific Decadal Oscillation (PDO; D'Arrigo et al. 2001) was weakly correlated with the second principal component ($r = 0.17$, $p < 0.01$). Moreover, an independent tree-ring width reconstruction of the Atlantic Multidecadal Oscillation (AMO; Gray et al. 2004) appeared to be associated with

periods of maximum coherence (cross correlations) among the fire-scar chronologies during warm phases of the AMO, and minimum coherence during cool phases. The longest and coldest AMO phase occurred during the period 1750–1849, encompassing the fire-scar gap observed in many of the sites in the network. These findings corroborate and expand a growing list of tree-ring studies demonstrating fire-climate teleconnections at mountain range to subregional scales in the western United States involving ENSO (e.g., Swetnam and Betancourt 1990; Veblen et al. 1999, 2000; Donnegan et al. 2001; Heyerdahl et al. 2002; Norman and Taylor 2003; Schoennagel et al. 2005), PDO (e.g., Norman and Taylor 2003; Westerling and Swetnam 2003; Hessl et al. 2004; Taylor and Beaty 2005; Schoennagel et al. 2005), and AMO (Brown 2006; Sibold and Veblen 2006).

9.4 Ecologically Effective Climate Change

It appears likely that changes in both fire regimes and increases in tree recruitment during the early nineteenth century in western North America and South America are related to changes in timing and strength of ENSO events (Brown and Wu 2005), with further possible modulation of the effects of ENSO (at least in North America) by the AMO (Kitzberger et al. 2007). The early 1800s regional cohort synchrony (Fig. 9.10) may be the best example of the contingency of favorable regional climate and fire conditions occurring together to promote successful establishment; i.e., wetter conditions and longer fire intervals (e.g., Figs. 9.8, 9.11, and 9.12). We suggest that overall, these findings and the widespread occurrence of the 'gap' in fire-scar chronologies in North and South America are compelling examples of an 'ecologically effective climate change' deserving of more focused analysis by paleoclimatologists and others. In particular, we posit that these ecological responses that occurred at the turn of the eighteenth to nineteenth centuries reflect one of the most important and ecologically effective climatic changes in the past three centuries in western North America and southern South America, causing changes in forest structure that persist to the present.

Most dendroecological studies involving climatic analysis, and most of the preceding examples in this chapter, focus primarily on the ecological implications of the responses of disturbances or demographic processes to climate variations and changes. This is natural and appropriate as a focus of dendroecological research. However, now that numerous case studies have been conducted demonstrating and evaluating ecological responses to climate, and broadscale network approaches using dendroecological data are increasingly feasible (and with regional datasets starting to become available), we propose that such dendroecological datasets and analyses be used more broadly for identifying important climatological events and processes. Glacier- and lake-level fluctuations are commonly used by dendroclimatologists and paleoclimatologists as corroborating lines of evidence for identifying climate events and changes. Fire and other dendroecological evidence are used less frequently for such validation (but see Cook et al. 2004 for an example

where both fire-scar and lake-level data were compared with tree-ring climate reconstructions). In some cases, regional ecological time series may be less noisy and/or higher-resolution indicators of climate variability than glacier- and lake-level fluctuations.

It is clear that dendroecological data, especially networks of such data, can be very useful for clarifying and identifying climatic variations and changes *that are important to ecosystems*. We refer to this as 'ecologically effective climate change,' and we think that this category of climatic variability deserves special attention by ecologists and other researchers. As climate change due to greenhouse gas–induced warming continues and perhaps accelerates, it will be increasingly important that climatologists, ecologists, managers, policy makers, and the public focus their attention on understanding and anticipating the impacts of climatic change on ecosystems. This will require more effective integration and comparative analyses of dendroclimatic and dendroecological studies. It may well be that the ecologically effective climatic changes that dendroecology can address will provide some of the most sensitive and insightful information about climate change impacts. The great potential for ecological indicators is exemplified by time series of plant phenology, such as the timing of plant flowering (Cayan et al. 2001). These records (especially in networks) are now widely recognized and embraced as a key and valuable ecological indicator of climate change.

The final example we offer of the potential of using dendroecological responses to identify ecologically effective climate changes for guiding future research, and for applications, is the finding of the importance of wet/dry oscillations in fire occurrence in the western United States (e.g., Fig. 9.4). It was tree-ring analysis that first identified a strong statistical association between the wet/dry sequence of 1–3 wet years, followed by a dry year, and widespread fire occurrence during the dry year (Baisan and Swetnam 1990; Swetnam and Betancourt 1992; Swetnam and Baisan 1996). This finding has been replicated by numerous dendroecology studies, particularly in relatively dry ponderosa pine ecosystems where grass and other fine fuel production was important for historical fire ignition and spread (e.g., Veblen et al. 2000; Brown et al. 2001; Donnegan et al. 2001; Stephens et al. 2003; Brown and Wu 2005). Subsequently, analysis of modern fire and climate records (i.e., twentieth- and twenty-first-century data) confirmed that this pattern was important over large portions of the western United States during recent times (Knapp 1995; Westerling et al. 2002, 2003; Crimmins and Comrie 2004). Now, this wet/dry pattern, in combination with ENSO-based climate forecasts (and ENSO-fire associations), is used to develop seasonal 'outlook' (forecasting) products for fire managers (see Predictive Services at National Interagency Coordination Center, Boise, Idaho: http://www.nifc.gov/nicc/predictive/outlooks/outlooks.htm).

In conclusion, we are optimistic that dendroecological contributions to dendoclimatological research, and vice versa, will greatly expand in coming years. The interest in ecological responses to climatic variability and change is already very large and will certainly increase as global warming continues and its impacts increase. The signs of this scientific interest are already evident in increasing numbers of dendroclimatic and dendroecological papers with a climate focus in

leading forest science, ecology, and climatology journals. A challenge to dendroecologists is to work collaboratively and to promptly contribute datasets to publicly accessible archives, in the same generous, ethical, and forward-looking spirit as the hundreds of dendrochronologists around the world who have contributed ring width and ring density chronologies to the International Tree-Ring Data Bank. A challenge to dendroclimatologists is to focus their studies on parameters and questions with relevance to ecologists, and in turn to utilize the climatically relevant findings and datasets that dendroecologists are developing to address new questions in historical climatology.

Acknowledgements We are grateful to all of the many students and colleagues who have contributed to the collection and development of the dendroecological and dendroclimatological datasets that we describe and illustrate in this chapter. Our research over the past three decades has been supported primarily by The University of Arizona, US Forest Service, US Geological Survey, National Park Service, The Nature Conservancy, and the National Science Foundation.

References

Abolt RA (1997) Fire histories of upper elevation forests in the Gila Wilderness, New Mexico via fire-scar analysis and stand age structure analysis. MS thesis, The University of Arizona, Tucson, Arizona

Baisan CH, Swetnam TW (1990) Fire history on a desert mountain range: Rincon Mountain Wilderness, Arizona, USA. Can J Forest Res 20:1559–1569

Barton AM, Swetnam TW, Baisan CH (2001) Arizona pine (*Pinus arizonica*) stand dynamics: local and regional factors in a fire-prone Madrean gallery forest of southeast Arizona, USA. Landscape Ecol 16: 51–369

Baumgartner TR, Michaelsen J, Thompson LG, Shen GT, Soutar A, Casey RE (1989) The recording of interannual climatic change by high-resolution natural systems: tree rings, coral bands, glacial ice layers, and marine varves. In: Peterson DH (ed) Aspects of climatic variability in the Pacific and the western Americas. Geophys Monogr 55:1–14

Blackburn WH, Tueller PT (1970) Pinyon and juniper invasion in black sagebrush communities in east-central Nevada. Ecology 51:841–848

Blais JR (1981) Recurrence of spruce budworm outbreaks for 200 years in western Quebec. Forest Chron 57:273–275

Boyden S, Binkley D, Shepperd W (2005) Spatial and temporal patterns in structure, regeneration, and mortality of an old-growth ponderosa pine forest in the Colorado Front Range. Forest Ecol Manag 219:43–55

Breshears DD, Cobb NS, Rich PM, Price KP, Allen CD, Balice RG, Romme WH, Floyd ML, Belnap J, Anderson JJ, Myers OB, Meyer CW (2005) Regional vegetation die-off in response to global-change-type drought. Proc Natl Acad Sci USA 102:15144–15148

Briffa KR, Jones PD, Schweingruber FH (1994) Summer temperatures across northern North America: regional reconstructions from 1760 using tree-ring densities. J Geophys Res 99:25835–25844

Brown JH (1995) Macroecology. University of Chicago Press, Chicago, Illinois

Brown PM (2006) Climate effects on fire regimes and tree recruitment in Black Hills ponderosa pine forests. Ecology 87:2500–2510

Brown PM, Cook B (2006) Early settlement forest structure in Black Hills ponderosa pine forests. Forest Ecol Manag 223:284–290

Brown PM, Shepperd WD (2001) Fire history and fire climatology along a 5° gradient in latitude in Colorado and Wyoming, USA. Palaeobotanist 50:133–140

Brown PM, Wu R (2005) Climate and disturbance forcing of episodic tree recruitment in a southwestern ponderosa pine landscape. Ecology 86:3030–3038
Brown PM, Kaye MW, Huckaby LS, Baisan CH (2001) Fire history along environmental gradients in the Sacramento Mountains, New Mexico: influences of local and regional processes. Ecoscience 8:115–126
Cayan DR, Kammerdiener SA, Dettinger MD, Caprio JM, Peterson DH (2001) Changes in the onset of spring in the western United States. B Am Meteorol Soc 82:399–415
Clark NE, Blasing TJ, Fritts HC (1975) Influence of interannual climatic fluctuations on biological systems. Nature 256(5515):302–305
Cook ER (1990) A conceptual linear aggregate model for tree rings. In: Cook ER, Kairiukstis LA (eds) Methods of dendrochronology: applications in the environmental sciences. International Institute for Applied Systems Analysis, Kluwer, Boston, Massachusetts, pp 98–104
Cook ER (2000) NINO3 index reconstruction. International Tree-Ring Data Bank. IGBP PAGES/World Data Center-A for Paleoclimatology data contr. ser. #2000-052. NOAA/NGDC Paleoclimatology Program, Boulder Colorado, USA
Cook ER, Meko DM, Stahle DW, Cleaveland MK (1999) Drought reconstructions for the continental United States. J Climate 12:1145–1162
Cook ER, Woodhouse CA, Eakin CM, Meko DM, Stahle DW (2004) Long-term aridity changes in the western United States. Science 306:1015–1018
Cooper CF (1960) Changes in vegetation, structure, and growth of southwestern pine forests since white settlement. Ecol Monogr 30:129–164
Crimmins MA, Comrie AC (2004) Interactions between antecedent climate and wildfire variability across southeastern Arizona. Int J Wildland Fire 13:455–466
D'Arrigo R, Villalba R, Wiles G (2001) Tree-ring estimates of Pacific decadal climate variability. Clim Dynam 18:219–224
D'Arrigo R, Cook ER, Wilson RJ, Allan R, Mann ME (2005) On the variability of ENSO over the past six centuries. Geophys Res Lett 32(3). doi:10.1029/2004GL022055: Art. no. L03711
Donnegan JA, Veblen TT, Sibold JS (2001) Climatic and human influences on fire history in Pike National Forest, central Colorado. Can J Forest Res 31:1526–1539
Dunbar R, Wellington GM, Colgan MW, Glynn PW (1994) Eastern Pacific sea surface temperature since 1600 AD: the $d^{18}O$ record of climate variability in Galapagos corals. Paleoceanography 9:291–316
Esper J, Buntgen U, Frank DC, Nievergelt D, Liebhold A (2007) 1,200 years of regular outbreaks in alpine insects. Proc R Soc B Bio 274:671–679. doi:10.1098/rspb.2006.0191
Frelich LE, Graumlich LJ (1994) Age-class distribution and spatial patterns in an old-growth hemlock-hardwood forest. Can J Forest Res 24:1939–1947
Fritts HC (1976) Tree rings and climate. Academic, New York, 567 pp
Fritts HC (1991) Reconstructing large-scale climatic patterns from tree-ring data. The University of Arizona Press, Tucson, 286 pp
Fritts HC, Swetnam TW (1989) Dendroecology: a tool for evaluating variations in past and present forest environments. Adv Ecol Res 19:111–189
Fule PZ, Covington WW, Moore MM, Heinlein TA, Waltz AEM (2002) Natural variability in forests of the Grand Canyon, USA. J Biogeogr 29:31–47
Gray ST, Graumlich LJ, Betancourt JL, Pederson GD (2004) A tree-ring based reconstruction of the Atlantic Multidecadal Oscillation since 1567 AD. Geophys Res Lett 31:L12205. doi:10.1029/2004GL019932
Grissino-Mayer HD (1996) A 2,129-year reconstruction of precipitation for northwestern New Mexico, USA. In: Dean JS, Meko DM, Swetnam TW (eds) Tree rings, environment, and humanity. Radiocarbon, Tucson, AZ, pp 191–204
Grissino-Mayer HD, Swetnam TW (2000) Century-scale climate forcing of fire regimes in the American Southwest. Holocene 10:213–220
Hadley KS, Veblen TT (1993) Stand response to western spruce budworm and Douglas-fir bark beetle outbreaks, Colorado Front Range. Can J Forest Res 23:479–491

Harper JL (1977) Population biology of plants. Academic, London, 892 pp
Hawkins BA, Holyoak M (1998) Transcontinental crashes of insect populations? Am Nat 152(3):480–484
Henry JD, Swan JMA (1974) Reconstructing forest history from live and dead plant material—an approach to the study of forest succession in southwest New Hampshire. Ecology 55:772–783
Hessl AE, McKenzie D, Schellhaas R (2004) Drought and Pacific Decadal Oscillation linked to fire occurrence in the inland Pacific Northwest. Ecol Appl 14:425–442
Heyerdahl EK, Brubaker LB, Agee JK (2002) Annual and decadal climate forcing of historical fire regimes in the interior Pacific Northwest, USA. Holocene 12:597–604
Jardon Y (2001) Analyses temporelles et spatiales des épidémies de la tordeuse des bourgeons de l'épinette au Québec. PhD dissertation, Université du Québec, Montreal, QC, 157 pp
Johnson EA, Miyanishi K, Kleb H (1994) The hazards of interpretation of static age structures as shown by stand reconstructions in a Pinus contorta, Picea engelmannii forest. J Ecol 82:923–931
Kitzberger T, Veblen TT (1998) Influences of humans and ENSO on fire history of Austrocedrus chilensis woodlands in northern Patagonia, Argentina. Ecoscience 4:508–520
Kitzberger T, Veblen TT, Villalba R (1997) Climatic influences on fire regimes along a rain forest to xeric woodland gradient in northern Patagonia, Argentina. J Biogeogr 24:35–47
Kitzberger T, Swetnam TW, Veblen TT (2001) Interhemispheric synchrony of forest fires and the El Niño/Southern Oscillation. Global Ecol Biogeogr 10:315–326
Kitzberger T, Brown PM, Heyerdahl EK, Swetnam TW, Veblen TT (2007) Contingent Pacific-Atlantic Ocean influence on multicentury wildfire synchrony over western North America. Proc Natl Acad Sci USA 104(2):543–548
Knapp PA (1995) Intermountain west lightning-caused fires: climatic predictors of area burned. J Range Manage 48:85–91
Kneeshaw DD, Bergeron Y (1998) Canopy gap characteristics and tree replacement in the southeastern boreal forest. Ecology 79:783–794
Koenig WD, Knops JMH (1998) Scale of mast-seeding and tree-ring growth. Nature 396:225–226
Krause C (1997) The use of dendrochronological material from buildings to get information about past spruce budworm outbreaks. Can J Forest Res 27:69–75
League K, Veblen TT (2006) Climatic variability and episodic Pinus ponderosa establishment along the forest-grassland ecotones of Colorado. Forest Ecol Manag 228:98–107
Levin SA (1992) The problem of pattern and scale in ecology: the Robert H. MacArthur award lecture. Ecology 73:1943–1967
Logan JA, Régnière J, Powell JA (2003) Assessing the impacts of global warming on forest pest dynamics. Front Ecol Environ 1:130–137
Lorimer CG (1985) Methodological considerations in the analysis of forest disturbance history. Can J Forest Res 15:200–213
Mann ME, Bradley RS, Hughes MK (1998) Global-scale temperature patterns and climate forcing over the past six centuries. Nature 392:779–787
Mann ME, Bradley RS, Hughes MK (1999) Northern hemisphere temperatures during the past millennium: inferences, uncertainties, and limitations. Geophys Res Lett 26:759–762
Margolis EQ, Swetnam TW, Allen CD (2007) A stand-replacing fire history in upper montane forests of the southern Rocky Mountains. Can J Forest Res 37:2227–2241
Martinat PJ (1987) The role of climatic variation and weather in forest insect outbreaks. In: Barbosa P, Schultz JC (eds) (1987) Insect outbreaks. Academic Press, San Diego, pp 241–268
Mast JN, Wolf JJ (2004) Ecotonal changes and altered tree spatial patterns in lower mixed-conifer forests, Grand Canyon National Park, Arizona, USA. Landscape Ecol 19:167–180
Mast JN, Fule PZ, Moore MM, Covington WW, Waltz AME (1999) Restoration of presettlement age structure of an Arizona ponderosa pine forest. Ecol Appl 9:228–239
Mattson WJ, Haack RA (1987) The role of drought in outbreaks of plant-eating insects. Bioscience 37:110–118

Michaelsen J, Thompson LG (1992) A comparison of proxy records of El Niño/Southern Oscillation. In: Diaz HF, Markgraf V (eds) El Niño: historical and paleoclimatic aspects of the Southern Oscillation, Cambridge University Press, Cambridge, UK, pp 323–348
Moran PAP (1953) The statistical analysis of the Canadian lynx cycle. Aust J Zool 1:291–298
Morin H, LaPrise D, Bergeron Y (1993) Chronology of spruce budworm outbreaks near Lake Duparquet, Abitibi region, Quebec. Can J Forest Res 23:1497–1506
Morneau C, Payette S (2000) Long-term fluctuations of a caribou population revealed by tree-ring data. Can J Zool 78:1784–1790
Morrow PA, LaMarche VC Jr (1978) Tree-ring evidence for chronic insect suppression of productivity in subalpine eucalyptus. Science 201:1244–1246
Myers JH (1998) Synchrony in outbreaks of forest Lepidoptera: a possible example of the Moran effect. Ecology 79:1111–1117
Norman SP, Taylor AH (2003) Tropical and north Pacific teleconnections influence fire regimes in pine-dominated forests of northeastern California, USA. J Biogeogr 30:1081–1092
Pearson GA (1950) Management of ponderosa pine in the Southwest, as developed by research and experimental practice. Agriculture monograph 6, US Department of Agriculture, Forest Service, Washington, DC
Perkins D, Swetnam TW (1996) A dendroecological assessment of whitebark Pine (*Pinus albicaulis*) in the Sawtooth–Salmon River region of Idaho. Can J Forest Res 26:2123–2133
Quinn WH, Neal VT (1992) The historical record of El Niño events. In: Bradley RS, Jones PD (eds) Climate since AD 1500. Routledge, London, pp 623–646
Ranta E, Kaitala V, Lindstrom J, Helle E (1997) The Moran effect and synchrony in population dynamics. Oikos 78:136–142
Ricklefs RE (1987) Community diversity: relative roles of local and regional processes. Science 235:167–171
Royama T (1984) Population dynamics of the spruce budworm Choristoneura fumiferana. Ecol Monogr 54:429–462
Ryerson DE, Swetnam TW, Lynch AM (2003) A tree-ring reconstruction of western spruce budworm outbreaks in the San Juan Mountains, Colorado, USA. Can J Forest Res 33:1010–1028
Savage M (1991) Structural dynamics of a southwestern pine forest under chronic human influence. Ann Assoc Am Geogr 81:271–289
Savage M, Brown PM, Feddema J (1996) The role of climate in a pine forest regeneration pulse in the southwestern United States. Ecoscience 3:310–318
Schoennagel T, Veblen TT, Romme WH, Sibold JS, Cook ER (2005) ENSO and PDO variability affect drought-induced fire occurrence in Rocky Mountain subalpine forests. Ecol Appl 15(6):2000–2014
Schulman E (1956) Dendroclimatic changes in semiarid America. The University of Arizona Press, Tucson, Arizona, 142 pp
Schweingruber FH (1996) Tree rings and environment dendroecology. Paul Haupt, Berne, Switzerland
Sibold JS, Veblen TT (2006) Relationships of subalpine forest fires in the Colorado Front Range with interannual and multidecadal-scale climatic variation. J Biogeogr 33:833–842
Sinclair ARE, Gosline JM (1997) Solar activity and mammal cycles in the Northern Hemisphere. Am Nat 149:776–784
Sinclair ARE, Gosline JM, Holdsworth G, Krebs CJ, Boutin S, Smith JNM, Boonstra R, Dale M (1993) Can the solar cycle and climate synchronize the snowshoe hare cycle in Canada? Evidence from tree rings and ice cores. Am Nat 141:173–182
Speer JH, Swetnam TW, Wickman BE, Youngblood A (2001) Changes in Pandora moth outbreak dynamics during the past 622 years. Ecology 82:679–697
Spencer DA (1964) Porcupine population fluctuations in past centuries revealed by dendrochronology. J Appl Ecol 1:127–149
Stahle DW, D'Arrigo RD, Krusic PJ, Cleaveland MK, Cook ER, Allan RJ, Cole JE, Dunbar RB, Therrell MD, Gay DA, Moore MD, Stokes MA, Burns BT, Villanueva-Diaz J, Thompson LG

(1998) Experimental dendroclimatic reconstruction of the Southern Oscillation. B Am Meteorol Soc 79:2137–2152
Stephens SL, Skinner CN, Gill SJ (2003) Dendrochronology-based fire history of Jeffrey pine–mixed conifer forests in the Sierra San Pedro Mártir, Mexico. Can J Forest Res 33:1090–1101
Stokes MA, Smiley TL (1968) An introduction to tree-ring dating. University of Chicago Press, Chicago, Illinois, 73 pp
Swetnam, TW (1993) Fire history and climate change in giant sequoia groves. Science 262: 885–889
Swetnam TW, Baisan CH (1996) Fire effects in southwestern forests. Proceedings of the second La Mesa fire symposium, Los Alamos, New Mexico, March 29–31, 1994. USDA Forest Service general technical report RM-GTR-286
Swetnam TW, Baisan CH (2003) Tree-ring reconstructions of fire and climate history in the Sierra Nevada and southwestern United States. In: Veblen TT, Baker W, Montenegro G, Swetnam TW (eds) Fire and climatic change in temperate ecosystems of the western Americas. Ecological studies, vol 160. Springer, New York, pp 158–195
Swetnam TW, Betancourt JL (1990) Fire–Southern Oscillation relations in the southwestern United States. Science 249:1017–1020
Swetnam TW, Betancourt JL (1992) Temporal patterns of El Niño/Southern Oscillation: wildfire patterns in the southwestern United States. In: Diaz HF, Markgraf VM (eds) El Niño: historical and paleoclimatic aspects of the Southern Oscillation. Cambridge University Press, Cambridge, UK, pp 259–270
Swetnam TW, Betancourt JL (1998) Mesoscale disturbance and ecological response to decadal climatic variability in the American Southwest. J Climate 11:3128–3147
Swetnam TW, Dieterich JH (1985) Fire history of ponderosa pine forests in the Gila Wilderness, New Mexico. In: Lotan JE, Kilgore BM, Fischer WC, Mutch RW (tech coords) Proceedings—symposium and workshop on wilderness fire, November 15–18, 1983, Missoula, Montana. USDA Forest Service general technical report INT-182, pp 390–397
Swetnam TW, Lynch AM (1993) Multicentury, regional-scale patterns of western spruce budworm outbreaks. Ecol Monogr 63:399–424
Swetnam TW, Thompson MA, Sutherland EK (1985) Using dendrochronology to measure radial growth of defoliated trees. USDA Forest Service agricultural handbook 639:1–39
Swetnam TW, Wickman BE, Paul HG, Baisan CH (1995) Historical patterns of western spruce budworm and Douglas-fir tussock moth outbreaks in the northern Blue Mountains, Oregon, since AD 1700. Research paper PNW-RP-484. US Department of Agriculture, Forest Service, Pacific Northwest Research Station, Portland, Oregon, 27 pp
Swetnam TW, Allen CD, Betancourt JL (1999) Applied historical ecology: using the past to manage for the future. Ecol Appl 9:1189–1206
Taylor AH, Beaty RM (2005) Climatic influences on fire regimes in the northern Sierra Nevada mountains, Lake Tahoe basin, Nevada, USA. J Biogeogr 32:425–438
Trotter RT, Cobb NS, Whitham TG (2002) Herbivory, plant resistance, and climate in the tree-ring record: interactions distort climate reconstructions. Proc Natl Acad Sci USA 99:10197–10202
Turner MG, Romme WH, Gardner RH, O'Neill RV, Kratz TK (1993) A revised concept of landscape equilibrium: disturbance and stability on scaled landscapes. Landscape Ecol 8:213–227
Veblen TT, Kitzberger T (2002) Interhemispheric comparison of fire history: the Colorado Front Range, USA, and the northern Patagonian Andes, Argentina. Plant Ecol 163:187–207
Veblen TT, Kitzberger T, Villalba R, Donnegan J (1999) Fire history in northern Patagonia: the roles of humans and climatic variation. Ecol Monogr 69:47–67
Veblen TT, Kitzberger T, Donnegan J (2000) Climatic and human influences on fire regimes in ponderosa pine forests in the Colorado Front Range. Ecol Appl 10:1178–1195
Veblen TT, Baker WL, Montenegro G, Swetnam TW (eds) (2003) Fire and climatic change in temperate ecosystems of the western Americas. Ecological studies, vol 160. Springer, New York, 444 pp

Villalba R (1994) Tree-ring and glacial evidence for the Medieval Warm Epoch and the Little Ice Age in southern South America. Climatic Change 26:183–197
Villalba R, Veblen TT (1997a) Regional patterns of tree population age structures in northern Patagonia: climatic and disturbance influences. J Ecol 85:113–124
Villalba R, Veblen TT (1997b) Improving estimates of total tree ages based on increment core samples. Ecoscience 4:534–542
Weber UM (1997) Dendroecological reconstruction and interpretation of larch budmoth (*Zeiraphera diniana*) outbreaks in two central alpine valleys of Switzerland from 1470–1990. Trees-Struct Funct 11:277–290
Westerling AL, Swetnam TW (2003) Interannual to decadal drought and wildfire in the western US. Eos 84(49):545–560
Westerling AL, Gershunov A, Cayan DR, Barnett TP (2002) Long lead statistical forecasts of area burned in western United States wildfires by ecosystem province. Int J Wildland Fire 11:257–266
Westerling AL, Gershunov A, Brown TJ, Cayan DR, Dettinger MD (2003) Climate and wildfire in the western United States. B Am Meteorol Soc, May 2003:595–604
Westerling AL, Hidalgo HG, Cayan DR, Swetnam TW (2006) Warming and earlier spring increase western U.S. wildfire activity. Science 313:940–943
White TCR (1976) Weather, food and plagues of locusts. Oecologia 22:119–134

Chapter 10
North American Tree Rings, Climatic Extremes, and Social Disasters

David W. Stahle and Jeffrey S. Dean

Abstract Tree-ring reconstructed climatic extremes contemporaneous with severe socioeconomic impacts can be identified in the modern, colonial, and precolonial eras. These events include the 1950s, Dust Bowl, mid- and late-nineteenth century Great Plains droughts, El Año del Hambre, and the seventeenth and sixteenth century droughts among the English and Spanish colonies. The new tree-ring reconstructions confirm the severe, sustained Great Drought over the Colorado Plateau in the late thirteenth century identified by A.E. Douglass and document its spatial impact across the cultural heartland of the Anasazi. The available tree-ring data also indicate a succession of severe droughts over the western United States during the Terminal Classic Period in Mesoamerica, but these droughts are located far from the centers of Mesoamerican culture and their extension into central Mexico needs to be confirmed with the new suite of millennium-long tree-ring chronologies now under development in the region. The only clear connections between climate extremes and human impacts are found during the period of written history, including the prehispanic Aztec era where codices describe the drought of One Rabbit in Mexico and other precolonial droughts. The link between reconstructed climate and societies in the prehistoric era may never be made irrefutably, but testing these hypotheses with improved climate reconstructions, better archaeological data, and modeling experiments to explore the range of potential social response have to be central goals of archaeology and high-resolution paleoclimatology.

Keywords Climate · Dendrochronology · Drought · Epidemic disease · Human impacts · Megadrought · Palmer Drought Severity Index · PDSI · North America famines

D.W. Stahle (✉)
Department of Geosciences, University of Arkansas, Fayetteville, AR 72701, USA
e-mail: dstahle@uark.edu

M.K. Hughes et al. (eds.), *Dendroclimatology*, Developments in Paleoenvironmental Research 11, DOI 10.1007/978-1-4020-5725-0_10,

10.1 Introduction

The impact of climate on society has been a controversial research focus from the early days of dendrochronology. A.E. Douglass (1935) noted the coincidence between tree-ring-dated climate extremes and prehistoric Anasazi activities on the Colorado Plateau, including an increase in tree-ring-dated building activity during wet years and decreased activity or complete village abandonment in dry years. 'The great drouth from 1276 to 1299 was the most severe of all those represented in this 1200-year record and undoubtedly was connected with extensive disturbances in the welfare of the Pueblo people' (Douglass 1935, p. 49). 'Pueblo III, the golden age of southwestern prehistory, took its early form in Chaco Canyon about 919 AD, reached its local climax in the late eleventh century, and probably closed with the great drouth of 1276–1299' (Douglass 1935, p. 41). The first long tree-ring chronology developed by Douglass for the American Southwest has been replicated by more than 850 tree-ring chronologies now available for North America (Cook et al. 2004), and Douglass' 'great drouth' of the late thirteenth century has been verified as one of the most severe and protracted of the past 1000 years (Grissino-Mayer et al. 1997). However, the precise role of prolonged drought in the welfare of the Anasazi and their ancient migrations remains an interesting and provocative research question.

There have been a number of more recent attempts to link paleoclimatic extremes to famine, disease, and the collapse of human societies (Keys 1999; Diamond 2005). These catastrophe scenarios have been fiercely controversial among anthropologists, historians, and social theorists, and include viewpoints involving climate determinism, Malthusian demographics, a famine-prone peasantry, and Marxist and entitlement economic theory (Arnold 1988). Elements of each viewpoint are evident in many recent famines, and a loose consensus on the causes of *modern* hunger now includes environmental hazards, food system breakdowns, and entitlement failure. The impact of climatic hazards may have been greater among simple premodern societies, but under some circumstances even modern, more complex societies can suffer extreme climatic disruption. However, the impacts of climate and other geophysical hazards do tend to be greatest among impoverished segments of societies (Ingram et al. 1981; Mutter 2005), as has been demonstrated by the effects of the southeastern Asia tsunami and hurricanes Katrina and Rita. It is anticipated that the consequences of future anthropogenic climate change will continue to be greatest among the poor (Houghton 1997).

Two of the worst famines in world history illustrate the complex environmental, socioeconomic, and political dimensions of these catastrophes. The so-called 'late Victorian famines' of 1876–1879 across India, northern China, and Brazil—when an estimated 16–31 million people perished—were initiated by a strong El Niño event and extreme drought across the Indo-Pacific realm; the human tragedy, however, appears to have been aggravated by poverty, unrestrained market forces, and incompetent government (Davis 2001). Likewise, the catastrophic Chinese famines of 1958–1961 that attended the 'Great Leap Forward'—when 16–30 million 'excess deaths' occurred—began with drought but seem to have been magnified by Mao Zedong's social experiments and failed centralization of Chinese agriculture (Davis

2001). Analyses of these and other nineteenth- and twentieth-century famines indicate that the role of climatic extremes in economic system collapse and starvation has been complex, nonlinear, and strongly subject to prevailing social and technological conditions. The climatic sensitivity of premodern agrarian societies was likely increased by simpler trade and transportation systems, smaller-scale water control systems, and the absence of immunization against disease.

The variable social impacts of climatic extremes also were evident during the major decadal moisture regimes witnessed over North America during the modern era. The Dust Bowl drought of the 1930s (Figs. 10.1 and 10.2a) included the most extreme annual to decadal moisture shortfalls measured in the United States or Canada during the instrumental period (Fye et al. 2003). The Dust Bowl drought interacted with poor land use practices to produce massive dust storms and the most famous environmentally mediated migration in American history. The social costs of environmental change in the 1930s have not been fully separated from the technological and economic changes in Great Plains agriculture during the Depression, but the drought and dust storms certainly contributed to the heavy depopulation of the hard-hit areas on the southern High Plains (Worster 1979). The impact of the Dust Bowl was also mediated by a massive federal relief effort, and President Roosevelt's New Deal Policies 'ensured that the "catastrophe" of the 1930s was a large ripple

Fig. 10.1 A 'Dust Bowl farm' north of Dalhart, Texas, photographed during the June growing season of 1938 by Dorothea Lange (Library of Congress, Prints and Photographs Division, reproduction number LC-DIG-fsa-8b32396). The decadal drought of the 1930s contributed to one of the greatest environmental and social disasters in American history. The house illustrated here was still occupied, but most in the district had been abandoned by 1938

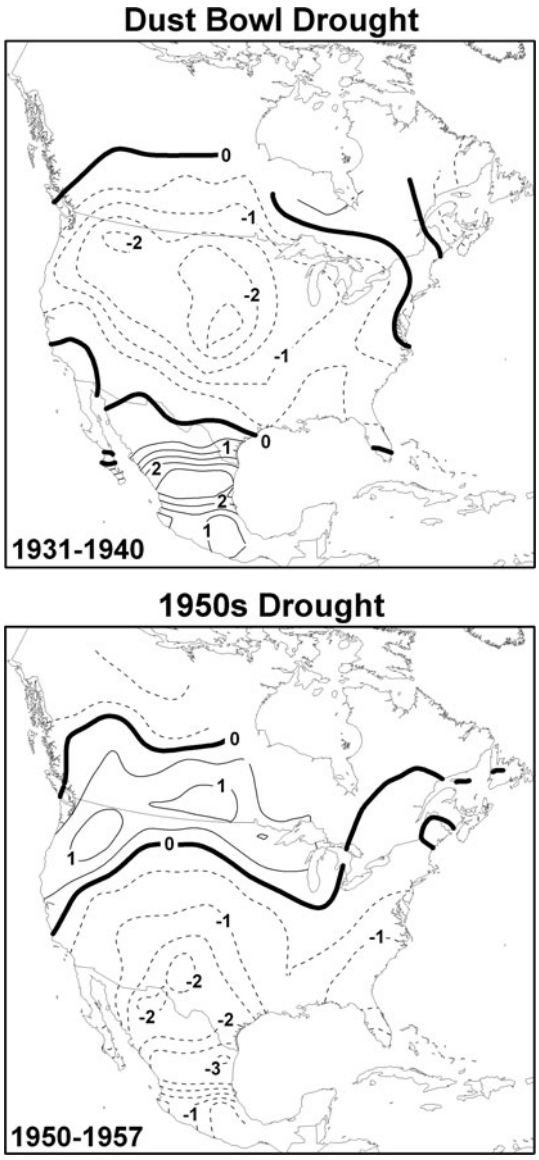

Fig. 10.2 Instrumental summer (June–July–August, JJA) Palmer Drought Severity Index averaged at each of the 286 grid points for North America (the 2.5° × 2.5° latitude/longitude grid from Cook et al. 2004, 2007) and then mapped for the Dust Bowl (**a**, 1931–1940) and 1950s (**b**, 1950–1957) droughts. The PDSI is an integration of monthly precipitation and temperature effects on available soil moisture, and it has proved to be a good model for the effects of climate on tree growth at moisture-limited sites. The 10-year average summer PDSI fell to −2.5 over the central Great Plains and reached above +2.5 over Mexico during the 1930s (a; contour interval is 0.5 PDSI units; *dashed lines* = negative PDSI and dry; *solid lines* = positive PDSI and wet). Note the changing geographical focus of decadal drought from the 1930s through the 1950s

through the national economy, rather than the tidal wave of system collapse on the entire western front of the Plains as in the 1890s' (Bowden et al. 1981).

By contrast, the severe drought of the 1950s, which impacted the southern Plains, Southwest, and Mexico (Fig. 10.2b), lasted nearly as long and impacted a region nearly as large as the Dust Bowl drought (Fig. 10.2a), but did not produce a fraction of the social consequences associated with the Dust Bowl in the United States (e.g., Warrick and Bowden 1981). Out migration from the hard-hit southern Plains

was less than 10% for the 1950s, comparable to emigration during wet decades (Bowden et al. 1981). The ranching (Kelton 1984) and dry farming (Rautman 1994) economies of the Southwest were hard-hit, but the postwar economy of the United States was booming and the drought had little economic impact at the national level. The 'Sun Belt miracle' of Southwestern population growth and intensive water and energy demand had yet to occur. However, Mexico experienced 'national drought' during the 1950s that had severe impacts on rural farming and ranching, highlighting international differences in the economic environments in which this severe regional drought developed (Florescano 1980).

The first major drought of the twenty-first century (Seager 2007), which began in 1999 and currently afflicts much of the western United States and northern Mexico, already has had major environmental and human consequences. Severe precipitation shortfalls have caused crop failures and cutbacks in both small- and large-scale dryland farming. Irrigation agriculture, municipal water supplies, and the generation of electricity have been threatened by unprecedented low water levels in Southwestern reservoirs. All this has occurred at a time when skyrocketing human population is vastly increasing demand for water and electricity and driving fierce competition among the affected groups, cities, and states. Massive fires have consumed more than a million acres of desiccated forests, fueled by living trees with moisture levels below that of kiln-dried lumber. These catastrophic fires have been linked with drought and regional climate change (Westerling and Swetnam 2003; Westerling et al. 2006) and have displaced burned-out communities, destroyed watersheds, and ravaged the tourist and lumber industries. Millions of moisture-stressed conifers (especially pinyon) have succumbed to the drought, or insect infestations, or the lethal combination of both, leaving barren landscapes exceptionally vulnerable to fire and erosion. The current forest dieback appears to exceed the mortality associated with the 1950s drought (Breshears et al. 2005), which had major ecological consequences across the Southwest (Swetnam and Betancourt 1998). Tree-ring data suggest that other major forest mortality events may have occurred during the droughts of the late thirteenth and sixteenth centuries (Swetnam and Betancourt 1998, Fig. 15), but the extent to which the current dieback is related simply to drought or may also reflect other human impacts on Western woodlands has not been determined.

Wet climate extremes may also have significant long-term socioeconomic consequences, as was illustrated from 1905 through 1917 during the early twentieth-century pluvial (Fye et al. 2003). The most recent assessment of the available tree-ring data for the western United States indicates that the first two decades of the twentieth century was the wettest multiyear episode in the past 1200 years (Cook et al. 2004). The tree-ring-reconstructed Palmer Drought Severity Indices (PDSIs; defined in Fig. 10.2) during the wettest decade of the twentieth-century pluvial (1907–1916) indicate prolonged wetness from Baja California across the Rockies to the Canadian border (Fig. 10.3). In fact, Stockton (1975) reconstructed Colorado River streamflow at Lees Ferry, Arizona, to arrive at perhaps the most famous number ever calculated with tree-ring data, a long-term mean annual flow of only 13×10^6 acre feet/year compared with 16.4×10^6 acre feet/year estimated by

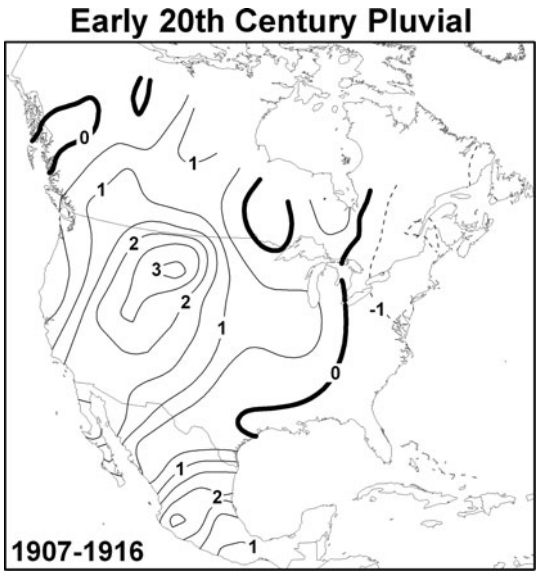

Fig. 10.3
Tree-ring-reconstructed summer PDSI averaged at each of the 286 grid points and mapped for the 10 most extreme consecutive years of the early twentieth-century pluvial (1907–1916; same mapping conventions as in Fig. 10.2). Note the two cells of reconstructed wetness over the central Rocky Mountains and Mexico

the Bureau of Reclamation from discharge data compiled during the twentieth-century pluvial (Hundley 1975; Fye et al. 2003; see Woodhouse et al. 2006 for a recent reanalysis). Streamflow reconstructions for the Salt, Verde, and Gila Rivers (Graybill 1989; Graybill et al. 2006) show a similar positive anomaly for the Colorado River drainage below Lees Ferry. The early twentieth-century period of elevated flow was certainly not sustained, but it coincided with the negotiations that led to the Colorado River Compact, which over-allocated the flow of the Colorado River among the basin states and later included Mexico (Brown 1988). This wet period also coincided with massive ecological changes on the forest and rangelands of the West, and even in the absence of human activities would have favored reduced fire and a pulse of forest regeneration (Swetnam and Betancourt 1998; Westerling and Swetnam 2003). These favorably wet conditions may have contributed to the 'unhealthy' overstocked forests with elevated fire risks in the West that also have been encouraged by overgrazing, deliberate fire exclusion, and anthropogenic warming associated with warmer spring temperatures and earlier snowmelt (Westerling et al. 2006).

This chapter cites a selection of tree-ring studies of climate extremes with demonstrated or *suspected* societal impacts, including both moisture and temperature extremes. We then use the gridded tree-ring reconstructions of the summer PDSI for North America (Cook et al. 1999, 2004; Cook and Krusic 2004) and other regional climate reconstructions to estimate the intensity and spatial extent of selected drought and wetness extremes that are related at least chronologically, if not causally, to major societal changes in parts of North America. This retrospective discussion begins with the data-rich modern era, for which we know much more about the impacts of climatic extremes on society; it then extends back in time to

consider examples from the historic, colonial, and prehispanic eras. The climate and social associations witnessed during the modern and historic eras provide a proof of concept for the possible role of climatic extremes in selected social changes in prehistory. Further documentary and archaeological research will be needed to help test these climatic hypotheses of social change during the historic, colonial, and prehispanic eras.

10.2 Tree-Ring Analyses of Climate Extremes and Human Impacts

A.E. Douglass pioneered the use of proxy climate data from tree rings to study cultural change. Douglass documented severe multiyear drought over the Colorado Plateau dating from AD 1276 to 1299 and speculated on the hardships such an extended dry spell must have had on the Anasazi ancestors of the modern Pueblo Indians (Fig. 10.4; Douglass 1929). In fact, the first absolute tree-ring dating chronology for the Southwest was based on living trees and wood and charcoal recovered from historic and prehistoric sites (Douglass 1929). The exact chronological link between the living tree record and the archaeological time series was complicated by the prehistoric migration of people and the abandonment of

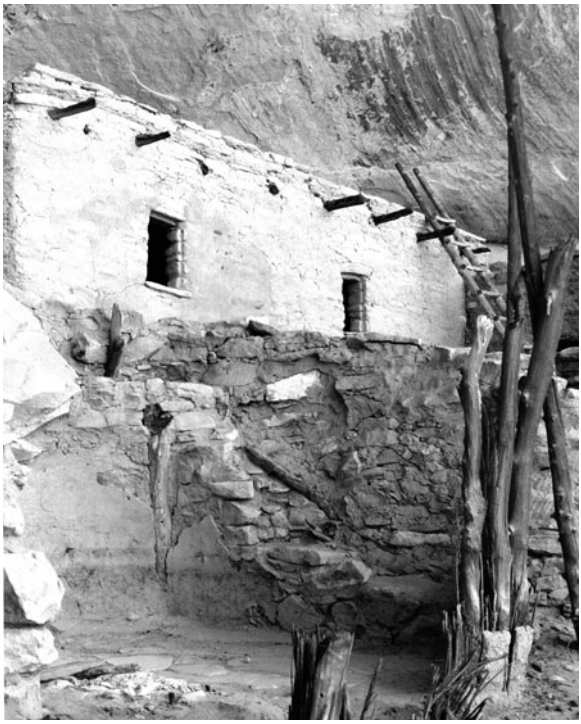

Fig. 10.4 Rooms 44, 45, and 74 (rear *right*, rear *left*, and *foreground*, respectively) at Keet Seel in northeastern Arizona, one of many Southwestern sites abandoned during Douglass' Great Drought (AD 1276–1299). Room 74 is an annex to the adjacent kiva (a ceremonial structure). Grooved door jambs identify Rooms 44 and 45 as granaries built in 1275 to store food against future shortages (Dean 1969)

village sites during the Great Drought of the late thirteenth century (Douglass 1935). Datable timbers from the late thirteenth and early fourteenth centuries were scarce in the region. Douglass and his collaborators finally found charcoal samples bridging the gap between the modern and archaeological chronologies south of the classic Anasazi heartland near Jeddito Wash and along the Mogollon Rim, in fourteenth- and fifteenth-century archaeological sites believed to have grown in part by immigrants from sites abandoned in the Four Corners area (Haury and Hargrave 1931; Haury 1962; Adams 2002).

The causes of regional abandonment on the Colorado Plateau are still debated, but experiments have shown that the tree-ring record is well correlated with dryland crop yields in the Four Corners region (Burns 1983; Van West 1994), suggesting a drought sensitivity of the Anasazi practicing dryland agriculture. Burns (1983) used tree-ring-reconstructed crop yields to simulate food storage shortfalls and surpluses that identified probable famine among the Mesa Verde Anasazi during droughts, and expanded construction activity during periods of surplus crops, just as Douglass had suggested in 1935.

A number of other provocative studies describing tree-ring evidence for climate impacts on society in Europe and elsewhere have been published. Le Roy Ladurie (1971), for example, linked the period of exceptional growth from 1312 to 1319 in oak chronologies from southern Germany developed by Bruno Huber with flooding, harvest failure, and famine across France and England during one of the most severe periods of famine of the Middle Ages. Lamb (1995) discussed a number of climate inferences based on tree-ring data from Europe and North America, including a shift to colder conditions in the fifth century AD contemporaneous with Roman decline in western Europe.

Perhaps the most unambiguous link between tree-ring data, climate effects, and societal impacts has been demonstrated with frost-damaged rings. LaMarche and Hirschboeck (1984) and Salzer (2000) linked bristlecone pine records of frost rings in the western United States to large-magnitude volcanic eruptions through dust veil effects on the global climate system. The bristlecone pine records include frost rings in 1817 and 1884, following the eruptions of Tambora in 1815 and Krakatau in 1883. These were two of the largest volcanic eruptions in the past 500 years, and both had global-scale climatic and societal impacts. LaMarche and Hirschboeck (1984) tentatively linked the severe frost-ring event dated to 1626 BC in the White Mountain region of California to archaeological and radiocarbon evidence for the destruction of the late Bronze Age site of Akrotiri by the cataclysmic eruption of Thera (Santorini), an assignment that still generates heated debate (Manning 1999).

Baillie (1994, 1999) compiled evidence for profoundly suppressed growth in temperature-sensitive tree-ring chronologies from Europe, North America, and South America during the period AD 536–545. This evidence for anomalous cold was supported by early documentary references to severe cold, crop failure, and dry fogs, suggesting the global climatic effects of a cataclysmic volcanic eruption or the impact of an extraterrestrial object. The societal impacts of the cold climate conditions in the mid-sixth century appear to have been severe and included famine, pandemics (e.g., the Justinian Plague occurred in the 540s), and widespread

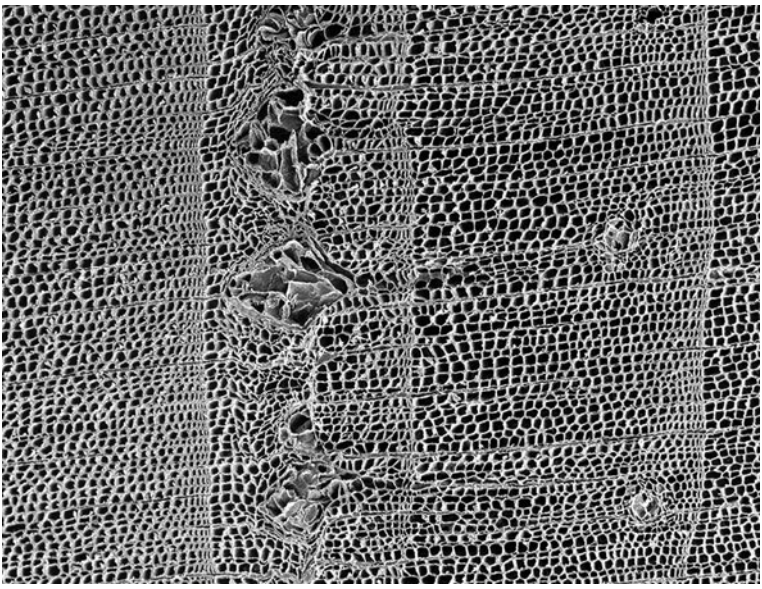

Fig. 10.5 A scanning electron micrograph by Dee Breger (2003), illustrating the annual growth rings from a Siberian pine (*Pinus sibirica* Du Tour) from AD 535 to 539, including the corrupted latewood during the extraordinary growing season freeze event of 536 (i.e., frost ring; D'Arrigo et al. 2001). The 536 event has been linked to an atmospheric dust veil arising from a massive volcanic eruption or extraterrestrial impact event and had global-scale climatic and societal effects (Baillie 1999)

mortality (Baillie 1999; Keys 1999). D'Arrigo et al. (2001) found severe frost damage in the rings of Siberian pine from Mongolia for AD 536 (Fig. 10.5), which was associated with documentary references to the attenuation of starlight, summer frost, crop failure, and famine in northern China from AD 536 to 537. The causes of the extraordinarily cold conditions during the mid-sixth century remain unclear, but they do appear to have occurred at the global scale and had severe societal impacts.

Brunstein (1995, 1996) significantly expanded the bristlecone pine frost-ring record for the Rocky Mountains and described the 'near extinction' of large animals on the High Plains of Colorado and Wyoming during the catastrophic winters of AD 1842–1845, which caused hunger and sickness among the southern Cheyenne. Stahle (1990) described the synoptic climatology and social impacts of the spring freeze events recorded by post oak frost rings from the southern Great Plains, including the epic spring cold wave of 1828: record-setting winter warmth was followed by an arctic outbreak of subfreezing temperatures in April that damaged fruit trees and crops across much of the eastern United States (Ludlum 1968; Mock et al. 2007). St George and Nielsen (2000) used the frequency of 'flood rings' in bur oak to estimate high-magnitude floods on the Red River in Manitoba. The most extreme flood ring in the 500-year record occurred in 1826, when the largest known flood in the history of the region nearly wiped out the Red River Settlement. The recurrence

of a flood of this magnitude would exceed the design capacity of the flood protection system for Winnipeg, force extensive evacuations, and cause extensive property damage (St George and Neilsen 2000).

Other interesting tree-ring studies of climatic extremes and social impacts include Jacoby et al. (1999), who used white spruce ring density data to reconstruct extremely cold conditions following the Laki eruption of 1783, when hundreds of Inuit people perished of famine in northwestern Alaska. Gil Montero and Villalba (2005) used moisture-sensitive tree-ring chronologies of *Juglans australis* and *Polylepis tarapacana* as proxies of drought and rural socioeconomic stress in northwestern Argentina. They note a relationship between severe, sustained, and spatially extensive drought beginning in the 1860s and heavy human mortality. The effects of prolonged drought on human mortality appear to have been leveraged by the decreasing availability of water, which concentrated humans and livestock around the few remnant water sources. This concentration favored the spread of epidemic diphtheria, which in the absence of an effective response by governmental authorities, contributed to the mortality and depopulation of the region (Gil Montero and Villalba 2005).

Severe nineteenth-century droughts have been identified in the documentary record for Africa (e.g., Nicholson 1994; Endfield and Nash 2002), including a decadal drought from 1857 to 1865. Food was very scarce and from 'the sea coast to the Zambesi, fountains, streams, and pools have dried up. . .cattle of all descriptions died everywhere from sheer poverty, and the losses of draught oxen to travelers, hunters and traders have been very severe' (London Missionary Society, quoted by Nash and Endfield 2002). A new tree-ring reconstruction of rainfall based on African bloodwood (*Pterocarpus angolensis*) identifies the period from 1859 to 1868 as the driest decade in the past 200 years in western Zimbabwe (Therrell et al. 2006); the reconstruction also highlights the potential for using tree-ring chronologies from deciduous hardwoods in seasonally dry tropical woodlands to help document the historical impacts of climate extremes.

Extreme climate has been implicated in many other important historical events, and the developing network of climate-sensitive tree-ring chronologies worldwide may allow new insight into these debates. For example, the decline of the Ming Dynasty in China has been linked in part to severe drought extending from AD 1637 to 1644 (Davis 2001). This drought and the associated socioeconomic impacts have been identified with documentary sources, but the new moisture-sensitive chronologies from Asia (e.g., Buckley et al. 1995; Pederson et al. 2001; Liu et al. 2004) will help researchers determine the intensity and spatial impact of this drought and of other climatic extremes over the past several centuries.

Kiracofe and Marr (2002) suggest that the devastating epidemic of ca. 1524 among the Inca of Peru, which killed a reported 200,000 people just prior to the Spanish conquest, was probably caused by bartonellosis (*Bartonella bacilliformis*) transmitted by infected sand flies (*Lutzomyia* sp.). Climate anomalies associated with El Niño events have been linked with a huge increase in the numbers of infected sand flies in the areas of Peru affected by bartonellosis. The co-occurrence of El Niño–related climate extremes during the suspected outbreak of 1524 might be

tested with the expanding network of tree-ring chronologies for South America. The discovery of the dendroclimatic value of *Polylepis tarapacana*, a small arid-site tree of the Andes, which grows at the highest elevations of any tree species on earth, is one of the most interesting recent developments in dendrochronology (Argollo et al. 2006). These *Polylepis* chronologies may help test the 1524 climate-bartonellosis hypothesis if time series of sufficient length can be developed.

10.3 Social Impacts of Climate Extremes During the Historic Era

The gridded tree-ring reconstructions of the summer Palmer Drought Severity Index for North America recently produced by E.R. Cook and colleagues provide an exactly dated, spatially detailed record of the hydroclimatic conditions attending many tumultuous events in American history and prehistory (Cook et al. 2007). To highlight the selected climatic extremes, we used the time series of tree-ring-reconstructed summer PDSIs (e.g., Cook et al. 2004) averaged from all 286 individual grid point reconstructions across North America for the past 500 years (Fig. 10.6). This reconstruction highlights the most important continent-wide annual to decadal dry and wet regimes and is highly correlated with the continent-wide average of summer PDSIs based on the instrumental data ($r = 0.84$ for 1900–1978). We then mapped the patterns of reconstructed PDSIs during the specific time periods of interest to estimate the intensity and spatial distribution of these climate extremes. Multiyear droughts with severe social impacts in the new North American PDSI reconstructions include, or are suspected of including, the late nineteenth-century drought over the central and northern Great Plains, the mid-nineteenth-century drought focused over the central Great Plains, the late

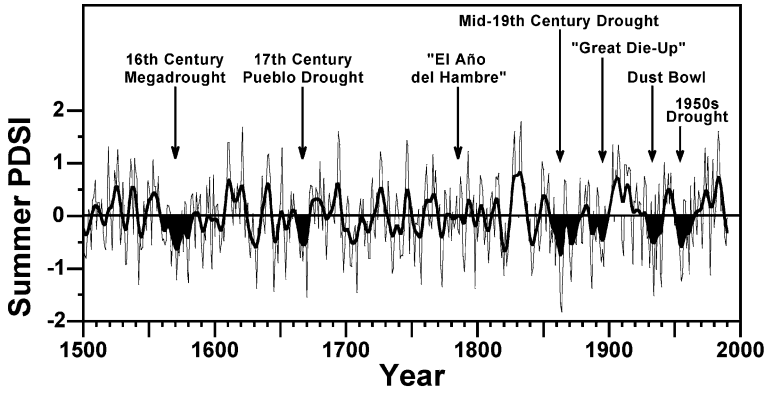

Fig. 10.6 The time series of tree-ring-reconstructed summer PDSI averaged each year for all 286 North American grid points (from Cook et al. 2004), illustrating continent-wide wet and dry spells from AD 1500 through 1990. Selected severe droughts of the past 500 years are highlighted and discussed in the text

eighteenth-century drought over the southern Plains and Mexico (including 'El Año de Hambre'), the seventeenth-century Pueblo drought over the Southwest, the early seventeenth-century Jamestown drought in Virginia, and the sixteenth-century megadrought across North America. We also discuss the Aztec drought of 'One Rabbit' in the mid-fifteenth century, the late thirteenth-century Great Drought first documented and discussed by Douglass, and the prolonged droughts contemporaneous with the Classic Period decline in Mesoamerica late in the first millennium AD. Many of the wettest years now evident in the North American PDSI reconstructions also had significant social consequences, including the early nineteenth-century pluvial, one of the wettest episodes in the tree-ring record for western North America in 500 years (Fig. 10.6).

In the dendroclimatic perspective of the past 500 years, the twentieth century was unusually wet, in spite of the Dust Bowl and 1950s droughts. The nineteenth century was drier, punctuated by several prolonged droughts that we know had significant socioeconomic and environmental impacts, magnified in part by human activities (Fig. 10.6). The so-called 'Great Die-Up' during the blizzards of 1886–1887 occurred during widespread drought in the central and northern Great Plains from 1886 through 1890 (Fig. 10.7). The drought appears to have been most severe over the Dakotas and Canadian prairies; it is reported to have degraded the forage value of the grasslands and contributed to the poor condition and subsequent mortality of cattle and to the ultimate collapse of the speculative, overstocked High Plains cattle empire in the late nineteenth century (Stegner 1954). The heavy mortality of cattle during the drought and blizzards of 1886–1887, which extended into the southern Great Plains (e.g., Wheeler 1991), was made famous by Charley Russell's

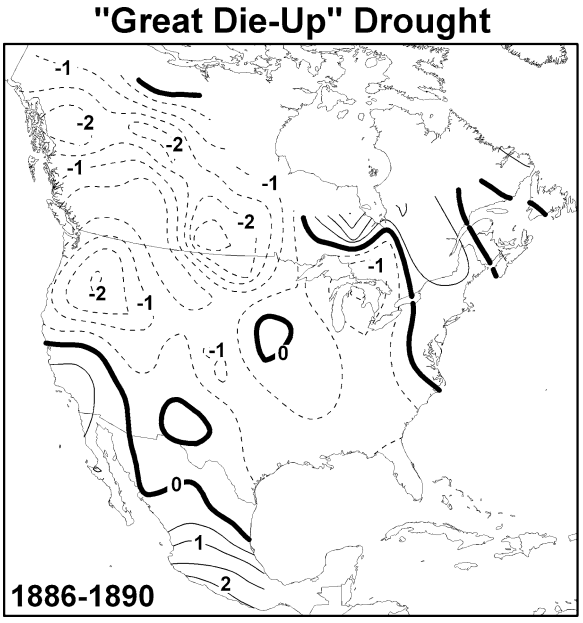

Fig. 10.7 Tree-ring-reconstructed summer PDSI averaged and mapped for the 5-year period from 1886 to 1890, and indicating prolonged drought over the northern Plains and Pacific Northwest (see Fig. 10.2 for mapping details). The impacts of this dry period were magnified by the extreme blizzards of 1886, which resulted in the 'Great Die-Up' of range cattle across the Great Plains

painting 'Waiting for a Chinook,' a grim portrait of a starving steer confronting a pack of wolves in a bleak winter landscape.

The Great Plains homesteaders also suffered in the blizzard and drought, as described by Wallace Stegner (1954): 'In some of the shacks, after five days, a week, two weeks, a month of inhuman weather, homesteaders would be burning their benches and tables and weighing the chances of a desperate dash to town—lonely, half-crazed Swedes, Norwegians, Russians, Americans, pioneers of the sod house frontier. Sometimes they owned a team, a cow, a few chickens; just as often they had nothing but a pair of hands, a willingness to borrow and lend, a tentative equity in 160 acres of Uncle Sam's free soil, a shelf full or partly full or almost empty of dried apples, prunes, sardines, crackers, coffee, flour, potatoes, with occasionally a hoarded can of Copenhagen *snus* or a bag of sunflower seeds. More than one of them slept with his spuds to keep them from freezing. More than one, come spring, was found under his dirty blankets with his bearded grin pointed at the ceiling, or halfway between house and cowshed where the blizzard had caught him' (Stegner 1954, p. 294). The drought, which began in 1886, 'was a slow starvation for water, and it lasted through 1887, 1888, 1889, into the eighteen-nineties. Homesteader hopes survived the first year; in fact, the speculative prices of land in eastern Dakota continued to spiral upward, and the rush to Indian Territory took place in the very heart of the dry years. By the second year the marginal settlers had begun to suffer and fall away; by the third year the casualties were considerable. By the fourth it was clear to everybody that this was a disaster, a continuing disaster. What began in 1886 was a full decade of drouth, the cyclic drying-out that [John Wesley] Powell had warned of in 1878' (Stegner 1954, p. 296).

The drought of the 1880s and 1890s was part of a recurring pattern of surplus and deficit moisture on the Great Plains that contributed to the waxing and waning of nonirrigated farms in the uplands. To describe the social impacts of these recurrent Great Plains droughts, Walter Prescott Webb (1931, p. 343) quoted A.M. Simons: 'following the times of occasional rainy season, this line of social advance rose and fell with rain and drought, like a mighty tide beating against the tremendous wall of the Rockies. And every such wave left behind it a mass of human wreckage in the shape of broken fortunes, deserted farms, and ruined homes.' The population losses in the dry-farming margins of the Great Plains were extreme in the 1890s (integrating the impacts of both the late 1880s through early 1890s and subsequent dry years in the 1890s), when some regions lost 50–75% of their citizens (Bowden et al. 1981). As Stegner noted, Cyrus Thomas coined the phrase 'rain follows the plow' in 1868, but 'by 1888 he knew better' (Stegner 1954, p. 298).

The most severe and long-lasting tree-ring-reconstructed drought of the nineteenth century occurred with little relief from 1841 through 1865, closely following the early nineteenth-century pluvial, one of the wettest periods in the past 500 years (Figs. 10.6 and 10.8). The center and intensity of the mid-nineteenth-century drought shifted over time and was interrupted by a few wet years (e.g., Woodhouse et al. 2002), but the western United States, Canada, and the borderlands of northern Mexico are estimated to have averaged incipient drought or worse for the entire 25-year period. This multidecadal drought appears to have been most extreme

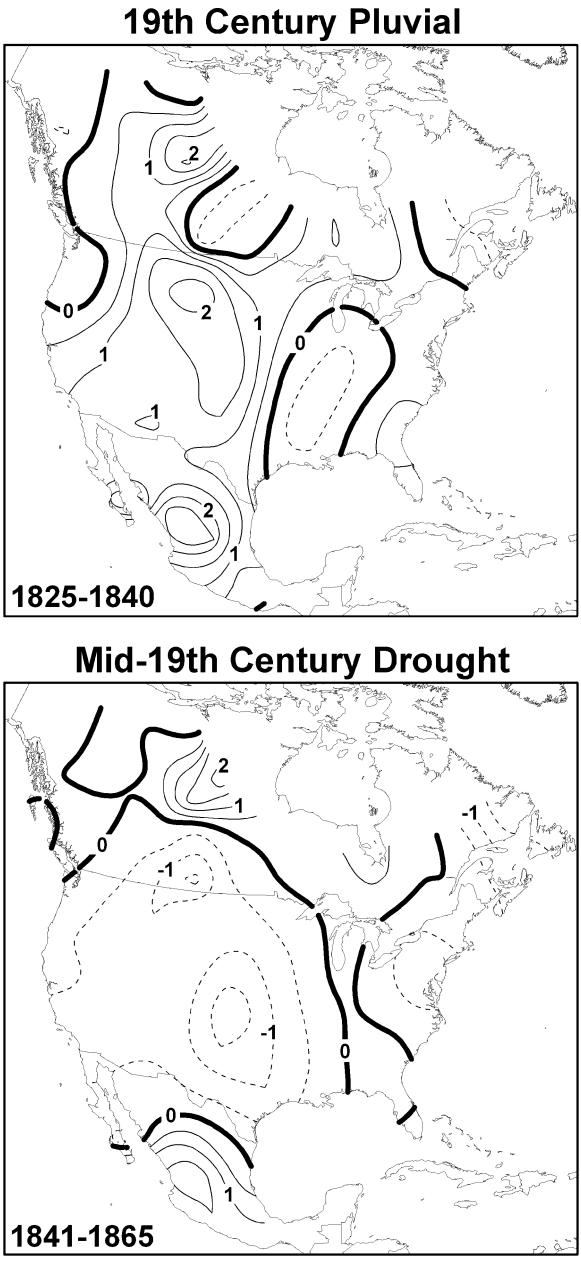

Fig. 10.8
Tree-ring-reconstructed summer PDSI averaged and mapped for the 'environmental crisis' of the mid-nineteenth century, when a pluvial (**a**, 1825–1840) was followed by a 25-year-long dry period (**b**, 1841–1865), which West (1995) argues interacted with overgrazing of vital riparian corridors by Native American ponies and Euroamerican stock animals to contribute to the extirpation of bison from the central High Plains

over the central Great Plains (Fig. 10.8), where an 'environmental crisis' described by West (1995) afflicted the Arapaho and Cheyenne Indians and interacted with their newly adopted horse culture and with the stock animals of Euroamerican overlanders to degrade critical riparian habitat and lead to the extirpation of the bison from the central High Plains.

The Arapaho and Cheyenne adopted the horse culture and bison hunting in the eighteenth century and migrated from the Great Lakes region into the central High Plains by 1800. They participated in trade with Spanish outposts at Santa Fe and Taos during a time of generally favorable climate, including the early nineteenth-century pluvial. Vivid descriptions by Henry Dodge and other explorers describe scenes of incredible abundance on the central High Plains, including vast herds of bison (West 1995). However, West argues that the Arapaho and Cheyenne became victims of their own technological innovation and ultimately came into competition with the very animal upon which they depended, the bison. The riparian corridors of the Platte, Republican, Smoky Hill, Arkansas, and Cimarron Rivers were key to the High Plains adaptation of the bison, providing water, nutritious winter forage, and shelter from winter storms. But the Native Americans and their ponies required these same resources, as did the stock animals of the Euroamerican overlanders. West (1995) chronicles the increasing use of the riparian resources during the 1840s and 1850s, the same period when the prolonged wet conditions of the early nineteenth-century pluvial were shifting into the persistent drought regime of the mid-nineteenth century. He argues that it was the convergence of Native American bison hunting, human utilization and degradation of the riparian 'habitat islands' of the High Plains, and the onset of multidecadal drought that led to the extirpation of the bison from the central High Plains by 1860, long before the rapacious market hunting of bison following the Civil War. The catastrophic winters of 1842–1845 must have contributed to the bison decline as well (Brunstein 1996).

El Año del Hambre, the year of hunger, described by Gibson (1964) as the 'most disastrous single event in colonial maize agriculture' in Mexico, occurred in 1786 after the August frost of 1785 in highland Mexico and during the severe 3-year drought of 1785–1787 (Therrell 2005). The gridded PDSI reconstructions indicate moderate drought (or worse) for this 3-year average extending from central Mexico into Texas (Fig. 10.9). Some 300,000 people are reported to have perished in the famine and epidemic disease that followed the frost, drought, and crop failures (Florescano 1980; Garcia Acosta 1995). The value of tithes paid to the Church inflated during the drought and frost of 1785–1787 due to the crop failures and increased cost of grain (Therrell 2005). Before El Año del Hambre, substantial droughts in Sonora were accompanied by crop failures, famine, disease outbreaks, and insurrections among the Yaqui, Pimas Bajos, and Seri Indians in 1740, 1737, and 1729, respectively (Brenneman 2004).

A severe 6-year drought occurred across the Southwest and into the central Plains from 1666 through 1671 (Fig. 10.10). A series of disasters among the Pueblo societies of New Mexico in the seventeenth century—including Apache raids, drought, famine, and disease—led to great population loss and submission to Spanish missionary control (Sauer 1980; Barrett 2002). As the drought progressed to 1670, the Pueblos and Spaniards were both reduced to eating 'hides and straps boiled with herbs and roots,' and 950 inhabitants of the Jumanos Pueblos died of starvation (Sauer 1980, p. 66). A great pestilence broke out in 1671 among the Pueblos and their cattle, and more than 400 people perished in one village. Documentary information on crop production during the Spanish occupation of the region is correlated with regional tree-ring estimates of precipitation (Barrett 2002; Parks et al.

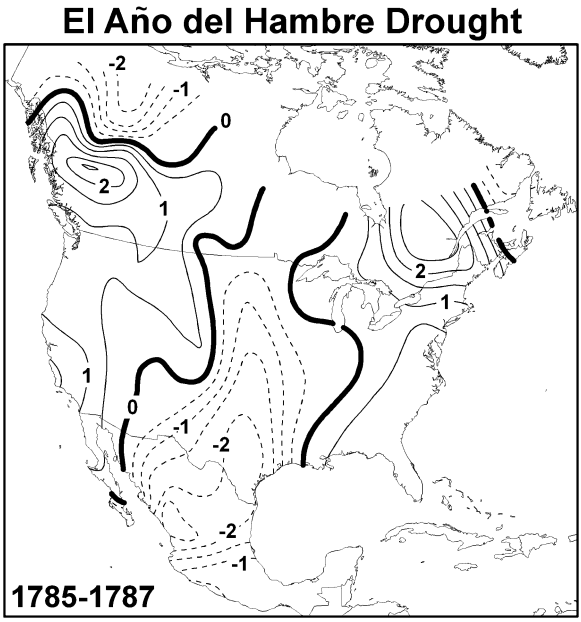

Fig. 10.9
Tree-ring-reconstructed summer PDSI mapped for the 3-year period (1785–1787) coinciding with El Año del Hambre (1786–1787) in Mexico, one of the most famous famines in Mexican history, resulting from a drought- and frost-induced crop failure

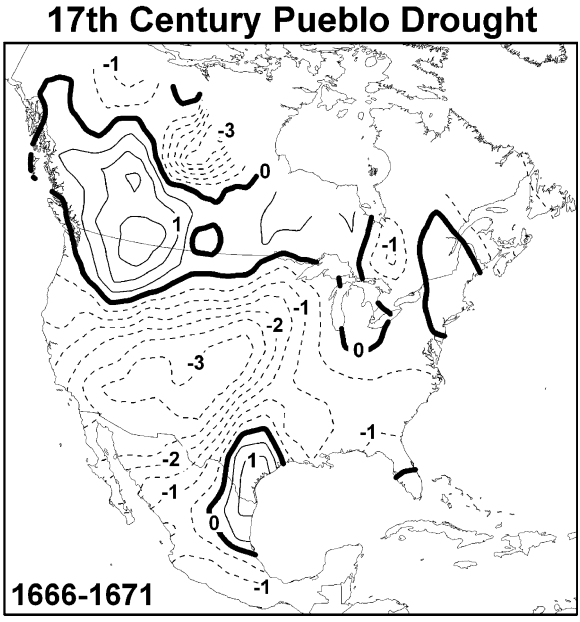

Fig. 10.10
Tree-ring-reconstructed summer PDSI mapped for the severe seventeenth-century drought, which lasted 6 years (1666–1671) and contributed to famine, disease, death, and village abandonment among the Pueblo societies of New Mexico

2006) illustrating the apparent sensitivity of the seventeenth-century economy in New Mexico to severe drought. Indeed, the hardship associated with this dry spell may have helped trigger the Pueblo Revolt of 1680, which drove the Spaniards out of New Mexico for more than a decade. This seventeenth-century 'Pueblo' drought, named for the region where the socioeconomic impacts have been documented in greatest detail, may serve as a useful model for the environmental and agricultural impacts of protracted drought among prehispanic Puebloan societies. These impacts may include the controversial effects of the Great Drought on the Anasazi societies of the Colorado Plateau, although the Anasazi did not suffer Apache raids or Spanish colonization in the late thirteenth century. The seventeenth-century Pueblo drought also offers a vivid spatial contrast to the geographical distribution of the early twentieth-century pluvial (Fig. 10.3), but it reproduces reasonably well the intensity, duration, and spatial impact of the recent drought over the Southwest that began in 1999 (Drought Monitor 2004).

Bald cypress tree-ring data from the Tidewater region of Virginia provide an interesting perspective on the human impact of drought extremes during the early English settlement of North America. Jamestown was founded in April 1607, the second year of a 7-year regional drought more severe and long-lasting than any other such event in more than 700 years (Stahle et al. 1998). The tree-ring data were calibrated with the Palmer Hydrological Drought Index (PHDI; Stahle et al. 1998) and, along with archival information on mortality among the colonists, provide statistical evidence for the sensitivity of this early English colony to drought. Mortality and the reconstructed PHDI for the Tidewater region of Virginia and North Carolina are significantly correlated for the first 18 years of English occupation, with most deaths arising from starvation and disease in drought years (Fig. 10.11; $r = 0.71$; $P < 0.001$, for 1608–1624 at Jamestown and including 1586, the one year with mortality data from the Roanoke Colony [Stahle et al. 1998]). In fact, just 38 of the initial 104 colonists survived the first year at Jamestown, and only 1200 out of the 6000 settlers sent to Jamestown in the first 18 years of settlement were still living by 1624.

The drought sensitivity of the early English settlers at Jamestown seems to have been heightened by their dependence on the trade and tribute of food supplies from the native Algonquin. The Spanish sphere of influence in North America during the sixteenth century extended from Mexico and Florida northward up the Atlantic coastline into the Chesapeake Bay, and it included missionary settlements in modern South Carolina (Paar 1999) and Virginia (Lewis and Loomis 1953). Father Juan Bautista de Segura at the Chesapeake Bay and authorities at the Santa Elena colony in South Carolina both referred to extended drought, parched soil, food shortages, famine, and death in the 1560s (Lewis and Loomis 1953; Anderson et al. 1995). These accounts refer to the hardships and food shortages suffered by the native people during drought well before the settlement of Jamestown, but this drought sensitivity would presumably have been shared by Spanish or English colonists who depended on the natives for their food supply.

The drought sensitivity of the early English settlers at Jamestown also arose from the specific location of the colony on the lower James River estuary near the

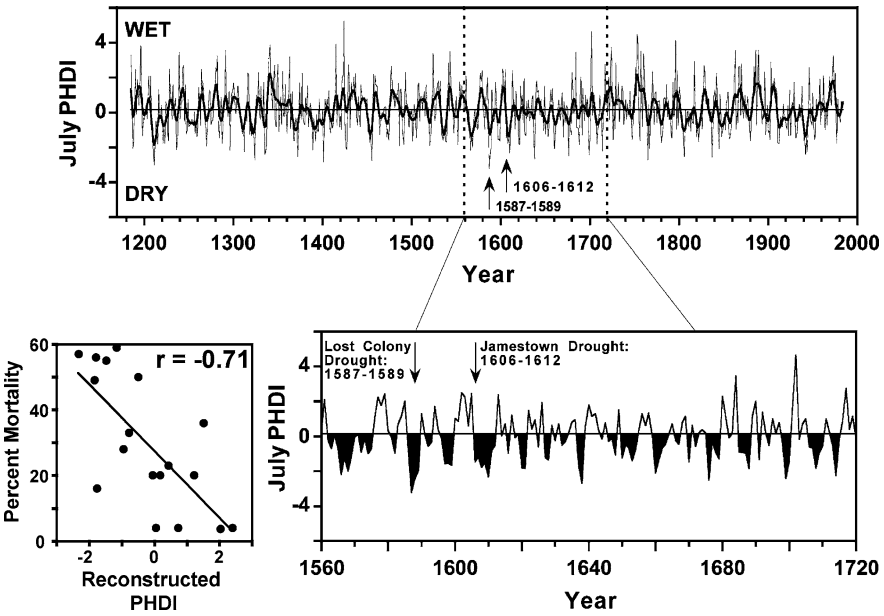

Fig. 10.11 This tree-ring reconstruction of the Palmer Hydrological Drought Index for the Tidewater region of Virginia and North Carolina extends from AD 1200 to 1985 and illustrates record drought during the initial English attempts to colonize America (Stahle et al. 1998). The Lost Colony of Roanoke Island disappeared during the most extreme reconstructed drought in 800 years (1587–1589), and the first successful settlement at Jamestown suffered prolonged drought from 1606 to 1612. Thousands of settlers died during the first two decades of English colonization, and the percent mortality was correlated with growing season moisture conditions (June PHDI, inset *left*)

brackish water/freshwater front. The location of this salinity gradient in the James River is sensitive to precipitation and streamflow (Prugh et al. 1992). In dry years, brackish water extends well upstream from Jamestown, and we know from firsthand accounts that the settlers suffered poor water quality and ill health during these dry years (Stahle et al. 1998). The Jamestown colony ultimately survived the drought and suffering during the first two decades of settlement to become the first successful English settlement in America. The drought sensitivity of the colony appears to have been lessened by increased support from England, expanded agricultural production, an improved water supply, and the development of the tobacco trade.

The drought of the 1560s in the Carolinas and Virginia was part of a severe, long-lasting drought that impacted much of the North American continent during the sixteenth century. This multidecadal sixteenth-century megadrought was focused over Mexico and the Southwest and persisted with little relief in some areas for nearly 30 years (Fig. 10.12). The drought appears to have developed over the far West in the 1540s, moved into the Great Plains during the 1550s, was most intense over Mexico and the eastern United States in the 1560s, expanded into the southwestern United States during the 1570s, and culminated in the 1580s over the Rocky

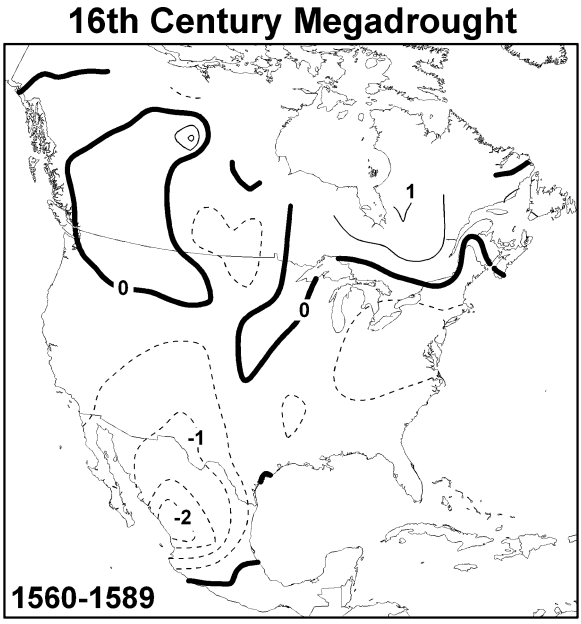

Fig. 10.12 Tree-ring-reconstructed summer PDSI during the sixteenth-century megadrought (see Fig. 10.2 for map details), the most severe sustained North American drought evident in the tree-ring record for the past 500 years (Stahle et al. 2000, 2007). Dry conditions prevailed for 30 years (1560–1589), but the epicenter of decadal drought shifted across the continent during the late sixteenth century (not shown)

Mountains (Stahle et al. 2007). During its most intense phase, the sixteenth-century megadrought appears to have exceeded the severity and geographical coverage of the Dust Bowl drought and may have been the worst drought over North America in the past 500 years (Stahle et al. 2000).

Significant environmental and socioeconomic impacts of the sixteenth-century megadrought have been reported for Mexico, the southwestern United States, and the Spanish and English colonies in the southeastern United States. Sir Walter Raleigh's colony on Roanoke Island (North Carolina) disappeared in 1587, which tree-ring data suggest was the driest single year in 800 years for the Tidewater region of Virginia and North Carolina (Stahle et al. 1998). The Spanish colony at Santa Elena, South Carolina, occupied during 1565–1587, endured many hardships associated with drought during the 1560s. The Juan Pardo expedition into the interior of the Carolinas and Tennessee during 1567–1568 was organized in part to seek food supplies for the colony (Anderson et al. 1995). In northern New Mexico, some pueblos were abandoned during the sixteenth-century drought (Schroeder 1968, 1992). Many of these settlements relied on rainfall agriculture and evidently could not be sustained during the extended drought.

The most severe impacts of the sixteenth-century drought appear to have occurred in Mexico, where extreme drought interacted with conquest, colonization, harsh treatment of the native people under the encomienda system of New Spain, poor crop yields, and epidemic disease to result in one of the worst demographic catastrophes in world history. The size of the native population of Mexico at the time of European contact is controversial, with the low count of 'minimalists' such as Angel Rosenblatt estimating some 8 million inhabitants, and the high count of

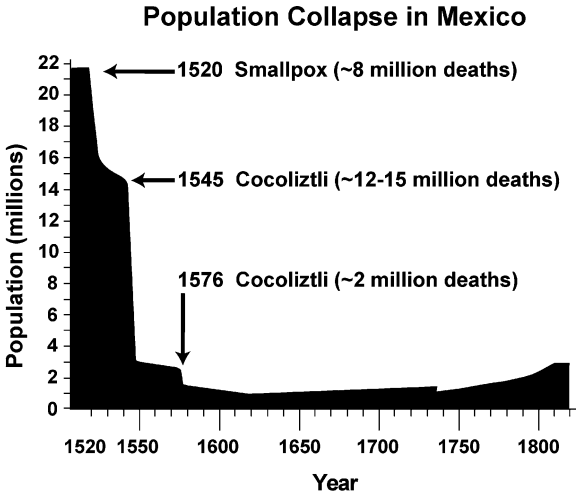

Fig. 10.13 The demographic collapse in Mexico following conquest in the sixteenth century is illustrated with population estimates from Cook and Simpson (1948) and Gerhard (1993). The heavy mortality in the 1540s and 1570s has been linked to indigenous hemorrhagic fevers (i.e., 'cocoliztli') and climate extremes by Acuna-Soto et al. (2002). The population of Mexico did not return to pre-conquest levels until the twentieth century

'maximalists' such as Sherburne Cook and Woodrow Borah estimating 15–20 million (Cook and Simpson 1948). The weight of opinion seems to favor the high count, and the population estimates for Mexico shown in Fig. 10.13 are based on the work of Cook and Borah (Gerhard 1993).

The epidemic of 1519–1520 was certainly caused by smallpox and killed an estimated 8 million native Mexicans during the war of conquest with Cortez (Acuna-Soto et al. 2002; Fig. 10.13). The conventional wisdom has been that the catastrophic epidemics of 1545–1548 and 1576–1580, which killed an estimated 12–15 million and 2–2.5 million people, respectively, were also the result of introduced European or African diseases such as measles, smallpox, and typhus (Acuna-Soto et al. 2000; Marr and Kiracofe 2000). The epidemic of 1545–1548 killed an estimated 80% of the native population of Mexico, which in absolute and percentage terms approaches the severity of the Black Death of bubonic plague from 1347 to 1351, when, conservatively, 25 million people perished in western Europe, or about 50% of the population. But the devastating Mexican epidemics of 1545 and 1576 are now believed by some epidemiologists to have been indigenous hemorrhagic fevers called 'cocoliztli' and later 'matlazahuatl' (Nahuatl terms for 'pest'). These epidemics may have been misdiagnosed as smallpox and typhus due in part to mistranslations of contemporary descriptions and the repetition of historical error. Two recent articles in the epidemiological literature cite new translations from the original Latin texts to make the convincing argument that the catastrophes of 1545 and 1576 were hemorrhagic fevers—probably caused by an indigenous agent, possibly with a rodent vector—that was leveraged by a sequence of climatic extremes and aggravated by the appalling living conditions of the native people under the encomienda system of New Spain.

Acuna-Soto et al. (2000) and Marr and Kiracofe (2000) cite descriptions of cocoliztli by Dr. Francisco Hernandez, the proto-medico of New Spain and former

personal physician of King Phillip II. Dr. Hernandez, who was in Mexico during the epidemic of 1576, described the symptoms of cocoliztli with clinical accuracy and detail. The symptoms included acute fever; intense headache; vertigo; and great effusions of blood from all body openings, especially the nose, ears, eyes, etc. Also reported were black tongue, green urine and skin, a net-like rash, abscesses behind the ears that invaded the neck and face, acute neurological disorder, insanity, and frequently death in 3 or 4 days (Acuna-Soto et al. 2000). Upon autopsy, the heart was found to be black and drained yellow and black blood, the liver was enlarged, and the lungs and spleen were semi-putrefied (Acuna-Soto et al. 2000). These symptoms do not describe smallpox, typhus, or any other European disease known to Dr. Hernandez, but more resemble a hemorrhagic fever such as Ebola or hemorrhagic forms of hantavirus. The mortality during these cocoliztli epidemics reflected the social order of sixteenth-century Mexico; deaths were highest among the native people, then the Indian-African mestizos, the Indian-European mestizos, the Africans, and finally even some Europeans died of this disease (Acuna-Soto et al. 2000). The severity of the epidemic may have been magnified among the native people by their poor living conditions, poor diet, and their overwork incumbent on providing tribute under the encomienda system. The geography of the 1545 and 1576 epidemics is also interesting, indicating a preference for the highland areas of Mexico and an absence from the warm low-lying coastal plains (Acuna-Soto et al. 2000, 2004).

Tree-ring data for Mexico during and after the sixteenth century support the hypothesis that unusual climatic conditions may have aggravated the four worst epidemics of cocoliztli, which began in the years 1545, 1576, 1736, and 1813. The epidemics in 1545 and 1576 occurred during the sixteenth-century megadrought, but all four of these most extreme cocoliztli epidemics actually occurred in wet years following intense droughts (Figs. 10.13 and 10.14; Acuna-Soto, personal communication). This sequence of climatic extremes, particularly the drought years followed

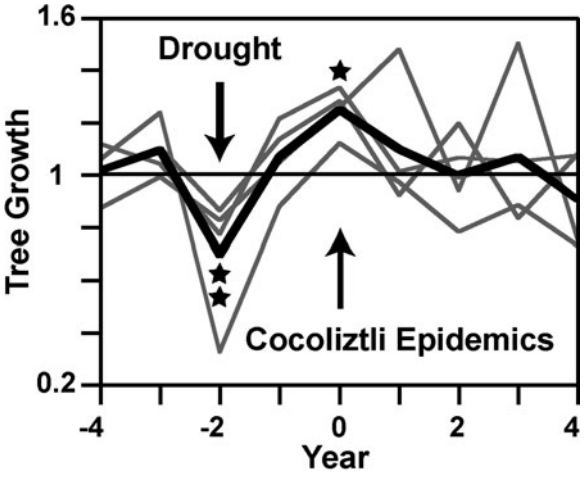

Fig. 10.14 The four most severe epidemics of cocoliztli (hemorrhagic fever) in Mexican history occurred in 1545, 1576, 1736, and 1813. In each case, these epidemics occurred in tree-ring-estimated wet years following severe drought. This superposed epoch analysis indicates that tree growth (mean = 1.0) in Mexico was significantly depressed 2 years prior to the outbreak and elevated during the year of outbreak during these four epidemics (* = $P < 0.05$; ** = $P < 0.01$)

by unusual wetness, has been witnessed during other infectious disease events (Epstein 2002), including the hantavirus outbreaks on the Colorado Plateau in 1993 and 1998 (Hjelle and Glass 2000). In the case of hantavirus, the incidence of infection in the rodent host is believed to have been magnified by a population bottleneck during drought. During the subsequent wet conditions, rodent populations expanded and infection was spread to human populations through rodent excreta. The agent responsible for the cocoliztli epidemics of sixteenth-century Mexico has not been identified. However, the tree-ring data suggest that extreme climate conditions may have magnified the impact of these disease catastrophes.

10.4 Suspected Social Impacts of Drought Extremes During the Precolonial Era

The native populations of Mesoamerica developed calendrical and hieroglyphic writing systems centuries before the arrival of Cortez. The Aztec calendar was based on the combination of a 260-day religious calendar and a 360-day solar calendar. The Aztec year was divided into 18 ‘months,’ each 20 days long, leaving 5 days each year that were not included in the formal calendar and were considered bad luck by the superstitious Aztecs (Caso 1971; Keber 1995). The religious and solar calendars rotated through all 18,980 unique daily combinations, resulting in one complete cycle of the two counting systems every 52 years. Each year of the 52-year cycle was identified by one of four possible iconic symbols, which were rabbit, reed, flint knife, and house (Keber 1995). The individual years were then numbered consecutively as follows: the year One Rabbit, Two Reed, Three Flint Knife, Four House, Five Rabbit, Six Reed, Seven Flint Knife, Eight House, Nine Rabbit, etc., until the 52-year cycle was completed with the year Thirteen House. The sequential order of each unique 52-year cycle is not obvious from the Aztec calendar alone, but the sequence of cycles was specified by the Aztec scribes according to royal succession and major political events. Each cycle was then related to the Julian calendar by Jesuits and surviving Aztec scribes during the mid-sixteenth century, so that every year of Aztec traditional history can be tentatively linked to a specific year in the Western calendar, especially during the 14^{th}, 15^{th}, and 16^{th} centuries preceding Conquest.

The Aztecs recorded notable political, celestial, and environmental events with pictorial images linked to specific calendar year signs in ancient diaries known as codices. Codices were prepared by scribes for each city-state of the Aztec empire, but they were considered blasphemous by the Spaniards, and most were destroyed soon after the conquest (Keber 1995). Nevertheless, a few important codices survive and with them fragments of recorded Aztec history. Therrell et al. (2004) noted 13 events specifically identified in the codices as dry years and used independent tree-ring data from Mexico to substantiate most of these Aztec droughts.

Perhaps the most extreme drought of the prehispanic Aztec era occurred in the year of One Rabbit in 1454, for which the codices indicate parched fields, wilted crops, and human corpses littering the ground (Therrell et al. 2004). The tree-ring

data from Durango, Mexico, indicate intense drought spanning the period 1453–1455, being most intense in 1454. The 'Drought of One Rabbit' in 1454 seems to have contributed to the Aztec superstition regarding all One Rabbit years, which were feared for their association with famine and calamity. The available tree-ring data from Mexico supply some substance to this superstition, indicating that drought occurred in most of the Thirteen House years immediately prior to the One Rabbit years of the Aztec traditional history (10 of 13 cases from AD 882 to 1558), which would have reduced crop yields and could have contributed to hunger and hardship during the subsequent One Rabbit years (Therrell et al. 2004).

The network of 850 climate-sensitive tree-ring chronologies developed across North America by the dendrochronological community, and used by Cook et al. (2004) to reconstruct the summer PDSI, fulfills the potential demonstrated by Douglass (1929, 1935) when he compiled the first master tree-ring chronology based on living trees and archaeological timbers. The new network and the derived reconstructions confirm the Great Drought in the late thirteenth century, which was most intense over the Anasazi cultural area on the Colorado Plateau and persisted for at least 21 years (Fig. 10.15). However, the precise role of climate in the development and decline of the Anasazi on the Colorado Plateau remains controversial. Paleoenvironmental information, including tree-rings, indicates that environmental conditions of the period 950–1130 were relatively favorable (Dean 1988, 1996; Dean and Funkhouser 1995). During this interval, Anasazi populations expanded to their maximum geographical extent and achieved their greatest sociocultural complexity in the regional interaction system focused on Chaco Canyon, New Mexico

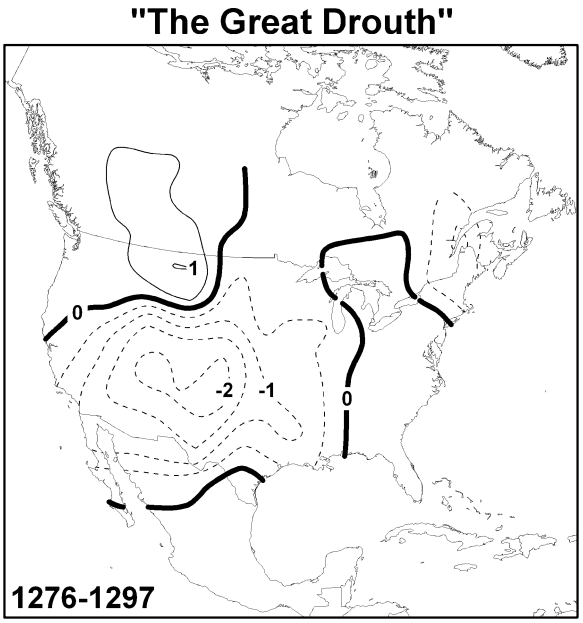

Fig. 10.15 Tree-ring-reconstructed summer PDSI is mapped from 1276 to 1297 (see Fig. 10.2) and illustrates moderate drought or worse for the entire 21-year episode centered over the Anasazi cultural area, as first documented by A.E. Douglass (1929, 1935). This drought has been implicated in environmental degradation and Anasazi abandonment across much of the Four Corners region

(Vivian 1990; Noble 2004). At the same time, Hohokam populations developed immense irrigation systems and a complex social organization in the Sonoran Desert (Reid and Whittlesey 1997, pp. 69–110).

A prolonged bimodal drought from about 1130 to 1180 was associated chronologically with a series of human behavioral and organizational changes throughout the Southwest: Anasazi groups withdrew from the peripheries of their maximum range and from upland areas as previously scattered groups aggregated into larger settlements in better watered lowland localities, the Chacoan regional system ended with the depopulation of its Chaco Canyon core to be succeeded by more localized polities, the Hohokam Sedentary Period pattern gave way to that of the Classic Period, and many others. The late thirteenth century saw widespread environmental degradation, including massive arroyo cutting, falling alluvial groundwater levels, decreased effective moisture, and Douglass' Great Drought (Fig. 10.15). Anasazi emigration from the Four Corners area began before the environmental crisis of the late 1200s, and by the close of the thirteenth century much of the Anasazi cultural area on the Colorado Plateau was abandoned. Although highly unfavorable environmental conditions can certainly be documented for that time, agent-based modeling of environmental and social interactions among Anasazi households in Long House Valley, Arizona (Dean et al. 2000; Gumerman et al. 2003), indicates that the carrying capacity of the environment was not entirely depleted by the end of the thirteenth century. This outcome suggests that the Anasazi abandonment of the Four Corners area must have involved social or cultural considerations in addition to the environmental crisis of the time.

One of the most challenging problems in American archaeology concerns the decline of Classic Period city-states in Mesoamerica during the late first millennium AD, including the abandonment of Teotihuacan in central Mexico (ca. AD 750) and the large urban centers in the Mayan lowlands (ca. AD 770–950). The Terminal Classic Period (AD 750–950) has been recognized in the archaeological record by a decline in the production of fine manufactured goods, the end of large construction projects, the collapse of large-scale trade networks, the abandonment of large urban centers, and the general depopulation of the region. The cause of Classic Period decline is unclear, but drought, human degradation of the environment, disease, warfare, and collapse of the social order needed to sustain the complex exchange networks and urban infrastructure have been implicated (e.g., Millon 1970; Sharer 1994; Gill 2000).

The North American tree-ring network for the first millennium is extremely sparse and limited largely to the American West. No tree-ring chronologies more than 1000 years long have yet been developed for Mesoamerica near the center of the cultural changes during the Terminal Classic Period. Many of the longest Western chronologies have been developed for high-elevation conifers such as bristlecone pine and limber pine, some of which exhibit ambiguous growth responses to climate. However, Grissino-Mayer (1996) developed a long, precipitation-sensitive tree-ring chronology at El Malpais, New Mexico, arguably one of the most important tree-ring chronologies ever produced. The El Malpais chronology is based on long-lived Douglas-fir and ponderosa pine trees and

subfossil logs of both species, which allowed Grissino-Mayer to develop an exactly dated chronology extending continuously from 136 BC to AD 1992, for a total length of 2129 years.

El Malpais is an extreme moisture-limited site, and the derived chronology has been used to estimate annual rainfall totals over west-central New Mexico for the past two millennia (Grissino-Mayer 1996). The El Malpais reconstruction suggests that the multidecadal droughts in the eighth and sixteenth centuries may have been the most severe and sustained droughts to impact the Southwest in the past 1500 years. The eighth-century megadrought extended from AD 735 to 765 at El Malpais, coincidental with the approximate timing of the abandonment of Teotihuacan, 600 km to the southeast on the Mesa Central of Mexico. We do not know that the eighth-century drought extended into central Mexico (Fig. 10.16), but the 1950s drought in the instrumental record (Fig. 10.2) and a few other tree-ring-reconstructed droughts (e.g. Figs. 10.9, 10.10, and 10.12) indicate that annual and decadal droughts can simultaneously impact the entire region from New Mexico and Texas down into central Mexico (Acuna-Soto et al. 2005).

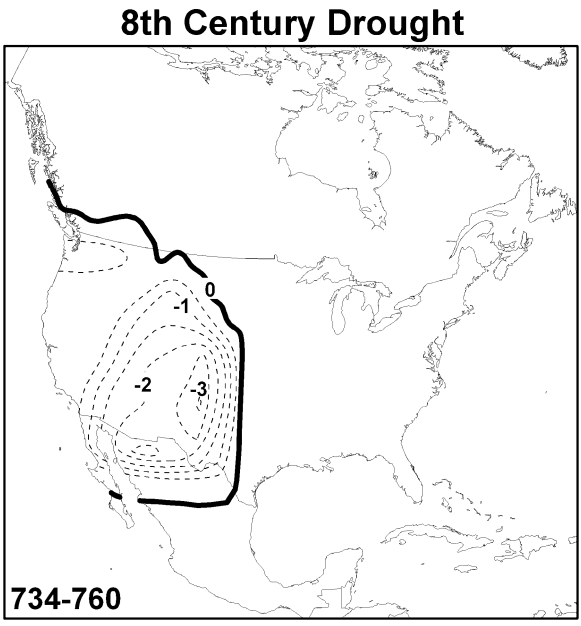

Fig. 10.16 Tree-ring-reconstructed summer PDSI is mapped across the available grid points for the severe sustained drought during the mid-eighth century (AD 734–760; see Fig. 10.2 for mapping details). The predictor tree-ring chronologies are restricted to the western United States, North Carolina, and West Virginia during this time period, and the eastern and southern margins of this drought are not well defined by the available data. The sharp decline in reconstructed summer PDSI in northern Mexico is entirely an artifact of the mapping software and the absence of tree-ring chronologies. Other proxies indicate drought conditions over Mesoamerica from AD 750 to 950 and have implicated climate in the decline of Classic Period cultures (e.g., Hodell et al. 1995, 2005; Gill 2000; Haug et al. 2003)

Evidence for the geographical impact of the eighth-century drought is limited, but tree-ring and lake sediment data indicate that multidecadal drought centered near AD 750 extended from the northern Great Plains, across the southwestern United States, and into central Mexico (e.g., Fig. 10.16). Haug et al. (2003) and Peterson and Haug (2005) documented multidecadal pulses of drought over northern Venezuela and the Caribbean Sea in the sediment record of the Cariaco Basin, beginning in the eighth century and extending into the mid-tenth century. They argued that the anomalies in the Intertropical Convergence Zone (ITCZ) implied by this record would have impacted rainfall over the Mayan lowlands. Intense drought during the Terminal Classic Period has been reconstructed by Hodell et al. (1995, 2005) in lake sediment records from the Yucatan, and it has been implicated in the Mayan collapse (Hodell et al. 1995; Gill 2000). Hunt and Elliott (2005) have simulated severe multidecadal drought over the Mesoamerican sector in a 10,000-year run of the CSIRO Mark 2 global coupled climatic model based only on naturally occurring global climatic variability, demonstrating the plausibility of the prolonged drought identified in the proxy records from the Yucatan Peninsula and elsewhere.

These are interesting *potential* associations between the Classic Period decline and drought. The only certainty is that the eighth-century megadrought—and subsequent droughts in the ninth and tenth centuries evident in the North American, Yucatan, and Cariaco records—*may* have interacted with anthropogenic environmental degradation, epidemic disease, and social upheaval to contribute to the collapse of the Classic Period in Mesoamerica. More paleoclimatic and archaeological information will be required to constrain these hypotheses, including the development of long, climate-sensitive tree-ring chronologies for Mesoamerica and realistic agent-based modeling of Classic Period societies.

10.5 Summary

Tree-ring-reconstructed climatic extremes contemporaneous with severe socioeconomic impacts can be identified for the modern, colonial, and precolonial eras. These events include the drought of the 1950s, the 1930s Dust Bowl, mid- and late nineteenth-century Great Plains droughts, El Año del Hambre, and the seventeenth- and sixteenth-century droughts in the English and Spanish colonies. The new tree-ring reconstructions confirm the severe, sustained Great Drought over the Colorado Plateau in the late thirteenth century identified by Douglass (1935), and they document its spatial impact. The available tree-ring data indicate a succession of severe droughts over the western United States during the Mesoamerican Terminal Classic Period, but these are located far from the cultural heartland of Mesoamerica. Recently, Montezuma bald cypress (*Taxodium mucronatum*) more than 1000 years old have been discovered in central Mexico (Villanueva et al. 2004), and if they can be exactly dated may provide tree-ring reconstructions of precipitation useful for testing the role of drought in cultural decline during the Classic Period.

The only clear connections between climate extremes and impacts on humans are found during the period of written history—including the prehispanic Aztec

era codices, which describe the drought of One Rabbit in Mexico and other pre-colonial droughts. The links between reconstructed climate and societies in the prehistoric era may never be made irrefutably, but testing these hypotheses with improved climate reconstructions, better archaeological data, and modeling experiments to explore the range of potential social responses have to be central goals of archaeology and high-resolution paleoclimatology.

Acknowledgements We thank E.R. Cook, F.K. Fye, and R.D. Griffin for advice and assistance, and Dee Breger for permission to reproduce Fig. 10.5. Funding from the National Science Foundation, Earth System History Program (Grant number ATM-0400713, DWS), and the Archaeology and Archaeometry Program (several grants, JSD), is gratefully acknowledged.

References

Acuna-Soto R, Calderón-Romero L, Maguire J (2000) Large epidemics of hemorrhagic fevers in Mexico 1545–1815. Am J Trop Med Hyg 62:733–739

Acuna-Soto R, Stahle DW, Cleaveland MK, Therrell MD (2002) Megadrought and megadeath in sixteenth-century Mexico. Emerg Infect Dis 8:360–362

Acuna-Soto R, Stahle DW, Therrell MD, Griffin RD, Cleaveland MK (2004) When half of the population died: the epidemic of hemorrhagic fevers of 1576 in Mexico. FEMS Microbiol Lett 240:1–5

Acuna-Soto R, Stahle DW, Therrell MD, Gomez Chavez S, Cleaveland MK (2005) Drought, epidemic disease, and the fall of Classic Period cultures in Mesoamerica (AD 750–950), hemorrhagic fevers as a cause of massive population loss. Med Hypotheses 65:405–409

Adams EC (2002) Homol'ovi: an ancient Hopi settlement cluster. University of Arizona Press, Tucson

Anderson DG, Stahle DW, Cleaveland MK (1995) Paleoclimate and the potential food reserves of Mississippian societies: a case study from the Savannah River valley. Am Antiquity 60:258–286

Argollo J, Solis C, Pacajes J (2006) Dendroclimatology of *Polylepis tarapacana* in the central Andes of Bolivia. CONCORD Symposium on Climate Change, Mendoza, Argentina, April 4–6, 2006 (abstract)

Arnold D (1988) Famine. Blackwell, New York

Baillie MGL (1994) Dendrochronology raises questions about the nature of the AD 536 dust-veil event. Holocene 4:212–217

Baillie MGL (1999) Exodus to Arthur: catastrophic encounters with comets. Batsford, London

Barrett EM (2002) Conquest and catastrophe: changing Rio Grande pueblo settlement patterns in the sixteenth and seventeenth centuries. University of New Mexico Press, Albuquerque

Bowden MJ, Kates RW, Kay PA, Riebsame WE, Warrick RA, Johnson DL, Gould HA, Weiner D (1981) The effect of climate fluctuations on human populations: two hypotheses. In: Wigley TML, Ingram MJ, Farmer G (eds) Climate and history. Cambridge University Press, Cambridge, pp 479–513

Breger D (2003) Mongolian frost rings. Science 301:1472

Brenneman DS (2004) Climate of rebellion: the relationship between climate variability and indigenous uprisings in mid-eighteenth-century Sonora. PhD dissertation, University of Arizona, Tucson

Breshears DD, Cobb NS, Rich PM, Price KP, Allen CD, Balice RG, Romme WH, Kastens JH, Floyd ML, Belnap J, Anderson JJ, Myers OB, Meyer CW (2005) Regional vegetaion die-off in response to global-change-type drought. Proc Natl Acad Sci USA 102:15144–15148

Brown BG (1988) Climate variability and the Colorado River Compact: implications for responding to climatic change. In: Glantz MH (ed) Societal responses to regional climatic change. Westview, Boulder, Colorado, pp 279–304

Brunstein FC (1995) Bristlecone pine frost-ring and light-ring chronologies, from 569 BC to AD 1993, Colorado. Open-File Report 95-63, US Geological Survey, Denver
Brunstein FC (1996) Climatic significance of the bristlecone pine latewood frost-ring record at Almagre Mountain, Colorado, USA. Arctic Alpine Res. 28:65–76
Buckley BM, Barbetti M, Watanasak M, D'Arrigo R, Boonchirdchoo S, Sarutanon S (1995) Dendrochronological investigations in Thailand. IAWA J 16:393–409
Burns BT (1983) Simulated Anasazi storage behavior using crop yields reconstructed from tree rings: AD 652–1968. PhD dissertation, University of Arizona, Tucson
Caso A (1971) Calendrical systems of central Mexico. In: Ekholm GF, Bernal I (eds) Archaeology of northern Mesoamerica, part I. University of Texas Press, Austin, pp 333–348
Cook ER, Krusic PJ (2004) North American Drought Atlas. Lamont-Doherty Earth Observatory and the National Science Foundation. http://iridl.ldeo.columbia.edu/SOURCES/.LDEO/.TRL/.NADA2004/.pdsi-atlas.html
Cook ER, Meko DM, Stahle DW, Cleaveland MK (1999) Drought reconstructions for the continental United States. J Climate 12:1145–1162
Cook ER, Woodhouse CA, Eakin CM, Meko DM, Stahle DW (2004) Long-term aridity changes in the western United States. Science 306:1015–1018
Cook ER, Seager R, Cane MA, Stahle DW (2007) North American drought: reconstructions, causes, and consequences. Earth Sci Rev 81:93–134
Cook SF, Simpson LB (1948) The population of central Mexico in the sixteenth century. Ibero Americana, vol 31. University of California Press, Berkeley
D'Arrigo RD, Frank D, Jacoby G, Pederson N (2001) Spatial response to major volcanic events in or about AD 536, 934, and 1258: frost rings and other dendrochronological evidence from Mongolia and northern Siberia. Climatic Change 49:239–246
Davis M (2001) Late Victorian holocausts. Verso, London
Dean JS (1969) Chronological analysis of Tsegi Phase sites in northeastern Arizona. Papers of the Laboratory of Tree-Ring Research, No. 3, University of Arizona Press, Tucson
Dean JS (1988) Dendrochronology and paleoenvironmental reconstruction on the Colorado Plateaus. In: Gumerman GJ (ed) The Anasazi in a changing environment. Cambridge University Press, Cambridge, pp 119–167
Dean JS (1996) Demography, environment, and subsistence stress. In: Tainter JA, Tainter BB (eds) Evolving complexity and environmental risk in the prehistoric Southwest. Santa Fe Institute studies in the sciences of complexity. Addison-Wesley, Reading, Massachusetts, pp 25–56
Dean JS, Funkhouser GS (1995) Dendroclimatic reconstructions for the southern Colorado Plateau. In: Waugh WJ (ed) Climate change in the Four Corners and adjacent regions: implications for environmental restoration and land-use planning. US Department of Energy, Grand Junction Projects Office, Grand Junction, Colorado, pp 85–104
Dean JS, Gumerman GJ, Epstein JM, Axtell RL, Swedlund AC, Parker MT, McCarroll S (2000) Understanding Anasazi culture change through agent-based modeling. In: Kohler TA, Gumerman GJ (eds) Dynamics in human and primate societies: agent-based modeling of social and spatial processes. Santa Fe Institute studies in the sciences of complexity. Oxford University Press, New York, pp 179–205
Diamond J (2005) Collapse: how societies choose to fail or succeed. Viking, New York
Douglass AE (1929) The secret of the Southwest solved by talkative tree rings. Natl Geogr 56: 736–770
Douglass AE (1935) Dating Pueblo Bonito and other ruins of the Southwest. National Geographic Society Contributed Technical Papers, Pueblo Bonito series 1:1–74
Drought monitor (2004) North American drought monitor, August 2004. http://www.ncdc.noaa.gov/nadm.html
Endfield GH, Nash DJ (2002) Drought, desiccation and discourse: missionary correspondence and nineteenth-century climate change in central southern Africa. Geogr J 168:3–47
Epstein PR (2002) Shifting times and paradigms: climate change and public health. In: Leroy S, Stewart IS (eds) Environmental catastrophes and recovery in the Holocene, abstracts volume, Brunel University, London, pp 30–31

Florescano E (1980) Análisis Histórico de las Sequías en México. Comisión del Plan Nacional Hidráulico, México City
Fye FK, Stahle DW, Cook ER (2003) Paleoclimatic analogs to twentieth-century moisture regimes across the United States. B Am Meteorol Soc 84:901–909
Garcia Acosta V (1995) Los Precios de Alimentos y Manufacturas Novohispanos. Comité Mexicano de Estudios Superiores, Instituto de Investigaciones Históricas, UNAM, Mexico City
Gerhard P (1993) A guide to the historical geography of New Spain. University of Oklahoma Press, Norman
Gibson C (1964) The Aztecs under Spanish rule: a history of the Indians of the Valley of Mexico. Stanford University Press, California
Gil Montero R, Villalba R (2005) Tree rings as a surrogate for economic stress: an example from the Jujuy, Argentina, in the 19th century. Dendrocronologia 22:141–147
Gill R (2000) The Great Maya droughts. University of New Mexico Press, Albuquerque
Graybill DA (1989) The reconstruction of prehistoric Salt River streamflow. In: Graybill DA, Gregory DA, Nials FL, Fish SK, Gasser RE, Miksicek CH, Szuter CR, The 1982 excavations at Las Colinas: environment and subsistence. Arizona State Museum archaeological series 162, vol 5. Tucson, pp 25–38
Graybill DA, Gregory DA, Funkhouser GS, Nials FL (2006) Long-term streamflow reconstructions, river channel morphology, and aboriginal irrigation systems along the Salt and Gila Rivers. In: Doyel DE, Dean JS (eds) Environmental change and human adaptation in the ancient American Southwest. University of Utah Press, Salt Lake City, 69–123
Grissino-Mayer HD (1996) A 2129-year reconstruction of precipitation for northwestern New Mexico. In: Dean JS, Meko DM, Swetnam TW (eds) Tree rings, environment and humanity. Proceedings of the International Conference, Tucson, Arizona, 17–21 May 1994. Radiocarbon, Tucson, pp 191–204
Grissino-Mayer HD, Baisan CH, Swetnam TW (1997) A 1,373 year reconstruction of annual precipitation for the southern Rio Grande basin. Final report submitted to the Directorate of Environment, Natural Resources Division, Fort Bliss, Texas, for the Legacy Program. Laboratory of Tree-Ring Research, University of Arizona, Tucson
Gumerman GJ, Swedlund AC, Dean JS, Epstein JM (2003) The evolution of social behavior in the prehistoric American Southwest. Artif Life 9:435–444
Haug G, Gunter D, Peterson L, Sigman D, Hughen K, Aeschilmann B (2003) Climate and the collapse of Maya civilization. Science 299:1731–1735
Haury EW (1962) HH-39: recollections of a dramatic moment in Southwestern archaeology. Tree-Ring Bull 24(3–4):11–14
Haury EW, Hargrave LL (1931) Recently dated pueblo ruins in Arizona. Smithsonian miscellaneous collections, vol 82, no 11. Smithsonian Institution, Washington, DC
Hjelle B, Glass GE (2000) Outbreak of hantavirus infection in the Four Corners region of the United States in the wake of the 1997–1998 El Niño–Southern Oscillation. J Infect Dis 81:1569–1573
Hodell DA, Curtis JH, Brenner M (1995) Possible role of climate in the collapse of Classic Maya civilization. Nature 375:391–394
Hodell DA, Brenner M, Curtis JH (2005) Terminal classic drought in the northern Maya lowlands inferred from multiple sediment cores in Lake Chichancanab (Mexico). Quaternary Sci Rev 24:1413–1427
Houghton J (1997) Global warming: the complete briefing. Oxford University Press, Oxford
Hundley N Jr (1975) Water and the West. University of California Press, Berkeley
Hunt BG, Elliott TI (2005) A simulation of the climatic conditions associated with the collapse of the Maya civilization. Climatic Change 69:393–407
Ingram MJ, Farmer G, Wigley TML (1981) Past climates and their impact on man: a review. In: Wigley TML, Ingram MJ, Farmer G (eds) Climate and history. Cambridge University Press, Cambridge, pp 479–513
Jacoby GC, Workman KW, D'Arrigo RD (1999) Laki eruption of 1783, tree rings, and disaster for northwest Alaskan Inuit. Quaternary Sci Rev 18:1365–1371

Keber EQ (1995) Codex Telleriano-Remensis: Ritual, Divination, and History in a Pictorial Aztec Manuscript. University of Texas Press, Austin
Kelton E (1984) The time it never rained. Texas Christian University Press, Fort Worth
Keys D (1999) Catastrophe: an investigation into the origins of the modern world. Ballantine, New York
Kiracofe JB, Marr JS (2002) Andean epidemic, 1524–25, smallpox or bartonellosis? Paper presented at the conference on disease and disaster in pre-Columbian and colonial America, Inter-American Institute for Advanced Studies in Cultural History, Navy Memorial Auditorium, 13–14 April 2002. http://www.interamericaninstitute.org/2002_conference.htm
LaMarche VC, Hirschboeck KK (1984) Frost rings in trees as records of major volcanic eruptions. Nature 307:121–126
Lamb HH (1995) Climate, history and the modern world. Routledge, London
Le Roy Ladurie E (1971) Times of feast, times of famine. Doubleday, New York
Lewis C, Loomis A (1953) The Spanish Jesuit mission in Virginia, 1570–1572. University of North Carolina Press, Chapel Hill
Liu WG, Feng XH, Liu Y, Zhang QG, An ZS (2004) Delta O-18 values of tree rings as a proxy of monsoon precipitation in northwest China. Chem Geol 206:73–80
Ludlum DM (1968) Early American winters II, 1821–1870. American Meteorological Society, Boston
Manning SW (1999) A test of time: the volcano of Thera and the chronology and history of the Aegean and east Mediterranean in the mid second millennium BC. Oxbow, Oxford
Marr JS, Kiracofe ER (2000) Was the huey cocoliztli a hemorrhagic fever? Medical History 44:341–362
Millon R (1970) Teotihuacan: completion of map of a giant ancient city in the Valley of Mexico. Science 170:1070–1082
Mock CJ, Mojzisek J, McWaters M, Chenoweth M, Stahle DW (2007) The winter of 1827–1828 over eastern North America: a season of extraordinary climatic anomalies, societal impacts, and false spring. Climatic Change 83:87–115
Mutter JC (2005) The earth sciences, human well-being and the reduction of global poverty. Eos 86:157, 164–165, 9 April.
Nash DJ, Endfield GH (2002) A nineteenth-century climate chronology for the Kalahari region of central southern Africa derived from missionary correspondence. Int J Climatol 22:821–841
Nicholson SE (1994) Recent rainfall fluctuations in Africa and their relationship to past conditions over the continent. Holocene 4:121–131
Noble DG (ed) (2004) In search of Chaco: new approaches to an archaeological enigma. School of American Research Press, Santa Fe
Paar KL (1999) To settle is to conquer: Spaniards, Native Americans, and the colonization of Santa Elena in sixteenth-century Florida. PhD dissertation, University of North Carolina, Chapel Hill
Parks JA, Dean JS, Betancourt JL (2006) Tree-rings, drought, and the Pueblo abandonment of south-central New Mexico. In: Doyel DE, Dean JS (eds) Environmental change and human adaptation in the ancient American Southwest. University of Utah Press, Salt Lake City, pp 214–227
Pederson N, Jacoby GC, D'Arrigo R, Buckley B, Dugarjav C, Mijiddorj R (2001) Hydrometeorological reconstructions for northeastern Mongolia derived from tree rings: AD 1651–1995. J Climate 14:872–881
Peterson LC, Haug GH (2005) Climate and the collapse of Maya civilization. Am Sci 93:322–329
Prugh BJ, Herman PE, Belval DL (1992) Water-data report VA-91-1. US Geological Survey (USGS), Richmond, Virginia
Rautman AE (1994) Regional climate records and local experience: 'drought' and the decline of dryfarming in central New Mexico. C&A: Culture and agriculture, B Cult Agr Group 49:12–15
Reid J, Whittlesey S (1997) The archaeology of ancient Arizona. University of Arizona Press, Tucson
Salzer MW (2000) Dendroclimatology in the San Francisco Peaks region of northern Arizona, USA. PhD dissertation, University of Arizona, Tucson

Sauer CO (1980) Seventeenth-century North America. Turtle Island, Berkeley, California
Schroeder AH (1968) Shifting for survival in the Spanish Southwest. New Mex Hist Rev XLIII 4:291–310
Schroeder AH (1992) Prehistoric Pueblo demographic changes. In: Vierra BJ (ed) Current research on the late prehistory and early history of New Mexico. Special publication 1. New Mexico Archaeological Council, Albuquerque, pp 29–35
Seager R (2007) The turn of the century drought across North America: global context, dynamics and past analogues. J Climate 20:5527–5552
Sharer RJ (1994) The ancient Maya. Stanford University Press, Stanford, California
Stahle DW (1990) The tree-ring record of false spring in the south-central USA. PhD dissertation, Arizona State University, Tempe
Stahle DW, Cleaveland MK, Blanton DB, Therrell MD, Gay DA (1998) The Lost Colony and Jamestown droughts. Science 280:564–567
Stahle DW, Cook ER, Cleaveland MK, Therrell MD, Meko DM, Grissino-Mayer HD, Watson E, Luckman BH (2000) Tree-ring data document sixteenth-century megadrought over North America. Eos 81:121–125
Stahle DW, Fye FK, Cook ER, Griffin RD (2007) Tree-ring-reconstructed megadroughts over North America since A.D. 1300. Climatic Change 83:133–149
Stegner W (1954) Beyond the hundredth meridian. Penguin, New York
St George S, Nielsen E (2000) Signatures of high-magnitude nineteenth-century floods in *Quercus macrocarpa* (Michx.) tree rings along the Red River, Manitoba, Canada. Geology 28:899–902
Stockton CW (1975) Long-term streamflow records reconstructed from tree rings. Papers of the Laboratory of Tree-Ring Research, no 5. University of Arizona Press, Tucson
Swetnam TW, Betancourt JL (1998) Mesoscale disturbance and ecological response to decadal climatic variability in the American Southwest. J Climate 11:128–3147
Therrell MD (2005) Tree rings and 'El Año del Hambre' in Mexico. Dendrochronologia 22:03–207
Therrell MD, Stahle DW, Acuna-Soto R (2004) Aztec drought and the 'curse of one rabbit.' B Am Meteorol Soc 85:263–1271
Therrell MD, Stahle DW, Ries LP, Shugart HH (2006) Tree-ring-reconstructed rainfall variability in Zimbabwe. Clim Dynam 26:77–685
Van West CR (1994) Modeling prehistoric agricultural productivity in southwestern Colorado: a GIS approach. Reports of investigations 67. Department of Anthropology, Washington State University, Pullman, Crow Canyon Archaeological Center, Cortez, Colorado
Villanueva Diaz J, Cerano Paredes J, Stahle DW, Therrell MD, Cleaveland MK, Sanchez Cohen I (2004) Elementos basicos de la dendrocronologia y sus applicaciones en Mexico. INIFAP Folleto Tecnico no 2. Gomez Palacio, Durango, Mexico
Vivian RG (1990) The Chacoan prehistory of the San Juan basin. Academic, San Diego
Warrick RA, Bowden MJ (1981) The changing impacts of droughts in the Great Plains. In: Lawson MP, Baker ME (eds) The Great Plains, perspectives and prospects. University of Nebraska Press, Lincoln
Webb WP (1931) The Great Plains. Grossett & Dunlap, New York
West E (1995) The way to the West. University of New Mexico Press, Albuquerque
Westerling AL, Swetnam TW (2003) Interannual to decadal drought and wildfire in the western United States. Eos 84:45–555
Westerling AL, Hidalgo HG, Cayan DR, Swetnam TW (2006) Warming and earlier spring increases western U.S. forest wildfire activity. Science 313:940–943
Wheeler DL (1991) The blizzard of 1886 and its effect on the range cattle industry in the southern Plains. Southwest Hist Quart 94:0–80
Woodhouse CA, Lukas JJ, Brown PM (2002) Mid-nineteenth-century Colorado drought. B Am Meteorol Soc 83:484–1493
Woodhouse CA, Gray ST, Meko DM (2006) Updates streamflow reconstructions for the upper Colorado River basin. Water Resour Res 42, W05415
Worster D (1979) Dust Bowl. Oxford University Press, Oxford

Part V
Overview

Chapter 11
Tree Rings and Climate: Sharpening the Focus

Malcolm K. Hughes, Henry F. Diaz, and Thomas W. Swetnam

Abstract A brief overview is given of the major contributions of dendroclimatology to current knowledge and understanding of climate variability and change. Particular attention is given to: (1) greatly enhanced information on the spectrum of climate variability, especially on interannual, decadal, and multidecadal timescales; (2) the history of regional to hemispheric temperatures over recent centuries; (3) the probable causes of the variability seen in tree-ring and other records over the past millennium; (4) attempts to determine the quantity 'climate sensitivity' of the Earth's climate system; and (5) reconstructions of the behavior of circulation features and of regional climates, notably drought. Emphasis is given to the importance of regional, continental, and broader-scale networks, as well as to a wide array of technical advances, in making these achievements possible. Then an impressive array of applications is discussed, ranging from ecology and hydrology to anthropology and archaeology. Finally, attention is given to the prospects for dendroclimatology, and in particular to suggestions for making best use of its strengths and for overcoming its weaknesses.

Keywords Dendroclimatology · Tree rings · Climate reconstruction · Climate variability · Climate change

11.1 Introduction

In the past four decades, dendroclimatology has made valuable contributions to a greatly improved understanding of climate variability over recent centuries. In the early 1970s, there was little systematic knowledge of the nature and causes of climate variability on multiannual to multicentennial timescales, and little more than speculation existed concerning the course of hemispheric-scale temperatures over

M.K. Hughes (✉)
Laboratory of Tree-Ring Research, University of Arizona, Tucson, AZ 85721, USA
e-mail: mhughes@ltrr.arizona.edu

M.K. Hughes et al. (eds.), *Dendroclimatology*, Developments in Paleoenvironmental Research 11, DOI 10.1007/978-1-4020-5725-0_11,

the past few hundred years. Knowledge of the variability of circulation features and its impact on regional climates depended almost entirely on the century or less of direct meteorological observations available for most locations. Great progress has been made on all three of these issues, and this progress will be briefly discussed here with particular emphasis on the role of dendroclimatology. Then we will consider the growth in recent decades of applications of dendroclimatology to other fields, including ecology, hydrology, and the study of interactions between human societies and climate. Finally, we will look to the future of dendroclimatology—in particular, we will call for a reframing of the way we use tree rings as archives of past climate. This recommendation arises from a maturing understanding of the strengths and limitations of dendroclimatology as it is currently practiced.

11.2 Spectrum of Climate Variability

In the mid-twentieth century, a notional spectrum of climate variability would have had no robust features between the annual cycle and those related to celestial mechanics on millennial and multimillennial timescales. For example, Kutzbach and Bryson (1974) pointed out the lack of information on Holocene climatic variability at what they called intermediate frequencies or timescales—the interval of the variance spectrum ranging in periods from about 100 to 1000 years. Furthermore, because of the relative shortness of the instrumental record, estimates of periodicities greater than about 30 years were deemed to have large uncertainties. The authors expressed an expectation that tree rings and other high-resolution proxy climate records would play an important role in defining details of the climatic spectrum at these intermediate timescales (see also Mitchell 1976). Indeed, that expectation has proven justified, as multiple authors, using both instrumental and proxy records, including tree rings, have documented the existence of robust features of variability on multidecadal (e.g., Schlesinger and Ramankutty 1994; Mann and Park 1994; Cayan et al. 1998; Allan 2000; Delworth and Mann 2000; Briffa et al. 2001; Gray et al. 2003; Villalba et al. 2003) and longer timescales (e.g., Mann et al. 1995, 1998, 2000, 2008; Cobb et al. 2003; Cook et al. 2004b; Graham et al. 2007).

Following the very strong El Niño event of 1982–1983 (Kiladis and Diaz 1986), the connection between the El Niño/Southern Oscillation (ENSO) and climate anomalies worldwide (Kiladis and Diaz 1989) had been demonstrated. Reconstructions of a number of ENSO indices have been published, using networks of tree-ring chronologies and in some cases, other proxies such as coral annual band properties (Lough and Fritts 1985; Stahle and Cleaveland 1993; Stahle et al. 1998; Cook 2000; Mann et al. 2000, 2009; D'Arrigo et al. 2005a). These reconstructions were based on the strength of the large-scale associations between ENSO and local climate patterns. They extended the available record of El Niño events with annual resolution back several hundred years. Tree rings have also been used to reconstruct other aspects of climate variability on these timescales (see, for example, Cayan et al. 1998; Dettinger et al. 1998).

In the 1990s, scientific interest in the nature of decadal-scale climate variability rose with analyses that highlighted the lower-frequency (decadal and longer) aspects of climatic variability (e.g., Graham 1994; Mantua et al. 1997; Zhang et al. 1997; Gershunov and Barnett 1998; Enfield and Mestas-Nuñez 2000; Enfield et al. 2001). This interest, in turn, led to efforts to extend the records of indices such as the Pacific Decadal Oscillation (PDO), the Atlantic Multidecadal Oscillation (AMO), and the North Atlantic Oscillation (NAO) using networks of tree-ring chronologies (for example, Cook et al. 1998; Biondi et al. 2001; D'Arrigo et al. 2001, 2005b; Gedalof et al. 2002; Villalba et al. 2001; Gray et al. 2004).

Villalba et al. (2001; Chapter 7, this volume) demonstrate the existence of substantial synchrony on multiyear to multidecadal timescales in the spatial and temporal patterns of temperature variability along the American Cordillera in connection with sea surface temperature (SST) variability throughout the Pacific Ocean (see also Dettinger et al. 2001). This finding has been possible as a result of the continued development of dendroclimatic networks. The association, or teleconnection, between SST variability in the Pacific and temperature and precipitation changes along the entire American Cordillera has been related to forced large-scale modes of the atmospheric circulation, such as the northern and southern annular modes (Thompson and Wallace 2000; Thompson et al. 2000) and to planetary wave structures due to changes in diabatic heating of the atmosphere associated with the SST changes (Horel and Wallace 1981; Karoly 1989; Hoerling and Kumar 2000; Diaz et al. 2001).

11.3 Reconstruction of Regional to Hemispheric Temperature for Recent Centuries

Early efforts to constrain the range of natural variability from regional to global scales are discussed in the volume *Global Changes of the Past* (Bradley 1991). Webb (1991) and Wigley (1991) estimated the natural variability of global temperatures to be in the range of 1.0–1.5°C in the past 1000 years. With regard to regional spatial scales, Overpeck (1991) estimated that Little Ice Age (LIA) temperatures were within about 2°C of mid-twentieth-century levels, but he also noted that 'the exact geographic and temporal character of the LIA has not yet been established. . .'

Attention was focused on the so-called medieval period in a workshop reported as a series of papers in the journal *Climatic Change* in 1994. This workshop represented a continuing effort to evaluate the amplitude and extent of episodes of multidecadal to century-scale climatic variations in the historical and high-resolution paleoclimate record. Hughes and Diaz (1994) evaluated the following statement found in a US Department of Energy (1989) report: 'A thousand years ago, climate in the North Atlantic regions was perhaps 1°C warmer than now. . .' Based on an extensive review of the literature, together with the findings of the other papers published in this special issue of *Climatic Change*, Hughes and Diaz concluded, '[T]he available evidence does not support a global Medieval Warm Period. . .'

However, the review did indicate that for some areas of the globe, 'temperatures appeared to have been warmer than mid-twentieth century values, although these warmer regional episodes were not strongly synchronous.' Even so, the authors pointed out that 'far more high-quality records of the climate of recent millennia would be needed to provide a definitive answer to the question: was there a Medieval Warm Period and if so, where and when?'

More than a decade after the *Climatic Change* volume, the report of Working Group I of the Fourth Assessment Report (AR4) of the Intergovernmental Panel on Climate Change (IPCC) came to a broadly similar conclusion regarding the question addressed by Hughes and Diaz (1994) (Jansen et al. 2007, Box 6.4), even though considerably more data (including many tree-ring data) were by then available, and major progress had been made in improving methods. AR4 stated that, 'In medieval times, as now, climate was unlikely to have changed in the same direction, or by the same magnitude, everywhere ... At some times, some regions may have experienced even warmer conditions than those that prevailed throughout the twentieth century ...' AR4 then went on to make the important point that, 'Regionally restricted evidence by itself, ... is of little practical relevance to the question of whether climate in medieval times was globally as warm or warmer than today. Local climate variations can be dominated by internal climate variability, often the result of the redistribution of heat by regional climate processes.'

The AR4 continues, 'Only very large-scale climate averages can be expected to reflect global forcings over recent millennia ... To define medieval warmth in a way that has more relevance for exploring the magnitude and causes of recent large-scale warming, widespread and continuous palaeoclimatic evidence must be assimilated in a homogeneous way and scaled against recent measured temperatures to allow a meaningful quantitative comparison against twentieth-century warmth ... A number of studies that have attempted to produce very large spatial-scale reconstructions have come to the same conclusion: that medieval warmth was heterogeneous in terms of its precise timing and regional expression ...'

It is noteworthy that most of these climate reconstructions have used tree-ring records. Several have been based solely on tree-ring evidence (for example, Briffa et al. 2001; Esper et al. 2002; Cook et al. 2004a; D'Arrigo et al. 2006), and others have combined tree rings with other annual- or decadal-resolution proxy climate records, such as varved sediments, ice cores, coral growth bands, and historical documents (for example, Kaufman et al. 2009; Mann et al. 1998, 1999, 2000, 2008, 2009; Mann and Jones, 2003; Moberg et al. 2005). A few have used no tree rings (Huang et al. 2000; Oerlemans 2005). Most of the tree-ring data used have been derived from ring widths, but an important body of work has been based on maximum latewood density (MXD; see Briffa et al. 2001). In general, tree rings provide the largest number of proxy records available for these reconstructions, and they have the widest geographical distribution.

While commenting that, 'The uncertainty associated with present palaeoclimate estimates of NH mean temperatures is significant, especially for the period prior to 1600 when data are scarce ...' AR4 (Jansen et al. 2007) noted that the warmest

period at the hemispheric level 'prior to the twentieth century very likely occurred between 950 and 1100, but temperatures were probably between 0.1 and 0.2°C below the 1961–1990 mean and significantly below the level shown by instrumental data after 1980.' Further, 'The evidence currently available indicates that NH mean temperatures during medieval times (950–1100) were indeed warm in a 2-kyr context and even warmer in relation to the less sparse but still limited evidence of widespread average cool conditions in the 17th century … However, the evidence is not sufficient to support a conclusion that hemispheric mean temperatures were as warm, or the extent of warm regions as expansive, as those in the twentieth century as a whole, during any period in medieval times …'. In summarizing all the reconstructions they considered (see their Fig. 6.10c), AR4 concluded that for the Northern Hemisphere there were 'relatively cool conditions in the 17th and early nineteenth centuries and warmth in the 11th and early 15th centuries, but the warmest conditions are apparent in the twentieth century.' These features are consistently represented in most of the published reconstructions (see AR4 Fig. 6.10c), and their scale in the last 3 or 4 centuries seems to be remarkably consistent, even when quite different types of records have been used; for example, documentary evidence, early instrumental measurements, or glacier dynamics (e.g., Luterbacher et al. 2004; Oerlemans 2005). As will be discussed below, the global climate of the period between roughly AD 500 and AD 1500 turns out to be much more interesting than a simple 'Warm Period,' and that finding owes much to dendroclimatology.

11.4 Causes of Climate Variability in the Past Millennium

Using statistical comparisons, Mann et al. (1998) attributed much of the hemispheric-scale patterns of temperatures of the last 400 years to solar and volcanic forcing, with greenhouse gas concentrations 'emerging as the dominant factor in the twentieth century.' By the time of the writing of the AR4 report (Jansen et al. 2007), a number of climate model runs had been performed forced by estimates of natural and anthropogenic forcing factors and building on earlier modeling work by, for example, Crowley (2000). The forcing factors included solar radiation, volcanic gases and ash, and greenhouse gases in every case, and some combination of tropospheric sulfate aerosols, tropical and/or stratospheric ozone changes, and/or halocarbons, and land use changes. A variety of models were used, including coupled global climate models (GCMs), energy balance models (EBMs), and earth system models of intermediate complexity (EMICS). Remarkably, a fairly consistent picture of simulated temperature over the past 1000 years or so emerges. 'Despite differences in the detail and implementation of the different forcing histories, there is generally good qualitative agreement between the simulations regarding the major features' (Jansen et al. 2007). Further, most of the common major features of the simulations are seen in the 'ensemble view' of the then available reconstructions, and the simulations largely fall within the envelope of the various reconstructions and their uncertainties (AR4, Fig. 6.13d). These results

support the proposition that hemispheric- or larger-scale temperature fluctuations on timescales from multiyear to centuries are largely determined by changes in radiative forcing.

In fact, the AR4 comparisons between the reconstructions (largely tree-ring based) and climate model runs yielded a result that supported and extended the conclusion of Mann et al.'s (1998) statistical comparison of the Northern Hemisphere temperature reconstruction with estimates of solar, volcanic, and greenhouse gas forcing. Simulations were run on EBM and EMIC models, using differing histories of forcing. One set was run using all available forcing, whereas another had the anthropogenic forcings rendered flat from 1765 on. Each set included runs with different strengths of solar irradiance forcing. All were rather similar for the period before 1765, but only the simulations in which the observed history of variation in the anthropogenic factors was applied after 1765 tracked the reconstructed and observed Northern Hemisphere temperature out to the late twentieth century (AR4, Fig. 6.14d). As in Mann et al. (1998), natural forcings, primarily solar and volcanic, account for the reconstructed hemispheric temperature history for most of the past millennium, but it is not possible to account for late-nineteenth- and twentieth-century values without the anthropogenic forcings. This is a particularly compelling finding because it is based on current knowledge of the mechanisms of the climate system as incorporated in the models rather than a solely statistical analysis.

11.5 Climate Sensitivity

There is a challenge that high-resolution paleoclimatology has yet to meet. Bradley (Chapter 1, this volume) expressed the expectation that meaningful estimates of climate sensitivity in pre-industrial times will be made in the next decade. Climate sensitivity is the global surface temperature change associated with a doubling in the atmospheric carbon dioxide equivalent. Specifically, Jansen et al. (2007) wrote in AR4 (Section 6.6.4) that, 'It is difficult to constrain the climate sensitivity from the proxy records of the past millennium.' As they stand, reconstructions of global temperature and estimates of forcings are too uncertain to permit this. In particular, Jansen et al. (2007) note that the magnitudes of low-frequency variations in hemispheric temperature reconstructions differ by 'up to about a factor of two for different reconstructions' and that the reconstructions of natural forcings (solar and volcanic) are uncertain for this period. As Bradley points out, dendroclimatology can play a role in reducing the uncertainty of these temperature reconstructions by increasing the number, quality, temporal extent, and geographic coverage of the global network of tree-ring chronologies useful in dendroclimatology research. It should be added that dendrochronology in the broader sense plays a role in improving estimates of forcing; for example, by improving the chronology of climatically effective volcanic eruptions (e.g., Larsen et al. 2008; Salzer and Hughes 2007) and as a source of information on cosmogenic isotopes as proxies for solar activity (e.g., Bond et al. 2001).

It is important to note that most of the reconstructions referred to above were based either completely or substantially on tree-ring data and on the work of dendroclimatologists. Even so, the major conclusions are robust to the exclusion of tree-ring data. Mann et al. (2008) brought together the largest dataset of tree-ring and other annual- and decadal-resolution proxy data so far used for a hemispheric reconstruction, and they compared alternative algorithms for extracting a reconstruction of Northern Hemisphere temperature since the mid-first millennium AD. They conclude that, 'Recent warmth [the past decade] appears anomalous for at least the past 1300 years whether or not tree-ring data are used. If tree-ring data are used, the conclusion can be extended to at least the past 1700 years, but with additional strong caveats. The reconstructed amplitude of change over past centuries is greater than hitherto reported, with somewhat greater medieval warmth in the Northern Hemisphere, albeit still not reaching recent levels.' The strong caveats referred to concern decreasing numbers of records for earlier times, the effects of the 'segment length curse' on the capacity of tree-ring chronologies to conserve century- to multicentury-scale variability, and time-dependent biases introduced by standardization procedures (see Hughes, Chapter 2, this volume, and Briffa and Melvin, Chapter 5, this volume).

The Mann et al. (2008) results suggest that, at least for the past 1300 years, these effects do not produce a different general pattern of hemispheric temperature variability than is found with the other proxies used (namely, marine and lacustrine sediments, speleothems, ice cores, corals, and historical documentary series). This fact, combined with the general agreement between climate model results and the existing, largely tree-ring-based, literature of hemispheric temperature reconstructions, suggests not only that tree rings, appropriately handled, are no worse than other proxies, but also that it will be worth the effort to extend and expand the global dendroclimatic network back in time, out to the present, and to presently uncovered regions.

11.6 Circulation Features and Regional Climates

Although hemispheric or global mean temperature reconstructions have special value for studying the effects of changing radiative forcings—such as solar irradiance, volcanic gases and ash, and greenhouse gases—and eventually for estimating climate sensitivity, they conceal a rich history of regional variations. It is this that we referred to at the end of Section 11.3. At very large scales, it has recently emerged that, far from conditions being uniformly warm in so-called 'medieval' times, some large regions of the globe experienced relatively cool sea surface temperatures, as recorded in coral skeletons, compared to modern values (Cobb et al. 2003). Stine (1994), using geomorphic data, identified century-long extreme low stands in Mono Lake, California, and other midlatitude locations in both North and South America for the tenth through fourteenth centuries. He believed these low stands to be so unusual as to merit the designation of this period as the 'Medieval Climate

Anomaly' (MCA), and he proposed a mechanism of changed atmospheric circulation. These lake low stands corresponded with sustained periods of dryness recorded in rings of lower forest border bristlecone pine in the nearby Great Basin (LaMarche 1974; Hughes and Graumlich 1996; Hughes and Funkhouser 1998, 2003). Graham and Hughes (2007) used tree rings to achieve a more direct confirmation of Stine's Mono Lake low stands by driving a hydrographic model of Mono Lake with reconstructed inflow rates derived from tree-ring chronologies. Cook et al. (2004b), also using tree rings and comparisons with other proxy records (e.g., lake level and wildfire reconstructions from fire scars in tree rings and charcoal in sediments), showed that this period was indeed anomalous across much of western North America, such that a markedly greater portion of the area tended to be experiencing drought conditions in the centuries before the mid-second millennium AD than since then. Recent Colorado River flow tree-ring-based reconstructions with good sample depth through the past millennium identify extraordinary, multidecadal drought during the mid-twelfth century (Meko et al. 2007).

Taken together, these findings support Stine's (1994) designation of this period as being anomalous in western North America. The question then arises, what caused this? Graham et al. (2007) found that climate between approximately AD 500 and 1350 was marked by generally arid conditions on land in much of western North America and cool sea surface temperatures along the California coast. They were able to link this Medieval Climate Anomaly to large-scale circulation features revealed by tree rings and by other proxy climate records such as coral bands and ocean sediments. This was in part achieved by reference to analogous patterns seen in transient climate model runs. According to Graham et al. (2007), the Medieval Climate Anomaly was followed by wetter conditions in western North America and warming coastal SSTs during the transition into the Little Ice Age. In concert with these midlatitude changes, they reported that proxy records from the tropical Pacific Ocean show contemporaneous changes indicating cool central and eastern tropical Pacific SSTs during the MCA, with warmer than modern temperatures in the western equatorial Pacific.

This pattern of midlatitude and tropical climate conditions is consistent with the hypothesis that a dry MCA in the western United States resulted (at least in part) from tropically forced changes in Northern Hemisphere circulation patterns like those associated with modern La Niña episodes (Cook et al. 2007). Building on results reported by Graham et al. (2007) concerning the MCA/LIA transition in the north Atlantic region, Trouet et al. (2009) combined tree-ring records from north Africa with speleothems from northern Europe to reconstruct a major shift in the North Atlantic Oscillation at the time of this transition. The Graham et al. and Trouet et al. studies used relatively small numbers of proxy climate records, including long tree-ring chronologies, along with climate models, to infer shifts of climate regimes on very large spatial scales. Their results are largely consistent with those obtained in a very different manner by Mann et al. (2009). In this case, the methods of statistical climate field reconstruction (CFR) were used to examine the differences between two reconstructed global temperature fields, one for the MCA (here AD 950–1250), the other for the LIA (here AD 1400–1700). This was

done by using the very large dataset of tree-ring and other annual- to bidecadal-resolution proxy records already used by Mann et al. (2008) to reconstruct mean Northern Hemisphere temperature (see above). Their MCA showed a tendency for La Niña–like conditions in the tropical Pacific. The reconstructed spatial patterns of temperature change implied particular dynamical responses of climate to natural radiative forcing changes that would involve the El Niño/Southern Oscillation and the North Atlantic Oscillation/Arctic Oscillation. The work of Cook et al. (2007), Goosse et al. (2008), Graham et al. (2007), and Mann et al. (2009) represents a new stage in the development of high-resolution paleoclimatology, including dendroclimatology, in which reconstructions of past climate are interpreted in the light of climate model simulations, and simulations may be constrained by proxy records or reconstructions based on them. The results of this work are likely to have considerable implications for the understanding of future climate changes; in particular, the consequences of anthropogenic climate change for regional climatic phenomena such as drought.

11.7 The Current State of Play

It is clear that dendroclimatology has made major and unique contributions on all three fronts mentioned: the spectrum of climate variability, hemispheric mean temperature over recent centuries and millennia, and the relationships between global or hemispheric features, circulation patterns, and regional to local climate variability and change. As a result, a new paradigm of climate variability and change in recent centuries and millennia is emerging, which is distinct in a number of respects from the paleoclimatology of longer timescales and more dramatic shifts in the boundary conditions of the climate system. It is a paradigm in which the spatial and temporal specificity of high-resolution archives such as tree rings permit a seamless approach to the linking of the effects of radiative forcing at global scale with regional and local climate patterns combining forced and natural internal variability (Hughes and Ammann 2009). On the one hand, reconstructions of decadal to multicentennial changes at hemispheric or global scales provide a test for models of radiatively forced climate variability and change, whereas spatiotemporal patterns at these and shorter timescales and smaller, regional spatial scales represent the combined effects of forced and internal variability. Such regional reconstructions, however, also constitute a rich resource from which it is possible ‘to isolate systematic regional climate responses to repeated forcing events’ (Hughes and Ammann, 2009); for example, climatically effective volcanic eruptions. Such analyses have the potential to contribute to the untangling of the effects of forced and unforced climate variability at regional scales. The approach is increasingly integrated into climate science, contributing otherwise unavailable insights, and in turn benefiting from new challenges.

These contributions, and the many other achievements discussed in this volume, have been possible because of decades of conceptual and technical development,

as well as the building of networks of chronologies according to largely consistent protocols. A number of the basic concepts are discussed by Hughes (Chapter 2, this volume), and the development of the networks was described by Hughes (2002). An apparent tension has emerged between the empirical-statistical approach, on which most of the achievements of dendroclimatology have been based, and process-based modeling. Vaganov et al. (2006, p. 308) suggest that process-based modeling (see Vaganov et al. Chapter 3, this volume) should be viewed as a complement to empirical-statistical techniques (see Cook and Pederson, Chapter 4, this volume), not as a substitute. Following Harte (2002), they assert that, 'Empirical-statistical tools are of great value in dealing with particularity and contingency, just as process-based modeling may be a way of approaching generality and simplicity.'

So it is that the building and analysis of networks of dendroclimatic records have brought to light emergent phenomena (see Cook and Pederson, Chapter 4, this volume) that would likely not have been anticipated based only on the available state of knowledge of mechanisms; for example, elements of synchrony in drought between the midlatitudes of North and South America over several centuries (see Villalba et al. Chapter 7, this volume), or the possible existence of two continental-scale modes of drought in North America (Woodhouse et al. 2009). The solutions to some of the most pressing problems in dendroclimatology, however, must lie in better understanding of mechanisms; for example, of possible changing of climate control of ring growth (as in the 'divergence' problem; see Vaganov et al. Chapter 3, this volume; Briffa et al. 1998; D'Arrigo et al. 2008), in the effects of stand dynamics, or in the mechanics and geometry of tree development. It is, of course, also necessary to identify and deal with artifacts produced by combinations of chronology composition and standardization techniques (see Briffa and Melvin, Chapter 5, this volume).

11.8 The Importance of Networks

Modern dendroclimatology has only been possible because of the development of networks of chronologies at local, regional, continental, and hemispheric scale (see Hughes, Chapter 2, this volume, for a discussion of the centrality of networks to dendroclimatology). Schulman (1956) systematically built networks of tree-ring chronologies collected as records of hydroclimate, demonstrating a strong common signal across hundreds of kilometers. This development was expanded further by Fritts and colleagues (Fritts 1965, 1976; Fritts et al. 1971, 1976; LaMarche and Fritts 1971; Blasing and Fritts 1976), who used a distributed network of tree-ring sites to reconstruct spatiotemporal patterns of regional climatic variability prior to the beginning of instrumental observations. They developed methods for mapping temporal and spatial variations of tree-ring growth for a network of western US conifers that they linked to changes in large-scale atmospheric circulation patterns (sea level pressure [SLP], cyclone frequency) in the north Pacific. Fritts (1991) summarizes the basic approach and provides examples of the application of these techniques to

enhance understanding of secular variability in large-scale climate patterns prior to the start of instrumental records.

The North American network of moisture-sensitive trees is now much more widespread and heavily replicated than that used by Fritts (Meko et al. 1993; Cook et al. 2004b; Kipfmueller and Salzer, 2010). It extends well into Canada and to central Mexico (St. George et al. 2009; Stahle et al. 1999, 2007; Villanueva-Diaz et al. 2007). Major tree-ring networks have been established in South America (see Villalba et al. Chapter 7, this volume); Siberia (for example, Vaganov et al. 1996; Esper et al. 2009); the eastern Mediterranean and North Africa (Touchan et al. 2005, 2008); many regions of Europe (for example, Büntgen et al. 2006; Helama et al. 2005); Australasia, especially New Zealand (for example, Fowler et al. 2008) and Tasmania (Cook et al. 2006); central Asia and China (for example, Jacoby et al. 2003; Garfin et al. 2005; Yin et al. 2008) and the Himalayan region (for example, Hughes 1992, 2001; Borgaonkar et al. 1996; Yadav and Singh 2002); as well as the lands around the north Pacific (for example, D'Arrigo et al. 2001). In addition to these networks, which are based mainly on ring widths, Schweingruber and his colleagues have established a network of maximum latewood density chronologies that covers most of the boreal forest and much of the alpine forest of the Northern Hemisphere, with significant collections outside those regions, too (Schweingruber and Briffa 1996).

There is still great potential for dendroclimatological network building and for the intensification and updating of existing networks. Numerous regions are still radically under sampled; for example, the tropics, including most of Africa; much of central Asia; and other, smaller pockets, such as European Russia. Data on some of the major networks were collected in the 1970s and 1980s, and they should be updated. Given the unusual climate changes in many parts of the globe in recent decades, tree-ring chronology updating would be particularly valuable in evaluating potential changes in climate–tree growth responses during this period. It could well be the case that sample numbers should be greater than has been the case in the past. It is clearly the case that greatly improved metadata on collection sites and their topographic, geologic, and ecological context may now be collected by using modern geospatial technology, and that the interpretation of the ring record would be greatly improved as a result.

11.9 Growth in the Applications of Dendroclimatology: the 1990s to Present

Here we consider some exciting new climatic applications of dendrochronology in the fields of water resources management, wildfire history and risks in western North America forests, ecological impacts of climatic changes, and the application of new tools in connection with traditional uses of dendrochronology in archaeological work. Similar applications are being made in other regions, and our account is meant to be indicative, not exhaustive.

Dendroclimatology has experienced explosive growth since the late 1980s, with a great number of published papers documenting regional- to hemispheric-scale climatic variability over the past several centuries. Its results and insights have been applied to scientific and practical problems in ecology and hydrology; for example, issues with important policy and management implications.

Swetnam and Brown (Chapter 9, this volume) review the parallel strategy of network development that ecological tree-ring studies have pursued in recent decades, building from local scales to networks of ecological histories at regional to continental scales. At these broader scales, chronology networks reveal emergent patterns of spatial and temporal synchrony of forest fires, insect outbreaks, and tree demography (natality and mortality) reflecting climatic drivers (e.g., Swetnam and Betancourt 1990, 1998; Kitzberger et al. 2007). The existence of independently derived climatic proxies from ring-width and density chronologies has greatly facilitated this new development in 'macroecology.' Moreover, the remarkably strong association between extreme years in the regional fire history networks and the drought and ENSO reconstructions, for example, provide significant assurance that both types of networks have captured the most extensive and highest magnitude climate and fire events (e.g., Fig. 9.3 in Swetnam and Brown, Chapter 9, this volume; Swetnam and Betancourt 1990, 1998).

Although tree-ring ecological and climate networks have, so far, been assembled and used jointly primarily at regional scales, hemispheric and global scales are feasible. Following the work of Villalba and colleagues regarding evidence for synchronicity of dendroclimatic responses to Pacific Ocean SST changes on multiple timescales, Kitzberger et al. (2001) showed that forest fire histories in North and South America shared similar histories and relationships to ENSO. The newest and perhaps most promising approach for reconstructing regional to continental (and perhaps global) forest fire histories involves an adaptation of the classic dendroclimatic regression methods of calibration and verification. Combinations of modern-area-burned time series (from forest fire records and atlases), independent networks of tree-ring width chronologies, and tree-ring dated fire-scar based fire chronologies are used to reconstruct and test multicentury histories of wildfire at regional and continental scales (Westerling and Swetnam 2003; Girardin 2007; Girardin and Sauchyn 2008).

The Girardin (2007) and Girardin and Sauchyn (2008) studies have been particularly valuable in evaluating the rise in area burned in Canada in recent decades in the context of multiple centuries, and in association with warming trends, as observed in twentieth-century data for both Canada and the western United States (Gillett et al. 2004; Westerling et al. 2006). The values and uses of these ecological disturbance and climate studies from tree rings have expanded from improved basic understanding of large-scale processes to new insights with applications in management. For example, applications have included the development of predictive models of seasonal fire activity based on the state of the ENSO and prior season rainfall and drought conditions (Corringham et al. 2008).

During past few decades, a significant amount of work regarding hydrologic aspects of climatic variability throughout the world on interannual to century

timescales has used tree-ring networks (for example, Stockton and Meko 1975, 1983; Stahle and Cleaveland 1992; Hughes and Brown 1992; Graumlich 1993; Villalba et al. 1998; Hughes and Funkhouser 1998; Cook et al. 1999, 2004b; Stahle et al. 2000, 2007; Meko and Woodhouse 2005; Ni et al. 2002; Touchan et al. 2005, 2008; Woodhouse et al. 2006; Davi et al. 2006; Meko et al. 2007; Christie et al. 2009; Le Quesne et al. 2009). For obvious reasons, drought has been a major focus of most of these studies; however, more recently, streamflow reconstruction has received greater attention (Stockton and Jacoby 1976; Cook and Jacoby 1983; Cleaveland and Stahle 1989; Andreev et al. 1999; Case and Macdonald 2003; Meko et al. 2001, 2007; Meko and Woodhouse 2005; Graham and Hughes 2007; Gou et al. 2007; Lara et al. 2008), as warming trends in various parts of the world, coupled with persistent drought conditions, have sparked the interest of water resources managers and policy makers (Meko and Woodhouse, Chapter 8, this volume).

Severe and persistent drought has been commonplace in the western United States throughout much of the first decade of the twenty-first century, and this has led to concerns about declining snow packs (Mote et al. 2005), diminished streamflow (Stewart et al. 2005), and lowering reservoirs (Pulwarty et al. 2005). In the face of climate change analyses (Barnett et al. 2008), these concerns have spurred water resources managers to evaluate longer hydrological baselines that are possible through tree-ring reconstructions. Studies such as those of Woodhouse (2003); Woodhouse et al. (2006), and Meko et al. (2007) have helped reservoir managers across the western United States gain a better understanding of the historical range of climate variability in the region—which has exhibited larger fluctuations than anything experienced in historical times (Stine 1994; Cook et al. 2004b; Graham and Hughes 2007; Graham et al. 2007).

In parallel to these tree-ring-based studies focused on developing longer baselines for assessing current and future hydroclimatic changes in the western United States, some innovative studies using tree rings and other paleoenvironmental proxy records suggest that abandonment of the Four Corners Pueblo cultures in the southwest United States may have resulted from reductions in both cool and warm season precipitation, leading to low maize yields and the collapse of settlements (Benson et al. 2007). Likewise, Stahle et al. (2007) show that megadroughts occurred several times in the prehistoric tree-ring-based record in the western United States, with enormous consequences for the indigenous peoples in the region. In the sixteenth century, drought affected large portions of North America (including Mexico). Other notable works are those of Stahle et al. (2000), Acuña Soto et al. (2002), and Therrell et al. (2004), who establish a plausible link between severe pre- and post-Columbian droughts in Mexico and pandemic outbreaks of diseases that likely led to the deaths of millions of people. Of historical interest in the United States is the study by Stahle et al. (1998), which documents the occurrence (using tree-ring reconstructions) of a historically extreme drought in the middle Atlantic region coincident with the attempted establishment of English settlements in the New World. Stahle and Dean (Chapter 10, this volume) further discuss the nexus between climate extremes and social disasters.

Thus, tree-ring, historical-documentary, and archeological lines of evidence can be combined in the evaluation of past human societal and behavioral responses to climate variability and change (e.g., see Stahle and Dean, Chapter 10, this volume). Potential exists to further develop such interdisciplinary studies in various areas of the world having rich human histories and tree-ring resources. These narratives are of great interest to the public and have potential to offer new insights into human history and our role in both causing and responding to environmental change.

11.10 Prospects for Dendroclimatology

In a review of the 'state of the art' of dendrochronology in climatology, Hughes (2002), referring to tree rings as natural archives of climate variability, stated:

> The greatest strengths are: the capability to date tree rings to the calendar year, with a very high degree of confidence; the existence of large geographic-scale patterns of common year-to-year tree-ring variability; the development of very extensive, shared networks of tree-ring chronologies meeting common standards; the surprising effectiveness of very simple linear models of tree-ring/climate relationships; and the growing understanding of the mechanisms leading to variability in tree ring features.

During the past 1–2 decades, these strengths have been put to good use by many researchers to provide relatively robust climate reconstructions on large regional to hemispheric spatial scales for the past several centuries to millennia.

Improvement of such reconstructions is limited by the relative lack of high-quality records in important regions, especially in the tropics, and for times before the past five or six centuries. Without adequate networks, knowledge of such regions and times cannot benefit from the robust spatiotemporal patterns tree rings can provide for climate reconstruction. With them, the prospects for climate reconstruction are greatly improved. The accelerating pace of network building and temporal extension of chronologies exemplified in Villalba et al. (Chapter 7, this volume) augurs well for the continued contribution of dendroclimatology to knowledge of Late Holocene and recent climate. Moreover, new kinds of records based on ratios of stable isotopes are emerging that provide information not available from ring-width and density records, in boreal, temperate, and tropical regions (see Gagen et al. Chapter 6, this volume). The experience of recent decades also suggests that there are many other new tree-ring archives of past climate to be discovered and developed, even in regions where dendrochronologists have been active for some decades.

Hughes (2002) also summarized the major weaknesses of dendrochronology in the study of climate:

> [T]ree-ring chronologies only capture a fraction of climate variability; their response may be limited to specific seasonal 'windows'; some do not respond directly to a single monthly or even seasonal climate variable. . .their use to reconstruct past climate is based on the assumption that the same factors, acting in the same way, controlled the formation of tree rings in the past as in the twentieth century and, the techniques used to remove non-climatic

variability, such as that caused by tree age/size trend and interactions with neighbors, limit the faithful representation of climate variations on centennial and longer timescales in many cases.

Overcoming the weaknesses of dendroclimatology may require more creativity than making best use of its strengths. It is time to reframe the way tree rings are used as natural archives. Specifically, this reframing would involve:

1. Thinking of the tree ring as a natural archive that contains several potential proxy records of climate, whose mutual relations contain information about multiple environmental factors; these would include total and partial ring widths, density variables, microanatomical measurements, ratios of stable isotopes (see Gagen et al. Chapter 6, this volume), and potentially trace chemistry.
2. Using a combination of improved process-based modeling and empirical-statistical approaches to produce an integrated understanding of why the various proxy records in a ring vary through time and within the tree; this would include consideration not only of the mechanisms producing interannual variations in the various proxies (see Cook and Pederson, Chapter 4, this volume; Vaganov et al. Chapter 3, this volume), but also how and why this interannual variability changes according to cambial age and tree geometry (see Briffa and Melvin, Chapter 5, this volume).
3. Placing these processes in a spatially explicit context of the forest and the landscape; events in neighboring trees, and in the forest and landscape more broadly, clearly influence ring formation, and the character of each tree-ring record (see Swetnam and Brown, Chapter 9, this volume). Given recent developments in the modeling of forest dynamics, remote sensing, and geospatial analytical techniques, it should be possible to put the treatment of these influences on a more quantitative basis than hitherto.
4. Using ecological information based on dendrochronology as a source of climate information with relevance to forests and woodlands (see Swetnam and Brown, Chapter 9, this volume); there is particular promise in developing understanding of fire climatology and expanding dendroecological fire history networks to continental and global scales.
5. Reconciling the multiple proxies available from a tree-ring record internally in terms of mechanisms and known relationships, and then reconciling them with independent proxies from other natural archives; in the best case, this will involve tree-ring proxies and independent proxies providing estimates of processes linked by known, measurable mechanisms—for example, linking a tree-ring-based precipitation reconstruction through streamflow to the variation of lake levels recorded by geomorphic or sediment isotope records (for example, Andreev et al. 1999; Graham et al. 2007; Graham and Hughes, 2007; Luckman and Wilson 2005; Solomina et al. 2005). By linking independent reconstructions of different components of a system, such as precipitation in the headwaters and the level of a receiving lake, it is possible to test the mutual consistency of the reconstructions quantitatively, and not merely to track covariation. Did, for example, the precipitation as reconstructed vary enough and at the right time to

produce the lake level changes as independently reconstructed, given the present state of knowledge of the watershed and the lake? Given the impossibility of calibrating multidecadal- and century-scale variability, such reconciliations offer a way of checking the magnitudes of these changes.

6. Reaching beyond the present paradigm, in which tree rings are seen as imperfect thermometers or rain gauges, to one in which fields of proxy data (for example, annual maps of maximum latewood density, ring width, or an isotopic ratio) are used 'as is' to constrain models of climate, or to enhance sparse instrumental records through data assimilation schemes (Hughes and Ammann 2009). This approach has the potential to provide resolution to some problems of nonstationary response, and of changing environment, as well as acknowledging the potential for nonlinear responses.

In his 2002 review, Hughes concluded: '[T]he overall assessment [of the role of dendrochronology in climatology] is that it is vibrant, with much robust debate and innovative work.' The chapters in this book represent a cross section of the exciting dendroclimatology work being carried out throughout the world. It also points to some of the key areas for future inquiry. As was the case with *Tree Rings, Environment and Humanity* (Dean et al. 1996), this volume points to the future as much as it takes a look back at some of the notable accomplishments of our discipline. B. Luckman pointed out in his contribution to the 1996 volume, that dendrochronology had a great opportunity to make significant contributions within global change research. The record of the past 15 years bears that prediction out. The expansion of research and the development of practical applications using tree rings as proxies of past climatic variability is pointing to exciting new developments for dendroclimatology—which likely will continue to grow. As human pressures on the environment and the emerging signals of global climate change begin to impact societies more heavily, there is a need for a greater understanding of the historic nature and range of climatic variability on regional scales. Dendrochronology will continue to be one of the best tools available for providing a comparative context for future changes in climate.

References

Acuña Soto R, Stahle DW, Cleaveland MK, Therrell MD (2002) Megadrought and megadeath in 16th century Mexico. Emerg Infect Dis 8:360–362

Allan RJ (2000) ENSO and climatic variability in the past 150 years. In: Diaz HF, Markgraf V (eds) El Niño and the Southern Oscillation: multiscale variability and global and regional impacts. Cambridge University Press, New York, pp 3–55

Andreev SG, Vaganov EA, Naurzbaev MM, Tulokhonov AK (1999) Registration of long-term variations in the atmospheric precipitation, River Selenga runoff, and Lake Baikal level by annual pine tree rings. Dokl Earth Sci 368:1008–1011

Barnett TP, Pierce DW, Hidalgo HG, Bonfils C, Santer BD, Das T, Bala G, Wood AW, Nozawa T, Mirin AA, Cayan DR, Dettinger MD (2008) Human-induced changes in the hydrology of the western United States. Science 319:1080–1083

Benson LV, Berry MS, Jolie EA, Spangler JD, Stahle DW, Hattori EM (2007) Possible impacts of early-11th-, middle-12th-, and late-13th-century droughts on western Native Americans and the Mississippian Cahokians. Quaternary Sci Rev 26:336–350

Biondi F, Gershunov A, Cayan DR (2001) North Pacific decadal climate variability since AD 1661. J Climate 14:5–10

Blasing TJ, Fritts HC (1976) Reconstructing past climatic anomalies in the North Pacific and western North America from tree-ring data. Quaternary Res 6:563–579

Bond G, Kromer B, Beer J, Muscheler R, Evans MN, Showers W, Hoffmann S, Lotti-Bond R, Hajdas I, Bonani G (2001) Persistent solar influence on North Atlantic climate during the Holocene. Science 294:2130–2136

Borgaonkar HP, Pant GB, Kumar KR (1996) Ring-width variations in *Cedrus deodara* and its climatic response over the western Himalaya. Int J Climatol 16:1409–1422

Bradley RS (1991) Global changes of the past. UCAR/Office for Interdisciplinary Earth Studies, Boulder, Colorado

Briffa KR, Schweingruber FH, Jones PD, Osborn TJ, Shiyatov SG, Vaganov EA (1998) Reduced sensitivity of recent tree-growth to temperature at high northern latitudes. Nature 391:678–682

Briffa KR, Osborn TJ, Schweingruber FH, Harris IC, Jones PD, Shiyatov SG, Vaganov EA (2001) Low-frequency temperature variations from a northern tree ring density network. J Geophys Res 106:2929–2941

Büntgen U, Frank DC, Nievergelt D, Esper J (2006) Summer temperature variations in the European Alps, AD 755–2004. J Climate 19:5606–5623

Case RA, Macdonald GM (2003) Tree ring reconstructions of streamflow for three Canadian prairie rivers. J Am Water Resour As 39:703–716

Cayan DR, Dettinger MD, Diaz HF, Graham NE (1998) Decadal variability of precipitation over western North America. J Climate 11:3148–3166

Christie DA, Lara A, Barichivich J, Villalba R, Morales MS, Cuq E (2009) El Niño-Southern Oscillation signal in the world's highest-elevation tree-ring chronologies from the Altiplano, central Andes. Palaeogeogr Palaeocl 281:309–319

Cleaveland MK, Stahle DW (1989) Tree ring analysis of surplus and deficit runoff in the White River, Arkansas. Water Resour Res 25:1391–1401

Cobb K, Charles C, Cheng H, Edwards R (2003) El Niño/Southern Oscillation and tropical Pacific climate during the last millennium. Nature 424:271–276

Cook ER (2000) Niño-3 index reconstruction. International Tree-Ring Data Bank, IGBP PAGES/World Data Center-A for Paleoclimatology. NOAA/NGDC Paleoclimatology Program, Data Contribution Series 2000–052

Cook ER, Jacoby GC (1983) Potomac River streamflow since 1730 as reconstructed by tree rings. J Clim Appl Meteorol 22:1659–1672

Cook ER, D'Arrigo RD, Briffa KR (1998) A reconstruction of the North Atlantic Oscillation using tree-ring chronologies from North America and Europe. Holocene 8:9–17

Cook ER, Meko DM, Stahle DW, Cleaveland MK (1999) Drought reconstructions for the continental United States. J Climate 12:1145–1162

Cook ER, Esper J, D'Arrigo RD (2004a) Extra-tropical Northern Hemisphere land temperature variability over the past 1000 years. Quaternary Sci Rev 23[20–22]:2063–2074

Cook ER, Woodhouse CA, Eakin CM, Meko DM, Stahle DW (2004b) Long-term aridity changes in the western United States. Science 306:1015–1018

Cook ER, Buckley BM, Palmer JG, Fenwick P, Peterson MJ, Boswijk G, Fowler A (2006) Millennia-long tree-ring records from Tasmania and New Zealand: a basis for modelling climate variability and forcing, past, present and future. J Quaternary Sci 21:689–699

Cook ER, Seager R, Cane MA, Stahle DW (2007) North American drought: reconstructions, causes, and consequences. Earth-Sci Rev 81:93–134

Corringham TW, Westerling AL, Morehouse BJ (2008) Exploring use of climate information in wildland fire management: a decision calendar study. J Forest 106:71–77

Crowley TJ (2000) Causes of climate change over the past 1000 years. Science 289:270–277

D'Arrigo R, Villalba R, Wiles G (2001) Tree-ring estimates of Pacific decadal climate variability. Clim Dynam 18:219–224

D'Arrigo R, Cook E, Wilson R, Allan R, Mann M (2005a) On the variability of ENSO over the past six centuries. Geophys Res Lett 32:L03711. doi:10.1029/2004GL022055

D'Arrigo R, Wilson R, Deser C, Wiles G, Cook E, Villalba R, Tudhope A, Cole J, Linsley B (2005b) Tropical–North Pacific climate linkages over the past four centuries. J Climate 18:5253–5265

D'Arrigo R, Wilson R, Jacoby G (2006) On the long-term context for late twentieth century warming. J Geophys Res-Atm 111. doi:10.1029/2005JD006352

D'Arrigo R, Wilson R, Liepert B, Cherubini P (2008) On the 'divergence problem' in northern forests: a review of the tree-ring evidence and possible causes. Global Planet Change 60: 289–305

Davi NK, Jacoby GC, Curtis AE, Baatarbileg N (2006) Extension of drought records for central Asia using tree rings: west-central Mongolia. J Climate 19:288–299

Dean JS, Meko DM, Swetnam TW (eds) (1996) Tree rings, environment and humanity. Radiocarbon, Tucson, Arizona, xiii + 889 pp

Delworth TL, Mann ME (2000) Observed and simulated multidecadal variability in the Northern Hemisphere. Clim Dynam 16:661–676

Dettinger MD, Cayan DR, Diaz HF, Meko DM (1998) North-south precipitation patterns in western North America on interannual-to-decadal time scales. J Climate 11:3095–3111

Dettinger MD, Battisti DS, McCabe GJ, Bitz CM, Garreaud RD (2001) Interhemispheric effects of interannual and decadal ENSO-like climate variations on the Americas. In: Markgraf V (ed) Interhemispheric climate linkages. Academic Press, San Diego, pp 119–140

Diaz HF, Hoerling MP, Eischeid JK (2001) ENSO variability, teleconnections, and climate change. Int J Climatol 21:1845–1862

Enfield DB, Mestas-Nuñez AM (2000) Global modes of ENSO and non-ENSO sea surface temperature variability and their associations with climate. In: Diaz HF, Markgraf V (eds) El Niño and the Southern Oscillation: multiscale variability and global and regional impacts. Cambridge University Press, New York, pp 89–112

Enfield DB, Mestas-Nuñez AM, Trimble PJ (2001) The Atlantic multidecadal oscillation and its relation to rainfall and river flows in the continental US. Geophys Res Lett 28:2077–2080

Esper J, Cook ER, Schweingruber FH (2002) Low-frequency signals in long tree-ring chronologies for reconstructing past temperature variability. Science 295:2250–2253

Esper J, Frank D, Büntgen U, Verstege A, Hantemirov R, Kirdyanov AV (2009) Trends and uncertainties in Siberian indicators of twentieth century warming. Glob Change Biol. doi:10.1111/j.1365–2486.2009.01913.x :1–14

Fowler AM, Palmer J, Fenwick P (2008) An assessment of the potential for centennial-scale reconstruction of atmospheric circulation from selected New Zealand tree-ring chronologies. Palaeogeogr Palaeocl 265:238–254

Fritts HC (1965) Tree-ring evidence for climatic changes in western North America. Mon Weather Rev 93:421–443

Fritts HC (1976) Tree rings and climate. Academic Press, London, xii + 567 pp

Fritts HC (1991) Reconstructing large-scale climatic patterns from tree-ring data. The University of Arizona Press, Tucson, 286 pp

Fritts HC, Blasing TJ, Hayden BP, Kutzbach JE (1971) Multivariate techniques for specifying tree-growth and climate relationships and for reconstructing anomalies in paleoclimate. J Appl Meteorol 10:845–864

Fritts HC, Lofgren GR, Gordon GA (1976) Variations in climate since 1602 as reconstructed from tree rings. Quaternary Res 12:18–46

Garfin GM, Hughes MK, Yu L, Burns JM, Touchan R, Leavitt SW, An ZS (2005) Exploratory temperature and precipitation reconstructions from the Qinling Mountains, north-central China. Tree-Ring Res 61:59–72

Gedalof Z, Mantua NJ, Peterson DL (2002) A multi-century perspective of the variability in the Pacific Decadal Oscillation: new insights from tree rings and coral. Geophys Res Lett 29(24):2204. doi:10.1029/2002GL015824

Gershunov A, Barnett TP (1998) Interdecadal modulation of ENSO teleconnections. B Am Meteorol Soc 79:2715–2726

Gillett NP, Weaver AJ, Zwiers FW, Flannigan MD (2004) Detecting the effect of climate change on Canadian forest fires. Geophys Res Lett 31, ISI 000224408400005

Girardin MP (2007) Interannual to decadal changes in area burned in Canada from 1781 to 1982 and the relationship to Northern Hemisphere land temperatures. Global Ecol Biogeogr 16: 557–566

Girardin MP, Sauchyn D (2008) Three centuries of annual area burned variability in northwestern North America inferred from tree rings. Holocene 18:205–214

Goosse H, Mann ME, Renssen H (2008) Climate of the past millennium: combining proxy data and model simulations. In: Battarbee RW, Binney HA (eds) Natural climate variability and global warming: a Holocene perspective. Wiley-Blackwell, Chichester, UK, pp 163–188

Gou XH, Chen FH, Cook E, Jacoby G, Yang MX, Li JB (2007) Streamflow variations of the Yellow River over the past 593 years in western China reconstructed from tree rings. Water Resour Res 43, ISI 000247698100007

Graham NE (1994) Decadal-scale climate variability in the 1970s and 1980s: observations and model results. Clim Dynam 10:135–162

Graham NE, Hughes MK (2007) Reconstructing the mediaeval low stands of Mono Lake, Sierra Nevada, California. Holocene 17:1197–1210

Graham NE, Hughes MK, Ammann CM, Cobb KM, Hoerling MP, Xu T, Kennett DJ, Kennett JP, Rein B, Stott L, Wigand PE (2007) Tropical Pacific-mid-latitude teleconnections in medieval times. Clim Change 83. doi:10.1007/s10584-007-9239-2

Graumlich L (1993) A 1000-year record of temperature and precipitation in the Sierra Nevada. Quaternary Res 39:249–255

Gray ST, Betancourt JL, Fastie CL, Jackson ST (2003) Patterns and sources of multidecadal oscillations in drought-sensitive tree-ring records from the central and southern Rocky Mountains. Geophys Res Lett 30(6):1316. doi:10.1029/2002GL016154

Gray ST, Graumlich LJ, Betancourt JL, Pederson GT (2004) A tree-ring based reconstruction of the Atlantic Multidecadal Oscillation since AD 1567. Geophys Res Lett 31:L12205. doi:10.1029/2004GL019932

Harte J (2002) Toward a synthesis of the Newtonian and Darwinian worldviews. Phys Today 55:29–34

Helama S, Timonen M, Lindholm M, Merilainen J, Eronen M (2005) Extracting long-period climate fluctuations from tree-ring chronologies over timescales of centuries to millennia. Int J Climatol 25:1767–1779

Hoerling MP, Kumar A (2000) Understanding and predicting extratropical teleconnections related to ENSO. In: Diaz HF, Markgraf V (eds) El Niño and the Southern Oscillation: multiscale variability and global and regional impacts. Cambridge University Press, New York, pp 57–88

Horel JD, Wallace JM (1981) Planetary-scale atmospheric phenomena associated with the Southern Oscillation. Mon Weather Rev 109:813–829

Huang S, Pollack HN, Shen P-Y (2000) Temperature trends over the past five centuries reconstructed from borehole temperatures. Nature 403:756–758

Hughes MK (1992) Dendroclimatic evidence from the western Himalaya. In: Bradley RS, Jones PD (eds) Climate since AD 1500. Routledge, London, pp 415–431

Hughes MK (2001) An improved reconstruction of temperature at Srinaga, Kashmir since AD 1660 based on tree-ring width and maximum latewood density of *Abies pindrow* [Royle] Spach. Palaeobotanist 50:13–19

Hughes MK (2002) Dendrochronology in climatology: the state of the art. Dendrochronologia 20:95–116

Hughes MK, Ammann CM (2009) The future of the past: an earth system framework for high resolution paleoclimatology: editorial essay. Clim Change 94:247–259
Hughes MK, Brown PM (1992) Drought frequency in central California since 101 BC recorded in giant sequoia tree rings. Clim Dynam 6:161–167
Hughes MK, Diaz HF (1994) Was there a 'Medieval Warm Period,' and if so, where and when? Clim Change 26:109–142
Hughes MK, Funkhouser G (1998) Extremes of moisture availability reconstructed from tree rings for recent millennia in the Great Basin of western North America. In: Beniston M, Innes JL (eds) The impacts of climate variability on forests. Springer, Berlin, pp 99–107
Hughes MK, Funkhouser G (2003) Frequency-dependent climate signal in upper and lower forest border tree rings in the mountains of the Great Basin. Clim Change 59:233–244
Hughes MK, Graumlich LJ (1996) Multimillennial dendroclimatic records from western North America. In: Bradley RS, Jones PD, Jouzel J (eds) Climatic variations and forcing mechanisms of the last 2000 years. Springer Verlag, Berlin, pp 109–124
Jacoby G, Pederson N, D'Arrigo R (2003) Temperature and precipitation in Mongolia based on dendroclimatic investigations. Chinese Sci Bull 48:1474–1479
Jansen E, Overpeck J, Briffa KR, Duplessy J-C, Joos F, Masson-Delmotte V, Olago D, Otto-Bliesner B, Peltier WR, Rahmstorf S, Ramesh R, Raynaud D, Rind D, Solomina O, Villalba R, Zhang D (2007) Palaeoclimate. In: Solomon S, Qin D, Manning M, Chen Z, Marquis M, Avery KB, Tignor M, Miller HL (eds) Climate change 2007: the physical science basis. Contribution of Working Group I to the Fourth assessment report of the Inter-governmental Panel on Climate Change. Cambridge University Press, Cambridge, UK, and New York, USA
Karoly D (1989) Southern Hemisphere circulation features associated with El Niño–Southern Oscillation. J Climate 2:1239–1252
Kaufman DS, Schneider DP, Mckay NP, Ammann CM, Bradley RS, Briffa KR, Miller GH, Otto-Bliesner BL, Overpeck JT, Vinther BM (2009) Recent warming reverses long-term Arctic cooling. Science 325:1236–1239
Kiladis GN, Diaz HF (1986) An analysis of the 1877–78 ENSO episode and comparison with 1982–83. Mon Weather Rev 114:1035–1047
Kiladis GN, Diaz HF (1989) Global climatic anomalies associated with extremes in the Southern Oscillation. J Climate 2:1069–1090
Kipfmueller KF, Salzer MW (2010) Linear trend and climate response of five-needle pines in the western United States related to treeline proximity. Can J Forest Res 40:134–142
Kitzberger T, Swetnam TW, Veblen TT (2001) Inter-hemispheric synchrony of forest fires and the El Niño-Southern Oscillation. Global Ecol Biogeogr 10:315–326
Kitzberger T, Brown PM, Heyerdahl EK, Swetnam TW, Veblen TT (2007) Contingent Pacific–Atlantic Ocean influence in multicentury wildfire synchrony over western North America. Proc Natl Acad Sci USA 104:543–548
Kutzbach JE, Bryson RA (1974) Variance spectrum of Holocene climatic fluctuations in the North Atlantic sector. J Atmos Sci 31:1958–1963
LaMarche VC (1974) Paleoclimatic inferences from long tree-ring records. Science 183: 1043–1088
LaMarche VC, Fritts HC (1971) Anomaly patterns of climate over the western United States, 1700–1930, derived from principal component analysis of tree-ring data. Mon Weather Rev 99:138–142
Lara A, Villalba R, Urrutia R (2008) A 400-year tree-ring record of the Puelo River summer-fall streamflow in the Valdivian Rainforest eco-region, Chile. Clim Change 86:331–356
Larsen LB, Vinther BM, Briffa KR, Melvin TM, Clausen HB, Jones PD, Siggaard-Andersen ML, Hammer CU, Eronen M, Grudd H, Gunnarson BE, Hantemirov RM, Naurzbaev MM, Nicolussi K (2008) New ice core evidence for a volcanic cause of the AD 536 dust veil. Geophys Res Lett 35. doi:10.1029/2007GL032450
Le Quesne C, Acuna C, Boninsegna JA, Rivera A, Barichivich J (2009) Long-term glacier variations in the central Andes of Argentina and Chile, inferred from historical records and tree-ring reconstructed precipitation. Palaeogeogr Palaeocl 281:320–333

Lough JM, Fritts HC (1985) The Southern Oscillation and tree rings: 1600–1961. J Clim Appl Meteorol 24:952–966
Luckman BH (1996) Dendrochronology and global change. In: Dean JS, Meko DM, Swetnam TW (eds) Tree rings, environment and humanity. Radiocarbon, Tucson, AZ, pp 1–24
Luckman BH, Wilson RJS (2005) Summer temperatures in the Canadian Rockies during the last millennium: a revised record. Clim Dynam 24:131–144
Luterbacher J, Dietrich D, Xoplaki E, Grosjean M, Wanner H (2004) European seasonal and annual temperature variability, trends, and extremes since 1500. Science 303:1499–1503
Mann ME, Jones PD (2003) Global surface temperatures over the past two millennia. Geophys Res Lett 30:1820. doi:10.1029/2003GL017814
Mann ME, Park J (1994) Global-scale modes of surface temperature variability on interannual to century timescales. J Geophys Res 99:25819–25833
Mann ME, Park J, Bradley RS (1995) Global interdecadal and century-scale climate oscillations during the past five centuries. Nature 378:266–270
Mann ME, Bradley RS, Hughes MK (1998) Global-scale temperature patterns and climate forcing over the past six centuries. Nature 392:779–787
Mann ME, Bradley RS, Hughes MK (1999) Northern Hemisphere temperatures during the past millennium: inferences, uncertainties, and limitations. Geophys Res Lett 26:759–762
Mann ME, Bradley RS, Hughes MK (2000) Long-term variability in the ENSO and associated teleconnections. In: Diaz HF, Markgraf V (eds) El Niño and the Southern Oscillation: multi-scale variability and global and regional impacts. Cambridge University Press, New York, pp 357–412
Mann ME, Zhang Z, Hughes MK, Bradley RS, Miller SK, Rutherford S, Ni F (2008) Proxy-based reconstructions of hemispheric and global surface temperature variations over the past two millennia. Proc Natl Acad Sci USA 105:13252–13257
Mann ME, Zhang Z, Rutherford S, Bradley RS, Hughes MK, Shindell D, Ammann C, Faluvegi G, Ni F (2009) Global signatures and dynamical origins of the 'Little Ice Age' and 'Medieval Climate Anomaly.' Science 326:1256–1260
Mantua NJ, Hare SR, Zhang Y, Wallace JM, Francis RC (1997) A Pacific interdecadal climate oscillation with impacts on salmon production. B Am Meteorol Soc 78:1069–1079
Meko DM, Woodhouse CA (2005) Tree-ring footprint of joint hydrologic drought in Sacramento and upper Colorado River basins, western USA. J Hydrol 308:196–213
Meko DM, Cook ER, Stahle DW, Stockton CW, Hughes MK (1993) Spatial patterns of tree-growth anomalies in the United States and southeastern Canada. J Climate 6:1773–1786
Meko DM, Therrell MD, Baisan CH, Hughes MK (2001) Sacramento River flow reconstructed to AD 869 from tree rings. J Am Water Resour As 37:1029–1039
Meko DM, Woodhouse CA, Baisan CA, Knight R, Lukas JL, Hughes MK, Salzer MW (2007) Medieval drought in the upper Colorado River basin. Geophys Res Lett 34:L10705. doi:10.1029/2007GL029988
Mitchell JM (1976) An overview of climatic variability and its causal mechanisms. Quaternary Res 6:481–493
Moberg A, Sonechkin DM, Holmgren K, Datsenko NM, Karlen W (2005) Highly variable Northern Hemisphere temperatures reconstructed from low- and high-resolution proxy data. Nature 433:613–617
Mote PW, Hamlet AF, Clark MP, Lettenmaier DP (2005) Declining mountain snowpack in western North America. B Am Meteorol Soc 86:39–49
Ni FB, Cavazos T, Hughes MK, Comrie AC, Funkhouser G (2002) Cool-season precipitation in the southwestern USA since AD 1000: comparison of linear and nonlinear techniques for reconstruction. Int J Climatol 22:1645–1662
Oerlemans J (2005) Extracting a climate signal from 169 glacier records. Science 308:675–677
Overpeck JT (1991) Century- to millennium-scale climatic variability during the Late Quaternary. In: Bradley RS (ed) Global changes of the past. UCAR Office of Interdisciplinary Earth Studies, Boulder, Colorado, pp 139–173

Pulwarty R, Jacobs K, Dole R (2005) The hardest working river: drought and critical water problems on the Colorado. In: Wilhite D (ed) Drought and water crises: science, technology and management. Taylor and Francis, Boca Raton, Florida, pp 249–285

Salzer MW, Hughes MK (2007) Bristlecone pine tree rings and volcanic eruptions over the last 5000 yr. Quaternary Res 67:57–68

Schlesinger ME, Ramankutty N (1994) An oscillation in the global climate system of period 65–70 years. Nature 367:723–726

Schulman, E. (1956) Dendroclimatic Changes in Semiarid America. University of Arizona Press, Tucson, AZ, 142 pp

Schweingruber FH, Briffa KR (1996) Tree-ring density networks for climate reconstruction. In: Jones PD, Bradley RS, Jouzel J (eds) Climatic variations and forcing mechanisms of the last 2000 years. Springer, Berlin, pp 43–66

Solomina ON, Davi N, D'Arrigo R, Jacoby G (2005) Tree-ring reconstruction of Crimean drought and lake chronology correction. Geophys Res Lett 32, ISI 000232551900002

St. George S, Meko DM, Girardin MP, Macdonald GM, Nielsen E, Pederson GT, Sauchyn DJ, Tardif JC, Watson E (2009) The tree-ring record of drought on the Canadian prairies. J Climate 22:689–710

Stahle DW, Cleaveland MK (1992) Reconstruction and analysis of spring rainfall over the southeastern US for the past 1000 years. B Am Meteorol Soc 73:1947–1961

Stahle DW, Cleaveland MK (1993) Southern Oscillation extremes reconstructed from tree rings of the Sierra Madre Occidental and southern Great Plains. J Climate 6:129–140

Stahle DW, Cleaveland MK, Blanton DB, Therrell MD, Gay DA (1998) The lost colony and Jamestown droughts. Science 280:564–567

Stahle DW, Cleaveland MK, Therrell MD (1999) Tree-ring reconstruction of winter and summer precipitation in Durango, Mexico, for the past 600 years. In: 10th Symposium on Global Change Studies, American Meteorological Society

Stahle DW, Cook ER, Cleaveland MK, Therrell MD, Meko DM, Grissino-Mayer HD, Watson E, Luckman BH (2000) Tree-ring data document sixteenth century megadrought over North America. Eos 81:121–125

Stahle DW, Fye FK, Cook ER, Griffin RD (2007) Tree-ring reconstructed megadroughts over North America since AD 1300. Clim Change 83:133–149

Stewart IT, Cayan DR, Dettinger MD (2005) Changes toward earlier streamflow timing across western North America. J Climate 18:1136–1155

Stine S (1994) Extreme and persistent drought in California and Patagonia during mediaeval time. Nature 269:546–549

Stockton CW, Jacoby GC (1976) Long-term surface water supply and streamflow levels in the upper Colorado River basin. Lake Powell Research Project Bulletin 18, 70 pp

Stockton CW, Meko DM (1975) A long-term history of drought occurrence in western United States inferred from tree rings. Weatherwise 28:244–249

Stockton CW, Meko DM (1983) Drought recurrence in the Great Plains as reconstructed from long-term tree-ring records. J Clim Appl Meteorol 22:17–29

Swetnam TW, Betancourt JL (1990) Fire–Southern Oscillation relations in the southwestern United States. Science 249:1017–1020

Swetnam TW, Betancourt JL (1998) Mesoscale disturbance and ecological response to decadal climatic variability in the American Southwest. J Climate 11:3128–3147

Therrell MD, Stahle DW, Acuña Soto R (2004) Aztec drought and 'Curse of One Rabbit.' B Am Meteorol Soc 85:1263–1272

Thompson DWJ, Wallace JM (2000) Annular modes in the extratropical circulation. Part I: Month-to-month variability. J Climate 13:1000–1016

Thompson DWJ, Wallace JM, Hegerl GC (2000) Annular modes in the extratropical circulation. Part II: Trends. J Climate 13:1018–1036

Touchan R, Xoplaki E, Funkhouser G, Luterbacher J, Hughes MK, Erkan N, Akkemik U, Stephan J (2005) Reconstructions of spring/summer precipitation for the eastern Mediterranean from tree-ring widths and its connection to large-scale atmospheric circulation. Clim Dynam 25:75–98

Touchan R, Anchukaitis KJ, Meko DM, Attalah S, Baisan C, Aloui A (2008) Long term context for recent drought in northwestern Africa. Geophys Res Lett 35, ISI 000257738500005

Trouet V, Esper J, Graham NE, Baker A, Scourse JD, Frank DC (2009) Persistent positive North Atlantic Oscillation mode dominated the medieval climate anomaly. Science 324:78–80

US Department of Energy (1989) Atmospheric carbon dioxide and the greenhouse effect. National Technical Information Service, Springfield, Virginia, 36 pp

Vaganov EA, Shiyatov SG, Mazepa VS (1996) Dendroclimatic study in Ural-Siberian subarctic. 'Nauka' Siberian Publishing Firm RAS, Novosibirsk

Vaganov EA, Hughes MK, Shashkin AV (2006) Growth dynamics of conifer tree rings: images of past and future environments. Springer, Berlin Heidelberg New York

Villalba R, Grau HR, Bonisegna JA, Jacoby GC, Ripalta A (1998) Tree-ring evidence for long-term precipitation changes in subtropical South America. J Biogeogr 18:1463–1478

Villalba R, D'Arrigo RD, Cook ER, Wiles G, Jacoby GC (2001) Decadal-scale climatic variability along the extratropical western coast of the Americas: evidences from tree-ring records. In: Markgraf V (ed) Interhemispheric climate linkages. Academic Press, San Diego, pp 155–172

Villalba R, Lara A, Boninsegna JA, Masiokas M, Delgado S, Aravena JC, Roig FA, Schmelter A, Wolodarsky A, Ripalta A (2003) Large-scale temperature changes across the southern Andes: twentieth-century variations in the context of the past 400 years. Clim Change 59:177–232

Villanueva-Diaz J, Stahle DW, Luckman BH, Cerano-Paredes J, Therrell MD, Cleaveland MK, Cornejo-Oviedo E (2007) Winter-spring precipitation reconstructions from tree rings for northeast Mexico. Clim Change 83:117–131

Webb T (1991) The spectrum of temporal climatic variability: current estimates and the need for global and regional time series. In: Bradley RS (ed) Global changes of the past. UCAR Office of Interdisciplinary Earth Studies, Boulder, Colorado, pp 61–81

Westerling AL, Swetnam TW (2003) Interannual to decadal drought and wildfire in the western US. Eos 84:545–560

Westerling AL, Hidalgo HG, Cayan DR, Swetnam TW (2006) Warming and earlier spring increase in western US forest wildfire activity. Science 313:940–943

Wigley TML (1991) Climate variability on the 10–100-year time scale: observations and possible causes. In: Bradley RS (ed) Global changes of the past. UCAR Office of Interdisciplinary Earth Studies, Boulder, Colorado, pp 83–101

Woodhouse CA (2003) A 431-yr reconstruction of western Colorado snowpack from tree rings. J Climate 16:1551–1561

Woodhouse CA, Gray ST, Meko DM (2006) Updated streamflow reconstructions for the upper Colorado River basin. Water Resour Res 42:W05415. doi:10.1029/2005WR004455

Woodhouse CA, Russell JL, Cook ER (2009) Two modes of North American drought from instrumental and paleoclimatic data. J Climate 22:4336–4347

Yadav RR, Singh J (2002) Tree-ring-based spring temperature patterns over the past four centuries in western Himalaya. Quaternary Res 57:299–305

Yin ZY, Shao XM, Qin NS, Liang E (2008) Reconstruction of a 1436-year soil moisture and vegetation water use history based on tree-ring widths from Qilian junipers in northeastern Qaidam Basin, northwestern China. Int J Climatol 28:37–53

Zhang Y, Wallace JM, Battisti DS (1997) ENSO-like interdecadal variability: 1900–93. J Climate 10:1004–1020

Index

M.K. Hughes et al. (eds.), *Dendroclimatology*, Developments in Paleoenvironmental Research 11, DOI 10.1007/978-1-4020-5725-0,